

Cooperative Institute for Mesoscale Meteorological Studies

Annual Report

Prepared for the
National Oceanic and Atmospheric Administration
Office of Oceanic and Atmospheric Research

Cooperative Agreement NA11OAR4320072

Fiscal Year – 2016

Cover figure – RaXPol 1.7degree radar reflectivity (dBZ) at 2308 UTC with corresponding EnKF analysis ensemble mean convergence (s^{-1}) overlain in blue contours, dashed contours represent negative values. Ensemble mean wind vectors are plotted in white with regions where wind speed is greater than 25 m s^{-1} shaded white. The rear-flank downdraft (RFD) gust front and broad downdraft extending through the forward flank are annotated. For more on this project involving Patrick Skinner and Jeffrey Snyder (CIMMS at NSSL), Louis Wicker (NSSL), and Howard Bluestein and Kyle Thiem (OU School of Meteorology), see pages 153-154.

Table of Contents

Introduction	4
General Description of CIMMS and its Core Activities	4
Management of CIMMS, including Mission and Vision Statements, and Organizational Structure	5
Executive Summary Listing of Activities during FY2015	6
Distribution of NOAA Funding by CIMMS Task and Research Theme	12
CIMMS Executive Board and Assembly of Fellows Meeting Dates and Membership	13
General Description of Task I Expenditures and All NOAA Expenditures	16
Research Performance	17
Theme 1 – Weather Radar Research and Development	17
Theme 2 – Stormscale and Mesoscale Modeling Research and Development	138
Theme 3 – Forecast and Warning Improvements Research and Development	193
Theme 4 – Impacts of Climate Change Related to Extreme Weather Events	285
Theme 5 – Societal and Socioeconomic Impacts of High Impact Weather Systems	289
Public Affairs and Outreach	306
Appendix A – Awards and Honors	309
Appendix B – Publication Summary	313
Appendix C – Personnel Summary – NOAA Funded Research Only	314
Appendix D – Compilation of CIMMS-Related Publications 2014-2015	315
Appendix E – NOAA Competitive Award Recipient Reports and NOAA Hurricane Sandy Competitive Award Recipient Reports	324

**COOPERATIVE INSTITUTE FOR MESOSCALE METEOROLOGICAL STUDIES
THE UNIVERSITY OF OKLAHOMA**

**Annual Report of Research Progress Under
Cooperative Agreement NA11OAR4320072
During the 2016 Fiscal Year**

*Randy A. Pepler, Interim Director
Tracy L. Reinke, Executive Director of Finance and Operations
Sebastian Torres, Assistant Director for NOAA Relations*

INTRODUCTION

General Description of CIMMS and its Core Activities

The Cooperative Institute for Mesoscale Meteorological Studies (CIMMS) was established in 1978 as a cooperative program between the National Oceanic and Atmospheric Administration (NOAA) and The University of Oklahoma (OU). CIMMS provides a mechanism to link the scientific and technical resources of OU and NOAA to create a center of research excellence in weather radar, stormscale meteorological phenomena, regional climate variations, and related subject areas – all with the goal of helping to produce better forecasts and warnings that save lives and protect property.

CIMMS promotes cooperation and collaboration on problems of mutual interest among university researchers and the NOAA Office of Oceanic and Atmospheric Research (OAR) National Severe Storms Laboratory (NSSL), National Weather Service (NWS) Radar Operations Center (ROC) for the WSR-88D (NEXRAD) Program, NWS NCEP (National Centers for Environmental Prediction) Storm Prediction Center (SPC), NWS Warning Decision Training Division (WDTD), NWS Norman Forecast Office (OUN), and NWS Training Center (NWSTC) in Kansas City, Missouri. Late in FY16, CIMMS established a relationship with the NOAA Air Resources Laboratory's Atmospheric Turbulence and Diffusion Division, in an agreement with Oak Ridge Associated Universities (ORAU).

CIMMS research contributes to the NOAA mission through improvement of the observation, analysis, understanding, and prediction of weather elements and systems and climate anomalies ranging in size from cloud nuclei to multi-state areas. Advances in observational and analytical techniques lead to improvements in understanding of the evolution and structure of these phenomena. Understanding provides the foundation for more accurate prediction of hazardous weather and anomalous regional climate. Better prediction contributes to improved social and economic welfare. Because small-, meso-, and regional-scale phenomena are also important causes and manifestations of climate, CIMMS research is contributing to improved understanding of the global climate system and regional climate variability and change. CIMMS promotes research collaboration between scientists at OU and NOAA by providing a center where government and

academic scientists may work together to learn about and apply their knowledge of stormscale weather and regional-scale climate processes.

CIMMS is part of the National Weather Center, a unique confederation of federal, state, and OU organizations that work together in partnership to improve understanding of the Earth's atmosphere. Recognized for its collective expertise in severe weather, many of the research and development activities of the Center have served society by improving weather observing and forecasting, and thus have contributed to reductions in loss of life and property.

In addition to CIMMS, National Weather Center organizations include:

- NOAA OAR National Severe Storms Laboratory (NSSL)
- NOAA NWS Warning Decision Training Division (WDTD)
- NOAA NWS NCEP Storm Prediction Center (SPC)
- NOAA NWS Radar Operations Center (ROC)
- NOAA NWS Norman Forecast Office (OUN)
- Oklahoma Climatological Survey (OCS)
- OU Center for Analysis and Prediction of Storms (CAPS)
- OU Advanced Radar Research Center (ARRC)
- OU College of Atmospheric and Geographic Sciences
- OU School of Meteorology
- OU Department of Geography and Environmental Sustainability

CIMMS concentrates its research and outreach efforts and resources on the following principal themes: (1) weather radar research and development, (2) stormscale and mesoscale modeling research and development, (3) forecast and warning improvements research and development, (4) impacts of climate change related to extreme weather events, and (5) societal and socioeconomic impacts of high impact weather systems.

This report describes NOAA-funded research and outreach progress made by CIMMS scientists at OU and those assigned to our collaborating NOAA units under cooperative agreement NA11OAR4320072 during 1 July 2015 through 30 June 2016. Publications written, awards received, and employee and funding statistics are presented in Appendices.

Management of CIMMS, including Mission and Vision Statements, and Organizational Structure

An Executive Board and Council of Fellows help advise CIMMS.

The CIMMS Executive Board is to meet quarterly to provide advice and recommendations to the Director of CIMMS regarding appointments, procedures, and policies; to review and adopt bylaws; and to periodically review the accomplishments and progress of the technical and scientific programs and projects of the CIMMS.

The Council of Fellows meets as needed and is composed of a cross-section of local and national scientists who have expertise relevant to the research themes of CIMMS and are actively involved in the programs and projects of CIMMS. Appointment as a Fellow, by the CIMMS Executive Board, is normally for a two-year term, and reappointment is possible. Appointments may be made for a shorter period of time or on a part-time basis with the concurrence of the appointee and the CIMMS Executive Board. Fellows will review and suggest modifications of bylaws, participate in reviews of CIMMS activities, and elect two of their number to serve on the Executive Board. The Executive Board appoints Fellows.

The Mission and Vision Statements of CIMMS are as follows:

Mission – *To promote collaborative research among University and NOAA scientists on problems of mutual interest to improve basic understanding and to help produce better forecasts and warnings that save lives and property*

Vision – *A center of research excellence in mesoscale meteorology and related topics, fostering vibrant University-NOAA collaborations*

The organizational structure of CIMMS in FY16 included: Interim Director (Randy Pepler), Executive Director of Finance and Operations Director (Tracy Reinke), Assistant Director for NOAA Relations (Sebastian Torres), Account and Budget Representative (Jamie Foucher), and Staff Assistant (Tanya Riley). Scientists, students, and post-docs are housed on the OU campus in its National Weather Center (NWC) and at the NWSTC in Kansas City. Some CIMMS undergraduate students have duty stations off-campus at ROC in Norman.

Executive Summary Listing of Activities during FY2016

Theme 1 – Weather Radar Research and Development

At the very center of NOAA's mission are the objectives of achieving a "reduced loss of life, property, and disruption from high-impact weather events", "improved transportation efficiency and safety", and "improved freshwater resource management" (NOAA's *Next Generation Strategic Plan*, Long-Term Goal: Weather Ready Nation, pp. 10-14, December 2010). The weather systems involved include severe thunderstorms, tornadoes, tropical storms and hurricanes, and winter cyclones. Those systems produce the high intensity precipitation, strong winds, flooding, lightning strikes, freezing rain, and large snow accumulations that damage property, cost lives, disrupt transportation, and cause other economic dislocation. Reduction of these adverse impacts can result from the availability and use of accurate forecasts of the above weather systems and their associated phenomena, for future periods ranging from several days down to a few minutes. One of the essential starting points for developing those forecasts is the detailed observation of the present state of the atmosphere.

For almost 60 years, remote sensing via weather radar has been a vital source of the necessary observations. The present national weather radar system (WSR-88D) uses reflectivity and Doppler velocity measurements to document the location and movement of the above weather systems, and indicate the time evolution of their precipitation intensity and wind strength. However, this radar system soon will be as old (30 years) as the chronologically and technologically ancient system (WSR-57) that it replaced in 1988. This situation has two crucial implications for NOAA's continued pursuit of its above objectives to achieve a "reduced loss of life, property, and disruption from high impact weather events", "improved transportation efficiency and safety", and "improved freshwater management". First, NOAA and its partners must complete the recently initiated development of the new Multi-Function Phased Array Radar (MPAR) system that will replace the WSR-88D and is incorporating all relevant technological advances during the last 20+ years. Second, since completion of this development activity will require another 7-12 years at its current rate of progression, the ongoing current WSR-88D upgrades (especially Dual-Polarization) must be brought to fruition as soon as possible.

During the past year, research was conducted on:

- ***NSSL Project 1 – Advancements in Weather Radar***
 - WSR-88D Improvements
 - Dual-Polarization
 - MPAR Meteorology
 - MPAR Engineering

- ***NSSL Project 2 – Hydrometeorology Research***

- ***CIMMS Task III Projects***
 - ARRC R&D Activities for the Multi-Mission Phased Array Radar Program
 - Polarimetric Phased Array Radar Research in Support of MPAR Strategy

Theme 2 – Stormscale and Mesoscale Modeling Research and Development

Research and development for stormscale and mesoscale modeling are essential for NOAA's aforementioned objectives. Use of stormscale and mesoscale models is a major ingredient of the forecasting and nowcasting procedures for high impact weather events, and is expected to grow in the future. The initialization of those prediction models is depending increasingly on wind and other observations from the current weather radar systems. This dependence also is anticipated to expand and therefore is a principal motivation for the weather radar research and development proposed above -- to improve the initialization and hence performance of the prediction models. At the center of this radar-modeling interface is the manner in which radar data are ingested into the models, especially in combination with measurements from other platforms (e.g., satellite, rawinsonde, surface) via "assimilation" procedures. In addition to their predictive roles, stormscale and mesoscale models also are used extensively in a research mode to understand better the behavior of weather systems on those scales.

The atmospheric processes that receive particular attention in these simulations include mesoscale dynamics, convective initiation, cloud dynamics and microphysics, and the precipitation process. Also investigated is the sensitivity of the simulation results to the data assimilation procedures. The ultimate goal of such stormscale and mesoscale simulation research is to improve the performance of the operational forecasting models.

During the past year, research was conducted on:

- ***NSSL Project 3 – Numerical Modeling and Data Assimilation***
- ***NSSL Project 4 – Hydrologic Modeling Research***
- ***NSSL Project 7 – Synoptic, Mesoscale and Stormscale Processes Associated with Hazardous Weather***
- ***CIMMS Task III Projects***
 - Operation of VHF Lightning Mapping Systems to Provide Data for GOES-R GLM Verification and Algorithm Development and Testing
 - Using Total Lightning Data from BLM/GOES-R to Improve Real-Time Tropical Cyclone Genesis and Intensity Forecasts
 - Assimilating Satellite Data into NWP Models to Improve Forecasting of High Impact Weather Events
 - Hybrid Data Assimilation for Convective-Scale “Warn-on Forecast”
 - Objective Probabilistic Guidance for Severe Weather Outbreaks

Theme 3 – Forecast and Warning Improvements Research and Development

It is under this theme that the results of the research and development from the two preceding themes are integrated and converted into improved weather forecasts and warnings disseminated to the U.S. public. The ultimate outcome is to provide NWS forecasters routinely with enhanced information on which to base their forecasts. Two areas of highly innovative activity, anchored within the Hazardous Weather Testbed (HWT), dominate this effort – the Experimental Forecasting Program and the Experimental Warning Program. Activity within this theme also is dominated by the training activities of CIMMS scientists at the Warning Decision Training Branch.

During the past year, research and training were conducted on:

- ***NSSL Project 5 – Hazardous Weather Testbed***
- ***NSSL Project 6 – Development of Technologies and Techniques in Support of Warnings***

- ***ROC Project 10 – Analysis of Dual Polarized Weather Radar Observations of Severe Convective Storms to Understand Severe Storm Processes and Improve Warning Decision Support***
- ***SPC Project 11 – Advancing Science to Improve Knowledge of Mesoscale Hazardous Weather***
- ***WDTD Project 12 – Warning Decision-Making Research and Training***
- ***OST Project 13 – Research on Integration and Use of Multi-Sensor Information for Severe Weather Warning Operations***
- ***NWSTC Project 14 – Forecast Systems Optimization and Decision Support Services Research Simulation and Training***
- ***CIMMS Task III Projects***
 - The GOES-R GLM Lightning Jump Algorithm: A National Field Test for Operational Readiness
 - Development of Short-Range Real-Time Analysis and Forecasting System Based on the ARPS for Taiwan Region
 - Contribution to Model Development and Enhancement Research Team by the Center for Analysis and Prediction of Storms
 - Advanced Data Assimilation and Prediction Research for Convective-Scale “Warn-on-Forecast”
 - National Sea Grant Weather & Climate Extension Specialist Activities
 - Prototyping and Evaluating Key Network-of-Networks Technologies

Theme 4 – Impacts of Climate Change Related to Extreme Weather Events

Here, we are concerned with the regional and global climate system context of mesoscale and stormscale weather variability, and especially the functioning of what now is termed the weather-climate interface. The genesis and trends of extreme events are of particular interest, given society’s current concerns about climate maintenance and change. The optimum path forward will require an appropriate combination of observational (using fine resolution data) and modeling (emphasizing convection) research. This theme also addresses the NOAA objective of achieving “improved scientific understanding of the changing climate system and its impacts” and “assessments of current and future states of the climate system that identify potential impacts and inform science, services, and stewardship decisions” (*NOAA’s Next Generation Strategic Plan*, Long-Term Goal: Climate Adaptation and Mitigation, pp. 5-10, December 2010).

During the past year, research and outreach were conducted on:

- **CIMMS Task III Project**
 - The Assimilation, Analysis, and Dissemination of Pacific Rain Gauge Data (PACRAIN)

Theme 5 – Societal and Socioeconomic Impacts of High Impact Weather Systems

This theme contributes to several of NOAA’s objectives - - providing “mitigation and adaptation choices supported by sustained, reliable, and timely climate services”; achieving “a climate-literate public that understands its vulnerabilities to a changing climate and makes informed decisions”; and furnishing “services meeting the evolving demands of regional stakeholders” (*NOAA’s Next-Generation Strategic Plan*, Long-Term Goal: Climate Adaptation and Mitigation, pp. 5-10, December 2010). Much of the effort here is motivated and fed by results obtained under the Forecast and Warning Improvements and Extreme Weather-Climate Change Impacts themes that, in turn, are built around the core of the more basic Weather Radar and Stormscale/Mesoscale Modeling Research and Development. The goal here is to facilitate the mitigation (enhancement) of the adverse (beneficial) social and socioeconomic impacts of high-impact weather systems and regional/seasonal-scale climate variations. Thus, our contributions to this theme are part of NOAA’s crucial ultimate interface with society, and therefore will reflect the continuing and increasing involvement of OU social scientists.

During the past year, research and outreach were conducted on:

- **NSSL Project 8 – Warning Process Evolution and Effective Communication to the Public**
- **NSSL Project 9 – Evaluating the Impact of New Technologies, Data, and Information in the Operational Forecasting Environment**
- **CIMMS Task III Projects**
 - Collaborative Research: Understanding the Current Flow of Weather Information and Associated Uncertainty, and Their Effect on Emergency Managers and the General Public
 - Implementation of a Drought App for Mobile Devices
 - Drought Risk Management for the United States
 - Baseline of Public Responsiveness to Uncertainty in Forecasts

Public Affairs and Outreach

CIMMS education and outreach activities help NOAA achieve its objectives of providing “an engaged and educated public with an improved capacity to make scientifically informed environmental decisions” and making “full and effective use of international partnerships and policy leadership to achieve NOAA’s mission objectives” (*NOAA’s*

Next Generation Strategic Plan, Engagement Enterprise Objective, pp. 30-32, December 2010). CIMMS location and role within the OU-NOAA National Weather Center (NWC) has embedded it within a wide-ranging and ongoing set of education and outreach activities that will draw continuously on the knowledge developed within the five above research themes. Those activities (a) involve local and national outreach to the general public, (b) extend across all levels of formal education, and (c) provide post-doctoral and professional development opportunities for individuals in careers related to the atmospheric sciences.

During the past year, public affairs and outreach activities included:

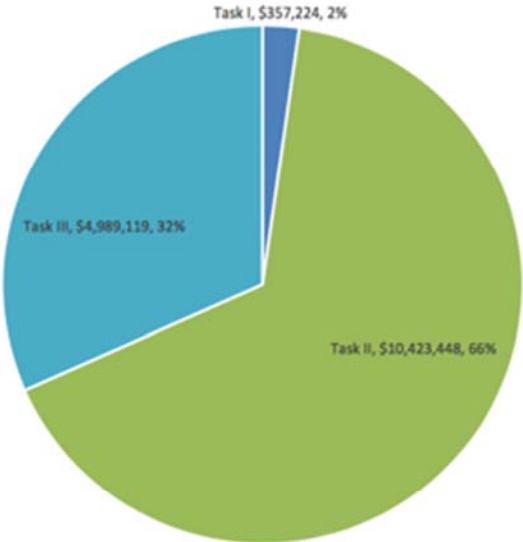
- NOAA Partners Communications, Public Affairs, and Outreach
- CIMMS at WDTD Outreach

Awards and Honors

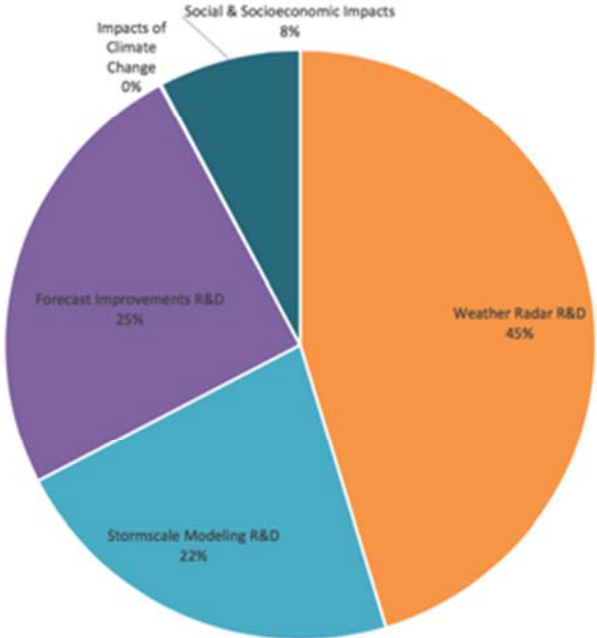
See Appendix A.

Distribution of NOAA Funding by CIMMS Task and Research Theme

NOAA Funding by Task FY16



NOAA Funding by Theme FY16



■ Weather Radar R&D
 ■ Stormscale Modeling R&D
 ■ Forecast Improvements R&D
 ■ Impacts of Climate Change
 ■ Social & Socioeconomic Impacts

CIMMS Executive Board and Council of Fellows Meeting Dates and Membership

Executive Board meetings were held on November 6, 2015 and March 25, 2016. No Council of Fellows meetings took place in FY16.

Executive Board membership for 2016 is as follows:

- Dr. Randy Pepler (Chair), Interim Director, CIMMS, and Lecturer, Department of Geography and Environmental Sustainability, OU
- Dr. Robert Palmer, Associate Vice President for Research, Executive Director, ARRC, and Professor and Tommy C. Craighead Chair, School of Meteorology, OU (Provost designated)
- Dr. Carol Silva, Director, CRCM, and Associate Professor of Political Science, OU (Provost designated)
- Dr. Kirsten de Beurs, Chair and Associate Professor, Department of Geography and Environmental Sustainability, OU (Provost designated)
- Mr. Lans Rothfusz, Deputy Director, NSSL (OAR designated)
- Dr. Jack Kain, Chief, Forecast Research and Development Division, NSSL (OAR designated)
- Mr. Richard Murman, Radar Operations Center Applications Branch (NWS designated)
- Dr. Steven Weiss, Chief, Science Support Branch, SPC (NWS designated)
- Dr. Boon Leng Cheong, Research Scientist, ARRC (Elected from Assembly of Fellows)
- Dr. David Turner, Research Meteorologist, NSSL (Elected from Assembly of Fellows)
- Mr. David Andra, Meteorologist-in-Charge, Norman NWS WFO (*ex-officio* member)
- Dr. Steven Koch, Director, NSSL (*ex-officio* member)
- Mr. Ed Mahoney, Director, WDTD (*ex-officio* member)
- Dr. Russell Schneider, Director, SPC (*ex-officio* member)
- Mr. Terry Clark, Director, ROC (*ex-officio* member)
- Dr. David Parsons, Chair, OU School of Meteorology, Associate Director, CAPS, and Mark and Kandi McCasland Professor of Meteorology (*ex-officio* member)

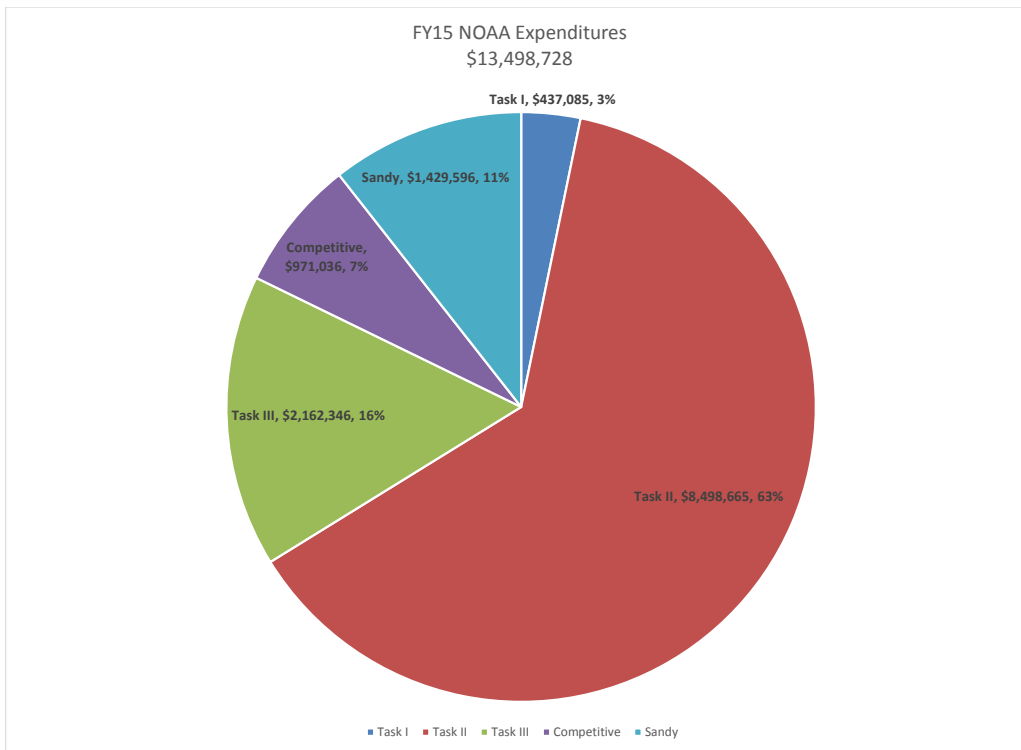
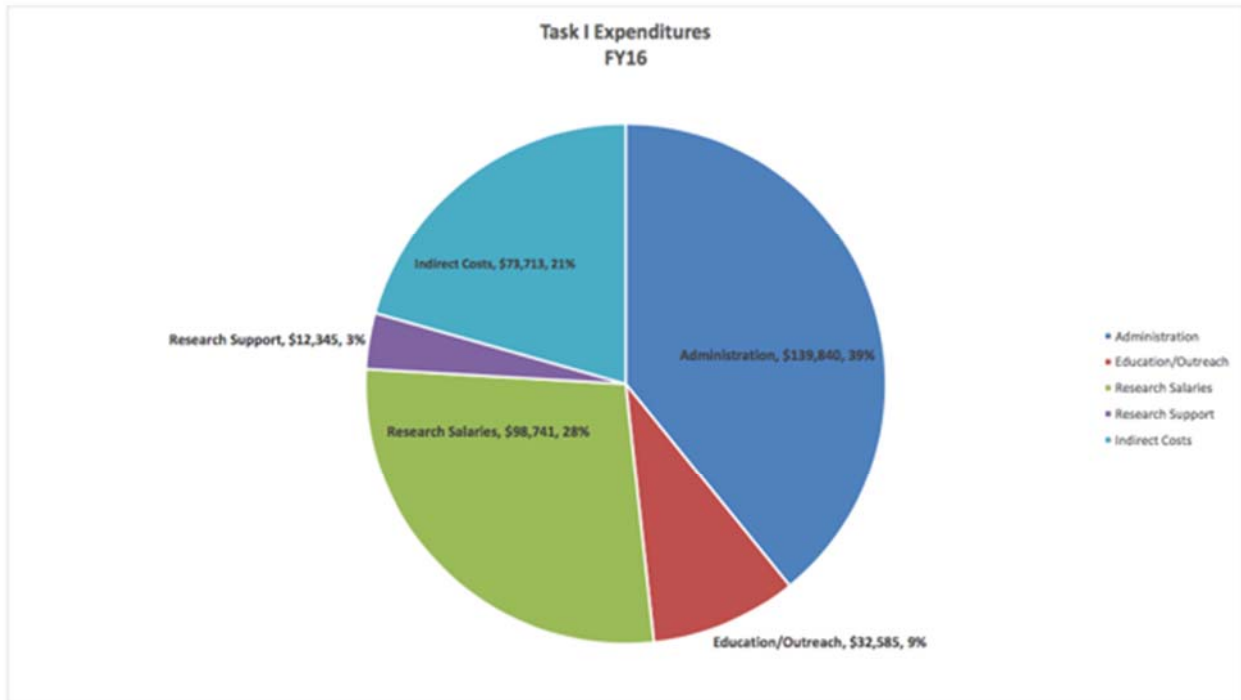
Council of Fellows membership for 2015-2017 is as follows:

- Dr. Jeffrey B. Basara, Associate Professor of Meteorology, OU
- Dr. William H. Beasley, Professor of Meteorology, OU
- Dr. Michael I. Biggerstaff, Professor of Meteorology, OU
- Dr. Howard B. Bluestein, George Lynn Cross Research Professor of Meteorology, OU
- Dr. Keith Brewster, Senior Scientist and Associate Director, CAPS, OU
- Dr. Harold E. Brooks, Research Meteorologist and Team Leader, Mesoscale Applications Group, NSSL, and Adjunct Professor of Meteorology, OU
- Dr. Frederick H. Carr, Professor of Meteorology OU
- Dr. Steven Cavallo, Assistant Professor of Meteorology, OU
- Dr. Boon Leng Cheong, Research Scientist, ARRC, OU
- Dr. Phillip Chilson, Professor of Meteorology, OU
- Dr. Adam J. Clark, Research Meteorologist, NSSL
- Mr. Terrence Clark, Director, ROC
- Dr. Michael Coniglio, Research Scientist, NSSL
- Dr. Kirsten de Beurs, Chair and Associate Professor of Geography and Environmental Sustainability, OU
- Dr. Michael W. Douglas, Retired Research Scientist, NSSL
- Dr. Richard J. Doviak, Senior Engineer, Doppler Radar and Remote Sensing Research Group, NSSL, and Affiliate Professor of Meteorology and of Electrical and Computer Engineering, OU
- Dr. Kelvin K. Droegemeier, Vice President for Research and Regents' Professor, OU
- Dr. Claude E. Duchon, Emeritus Professor of Meteorology, OU
- Dr. Chris Fiebrich, Associate Director, OCS
- Dr. Jack Friedman, Research Scientist, CASR, OU
- Dr. Caleb Fulton, Assistant Professor of Electrical and Computer Engineering, OU
- Dr. Jidong Gao, Research Scientist, NSSL
- Dr. Nathan Goodman, Associate Professor of Electrical and Computer Engineering, OU

- Dr. J.J. Gourley, Research Scientist, NSSL
- Dr. Pamela Heinselman, Research Scientist, NSSL
- Mr. Kurt Hondl, Research Meteorologist, NSSL
- Dr. Yang Hong, Associate Professor of Civil Engineering and Environmental Sciences, OU
- Mr. Ken Howard, Research Meteorologist, NSSL
- Mr. Michael Jain, Acting Chief, Radar Research & Development Division, NSSL
- Dr. Hank Jenkins-Smith, Associate Director, CASR, and Professor of Political Science, OU
- Dr. Israel Jirak, Science and Operations Officer, SPC
- Dr. David P. Jorgensen, Chief, Warning Research & Development Division, NSSL
- Dr. Jack Kain, Chief, Forecasting Research & Development Division, NSSL
- Dr. Petra Klein, E. K. Gaylord Presidential Professor and Associate Professor of Meteorology, OU
- Mr. Kevin E. Kelleher, Director, Global Systems Division, ESRL
- Dr. James F. Kimpel, Director, Emeritus NSSL, and Emeritus Professor of Meteorology, OU
- Dr. Kevin Kloesel, Director, OCS, and Associate Professor of Meteorology, OU
- Dr. Steven Koch, Director, NSSL
- Dr. Fanyou Kong, Research Scientist, CAPS, OU
- Dr. Daphne LaDue, Research Scientist, CAPS, OU
- Dr. Valliappa Lakshmanan, Director of Meteorology, The Climate Corporation
- Dr. S. Lakshmiarahan, George Lynn Cross Research Professor of Computer Science, OU
- Dr. Lance M. Leslie, Robert E. Lowry Chair and George Lynn Cross Professor of Meteorology, OU
- Dr. Donald R. MacGorman, Research Physicist, Convective Weather Research Group, NSSL, and Affiliate Professor of Meteorology and of Physics and Astronomy, OU
- Mr. Ed Mahoney, Chief, WDTD
- Dr. Edward Mansell, Research Scientist, NSSL
- Dr. Patrick Marsh, Techniques Development Meteorologist, SPC
- Dr. Elinor Martin, Assistant Professor of Meteorology, OU
- Dr. Amy McGovern, Associate Professor of Computer Science, OU
- Dr. Renee McPherson, Director of Research, South Central Climate Science Center, and Associate Professor of Geography and Environmental Sustainability, OU
- Dr. Berrien Moore III, Vice President for Weather and Climate Programs, Dean, College of Atmospheric and Geographic Sciences, Director, National Weather Center, and Chesapeake Professor of Meteorology, OU
- Dr. Mark L. Morrissey, Professor of Meteorology, OU
- Mr. Richard Murnan, Radar Meteorologist, ROC
- Mr. John Ogren, Acting Chief Learning Officer, NWS
- Dr. Robert D. Palmer, Associate Vice President for Research, Executive Director, ARRC, and Tommy Craighead Chair and Professor of Meteorology, and OU
- Dr. David Parsons, Director, School of Meteorology, Mark and Kandi McCasland Professor of Meteorology, OU
- Dr. Robert Rabin, Research Scientist, NSSL
- Dr. Michael B. Richman, E. K. Gaylord Presidential Professor of Meteorology, OU
- Mr. Lans Rothfusz, Deputy Director, NSSL
- Dr. Jessica Ruyle, Assistant Professor of Electrical and Computer Engineering, OU
- Dr. Jorge Salazar-Cerreno, Assistant Professor of Electrical and Computer Engineering, OU
- Dr. Russell Schneider, Director, SPC
- Dr. Mark Shafer, Director of Climate Services, OCS, and Assistant Professor of Geography and Environmental Sustainability, OU
- Dr. Alan M. Shapiro, American Airlines Professor and President's Associates Presidential Professor of Meteorology, OU
- Dr. Hjalti Sigmarsson, Assistant Professor of Electrical and Computer Engineering, OU
- Dr. Carol Silva, Director, CRCM, and Professor of Political Science, OU
- Dr. Paul Spicer, Professor of Anthropology, OU
- Dr. David J. Stensrud, Chair, Department of Meteorology, Pennsylvania State University
- Dr. Jerry M. Straka, Professor of Meteorology, OU
- Dr. Aondover A. Tarhule, Associate Dean, College of Atmospheric and Geographic Sciences, and Associate Professor, Department of Geography and Environmental Sustainability, OU
- Dr. David Turner, Research Scientist, Global Systems Division, ESRL
- Dr. Xuguang Wang, Associate Professor of Meteorology, and Presidential Research Professor, OU
- Mr. Steven J. Weiss, Chief, Science Support Branch, SPC

- Dr. Louis J. Wicker, Research Meteorologist, Convective Weather Research Group, NSSL, and Affiliate Associate Professor of Meteorology, OU
- Dr. Kimberly Winton, Director, South Central Climate Science Center, USGS
- Dr. Qin Xu, Research Meteorologist, Models and Assimilation Team, NSSL, and Affiliate Professor of Meteorology, OU
- Dr. Ming Xue, Director, CAPS, and Professor of Meteorology, OU
- Dr. Mark Yeary, Professor of Electrical and Computer Engineering, OU
- Dr. Tian-You Yu, Director of Operations, ARRC, and Professor of Electrical and Computer Engineering, OU
- Mr. Allen Zahrai, Team Leader, Radar Engineering and Development, NSSL
- Dr. Guifu Zhang, Professor of Meteorology, OU
- Dr. Jian Zhang, Research Hydrometeorologist, NSSL
- Dr. Yan Zhang, Associate Professor of Electrical and Computer Engineering, OU
- Dr. Conrad Ziegler, Research Meteorologist, Models and Assimilation Team, NSSL
- Dr. Dusan S. Zrnica, Senior Engineer and Group Leader, Doppler Radar and Remote Sensing Research Group, NSSL, and Affiliate Professor of Meteorology and of Electrical and Computer Engineering, OU

General Description of Task I Expenditures and All NOAA Expenditures



RESEARCH PERFORMANCE

Theme 1 – Weather Radar Research and Development

NSSL Project 1 – Advancements in Weather Radar

NOAA Technical Leads: Michael Jain, Kurt Hondl, Dusan Zrnić, Pamela Heinselman, and Allen Zahrai (NSSL)

NOAA Strategic Goal 2 – Weather-Ready Nation – Society is Prepared for and Responds to Weather-Related Events

Funding Type: CIMMS Task II

1. WSR-88D Improvements

Overall Objectives

Conduct research and development to provide improvements to the NWS operational radar (WSR-88D). This research explores ways to improve the detection of hazardous weather and improve the weather radar data quality.

Accomplishments

a. Ground Clutter Mitigation

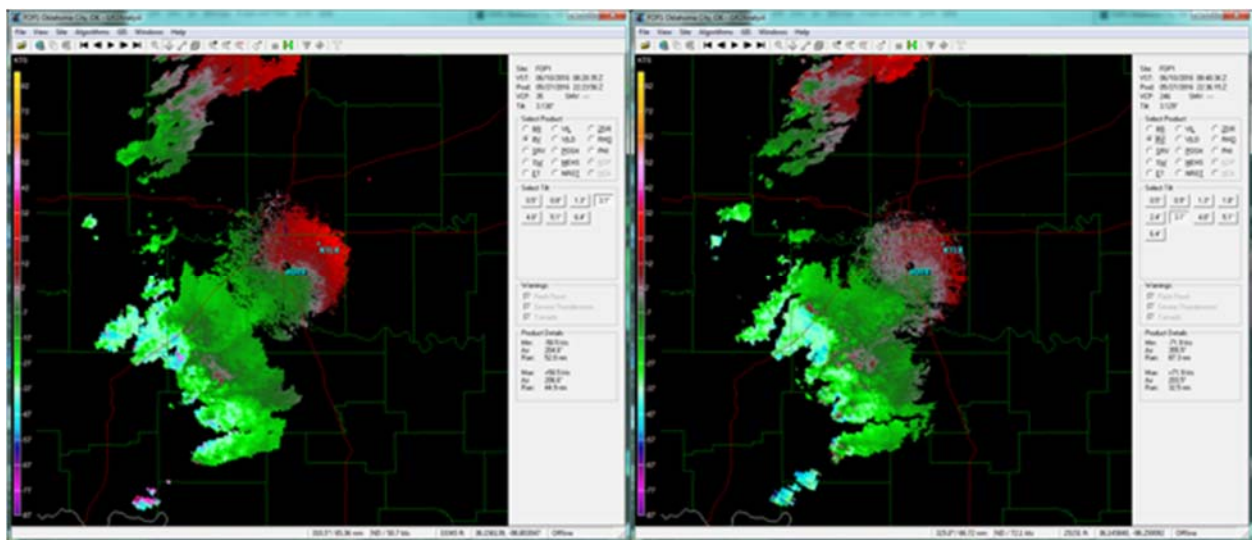
David Warde and Sebastian Torres (CIMMS at NSSL)

A common dilemma in obtaining good-quality meteorological-variable estimates using Doppler weather radar is the application (or misapplication) of ground clutter filters (GCF) to mitigate contamination from ground returns. Typically, weather radars use static clutter maps (i.e., pre-identified clutter contaminated regions) to control the application of the GCF. Ideally, the GCF should only be applied if the ground clutter contamination obscures the weather estimate. However, the problem of applying the GCF becomes very complex considering the dynamic atmospheric effects on radar beam propagation. The goal of this project is to develop efficient techniques that provide both automated detection and application of ground clutter filtering. The Clutter Environment Analysis using Adaptive Processing (CLEAN-AP) filter is a spectral technique for automatic detection and mitigation of ground clutter contamination. We had previously shown the clutter detection and mitigation performance of the CLEAN-AP filter using time-series data from the national network of weather surveillance radars (WSR-88D), the dual-polarized (DP) KOUN and OU Prime radars, and the NWRT PAR.

A common occurrence when trying to mitigate ground clutter is the loss of weather signals with low radial velocity especially when these weather signals have similar radar-observed ground-clutter characteristics as is typical in stratiform rain and snow events. Polarization diverse weather radars such as the newly upgraded NEXRAD

WSR-88D provide additional discriminating signatures which can assist in identification of low radial velocity weather signals. We developed the Weather Environment Thresholding (WET) algorithm to identify weather signals which reduces the ambiguity between low velocity weather signals and ground clutter. The WET algorithm when combined with CLEAN-AP was shown to enhance the ground clutter mitigation capability for a snow event where current NEXRAD WSR-88D ground clutter mitigation techniques had failed. Compared to current technologies used for ground clutter mitigation, the WET/CLEAN-AP filter provides a real-time, integrated clutter mitigation solution with: (a) improved ground clutter suppression, (b) effective ground clutter detection, and (c) dynamic ground clutter suppression characteristics optimally matched to the existing atmospheric environment.

In FY16, we continued optimization work on the window selection and notch width determination routines within CLEAN-AP. Additionally, we continued to support ROC engineers on the implementation, integration, and testing of CLEAN-AP in the Staggered PRT (SPRT) processing mode. During WSR-88D testing of SPRT, we noted decreased clutter suppression capability. Through analysis, we quickly identified that the Intermediate-Frequency Digital Receiver (IFDR) sampling frequency was not optimally set for the WSR-88D system. We recommended changing the IFDR sampling frequency within the RVP-900 architecture to better align it with the Coherent Oscillator (COHO) in the WSR-88D transmitter; this led to an immediate increase in ground clutter suppression capability of 5 dB.



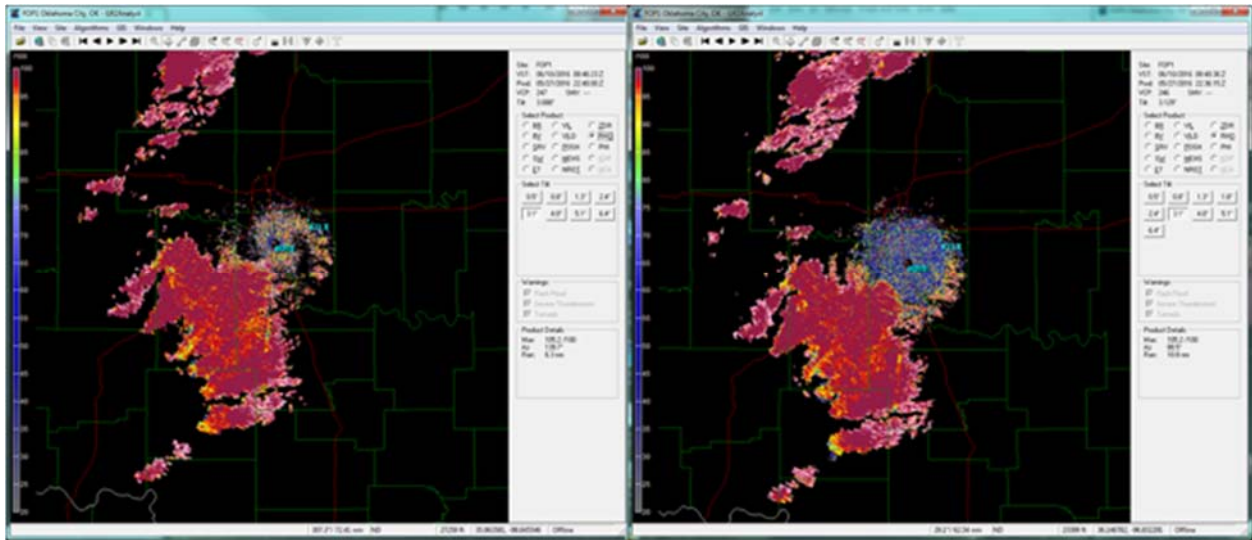
Comparison of filtered velocity estimates from Batch (left image using CMD/GMAP) and SPRT (right image using the CLEAN-AP filter) shows noticeable improvement in the recovery of estimates for the SPRT waveform when velocities are near zero knots. This is illustrated by lost estimates in the batch velocity estimates from the current WSR-88D identification/filtering process. Data was collected on the WSR-88D KCRI testbed in Norman, OK on May 27, 2016 with experimental VCP 247 (batch) and VCP 246 (SPRT).

b. Range-and-Velocity Ambiguity Mitigation: Staggered PRT

David Warde and Sebastian Torres (CIMMS at NSSL)

In pulsed Doppler weather radars, the range and Doppler velocity ambiguity problems are coupled so that trying to alleviate one of them worsens the other. Special techniques are necessary to resolve both range and velocity ambiguities to the levels required for the efficient observation of severe weather. Efforts in this area are expected to culminate in significantly improved WSR-88D data quality when implemented on the Radar Data Acquisition sub-system. The increased data quality will result in an improved ability for the WSR-88D to detect severe weather, flash floods, winter storms, and provide aviation forecasts. Over the last decade, two techniques have emerged as viable candidates to address the mitigation of range and velocity ambiguities in the WSR-88D, thus reducing the amount of purple haze obscuration currently encountered during the observation of severe phenomena. These are: systematic phase coding (SZ-2) and staggered pulse repetition time (SPRT). The two techniques are complementary since they offer advantages at specific elevation angles; hence, they can be simultaneously incorporated into the same volume coverage pattern. The first stage of upgrades that implemented SZ-2 is now complete and has been operational with great success for a number of years. The second stage of NEXRAD upgrades dealing with range and velocity ambiguities involves the operational implementation of SPRT. For ground clutter filtering SPRT data, we developed a novel spectral processing SPRT algorithm that incorporates the mature CLEAN-AP filter, range-overlaid recovery, dual polarization and a generalized PRT ratio.

In FY16, we continued to support ROC engineers on the implementation, integration, and testing of Staggered PRT (SPRT) processing mode. We are currently researching why there are increased numbers of velocity dealiasing errors in the SPRT velocity estimates as compared to batch velocity estimates. Thus far, we have re-verified the WSR-88D implementation of the algorithm and reprocessed Level-I data offline using both time-domain and frequency-domain processing. Additionally, we have compared the dealiasing technique used in the algorithm to other dealiasing techniques with no change in the number of dealiasing errors. We are continuing to assist in this analysis but have been limited by the number of data cases with sufficient weather to analyze. Furthermore, we have asked for new data cases with a different IFDR frequency change to reduce phase noise. On a positive note, Level-I data observed in the SPRT processing mode provides better performance in many aspects such as increased coverage for all fields (both due to no overlaid echoes and increased detectability at range), dual polarization and reflectivity fields with better quality, and, of course, larger maximum unambiguous velocity. It is worth noting that the dealiasing errors appear to be correctable in the post processing (Level-III) products using our suggested changes to the 2D-velocity-dealiasing algorithm.

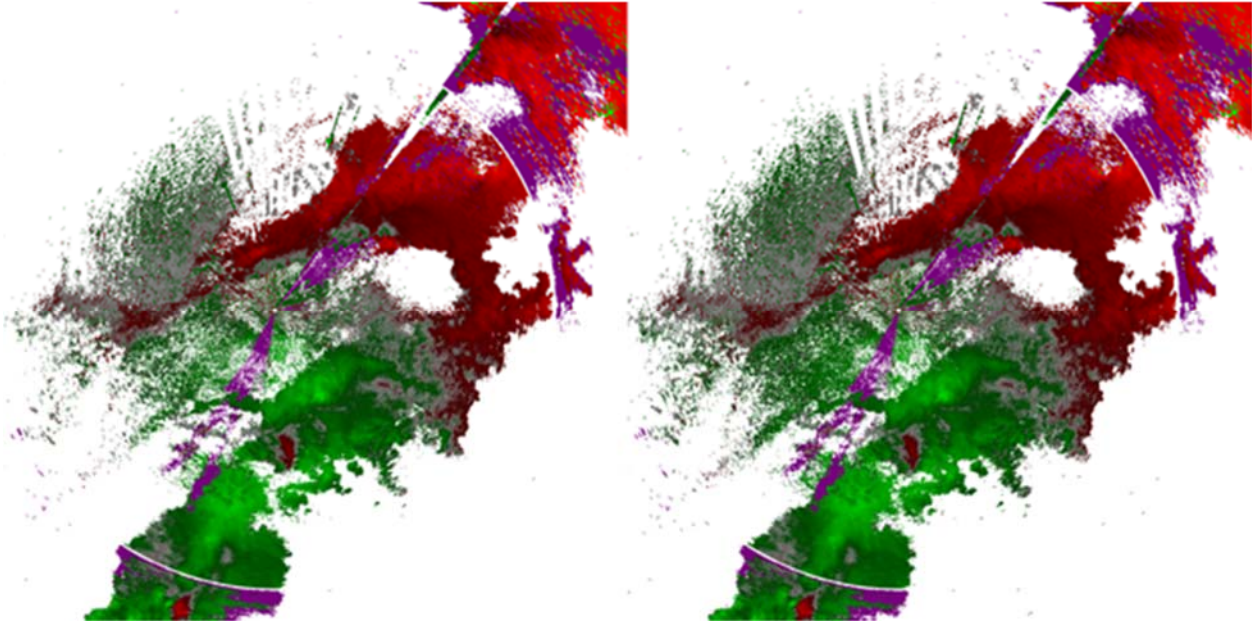


Comparison of correlation coefficient estimates from Batch (left image) and SPRT (right image) shows noticeable improvement in the estimates when using the SPRT waveform. Data was collected on the WSR-88D KCRI testbed in Norman, OK on May 27, 2016 with experimental VCP 247 (batch) and VCP 246 (SPRT).

c. Range-and-Velocity Ambiguity Mitigation: SZ-2

Sebastian Torres and David Warde (CIMMS at NSSL)

In FY16, we revised our recommendation for new SZ-2 recovery-region censoring thresholds and collaborated with ROC engineers to re-process the same data cases used in the initial evaluation. Based on this evaluation, we reassessed the integration of dB-for-dB censoring, coherency-based thresholding, and strong-point clutter filtering within the SZ-2 algorithm. We developed updated recommendations and provided an update of the SZ-2 Algorithm Description to the ROC that addresses the improved recovery-region censoring (new thresholds) and the integration of the techniques mentioned before. Also, to complement ROC's preliminary analysis of the performance of the SZ-2 algorithm with the updated thresholds, we developed and delivered a PowerPoint presentation that summarizes the recommended changes to the SZ-2 algorithm, provides examples from real data, and discusses the expected performance improvements. Based on this work, we recommended the implementation of the SZ-2 algorithm changes followed by a comprehensive validation of the algorithm. Additionally, we recommended that a change to the IFDR sampling frequency in the newly upgraded signal processor would benefit the decoding of SZ-2 phase-coded signals and contribute to improved performance of the SZ-2 algorithm.



Comparison of Coherency Based Thresholding (CBT) off (left image) and on (right image) while using SZ2 to recover overlaid velocity. Increased numbers of recovered velocity values are seen with CBT ON as compared with CBT OFF.

d. Correlation Coefficient Estimation

Igor Ivić (CIMMS at NSSL)

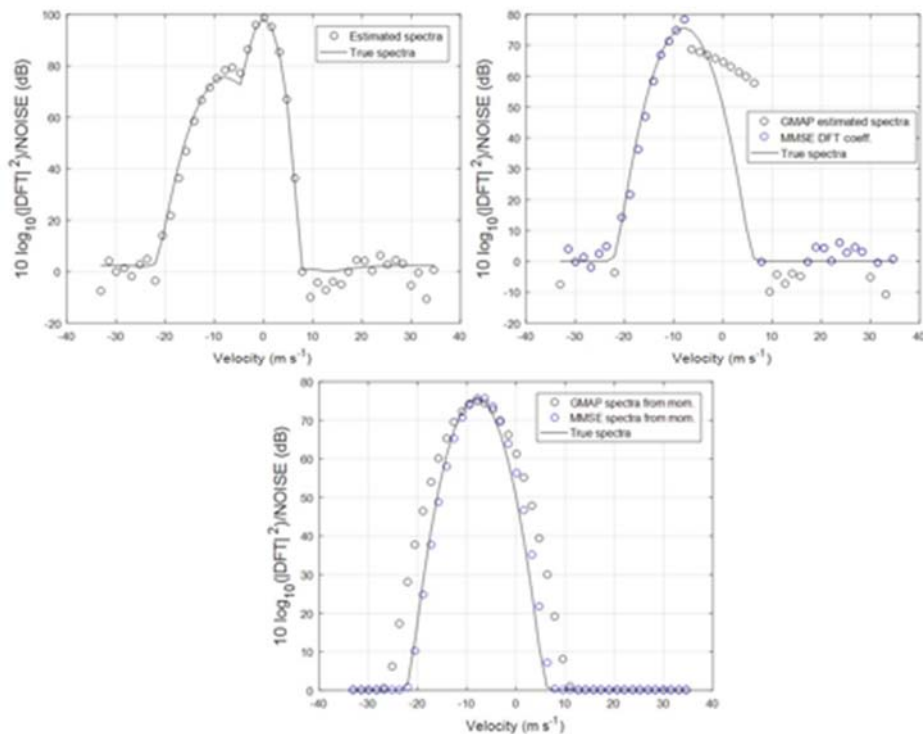
The co-polar correlation coefficient (CC) is one of the three polarimetric variables being produced by the WSR-88D. CC aids in the recognition of different types of radar echoes and in separation of returns from rain and snow. The latter requires precise measurements of CC in areas with low and moderate signal-to-noise ratios (SNR). Unfortunately, correlation coefficient estimates are unusable when they become larger than one, which is common when the number of samples per dwell is small and in areas with SNR less than ~15 dB. In addition, the current CC estimator is positively biased, especially when the number of samples per dwell is small. To mitigate these issues, a novel correlation coefficient estimation technique is being developed that has the potential of producing less biased estimates. Mitigating the CC bias will result in more accurate estimates, which will improve polarimetric recognition of echoes. It will also reduce the number of estimates that cannot be used for classification (i.e., invalid estimates). The improved CC estimator will provide improved accuracy while being computationally viable for easier operational implementation on the WSR-88D.

During FY16, details of the algorithm were further tuned by taking into account implementation aspects. The algorithm was presented to the ROC team at the Technical Interchange Meeting (TIM) as well as in the form of a peer reviewed publication (Ivić 2016).

e. Estimation from Ground Clutter Filtered Spectra

Igor Ivić (CIMMS at NSSL)

Radar returns from ground clutter contaminated weather signals can result in biased estimates of meteorological variables if not processed properly. A frequency domain ground-clutter filter (e.g., GMAP) is typically employed to remove this contamination. This usually results in less biased meteorological-variable estimates. However, if spectra of meteorological and ground clutter signals are overlaid (typical in stratiform rain and snow events), removal of the latter also removes portion of the useful signal. The result is that the estimates of Doppler moments may still be significantly biased in these cases. To mitigate this, an interpolation is typically used to replace the removed spectral coefficients. For this project, a novel approach is pursued whereby meteorological variables of interest are estimated only from spectral coefficients which are not removed by the ground clutter filter. This is achieved by determining the spectral coefficients with significant signal presence and iteratively finding the MMSE (Minimum Mean Square Error) fit to the model using these coefficients. During FY16, research was initiated on the theoretical background for this project along with development of software infrastructure.



True spectrum and an associated simulated realization (top leftmost panel) in the case of weather and ground clutter signal overlay. Same spectrum after removal of contaminated spectral coefficients by GMAP (top rightmost panel); spectral coefficients used for velocity and spectrum width estimation using the novel method are shown with blue circles. The bottom panel shows spectra produced from Doppler moments estimated using an interpolation (black circles) and the novel method (blue circles).

f. Hybrid-Scan Estimators

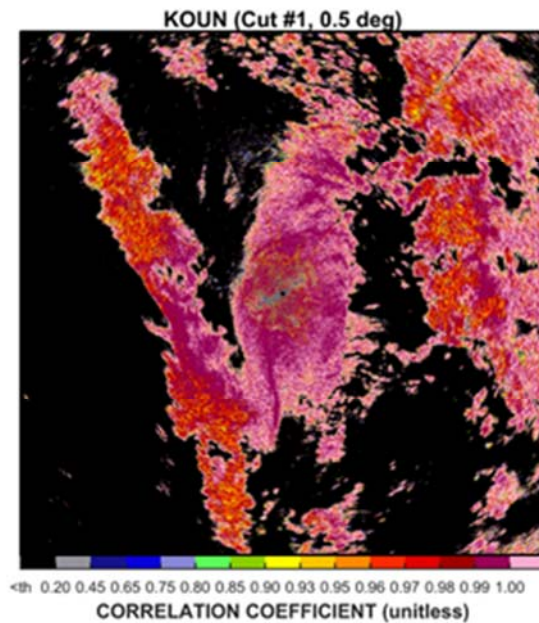
David Schwartzman, David Warde, and Sebastian Torres (CIMMS at NSSL)

Dual-polarization signal-processing techniques have remained essentially the same since the polarimetric upgrade of the WSR-88D network. Initial processing schemes were simple so as to avoid unnecessary complications during the first stages of operation. Since that time, large errors in the polarimetric variables have been routinely observed under certain conditions, and efforts to remove or reduce them are being explored. One such technique is the use of data from multiple scans to provide improved data quality, which is referred to as hybrid-scan estimation.

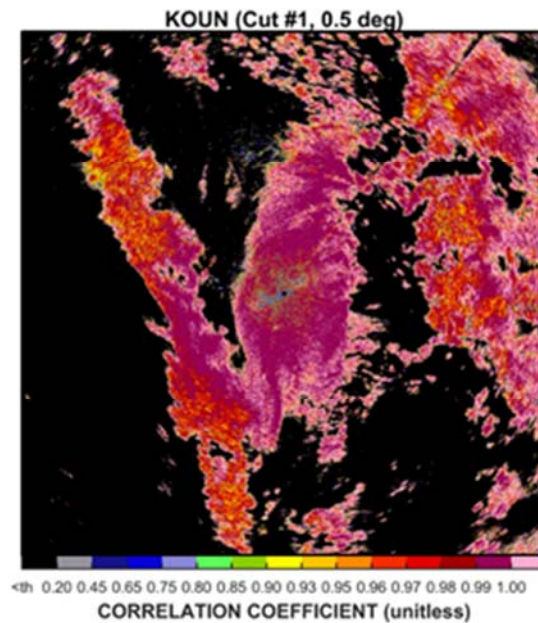
Split cuts consisting of one surveillance scan and one Doppler scan at the same elevation angle are typically used at the lowest tilts on operational Volume Coverage Patterns (VCP). Currently, reflectivity and polarimetric variables are obtained from the long-pulse-repetition-time (PRT) surveillance scan, whereas Doppler velocity and spectrum width are obtained from the short-PRT Doppler scan. While not currently used, polarimetric variables estimated from the Doppler scan could result in better estimates than those from the surveillance scan. For example, this could happen under several conditions: (a) when dwell times in the Doppler scan are longer than those in the surveillance scan, (b) at low-to-medium SNRs when the larger number of samples may help reduce statistical fluctuations, (c) for wide spectrum widths, or (d) in the case of ground-clutter contamination for which a larger number of samples typically results in improved mitigation. Thus, it is important to identify the situations for which estimates from the Doppler scan are better than those from the surveillance scan so that an estimator that selects the best data from both scans can be devised.

In the past year, we simulated dual-polarization data to assess the statistical performance of surveillance- and Doppler-scan estimates for a wide range of meteorological conditions. Using theoretical equations to compute bias and variance of polarimetric estimates, our algorithm chooses the estimate with better statistics from either the surveillance or Doppler scan. To validate the proposed algorithm, we processed several real-data cases with and without the *hybrid-scan* estimates and observed significant improvement in data quality when it is used. We prepared a presentation of the algorithm for the ROC Data Quality team, which included a flow chart of the algorithm. It also contained bias and standard deviation comparisons of Surveillance and Doppler scan data quality for the three polarimetric variables, which show meteorological conditions for which the Doppler scan data has better quality than that of the Surveillance scan. We also qualitatively analyzed real-data cases processed with the algorithm and quantified the amount of *pink fringe* (i.e., invalid correlation-coefficient estimates) reduction obtained when using this technique. Results indicate that the use of hybrid-scan estimators can significantly improve the quality of polarimetric variables.

Conventional ρ_{hv} Estimator



Hybrid-Scan ρ_{hv} Estimator



Plan-position-indicator (PPI) displays of conventional (left) and hybrid-scan (right) correlation-coefficient estimates from weather radar data for a convective storm. Three types of data quality improvements can be observed in hybrid-scan estimates: a smoother correlation coefficient field (which indicates a reduction in the variance of estimates), improved clutter suppression, and a significant reduction in the pink fringe (invalid estimates).

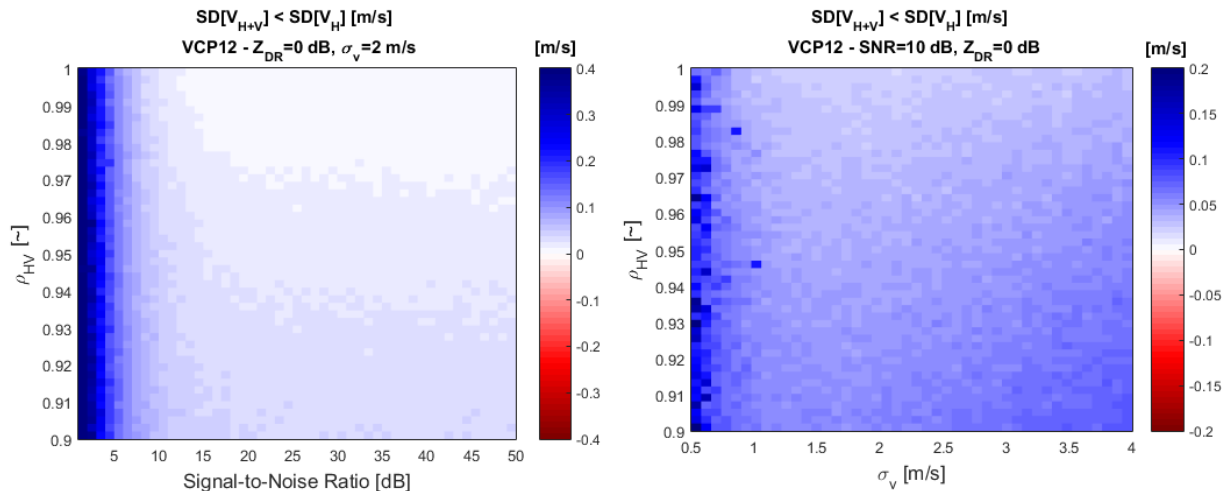
g. Dual-Polarization-Based Velocity Estimator

David Schwartzman, David Warde, and Sebastian Torres (CIMMS at NSSL)

Despite the introduction of dual-polarization capabilities to the WSR-88D network, many of the original spectral-moment estimators remain the same. For example, Doppler velocity estimates are calculated using information from only the horizontal channel and ignore the vertical-channel data, which could be used to improve its precision. In the most basic sense, the vertical channel provides additional samples (not necessarily independent from those in the horizontal channel) of the same radar volume, which could be used to reduce the standard deviation of the classical single-polarization velocity estimator. The goal of this project is to examine the performance of dual-polarization-based velocity estimators; i.e., those that make use of the horizontal- and vertical-channel data. However, combining estimates that exhibit different statistical characteristics can be challenging. For example, one issue with combining velocity estimates from both polarimetric channels arises when the differential reflectivity is large (either positive or negative in dB units) and the SNR is small. In the case of positive differential reflectivity, the signal in the vertical channel has a smaller SNR, leading to

estimates with higher standard deviation than those from the horizontal channel. The reverse is true for cases of negative differential reflectivity.

In the past year, we developed simulations to identify meteorological conditions for which the dual-polarization-based velocity estimator (i.e., the one that combines H and V estimates) is better than the classical single-polarization estimator (i.e., the one that uses H only estimates). The dual-polarization-based velocity estimator shows better statistics (bias and variance) at low-to-medium SNRs and also for the combination of low-to-medium correlation coefficients and medium-to-high spectrum widths. We explored several weighting techniques to combine the autocorrelation functions from which the estimates are computed: averaging, power-based, SNR-based, spectrum width-based, etc. Initial results show that weighting techniques have little effect on the improvement of the dual-polarization-based velocity estimate. Real data cases were processed and qualitatively analyzed using the dual-polarization-based velocity estimator. While this work is not yet finished, initial results do not reveal significant improvement of the proposed technique over the classical single-polarization velocity estimator.



Improvement in standard deviation obtained when using the dual-polarization-based velocity estimator over the classical single-polarization velocity estimator. Improvement as a function of the signal-to-noise ratio and the correlation coefficient is shown in the left panel. Improvement as a function of the spectrum width and the correlation coefficient is shown in the right panel. Results show that while the dual-polarization-based velocity estimate does improve the quality of estimates, the gain is not significant (at most ~0.4 m/s) for most meteorological conditions under consideration.

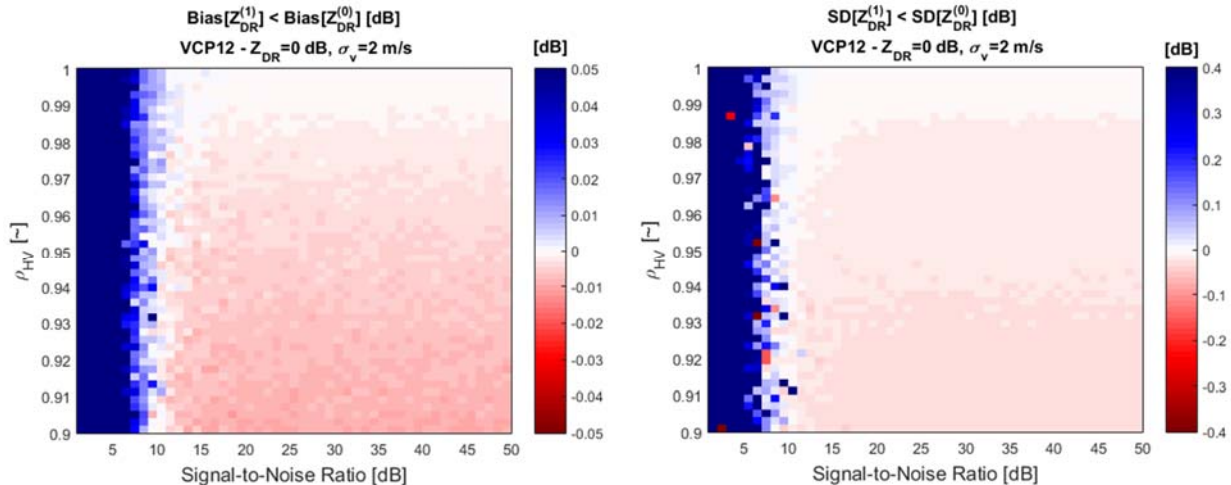
h. Hybrid Differential-Reflectivity Estimator

David Schwartzman, David Warde, and Sebastian Torres (CIMMS at NSSL)

Polarimetric-variable estimators exhibit relatively large statistical errors at low SNRs (below 10-15 dB). As a result, SNR censoring thresholds for the polarimetric variables should be on the order of 10 and 15 dB for differential reflectivity/phase and correlation

coefficient, respectively. Additionally, uncertainty in the noise estimates for the horizontal and vertical channels could introduce additional bias and standard deviation. To improve the accuracy and precision of the polarimetric variables at low SNR and to reduce the influence of incorrect noise estimates, alternative estimators have been previously suggested. Specifically, the lag-1 estimators discussed by Melnikov and Zrnic (2007) are free from influence of noise and are therefore more robust at lower SNRs. In this project, we propose a hybrid differential-reflectivity estimator that uses either the lag-1 estimator (at low-to-medium SNRs) or the lag-0 estimator (at medium-to-high SNR). Thus, one of the objectives of this study is to identify criteria to choose the appropriate estimator that leads to the best statistical performance.

During the report period, we developed simulations to identify the meteorological conditions for which the lag-1 differential-reflectivity estimator is better than the classical lag-0 estimator. We observed from the simulations that the performance is mostly controlled by signal-to-noise ratio, spectrum width, correlation coefficient, and dwell times. For lower signal-to-noise ratios, the noise introduced in the classic (lag-0) estimator significantly contaminates the signal, which leads to estimates with poor data quality. The lag-1 estimator shows better performance at low signal-to-noise ratio due to the fact that it uses the (noiseless but less correlated) lag-1 correlation to estimate powers. While this work is not yet finished, initial results reveal significant improvement can be obtained using the proposed hybrid estimator at low-to-medium signal-to-noise ratios.



Difference in bias (left) and standard deviation (right) between the lag-0 and the lag-1 differential reflectivity estimators as a function of the signal-to-noise ratio and the correlation coefficient. Areas with blue colors indicate conditions where the lag-1 estimator outperforms the lag-0 estimator, while areas with red colors mean the opposite. Results show that at low signal-to-noise ratio, differential reflectivity estimates can be improved in both bias and standard deviation by using a multi-lag estimator.

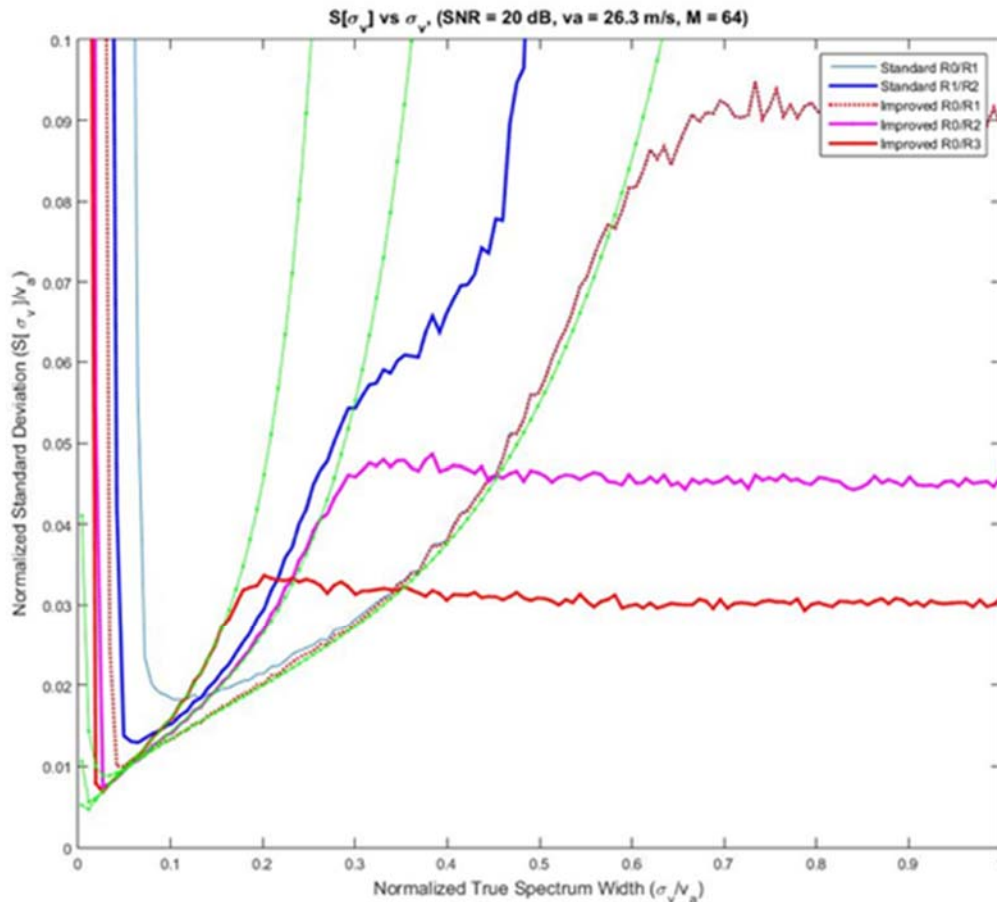
i. Spectrum Width Estimation

David Warde and Sebastian Torres (CIMMS at NSSL)

Improved quality of spectrum width estimates would enhance data assimilation (Warn on Forecast), storm feature identification (rear flank downdrafts, boundaries, tornado genesis, and hail spikes), and downstream algorithms (NEXRAD Turbulence Detection Algorithm, range oversampling, non-uniform beam filling, Bragg scatter identification). On Doppler weather radars, the spectrum width is commonly estimated from a ratio of autocorrelation estimates at two different lags. These estimators have been used for decades on operational weather radars and have well known properties. For example, the R0/R1 estimator, which is based on the ratio of lag-0 to lag-1 autocorrelations, performs the best for wide spectrum widths but has poor performance for narrow spectrum widths and depends on accurate noise measurements. The R1/R2, which is based on the ratio of lag-1 to lag-2 autocorrelations, and other estimators based on higher-lag autocorrelations provide better narrow spectrum-width estimates than the R0/R1 estimator and improve performance when accurate noise measurements are not available, but they are severely biased for wide spectrum widths. Thus, to provide better estimates over a wide range of spectrum widths, a few estimators can be suitably combined. This so-called hybrid spectrum-width estimator can take advantage of the best characteristics of each estimator for different regimes. We developed and formalized improvements to spectrum width estimation by combining ASD and Welch processing to create “matched” autocorrelations. The new estimators provide a larger span of unbiased estimates for narrow spectrum widths at lower sample sizes and with less variance than standard methods; wide spectrum width estimates are unaffected and perform comparable to the standard estimators. The new estimators were combined into a simple hybrid spectrum width estimator that showed improved performance over the current NEXRAD WSR-88D hybrid spectrum width estimator. We implemented the improved spectrum width estimators into the staggered PRT algorithm and provided the updated algorithmic description to the NWS Radar Operations Center for implementation into the NEXRAD WSR-88D. Additionally, we provided scientific and technical support to assist the National Center for Atmospheric Research and the NWS Radar Operations Center with incorporation of the improved estimators into the NEXRAD hybrid spectrum width estimator.

In FY16, we continued working with ROC software engineers to incorporate the Hybrid Spectrum Width Estimator for SPRT into the WSR-88D. Using perturbation analysis on a Gaussian shaped power spectrum, the spectrum width mean and standard deviation formulas of the new estimators were being formulated. Additionally, we provided recommended changes to the segment-III spectrum-width computation for the Hybrid Spectrum Width estimator. We also investigated the report of a small bias when combining power estimates from the short and long PRTs in either segment I or III for non-overlaid conditions. Currently, only the power estimate from the short (for segment I) or the long (for segment III) PRT is used for the spectrum width computation where overlaid conditions are guaranteed not to exist. However, in non-overlaid conditions, the spectrum width estimate would benefit from combining the powers from both PRTs. This

small power bias (less than a few 10ths of a dB) occurs when false detections of non-overlaid conditions occur and the power computation reverts back to the single-segment power computation. Due to the increased quality of the spectrum width estimates when using the combined powers in non-overlaid conditions and the small number false detections of non-overlaid conditions, these biases were deemed insignificant and the algorithm remains unchanged.



Comparison of the standard deviation of the improved spectrum width estimators (R0/R1 – red dotted line, R0/R2 maroon solid line, R0/R3 – red solid line) with the legacy spectrum width estimators (R0/R1 - thin blue solid line, R1/R2 – thick blue solid line) show improved performance at narrow spectrum widths without degradation at wider spectrum widths. The theoretical standard deviation (green dot-line) is shown for each of the improved estimators and matches well for narrow spectrum widths where the perturbation analysis is valid.

j. Range Oversampling Techniques

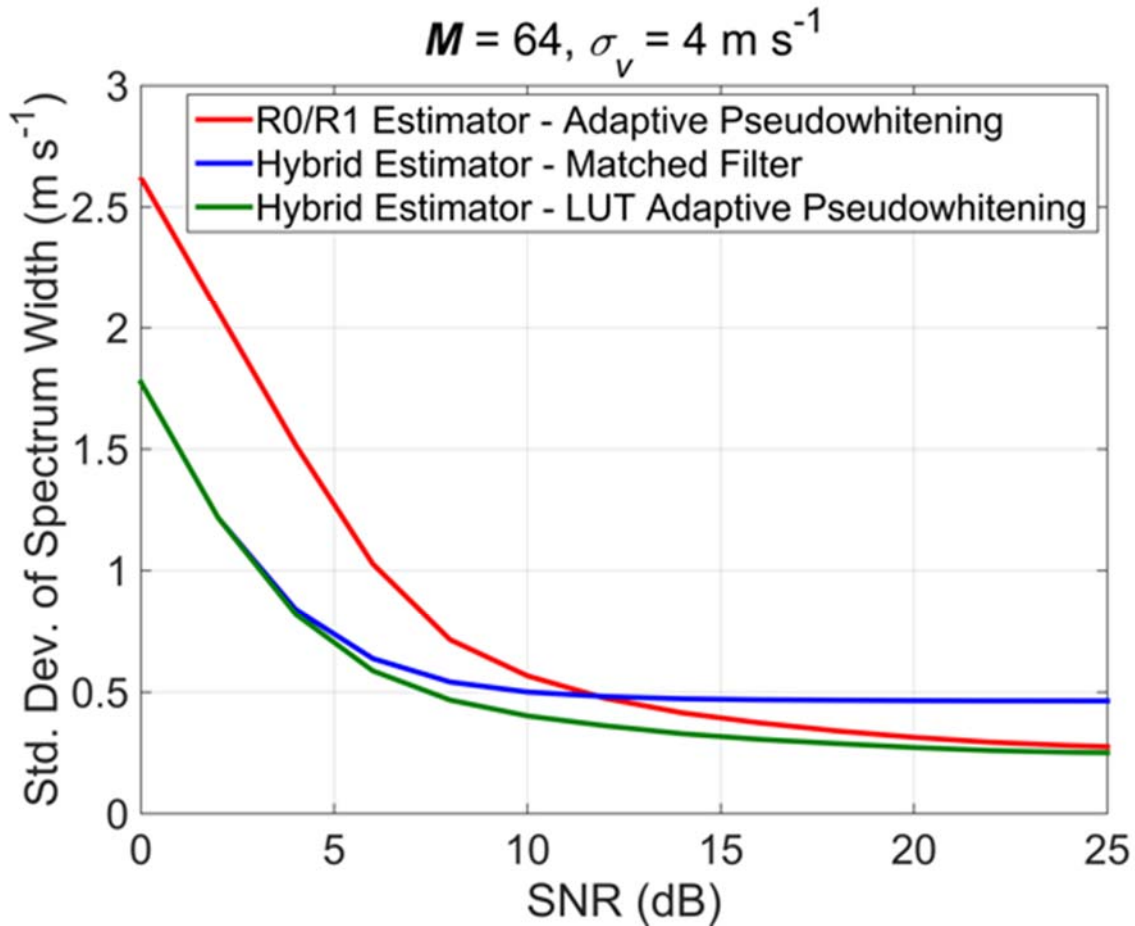
Sebastian Torres and Christopher Curtis (CIMMS at NSSL)

Obtaining radar data at faster rates can provide an important capability for the observation of rapidly evolving weather phenomena. When increasing data rates, the

conventional trade-off involves sacrificing either spatial coverage or data precision. With range oversampling, it is possible to add a new dimension to this trade-off: signal processing. Range oversampling allows us to either obtain data twice as fast with variances similar to conventional processing or improve data quality without sacrificing update time or spatial coverage. This type of processing has been used to significantly reduce update times on the National Weather Radar Testbed (NWRT) Phased Array Radar (PAR) and to improve polarimetric data quality on a NEXRAD research radar (KOUN). In FY16, we focused our efforts on implementing adaptive pseudowhitening with non-traditional estimators.

In the original implementation of adaptive pseudowhitening, we used explicit variance expressions for each estimator to choose a transformation that was appropriate for the weather signal characteristics. This worked well for traditional radar-variable estimators, but some of the new non-traditional estimators either do not have an explicit variance expression or have a difficult-to-derive expression. We formulated a lookup-table technique that uses Monte Carlo simulations to find the proper transformation without utilizing a variance expression. We presented the work at the 37th Conference on Radar Meteorology in Norman, OK and submitted a paper to the Journal of Atmospheric and Oceanic Technology, "Adaptive Range Oversampling Processing for Nontraditional Radar-Variable Estimators." We have received and responded to the initial round of peer reviews, and the paper should be published in FY17.

In addition to this research work, we also continued to work with Radar Operations Center engineers to determine how best to implement range oversampling processing on the NEXRAD network. This included a technical interchange meeting in December to give them a basic outline for adaptive pseudowhitening along with concerns about possible hardware limitations. We also met with them at the KOUN site in March to figure out how to set up the radar to effectively collect range-oversampled data.



Standard deviation of spectrum width versus signal-to-noise ratio (SNR) for three estimators: R0/R1 with Adaptive Pseudowhitening, Hybrid Estimator with Matched Filter, and Hybrid Estimator with Lookup Table (LUT) Adaptive Pseudowhitening. LUT adaptive pseudowhitening gives the high-SNR performance of the R0/R1 estimator and the low-SNR performance of the hybrid estimator for the best overall performance.

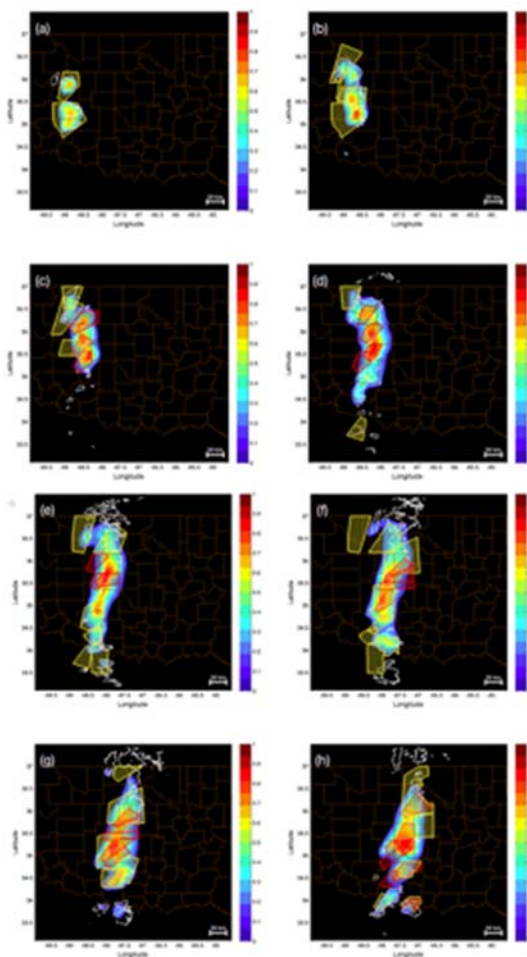
k. Weather Radar–Spatio Temporal Saliency

David Schwartzman and Sebastian Torres (CIMMS at NSSL), and Tian-You Yu (OU ARRC)

Forecasters often monitor and analyze large amounts of data especially during severe weather events, which can be overwhelming. Thus, it is important to effectively allocate their finite perceptual and cognitive resources on the most relevant information. For this purpose, we developed a novel analysis tool that quantifies the amount of spatial and temporal information in time-series of constant-elevation weather radar reflectivity images. The proposed Weather Radar–Spatio Temporal Saliency (WR–STS) is based on the mathematical model of the human attention system (referred to as saliency) adapted to radar reflectivity images and makes use of information-theory concepts. It was shown that WR–STS highlights spatially and temporally salient (attention attracting)

regions in weather radar reflectivity images, which can be associated with meteorologically important regions.

During FY16, we completed the performance analysis of WR-STS. Its skill to highlight current regions of interest was assessed by analyzing the WR-STS values within regions in which severe weather is likely to strike in the near future as defined by NWS forecasters. The performance of WR-STS was demonstrated for a severe weather case and analyzed for a set of ten diverse cases. Results support the hypothesis that WR-STS can identify regions with meteorologically important echoes and could assist in discerning fast changing, highly-structured weather echoes during complex severe-weather scenarios, ultimately allowing forecasters to focus their attention and spend more time analyzing those regions. A paper was submitted to the Journal of Oceanic and Atmospheric Technology on this topic and is currently under review.



WR-STS maps corresponding to the tornadic storm on 24 May 2011 obtained from the KTLX radar. Active tornado warning polygons (red), severe thunderstorm polygons (yellow), and 10-dBZ reflectivity contour lines (white) are overlaid on top of the WR-STS maps (a) 193207 UTC, (b) 195754 UTC, (c) 202743 UTC, (d) 205733 UTC, (e) 212720 UTC, (f) 215704 UTC, (g) 222648 UTC, and (h) 225633 UTC.

I. Real-Time Weather Signal Processing

Eddie Forren (CIMMS at NSSL)

Prior to this year, NSSL's real-time, radar independent signal processing software was able to process data for both KOUN and the NWRP phased array radars. Real-time processing on KOUN with a passive real-time data connection had been implemented, but the system had not been set up or tested. In the first half of the year, some small problems were resolved, and the 32-bit version of the software was set up with a passive data connection on KOUN. Testing revealed problems processing MESOSAILS VCPs that revisit the lower elevation cuts. An "LDM" connection was also set up to pull production KOUN data into WDSSII. Because of other priorities, a connection to ingest NSSL's experimental data stream into WDSSII was not set up and the problems with MESOSAILS VCPs were not addressed.

Because of needs from other projects, the real-time signal processing code was ported to 64-bit Linux late last year and some further testing occurred during this year. Additional bug fixes included corrections related to processing sector scan data, addressing threading/priority problems, and preventing failures due to DSP processing limitations. Options that use rotation rate were added to the NEXRAD/ORDA playback tool to help with processing KOUN sector data collections.

m. Hardware Development and Maintenance for KOUN and Mobile Radars

Danny Wasielewski and Mike Schmidt (CIMMS at NSSL), and Mike Shattuck (NSSL)

NSSL maintains several radar assets used by researchers, including both mobile radars and NSSL's research and development WSR-88D, KOUN. In addition to their use as meteorological and hydrological research instruments, these radar assets also serve as testbeds for technological research. Technologies prototyped on KOUN in particular are directly applicable to the WSR-88D network. Maintenance and continual improvement of these assets is essential to providing high quality instruments for new research and for supporting NSSL's commitment to R2O.

KOUN. During FY16, only minor changes were made to the configuration of KOUN. The Radar Operations Center continued to refine the hardware and software associated with prototyping the upcoming tech refresh of the WSR-88D network. Michael Shattuck (NSSL) performed restorative maintenance on the RF generator. Danny Wasielewski (CIMMS) found a bad network adapter on one of NSSL's processors and implemented a temporary workaround. The processor will be upgraded or replaced. The effort to demonstrate range oversampling continued in FY16. Progress was made on configuring the RVP9 processor to accommodate the range-oversampled data, particularly in adjusting the filter bandwidth. However, a major limitation was also discovered: experiment suggests that there may be a maximum number of bins per second that can be processed. While this does not technically prevent creating range-oversampled data,

it does limit the oversampling factor and/or maximum range. Currently, we are unaware of the source of this limit or any workaround.

Mobile Radars. Several improvements for usability were made on NOXP, NSSL's X-band polarimetric mobile radar. The computer equipment racks were rearranged and outfitted with dual monitors and a more functional keyboard-mouse console. The single uninterruptible power supply was replaced with two on separate 20A circuits, resolving a longstanding problem wherein power was lost when a user attempted to power external equipment from the same circuit as the processor racks. A networkable pan/tilt/zoom camera was added on a mast to the top of the truck cab, allowing a remote operator to monitor the antenna or surroundings. CIMMS staff explored several options to maintain power to the waveguide compressor-dehydrator during periods of inactivity (this would prevent the need to purge the waveguide prior to operation by keeping the humidity low); however, no practical option was found. Purge valves were added to the waveguide near the feed horn to maximize the length of waveguide purged. SR-1, OU's C-band non-polarimetric mobile radar, was decommissioned after the PECAN field experiment in 2015. CIMMS/NSSL and OU have received funding to build a new dual-polarization C-band mobile radar (branded SR-3) using the truck and antenna formerly belonging to SR-1. Work commenced in March 2016, beginning with refurbishing the truck and placing orders for the new magnetron transmitter and dual-polarization rotary joint. Rebuilding of the radar will continue through FY17.

n. Improving the Processing of Polarimetric Data for Operational WSR-88D Radars

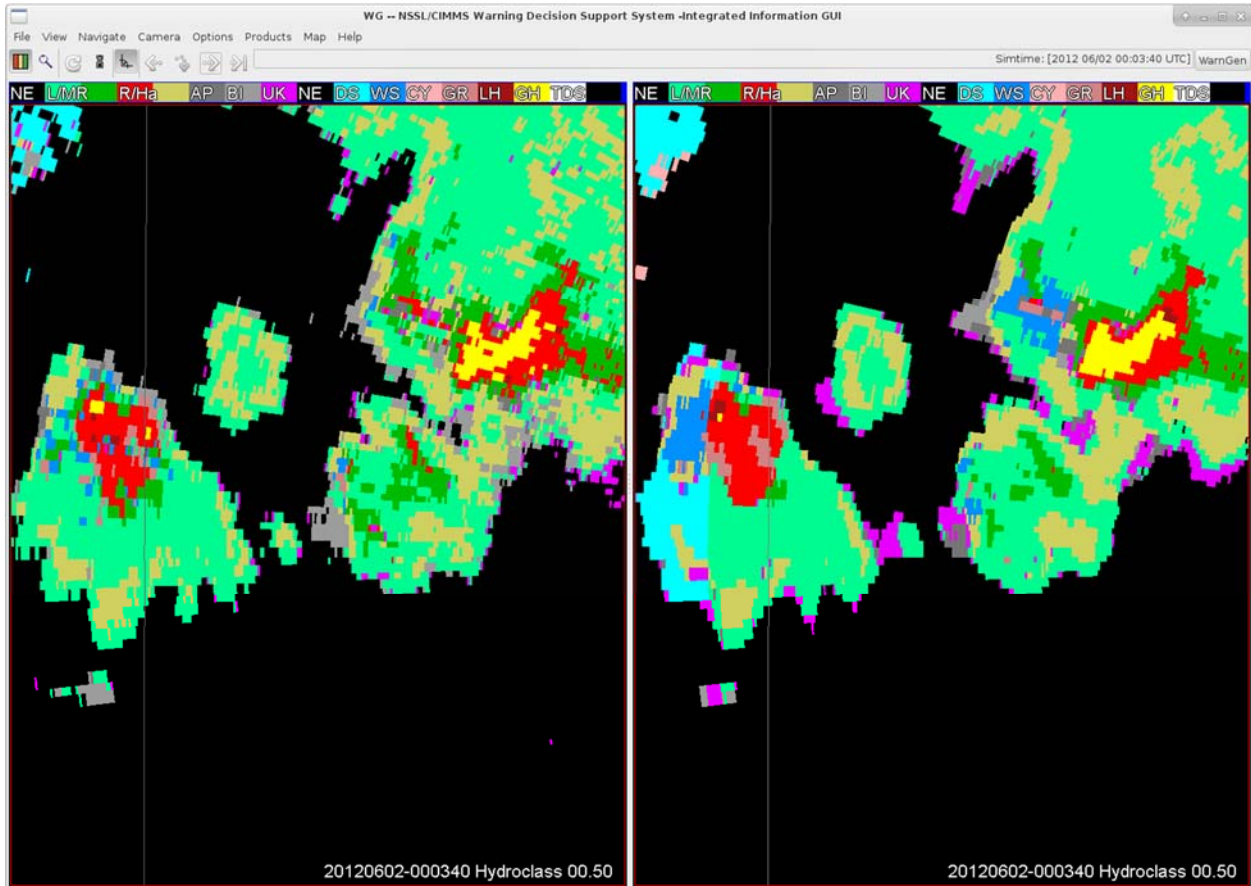
John Krause and Jeff Snyder (CIMMS at NSSL)

The processing of radar data collected by operational WSR-88D radars has been further refined. The work was primarily done in two directions: (a) discrimination between weather and non-weather radar signals and (b) using 2D processing routines instead of 1D processing procedures for which the information for a single radial of radar data has been processed independently from the one at adjacent radials.

Discriminating between meteorological and non-meteorological radar returns is necessary for a number of radar applications, including hydrometeor classification, quantitative precipitation estimation (QPE), and the computation of specific differential phase KDP. The algorithm proposed in Krause (2016), MetSignal, uses polarimetric radar data and is simple by design, allowing users to adjust its performance based on the location's specific needs. The MetSignal algorithm is a fuzzy logic technique with a few post-processing rules and has been selected for implementation on the WSR-88D network in the United States.

It is demonstrated that 2D processing and smoothing of the radar data notably suppresses the noise and better reveals coherent features of the storm (see figure below). A particular benefit of the 2D median smoothing is anticipated for estimation of the total span of differential phase $\Delta\Phi_{DP}$ which is a key variable for determination of the

specific attenuation A in the $R(A)$ algorithm which emerges as a primary QPE algorithm for NEXRAD.

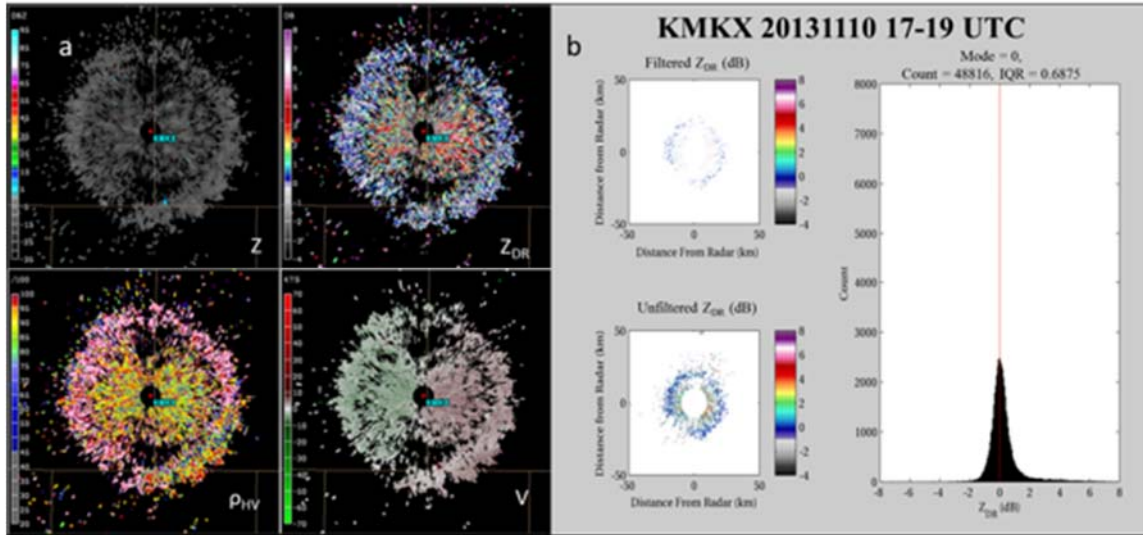


Comparison of the Hydroclass basic product (left panel) and its modification after 2D 2 km median smoothing is applied (right panel). No changes were made to the Hydrometeor Classification Algorithm itself. More coherent and realistic features of the storm structure are revealed after 2D median smoothing is applied.

o. Calibrating the Network of WSR-88D radars

Valery Melnikov (CIMMS at NSSL)

Differential reflectivity (Z_{DR}) values should be measured with accuracies not worse than 0.2 dB. To achieve this accuracy, observations of Bragg scatter were tested on the WSR-88D network. A filter to select Bragg scatter areas in the echoes from “clear air” was developed. The filter is going to be included into Build 18 of the RPG. The monitoring of Z_{DR} using Bragg scatter was performed in 2016 for more than 50 WSR-88D radars. An example of Bragg scatter areas seen by the WSR-88D and a histogram of measured Z_{DR} is shown in the figure below.



Bragg scatter from Milwaukee, WI (KMKX) on 10 November 2013. The WSR-88D PPI images (left panels) show Z (upper-left), Z_{DR} (upper-right), ρ_{HV} (lower-left), and Velocity (lower-right) from the 3.5° elevation angle at 18:52 UTC. Right panels show the range gates that pass the filter in the top-left panel (out to 50 km), all of the range gates within the bottom-left panel (out to 50 km), and the histogram of range gates that pass the filter in the right panel. Zero dB is marked by the red line in the histogram.

Publications

- Ivić, I. R., 2016: A technique to improve copolar correlation coefficient estimation. *IEEE Transactions on Geoscience and Remote Sensing*, **54**, 5776–5800.
- Torres, S. M. and C. D. Curtis, 2015: The impact of range oversampling processing on tornado velocity signatures obtained from WSR-88D super-resolution data. *Journal of Atmospheric and Oceanic Technology*, **32**, 1581-1592.

2. Dual-Polarization

Overall Objectives

Use dual-polarization radars for quantitative precipitation estimation, hydrometeor classification, and investigation of microphysical processes in clouds and precipitation.

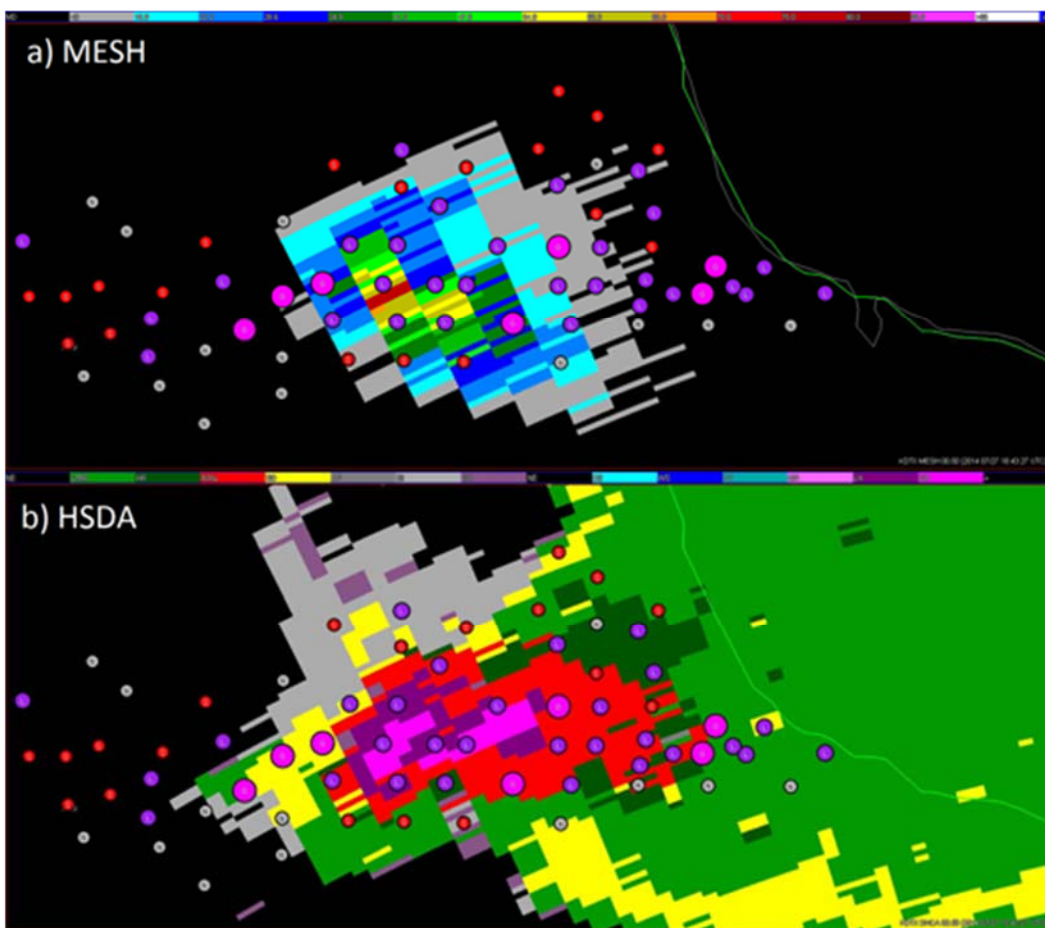
Accomplishments

a. Hail Size Discrimination Using Dual-Polarization Radars – Hail Size Discrimination Algorithm (HSDA)

Kiel Ortega, Holly Obermeier, Jeff Snyder, John Krause, and Alexander Ryzhkov (CIMMS at NSSL)

A hybrid single-radar and dual-polarization hail detection and sizing algorithm is being developed. The first step of the project was to adapt the existing Hail Detection Algorithm (HDA; Witt et al. 1998) to run in pixel-by-pixel framework on single radar data, instead of the storm-based framework it currently employs. This pixel-by-pixel algorithm

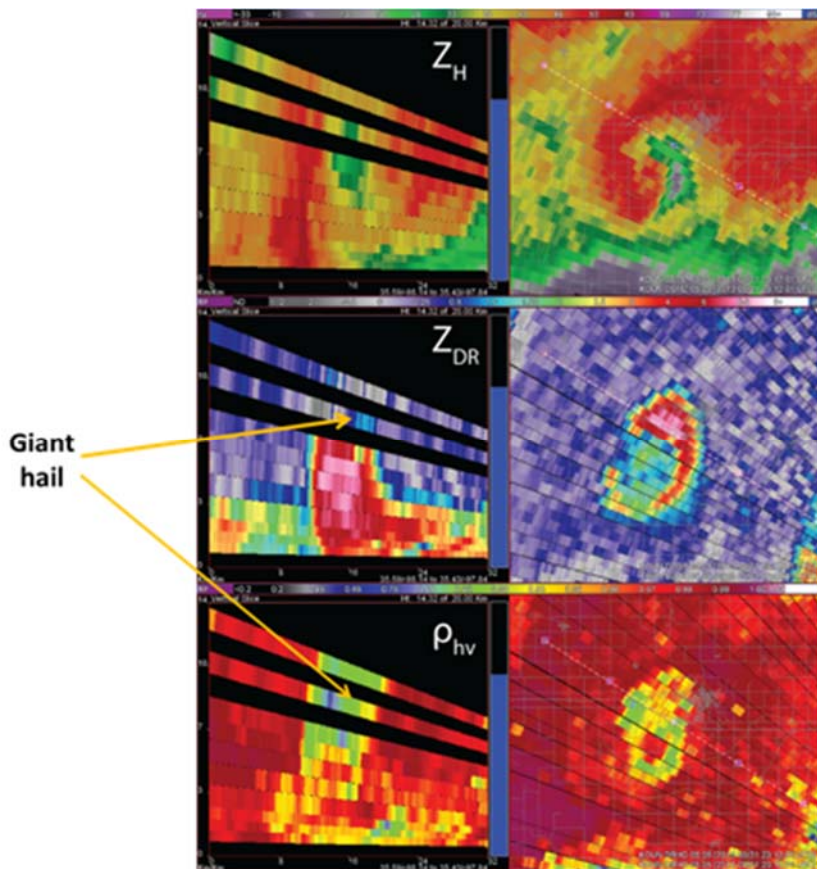
produces a Maximum Expected Size of Hail (MESH) value for each pixel in the radar domain (code drawn from NSSL's experimental MESH Algorithm). A second project step is to work with NSSL's experimental, Dual-Pol, Hydrometeor Classification Algorithm (HCA) that includes hail size estimates (small (<1 in), large (1-2 in), and giant (>2 in). It is called the Hail Size Discrimination Algorithm (HSDA; Ortega et al. 2016 (in press). Finally, a third step will be integrating MESH and HSDA outputs into a combined form. In order to develop and evaluate the new algorithm, 268 cases were chosen where the Severe Hazards Analysis and Verification Experiment (SHAVE) collected high-quality datasets. The Level-II radar data are processed through the operational dual-pol preprocessing algorithm and then the new MESH algorithm and the new HSDA Algorithm are run. Currently, values from the HSDA and MESH are being qualitatively compared to SHAVE hail reports (see figure below). The evaluations will help determine how to combine MESH and HSDA output into a single output.



Hail size estimates overlaid with verification for a hailstorm near Detroit, MI in July 2014. a) Single-radar MESH hail size estimates (scale at top in mm) for 1847 UTC. b) HSDA hydrometeor and hail size classifications (scale at top; R/Ha=small hail & rain, LH=large hail, and GH=giant hail) for 1847 UTC. SHAVE hail size verification data overlaid as circles of different sizes (N = none, S=small hail, L=large hail, and G=Giant hail).

HSDA attempts to identify large (i.e., equivolume diameter D of at least 2.5 cm) and giant (i.e., D of at least 5.0 cm) hail on a bin-by-bin basis using beam height, reflectivity (Z_H), differential reflectivity (Z_{DR}), and co-polar correlation coefficient (ρ_{hv}) information at each bin. Although the HSDA has shown skill at identifying regions of large and/or giant hail, it tends to be very sensitive to Z_{DR} miscalibration, and it may not identify hail where Z_H is relatively low (such as areas near the updrafts of strong supercells, where intense size sorting may produce extremely low number concentrations of giant hail).

Additional polarimetric radar signatures have been explored to identify giant hail. It was shown that the differential reflectivity Z_{DR} is usually negative (down to $-1 - 1.5$ dB) and the cross-correlation coefficient ρ_{hv} is anomalously low (e.g., less than -1 dB) in the areas where giant hail with diameter larger than 5 cm grows in a wet growth regime. These areas are commonly observed above the tops of the Z_{DR} columns signifying strong convective updrafts. Early detection of such zones aloft would facilitate nowcasting of giant hail at the surface with a lead time of 5 – 15 minutes.



(Left Column) Reconstructed RHIs and (right column) PPIs at 5.05° elevation angle showing (from top to bottom) Z_H , Z_{DR} , and ρ_{hv} from 31 May 2013 at 2312 UTC. The Z_{DR} column extends to ~8 km AGL and is nearly centered on the bounded weak echo region seen in Z_H and a column of reduced ρ_{hv} . Negative Z_{DR} of -1 to -2 dB associated with $\rho_{hv} < 0.8$ is found atop the Z_{DR} column (marked by arrows). This storm produced hail greater than 16.0 cm in diameter (Witt 2016).

b. Polarimetric Detection of Convective Updrafts

Jeff Snyder, Valery Melnikov, John Krause, and Alexander Ryzhkov (CIMMS at NSSL)

Observations collected over the past couple of decades and numerical model simulations in the past few years have shown the presence of an upward extension of positive Z_{DR} above the 0°C level in convective storm updrafts. More recently, Snyder et al. (2015) created an algorithm to quantify Z_{DR} column depth as a proxy for convective storm updraft intensity. This concept is becoming widely accepted in the community. However, owing to irregular vertical data coverage in operational WSR-88D volume coverage patterns and finite radar resolution the Z_{DR} columns associated with weaker updrafts are sometimes difficult to detect. In a warm-rain scenario, the Z_{DR} enhancement associated with convective updraft is rarely observed above the freezing level and is entirely attributed to the size sorting in pure rain below the melting layer. The corresponding drop size distributions are characterized by relative lack of small raindrops and abundance of large raindrops.

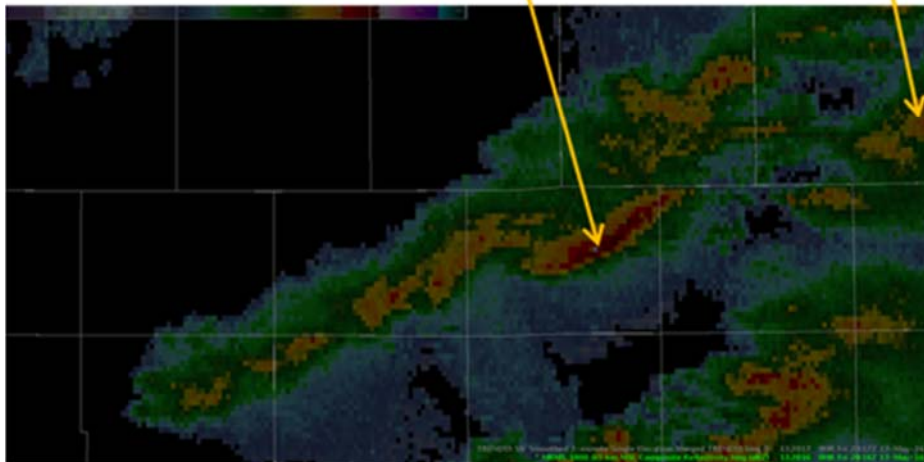
The size sorting (SS) signature below the freezing level is recognized as a combination of high Z_{DR} and low Z . It is identified by examining the $Z - Z_{DR}$ scatterplot at a given elevation sweep and locations with Z_{DR} significantly deviating from the median Z_{DR} vs Z dependency are recognized as SS. The Z_{DR} column product and SS signature can be combined in a “storm tendency” or TRENDSS (trend in the SS signature) product which identifies the convective updraft in a full depth of the atmosphere.

An example of the experimental TRENDSS product is shown in the figure below. The MRMS field of Z measured on 13 May 2016 at 1954 UTC with the TRENDSS product overlaid is displayed in Fig. 2b (white color, top panel). The color intensity of TRENDSS indicated the strength of the SS signature which is likely proportional to the updraft velocity. At 1954 UTC, the squall line was not formed yet but significant TRENDSS associated with relatively low Z shows updraft-related size sorting which can be used for nowcasting of a squall line development 22 minutes later (bottom panel).

1954 UTC



2016 UTC



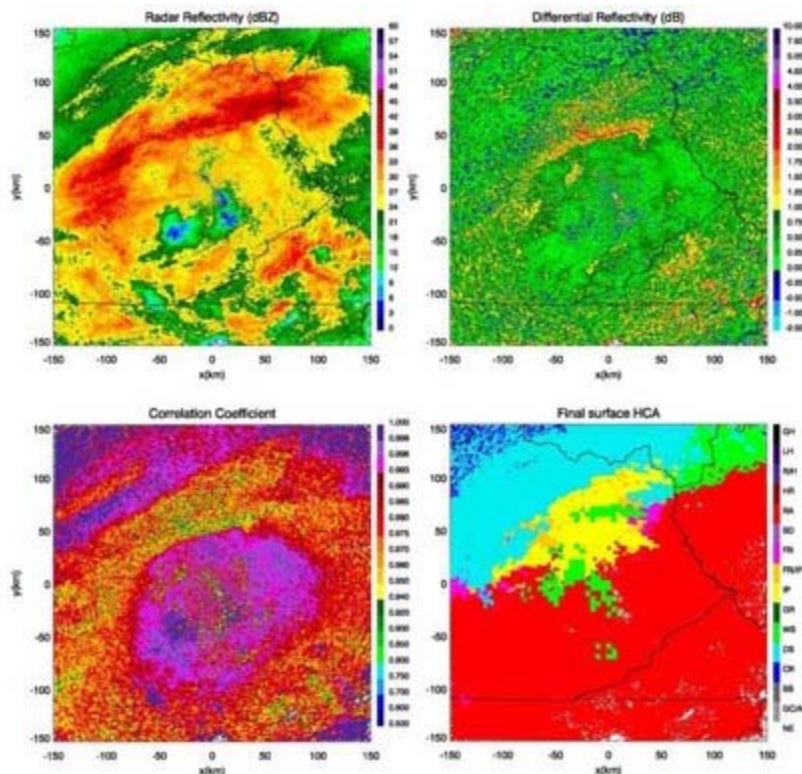
The MRMS field of radar reflectivity with the TRENDSS product overlaid on 13 May 2016 at 1954 UTC (top panel). The MRMS field of Z at 2016 when a strong squall line has formed in the location marked by the TRENDSS product 22 min earlier (bottom panel). The correspondence between enhanced TRENDSS at 1954 UTC and enhanced Z at 2016 UTC is indicated with arrows.

c. Development and Testing of a New Surface-based Hydrometeor Classification Algorithm

Terry Schuur, Alexander Ryzhkov, and John Krause (CIMMS at NSSL)

A new surface Hydrometeor Classification Algorithm (sHCA) that uses an improved “hybrid” Melting Layer Detection Algorithm (HMLDA) has been refined and tested against several published low-melting-layer, transitional winter weather events. The objective of the sHCA and HMLDA development is to use both WSR-88D polarimetric

radar observations and thermodynamic information form the High Resolution Rapid Refresh (HRRR) numerical model to produce a surface-based precipitation type classification that improves upon the radar-only Hydrometeor Classification Algorithm (HCA) precipitation type classification currently available on the WSR-88D network. The sHCA is designed to provide several advantages over previously presented classification methodologies, including 1) the use of advanced (spectral bin or random forest) background classification techniques that are better able to diagnose transitional precipitation types such as freezing rain and/or ice pellets than previously tested background classification algorithms, 2) a redesigned HMLDA that uses signal-to-noise ratio thresholds to combine radar-based ML detections at locations close to the radar with model-based at locations more distant from the radar, thereby providing a ML coverage map that is more consistent with observations, 3) a new methodology to determine the median ML height, which is used to determine where wet snow may be falling at the surface, and 4) a design that allows other products, such as Z_{DR} columns, hail sizes, and tornadic debris signatures, to be “plugged in” as additional classification categories. By projecting to the surface the results of the existing fuzzy-logic-based HCA for all locations where surface temperatures do not favor transitional winter weather precipitation types, the sHCA is further designed to be an all season (rather than just winter storm) algorithm that, rather than a separate product, can be presented as additional, surface-based layer to the existing HCA algorithm.



Radar reflectivity (upper left), differential reflectivity (upper right), correlation coefficient (lower left), and final surface-based precipitation type classification results (lower right) for a winter weather event observed by the KJKL (Jackson, Kentucky) radar at 045619 UTC on February 3, 2014. Classification categories in the lower right panel are no echo

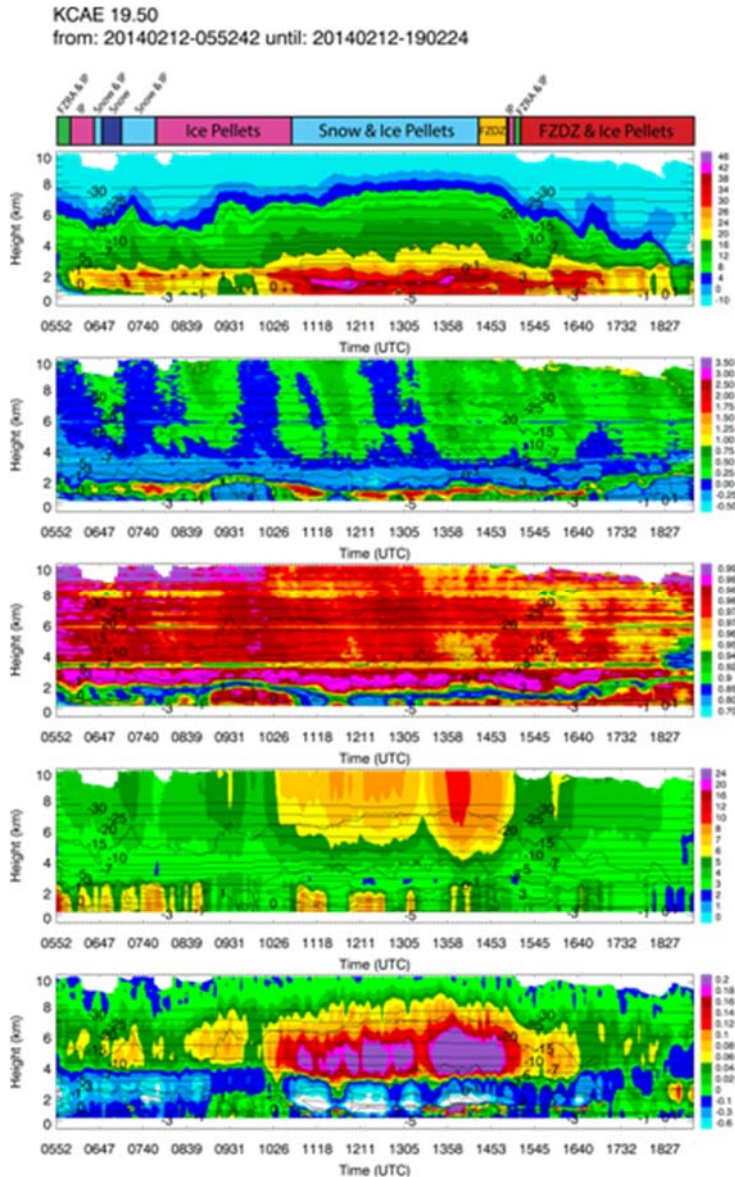
(NE), ground clutter and anomalous propagation (GC/AP), biological scatterers (BS), crystals (CR), dry snow (DS), wet snow (WS), graupel (GR), ice pellets (IP), freezing rain/ice pellet mix (FR/IP), freezing rain (FR), big drops (BD), rain (RA), heavy rain (HR), rain/hail mix (R/H), large hail (LH), and giant hail (GH). Precipitation type categories in the lower right panel indicate the presence of transitional winter precipitation types such as ice pellets and freezing rain that are not possible with the HCA that is currently deployed on the WSR-88D network.

d. Polarimetric and Microphysical Investigation of Winter Precipitation Using Quasi-Vertical Profiles (QVP) Methodology

Erica Griffin, Terry Schuur, and Alexander Ryzhkov (CIMMS at NSSL)

A catalogue of observed winter precipitation events and their associated polarimetric signatures and surface precipitation types has been created and maintained throughout the last several winter seasons. Quasi-vertical profiles (QVPs) of polarimetric variables have been generated for numerous events from this catalogue with the goal of investigating microphysical processes in winter precipitation. QVPs provide an unprecedented look into the microphysical processes within winter storms and are an efficient way to process and illustrate polarimetric WSR-88D data, by azimuthal averaging of radar reflectivity (Z), differential reflectivity (Z_{DR}), cross-correlation coefficient (ρ_{HV}), and differential phase (Φ_{DP}) at high antenna elevation. Their time vs. height format allows for observation of the temporal evolution of these microphysical processes. Φ_{DP} and K_{DP} processing was tested and updated, to obtain optimal display and accuracy of the QVP data. The signatures are analyzed alongside their associated environmental thermodynamic conditions and observed surface precipitation types.

Several intriguing and recurring polarimetric signatures have been observed in the QVPs, particularly in the Z_{DR} and K_{DP} profiles. These signatures include downward extensions of the melting layer (ML) to the surface, sagging MLs with potential riming aloft, rain-snow transition zones, refreezing, wet snow growth (δ profile in Φ_{DP}), and dendritic growth zones (DGZs). Increased ice concentrations are indicated by locally-enhanced Z_{DR} and Φ_{DP} , and reduced ρ_{HV} near cloud top. Analyses and observations reveal that high K_{DP} in the DGZ is usually associated with low Z_{DR} in the DGZ and taller, colder cloud tops, while the greatest Z_{DR} in the DGZ is typically observed for lower K_{DP} in the DGZ and shallow, warmer cloud tops. QVPs have also proven valuable for potentially distinguishing snow aggregation and riming processes. The most pronounced signatures occur in the DGZ and at the tops of clouds, while aggregation and riming dissolve prominent K_{DP} and Z_{DR} signatures below. It is also apparent that K_{DP} signatures in winter precipitation may contain important microphysical information. The QVP methodology allows us to better elucidate ice microphysical processes and their evolution, as QVPs of K_{DP} are particularly useful for quantification of ice. Accordingly, there is ample potential for polarimetric measurements to improve upon existing radar-based techniques to estimate IWC.



Time vs. height QVPs of polarimetric radar variables from the KCAE WSR-88D at 0552 – 1902 UTC on 12 February 2014, at 19.5° elevation. The panels, from top to bottom, are Z_H , Z_{DR} , ρ_{HV} , Φ_{DP} , and K_{DP} , respectively. Augmented Automated Surface Observing System (ASOS) precipitation type observations for the period are indicated in the annotated color bar, above the top panel. High-Resolution Rapid Refresh (HRRR) model wet-bulb temperature contours are overlaid in black. At approximately 1215 UTC, the MLBB descended and reached the surface, with potential riming aloft indicated by the slightly enhanced Z_H and reduced Z_{DR} directly above (at ~2 km) and the enhanced Z_{DR} and Z_H below. Also, during this sagging of the MLBB to the surface, K_{DP} was particularly enhanced ($> 0.2^{\circ}\text{km}^{-1}$) within the model-indicated -10 and -20°C wet-bulb temperature isotherms, suggesting increased IWC in that region. Directly below the layer of enhanced K_{DP} was a pronounced vertical Z_H gradient. ASOS observations indicate this winter event primarily produced ice pellets and snow at the surface.

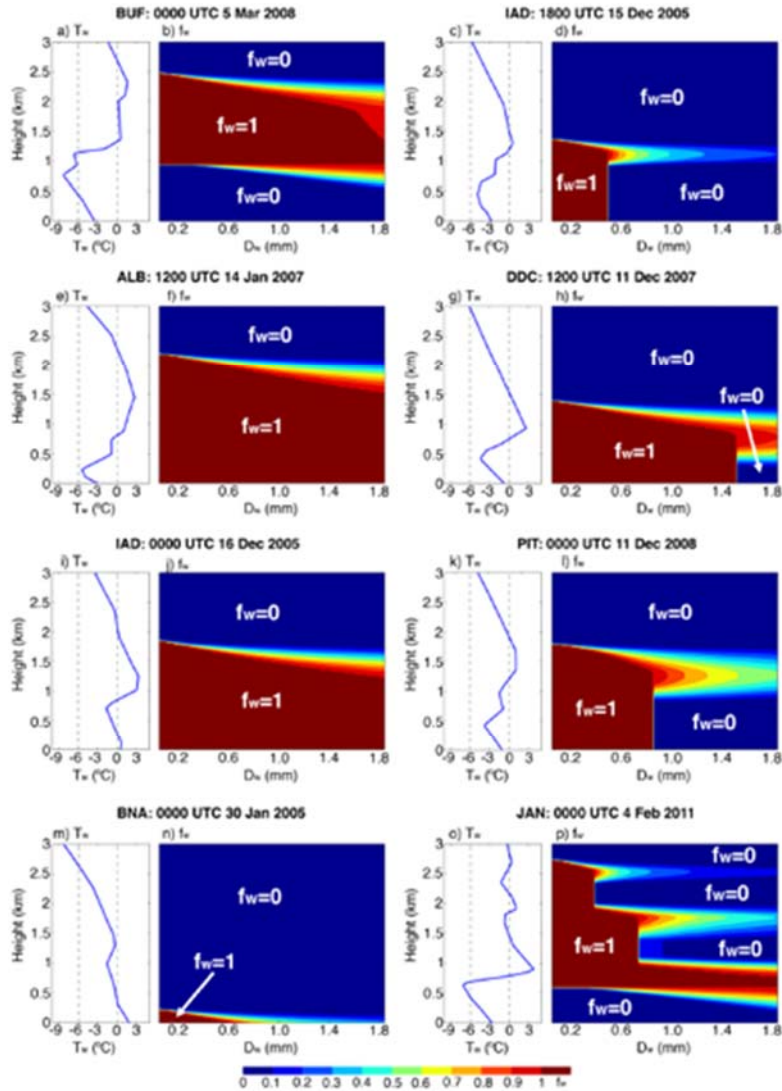
e. Development and Application of the Spectral Bin Classifier for Discrimination Between Different Types of Winter Precipitation

Heather Reeves, Alexander Ryzhkov, and John Krause (CIMMS at NSSL)

A new approach for distinguishing precipitation types at the surface, the spectral bin classifier (SBC) has been developed (Reeves et al. 2016). This algorithm diagnoses six categories of precipitation: rain (RA), snow (SN), a rain – snow mix (RASN), freezing rain (FZRA), ice pellets (PL), and a freezing rain – ice pellet mix (FZRAPL). It works by calculating the liquid water fraction f_w for a spectrum of falling hydrometeors given a prescribed temperature and humidity profiles. The relative precipitation rates of frozen and unfrozen content are then computed and used to determine the type of precipitation at the surface.

The SBC was applied to a collection of 1741 observed soundings associated with SN, RA, FZRA, and PL. The classifier performs very well with the detection of SN and RA, having PODs that range from 91.4% to 98.3%. Although the PODs are somewhat less for FZRA and PL (61.6% - 73.6%), comparison of the SBC detection to that from existing algorithms shows that the SBC has greater accuracy.

Large-scale maps of precipitation types covering middle and eastern US obtained from SBC initiated by the HRRR model output are generally consistent with the spatial distribution of precipitation documented by mPING reports. The SBC classifier has also been utilized in conjunction with the European COSMO-DE model for the Black Ice freezing rain event in Berlin, Germany and demonstrated very efficient performance identifying the freezing rain and its transition to ice pellets (Troemel et al. 2016).



Observed vertical profiles of wet bulb temperature T_w for different events and corresponding distributions of the mass water fraction of hydrometeors as functions of melted diameter D_w and height simulated by the SBC model (Reeves et al. 2016).

f. Hydrometeor Mixing Ratio Retrievals for Storm-Scale Radar Data Assimilation: Utility of Current Relations and Potential Benefits of Polarimetry

Jacob Carlin, Alexander Ryzhkov, and Jeff Snyder (CIMMS at NSSL)

The assimilation of radar data into storm-scale numerical weather prediction models has been shown to be beneficial for successfully modeling convective storms. Because of the difficulty of directly assimilating reflectivity (Z), hydrometeor mixing ratios, and sometimes rainfall rate, are often retrieved from Z observations using retrieval relations, and are assimilated as state variables. In the course of the study, the most limiting (although widely employed) cases of these relations are derived, and their assumptions and limitations have been examined. To investigate the utility of these retrieval relations

for liquid water content (LWC) and ice water content (IWC) in rain and hail as well as the potential for improvement using polarimetric variables, two models with spectral bin microphysics coupled with a polarimetric radar operator are used: a one-dimensional melting hail model and the two-dimensional Hebrew University Cloud Model.

The relationship between LWC and Z in pure rain varies spatially and temporally, with biases clearly seen using the normalized number concentration. Retrievals using Z perform the poorest while specific attenuation (A) and specific differential phase shift (K_{DP}) perform much better. Within rain–hail mixtures, separate estimation of LWC and IWC is necessary. Prohibitively large errors in the retrieved LWC may result when using Z . The quantity K_{DP} can be used to effectively retrieve the LWC and to isolate the contribution of IWC to Z . It is found that the relationship between Z and IWC is a function of radar wavelength, maximum hail diameter, and principally the height below the melting layer, which must be accounted for in order to achieve accurate retrievals.

g. Development of an Advanced Polarimetric Radar Forward Operator for Cloud Models with Spectral and Bulk Microphysics

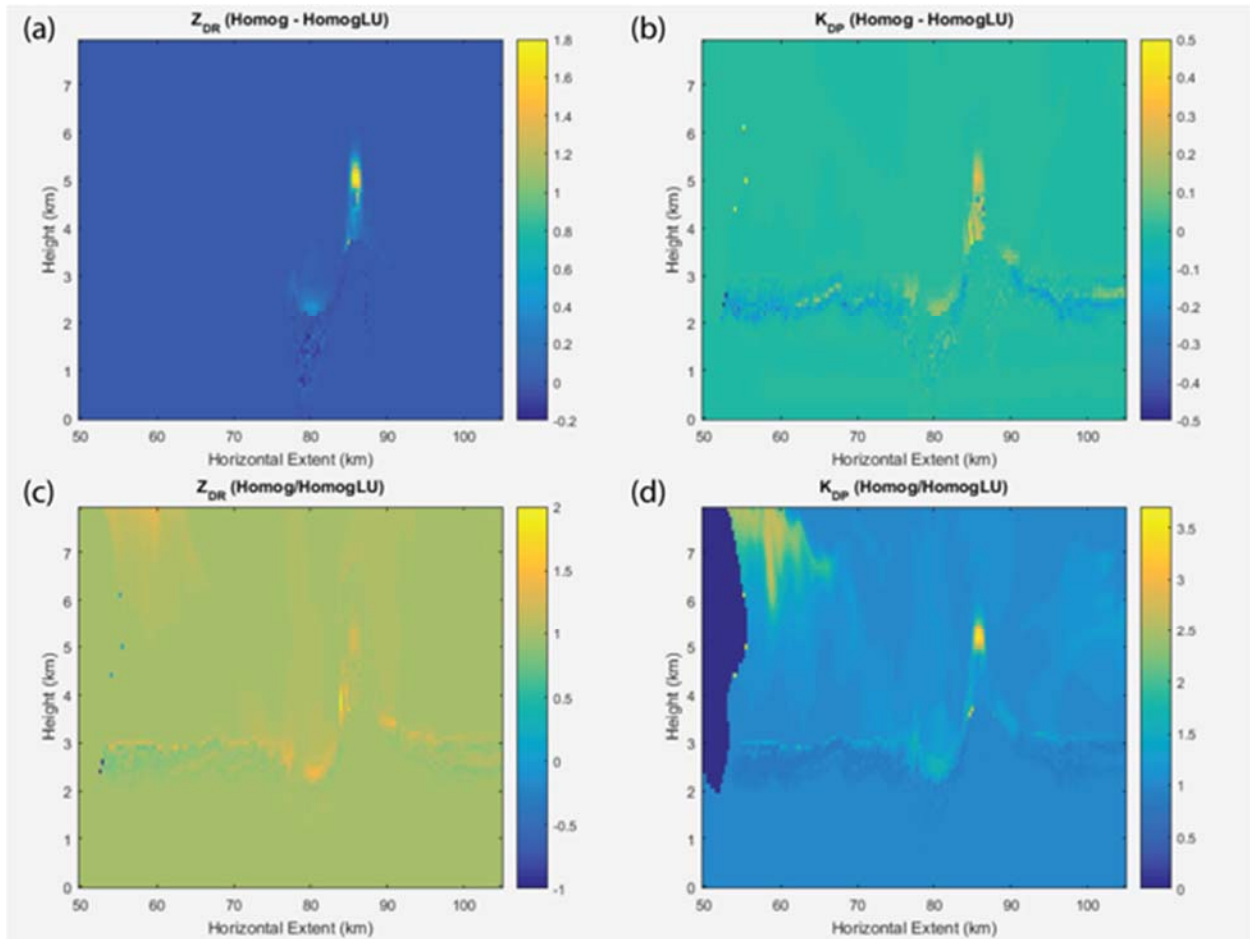
Jeff Snyder (CIMMS at NSSL)

A polarimetric radar forward operator can be an essential tool for comparing numerical model forecasts/output to polarimetric radar observations. The forward operator originally described in Ryzhkov et al. (2011) has seen steady development in the past several years. The forward operator currently operates with the bin microphysics scheme within the Hebrew University Cloud Model (HUCM). This microphysics package predicts, using 43 mass-doubling bins, concentration of liquid water (i.e., cloud droplets and raindrops), snow aggregates, three types of ice crystals (columns, plates, and dendrites), freezing drops, graupel, and hail. Liquid water fraction is predicted for snow aggregates, freezing drops, graupel, and hail; snow aggregates also track rime fraction as well. From these data, the forward operator calculates, amongst other quantities, radar reflectivity at horizontal and vertical polarizations (Z_H and Z_V , respectively), differential reflectivity (Z_{DR}), linear depolarization ratio (LDR), circular depolarization ratio (CDR), specific differential phase (K_{DP}), co-polar cross-correlation coefficient (ρ_{hv}), specific attenuation (A_H), and specific differential attenuation (A_{DP}).

In the past year, three significant modifications have been made to the forward operator, and one smaller modification was started. First, we have added flexibility to the forward operator by allowing the radar quantities to be calculated after the underlying numerical model has run; the forward operator has been separated from the numerical model. This addition allows a user to make minor modifications to the forward operator and re-calculate the radar quantities without having to re-run the entire model. This is also relevant because it is a beneficial step for moving the forward operator package over to another numerical model such as WRF. Second, we have created code to pre-compute scattering amplitudes for the differential hydrometeor species at an arbitrary array of temperatures and liquid water fractions; files containing these scattering amplitudes can subsequently be loaded by the forward operator, enabling the use of look-up tables that

very significantly reduces the computational expense compared to that required to compute the scattering amplitudes separately for each bin at each grid point for each hydrometeor species at each output time. Third, the two-layer T-matrix subroutine was integrated into the forward operator; this allows for more physically realistic modeling of the scattering properties of melting hydrometeors. A more minor modification, which began during the summer of 2016, allows the two-layer T-matrix subroutine to run with quadruple numerical precision (i.e., 16 byte floating point numbers); this modification was required for numerical stability purposes when the two-layer T-matrix method calculates the scattering amplitudes of electromagnetically large hydrometeors. This added level of precision is usually not required at S band (i.e., ~10-11 cm wavelength) but does become progressively more important at C (i.e., ~5.5 cm wavelength) and X (i.e., ~3 cm wavelength) bands.

The forward operator has been used for numerous projects, including the study of Z_{DR} and K_{DP} columns. In addition, we are currently investigating the errors associated with different assumptions and “short-cuts” that can be used to reduce computational expense. For example, the figure below shows the differences between a simulation using homogeneous-mixture T-matrix code (“Homog”) and using lookup tables based upon pre-computing scattering amplitudes using the same lookup table (“HomogLU”). The lookup tables assume a fixed temperature for water (20 C) and ice (0 C), which is relevant owing to the temperature sensitivity of the dielectric constant for water/ice; the liquid water fraction for each mixed-phase hydrometeor is rounded to the nearest 5% since the scattering amplitudes were pre-computed at mass water fraction intervals of 5%. The top row represents the differences between these two methods (i.e., Homog - HomogLU), whereas the bottom row represents the relative magnitudes of these methods (i.e., Homog/HomogLU). The left column shows ZDR; the right column shows KDP.



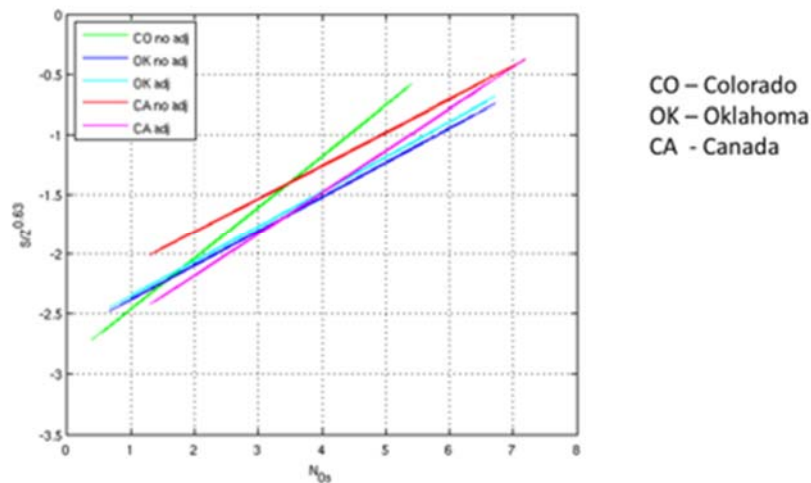
The above results show differences in (left column) ZDR and (right column) KDP for two versions of the forward operator – “Homog” (homogeneous T-matrix scattering calculations at each bin and grid-point) and “HomogLU” (lookup tables from pre-computed scattering amplitudes). The top row represents the mathematical difference in the two version of the operator; the bottom row represents the relative magnitude of Homog compared to that of HomogLU. The dielectric constant for water and ice is fixed in the HomogLU experiment, whereas it is allowed to vary in the Homog experiment. Liquid water fraction is allowed to vary completely in the Homog experiment, whereas it is rounded to the nearest 5% in the HomogLU experiment.

h. Investigation of Size Distributions and Radar Characteristics of Snow Using 2D-Video Disdrometer Data and Polarimetric Radar Measurements

Petar Bukovcic, Pengfei Zhang, and Alexander Ryzhkov (CIMMS at NSSL)

A detailed investigation of the 2D-video disdrometer data in snow combined with dual-polarization radar measurements has been carried out for a number of snowstorms in Oklahoma, Colorado, and Canada. Polarimetric radar data collected by two S-band WSR-88D radars in Oklahoma and Colorado and C-band King radar in Ontario during numerous snow events have been analyzed. It was confirmed that the power-law $S - Z$

relation between snow rate and radar reflectivity factor has to be parameterized by the intercept N_{0s} of the exponential size distribution of snowflakes as $S = \alpha N_{0s}^{0.37} Z^{0.63}$. An obvious correlation between N_{0s} and the magnitude of specific differential phase K_{DP} either next to the ground or in the dendritic growth layer aloft has been established from the analysis of the quasi-vertical profiles of polarimetric radar variables. This opens an opportunity for development of the polarimetric algorithm for quantification of snow. Large differences between the snow size spectra in synoptic snow and lake-effect snow have been discovered which are also reflected in the differences in the depth of the storms and prevailing values of K_{DP} and Z_{DR} with lake-effect snow exhibiting much higher N_{0s} , K_{DP} , and Z_{DR} .



Dependencies of $\log(S/Z^{0.63})$ on $\log(N_{0s})$ obtained from disdrometer measurements of snow in Oklahoma, Colorado, and Ontario (Canada).

i. Investigations of Microphysical Processes in Clouds Using Dual-Polarization Radars and *In Situ* Aircraft Measurements.

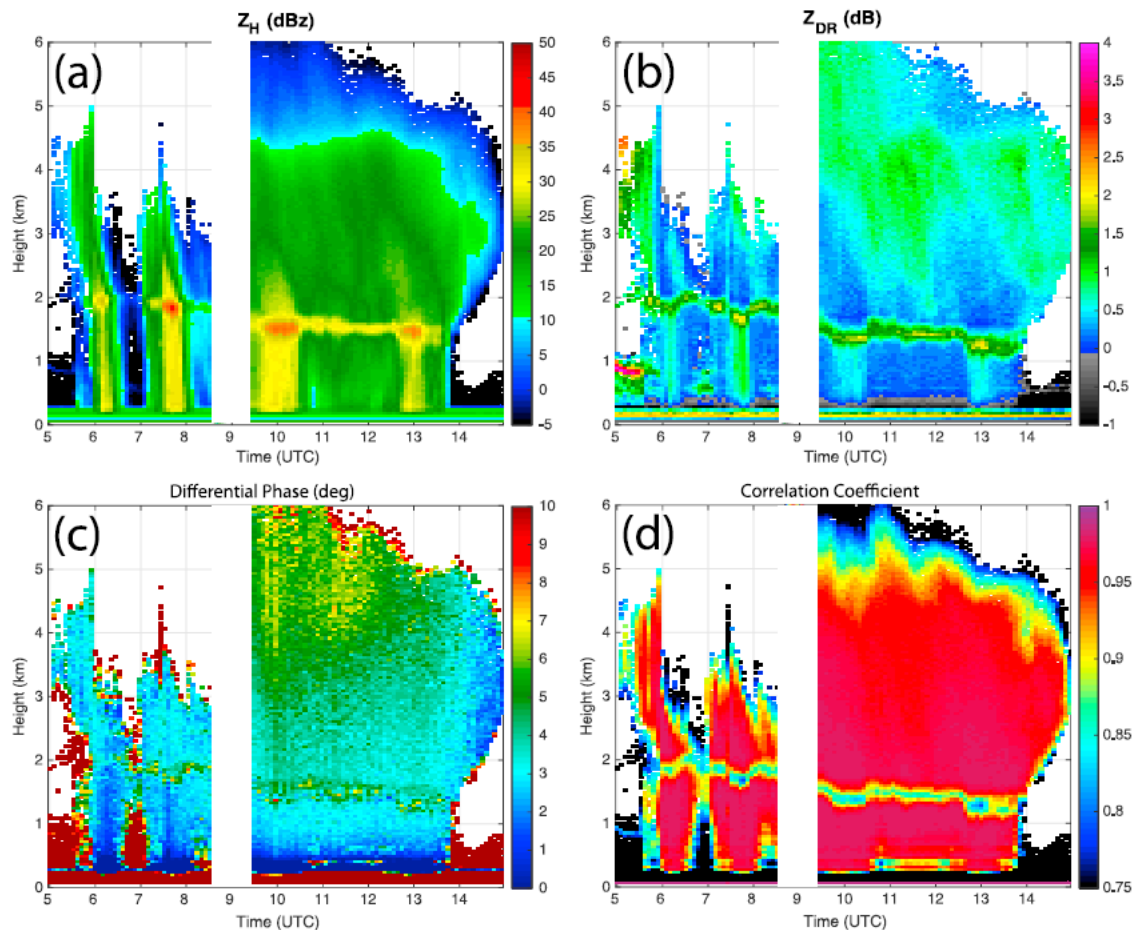
Alexander Ryzhkov (CIMMS at NSSL)

A detailed analysis of polarimetric radar signatures combined with in situ aircraft measurements has been performed for a number of storms observed during the MC3E field campaign held in northern Oklahoma in April – June 2011 as part of DOE ARS program. The focus was on better understanding of microphysical processes in the stratiform parts of mesoscale convective systems.

Quasi-vertical profiles of polarimetric radar variables in two MC3E stratiform precipitation events reveal episodic melting layer sagging. Integrated analyses using scanning and vertically pointing radar and aircraft measurements reveal that saggy bright band signatures are produced when dense, faster-falling, more isometric hydrometeors (relative to adjacent times) descend into the melting layer. In one case, strong circumstantial evidence for riming is found during bright band sagging times. A

spectral bin melting layer model successfully reproduces many aspects of the signature, supporting the observational analysis (Kumjian et al. 2016).

In the related study, aircraft spiral ascent and descent observations intercepting a transition to riming processes during widespread stratiform precipitation were investigated (Giangrande et al. 2016). The sequence was documented using collocated scanning and profiling radar, including longer-wavelength dual-polarization measurements and shorter-wavelength Doppler spectra. Riming regions were identified using aircraft measurements recording elevated liquid water concentrations, spherical particle shapes, and saturation with respect to water. Profiling cloud radar observations indicate riming regions during the event as having increasing particle fall speeds, rapid time-height changes, and bimodalities in Doppler spectra. These particular riming signatures are coupled to scanning dual-polarization radar observations of higher differential reflectivity Z_{DR} caused by secondary ice of highly nonspherical shape resulting from the Hallett - Mossop ice multiplication process. Needle-like ice splinters mixed with nearly spherical rimed ice produce elevated values of Z_{DR} .



Time series of quasi-vertical profiles of polarimetric radar variables from 27 April 2011. Data were collected using C-band radar at the ARM Southern Great Plains site during MC3E field campaign. “Sagging” of the melting layer due to riming is evident in the plots of Z_{DR} and ρ_{hv} (Kumjian et al. 2016).

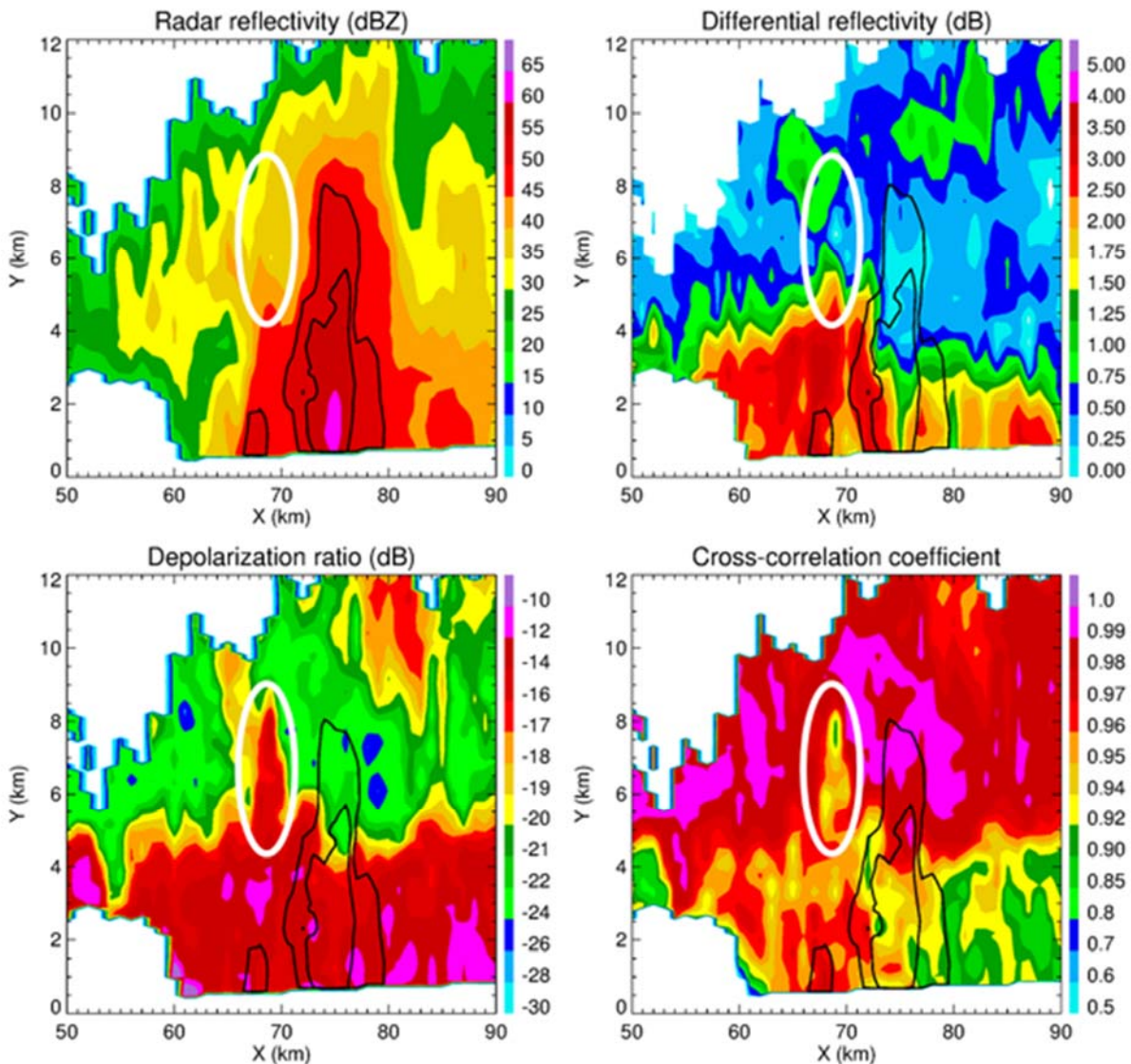
j. Estimation of Depolarization Ratio Using Radars with Simultaneous Transmission/Reception

Alexander Ryzhkov, Valery Melnikov, and Pengfei Zhang (CIMMS at NSSL)

A new methodology for estimating the Depolarization Ratio (DR) by dual-polarization radars with simultaneous transmission / reception of orthogonally polarized waves together with traditionally measured differential reflectivity Z_{DR} correlation coefficient ρ_{hv} , and differential phase Φ_{DP} in a single mode of operation is suggested. This depolarization ratio can serve as a proxy for circular depolarization ratio (CDR) measured by radars with circular polarization. The suggested methodology implies the use of a high-power phase shifter to control the system differential phase on transmission and a special signal processing to eliminate the detrimental impact of differential phase on the estimate of DR . As opposed to linear depolarization ratio LDR (which requires a special mode of operation), CDR (or DR) depends on hydrometeor orientation rather weakly and is less affected by noise.

The feasibility of the suggested approach has been demonstrated by retrieving DR from the standard polarimetric variables and the raw I and Q data, and by implementing the scheme on a C-band radar with simultaneous transmission / reception of horizontally and vertically polarized waves.

Possible practical implications of using DR include the detection of hail and the determination of its size above the melting layer, the discrimination between various habits of ice aloft, and the possible identification and quantification of riming which is associated with the presence of supercooled cloud water.



Composite RHI of Z , Z_{DR} , ρ_{hv} , and depolarization ratio DR is a hailstorm observed by the KOUN WSR-88D radar on 17 June 2005 at 0406 UTC and $Az = 305^\circ$. White oval encloses a convective updraft of a newly developing cell. The corresponding DR column is taller than the Z_{DR} column and better delineates a convective updraft.

Publications

- Bluestein, H., and J. Snyder, 2015: An observational study of the effects of dry air produced in dissipating convective storms on the predictability of severe weather. *Weather and Forecasting*, **30**, 79-114.
- Bluestein, H. B., J. C. Snyder, and J. B. Houser, 2015: A multi-scale overview of the El Reno, Oklahoma, tornadic supercell of 31 May 2013. *Weather and Forecasting*, **30**, 525-552.
- Bluestein, H., M. French, J. Snyder, and J. Houser, 2016: Doppler-radar observations of anticyclonic tornadoes in cyclonically rotating, right-moving supercells. *Monthly Weather Review*, **144**, 1591-1616.
- Boodoo, S., D. Hudak, A. Ryzhkov, P. Zhang, N. Donaldson, D. Sills, and J. Reid, 2015: Quantitative precipitation estimation from a C-Band Dual-polarized radar for the July 08 2013 flood in Toronto, Canada. *Journal of Hydrometeorology*, **16**, 2027-2044.

- Cao, Q., M. Knight, A. Ryzhkov, P. Zhang, and N. Lawrence, 2016: Differential phase calibration of linearly polarized weather radar for accurate measurements of circular depolarization ratio. *IEEE Transactions in Geosciences Remote Sensing*, Accepted.
- Carlin, J., 2015: Weather radar polarimetry. *Physics Today*. Available at <http://scitation.aip.org/content/aip/magazine/physicstoday/news/10.1063/PT.5.4011;jsessionid=4pginrtbms1m9.x-aip-live-02>.
- Carlin, J., A. Ryzhkov, J. Snyder, and A. Khain, 2016: Hydrometeor mixing ratio retrievals for storm-scale radar data assimilation: Utility of current equations and potential benefits of polarimetry. *Monthly Weather Review*, **144**, 2981-3001.
- Diederich, M., S. Troemel, A. Ryzhkov, P. Zhang, and C. Simmer, 2015: Use of specific attenuation for rainfall measurements at X-band radar wavelengths. Part I: Radar calibration and partial beam blockage estimation. *Journal of Hydrometeorology*, **16**, 487-502.
- Diederich, M., S. Troemel, A. Ryzhkov, P. Zhang, and C. Simmer, 2015: Use of specific attenuation for rainfall measurements at X-band radar wavelengths. Part II: Rainfall estimates and comparison with rain gauges. *Journal of Hydrometeorology*, **16**, 503-516.
- Giangrande, S., T. Toto, A. Bansemmer, M. Kumjian, S. Mishra, and A. Ryzhkov, 2016: Insights into riming and aggregation processes as revealed by aircraft, radar, and disdrometer observations for a 27 April 2011 widespread precipitation event. *Journal of Geophysical Research*, **121**, 5846-5863.
- Houser, J., H. B. Bluestein, and J. C. Snyder, 2015: Rapid-scan, polarimetric, Doppler radar observations of tornadogenesis and tornado dissipation in a tornadic supercell: the "El Reno, Oklahoma" storm of 24 May 2011. *Monthly Weather Review*, **143**, 2685-2710.
- Houser, J., H. Bluestein, and J. Snyder, 2016: A fine-scale radar examination of the tornadic debris signatures and weak reflectivity band associated with a large, violent tornado. *Monthly Weather Review*, In Press.
- Ilotoviz, E., N. Benmoshe, A. Khain, V. Phillips, and A. Ryzhkov, 2016: Effect of aerosols on freezing drops, hail, and precipitation in a mid-latitude storm. *Journal of Atmospheric Science*, **73**, 109-144.
- Kaltenboeck, R., and A. Ryzhkov, 2016: A freezing rain storm explored with a C-band polarimetric weather radar using the QVP methodology. *Meteorologische Zeitschrift*, Accepted.
- Krause, J., 2016: A simple algorithm to discriminate between meteorological and non-meteorological radar echoes. *Journal of Atmospheric and Oceanic Technology*, **33**, 1875-1885.
- Kumjian, M., S. Mishra, S. Giangrande, T. Toto, A. Ryzhkov, and A. Bansemmer, 2016: Polarimetric radar and aircraft observations of saggy bright band during MC3E. *Journal of Geophysical Research, Atmospheres*, **121**, 3584-3607.
- Lakshmanan, V., C. Karstens, J. Krause, K. Elmore, A. Ryzhkov, and S. Berkseth, 2015: Which polarimetric variables are important for weather / no-weather discrimination? *Journal of Atmospheric and Oceanic Technology*, **32**, 1209-1223.
- Melnikov, V., and D. S. Zrnić, 2015: On the alternate transmission mode for polarimetric phased array weather radar. *Journal of Atmospheric and Oceanic Technology*, **32**, 220-233.
- Melnikov, V., R. Doviak, and D. Zrnic, 2015: A method to increase the scanning rate of phased-array weather radar. *IEEE Transactions in Geosciences Remote Sensing*, **53**, Issue: 10, 5634-5643.
- Melnikov, V., D. Zrnić, D. Burgess, and E. Mansell, 2015: Vertical extent of thunderstorm inflows revealed by polarimetric radar. *Journal of Atmospheric and Oceanic Technology*, **32**, 1860-1865.
- Melnikov, V., M. Istok, and J. Westbrook, 2015: Asymmetric radar echo patterns from insects. *Journal of Atmospheric and Oceanic Technology*, **32**, 659-674.
- Ortega, K., J. Krause, and A. Ryzhkov, 2016: Polarimetric radar characteristics of melting hail. Part III: Validation of the algorithm for hail size discrimination. *Journal of Applied Meteorology and Climatology*, **55**, 829 – 848.
- Oue, M., M. Galletti, J. Verlinde, A. Ryzhkov, Y. Lu, and N. Bharadwaj, 2016: Use of X-band differential reflectivity measurements to study shallow Arctic mixed-phase clouds. *Journal of Applied Meteorology and Climatology*, **55**, 403-424.
- Phillips, V., A. Khain, N. Benmoshe, E. Ilotoviz, and A. Ryzhkov, 2015: Theory of time-dependent freezing. Part II. Scheme for freezing raindrops and simulations by a cloud model with spectral bin microphysics. *Journal of the Atmospheric Sciences*, **72**, 262-286.

- Reeves, H., A. Ryzhkov, and J. Krause, 2016: Discrimination between winter precipitation types based on spectral-bin microphysical modeling. *Journal of Applied Meteorology and Climatology*, **55**, 1747-1761.
- Ryzhkov, A., P. Zhang, H. Reeves, M. Kumjian, T. Tschallener, C. Simmer, and S. Troemel, 2016: Quasi-vertical profiles – a new way to look at polarimetric radar data. *Journal of Atmospheric and Oceanic Technology*, **33**, 551-562.
- Snyder, J., A. Ryzhkov, M. Kumjian, J. Picca, and A. Khain, 2015: Developing a Z_{DR} column detection algorithm to examine convective storm updrafts. *Weather and Forecasting*, **30**, 1819-1844.
- Snyder, J., and A. Ryzhkov, 2015: Automated detection of polarimetric tornado debris signatures. *Journal of Applied Meteorology and Climatology*, **54**, 1861-1870.
- Troemel, S., A. Ryzhkov, M. Diederich, K. Muhlbauer, C. Simmer, S. Kneifel, and J. Snyder, 2016: Multi-sensor characterization of mammatus clouds. *Monthly Weather Review*, Accepted.
- Wakimoto, R. M., N. T. Atkins, K. M. Butler, H. B. Bluestein, K. Thiem, J. C. Snyder, and J. B. Houser, 2015: Photogrammetric analysis of the 2013 El Reno tornado combined with mobile X-band polarimetric radar data. *Monthly Weather Review*, **143**, 2657-2683.
- Wakimoto, R., N. Atkins, K. Butler, H. Bluestein, K. Thiem, J. Snyder, J. Houser, and J. Wurman, 2016: Aerial damage survey of the 2013 El Reno tornado combined with mobile radar data. *Monthly Weather Review*, **144**, 1749-1776.
- Xie, X., R. Evaristo, S. Troemel, P. Saavedra, C. Simmer, and A. Ryzhkov, 2016: Radar observation of evaporation and implications for quantitative precipitation and cooling rate estimation. *Journal of Atmospheric and Oceanic Technology*, **33**, 1779-1792.
- Zrnich, D., V. Melnikov, R. Doviak, and R. Palmer, 2015: Scanning strategy for the Multifunction Phased-Array Radar to satisfy aviation and meteorological needs. *Geosciences Remote Sensing Letters, IEEE*, **12**, 204-208.

3. MPAR Meteorology

Accomplishments

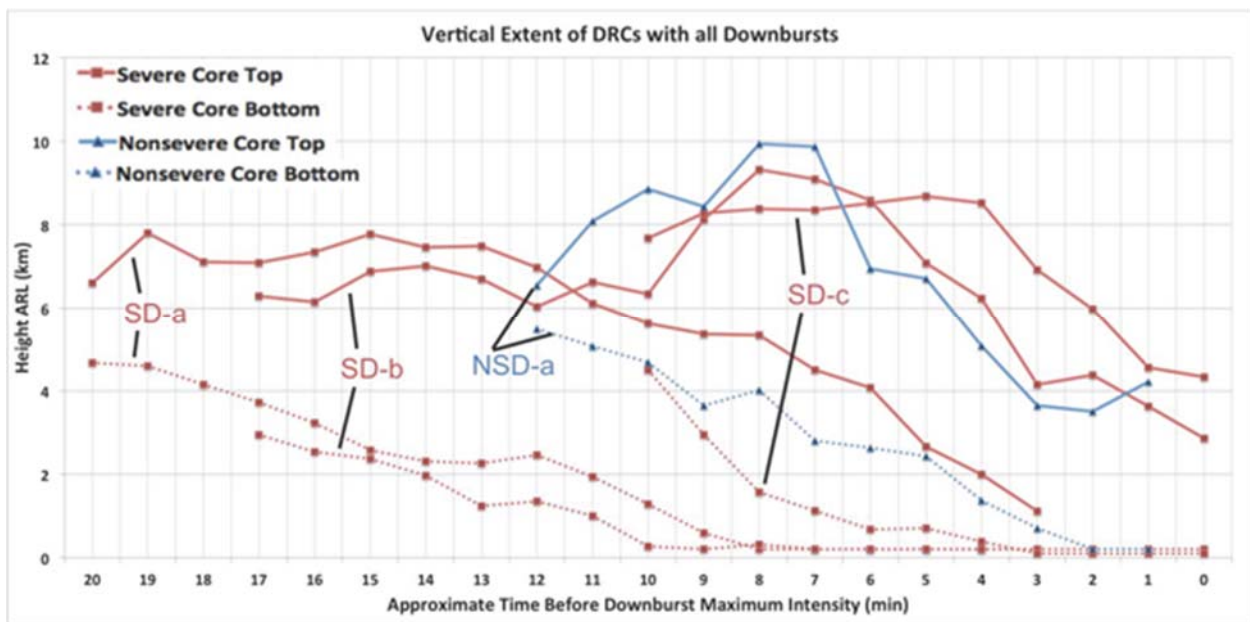
a. Advancements in Scientific Understanding of Storms Facilitated by Rapid-Update Radar Data

Charles Kuster and Terry Schuur (CIMMS at NSSL), and Pamela Heinselman (NSSL)

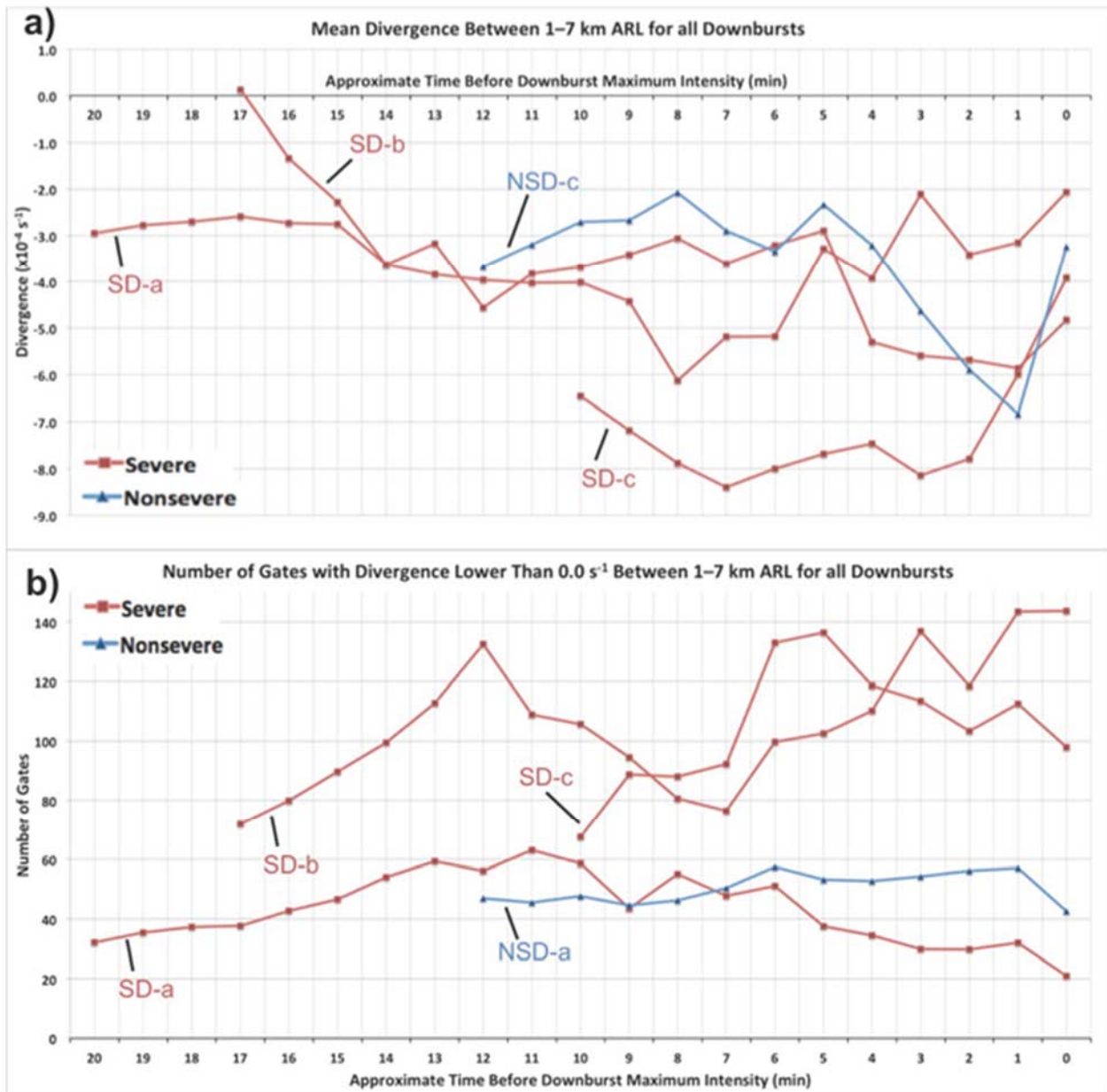
Rapid-update radar data is useful for sampling rapidly evolving storm-scale features such as downburst precursor signatures (e.g., descending reflectivity cores) and dual-polarization supercell signatures (e.g., Z_{DR} ring; Z_{DR} arc). To examine the impact of rapid-update radar data on observing downburst precursor signatures, we performed an in-depth case study of a storm that produced both severe and nonsevere downbursts within 50 km of NSSL's phased array radar located in Norman, Oklahoma. Precursor signatures typically evolved in time scales less than 10 min, thereby requiring rapid-update volumetric radar data for sufficient observations. These observations were important in this case because collapse and rapid descent of the high reflectivity core began 8.6 min prior to downburst maximum intensity on average, while increasing midlevel convergence size began 13.0 min prior to downburst maximum intensity on average (see figures below). Descending reflectivity core and midlevel convergence magnitude evolution was similar between the severe and nonsevere downbursts. However, midlevel convergence size evolution did differ. Midlevel convergence size observed with severe downbursts increased steadily and reached a clear peak, while convergence size observed with the nonsevere downburst remained steady (i.e.,

unchanging; Figure 2Kb). Observations of these trends may prove useful to forecasters issuing warnings for damaging winds produced by downbursts.

Special rapid-update sector scan data collected by KOUN provided an opportunity to examine the evolution of multiple dual-polarization supercell signatures (e.g., Z_{DR} ring; K_{DP} column; Z_{DR} arc) in a storm that produced a strong tornado on 31 May 2013. Magnitude and size of all signatures was calculated and them compared to the evolution of signatures such as mesocyclone intensity and upper-level reflectivity cores. No distinct relationship was found between any of the dual-polarization signatures and mesocyclone intensity or tornado development. A relationship did exist between Z_{DR} column growth and large hail production at the surface. Future research will continue to examine dual-polarization signatures and their potential benefits to forecasters tasked with issuing tornado warnings.



Evolution of the DRC for all analyzed severe (red lines) and nonsevere (blue line) downbursts on 14 June 2011. Solid lines are core top and dashed lines are core bottom.



Evolution of a) mean midlevel convergence and b) number of gates with divergence lower than 0.0 s^{-1} (i.e., convergence size) between 1.0(1.5)–7.0 km ARL for all analyzed severe (red lines) and nonsevere (blue line) downbursts on 14 June 2011. In a), negative divergence is convergence.

Publications

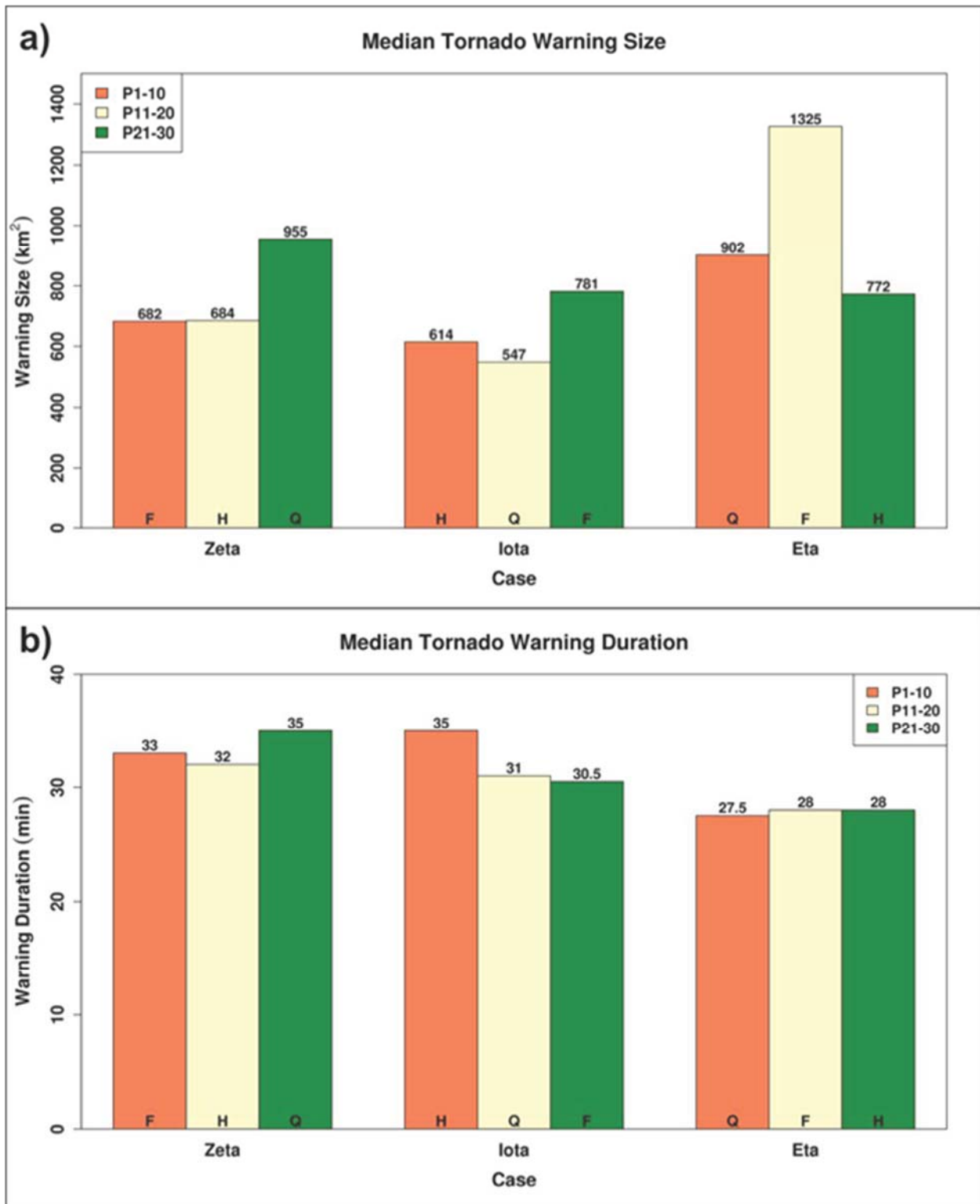
Kuster, C. M., P. L. Heinselman, and T. J. Schuur, 2016: Rapid-update radar observations of downbursts occurring within an intense multicell thunderstorm of 14 June 2011. *Weather and Forecasting*, **31**, 827–851.

b. Benefits of Rapid-Update Radar Data to NWS Forecasters and Emergency Managers

Charles Kuster and Katie Wilson (CIMMS at NSSL), Pamela Heinselman (NSSL), and Doug Speheger (OUN)

As part of the data collected during the 2015 Phased Array Radar Innovative Sensing Experiment (PARISE), we analyzed the characteristics (i.e., size and duration) of warnings issued by forecasters during the experiment. Warning size and duration varied most based on storm mode. For example, the largest tornado warnings were issued during the tornadic squall line case (see figure below). These warnings also had the shortest duration, which matched with forecaster perceptions that squall line tornadoes tend to be short-lived. There was no relationship between radar-update time and warning characteristics.

Emergency managers and public safety officials in Oklahoma use radar data to make life-saving decisions and are therefore an important user group to consider in the development of new radar technology and radar-based products. To collect input from this user group, we attended multiple meetings within the emergency management community and developed a survey that asked questions about the community's use of radar data, decisions they make using radar data, and their perceptions about the usefulness of various radar-based tornado track and intensity estimation products. Analysis of the data provided by 183 survey respondents as well as input from a focus group to be held in FY17 will inform ongoing research about rapid-update radar data and radar-based tornado products.



Median tornado warning a) size and b) duration for each participant group during 2015 PARISE. Median values are included near the top of each bar. Radar-update speed (F=Full, H=Half, and Q=Quarter) worked by each group for each case is included near the bottom of each bar.

4. MPAR Engineering

Objectives: Continue research and development in collaboration with NSSL and other government, industry, and university partners to determine the usefulness of phased array radars (PAR) for meteorological observations in a multifunction environment. The National Weather Radar Testbed Phased-Array Radar (NWRT/PAR) in Norman, OK was the first of its kind to study meteorological applications of this technology. It is now undergoing engineering upgrades to take advantage of modern PAR technology and to add a dual-polarization capability. Theoretical, simulation, and demonstration studies are being conducted to determine the feasibility of dual-polarized phased-array antenna systems along with the applications of using the radar for multiple functions (e.g., aircraft and weather surveillance). Other areas of research and development include design of novel fast and adaptive scanning techniques, pulse compression techniques, and advanced digital signal processing techniques.

Accomplishments

a. MPAR Advanced Technology Demonstrator

Hoyt Burcham, Christopher Curtis, Eddie Forren, Doug Forsyth, Igor Ivić, Rick Rhoton, David Schwartzman, Sebastian Torres, and Danny Wasielewski (CIMMS at NSSL), Mark Benner, Kurt Hondl, Micheal Shattuck, Allen Zahrai, and Dusan Zrnić (NSSL), and other government, industry, and university collaborators.

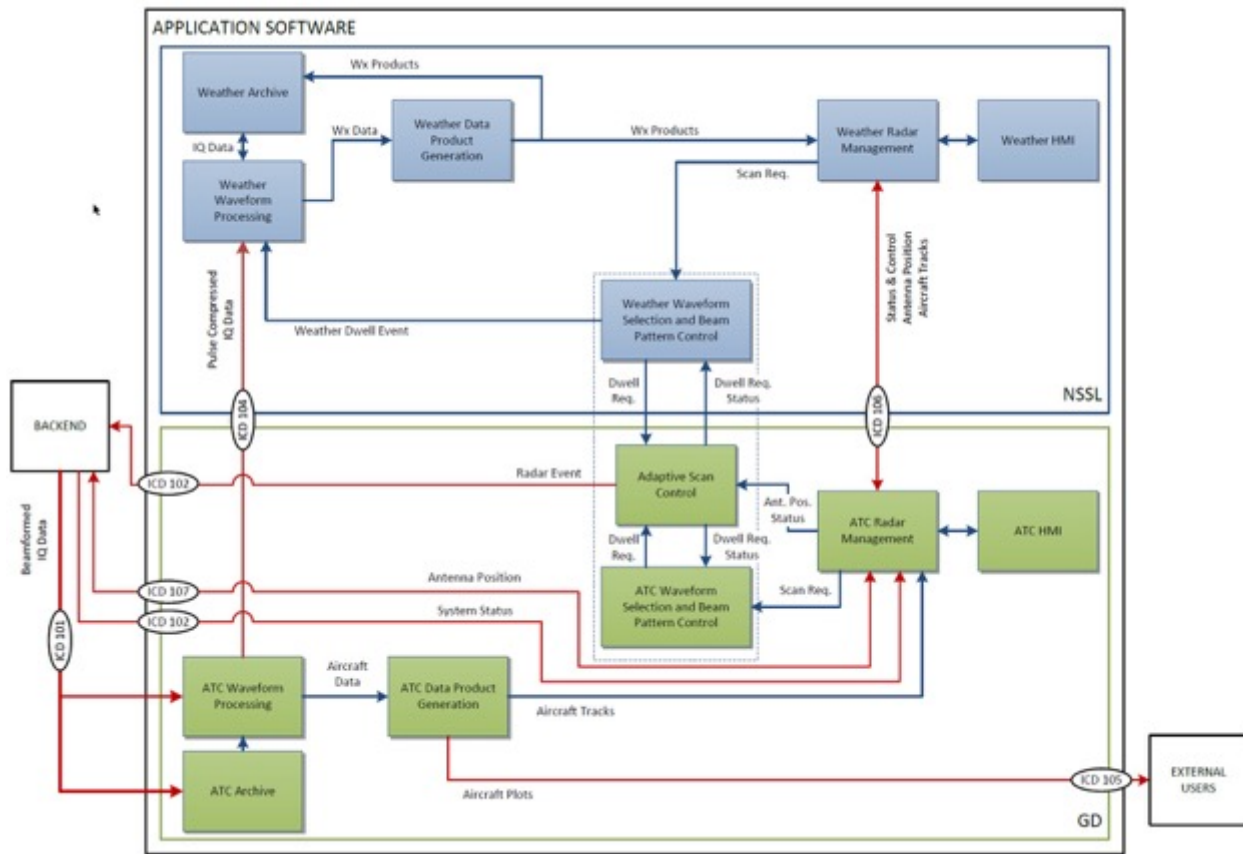
The Advanced Technology Demonstrator (ATD) is being developed to demonstrate Multifunction Phased-Array Radar (MPAR) risk reduction. It will replace the current SPY-1A antenna at the NWRT with an S-Band, 4-m diameter, dual-polarization, active phased array. The system's initial operating capabilities are intended to support the FAA investment decisions pertaining to the next generation of aircraft surveillance and weather sensing radar as well as to serve as a basis for ongoing meteorological research at NSSL. The ATD leverages several prior investments in order to provide a flexible, useful system while striving to keep cost and risk low. The antenna system is based around tile-able array panels developed under the MPAR Government Proof-of-Concept Technology Risk Reduction Program carried out by MIT/Lincoln Laboratory. The receiver and exciter electronics leverage work done by General Dynamics Advanced Information Systems (GDAIS) for the United States Navy in support of the Air and Missile Defense Radar development. The radar control system leverages the work done by GDAIS for the Office of Naval Research under the Digital Array Radar and Affordable Common Radar Architecture (ACRA) programs. Finally, the weather signal processor (including the inter-process-communication infrastructure, system control and monitoring, techniques, and algorithms) leverages the work done by CIMMS and NSSL for the original SPY-1A-based NWRT/PAR. Accomplishments by CIMMS staff in three main areas are described next: programmatic, application software, and facilities.

Programmatic Support. CIMMS staff supported programmatic ATD efforts by actively participating in several planning and design meetings, by providing input to scheduling and budget decisions, outlining and reviewing system requirements and system design documents, drafting and reviewing Interface Control Documents (ICD), and supporting programmatic milestones such as Preliminary and Critical Design Review meetings. In addition, the team continues to support regular conference calls for status updates and coordination of the entire ATD project.

Application Software. The Application Software portion of the ATD is being led by CIMMS staff and combines software developers and engineers from CIMMS and GDAIS. The required functionality of the Application Software includes generating weather- and aircraft-surveillance products, providing scan control and high-level radar control, system status monitoring, and archiving and display of data and products. The goal for the design of the Application Software is to maximally leverage existing NWRT/PAR and ACRA software to reduce the risk in meeting the FAA initial investment decision timeline. The figure below shows the functional architecture of the ATD Application Software and delineates responsibilities between the CIMMS/NSSL and GDAIS teams. During FY16, we developed concept-of-operations and design documentation to support the Preliminary Design Review (PDR), which occurred in August of 2015. In preparation for the next programmatic milestone, the Critical Design Review (CDR), we finalized ICDs, developed high-level mock-ups of Human-Machine Interface (HMI) screens derived from existing NWRT software, and prepared presentation materials covering functional requirements, functional architecture, schedule and risks, detailed design of weather scan generation, data ingest, signal processing, and radar management. The CDR was held in January of 2016. While the overriding design concept is to leverage as much existing software as possible and replace the NWRT real-time controller with an ACRA-based scheduler and radar management system, a concept of evolving the ATD processing system into an adaptive product database system that captures important changes that occur due to adaptive scanning was adopted. Additionally, ACRA aircraft tracking/processing software is being leveraged and enhanced by GDAIS for the purposes of supporting FAA multifunction demonstrations.

Software development work during the year started with reorganizing a 64-bit port of the NWRT software and merging the latest middleware changes from ORPG build 17 into our software baseline. A common repository with the reorganized software was established at GDAIS with remote access for CIMMS developers. A development system arrived at NSSL in March 2016, and the system was configured to get 128 weather DSP processes to execute on the few available computing nodes. Additionally, our scripts were modified to build and incorporate GDAIS's software into the software installation packages, and the install scripts were modified to install GDAIS's software and ours in a common environment on each computing node. The weather-scan-generation module that had been developed outside of the ACRA environment and was capable of generating weather dwell requests from hard-coded scan definition information, was then integrated into the ACRA scheduler and the ability to generate ACRA radar event messages (REM) from weather dwell requests was added and tested

by GDAIS in real time in the common software baseline. During this effort, a merged logging scheme was developed to allow the scheduler to transparently run in ACRA's or our environment with the appropriate logging mechanisms for each environment. Some low-level connectivity and messaging was established between the ACRA scheduler and our Java-based radar management server. Work on the weather digital signal processing (DSP) portion of the application software included implementation of dual-PRT processing, which required improvements to the data-ingest module. To obtain output results with realistic data, MATLAB I/Q data generated based on archived NEXRAD moment data was converted into an ATD-compatible format and fed into the real-time weather DSP data stream.



Functional block diagram of the ATD Application Software.

During FY16, CIMMS staff also continued to lead the design and development of the digital signal processing portion of the application software. This includes the weather signal processing that will be extended from the NWRT/PAR software and the air traffic control (ATC) software for detecting and tracking aircraft.

Facilities. The Facilities portion of the ATD continues to be led by CIMMS staff and combines engineers from CIMMS, NSSL, MIT/Lincoln Laboratory, and Regulus. During FY16, CIMMS staff members were involved in updating the Work Breakdown Structure

for the Facilities tasks to support the removal of the current NWRT SPY-1A antenna (that is scheduled for August 2016) and its replacement with the ATD. The team was involved in creating the Heavy Lift Plan for decommissioning the SPY-1A antenna and begun work on preparing the facilities infrastructure for the eventual installation of the ATD. In addition, we have been involved in the initial activities to move the 150-ft tower from the Radar Operations Center to Norman's fire station #7 for use as a calibration tower for the ATD. This has involved obtaining approvals from the FAA and working with the City of Norman on a suitable location for the tower.

b. MPAR Ten-Panel Dual-Polarization Demonstrator

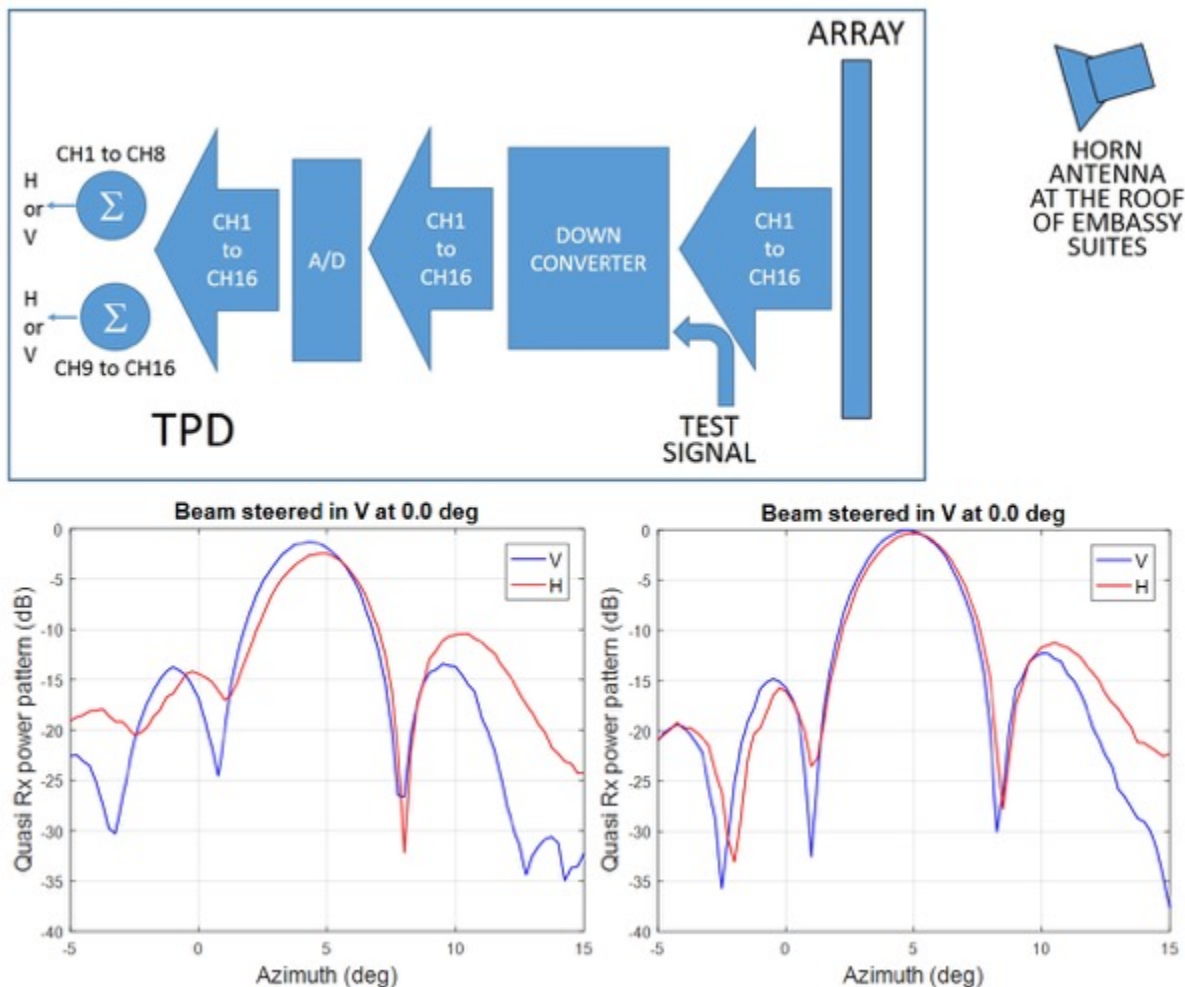
Igor Ivić and Daniel Wasielewski (CIMMS at NSSL), and Allen Zahrai (NSSL)

The NWRT/PAR has served as a valuable platform to demonstrate unique capabilities of phased array technology for weather observations. Additionally, advancements in the use of polarimetric radars for meteorological observations have become a staple of weather warning and forecasting. Thus, the future of weather radar lies in the combination of these two technologies. Current exploratory efforts have produced solutions that primarily focus on two designs: a conformal cylindrical phased array and a four-sided planar phased array. Prior to the commitment to one of these designs, significant analysis must be completed for each geometry. The goal of this project is to evaluate the performance of polarimetric planar phased array technology with respect to the national weather mission. For this purpose, NSSL and the FAA commissioned the construction of a 10-panel, mobile, polarimetric, phased-array system (referred to as the Ten Panel Demonstrator or TPD) by MIT/Lincoln Laboratory to be used as an evaluation platform to assess the polarimetric performance of the planar phased array technology. A test plan was developed that exercises the capabilities of the demonstration system, which focuses on absolute and relative accuracy measurements. Absolute measurements resolve the system's capability to accurately identify hydrometeors, while relative measurements examine the correct calibration of the system as well as off-broadside cross-polarization impacts. Comparisons with legacy systems (e.g., the polarimetric KOUN radar) are also important in developing a good understanding of the system capabilities and are built into the test plan. An analysis of the performance will play an ongoing important role in defining the expected performance of future systems, including the replacement of the SPY-1A antenna on the NWRT PAR (see previous project).

The construction of the dual-polarization demonstrator was completed by MIT/Lincoln Laboratory and delivered to NSSL in late FY15. During FY16, the development of the infrastructure for data ingestion, data processing, and display software in MATLAB was continued. Early data collections revealed many system-level issues that impeded the dual-polarization characterization work for which the TPD was intended. Poorly-shielded cables in the receiver chain were found to be a source of excess noise and were replaced, fragile printed circuit board (PCB) directional couplers (used only in near-field chamber testing) were removed, and amplifiers were added to each receiver chain to decrease the noise figure. The major challenge, however, was that channel-to-channel

phase differences among the receivers were found to be a function of temperature. To address this critical issue, we installed additional hardware and devised a scheme to measure and compensate for these phase fluctuations during operations. Several difficulties still remain at the system level, such as the matching between horizontal and vertical beam shapes and maintaining phase alignment among subarray data.

Having addressed the most pressing reliability issues, we made several attempts in May 2016 to collect data on stratiform precipitation for the purpose of assessing the dual-polarization system behavior. Unfortunately, we did not get the type of weather required for this work. Still, we have used the TPD to prototype calibration measurements that are planned for the ATD, including characterizing the receive paths using an external far-field continuous-wave (CW) transmitter, two-way (i.e., transmit and receive) path measurements using a delay line, and a scheme to map amplitude and phase of all individual elements. This work is ongoing.



An experimental setup used to collect test data (top panel). An improvement in the horizontal and vertical beam shapes resulting from an application of dynamic subarray phase matching (accounts for the phase drift in the downconverter hardware) is shown in the rightmost panel compared to the static phase matching in the leftmost panel.

c. MPAR Program Support

Sebastian Torres, Christopher Curtis, Igor Ivić, Danny Wasielewski, and Doug Forsyth (CIMMS at NSSL)

CIMMS continues to support the MPAR program and the MPAR program manager on several technical and programmatic fronts. Support consists of actively participating in the MPAR Government Engineering Team (GET), giving presentations at meetings with industry and other government organizations, reviewing proposal and technical documents, participating in internal and external technical discussions, and assisting the program manager with various programmatic issues.

d. PAR Dual Polarization

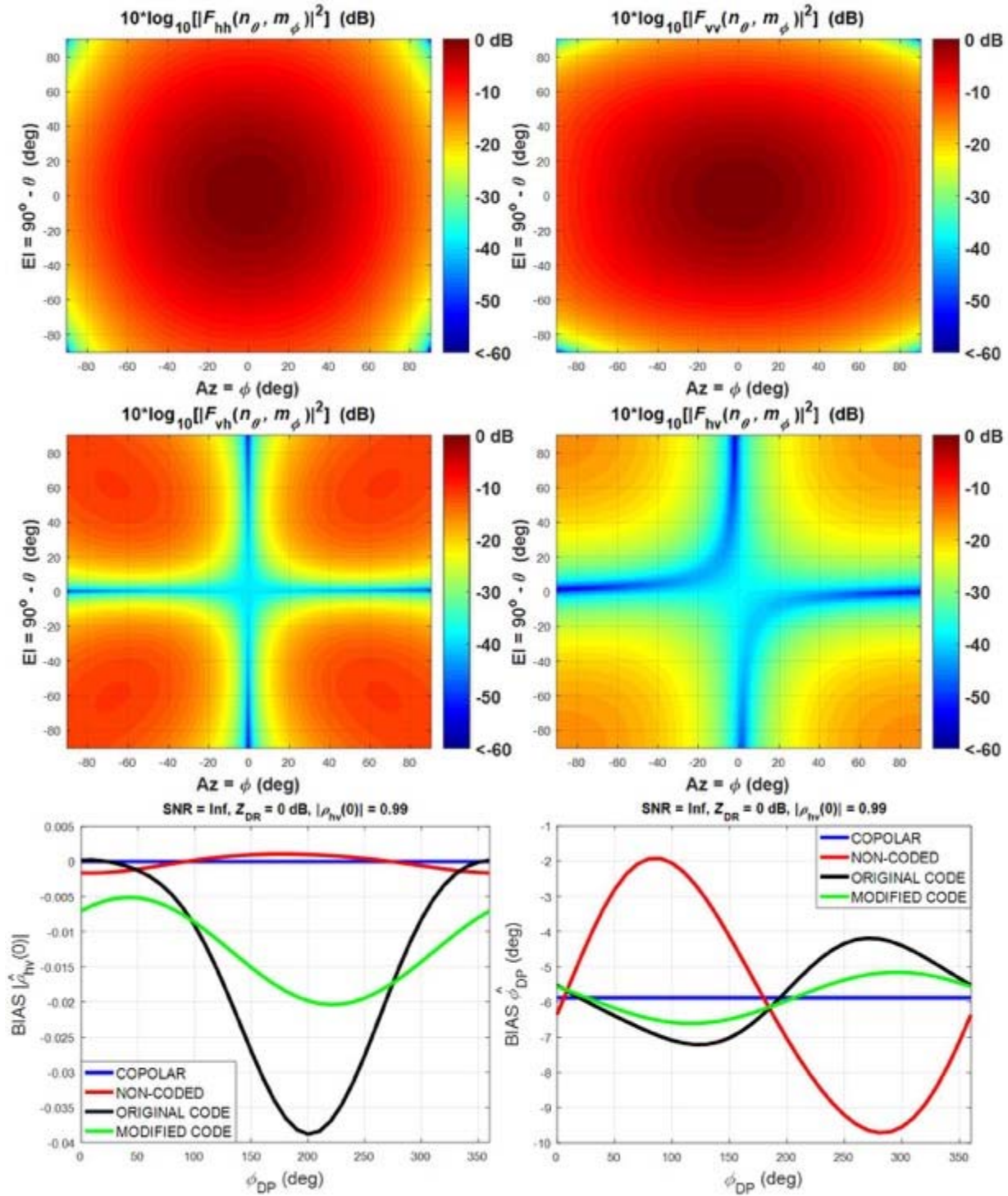
Igor Ivić and Djordje Mirković (CIMMS at NSSL), and Dušan Zrnić (NSSL)

NSSL and CIMMS scientists and engineers are investigating the replacement for the aging WSR-88D as part of a national interdepartmental collaboration to combine weather and air surveillance missions on a single platform. Promising is the Multifunction Phased Array Radar (MPAR), which incorporates high temporal and spatial resolution needed for improved weather sensing. The MPAR design will surely include a dual-polarization capability, as does the current WSR-88D system, allowing for improved rainfall estimation, hydrometeor classification, improved data quality, and enhanced weather hazard detection. One of the main challenges to the use of PAR technology for weather observations is the implementation of dual polarization with acceptable isolation between horizontal and vertical channels, which is essential for accurate interpretation of polarimetric variables.

Simulations and measurements on phased array antennas have shown that such isolation cannot be achieved only by the antenna hardware. Hence, additional modifications to the radar system are required to attain supplementary isolation of orthogonal channels. To achieve this, the following two options are being evaluated: (1) pulse-to-pulse (or interpulse) phase coding of the transmitted pulses in the horizontal and vertical channels, and (2) time-multiplexing (or quasi-simultaneous horizontal and vertical) in which the vertical transmitter port is immediately energized after energizing the horizontal port or vice versa. Both schemes were investigated using analytical derivations and simulated and real time-series data. Pulse-to-pulse phase coding was shown to provide additional isolation with a small increase in the standard deviation of estimates (compared to the perfect isolation between orthogonal channels). The time-multiplexing scheme was found to perform comparably to phase coding if the spatial gradients of reflectivity are small, but its performance degrades as gradients increase. It was observed that the time-multiplexing approach also introduces a significant increase in the standard deviation of estimates. During FY16, the pulse-to-pulse phase coding scheme was further investigated. We found that this approach mitigates the differential reflectivity bias but may increase the bias of copolar correlation coefficient estimates and, in some cases, the bias of the differential phase estimates. To mitigate this, a

modified phase code was proposed that maintains the differential reflectivity bias suppression but reduces the copolar correlation coefficient and differential phase bias with respect to the originally proposed phase code.

To facilitate the PAR dual-polarization evaluations, simulations using computational electromagnetics (CEM) tools were pursued. As part of this effort, a preliminary model of the ATD radiating element was developed. To evaluate the co- and cross-polar behavior of an array of radiation elements, this model was incorporated into a 5x5 element planar antenna array model. This work is ongoing.



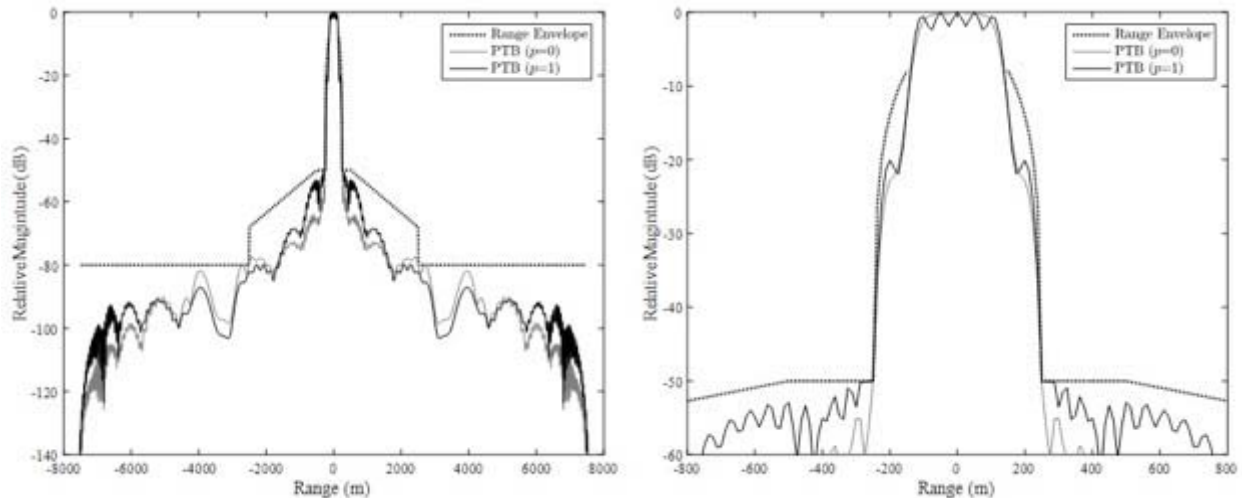
Copolar horizontal (top left panel) and vertical (top right panel) single-element radiation patterns and cross-polar horizontal (middle left panel) and vertical (middle right panel) single-element radiation patterns. Radiation patterns were simulated using the WiresPLate-Dielectrics (WIPL-D) software package, a commercial solver for electromagnetic structures. Copolar correlation coefficient (bottom left panel) and differential phase bias (bottom right panel).

e. PAR Pulse Compression

Sebastian Torres, Christopher Curtis, and David Schwartzman (CIMMS at NSSL)

Weather radars based on low-power solid-state transmitters typically use pulse compression as a means to achieve the required sensitivity to detect weaker returns. Pulse compression works by lengthening the transmitted pulse and modulating the transmitted waveform. A longer pulse leads to increased sensitivity due to the higher average power being transmitted, and frequency or phase modulation can be used to recover the original range resolution after processing. As such, pulse compression waveforms require a larger transmission bandwidth and result in an extended blind range (or dead time) close to the radar, which is typically mitigated by the addition of a fill-in pulse. Although the resulting range weighting function has a main lobe with the desired width, it typically contains sidelobes that extend a few kilometers in range. Range sidelobes can impact the range resolution of the radar and can be reduced by employing non-linear frequency-modulation (NLFM) transmission schemes at the price of an increased transmission bandwidth. Range oversampling processing has been used on radars with conventional high-power transmitters to reduce observation times without increasing the variance of estimates. It consists of sampling the received signals at a rate faster than the inverse of the transmitted pulse width thus producing complex voltages with a range correlation that depends on the modified pulse (i.e., the convolution of the transmitted pulse envelope and the receiver filter impulse response, which would include the effects of pulse compression). This a-priori information about the range correlation is used to devise transformations to decorrelate sets of range-oversampled signals from which auto- and cross-covariances are estimated. In turn, these are averaged to match conventional range sampling and are ultimately used to obtain more precise estimates of all radar variables.

During FY16, we developed a requirement-driven design approach for pulse-compression waveforms. Specifically, we addressed the mapping of high-level system requirements to constraints on the range weighting function, which includes the effects of pulse compression and range oversampling processing. The goal is to design minimum-bandwidth pulse-compression waveforms that are compatible with range oversampling processing and meet high-level system requirements. For this purpose, we developed a pulse-compression waveform optimization framework that incorporates the relevant metrics to explicitly define the optimization problem. In other words, the optimization problem assimilates the range-weighting-function constraints into a penalty function and accounts for the impacts of range-time signal processing. This work is applicable to the design of any weather radar system that uses pulse compression for enhanced sensitivity and needs range oversampling processing for faster updates such as the upcoming MPAR ATD.



Range weighting functions corresponding to a minimum-bandwidth (4.32 MHz) pulse-compression waveform obtained with our optimization framework (left panel). The optimum pulse-compression waveform is shown to satisfy a range-envelope requirement (dotted line) derived from high-level system requirements and is compatible with two cases of range oversampling processing: matched filtering ($p = 0$) and whitening ($p = 1$). Zoomed-in version of the left panel that highlights the performance of the optimum pulse-compression waveform close to the mainlobe (right panel).

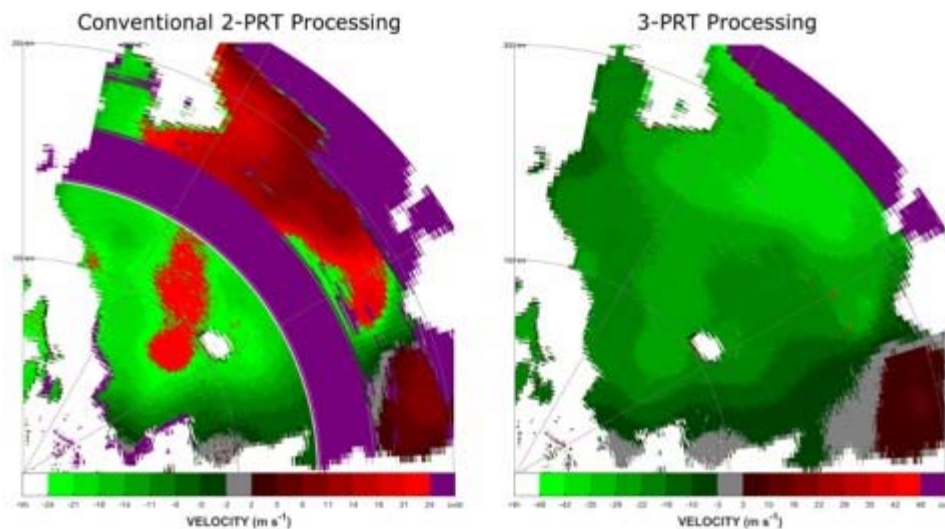
f. PAR Signal Processing: Addressing Issues with Pulse Compression on the ATD Using Triple-PRT Processing

Christopher Curtis (CIMMS at NSSL)

The ATD utilizes a modern active array antenna, which has many significant differences from a conventional dish antenna. Instead of using a single high-power transmitter, the ATD antenna has a separate solid-state transmitter for each radiating element. Even though the ATD antenna has over 4000 elements, each of the individual transmitters is relatively low power so that the total power transmitted from the array is less than a similar radar like the WSR-88D. In order to have sensitivity similar to the WSR-88D, the ATD will need to use a longer transmitted pulse. Thus, it will utilize pulse compression in order to have comparable range resolution. Pulse compression is a technique that uses a coded pulse with additional transmission bandwidth to provide the sensitivity and range resolution needed for a weather surveillance radar. Pulse compression allows radars with lower total power to have more sensitivity, but it also has some drawbacks. Because the pulse is longer, there is a larger blind range (i.e., more dead time) when the radar cannot receive backscattered signals. There is also dead time at the end of the reception period because of pulse compression processing. The standard way to deal with the dead time at the beginning of the reception period is to send another short pulse after the long pulse-compressed pulse (at a different frequency) to fill in the data that is missing. Unfortunately, this low-power fill pulse is unable to fill in the dead time at the end of the reception period because of significantly reduced sensitivity. These dead periods result in large gaps in the data that can cause problems with conventional processing.

The original plan for the ATD was to use conventional dual-PRT processing that uses data collected with a long pulse repetition time (PRT) for range coverage and data collected with shorter PRT for a larger unambiguous velocity. The long PRT data is then used to unfold the shorter PRT data, which puts the short PRT data at the proper range location. This works relatively well, but it does result in areas where the data cannot be unfolded properly. These areas of overlaid echoes show up as purple haze because there are radar returns from two or more range locations in the same range bin. When using pulse compression, the dead periods are also indicated using purple because there are no data collected at those range locations. This dead period is shown in the left panel of the figure below for conventional dual-PRT processing. The large purple band in the middle of the panel corresponds to data that is lost because of the dead time. The purple on the right side of the panel is from overlaid echoes. Because of the significant loss of data, a new type of processing strategy is needed for the ATD.

A triple-PRT strategy was developed in FY16 to address these large gaps in the data. An additional short-PRT dwell is utilized to fill in the data at range locations where the dual-PRT processing produces purple rings. This does lead to longer scan times, but it is worth it to avoid the data gaps. The result of the triple-PRT processing on the same data case is shown in the right panel of the figure below. The time-series data were simulated using the simulator described in a separate sub-project below. The large purple ring disappears, and the overlaid area is also smaller. Notice that the unambiguous velocity for triple-PRT processing is twice as large as that for dual-PRT processing, which leads to velocities with much less aliasing (this is indicated by red velocity values in the middle of the green values in the left panel). The triple-PRT processing will allow the ATD to produce data with much better quality. The long-term plan is to implement staggered-PRT strategies on the ATD to avoid the data gaps and reduce the scan times.



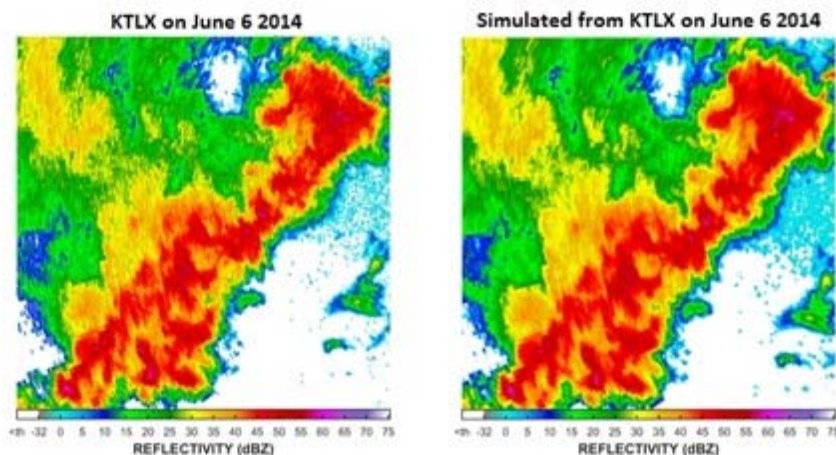
Plan-position indicator (PPI) plots of conventional dual-PRT processing (left panel) and triple-PRT processing (right panel) for the same simulated data case.

g. PAR Signal Processing: Dual-Polarization Time Series Simulator Using Archived NCDC Data

David Schwartzman, Christopher Curtis, and Sebastian Torres (CIMMS at NSSL)

The Advanced Technology Demonstrator (ATD) will replace the phased array antenna at the NWRT with a dual-polarization, active phased array antenna. The ATD is an ideal radar to demonstrate multi-function (simultaneous weather surveillance and aircraft tracking) and other unique capabilities of a phased array antenna. For example, exploiting the beam agility capability of phased arrays, we could reduce the update times from 5 minutes to 1 minute. However, the flexibility obtained with phased arrays makes them very complex systems. The goal of this research is to develop a two-dimensional, dual-polarization weather signal simulator to assess the performance of different radar scanning strategies, waveforms, and signal processing techniques. This will be directly applicable to the ATD but also to other types of radars.

The NCDC provides archived Level-II dual-polarization radar data from all of the WSR-88D radars in the NEXRAD network. Our weather signal simulator is able to ingest this dual-polarization data and simulate dual-polarization Level-I (time-series) data for the desired scanning parameters (e.g., pulse-repetition times, spatial resolution, waveform type). By processing the Level-I data provided by the simulator, we are able to qualitatively analyze the performance of different radar scanning strategies, waveforms, and signal processing techniques from any archived weather scenario. During FY16, we used the simulator to compare the performance of pulse-compressed, range-oversampled, bandwidth-optimum waveforms to the legacy WSR-88D conventional waveform. The combination of pulse compression and range oversampling is critical to achieve the ATD's goals of providing fast updates with good data quality.

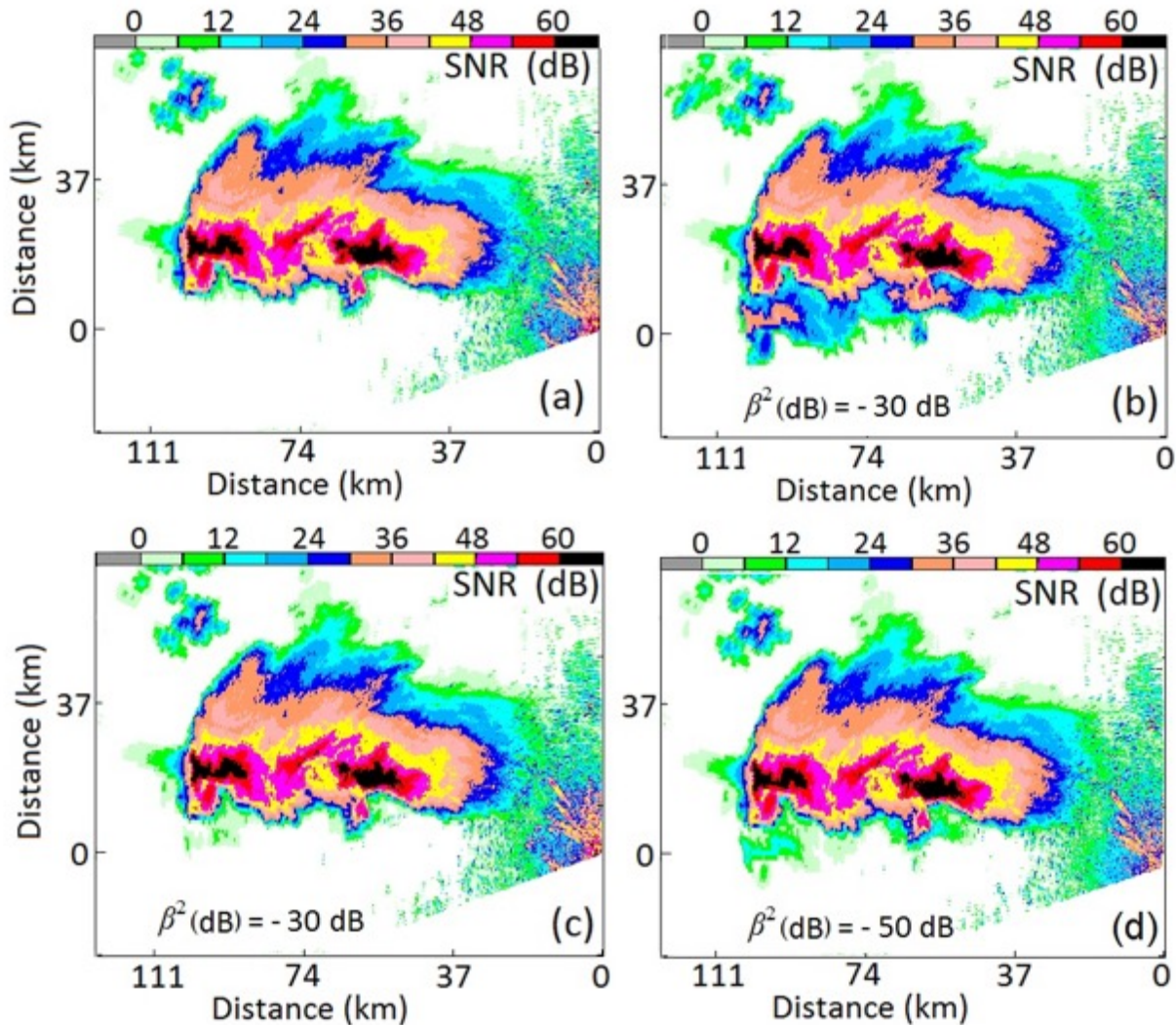


Original archived (left) and simulated (right) reflectivity fields corresponding to convective storm data collected with the KTLX on 06 June 2016 at ~11:10 UTC at an elevation of 0.5°. The simulated data was produced with a bandwidth-optimum, pulse compression waveform ($BW = 4.33$ MHz, $\tau = 50$ μ s) and processed using adaptive pseudowhitening range oversampling. Note that the adaptive pseudowhitening data looks smoother and has better data quality compared to the archived data.

h. PAR Scan Strategies: Faster Updates using a Two-Beam Scan Strategy

Valery Melnikov (CIMMS at NSSL), and Richard Doviak and Dusan Zrnić (NSSL)

Tornadoes and hail thunderstorms develop so quickly that their effective observation using radar requires the update time to be less than about a minute. Phased array technology allows transmitting two radar pulses into two different directions almost simultaneously. The technology also allows receiving signals from the same directions simultaneously. These capabilities can be used to scan two directions (or rays) simultaneously, which shortens the update time by a factor of two. The main challenge of this method is interference of signals received from the radiation pattern main lobe and its sidelobes when directed into two directions. This effect is the strongest in cases of high reflectivity gradients, which are frequently observed in radar echoes from severe weather. An approach to separate wanted contributions from two main lobes pointed into two directions and unwanted sidelobes contributions was developed. Some results are shown in the figure below where panel (a) shows a Signal-to-Noise-Ratio (SNR) field from a tornadic thunderstorm obtained with radar having a classical dish antenna with known sidelobe levels. This SNR field (a proxy for radar reflectivity) serves as a benchmark for the simulated PAR operations. Panel (b) shows a SNR field obtained with simulations of the two-beam scan strategy without resolving the main-lobe/sidelobe coupling. One can see ghost echoes to the south from two strong reflectivity cores (black color areas). Panel (c) shows a result of a partial separation of the main-lobe/sidelobe coupling. One can see some leftovers in the areas of ghost echoes. The full separation procedure makes the resulting field equal to the one shown in panel (a) with inaccuracies less than 1 dB. Parameter β^2 in the figure is the level of antenna sidelobes from the beam in the first direction in the direction of the second transmitted beam. This study shows a way to shorten the radar update time using PAR, which is needed to observe fast developing weather phenomena such as tornados and hail thunderstorms.



(a) “True” SNR (dB) field collected at an elevation angle of 1° with a WSR-88D KOUN on 31 March 2008 at 0334Z. (b) SNR field of the simulated dual-beam scan strategy and assuming $\beta^2 = -30$ dB where the contamination by mainlobe-sidelobe coupled power is evident. (c) Retrieved SNR field using the proposed two-term correction procedure for $\beta^2 = -30$ dB. (d) Same as in (b) but for $\beta^2 = -50$ dB.

Publications

- Ivić, I., and R. Doviak, 2016: Evaluation of phase coding to mitigate differential reflectivity bias in polarimetric PAR, *IEEE Transactions on Geoscience and Remote Sensing*, **54**, 431-451.
- Kuster, C. M., P. L. Heinselman, and M. Austin, 2015: 31 May 2013 El Reno tornadoes: Advantages of rapid-scan phased-array radar data from a warning forecaster’s perspective. *Weather and Forecasting*, **30**, 933-956.
- Melnikov, V., R. Doviak, and D. Znić, 2015: A method to increase the scanning rate of phased-array weather radar. *IEEE Transactions on Geoscience and Remote Sensing*, **53**, 5634-5643.
- Torres, S., R. Adams, C. Curtis, E. Forren, D. Forsyth, I. Ivić, D. Priegnitz, J. Thompson, and D. Warde, 2016: Adaptive-weather-surveillance and multifunction capabilities of the National Weather Radar Testbed Phased-Array Radar. *IEEE Proceedings*, **104**, 660-672.

NSSL Project 2 – Hydrometeorology Research

NOAA Technical Leads: Kenneth Howard and Jian Zhang (NSSL)

NOAA Strategic Goal 2 – *Weather-Ready Nation – Society is Prepared for and Responds to Weather-Related Events*

Funding Type: CIMMS Task II

Objectives

Hydrometeorology research objectives centered on dual polarized radar and quantitative precipitation estimations (QPEs). Specifically:

- The operational implementation of the MRMS system version 10.5The delivery of the MRMS system version 11.0 to NCEP
- The Virtual Multi-Radar Multi-Sensor (VMRMS) system
- Compiling technical information on individual radars that are participating in the Caribbean basin raw data assimilation project
- Enhancing the accuracy of radar snowfall estimation with new Z-S relationships
- Continued quality control advancements of hourly rain gauge observations
- Combining ground and radar-based precipitation estimates with rainfall climatologies to generate a merged quantitative precipitation estimation (QPE) product
- Integrating an evaporation correction scheme to real-time instantaneous radar rainfall rates
- Multi-sensor estimation of intense rainfall in complex terrain using GOES-R combined with ground and space-based radars
- Development and verification of new algorithm below the melting layer to estimate rainfall
- Evaluating MRMS QPE versus single-source radar QPE products
- The MRMS Experimental Testbed for Operational Products (METOP)
- The meteorological Phenomena Identification near the Ground (mPING) project
- mPING random forest research to develop an improved winter precipitation type algorithm
- Development of web-based tools and displays for real-time QPE and hydrologic analysis

Accomplishments

1. Operational Implementation of the Multi-Radar Multi-Sensor System v10.5

Carrie Langston, Karen Cooper, Darrel Kingfield, Heather Grams, Lin Tang, Jeff Brogden, and Ami Arthur (CIMMS at NSSL)

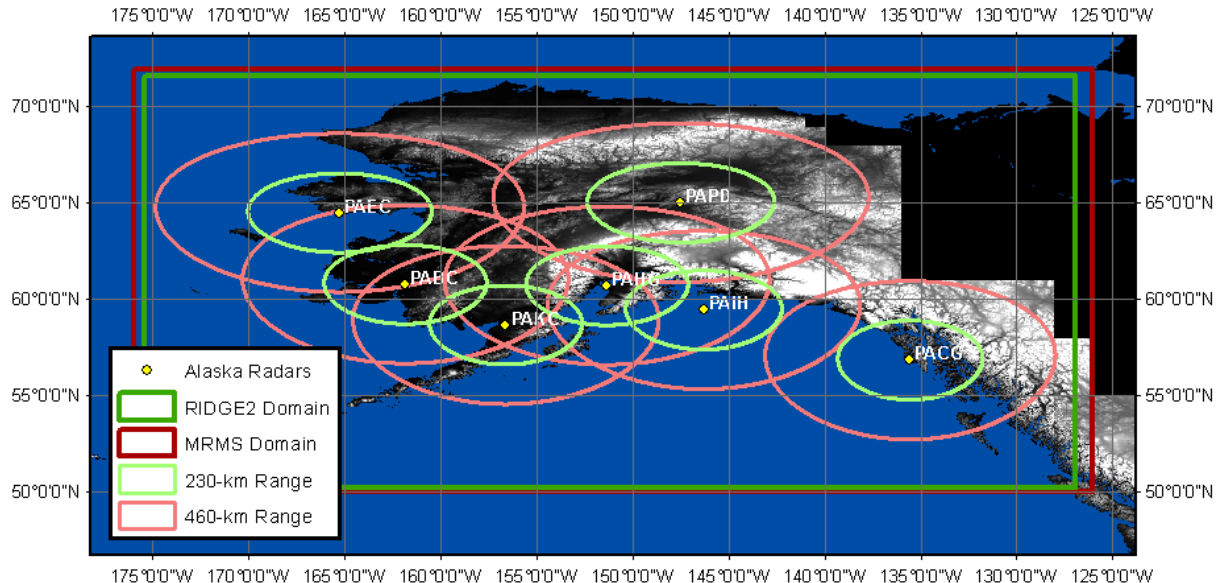
On December 15, 2015, the Multi-Radar Multi-Sensor (MRMS) system was upgraded from v10.0.1 to v10.5 at the National Centers for Environmental Prediction (NCEP)

Central Operations (NCO) as part of the Integrated Dissemination Program (IDP). While minor revisions were made to existing MRMS algorithms, the main purpose of the v10.5 update was generating images (geotiff) required by the Radar Integrated Display with Geospatial Elements version 2 (RIDGEII) program, which is currently managed by Southern Region Headquarters. The number of MRMS domains increased from one CONUS domain to include oCONUS domains (Alaska, Hawaii, Guam, Caribbean).

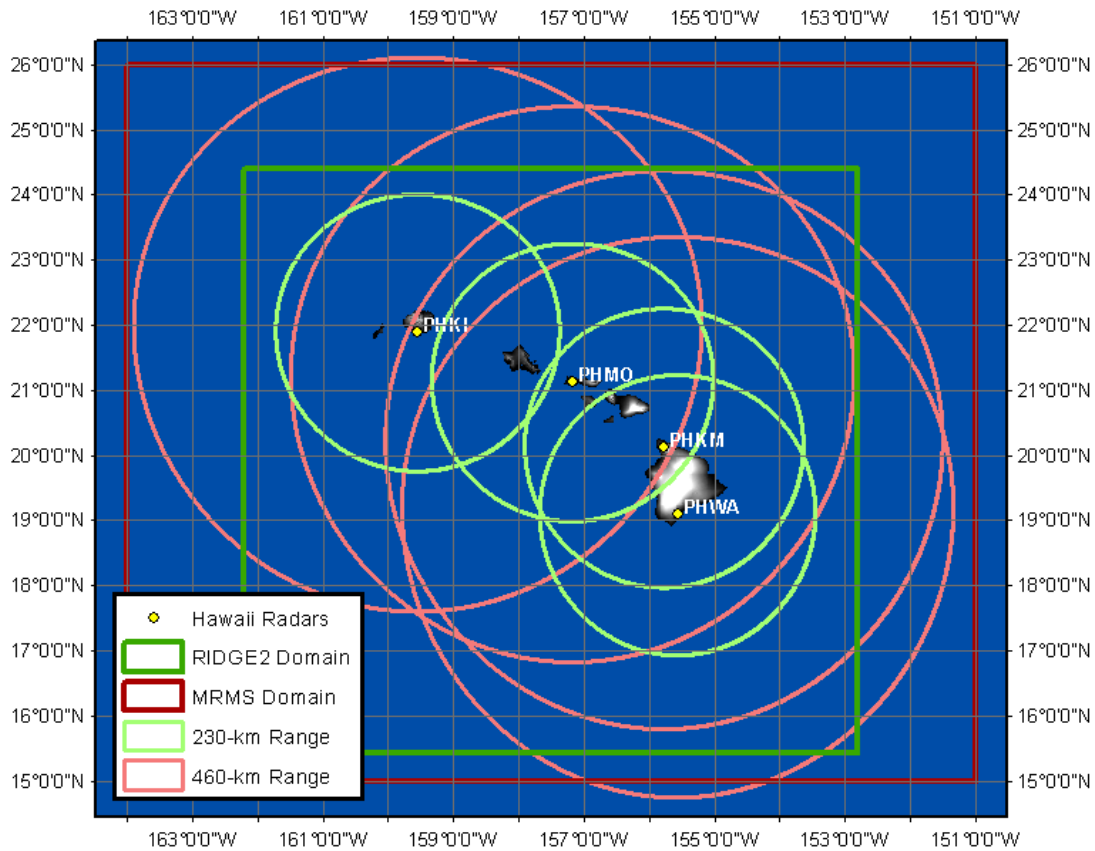
The CONUS domain continued to produce the full suite of MRMS products while the other oCONUS domains generated a reduced set of gridded products, which are as follows:

- Raw Base Reflectivity
- QC's Base Reflectivity
- Raw Composite Reflectivity
- QC'd Composite Reflectivity
- Echotop 18dBZ
- Base Hydrometeor Classification

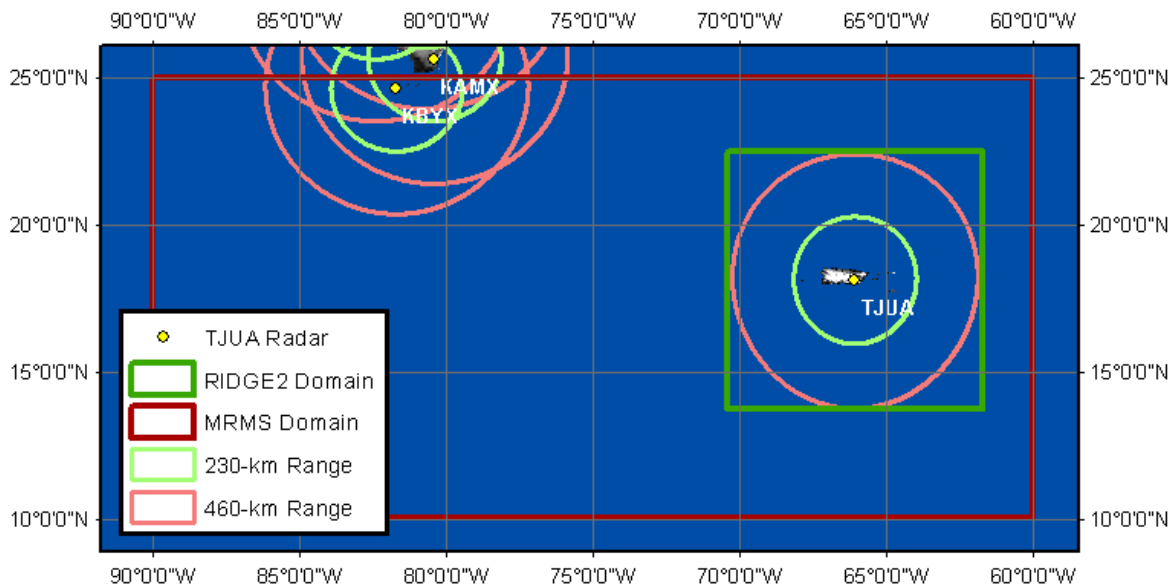
Of these products, Raw Base Reflectivity and Base Hydrometeor Classification are new to MRMS. The former was added to both the oCONUS and CONUS domains. The latter was added to oCONUS only. For CONUS, the MRMS PrecipFlag field proved sufficient and Base Hydrometeor Classification was not needed.



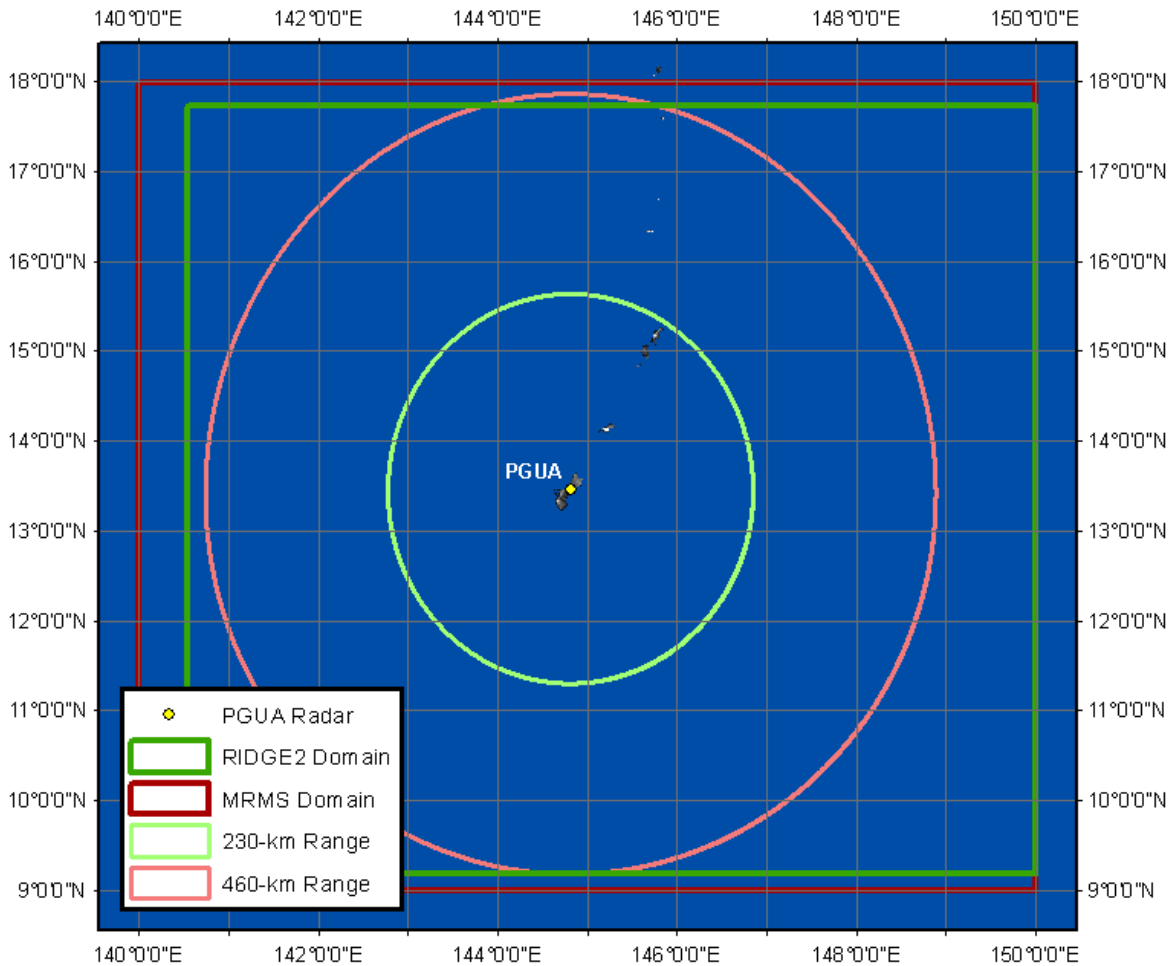
MRMS oCONUS domain for Alaska with radar coverage at ranges of 230 and 460 km



MRMS oCONUS domain for Hawaii with radar coverage at ranges of 230 and 460 km



MRMS oCONUS domain for the Caribbean with NWS radar coverage at ranges of 230 and 460 km



MRMS oCONUS domain for Guam with radar coverage at ranges of 230 and 460 km

In addition to gridded products for the CONUS and new oCONUS domains, RIDGEII also required a large number of single radar products in geotiff. All are listed below by radar/data type.

Radar/Data type	Products
TDWR (level III)	<ul style="list-style-type: none"> • SPG Long Range Base Reflectivity (TZL) • SPG Base Radial Velocity (TV0) • SPG One Hour Precipitation (N1P) • SPG Storm Total Precipitation (NTP) • SPG Vertical Integrated Liquid (NVL) • SPG Echo Tops (NET) • SPG Composite Reflectivity (NCR)
WSR-88D (level III)	<ul style="list-style-type: none"> • ORPG Base Reflectivity (N0Q) • ORPG Base Radial Velocity (NOU) • ORPG Storm Relative Mean Velocity (N0S) • ORPG One Hour Precipitation (N1P)

	<ul style="list-style-type: none"> • ORPG Storm Total Precipitation (NTP) • ORPG Hi-Res Vertical Integrated Liquid (DVL) • ORPG Enhanced Echo Tops (EET) • ORPG Composite Reflectivity (NCR) • ORPG Hydro Meteor Classification (N0H) [Dual-Pol] • ORPG Differential Reflectivity (N0X) [Dual-Pol] • ORPG Storm Total Precipitation (PTA) [Dual-Pol]
WSR-88D (level II)	<ul style="list-style-type: none"> • MRMS Raw Base Reflectivity (Super-Res) • MRMS Raw Base Radial Velocity (Super-Res)

The other updates to MRMS were minor improvements and are listed below:

- More correct inclusion of KLGX in 2D mosaics and QPE products
- Reduced internal system latency to more quickly produce some GRIB2 formatted product files
- Radar reflectivity quality control improvements
- Increased the number of HADS gauge observations to include those from Western Region burn areas.

The implementation of v10.5 required several new virtual machines (VMs). Working with NCO, ten VMs were created, configured and test. Three of the VMs generate the oCONUS data. The remainder VMs were used to convert Level III data to geotiffs for RIDGEII.

To assist NCO with testing and implementing MRMS v10.5, all standard MRMS documents were updated.

- *Software Design* -- Detailed definition of the MRMS data flow and processing modules
- *Build Instructions* -- Steps for compiling the various software components of MRMS
- *Implementation Instructions* -- Steps for installing and configuring MRMS on a server or virtual machine
- *Execution Instructions* -- Steps for starting, stopping and generally managing MRMS processes on a server or virtual machine.
- *Testing and Troubleshooting* -- Instructions for testing all the individual components of MRMS along with suggestions for troubleshooting common problems.
- *NCO server spreadsheet* -- A spreadsheet with three worksheets detailing on a virtual machine (VM) by VM basis the assigned processing, computing resources, lists of input and output data, and system configuration files.

In addition, two MRMS v10.5 specific documents were provided. The first outlined step by step instructions/recommendations for installing MRMS v10.5. The second provided NCO a test plan to help validate the update. In total, the MRMS on-boarding documentation consists of approximately 215 pages and three companion worksheets. A copy of the documentation can be made available if requested.

The MRMS v10.5 work is complete.

Publications

Zhang, J., K. Howard, C. Langston, B. Kaney, Y. Qi, L. Tang, H. Grams, Y. Wang, S. Cocks, S. Martinaitis, A. Arthur, K. Cooper, J. Brogden, and D. Kitzmiller, 2016: Multi-Radar Multi-Sensor (MRMS) quantitative precipitation estimation: Initial operating capabilities. *Bulletin of the American Meteorological Society*, **97**, 621-637.

2. Multi-Radar Multi-Sensor v11 Delivered to NCEP

Carrie Langston, Karen Cooper, Brian Kaney, Darrel Kingfield, Heather Grams, Lin Tang, Youcun Qi, Ami Arthur, Zac Flamig, and Jeff Brogden (CIMMS at NSSL)

In June 2016, the initial code drop for MRMS v11 was provided to NCO. Below is the list of changes. The new VMRMS system (see accomplishment #3) was heavily used in the development of the v11.

- **Infrastructure/System Changes**
 - Reduced overall system I/O by changing the data storage model from distributed to centralized.
 - Improved the MRMS system update process by centralizing software builds, scripts and configuration files.
- **Severe Weather Updates**
 - Lightning
 - Increased lightning product stability by switching input from a "data of opportunity" feed to an NCO operational feed.
 - The lightning density products were revised to not divide the number of flashes by the time interval over which the product is generated. NWS forecasters expressed concerns over the readability and interpretation of this product in the past and this is the first step in addressing their concerns. Furthermore, the lightning density algorithms now have a |5| kA threshold where CG strikes that are lower than this value are not counted as CGs.
 - AzShear and RotationTracks
 - The azimuthal shear products were improved in two main areas. First, the equation used to calculate azimuthal shear was updated to more accurately account for the weighting of individual velocity gates. This update addressed the issue associated with near radar performance of azimuthal shear, removing a once-

present region of false high azimuthal shear values that immediately surrounded the radar. The second improvement involved establishing an accurate method for calculating the vertical maximum value of azimuthal shear through a given layer of super resolution data. This allows a more complete use of all of the radials within an individual tilt. These two updates provide a more skillful rotation track product for use by operational forecasters and national centers.

- New Products
 - Added VII to NIDS data generated for the SPC
 - Added two new 5x5 km reflectivity products. The 1-km composite reflectivity and reflectivity at lowest altitude fields are resampled to 5-km and are provided to the SBN for dissemination. Their WMO codes are YAUC09 and YAUS01, respectively.
- **Hydromet Updates**
 - Model Usage
 - A higher resolution model (3 km HRRR) replaced the 13km RAP to provide atmospheric environmental data used in MRMS hydromet and severe algorithms. The RAP model is only used in areas with no HRRR coverage.
 - Radar Quality Control
 - Canada: A major improvement in the Canadian radar quality control to mitigate ground clutter contamination especially during anomalous propagation
 - WSR-88D: Several refinements were implemented to the dual-pol radar quality control to handle new scan modes (e.g., SAILS) of WSR-88Ds and to further improve the identification of melting layer in addition to wind farms.
 - Gauge Ingest and Quality Control
 - Gauge ingest process was refined to receive new gauge data more timely. Gauge QC process was modified to account for areas with no radar coverage and to improve gauge data quality associated winter precipitation.
 - Quantitative Precipitation Estimates (QPEs)
 - MRMS radar QPE was refined to minimize data voids near the radar sites and wind farms due to the clutter suppression. A climatology based tropical rain rate scheme was implemented to reduce a warm season wet bias in the MRMS radar QPE in the northern and central plains of US.
 - The local gauge correction (LGC) of radar QPE has been enhanced to account for potential sampling discrepancies between radar and gauge. A new product, Gauge Influence Index (GII), was implemented that depicts the gauge influence in the LGC product. The algorithm was further optimized to increase the computational and I/O efficiency.

- A radar based precipitation mask was removed from the Mountain Mapper to allow more gauge influence in areas with poor radar coverage.
 - New Products
 - Added a new product called Gauge Influence Index (GII) that depicts the influence of gauges in the gauge biased QPE fields. The GII is generated for each QPE accumulation period (1, 3, 6, 12, 24, 48, and 72H).
 - Increased the frequency of all 48 and 72H QPEs from daily at 12Z to hourly. Note that only the 12Z products will be sent via the SBN.
- **RIDGEII Updates**
 - Increased geoTIFF resolution for single radar products so they can be interrogated at their full native resolution.
- **New Algorithms**
 - AutoNowCaster (ANC)
 - ANC is an algorithm refined by MDL. It uses satellite, sounding, model and MRMS data to generate a Convective Likelihood and a Final Forecast (60-min forecast of reflectivity) product. Further ANC documentation can be found in VLab.
 - Flooded Location and Simulated Hydrographs (FLASH)
 - FLASH is an algorithm developed by NSSL and CIMMS. It uses Flash Flood Guidance, MRMS Radar-only precipitation rate and model data to generate several products such as Unit Streamflow, Streamflow, Soil Saturation, Precip Average Recurrence Interval, and QPE-to-FFG Ratio products. More information about FLASH and FLASH products can be found at <http://flash.ou.edu/>.

Providing an initial version to NCO is an accomplishment in of itself, but more work remains before v11 is operationally implemented in Fall 2016. Fiscal year 2017 will include an onsite visit to NCO, updates to the official documentation, and closely working with NCO onboarding staff to educate them about MRMS and help troubleshoot. The MRMS v11 work is ongoing.

3. Virtual Multi-Radar Multi-Sensor (VMRMS)

Karen Cooper, Carrie Langston, and Lin Tang (CIMMS at NSSL), and NSSL Information Technology Services (AceInfo Solutions) Staff

A key NSSL strategy to maintain the stability of MRMS for research and operational environments is to host development efforts on a computing infrastructure similar to what is used at NCO. To fill this need, a new development and testing system (called VMRMS) has been purchased, configured, tested and is now running in real time. The algorithms and configurations for the soon-to-be operational MRMS v11 were verified on VMRMS before they were given to NCO.

VMRMS at NSSL consists of:

- 3 Dell Chassis, with 24 Dell Blade Servers
- 246 Processors
- 9,216 GB of memory
- NetApp, Network Attached Storage, with over 40 TB of drive space with 10GB connectivity
- 75 VmWare Virtual machines

VMRMS went live on 1 May 2016. It provides a large CoNUS domain which includes the Southern section of Canada, as well as domains that include Alaska, Hawaii, Guam and Puerto Rico. This project is ongoing.

4. Caribbean Radar Data Assimilation Project

José Meitín, Karen Cooper, and Heather Reeves (CIMMS at NSSL)

NSSL is tasked with compiling the technical information on individual radars that are participating in the Caribbean basin raw data assimilation project. The earlier phase of the project involved high priority radar sites as determined by the National Hurricane Center. The following bullets describe the status of acquiring data from the various meteorological services across the Caribbean.

- Cayman Islands National Weather Service: We received approval to participate in the project from Cayman Islands government. The necessary equipment was shipped and installed at the Cayman Island radar site and the real time feed underwent a testing phase with preliminary products distributed to NCEP.
- Cuba Instituto de Meteorología (INSMET): At the request of the U.S. Department of State and NOAA headquarters, communications with the Cuban Meteorological Institute (INSMET) were suspended for over eight months until both governments recognize formal agreements. Once INSMET agreed to participate in the Caribbean mosaic project, we began testing the data transmission from two Cuban radar sites which provide coverage over most of the island.
- Jamaica Meteorological Service: Weather radar data products require a proprietary software license (Enterprise Corp) to reformat their base data files. Several weeks were spent negotiating access for a local site license. This effort failed due to the need for a recurring licensing fee for subsequent years. Our group technical staff proposed an alternate solution to the software license challenge but have been unable to receive support in implementation from the Jamaica local staff. Multiple telephone discussions and assurances have not yielded a positive result. We continue to explore options for this site.
- Bahamas Department of Meteorology: The existing radar at this location has been operating intermittently. Despite agreeing to participate in the project, we have not received any responses to our queries for several months. Through

discussion with the regional WMO representative and conversations with the department's interim director, we understand that the government is in negotiations to purchase a new radar(s) in the near future. We anticipate participation once the hardware issues are resolved.

This project is ongoing.

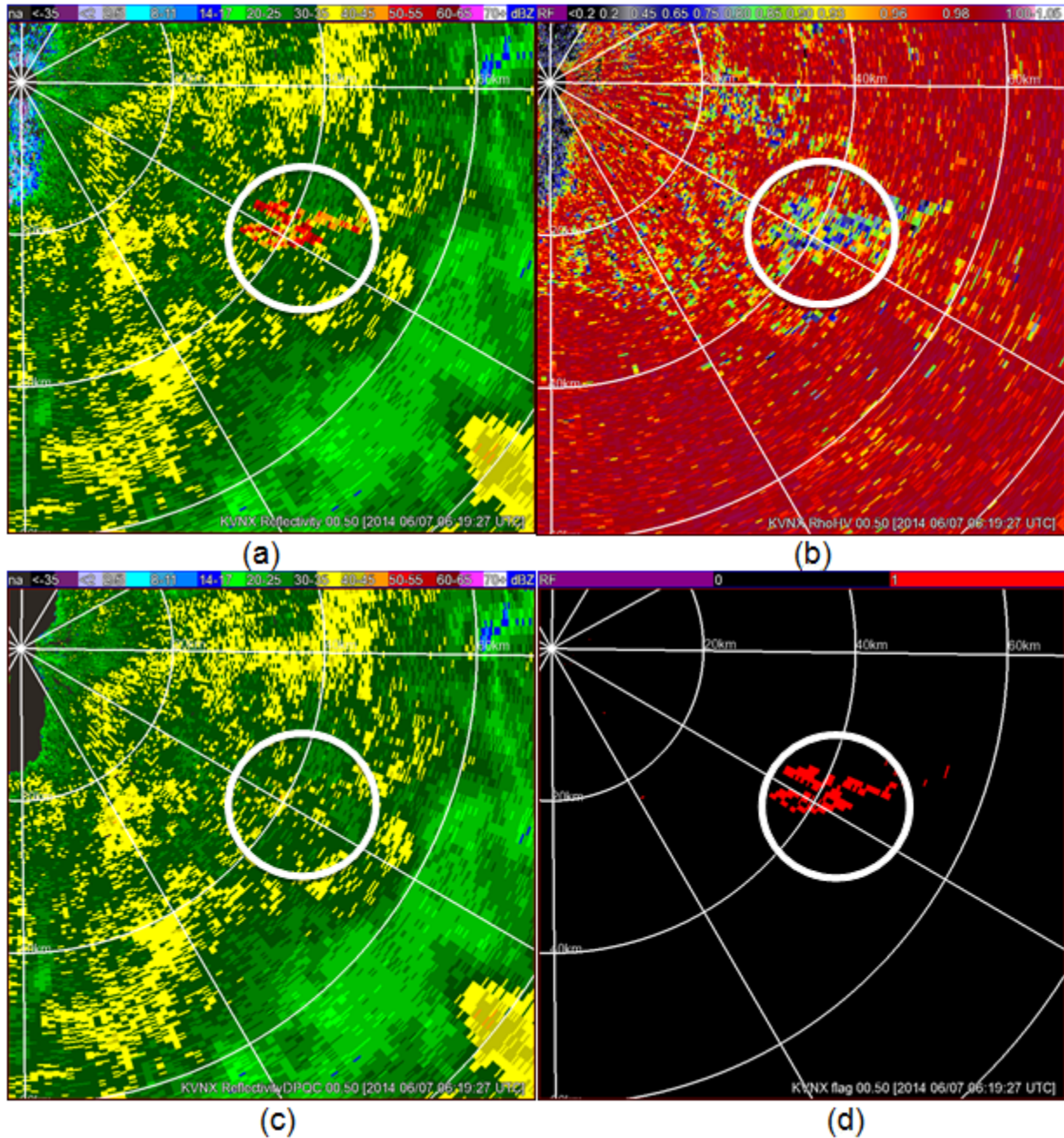
5. WSR-88D Data Quality Control Using Newly Upgraded Dual-Polarization Capabilities

Lin Tang and Carrie Langston (CIMMS at NSSL), and Jian Zhang and Kenneth Howard (NSSL)

The MRMS delivers high-quality severe weather and precipitation products for severe weather forecasts and warnings, hydrology, aviation and numerical weather prediction. It is important to effectively and accurately separate precipitation information from clutter contamination in the process of quantitative precipitation estimation. The quality control (QC) process of input radar data has been continuously improved to ensure its robust performance in various weather scenarios through real-time observation and users' feedbacks. In this year, the main focus has been clearance of the wind farm clutter and the bias correction.

It is challenging to differentiate the low ρ_{HV} associated with wind farms (WF) from precipitation (big drops, hails, and etc.) when the power returns from WF are embedded in convective storms. In the updated dpQC algorithm, the possible infected echoes from the wind turbine region are identified, base on the spatial dataset of U.S. wind turbine locations and associated wind turbine clutter as seen in MRMS radar-derived products. The contamination severity levels are different by cases depending on the environmental condition and radar beam propagation. The mean intensity (reflectivity) of the echoes from WF is compared with the neighboring echoes: 1) if the two values are comparable, then no severe contamination is observed and no correction is made; or 2) if the mean value from the WF location is much higher than the neighborhood, the pixels associated with decreased ρ_{HV} are flag out as WF contamination and the reflectivity is replaced with the mean neighboring intensity inside the studied regions. At the same time, as a reference for downstream process, a flag field is generated to mark out the pixels that are modified during the QC process, as demonstrated in the figures below. The QC refinement of wind turbines completely removes the WF clutter in clear air weather condition and corrects the returned echoes from wind farms with contaminated reflectivity measurement when they are embedded in storms. It benefits the accumulated QPE products in the MRMS system.

This project is complete.



(a) The raw Z field and (b) the associated ρ_{HV} field, (c) the quality controlled Z field with WF process, and (d) the flag field to mark out the pixels have been modified. The white circles highlight the location of wind farms. The fields are observed by KVNX at the elevation angle of 0.5° at UTC 06:19:27 UTC 7 June 2014.

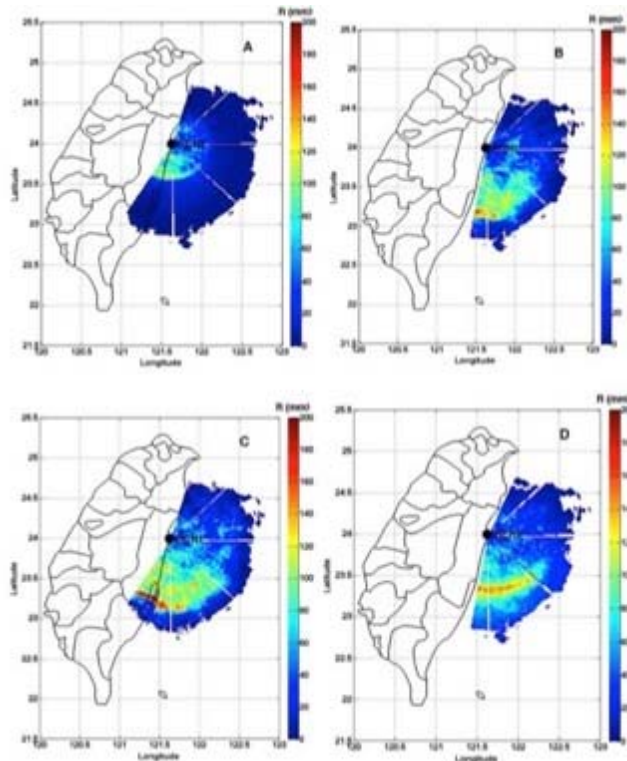
6. Radar Vertical Profile of Reflectivity Correction with Satellite Observations Using a Neural Network Approach

Yadong Wang (CIMMS at NSSL), Jian Zhang (NSSL), Pao-Liang Chang (Central Weather Bureau), and Qing Cao (Enterprise Electronics Corporation)

An artificial neural network (ANN) approach was developed to retrieve lower tilt radar reflectivity using higher tilts radar reflectivities and the satellite observations. This work can provide useful information when the lower tilt radar data is blocked by complex terrain and only higher tilts data is available. The neural network was further trained using more available data, and validated with more cases. This validation can further prove the feasibility of this approach. According to reviewers' comments, the following products were generated and tested using the data from Typhoon Tembin (23 August 2012):

- a.) The reflectivity from 6.0° is directly used in the rainfall rate estimation, which is used to simulate the radar based QPE when low tilt data is unavailable.
- b.) The rainfall rate is first calculated using the reflectivity data from 0.5° elevation angle. Since the reflectivity from Taiwan is unavailable because of the complex terrain, only the total rainfall from ocean region is used in this work. Moreover, for the comparison purpose, the rainfall is only calculated within the maximum of 6.0° elevation angle. This result is used as the "ground truth" in this test.
- c.) The 6.0° reflectivity is regenerated using the ANN VPR correction approach reported in the current work. It should be noted that the ANN is retrained using the data pairs from the ocean region.
- d.) The 6.0° reflectivity is again regenerated using the VPR derived from RCHL (VPR-RCHL) using the approach proposed by Zhang et al. (2009). It should be noted that the VPR-RCHL is derived using the radar data mainly from the ocean region (as emphasized in the manuscript). Therefore, the VPR-RCHL can catch the vertical structure of the reflectivity, and can produce good correction when applied on the ocean region.

Results indicated that 6.0° reflectivity field is disparate from the reflectivity from 0.5° tilt, and will bias the estimated rainfall when 6.0° tilt reflectivity if directly used in QPE. However, after the 6.0° reflectivity is corrected with VPR derived from RCHL (VPR-RCHL) or with the proposed ANN approach, the correlation between 6.0° and 0.5° tilts reflectivity increases.



24-h accumulated rainfall calculated using reflectivity from (a) 6.0° without correction, (b) 0.5° , (c) 6.0° with ANN-VPR correction, and (d) 6.0° with VPR-RCHL correction.

Publications

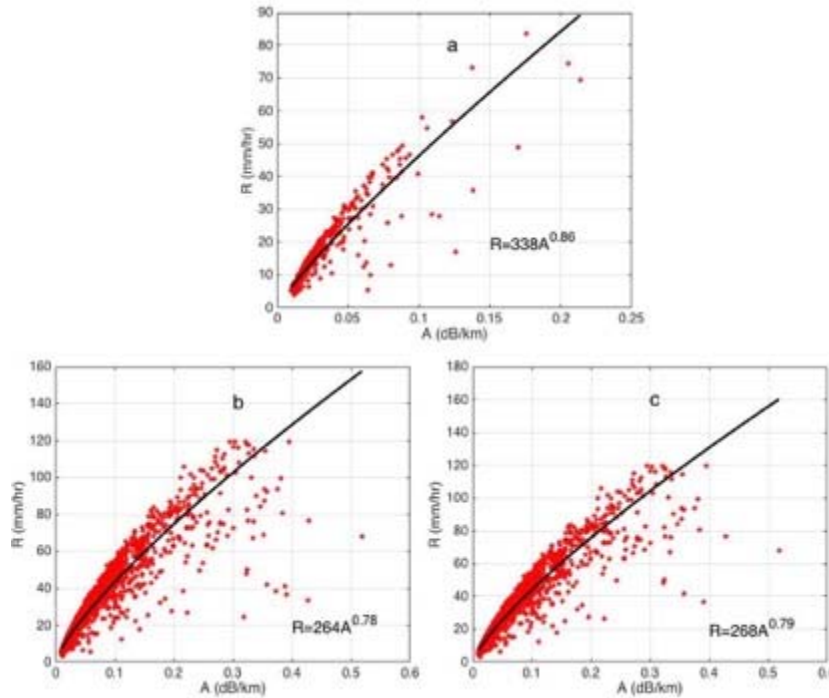
Wang, Y., J. Zhang, P.-L. Chang, and Q. Cao, 2015: Radar vertical profile of reflectivity correction with TRMM observations using a neural network approach. *Journal of Hydrometeorology*, **16**, 2230-2247.

7. Development of a Novel Radar QPE Approach Using Specific Attenuation for Two C-band Dual-Polarization Radar

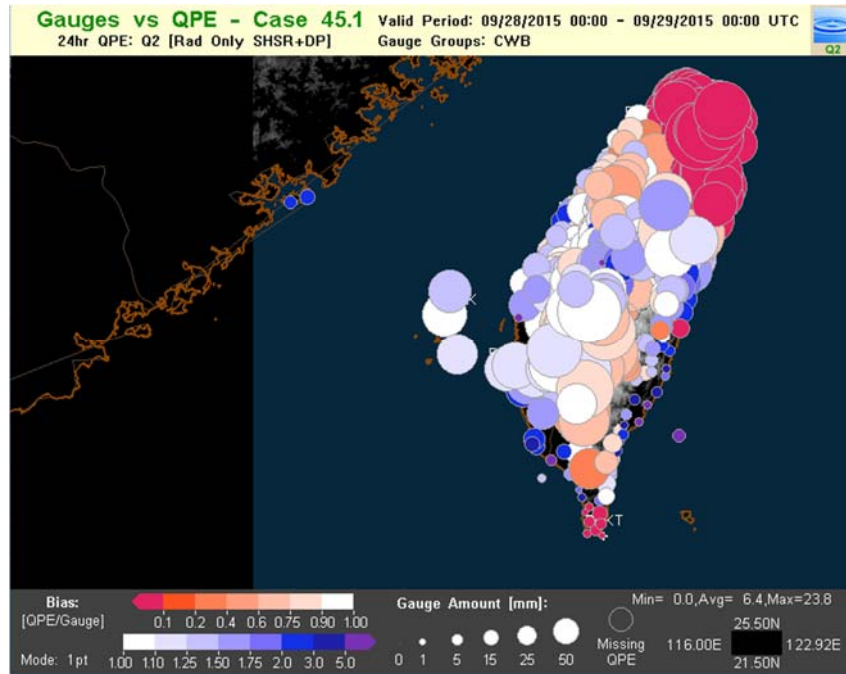
Yadong Wang, Pengfei Zhang, Alexander Ryzhkov, and Lin Tang (CIMMS at NSSL), and Jian Zhang (NSSL)

A novel Quantitative Precipitation Estimation (QPE) algorithm using the specific attenuation A has been developed. It was shown that the $R(A)$ estimate is less sensitive to the drop size distribution (DSD) variations compared to $R(Z)$ approach. However, including the precipitation category information into the $R=\gamma A^\Lambda$ relation can further enhance the accuracy of obtained rainfall rate estimation. The impacts of the precipitation type on the $R(A)$ relation are studied through simulation. There are total of 5851, 4016, and 3730 DSD data sets collected by four JWDs from stratiform, convective and tropical precipitations to generate the rainfall rate and specific attenuation. The relations between R and A are then obtained through the non-linearly fitting. It was found that the γ (Λ) for stratiform, convective and tropical precipitation are 338 (0.86), 264 (0.78), and 268 (0.79), respectively.

The performance of the modified $R(A)$ approach on one C-band dual-polarization radar (RCMK) was evaluated with a 24-h precipitation event ending 0000 UTC 29 September 2015 during Typhoon Dujuan. Based on the comparison results we could find that the modified $R(A)$ approach can provide good results with bias of 1.13, a correlation coefficient of 0.83, and a root mean square error of 63.24 mm.



Scatter plot of R vs. A . The scatters of R - A pairs are calculated based on the DSD data collected from stratiform (a), convective (b), and tropical (c) precipitations. The non-linearly fitting results are inserted as black lines and the obtained $R(A)$ relations are also included in the figure.



The comparison result between radar QPE ($R(A)$) and gauge observations. 24 hours accumulation ending 0000 UTC 29 September 2015 for Typhoon Dujuan was used in this study. The radar QPE is obtained through C-band dual-polarization radar (RCMK).

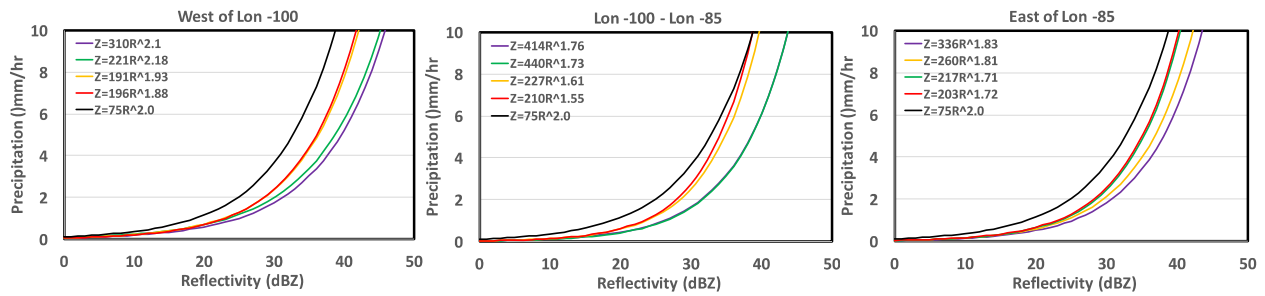
Publications

Wang, Y., J. Zhang, P. Chang, C. Langston, B. Kaney, L. Tang, 2016: Operational C-Band Dual-Polarization radar QPE for the subtropical complex terrain of Taiwan. *Advances in Meteorology*, 1-15.

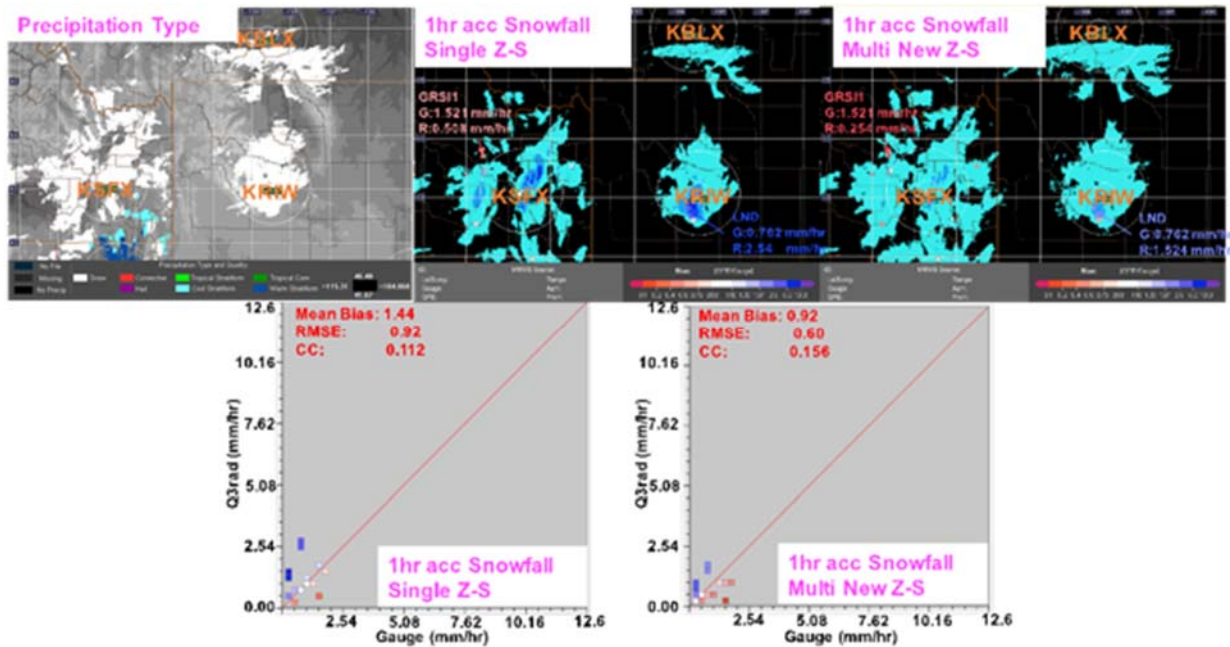
8. Enhance the Accuracy of Radar Snowfall Estimation with New Z-S Relationship

Youcun Qi (CIMMS at NSSL) and Jian Zhang (NSSL)

Snow may have negative effects on roadways and human lives, but the result of the melted snow/ice is good for farming and other water resources. For example, in the Southwest and West mountainous area of United States, water shortage is a very big concern. However, snowfall in the winter can provide humans, animals and crops an almost unlimited water supply. So, using radar to accurately estimate the snowfall is very important for human life and economic development in the water lacking area. The current study plans to analyze the characteristics of the horizontal and vertical variations of dry/wet snow using dual polarimetric radar observations, relative humidity and in situ snow water equivalent observations from the National Weather Service All Weather Prediction Accumulation Gauges (AWPAG) across the CONUS, and establish the relationships between the reflectivity (Z) and ground snow water equivalent (S). The new Z - S relationships will be evaluated with independent Community Collaborative Rain, Hail & Snow Network (CoCoRaHS) gauge observations and eventually implemented in the Multi-Radar Multi-Sensor system for improved quantitative precipitation estimation for snow. This project is ongoing.



New derived Z-S relationships for different domains



(Top left) surface precipitation type, (top middle) 1-h snowfall accumulation with single Z-S relationship, and (top right) 1-h snowfall accumulation with multiple Z-S relationships. Bottom row shows the scatter plots for (low left) single Z-S relationship and (top right) with multiple Z-S relationships.

9. Quality Control Advancements of Hourly Rain Gauge Observations

Steven Martinaitis, Stephen Cocks, and Youcun Qi (CIMMS at NSSL), and Jian Zhang and Kenneth Howard (NSSL)

Surface rain gauge observations are regarded as “ground truth” when used to verify and calibrate radar-derived quantitative precipitation estimates (QPE). However, gauges not properly vetted by a quality control (QC) procedure can introduce erroneous statistical results and bias calibration. Continued advancements were made to the rain gauge QC

algorithm to allow for a greater quantity of gauges to undergo QC and to modify decision-tree logic in the executable coding.

The QC algorithm was modified to better handle hourly snow-water equivalent gauge observations that were observed during winter precipitation events. A series of outlier functions and a threshold value of 0.25 inches were generated to ensure that gauges that recorded erroneous non-zero values were flagged in the QC process. The scripts used to run the real-time ingest of hourly gauges was modified to update the metadata file for the Hydrometeorological Automated Data System (HADS) gauge network every hour. This was done in response to a request by National Weather Service personnel in the Pacific Northwest for temporary emergency gauges that were being installed over recent wildfire burn scars. The ability to have the metadata file update every hour allows for the Multi-Radar Multi-System (MRMS) system to instantly add new gauges as they become operational.

Research has continued on the refinement of the gauge QC algorithm to ensure that quality observations are used in the generation and verification of MRMS products. Work has also begun on ingesting the gauge networks collected by the Meteorological Assimilation Data Ingest System (MADIS) into the operational MRMS system. Continuing long-term collaboration between the National Severe Storms Laboratory (NSSL) and other National Oceanic and Atmospheric Administration (NOAA) partners will address the collection and QC of gauge metadata, the identification of quality gauge observations within winter precipitation regimes, and the ability to display and assess the QC results and history. This project is ongoing.

Publications

- Martinaitis, S. M., S. B. Cocks, Y. Qi, B. T. Kaney, J. Zhang, and K. Howard, 2015: Understanding winter precipitation impacts on automated gauge observations within a real-time system. *Journal of Hydrometeorology*, **16**, 2345-2363.
- Qi, Y., S. Martinaitis, J. Zhang, and S. Cocks, 2016: A real-time automated quality control of hourly rain gauge data based on multiple sensors in MRMS system. *Journal of Hydrometeorology*, **17**, 1675-1691.

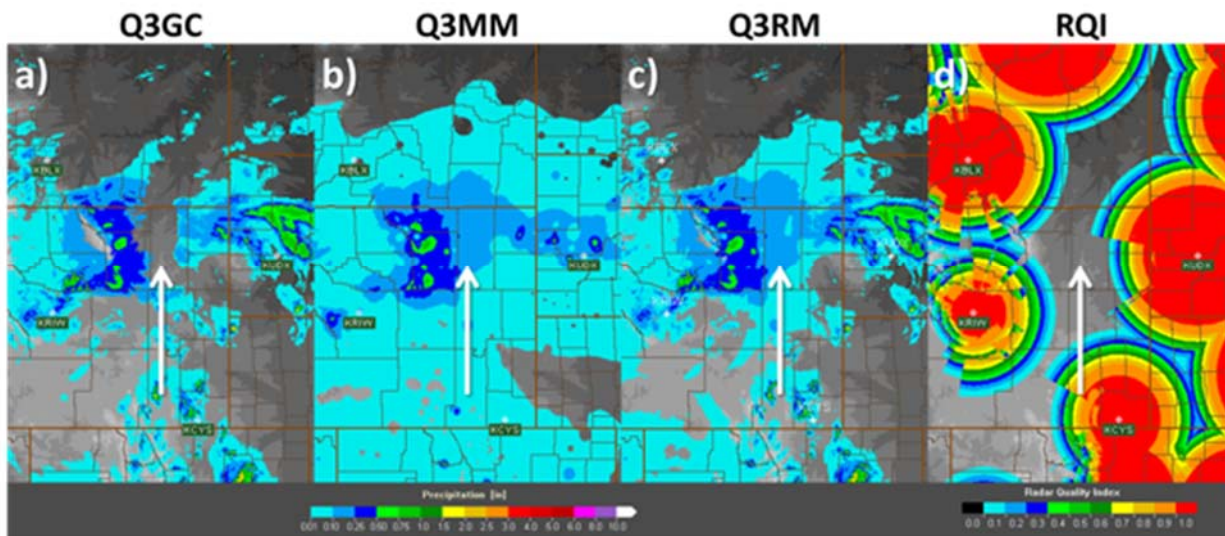
10. Combining Ground and Radar-Based Precipitation Estimates with Rainfall Climatologies to Generate a Merged QPE

Steven Martinaitis, Youcun Qi, and Stephen Cocks (CIMMS at NSSL), and Jian Zhang and Kenneth Howard (NSSL)

Different sources of QPE have varying strengths and challenges in generating deterministic surface precipitation values. These challenges are magnified in the western United States where there are significant gaps in radar coverage due to less dense coverage and beam blockage from complex terrain along with a sparse network of gauge observations. CIMMS scientists are developing a scheme to merge a radar-derived QPE with gauge observations and a climatology-based QPE to provide a more accurate and comprehensive QPE coverage across the conterminous United States.

The current scheme under development would merge the Multi-Radar Multi-Sensor (MRMS) local gauge corrected radar QPE (Q3GC) with the MRMS Mountain Mapper product (Q3MM), which is created by interpolating gauge observations onto the Parameter-elevation Relationships on Independent Slopes Model (PRISM) background rainfall climatology. The initial prototype merging scheme utilized the MRMS Radar Quality Index (RQI) as the primary weighting function to seamlessly blend the two QPE sources. Other factors that influenced the weight between Q3GC and Q3MM were the coverage of non-zero reflectivity values, the radius of influence of gauge observations, and surface model parameters from the Rapid Refresh (RAP) model. The initial results of the prototype merged scheme showed the value of using the Q3MM product to fill the gaps in radar coverage; however, limitations in the gauge QC and the coarse resolution of the RAP model data created areas of discontinuities or areas where observed winter precipitation was missing. To mitigate these limitations, the RQI product will be modified, which includes a greater product precision, and the gauge QC will be updated to better account for snow-water equivalent values in winter precipitation. This change in gauge QC will eliminate the need to use RAP model data in the QPE merging, which will mitigate the model-based discontinuities.

The merged QPE product will undergo extensive testing and evaluation prior to operational release, including case studies and real-time evaluations. This project is ongoing.



The source MRMS QPE sources a) Q3GC and b) Q3MM combined into the c) Q3RM QPE product as well as the d) RQI coverage of the radars over eastern Montana 1 h QPE ending 2100 UTC 24 May 2015. The white arrows represent areas where the merging of the QPE sources filled a significant gap in the radar coverage of QPE.

11. Integrating an Evaporation Correction Scheme to Real-Time Instantaneous Radar Rainfall Rates

Steven Martinaitis, Heather Grams, and Youcun Qi (CIMMS at NSSL), and Jian Zhang and Kenneth Howard (NSSL)

Multiple limitations still exist with radar sampling and radar-based quantitative precipitation estimation (QPE) that present challenges in creating accurate surface precipitation estimates. One such set of challenges is the overestimation of precipitation and false light precipitation echoes in sub-saturated environments. This is because the precipitation sampled aloft at the radar beam can be greatly reduced or even completely evaporated by the time it reaches the surface. An evaporation correction technique is being developed for the Multi-Radar Multi-Sensor (MRMS) system to help mitigate the impact of evaporation on precipitation between the radar beam level and the surface. The evaporation scheme is based on the derivations by Gregory (1995), which originated from the theory of evaporation of a water droplet or ice particle through the rate of mass diffusion with respect to time. Two different set of calculations are available for rain and snow.

The test evaporation correction scheme utilizes Rapid Refresh (RAP) model data to determine the precipitation type at the surface and to generate a three-dimensional profile of atmospheric conditions to modify the precipitation rate with respect to height. The different calculations for rain and snow are applied throughout the vertical column of each grid cell based upon the height of the freezing level and the lowest altitude of available radar data used to generate the instantaneous precipitation rate. A threshold with a linear reduction of the influence of evaporation for instantaneous rates is used to prevent the evaporation of more significant rain rates based on the assumption that the precipitation column containing these greater rates would saturate the environment at that particular location. A threshold with a linear reduction of the influence of evaporation was also used for the height above ground level to account for the radar potentially overshooting precipitation features, which would result in an initial underestimation of precipitation.

In the near future, the evaporation correction scheme will be tested through a number of case studies, and then eventually applied in a real-time environment. The goals for the evaporation correction scheme are to improve precipitation biases, remove false light precipitation, and improve gauge quality control with respect to the misclassification of false zero gauge observations. This project is ongoing.

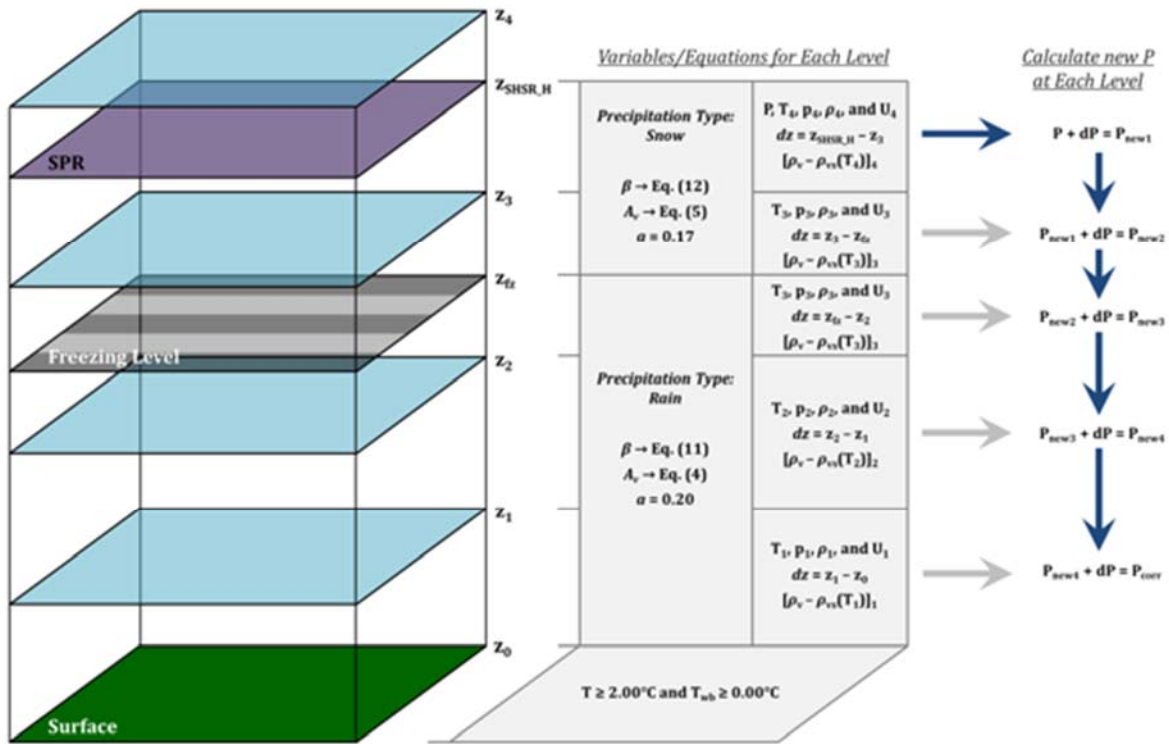


Diagram of calculating a new instantaneous precipitation rate (P_{corr}) for a single grid point for a situation where the available instantaneous precipitation rate was located above the freezing level and the estimated surface precipitation type was rain.

12. Multi-Sensor Estimation of Intense Rainfall in Complex Terrain using GOES-R Combined with Ground and Space-Based Radars

Heather Grams (CIMMS at NSSL), J.J. Gourley and Bob Rabin (NSSL), and Pierre Kirstetter (OU ARRC)

While the WSR-88D network provides fairly good spatial coverage over the eastern United States, gaps remain in the western U.S. where complex terrain limits how well ground-based radars can observe precipitation at low-levels. This limitation makes flash flood detection a significant challenge. Satellite-based rainfall products can provide much better spatial coverage, but coarse spatial and temporal resolutions have limited their usefulness at flash flood scales.

The Advanced Baseline Imager (ABI) set to launch on the GOES-R satellite will provide improved spatial resolution over current IR imagers (up to 2-km for some products), and the geostationary platform will allow for full CONUS scans at as high as a 5-minute time step. A new QPE product has been developed that uses a simple, steady state microphysics model to simulate near-surface drop size distribution moments (reflectivity and rain rate) in areas where radar coverage is poor or non-existent. The model is initialized from cloud top properties derived from the ABI, as well as analyses of

temperature and relative humidity from the High Resolution Rapid Refresh (HRRR) model.

During 2016, efforts were focused on QPE model improvements and validation against rain gauge observations and other satellite QPE algorithms. Once GOES-R is launched in late 2016, work will begin to adapt the prototype algorithm to use operational GOES-R data resolution and scan strategies. This project is ongoing.

Publications

Grams, H. M., P.-E. Kirstetter, and J. J. Gourley, 2016: Naive Bayesian precipitation type retrieval from satellite using a cloud top and ground radar matched climatology. *Journal of Hydrometeorology*, Accepted.

13. Development and Verification of New Algorithm to Estimate Rainfall

Yadong Wang, Pengfei Zhang, and Stephen Cocks (CIMMS at NSSL)

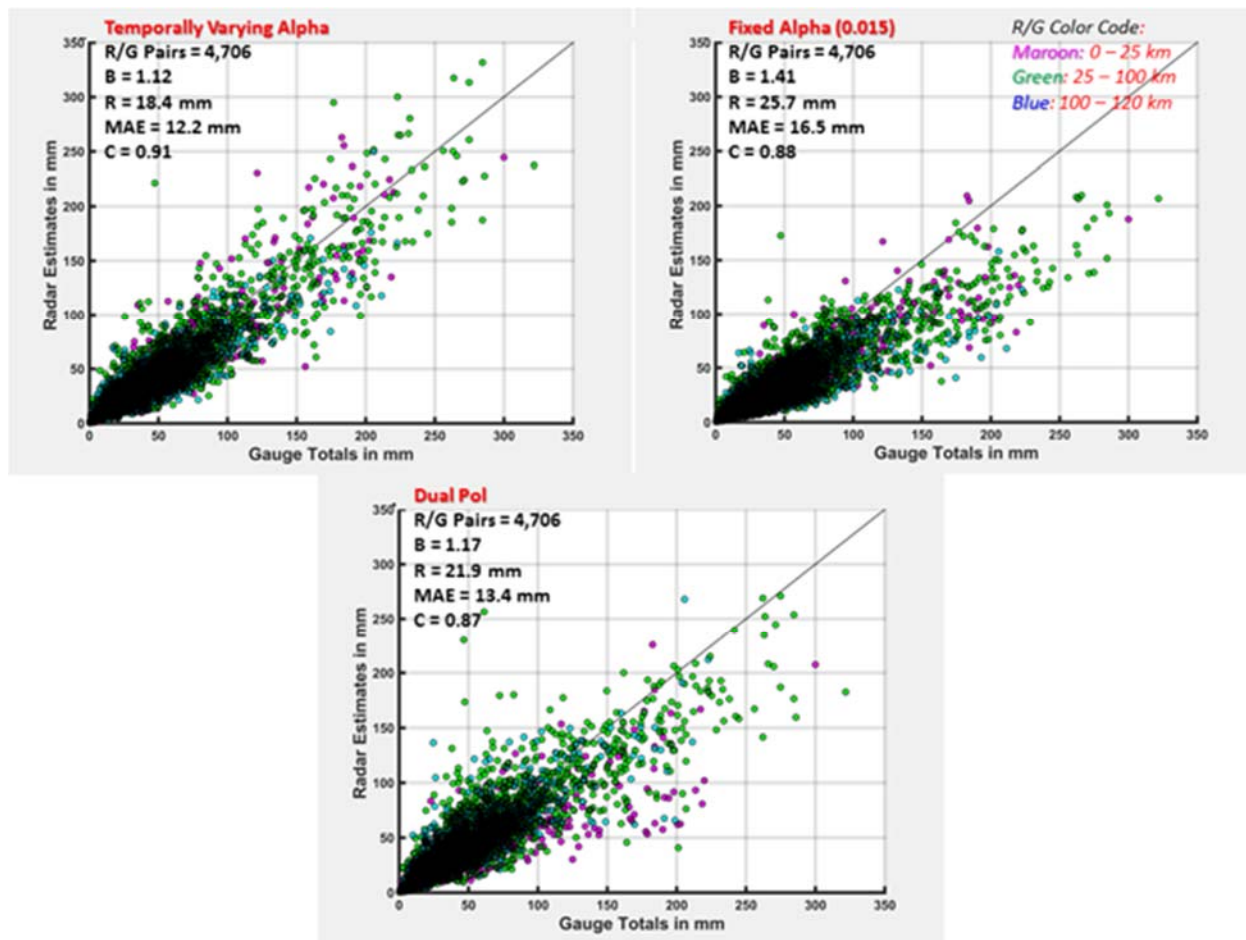
Work continued in developing a new algorithm to estimate rainfall below the melting layer that performs well under a variety of drop size distribution changes within a precipitation system. The algorithm uses a parameter called specific attenuation to estimate precipitation in pure rain and specific differential phase whenever hail is likely present (reflectivity greater than 50 dBZ). Key to estimates of precipitation in pure rain, was a parameter called Alpha. Alpha is nothing more than the ratio between the path integrated attenuation (caused by the presence of water droplets) and the specific differential phase along a given radar radial. Currently, a mathematical equation is used to estimate the alpha parameter via the use of ZDR to Z scatter plots. Alpha is estimated over the entire PPI and is updated every time step.

Overall, alpha appears to differentiate between typical mid-latitude Continental like rain events and those that are more precipitation efficient. The parameter tends to be lower in Continental like rain events (below 0.020) and higher in more precipitation efficient like rain events (e.g. tropical, values generally above 0.020). However, the presence of hail or any kind of frozen precipitation causes large errors; hence the use of specific differential phase when high reflectivity values are present.

The algorithm underwent a number of modifications over the past year. These modifications were tested on key benchmark tests until a stable robust code was developed that allowed the research operator to: 1) adjust the distance from the radar estimates are made in order to avoid the melting layer; 2) adjust the number of PPIs used to average the alpha parameter; 3) set the default value for the alpha parameter; 4) choose whether to use a linear or nonlinear equation to estimate alpha.

Once the code was ready, it was tested on 52 different precipitation events from the years of 2014, 2015, and 2016. As a test, we compared the $R(A) + R(KDP)$ algorithm's QPE, where alpha varies temporally, to QPE generated from the same algorithm except Alpha was kept constant and operational Dual Pol QPE. Performance statistics were generated by comparing QPE to quality controlled rain gauges. The early results clearly

showed reduced variability in the temporally varying R(A) + R(KDP) estimates when compared to the operational Dual Pol data. The temporally varying alpha R(A) + R(KDP) estimates were also superior to those where alpha was set to a constant. Work will continue on this project for the next fiscal year as we continue to refine and improve the precipitation estimates from this algorithm. This project is ongoing.



Scatter plot comparisons of a significant rain event using (top left) a temporally varying alpha value, (top right) a fixed alpha value of 0.015, and (bottom) dual-pol QPE.

14. Evaluating MRMS Quantitative Precipitation Estimates Versus Single Source Radar QPE Products

Stephen Cocks, Steven Martinaitis, and Youcun Qi (CIMMS at NSSL)

A systematic evaluation of MRMS QPE performance across the CONUS during the warm season was started during FY15 for five regions east of the Rocky Mountains: a) the Southern plains, b) the Southeast, c) the Northeast, d) the Great Lakes/Midwest, and e) and Northern and Central Plains. The study included precipitation events from 59 calendar days affecting 55 radars. Data was collected with reference to single radars to highlight the advantages of a mosaic versus single radar QPE. Additional work was completed in FY16 to finish this project. This included evaluating QPE product

performance below, within, and above the melting layer. An estimate of the distance from the radar of the minimum melting layer bottom (for a 24 hour period) was made using Dual Pol Rho HV data. This was used to differentiate between regions of pure rain and mixed hydrometeors within the melting layer. Inspection of the radar data for the precipitation events used in the study indicated that the radar beam was above the melting layer at distances greater than 200 km. Using this information, radar gauge pairs were separated into these various bins. In all the regions, MRMS QPE exhibited lower errors within and above the melting layer illustrating the utility of using a reflectivity mosaic that was bright band corrected to estimate precipitation.

As was discovered in FY15, MRMS QPE exhibited an overestimate bias within the northern interior the US that was related to often classifying radar echoes as tropical. An initial algorithm adjustment, involving a change to the creation of probability of warm rain fields, was developed to reduce the bias but further testing revealed that a different methodology was still needed. A new algorithm adjustment was made to reduce the bias by restricting the regions where a MRMS tropical climatological enhancement rate was applied. Previously, this enhancement rate, used only when radar echoes were classified as tropical, was applied over all regions east of the Rocky Mountains. However, this rate enhancement was specifically created to reduce underestimates caused when tropical systems moved across our coastlines. Therefore, the adjustment involved reducing the areas affected by the tropical climatological enhancement rate to over the Southeast and along the East Coast. Testing results indicated the bias is significantly reduced over the northern interior of the US. However, this adjustment does not address the overestimates that at times occur during the summer over the Southeast US and along the coast. The integration of the R(A) + R(KDP) algorithm into MRMS mosaics will eventually mitigate the bias over these regions as this algorithm should do a better job in estimating precipitation within tropical like systems. This project is ongoing.

Publications

Cocks, S. B., S. M. Martinaitis, B. Kaney, J. Zhang, and K. Howard, 2016: MRMS QPE performance during the 2013/14 cool season. *Journal of Hydrometeorology*, **17**, 791-810.

15. MRMS Experimental Testbed for Operational Products (METOP)

Youcun Qi, Brian Kaney, Steven Martinaitis, and Heather Grams (CIMMS at NSSL), and Jian Zhang and Ken Howard (NSSL)

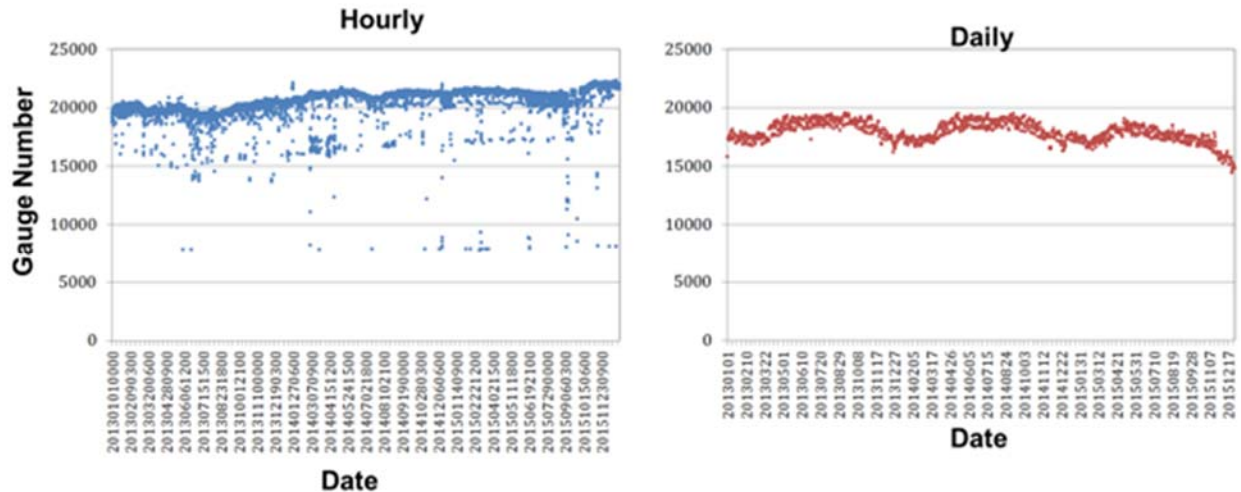
Accurate high-resolution quantitative precipitation estimation (QPE) at the continental scale is of critical importance to the nation's weather, water and climate services. To address this need, a Multi-Radar Multi-Sensor (MRMS) system was developed at the National Severe Storms Lab of National Oceanic and Atmospheric Administration that integrates radar, gauge, model and satellite data and provides a suite of QPE products at 1-km and 2-min resolution.

MRMS system consists of three components: 1) an operational system, 2) a real-time research system, and 3) an archive testbed. The operational system currently provides

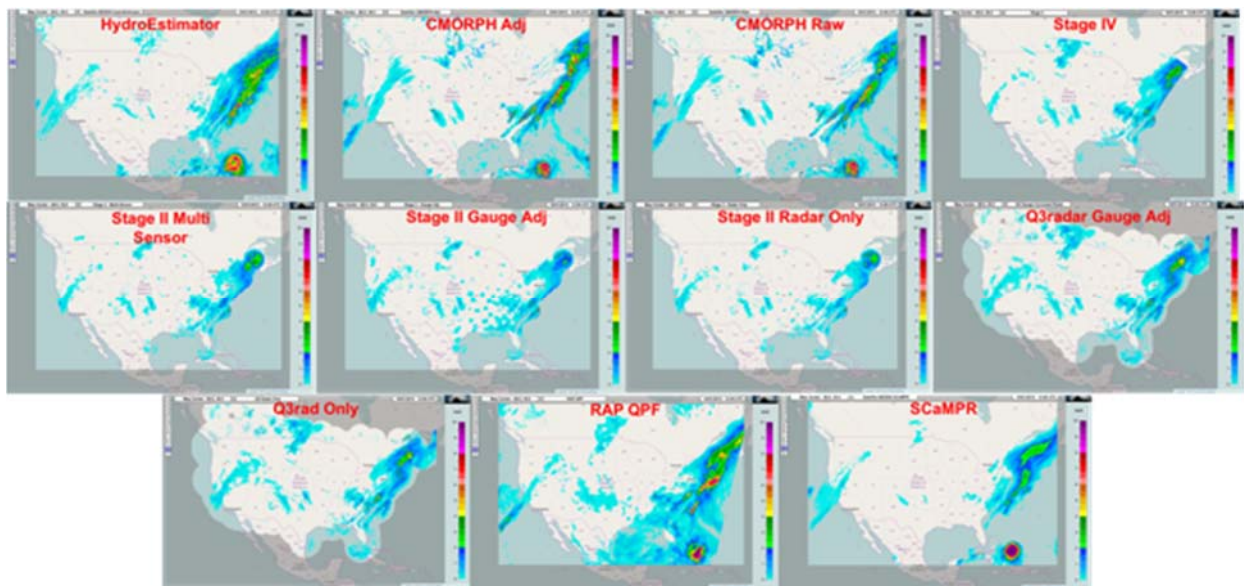
instantaneous precipitation rate, type and 1-h to 72-h accumulations for conterminous United States and southern Canada. The research system has the similar hardware infrastructure and data environment as the operational system, but runs newer and more advanced algorithms. The newer algorithms are tested on the research system for robustness and computational efficiency in a pseudo operational environment before they are transitioned into operations. The archive testbed, also called the MRMS Experimental Testbed for Operational Products (METOP), consists of a large database that encompasses a wide range of hydroclimatological and geographical regimes. METOP is for the testing and refinements of the most advanced radar QPE techniques, which are often developed on specific data from limited times and locations. The archive data includes quality controlled in-situ observations for the validation of the new radar QPE across all seasons and geographic regions. A number of operational QPE products derived from different sensors/models are also included in METOP for the fusion of multiple sources of complementary precipitation information. This project is ongoing.



Data availability of daily QPE and QPF Products



METOP hourly (left) and daily (right) gauge observations available



METOP QPE and QPF products

16. meteorological Phenomena Identification near the Ground (mPING)

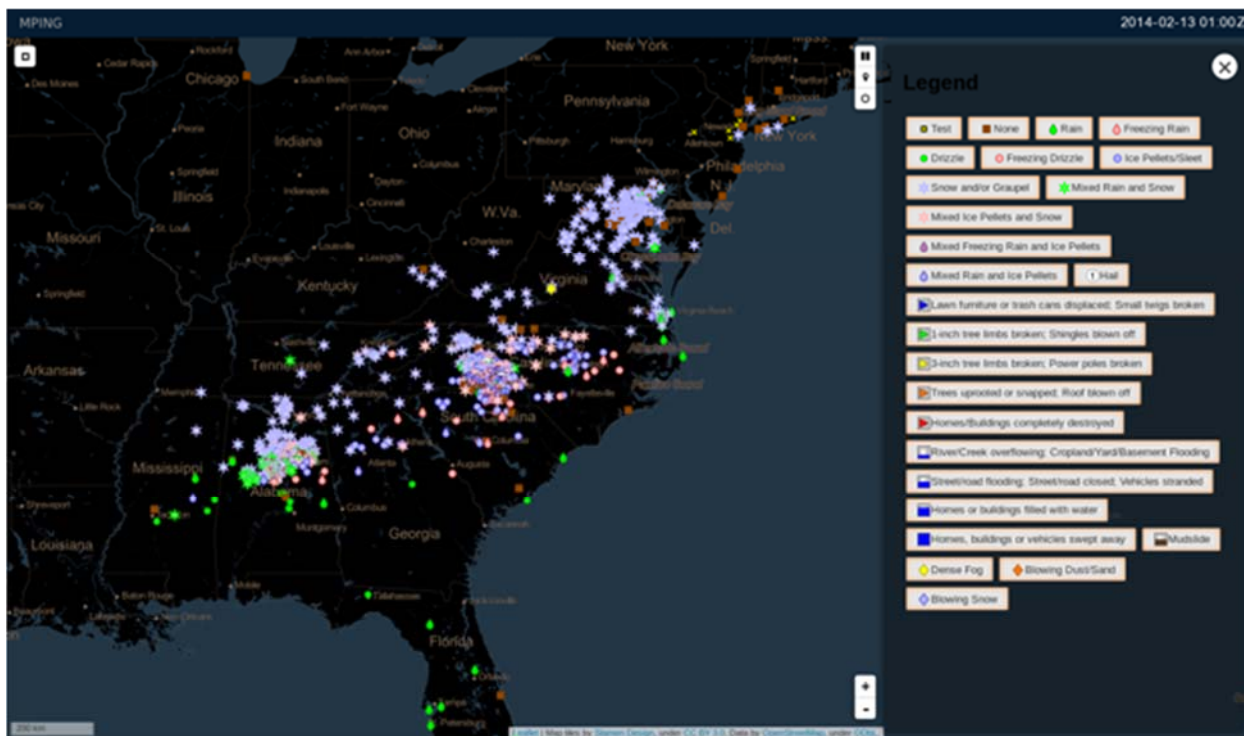
Kim Elmore, Heather Grams, and Jeff Brogden (CIMMS at NSSL)

The mPING (meteorological Phenomena Identification near the Ground) crowd-sourcing smart-phone app now has well over 100,000 downloads and has received over 1.100,000 report submissions. New versions of the app have been released that use HTTPS connections and that have identical look and feel. The data are now submitted to, housed within and backed up by OU Research Computing Services.

An application program interface has been fully released that allows mPING reporting capability to be embedded within any other app (such as for weather companies and

television stations). mPING has entered into an agreement with AccuWeather, who owns IP used by mPING, such that any government, educational, or research use of the data are free. Any commercial use is subject to terms and conditions from AccuWeather.

Data submission and access are controlled via an API key, which can be searched such that only submissions from a particular key can be displayed, a feature that may be useful to the NWS for identifying submissions from trained observers. A new public-facing display has also been developed that now has a global view. This means that observations from anywhere in the world can be displayed, and so observations from Alaska are now easily viewable from the public-facing display.



New mPING public display showing the new map projection and new precipitation type icons. The legend, which can be hidden allowing more screen space for data display, is shown on the right. This display loops over 4 h of data in 5 min intervals showing 1 hour of past data every 5 min.

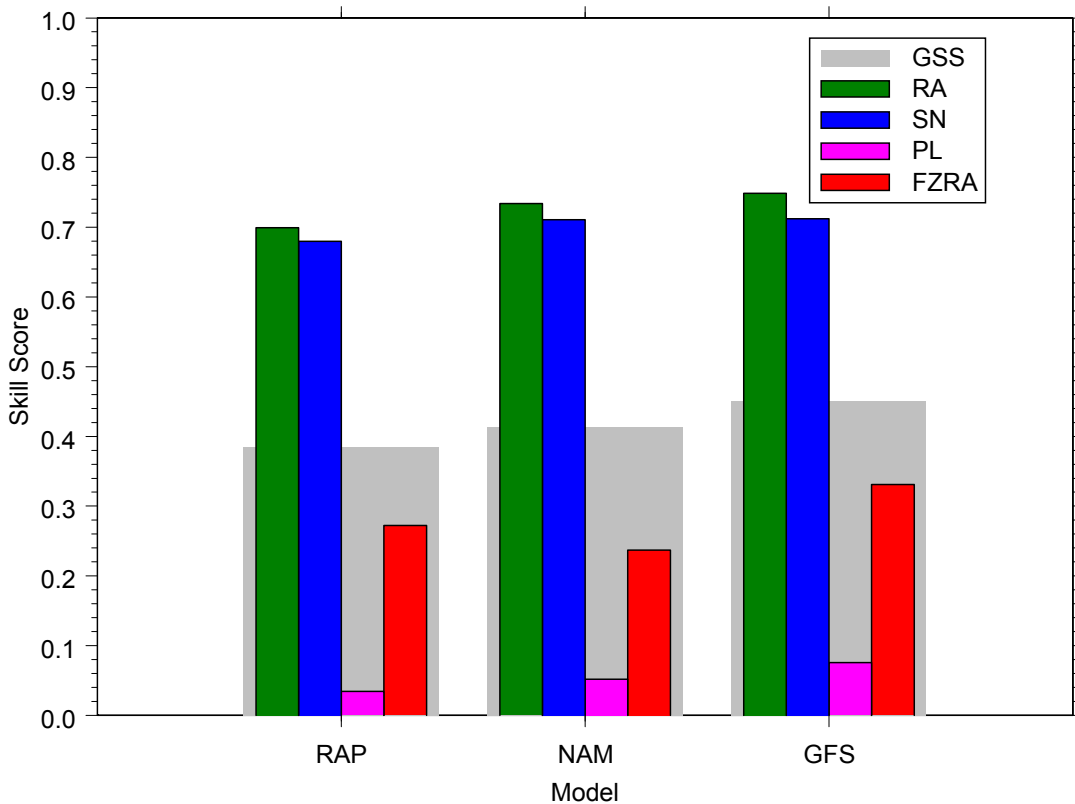
17. mPING Random Forest Research

Kim Elmore, Heather Grams, Hoyt Burcham, and John Krause (CIMMS at NSSL)

The random forest technique was applied to RAP, NAM and GFS forecast 6, 12 1nd 18 h pressure-level output. Only pressure level data are used because output in native vertical coordinates is unavailable. Results of this work reinforce the case for significantly better precipitation type *forecasts* may result from driving supervised machine learning algorithms, such as random forests, with mPING observations. This

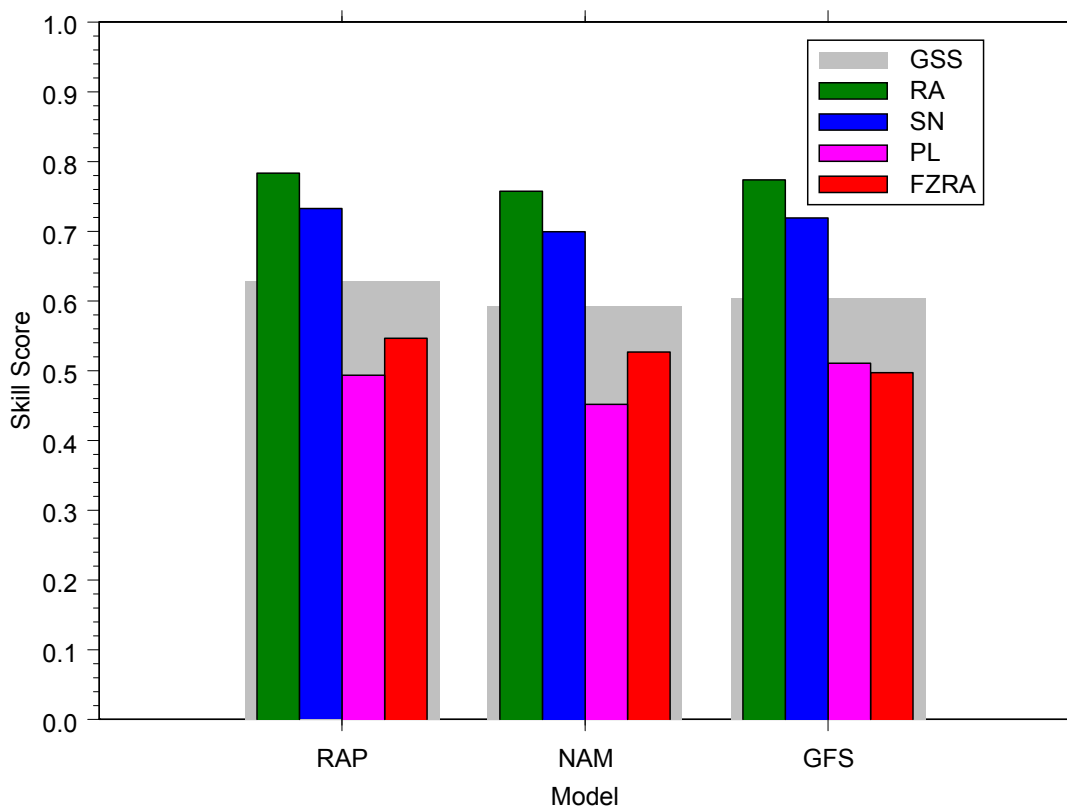
work also shows that the random forest created for each model is different and that a random forest created for one model does not work well when provided data from another model. Almost equivalent skill can be derived from each model even though the random forests are different and the most improvement is for the precipitation type for which the current operational algorithms do poorly: ice pellets and freezing rain. Finally, a multinomial logistic regression can be used to generate calibrated probabilities for each precipitation type such that probabilistic guidance for forecast precipitation type has been generated. Because the RAP did not change between the 2014-2015 and 2015-2016 winters, these probabilities will be validated using RAP forecast output for the 2015-2016 cold season.

Current Algorithms by Model



Current algorithm performance by model for the RAP, NAM and GFS. Colored bars are Peirce Skill Scores for rain (RA, green), snow (SN, blue), ice pellets (PL, magenta) and freezing rain (FZRA, red). The gray bars show the Gerrity score for the all four types taken together.

Random Forest Performance by Model



Same as previous figure, but for the random forest generated for each model. Little gain is apparent for RA and SN. The largest improvement is for PL and FZRA, but the overall Gerrity score is also much improved.

18. Development of Web-Based Tools and Displays for Real-Time QPE and Hydrologic Analysis

Brian Kaney and Carrie Langston (CIMMS at NSSL)

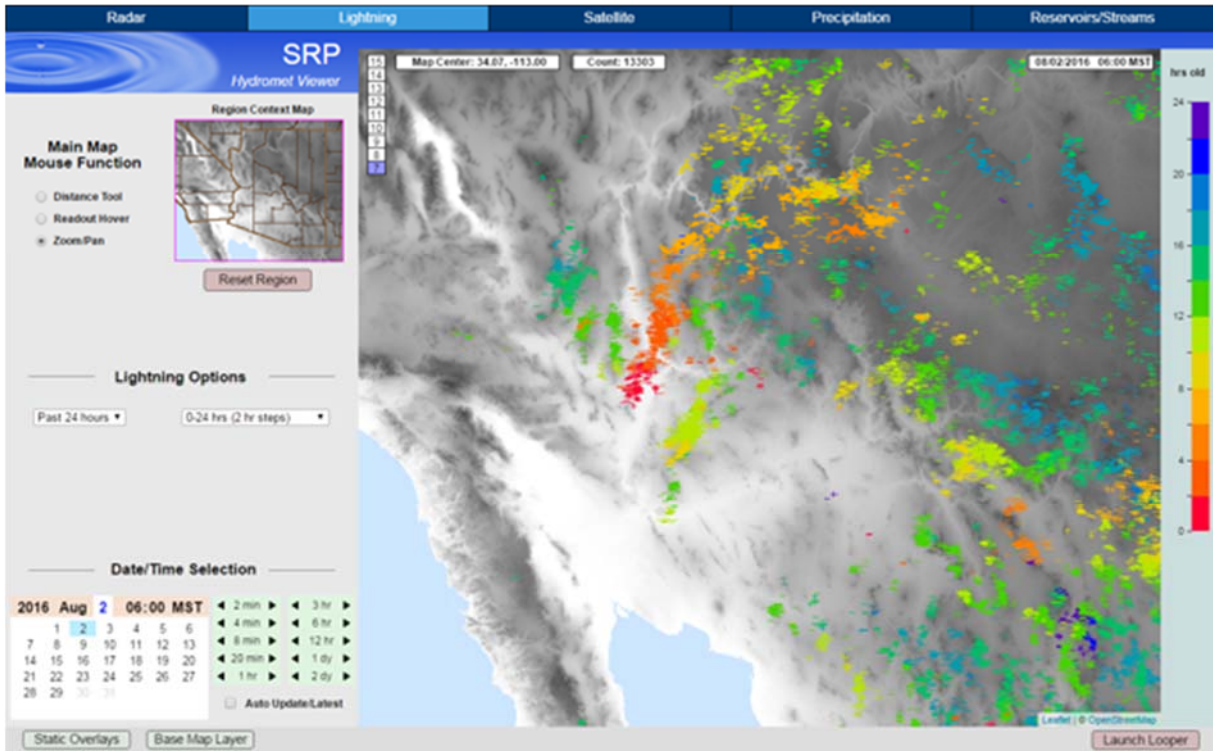
Within the hydrometeorology group, a cornerstone of all research and development has always been the evaluation of experimental products in real-time across the entire CONUS. The primary interfaces for this evaluation are the QPE Verification System (QVS; <http://mrms.ou.edu>) and the Radar Reflectivity Comparison Tool (RRCT; <http://rrct.nwc.ou.edu>). Several updates and improvements were made to both systems in FY 2016. This work is ongoing. A closely allied new project has been the Hydromet Viewer for Salt River Project in Phoenix. Although many details vary, the goal is for this development and the QVS to share as much common framework and code libraries and web strategies as possible.

a. Hydromet Viewer for Salt River Project

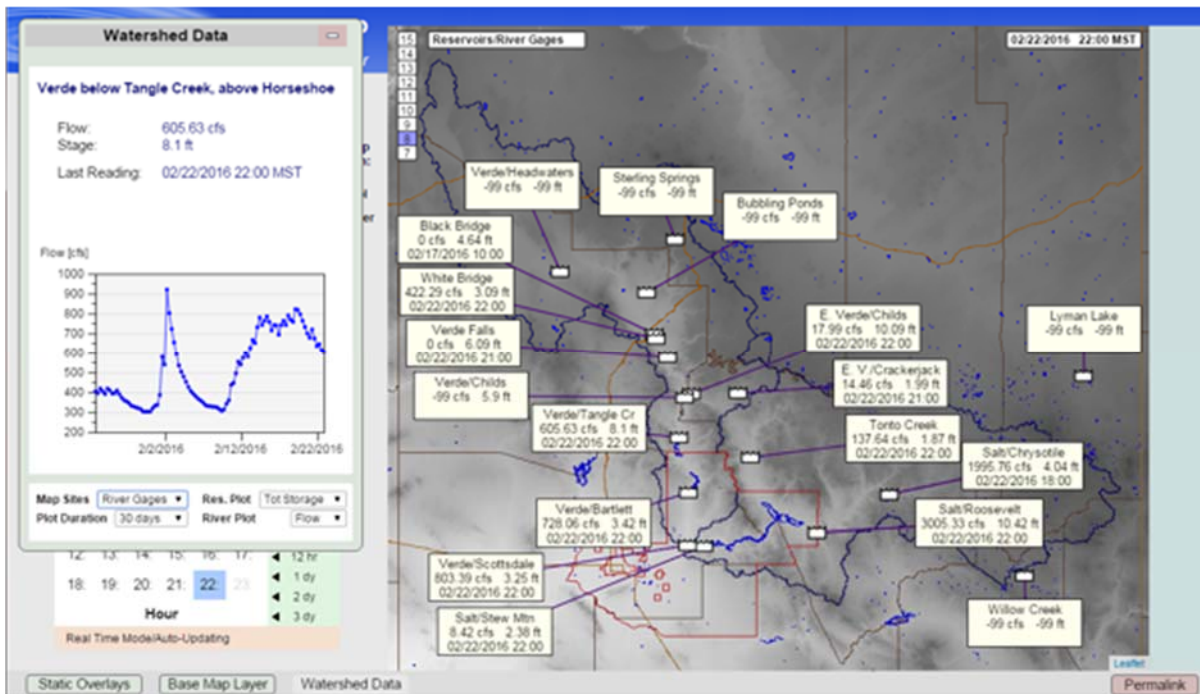
The Salt River Project (SRP) water and power utility operate in a very challenging QPE/QPF environment and had the first WSR-88D installation in the mountain west. With significant mountain blockages, complex terrain, large areas of orographically enhanced precipitation, significant winter precipitation from low based clouds, significant summer thunderstorms from high based clouds, and even tropical storm remnants, central Arizona is well suited to test the limits of multi-sensor QPE and the new dual-polarization capabilities in MRMS.

This project involves completely revamping the internal meteorology web tools used by SRP. New hardware was put in place and the latest version of the MRMS suite installed. The new Hydromet Viewer is intended as a one stop suite of tools to monitor weather in real-time, aid in weather related decision-making and facilitate post analysis. The MRMS products form a core for the Hydromet Viewer but the viewer also brings in satellite imagery, level 3 single radar products, lightning strike data, precipitation gauges, and lake/stream measurements into a single consistent framework. SRP also has an important network of automated surface weather stations (PRISMS) accurately monitoring several weather variables at high spatial and temporal resolution, which is also displayed in the new Hydromet Viewer.

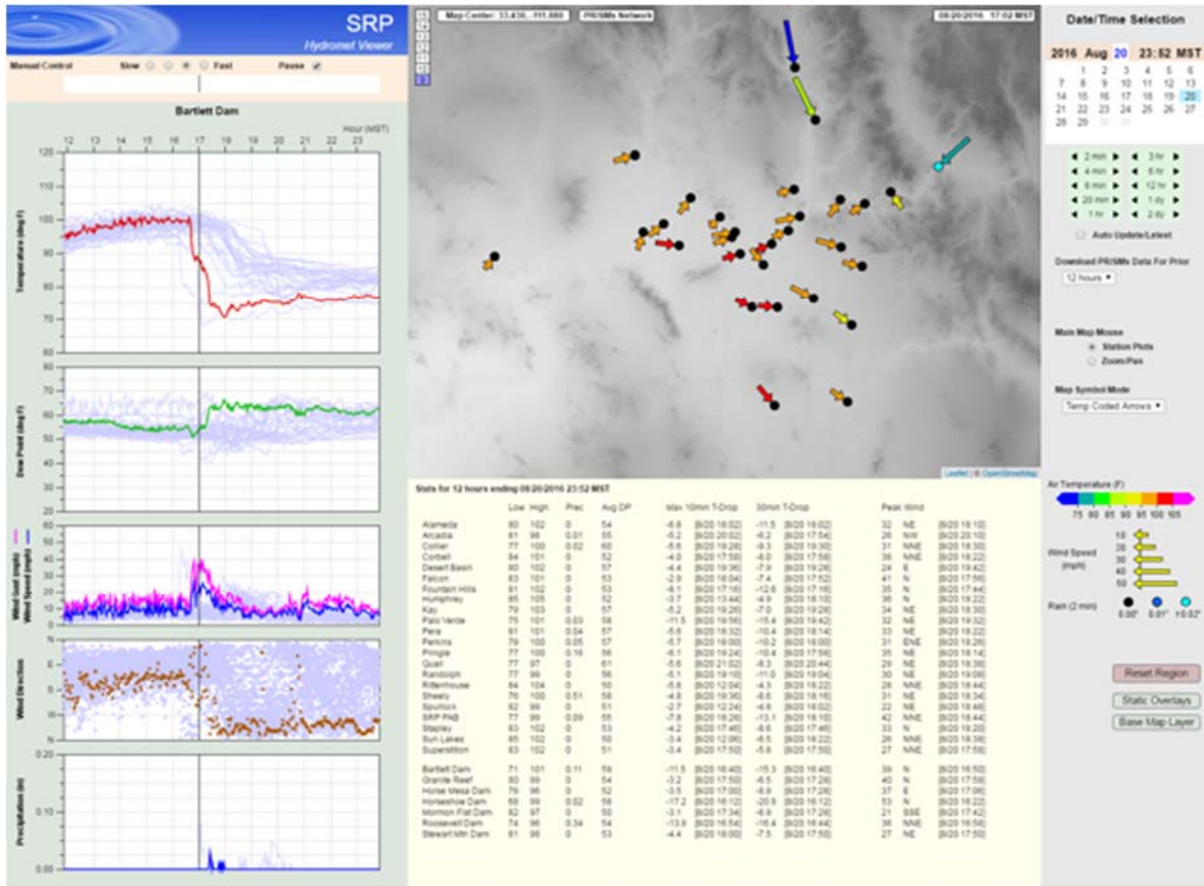
A PRISMS viewer is also available where the user can select from 1-h to 24-h worth of data from any time in the archive. The map shows the data in a spatial layout. There are also time series plot for many variables. The plots for the entire network are plotted in a subtle grey tone which shows at a glance the behavior of the entire network as a whole. But then one can highlight each station in turn and those plots stand out on top of the network background allowing one to quickly assess visually how that station compares with the rest. There is an entire section of important statistics such as high and low temp and time, direction and size of peak wind gust. And the entire data set can be animated in a time loop on the map allowing one to follow cool outflows and wind shift lines across multiple stations.



Sample image from the lightning strike display of the Salt River Project Hydromet Viewer. 24 hours of strikes are shown and color-coded for the time of day.



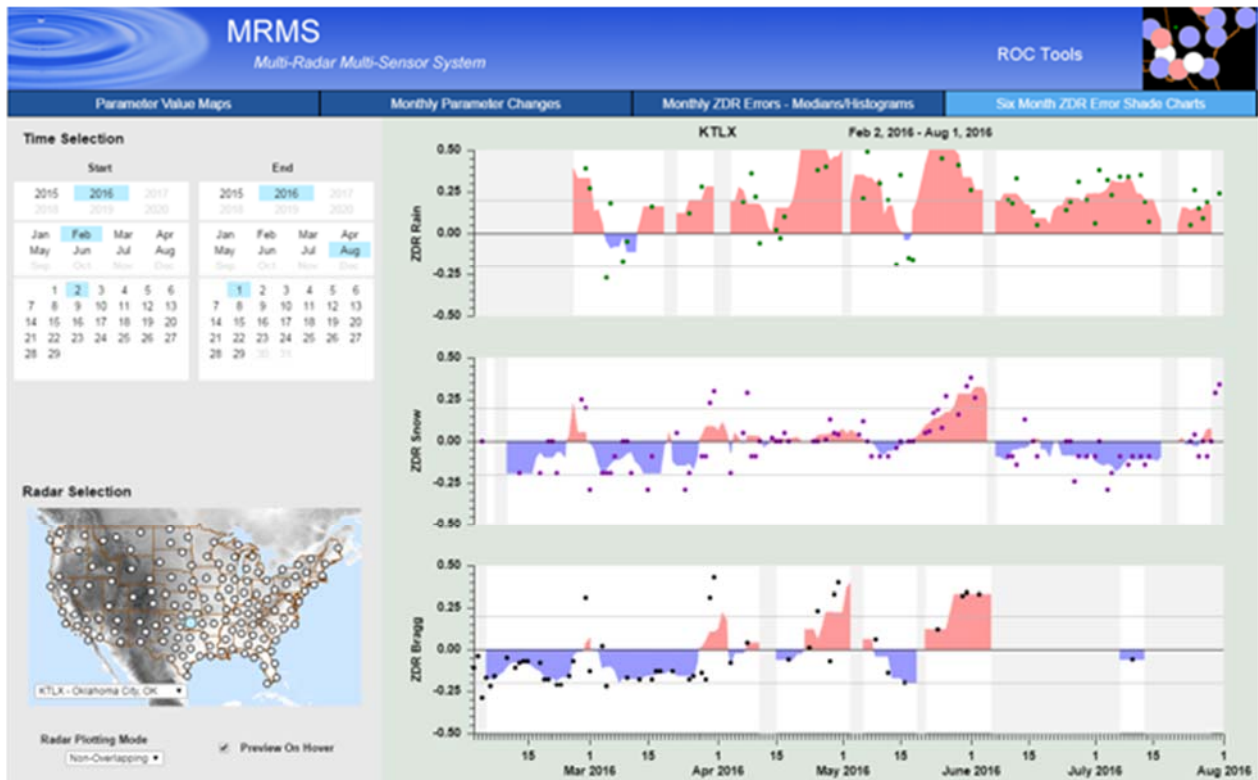
Sample screen from the reservoir and stream monitoring tool.



Sample screen from the PRISMS viewer.

b. Level 3 Adaptable Parameter Display Maintained for the Radar Operations Center

There was continued maintenance and minor work done on the suite of tools for monitoring the Level 3 single radar metadata. The code was updated to the latest techniques and libraries being used for QVS generally. And one major new tool was added. The Radar Operations Center (ROC) has historically generated a long time series of daily ZDR error values for all the WSR88D radars via three different methods. Plots of these time series could be viewed with a login at the ROC Hotline webpage. They had a very specific style of plot with daily points and a color-coded seven day running average that they referred to as a 'shade chart.' Our new tool greatly automated and simplified the process for generating these images. It allows users to view data for a user selectable time period instead of just the last 6 months and the navigation allows many radars to be viewed in rapid succession.



Sample view of the Level 3 adaptable parameters viewer

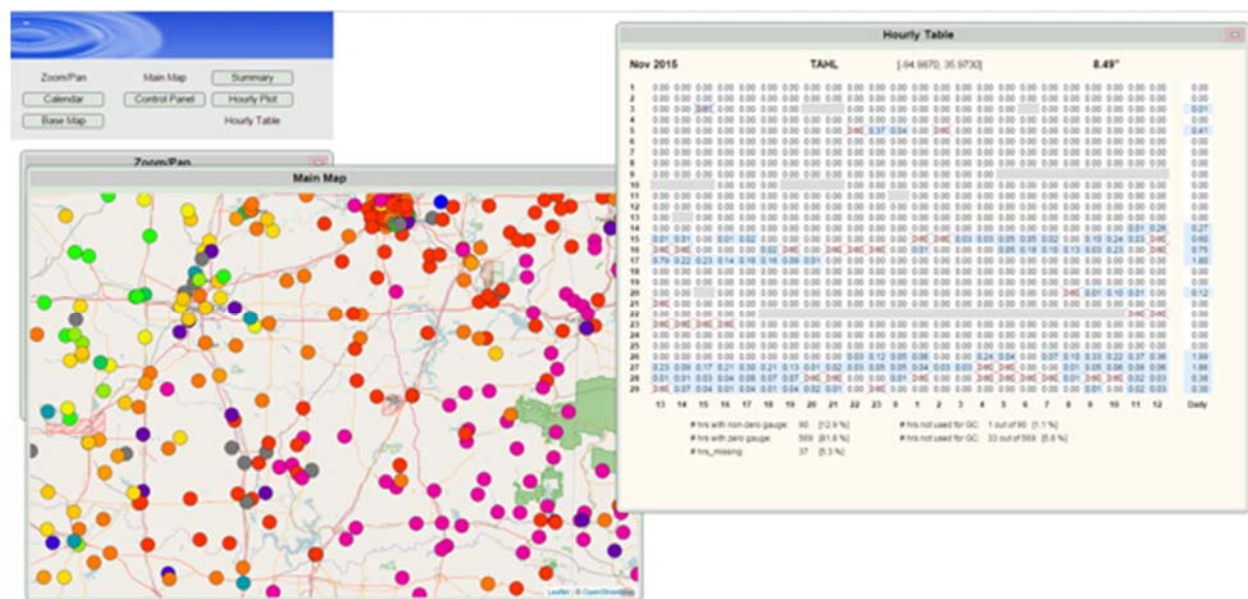
c. QVS Work for the Local VMRMS and Operational Version at the NCO

The QVS acronym originally came from QPE Verification System, where QPE itself stands for Quantitative Precipitation Estimate. Evaluating our precipitation products against other fields and ground truth is still a core purpose of the QVS. But as our methods for creating a precipitation field rely on many inputs there are also many variables, fields, and observations that can be brought to bear on post analysis. As such the term QVS has been used for a wide variety of web tools that aid our analyses in many different ways.

In FY2015, a significant overhaul was begun of the code libraries, web strategies and framework underlying the QVS. Much work has been completed but the process is ongoing and much remains to be finished. The latest QVS MRMS web maps are now built in layers which can include a Google or Open Street Maps base layer along with MRMS products and a variety of overlays and custom tool layers. The page is no longer constantly reloaded from scratch in response to a form submit button but instead only updates the minimum portion needed to respond to the user request. In technical terms, the web tools are now more fully AJAX applications, with the use of web services that return a JSON object.

FY2016 brought an expansion of the MRMS coverage into several domains outside the CONUS. In particular, there is coverage for Alaska, Hawaii, Guam and parts of the Caribbean. Prototype work is also being done with radar data from Korea.

A major QVS addition in FY2016 is the ability to view and assess the new QC flags that have been developed for precipitation gauges when they are used in the MRMS gauge adjusted radar QPE product. These flags are generated hourly for several thousand gauges across the CONUS. A new tool in the QVS allows one to look at the hourly gauges for an entire month for a given gauge and see a detailed report of the precipitation and the QC flags. Many gauges in the same region can be queried easily with a variety of ways to view the data.



Sample image of gauge display with gauge observations color-coded to precipitation value and a monthly table of hourly values for a specific gauge. Observations overlaid by a red 'X' means the value was removed by QC.

CIMMS Task III Project – ARRC R&D Activities for the Multi-Mission Phased Array Radar Program

NOAA Technical Leads: Chris Curtis, Sebastian Torres, and Igor Ivic (CIMMS at NSSL), Richard Doviak, Kurt Hondl, Allen Zahrai, and Dusan Zrnica (NSSL), and Mark Weber (CIMMS/NSSL IPA)

NOAA Strategic Goal 2 – Weather Ready Nation: Society is Prepared for and Responds to Weather-Related Events

Funding Type: CIMMS Task III

Overall Objectives

Develop several complementary technologies that are essential to the forward progress of multi-mission phased array systems. The projects described below are ongoing.

1. Effects of Transmit Schemes on Polarimetric Variables

Boon Leng Cheong and Nik Luetkemeyer (OU ARRC/ECE), and Igor Ivic (CIMMS at NSSL)

Objectives

Develop, implement and evaluate the feasibility of increasing polarimetric isolation between the horizontal and vertical channels using non-traditional transmit schemes, as one of the key requirements of the MPAR is the collection of polarimetric variables. Data collection using patched antennas presents a significant challenge in order to achieve cross-polar isolation on the orders of 30 dB like traditional dish reflectors. One solution to improve this deficiency is by using a transmit scheme that can help improve the isolation/minimize the coupling. For example, one could alternately transmit H & V pulses in order to reduce the cross-channel contamination (known as the AHV mode). Unfortunately, the AHV mode of operation presents numerous other challenges. The most important is that we would lose half of the samples and, thus, obtaining the dual-polarization variables with required quality while maintaining unambiguous range of ~300 km is extremely challenging. An alternative is to energize the V channel port immediately after the H port, referred to as the quasi-simultaneous horizontal and vertical (QSHV) transmission. Direct comparisons were made to the standard simultaneous horizontal and vertical (SHV) transmission.

Accomplishments

The digital transceiver of the PX-1000 was upgraded to perform the QSHV transmit scheme. Several datasets were collected using the PX-1000. It has been demonstrated that QSHV can be achieved in hardware and appreciable difference in ZDR measurements could be obtained (see Figure 1 below). A conference presentation was delivered at the 37th Conference on Radar Meteorology.

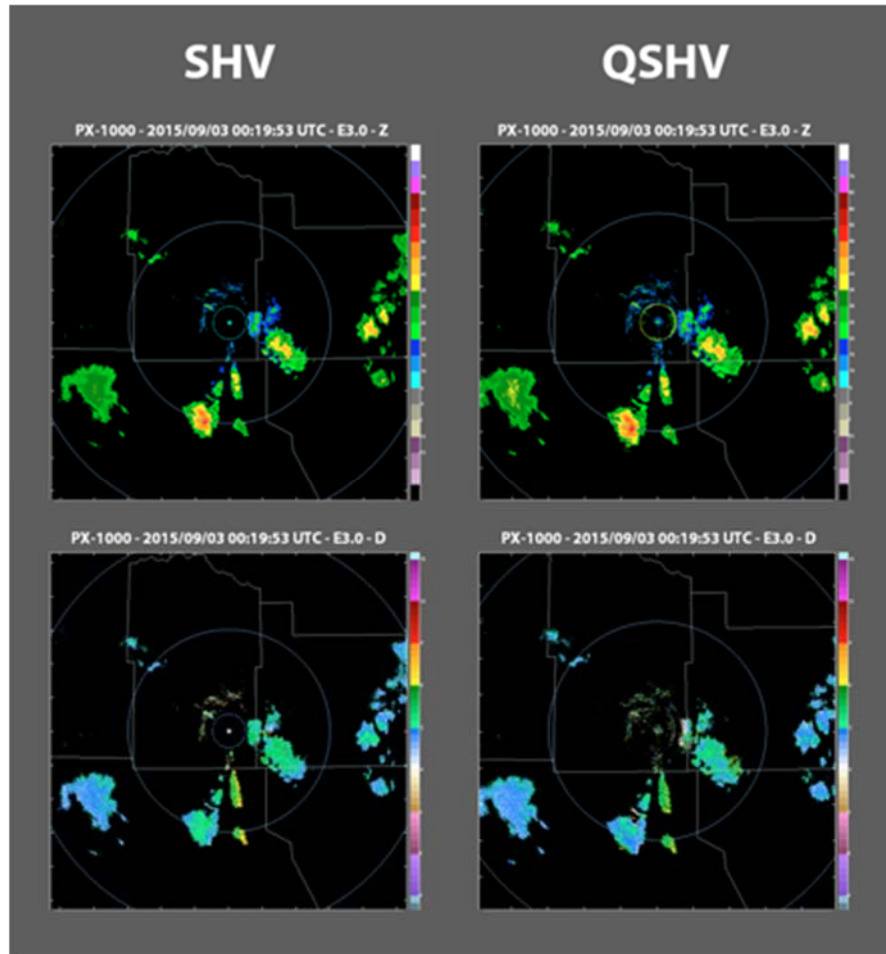


Figure 1. Comparison of the SHV and QSHV transmit schemes. The measured ZDR shows a significant difference, which corresponds to a lower bias.

2. Meeting the MPAR Timeline Using Simultaneous Receive Beams – The Role of Adaptive Beamspace Processing

Robert Palmer (OU ARRC/School of Meteorology/ECE), Sebastian Torres (CIMMS at NSSL), and Feng Nai (OU ARRC/ECE)

Objectives

The future MPAR system is required to concurrently perform aircraft and weather surveillance functions with update times of 4.8 seconds and one minute, respectively. To meet these demanding update-time requirements, an MPAR system will likely employ multiple simultaneous beams. One way to achieve this is to transmit a spoiled beam and use digital beamforming to form multiple simultaneous receive beams. However, this solution has difficulties in meeting the data-quality requirements for weather observations due to increased sidelobe levels in the two-way radiation pattern compared to similarly sized dished antennas. An alternative solution is to use adaptive beamforming so that the sidelobe levels are automatically lowered in the directions with significant weather return. Traditional adaptive beamforming algorithms are

computationally expensive, and their adaptive patterns cause significant challenge for reflectivity calibration. As a result, a calibrated and computationally efficient adaptive beamforming algorithm must be developed to help future MPAR system to meet its update-time and data quality requirements simultaneously.

Accomplishments

Adaptive beamspace processing has been proposed as an adaptive beamforming algorithm for phased-array weather radars that can produce accurate and calibrated estimates of weather radar variables while automatically rejecting interference signals from directions other than the pointing direction of the beam. Instead of operating on data from the receiving elements, adaptive beamspace processing first forms a set of deterministic beams and adaptively combines the output of these initial beams to perform interference rejection. Correlation between the output of the initial beams and their signal power are used to constrain the magnitude of the adaptive weights to prevent the algorithm from canceling the weather signal of interest. The initial beams also help to shape the final beam pattern to meet the assumptions required for calibration (i.e., estimating reflectivity from received signal power). Simulations have shown that adaptive beamspace processing can produce estimates of weather radar variables with small biases when compared to estimates produced by a system with a rotating dish antenna as shown in Figure 2 below. Furthermore, the adaptive algorithm has superior performance in reducing the impact of interference signal when compared to that of non-adaptive methods. The top panel of the figure shows the signal power estimates for a dish antenna system (black), Fourier beamforming, (blue), Capon beamforming (red), and adaptive beamspace processing (green). It is clear that Capon beamforming produces estimates that are negatively biased and the biases are not constant. The estimates of the other three methods are very similar except near the interference signal located at 0 degrees, where adaptive beamspace processing successfully mitigated the impact of the interference at angles near 0 degrees. The bottom panel shows the delta biases of the estimates of Fourier beamforming and adaptive beamspace processing, where the dish-antenna estimates are used as ground truth. This shows that the estimates produced by adaptive beamspace processing are close the dish-antenna estimates, and the delta-biases are less than 1 dB for the majority of steering angles. Doppler velocity and spectral width estimates show similar behavior. Figure 3 below shows an example of adaptive beamspace processing using real data collected by the Atmospheric Imaging Radar (AIR). It can be clearly seen that adaptive beamspace processing successfully mitigated the ground clutter contamination at higher elevations (due to the fan shaped transmit beam of the AIR) where aggressively tapered Fourier beamforming failed.

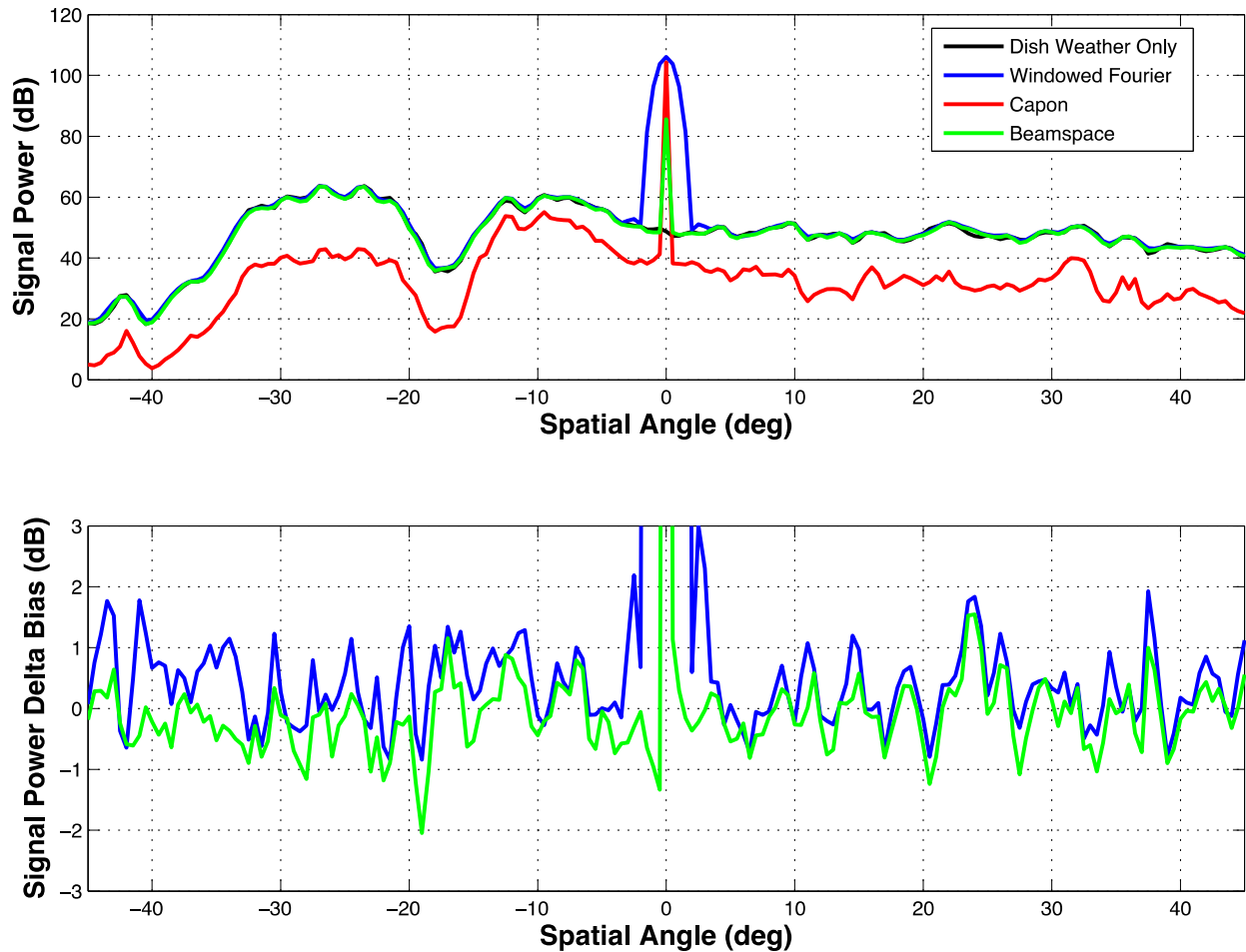


Figure 2. Mean signal power estimates (top panel) and signal-power delta bias (bottom panel) for the different beamforming methods from Nai et al. (2016), ©2016 IEEE. Capon beamforming has excellent interference rejection (the peak at 0 degrees is narrow), but its signal power estimates are significantly biased. The dish-weather-only (black line) estimates are covered up by the beamspace estimates except near 0 degrees. The windowed Fourier method and adaptive beamspace processing estimates have similar delta biases, but adaptive beamspace processing has superior interference rejection.

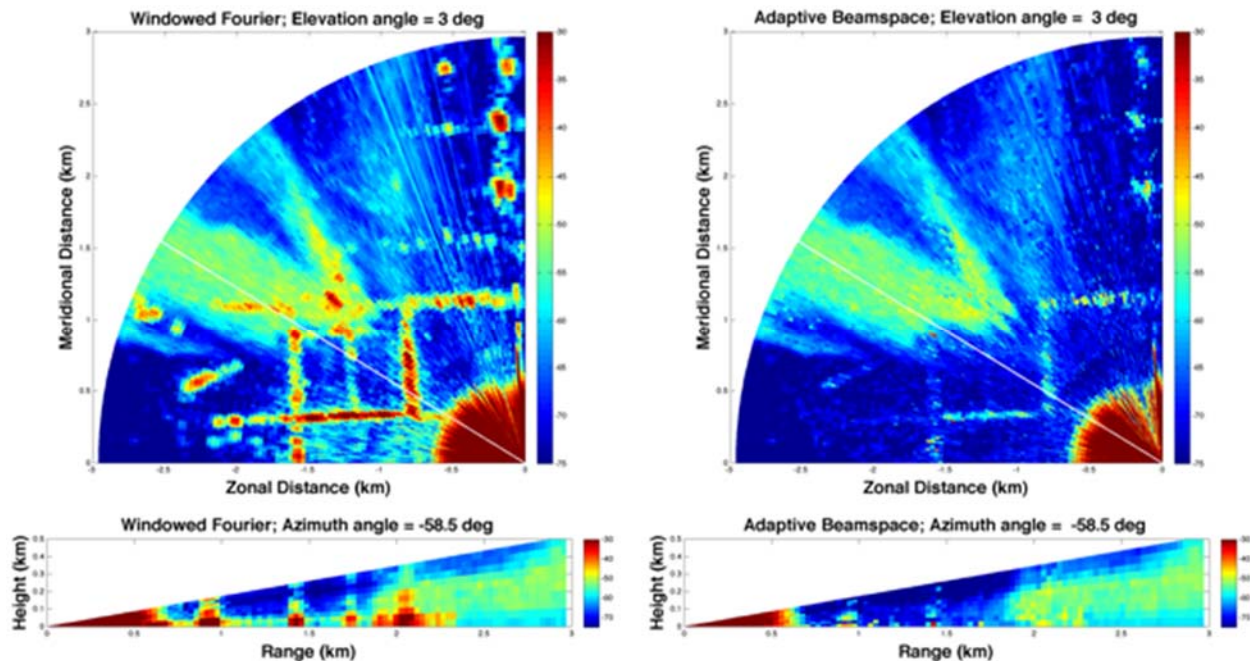


Figure 3. Real data example of adaptive beamspace processing from Nai et al. (2016), ©2016 IEEE. PPI and RHI fields corresponding to adaptive beamspace processing and windowed Fourier beamforming on data collected with the AIR on 16 May 2015 near Tipton, OK. The PPI plot shows the received signal power at 3 degrees in elevation, and the white line in the PPI plots indicates the azimuthal angle of the RHI plots. It can be clearly seen that adaptive beamspace processing successfully rejected the majority of the ground clutter signal that originated from lower elevation angles, and it performed much better than windowed Fourier beamforming.

3. Pulsed Interference Filters for MPAR

Mark Yeary and John Lake (OU ARRC/ECE), and Christopher Curtis (CIMMS at NSSL)

Objectives

The goals of this project were to analyze and improve various radio frequency interference (RFI) detection and mitigation techniques. Five algorithms were tested: the Interference Spike Detection Algorithms (ISDA), the electromagnetic interference filter (EMI), and the three RFI detection algorithms outlined by Vaisala in the RVP8 User's Manual. Additionally, several methods of data recovery were tested: interpolation in fast time, interpolation in slow time, and replacement.

Accomplishments

Multichannel receiver data collected from the National Weather Radar Testbed phased array radar was filtered for ground clutter, and a region containing, but not exclusively comprised of, weather was selected (see Figure 4). Subsequently, RFI with a known interference to noise ratio (INR) was injected at known locations into this data in locations with and without weather echoes present. This corrupted radar data was

subsequently fed to each of the algorithms, which performed RFI detection and RFI mitigation tasks (see Figure 5). The algorithms were not given any prior knowledge about the presence, strength, or location of RFI.

After execution of the algorithms, the radar data was processed as usual. Because the location and strength of the RFI was known to the researchers, statistics could be gathered and algorithm performance measured in statistics including probability of detection and bias.

Examinations of the statistics gave insight into algorithm performance, at least for the data set used. For probability of detection, at stricter false alarm rates, EMI performed best, followed by ISDA and then the three Vaisala algorithms; at less strict false alarm rates, ISDA outperformed the other algorithms (see Figure 6). In terms of bias remaining after data interpolation, all algorithms significantly reduced the bias left in the data. EMI and ISDA outperformed the Vaisala algorithms, and had a relatively flat performance with respect to INR, whereas the bias in the Vaisala algorithms increased with increasing INR (see Figure 7). Data recovery via slow-time interpolation (i.e. interpolation across pulses) seemed to perform better than simple replacement and fast-time interpolation (i.e. interpolation across range gates).

More work is still in progress. A better characterization of algorithm parameters and their relation to probability of false alarm is being undertaken, as is work on how phase-coded algorithms would be affected by these RFI mitigation algorithms.

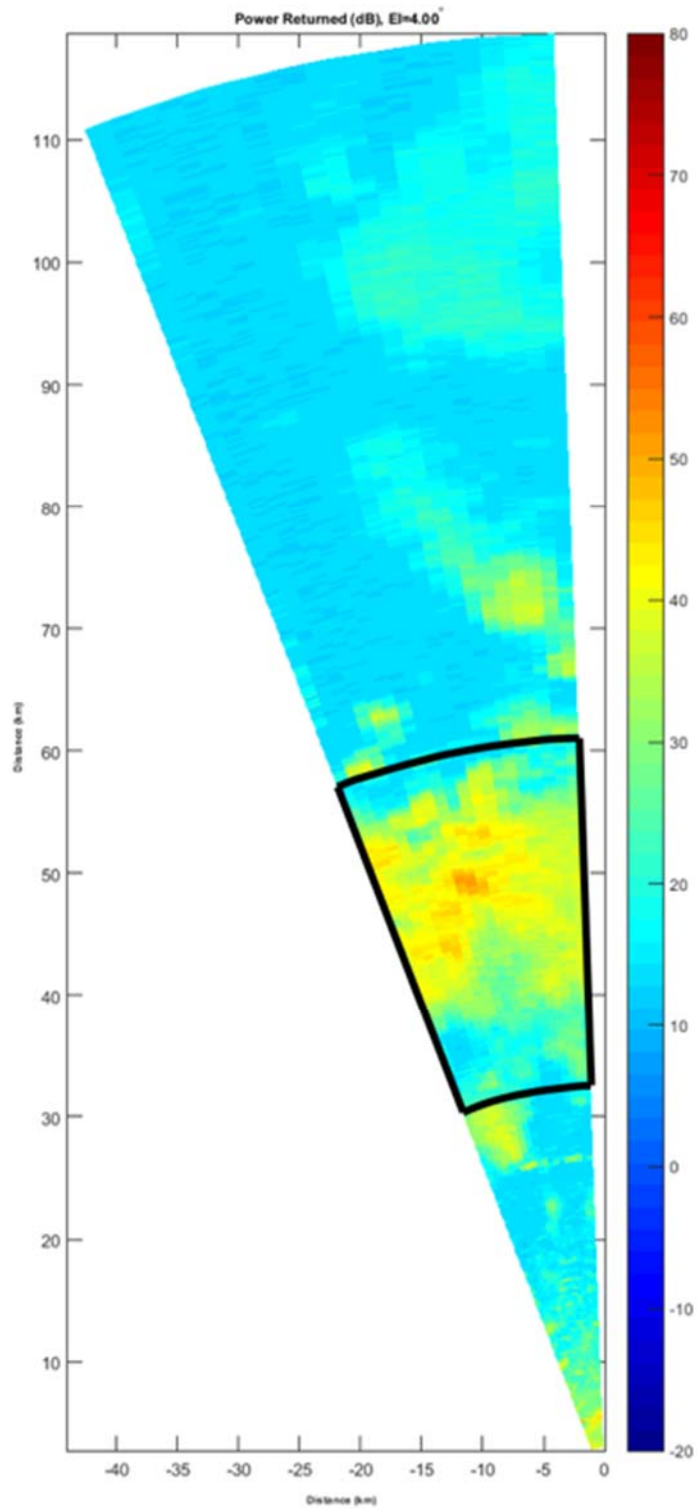


Figure 4. Data collected from the NWRT was filtered to mitigate ground clutter and a region comprised mostly of weather was selected.

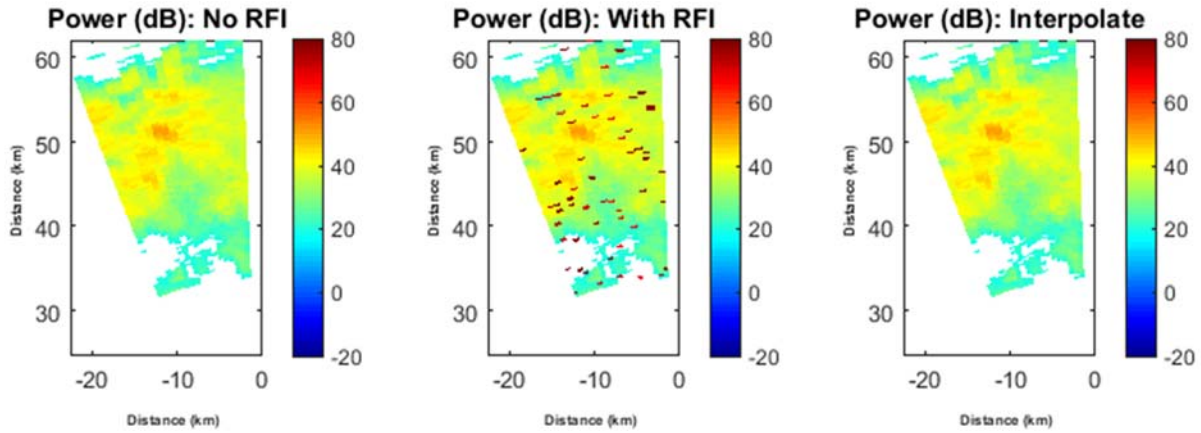


Figure 5. The data in this region (left) was corrupted with additive RFI at random locations and with random phase (center left). This corrupted data was given to a variety of RFI mitigation algorithms, which worked to eliminate the RFI, recovering the data (right).

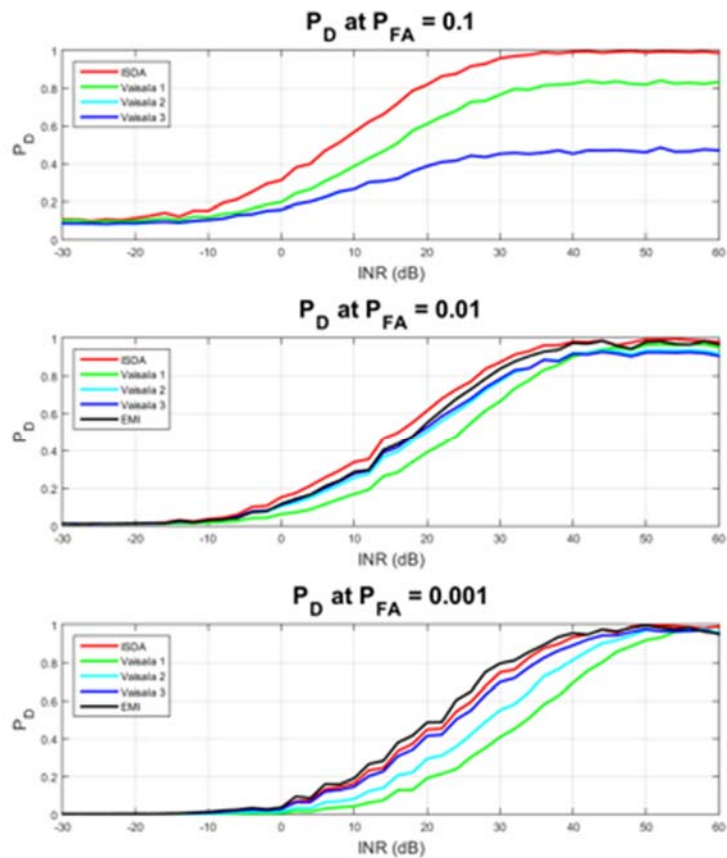


Figure 6. Because the location of the injected RFI was known, statistics on the probability of detection with respect to the probability of false alarm for the different algorithms could be collected. The EMI algorithm is not on the top graph because the probability of false alarm cannot be set to be less strict than 0.01.

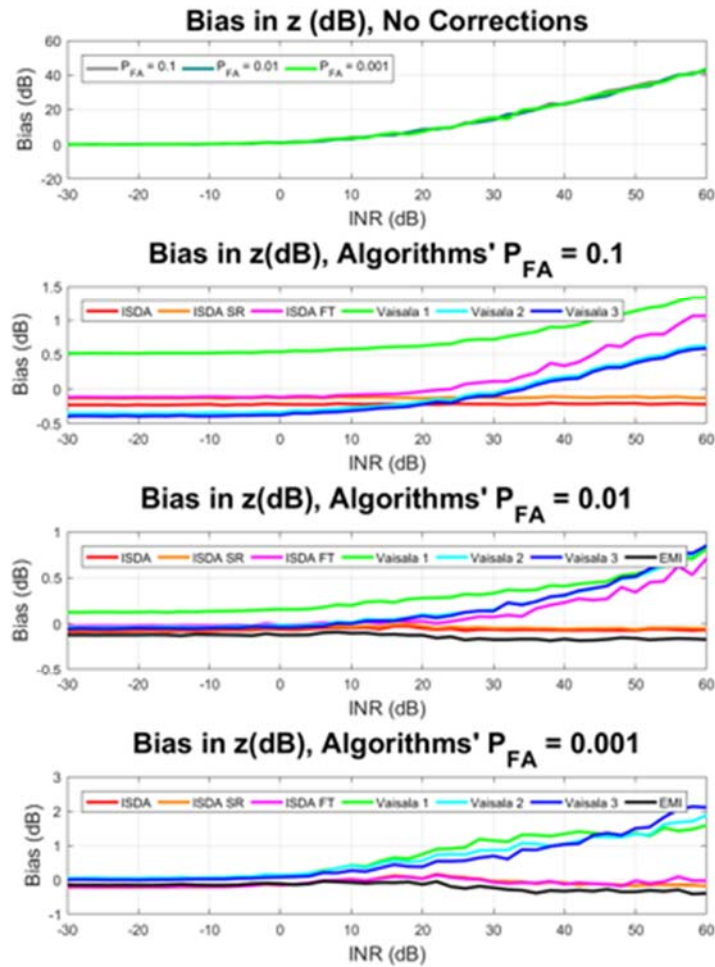


Figure 7. All algorithms tested did a good job of reducing the bias left over in the radar data. The Vaisala algorithms tended to have the most lingering bias after data recovery, though using fast-time interpolation seemed to also introduce problems at less strict false alarm rates. The EMI algorithm and the slow-time and simple replacement ISDA algorithms had a leftover bias that did not depend on the RFI interference to noise ratio.

4. RF Filters for Improved MPAR Interference Protection

Hjalti Sigmarsson, Caleb Fulton, and Shahrokh Saeedi (OU ARRC/ECE)

Objectives

In this task, the possibility of embedding RF filters into a phased array radar front-end module is being investigated. Substrate-integrated cavity filters are being embedded into the bottom two layers of the antenna stack-up without affecting the antenna performance but still providing significant improvement in the out-of-band interference rejection. The goal is to design filters that operate at 2.85 GHz, cover the entire band of

interest from 2.7 to 3 GHz, and add more than 30 dB of additional rejection while maintaining low loss. The full specifications of the filters are shown in the table below.

Filter specifications

Parameter	Target Value
Center Frequency	2.85 GHz
Bandwidth	350 MHz
Fractional BW	12%
Insertion Loss	< 1 dB
Rejection @ $(1 \pm 0.15) f_0$	> 30 dB

Accomplishments

The first step was to design a building block or a single embedded resonator. The resonator is formed by created plated vias through the substrate that form the walls of the cavity. Surface mount capacitors are used to load the cavity in order to miniaturize it. The current design is only 12.5 mm in diameter and still is able to achieve a measured quality factor greater than 150, which is sufficient for the desired insertion loss of less than 1 dB. Figure 8 shows a simulation model and the fabricated resonator prototype as well as the measured versus simulated frequency responses. The building block has been finalized and current emphasis is on the higher-order filter design.

In order to meet the desired specifications in Table 1, a fourth-order filter was selected. Two designs were synthesized: a traditional in-line configuration without any transmission zeros and an advanced configuration with strategically placed transmission zeros (Figure 9 and Figure 10).

The difference between the two designs is primarily in terms of the achievable isolation, where a 25 dB improvement is demonstrated at 2.4 GHz and nearly 13 dB at 3.3 GHz. The coupling matrix and the coupling routing diagram of the filter are shown in Figure 11, the simulation model in Figure 12, and the comparison between the synthesized filter response and the fullwave simulated results in Figure 13.

Current objective is to remove the second resonance within the cavity. Several methods have been explored which have resulted in various changed in the location and level of the second mode, but a complete solution has not been identified yet. The next steps are: changing the center post from a via cage to a large via and changing the shape of the post with the goal of moving the second mode while leaving the first mode unperturbed.

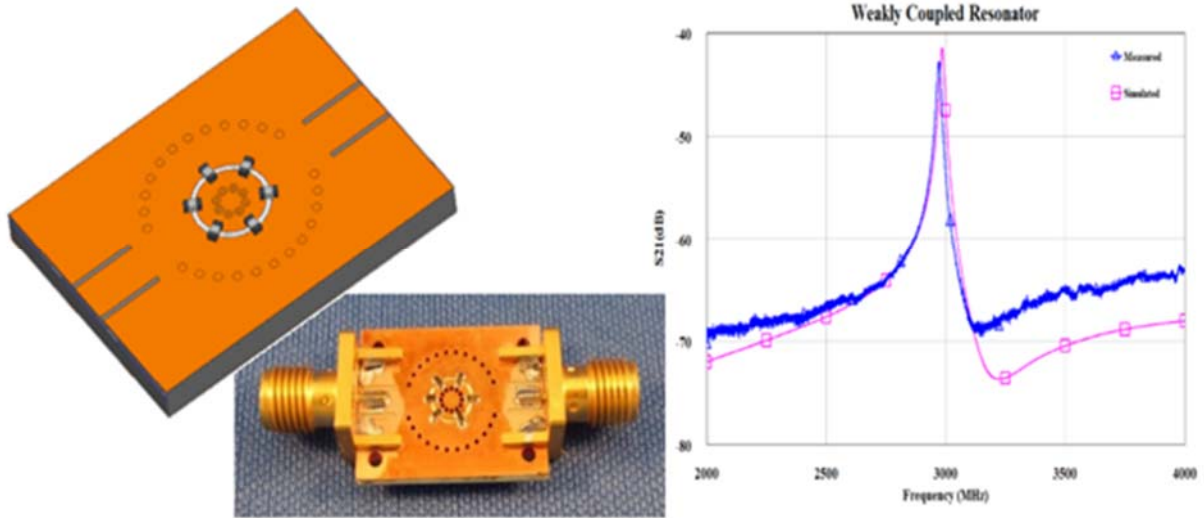


Figure 8. The evanescent-mode, substrate-integrated, cavity resonator used as the building block for the embedded filter design. Fullwave simulation model and the fabricated prototype on the left and the measured versus simulated frequency responses on the right.

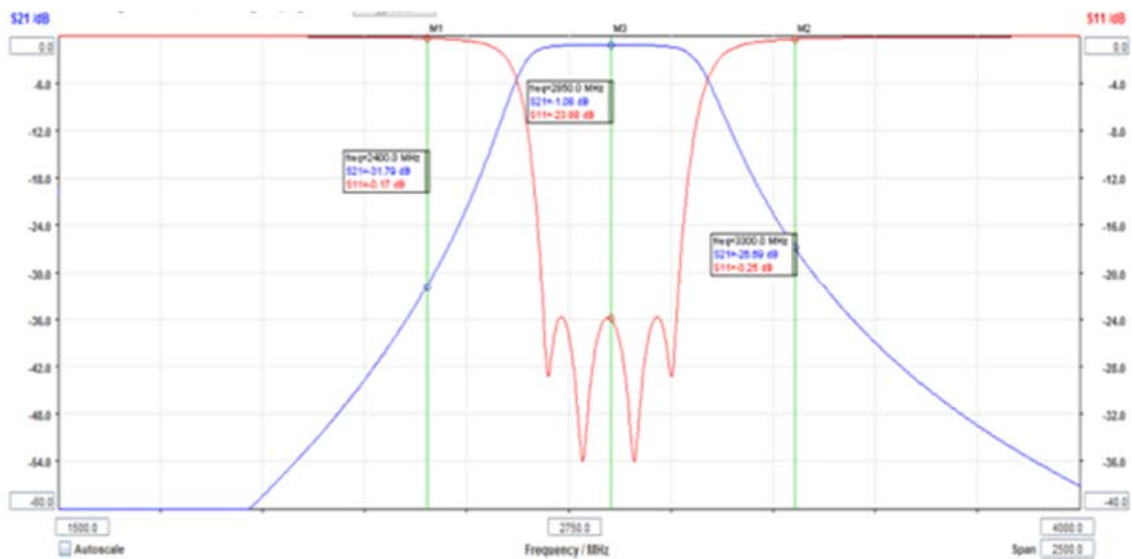


Figure 9: Frequency response of the synthesized 4th-order bandpass filter with no transmission zeros.

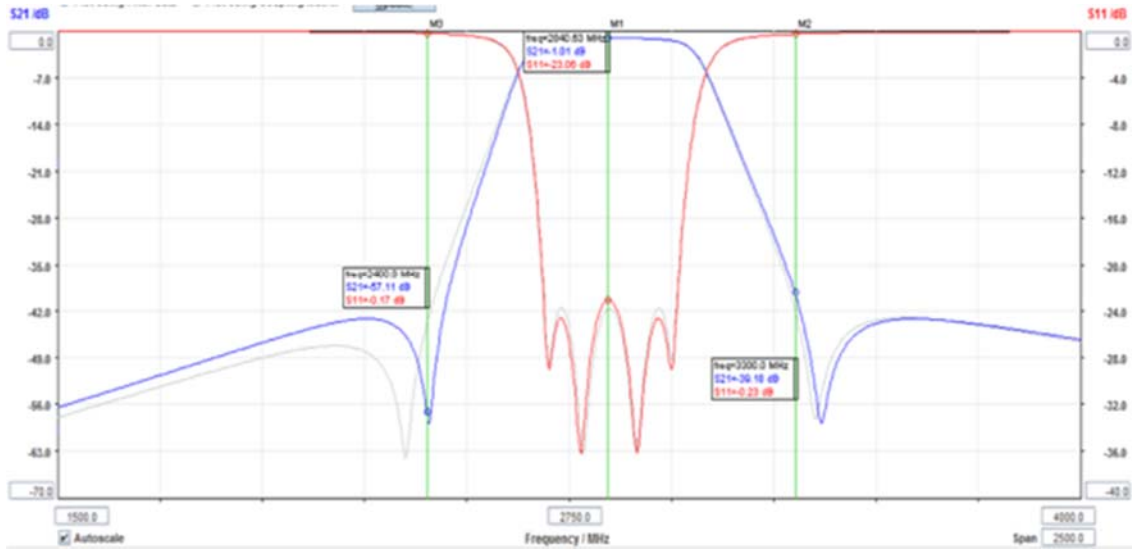


Figure 10. Frequency response of the synthesized 4th-order bandpass filter with two transmission zeros.

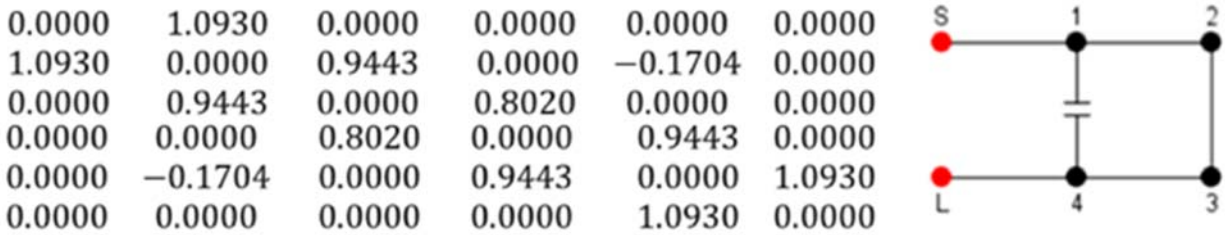


Figure 11. Coupling matrix and routing diagram for the 4th-order BPF with two transmission zeros.

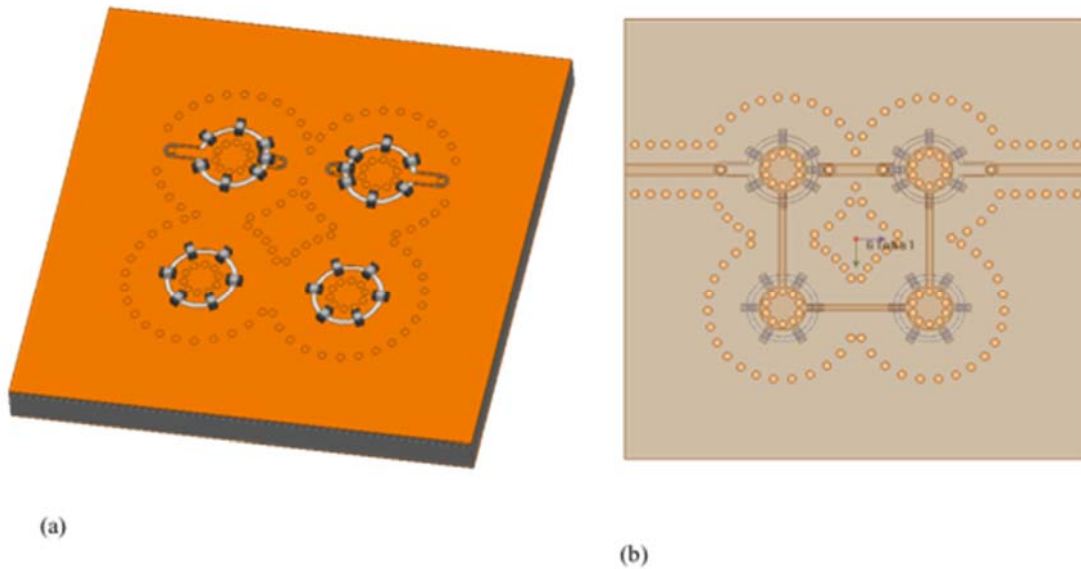


Figure 12. Capacitor-loaded SIW 4th-order bandpass filter model. a) 3D view, and b) top view.

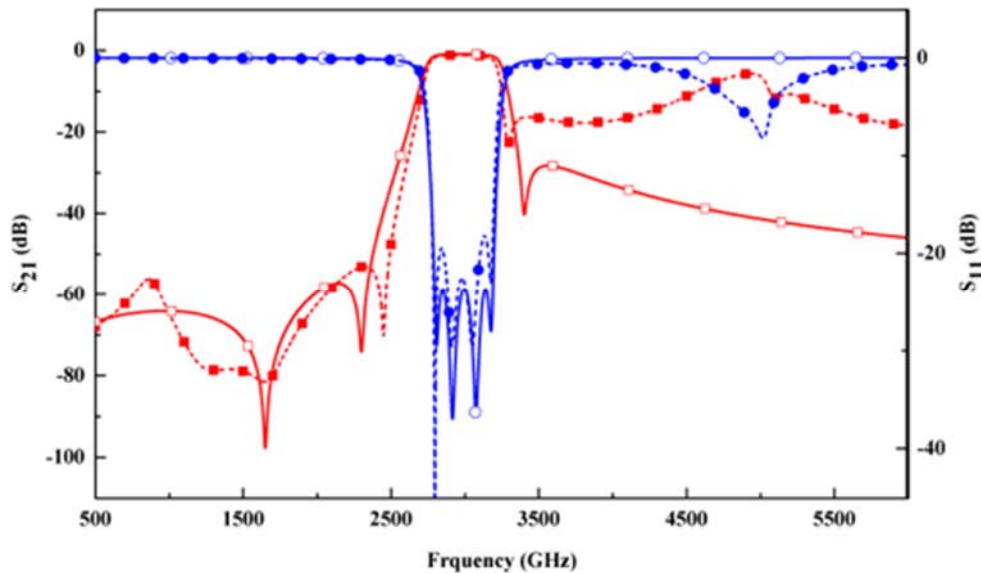


Figure 13. Frequency response of the 4th-order bandpass filter from EM simulation compared to synthesis.

5. Design and Characterization of a High-Performance S-Band Dual-Polarized Radiating Antenna Element Embedded in a Finite Array

Jorge Salazar, Caleb Fulton, and Jose Diaz (OU ARRC/ECE)

Objectives

The objectives of this project were to design and characterize a high performance dual-polarized S-band radiating antenna element in a finite array that will be part of a large-scale phased array radar for weather applications. In order to achieve high polarimetric performance over a desirable scanning range, our team included in the design and fabrication process several factors that mitigate the spurious radiation and help to improve the cross-polarization and matching of beam patterns at the element and array level. An antenna array was designed and prototyped to the operating band (2.7 - 2.9 GHz). The cross-polarization levels for the E-, D-, and H-planes is below -49 dB based on Ludwig's 3rd definition. Scanning performance of $\pm 60^\circ$ for all scanning ranges in the frequency band was achieved.

Accomplishments

Multiple factors in the antenna element were investigated during the design process of the 8x8 array in order to comply with the current antenna requirements of MPAR. These factors include: minimum spurious radiation from the feed network, a high degree of symmetry, large bandwidth, high port isolation, mitigation of reflected and diffracted fields at the internal and external edges of the array (large scale), mitigation of spurious radiation due to the excitation of higher modes, and a reliable fabrication process of the antenna boards. In order to prevent spurious radiation from the feed to the patches and allow high symmetry, a crossed aperture in the ground plane was used to excite the

principal and parasitic patch from the feed network. A fork feed network was designed for H and V in order to have a balanced feed. A high degree of symmetry at the element, subarray, and array level is taken into consideration to guarantee high cross-polarization and match antenna co-polarization patterns. A bandwidth of 10% was targeted to guarantee invariant impedance and gain loss for a large scanning range ($\pm 60^\circ$). A careful selection of antenna board materials was used in order to facilitate the PCB fabrication process and guarantee temperature stability under operation with high power amplifiers in the front-end modules. Two additional feed layers were incorporated in order to relocate the mechanical connections to the feed network of the array and provide more area for the electronics in the back of the array.

Figure 14a illustrates the mechanical stack-up, and Figure 14b shows the top view of the antenna element. Two subassemblies were considered, one for the antenna (based on Rogers 5880LZ) and the second one for the feed (based on Rogers 4350B). Figure 14c shows the return loss and isolation of an isolated antenna element. The overlapped bandwidth between the polarizations is roughly 400 MHz, and the isolation between the ports peaks at 2.97 GHz, around -48 dB.

Figure 15 shows numerical simulations in HFSS of radiation patterns for the antenna element. It is clear that the cross-polarization level across frequency is below -40 dB for both polarizations in the principal planes, with the exception of the V-polarization at 2.9 GHz. In the diagonal plane (D-Plane), levels are kept below -21 dB for all frequencies in a single element using the Ludwig-2 definition. The simulated active reflection coefficient (ARC) is presented in Figure 16. The element shows some degradation at the highest frequency (2.9 GHz); however, its performance exceeds the requirements for all scanning angles with reflections below -10 dB from 0 to $\pm 60^\circ$.

Measurements for the patterns were conducted in a far-field chamber using a customized NSI-RF-WR284 waveguide probe that operates in a frequency range from 2.6 to 3.95 GHz. A customized fixture (see Figure 17) constructed of high performance Rohacell 110 IG/A with a dielectric constant of 1.12 was used to support the array on a pedestal. This feature minimized reflections and disruption of patterns on the specular region of the far-field chamber. The antenna was attached to a solid aluminum plate that extended 1 inch from the border of the array, and the patterns were obtained at 3.0 GHz. Measurements for both polarizations were taken while exciting the two middle rows on the 8x8 array. Figure 18 shows the measured co- and cross-polarization patterns using Ludwig's 3rd definition. It can be seen that the cross-polarization level is below -44.5 dB for both polarizations in the measured planes from 45° in azimuth.

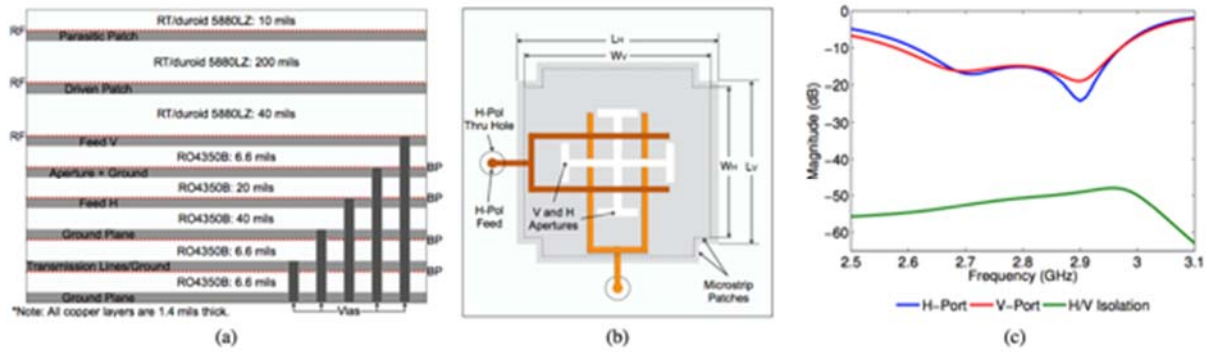


Figure 14. ARRC's Horus antenna element stack-up (a), top view (b), and S-parameters (c). The driven patch dimensions are $L_v = 32.7$ mm and $W_v = 22.7$ mm. For the parasitic patch, $L_h = 33.9$ mm and $W_h = 23.9$ mm. RF and BP refers to different prepreg layers. Drawings not to scale.

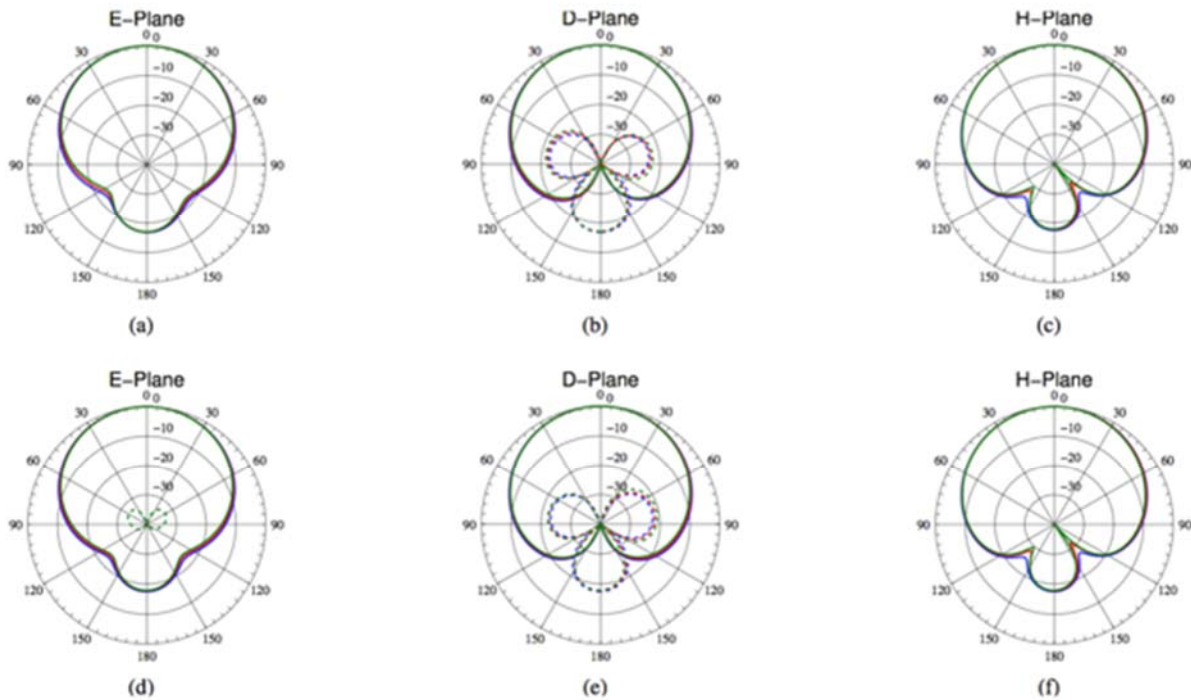


Figure 15. Simulated patterns for both H- (top row) and V-polarizations (bottom row) for the antenna. Solid (--) and dashed (--) lines refer to co- and cross-polarization, respectively (2.7 Blue, 2.8 Red, and 2.9 GHz Green).

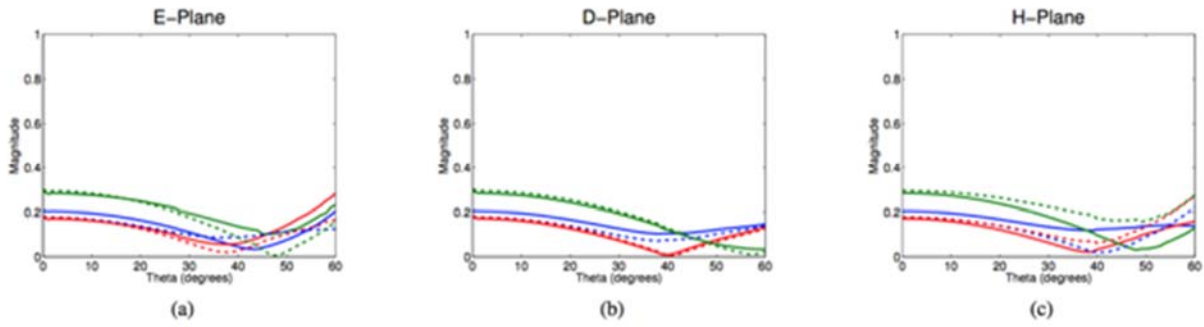


Figure 16. Simulated active reflection coefficients (ARCs) for the antenna, both H- and V-polarizations. Solid (–) and dashed (– –) lines refer to H and V (2.7 Blue, 2.8 Red, and 2.9 GHz Green). The unit cell size is 50.8mm on each side.

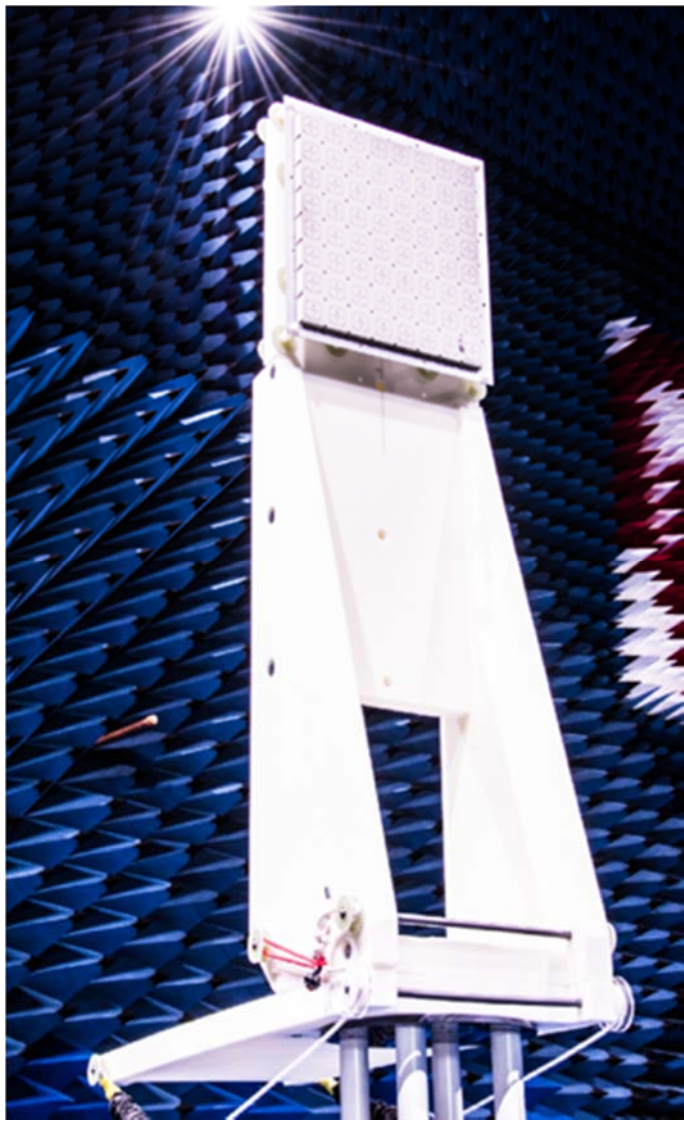


Figure 17. Antenna fixture in the ARRC's far-field chamber at The University of Oklahoma to measure the 8x8 array.

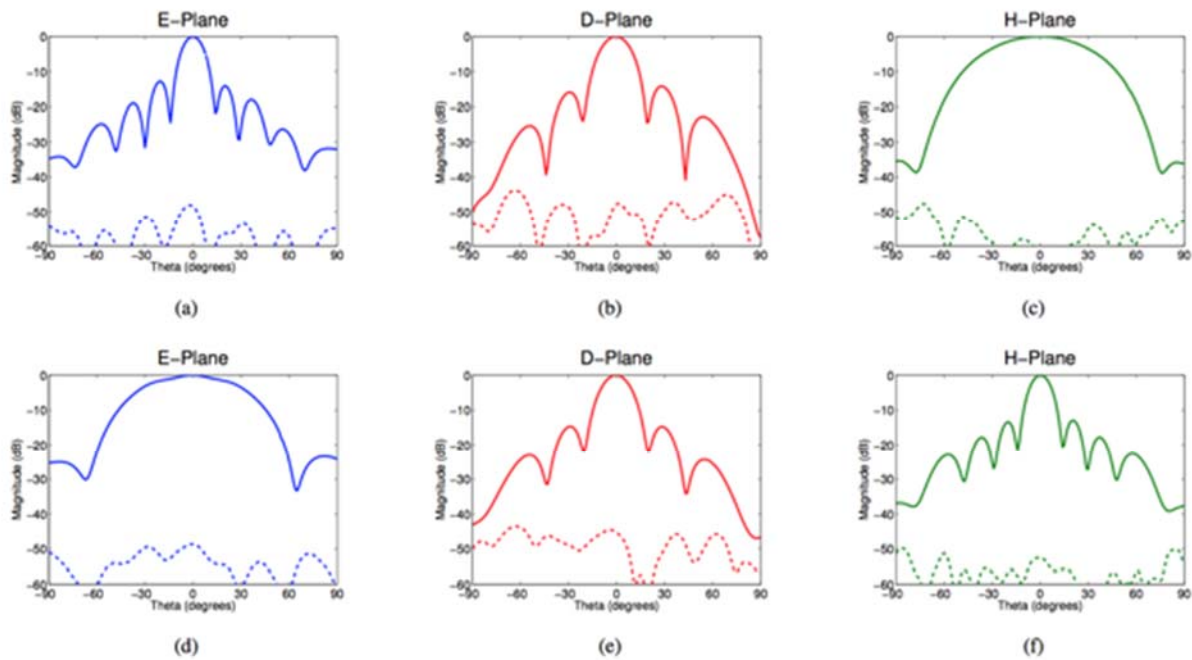


Figure 18. Measured patterns of Horus 8x8 array at 3 GHz while exciting the two middle rows for H-(top) and V-polarizations (bottom). Solid (—) and dashed (---) lines refer to co- and cross-polarization, respectively.

6. Electromagnetic Dipole-Based Dual-Polarized Radiating Elements – Improvements on the LMCO Design

Ridhwan Mirza and Yan (Rockee) Zhang (OU ARRC/ECE), and Dusan Zrnica and Richard Doviak (NSSL)

Accomplishments

The team has characterized and successfully improved the original EM dipole design from LMCO. Initial measurements and simulations validated the expected EM dipole radiating performance (Figure 19). More measurements and calibrations for array tests are needed in future studies. The graduate student supported through this study graduated with an MS degree in May 2016 and now works as an antenna engineer for a prestigious company.

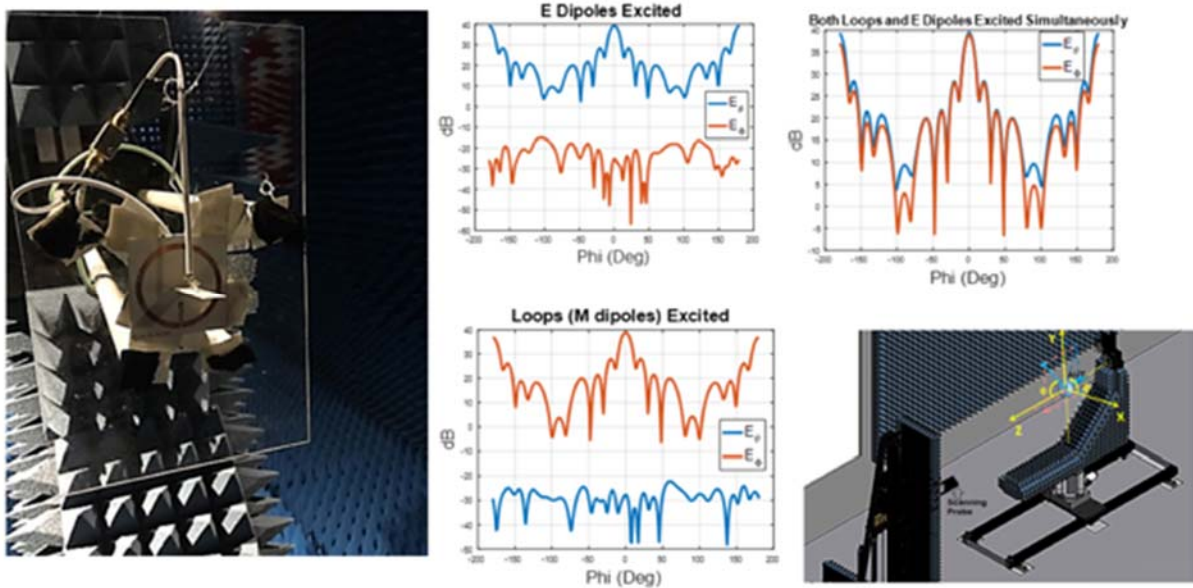


Figure 19. Electromagnetic dipole performance and measurements.

7. Impacts of Array Manifold on Polarimetric Steering Array Patterns – Comparative Measurements and Numeric Simulations

Sudantha Perera and Yan (Rockee) Zhang (OU ARRC/ECE), and Dusan Zrnica and Richard Doviak (NSSL)

Objectives

The team has performed scalable array system modeling and performance predictions using advanced computational EM tools and small-scale chamber measurements, and has undertaken a comparison of simulations and measurements.

Accomplishments

First, the FDTD algorithm for the non-orthogonal grid was implemented and successful simulation data has been collected. This simulation program can also be used in simulating faceted-cylindrical phased arrays (Perera 2016). Even though planar arrays and fully conformal arrays are successfully simulated using the FDTD algorithm for rectangular coordinate and cylindrical coordinate systems, respectively, this further improvement of our own CEM tool can be useful in many MPAR-related missions. Second, a new version of the CPPAR column antenna was measured in the far-field chamber. The measurements are plotted in different scanning directions. The NEXRAD feed antenna is also acquired, and will be used in CPPAR outdoor measurements. Third, in order to implement a new initial alignment algorithm for CPPAR, the existing python program was analyzed and a new software system design was initiated. The data was taken and analyzed for individual channel transmit and receive. Fourth, more small-scale modeling in near field measurements and derivation of knowledge for future CPPAR development was performed. Further validation of CEM simulation has been achieved (Figure 20).

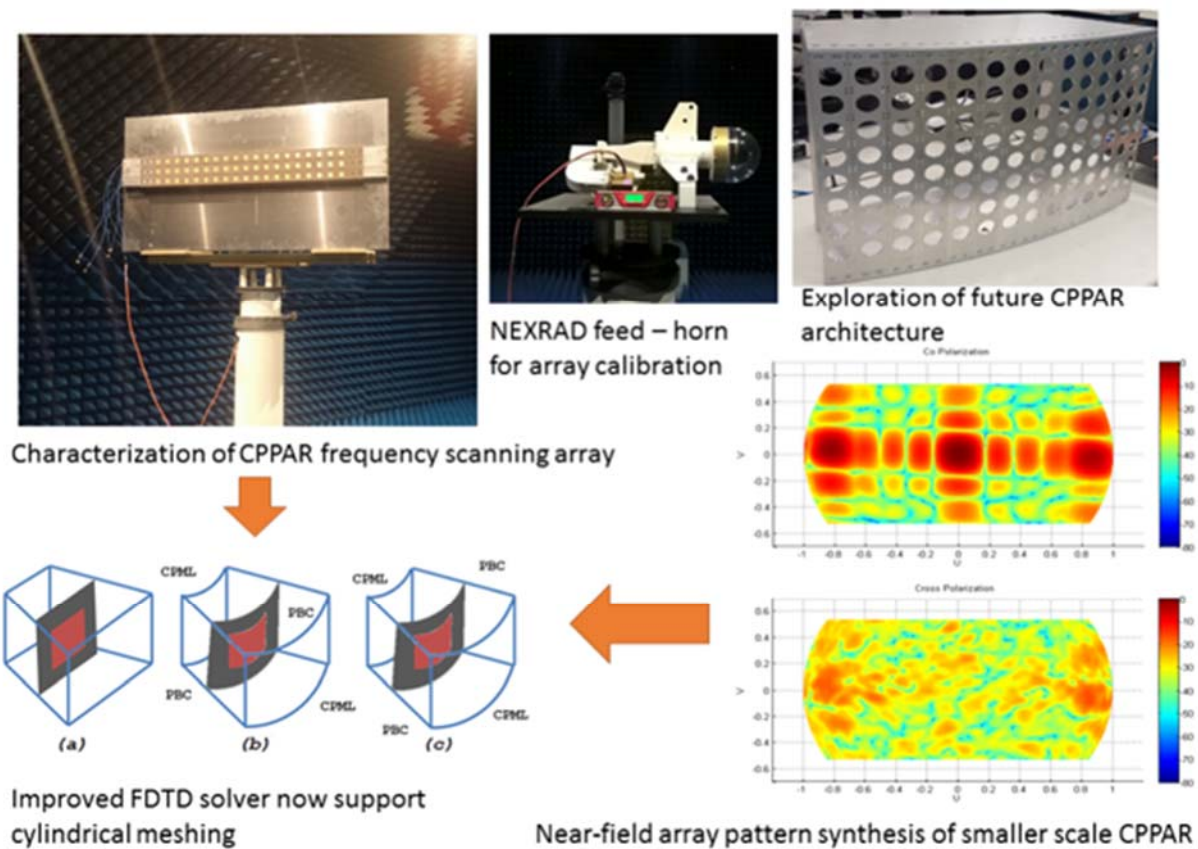


Figure 20. Summary of array system modeling and validation studies.

8. Impacts of Array Manifold on Polarimetric Steering Array Patterns – Comparative Measurements and Numeric Simulations

Xining Yu, Ankit Patel, Yan (Rockee) Zhang, and Hernan Suarez (OU ARRC/ECE), and Mark Weber and Allen Zahrai (NSSL)

Objectives

Investigate parallel MPAR backend signal and data processing schemes with a Serial-RapidIO based processor testbed and comparison with FPGA/GPU based options.

Accomplishments

The team has successfully achieved the FY16 project goal via the following. First, development of a new and scalable MPAR backend system testbed based on High Performance Embedded Computing (HPEC) architectures and serial RapidIO (SRIO) data communication, using hybrid backplane protocols and processing nodes (DSP/FPGA/GPU) has been completed (Figure 21). Second, a customized parallelism scheme was developed by the team, and it has been validated that the proposed backend system can handle basic MPAR backend processing chain (beamforming/pulse compression/Doppler processing), and can achieve hard real-time

performance of 20 ms for up to 700 digital array radar channels, by using DSP nodes only, which beats the performance of existing known schemes and parallelization tools on the market. Third, significant effort on using advanced FPGA devices for data transportation was undertaken, and the team validated that using our FPGA device, 80% protocol efficiency can be achieved for a 12 Gbit/s dual-lane SRIO link between FPGAs. The technologies from this project can be used directly in ATD, future MPAR, or CPPAR2 radar developments.

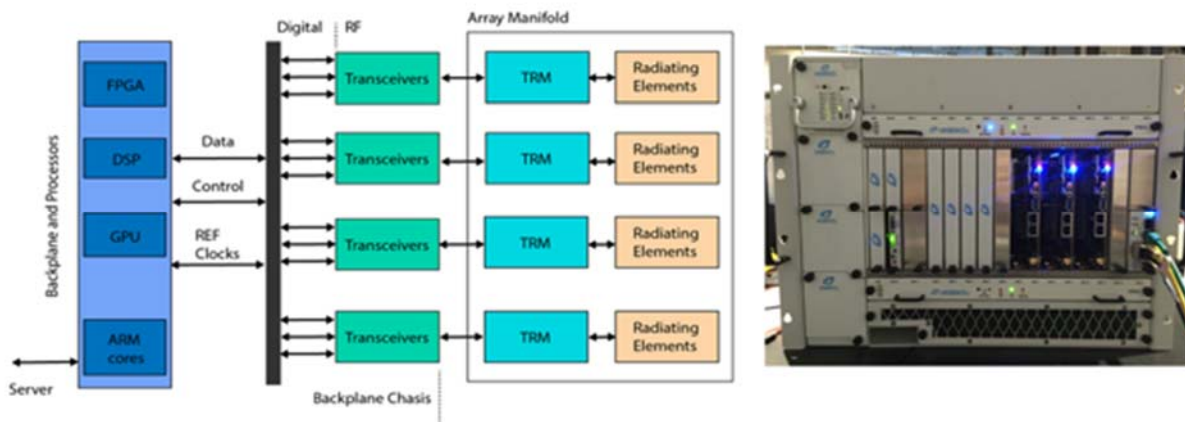


Figure 21. The new DSP-based MPAR backend testbed developed in FY2016.

9. CPPAR Demonstrator Calibration and Cylindrical Array Limitations Study

Caleb Fulton, Yan (Rockee) Zhang, and Jorge Salazar (OU ARRC/ECE), Guifu Zhang (OU ARRC/ECE/School of Meteorology), and Dusan Zrnica (NSSL)

Objectives

The objectives of this project were to refine the CPPAR Demonstrator’s hardware, to develop the software and hardware tools needed for its phased array and polarimetric calibration, to execute that calibration, to begin to use the system as a weather radar, and to better understand its pattern performance through simulations and fundamental analysis of the measured effects.

Accomplishments

Through a large effort on the part of the ARRC engineering team, faculty, and students involved – as well as several NSSL scientists – the CPPAR Demonstrator-related objectives have largely been accomplished over the previous year. These efforts and the current status are summarized herein, as well as the tasks that remain to further explore the engineering/science challenges and opportunities that this unique Demonstrator provides.

The ARRC engineering team developed and installed a far-field testbed for the CPPAR demonstrator that is based on a turntable, a far-field tower, and a long cable that connects the CPPAR to a far-field horn through custom switch boxes. Figure 22 summarizes this test setup. Custom software was developed that drives the turntable while commanding the CPPAR to store either column-level or beamformed pattern

measurements as made through the far-field tower. For receive operation, digital beamforming is executed in Matlab off-line based on an alternating projections synthesis technique that has been previously documented. Some example AZ-cut results are shown in Figure 23, for both the leftmost and center sector. These beams can be formed in parallel, since it is a digital beamformer. For transmit operation, the embedded pattern weights are similarly optimized offline in Matlab, but then an iterative mutual coupling-based algorithm (also previously-documented) is used to enforce these weights through the nonlinear amplifiers. Example transmit results are also shown in the figure, as well as the resulting two-way polarimetric pattern. This pattern (at least in one dimension) is very close to meeting even the previous MPAR objective thresholds for sidelobe levels and polarization matching, assuming the H and V patterns gains are known precisely on the calibration equipment itself (which as of now it is not).

Future and ongoing work to improve the pattern calibration process includes improved polarization calibration through careful characterization of this far-field test setup, replacement of the antennas in the coming months and filling out of the entire cylinder with “dummy” columns, and refinements to the mutual coupling algorithms to make use of in-situ probes that have recently been added to the edges of the CPPAR trailer to act as auxiliary coupling sources.

The embedded column patterns were previously simulated, as documented in previous reports, and are compared in detail to their measured patterns in Figure 24. There is clear agreement between the dominant behavior of these patterns, but the finite nature of the current CPPAR array (which will soon be ameliorated with the full population of the cylinder) and the presence of the backing tower and “absorbing wall” keep a precise comparison from being made. Nevertheless, the agreement as it stands suggests that early conclusions can be drawn from the current measurements. Namely, as shown in the bottom of Figure 24, it has been found that the dominant “source” of the back-radiation in the overall radiation patterns is the fields associated with the phase mode spectral coefficients that correspond to wave propagation around the cylinder at phase velocities that are near the speed of light. Current exploratory/fundamental research work is underway to determine whether or not the presence or absence of these (and other) spectral components can be engineered through proper antenna element (and dielectric stackup) design.

Finally, because the system has been sufficiently stable for the production of quality beams over small time scales (10s of minutes, at this point), we have been able to start a real weather radar measurement campaign. Figure 25 shows the early progress of this effort, comparing beamformed/calibrated reflectivity data collected by the CPPAR to the WSR-88D data as collected by KTLX, the nearest WSR-88D. Work is underway to investigate the dual polarization behavior of the system with respect to weather, and to continue to refine the system as described above to promote long-term system stability and reliability.

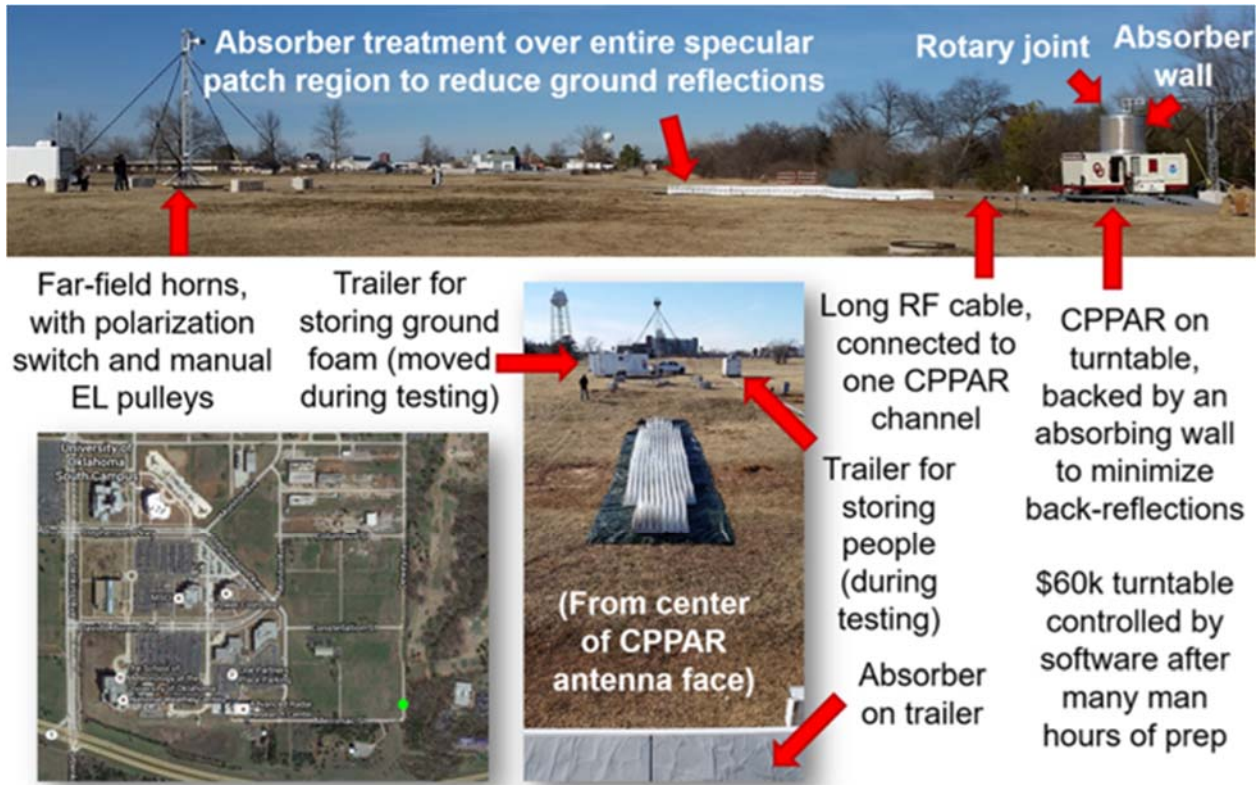


Figure 22. Far-field testbed that was developed for the CPPAR demonstrator.

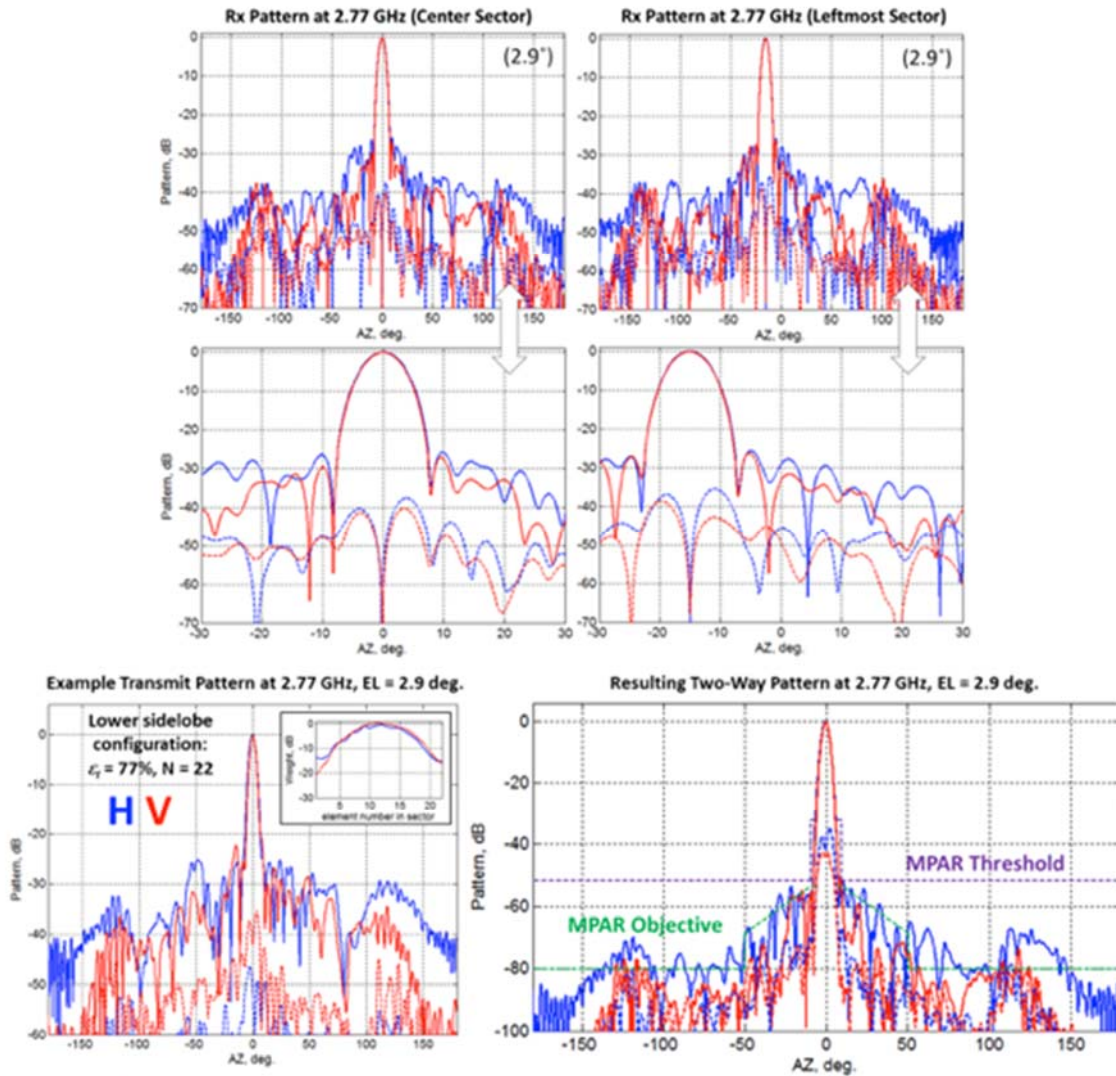


Figure 23. Pattern measurements made on the CPPAR demonstrator: (top) Receive patterns for two different sectors, including “zoomed in” view, and (bottom) measured transmit pattern and effective two-way pattern, the latter coming close to what appeared in the early MPAR “objective” requirements for sidelobe and polarization performance.

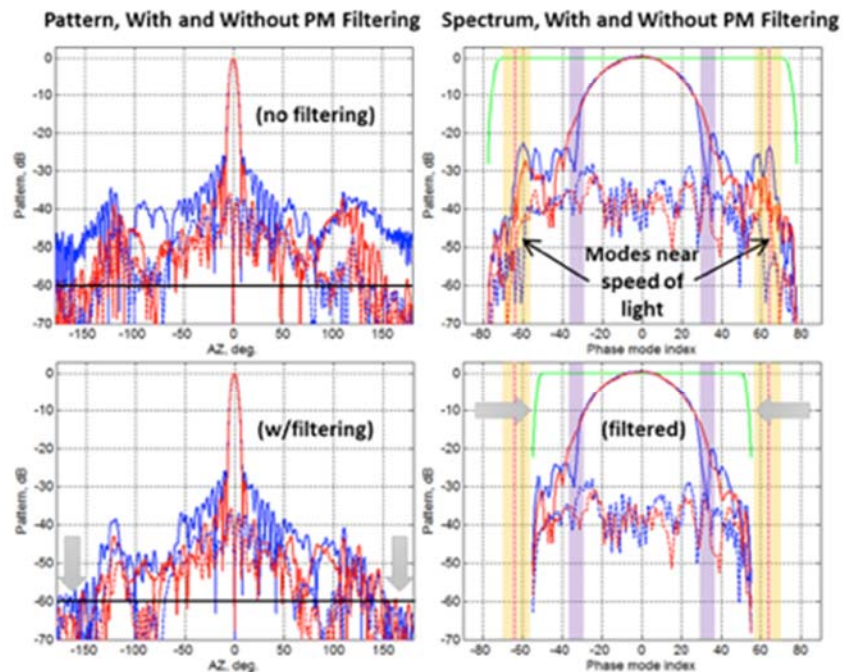
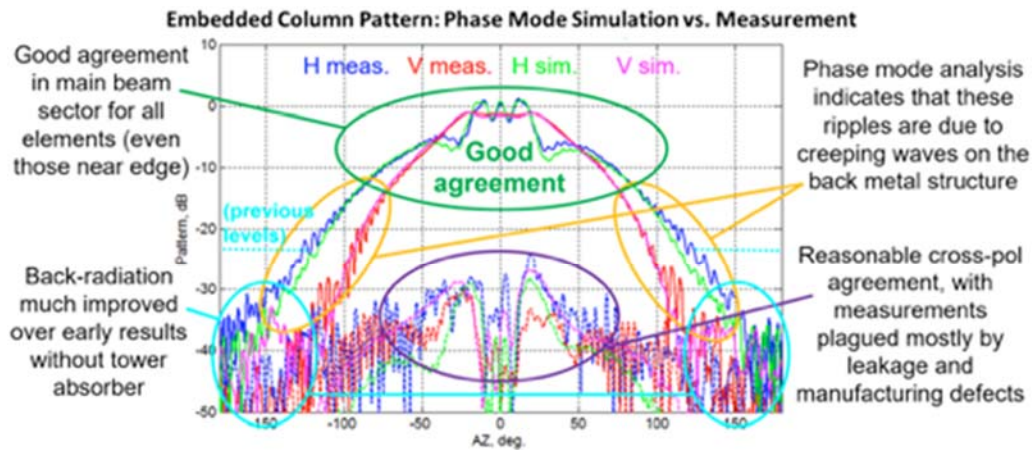


Figure 24. Investigation into fundamental behavior of CPPAR antenna, including (top) comparison between measurement and simulation as well as (bottom) investigation into how phase mode content near the speed of light is contributing to limitations to suppression of back-radiation.

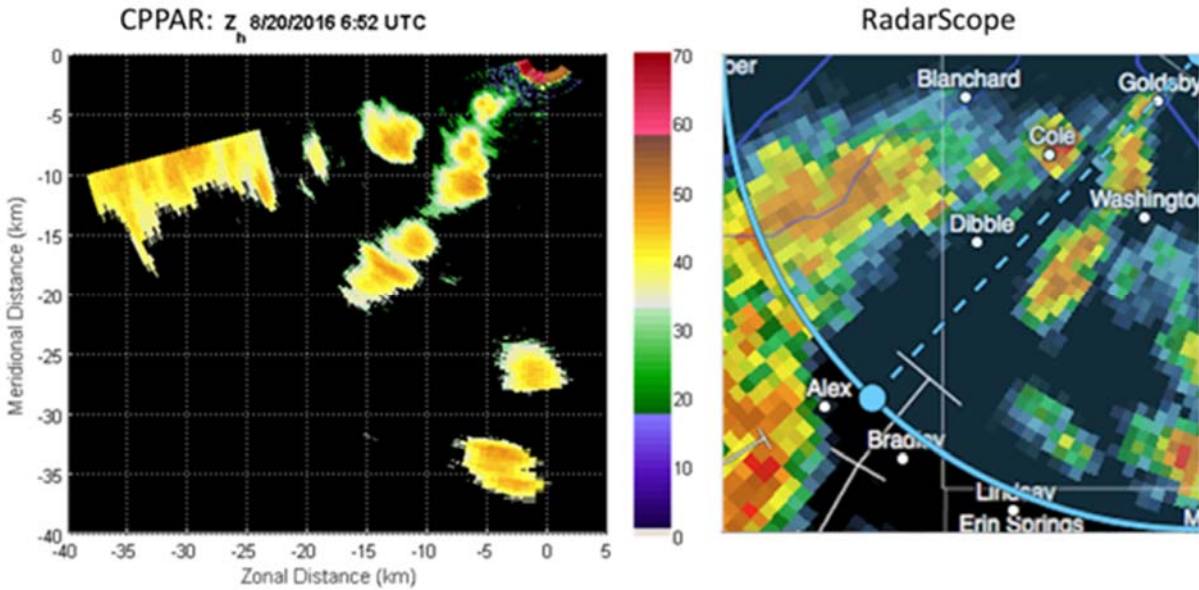


Figure 25. Early weather radar data from the CPPAR demonstrator, showing that it is clearly able to execute transmit and receive beamforming to produce reflectivity data; further work is underway to enable and optimize the measurement of dual-pol products.

10. Design and Development of an All-Digital Line Replaceable Unit – The HORUS Project

Caleb Fulton and Jorge Salazar (OU ARRC/ECE), and Robert Palmer (OU ARRC/School of Meteorology/ECE)

Objectives

The Horus project seeks to develop the world's first dual-pol, all digital weather radar to mitigate the associated risks in anticipation of a highly-digital MPAR/SENSR solution in the coming decade. The goal for the first year of this project was to pave the way towards a testbed-level demonstrator in 2016/2017 and a small-scale prototype system in 2018. In particular, this first year was dedicated to overall system design, first-pass custom antennas, and the procurement of long-lead items (such as the front-end).

Accomplishments

The Horus demonstrator, a 32x32-element (4x4 subarray) S-band digital dual-polarization phased array, was conceived following the OU/NSSL CPPAR Design Study as a means to capture the state-of-the-art in low-cost phased array technology in the context of the likely procurement of a large-scale, highly-digital MPAR/SENSR system in the coming decade. The reason for this is that even if the eventual system has digitization at the subarray level (instead of element level), it is clear that it will make use of low-cost transceiver electronics and will have a large number of digital channels. The electronics and digital systems described below that are being used in the 1024-element demonstrator are very much in line with such a system.

Figure 26 summarizes the expected system-level performance as a weather/hard-target radar, and shows a rendering of the overall aperture that will be developed in the coming years. The antenna, shown in Figure 27, has been designed to provide world-class polarimetric performance near the principal planes, and allows for the mechanical connectors and the electromagnetic lattice to be separable to promote upgrades, research, and flexibility in the coming years. It is detailed in the antenna section (Section V).

The heart of the Horus electronics lies in the Line Replaceable Unit (LRU), which consists of all of the transmitting, receiving, and digital processing electronics to provide core radar functionality for an 8x8 square of elements. Its block diagram and constituent components are shown in Figure 28. Inside its mechanical housing – which pairs with one of the 8x8 antenna panels – are eight independent “OctoBlades” which each drive eight dual-pol channels. The LRU also includes a “SuperBlade” as well as an analog bridge to distribute clocks and power to the OctoBlades. Each “blade” includes a liquid cooling manifold that provides an effective, lightweight, and scalable solution to the challenges presented by these high density electronics.

Figure 29 summarizes the current hardware development status in support of near-term demonstrations of representative electronics for the Horus LRU. The frontend prototypes, which feature a 10+ W amplifier for each polarization, are now fully integrated and tested in their final surface-mount packaging. The analog transceivers that are paired with these frontends, which are based on a state-of-the-art digital direct conversion IC, are currently being prototyped in a form factor that is amenable to the final LRU layout. On the digital side, a collection of FPGAs have been selected that will provide the core DSP and front-end control functionality needed to drive the radar electronics; representative hardware has been procured that will allow for testing of the requisite interfaces and processing functions. Additionally, a plan has been developed for larger-scale digital beamforming over Serial RapidIO interfaces on each OctoBlade.

System Performance Overview (16 Panel System)	
Operating Frequency Range	2.7-3.0 GHz
Element Polarization	Dual-Linear, RHCP, LHCP
Transmit Waveform Type	LFM/NLFM
Transmit Power (Single Element)	10.0 W (per Polarization)
Max Transmit Pulse Width	50.0 μ s
Max Transmit Duty Cycle	5.0 %
Max Transmit Waveform Bandwidth	50 MHz
Element Spacing (Horizontal x Vertical)	0.50 x 0.50 λ at 2.951 GHz
Radiator Panel Size (Elements)	8 x 8 (64) elements
Total Number of Panels	16 panels
Total Number of Radiating Elements	1024 elements
Maximum Elevation Scan Angle	60.0 deg
Horizontal Aperture	1.63 m (5.33 ft)
Vertical Aperture	1.63 m (5.33 ft)
Tx Aperture Gain (Uniform Excitation)	34.92 dBi
Rx Aperture Gain (Uniform Excitation)	32.12 dB
Total Assumed	Transmit 3.00 dB
SNR Losses	Receive 6.80 dB (Includes NF)
Min Beamwidth (Azimuth x Elevation)	4.38 x 4.38 deg at 0-deg EI
(1.38x Uniform Excitation Beamwidth)	4.38 x 8.76 deg at 60-deg EI
Sensitivity	Weather 3.5 dBz @ 30.0 km
(1 Pulse)	Hard Target 1.29E-03 m ² @ 30.0 km

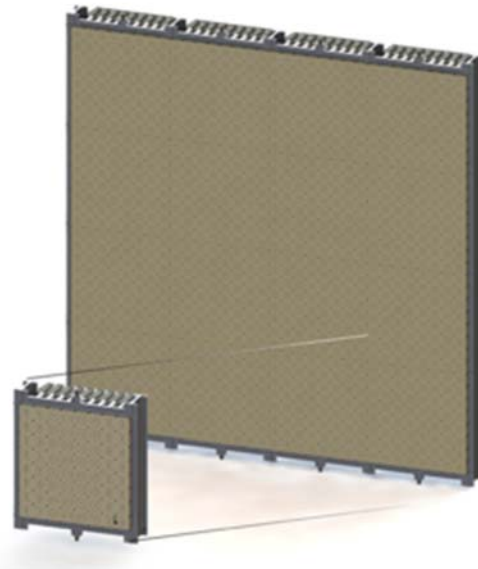


Figure 26. 4x4 Horus performance estimates and rendering of active digital aperture.

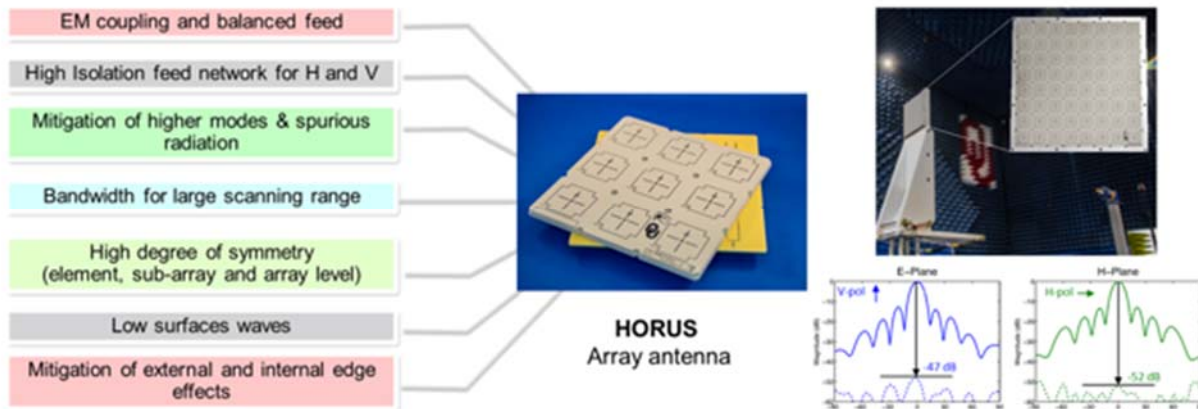


Figure 27. Horus antenna design and key performance advantages.

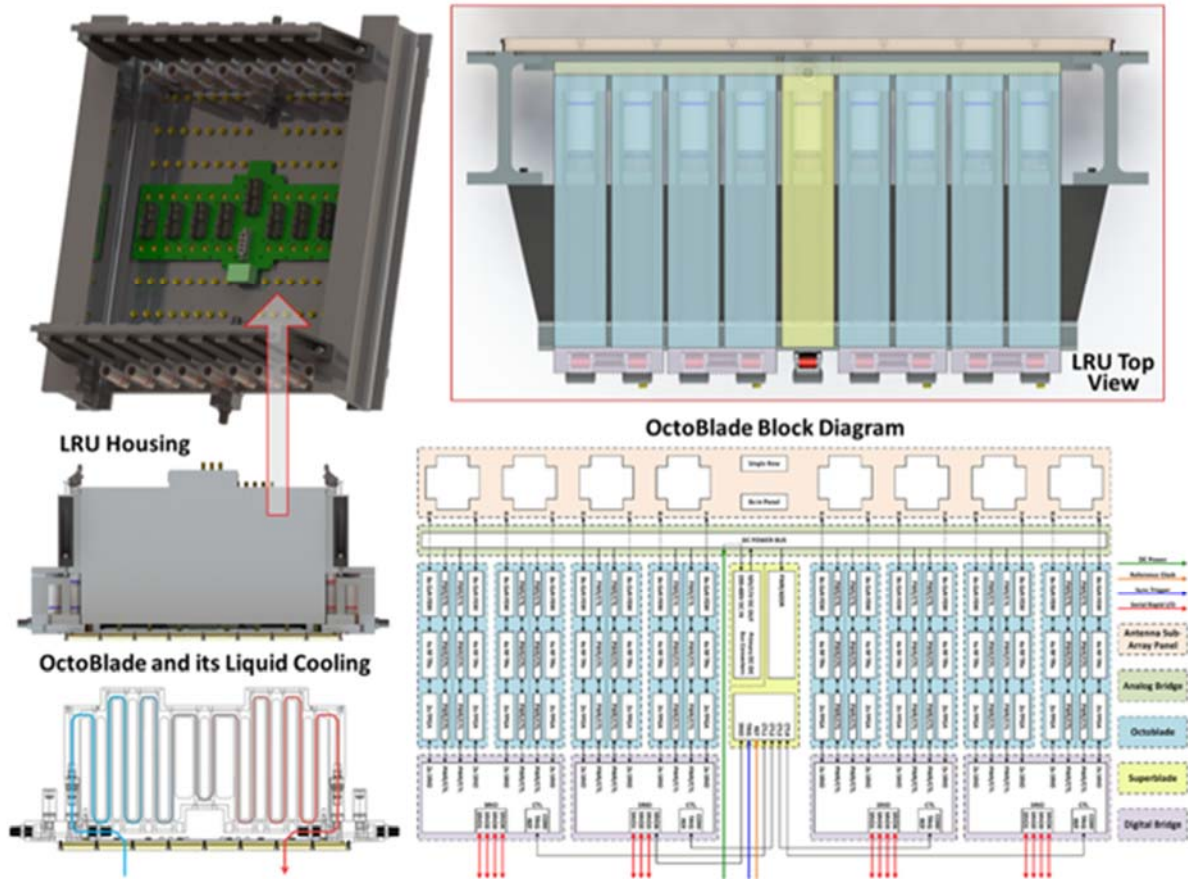


Figure 28. 4x4 Horus line replaceable unit (LRU) block diagram, including its housing structure, cooling mechanism, and view from the top of its 9 constituent “blades”.

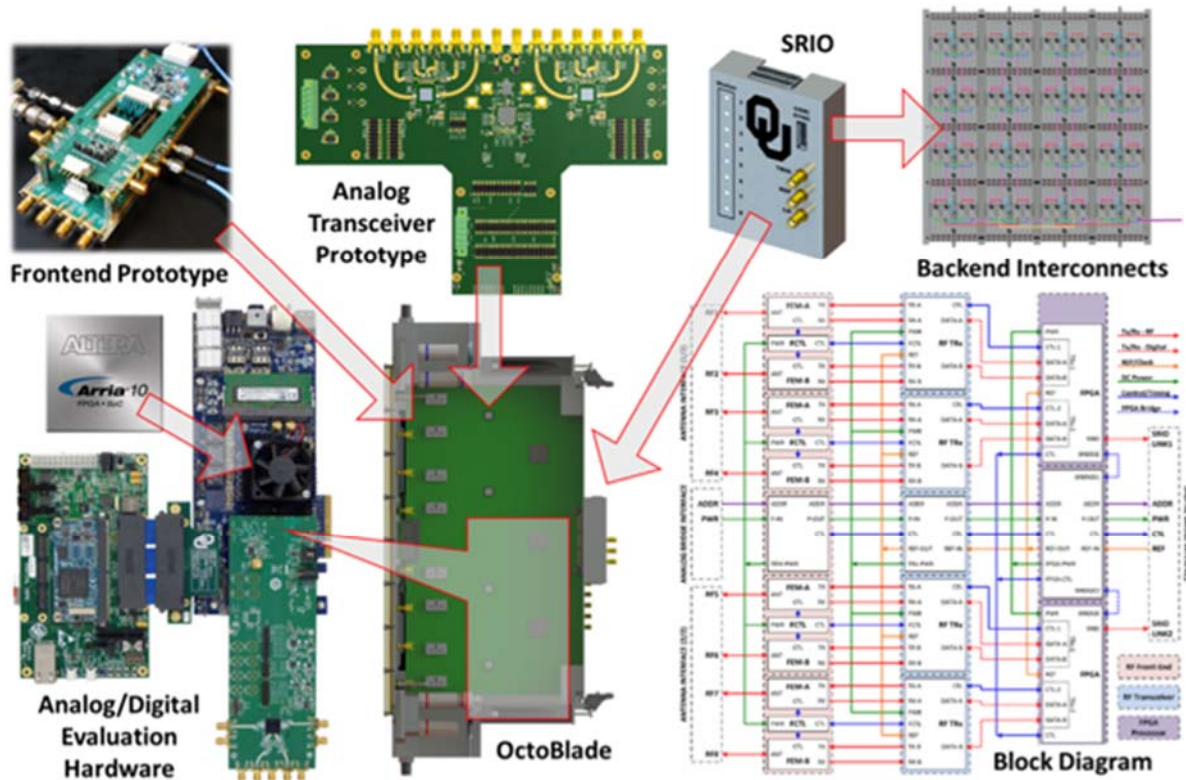


Figure 29. Current OctoBlade hardware and system development status and block diagram, including the evaluation board-based hardware that captures core digital transceiver and beamformer functionality.

Publications

- Curtis, C., M. Yeary, and J. Lake, 2016: Adaptive beamforming to mitigate ground clutter on the National Weather Radar Testbed phased array radar, *IEEE Transactions on Geoscience and Remote Sensing*, **54**, 1282-1291.
- Fulton, C., and A. Mirkamali, 2015: A computer-aided technique for the analysis of embedded element patterns of cylindrical arrays [EM Programmer's Notebook]. *IEEE Antennas and Propagation Magazine*, **57**, 132-138.
- Fulton, C., M. Yeary, D. Thompson, J. Lake, and A. Mitchell, 2016: Digital phased arrays: Challenges and opportunities. *Proceedings IEEE, Special Issue on Phased Arrays*, **104**, 487-503.
- Kurdzo, J. M., D. J. Bodine, B. L. Cheong, and R. D. Palmer, 2015: High-temporal resolution polarimetric X-band Doppler radar observations of the 20 May 2013 Moore, Oklahoma tornado. *Monthly Weather Review*, **143**, 2711-2735.
- Mirza, R., 2016: A Simple EM Dipole Radiating Element for Dual-Polarized Phased Array Weather Radars. M.S. Thesis, Department of Electrical and Computer Engineering, University of Oklahoma.
- Nai, F., S. M. Torres, and R. D. Palmer, 2016: Adaptive beamspace processing for phased-array weather radars. *IEEE Transactions on Geoscience and Remote Sensing*, **54**, 5688-5698.
- Yu, X., Y. Zhang, A. Patel, A. Zahrai, and M. Weber, 2016: An implementation of real-time phased array radar fundamental functions on DSP-focused, high-performance embedded computing platform. *Aerospace: Special Issue – Radar and Aerospace*, Accepted.

CIMMS Task III Project – Polarimetric Phased Array Radar Research in Support of MPAR Strategy

Guifu Zhang (ARRC at OU and OU School of Meteorology), Shaya Karimkashi (ARRC at OU), Richard Doviak, Allen Zahrai, and Dusan Zrnic (NSSL), Lesya Borowska and Said Abushamle (ARRC Post Docs), and Hadi Saeedimanesh, Mirhamed Mirmozafari, Thomas Grabow, and Mohammadhossein Golbonhaghighi (ARRC/ECE/SoM Students)

NOAA Technical Lead: Kurt Hondl (NSSL)

NOAA Strategic Goal 2 – *Weather Ready Nation: Society is Prepared for and Responds to Weather-Related Events*

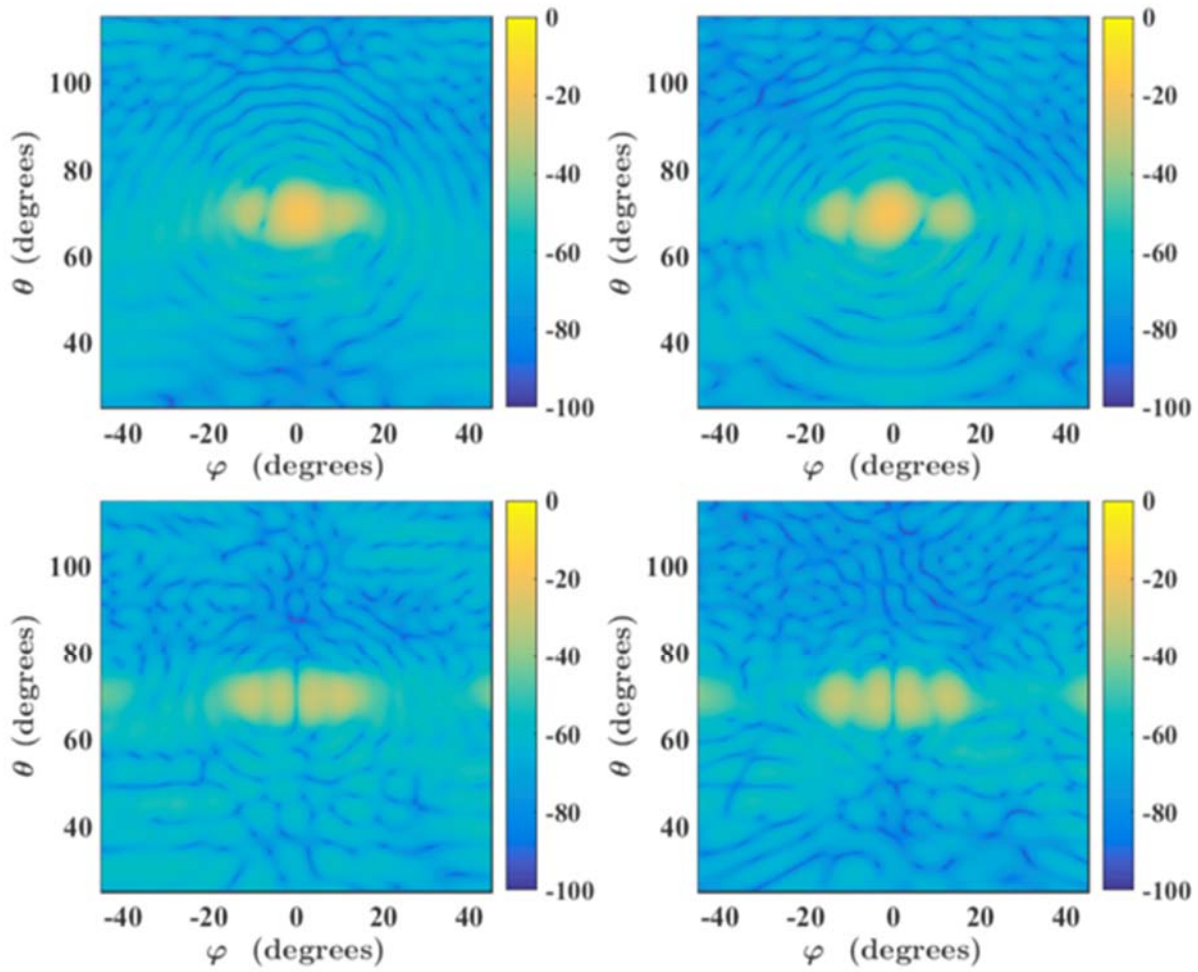
Funding Type: CIMMS Task III

Objectives

Conduct research on practical issues for designing and developing the Polarimetric Phased Array Radar (PPAR), including the Cylindrical Polarimetric Phased Array Radar (CPPAR), to better understand the scientific advantages, technical challenges & limitations and cost-performance tradeoffs, as well as to support MPAR strategy in decision making to sustain Norman's leadership in weather radar and to expand its radar expertise for broad research and multi-mission applications.

Accomplishments

This project team continues to work on i) CPPAR configuration, design and optimization, ii) radiating element design and testing, applicable to both the PPPAR and the CPPAR and iii) innovative signal processing. We made significant progresses in dual-polarization dipole antenna design and development, design and evaluation of image arrangements (figure below) and advanced signal processing for MPAR. Please see documented results from the listed publications



Comparison of CPPAR horizontal (left) and vertical (right) polarization, cross-polarization radiation pattern with (bottom) and without (top) image configuration at ($\theta = 70^\circ, \varphi = 0^\circ$).

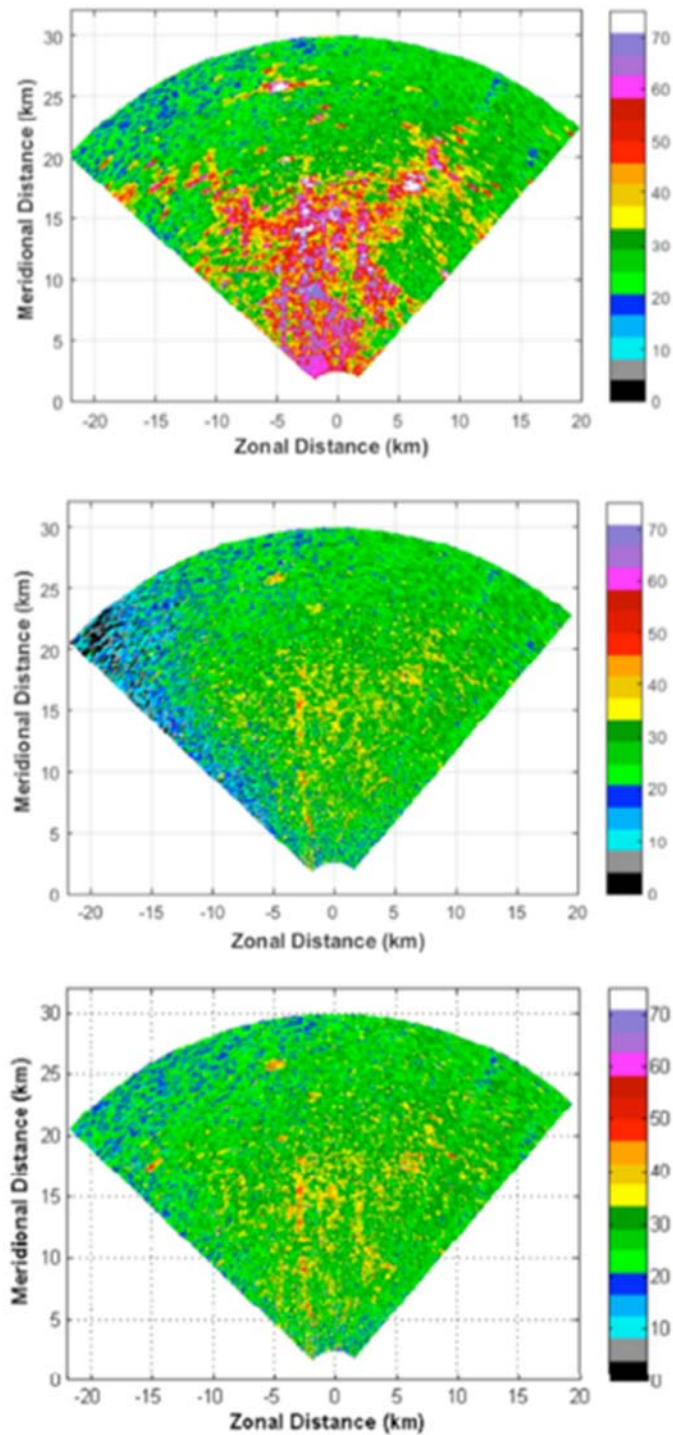


Illustration of step scan with joint signal processing with NWRP data: (a) Reflectivity field over a 90° sector scanned with the NWRP (PRT=0.8ms). Number of samples is 40. (b) Same as (a) but ground clutter has been removed by application of the CLEAN-AP procedure to the concatenated sequence (L=20, and M=60). (c) The field after application of the CLEAN-AP to the data but with L=8, M=24, and PRT=3.2ms.

Publications

- Borowska, L., G. Zhang, and D. S. Zrnic, 2015: Considerations for oversampling in azimuth on the phased array weather radar. *Journal of Atmospheric and Oceanic Technology*, **32**, 1614-1629.
- Borowska, L., G. Zhang, and D. S. Zrnic, 2016: Spectral processing for step scanning phased array radars, *IEEE Trans. On Geoscience and Remote Sensing*, **54**, 4534-4543.
- Karimkashi, S., and G. Zhang, 2015: Optimizing radiation patterns of a cylindrical polarimetric phased-array radar for multitemissions. *IEEE Transactions On Geoscience and Remote Sensing*, **53**, 2810-2818.
- Lei, L., G. Zhang, R. Doviak, and S. Karimkashi, 2015: Comparison of theoretical biases in estimating polarimetric properties of precipitation with weather radar using parabolic reflector, or planar and cylindrical arrays, *IEEE Transactions On Geoscience and Remote Sensing*, **53**, 4313-4327.
- Zhang, G. 2016: *Weather Radar Polarimetry*. CRC Press.

Theme 2 – Stormscale and Mesoscale Modeling Research and Development

NSSL Project 3 – Numerical Modeling and Data Assimilation

NOAA Technical Leads: Adam Clark, Pamela Heinselman, Jack Kain, Don MacGorman, Ted Mansell, Louis Wicker, and Conrad Ziegler (NSSL)

NOAA Strategic Goal 2 – *Weather-Ready Nation – Society is Prepared for and Responds to Weather-Related Events*

Funding Type: CIMMS Task II

Overall Objectives

Develop and test numerical weather prediction models, data assimilation techniques, and diagnostic, visualization, and verification methods to improve severe weather forecasts.

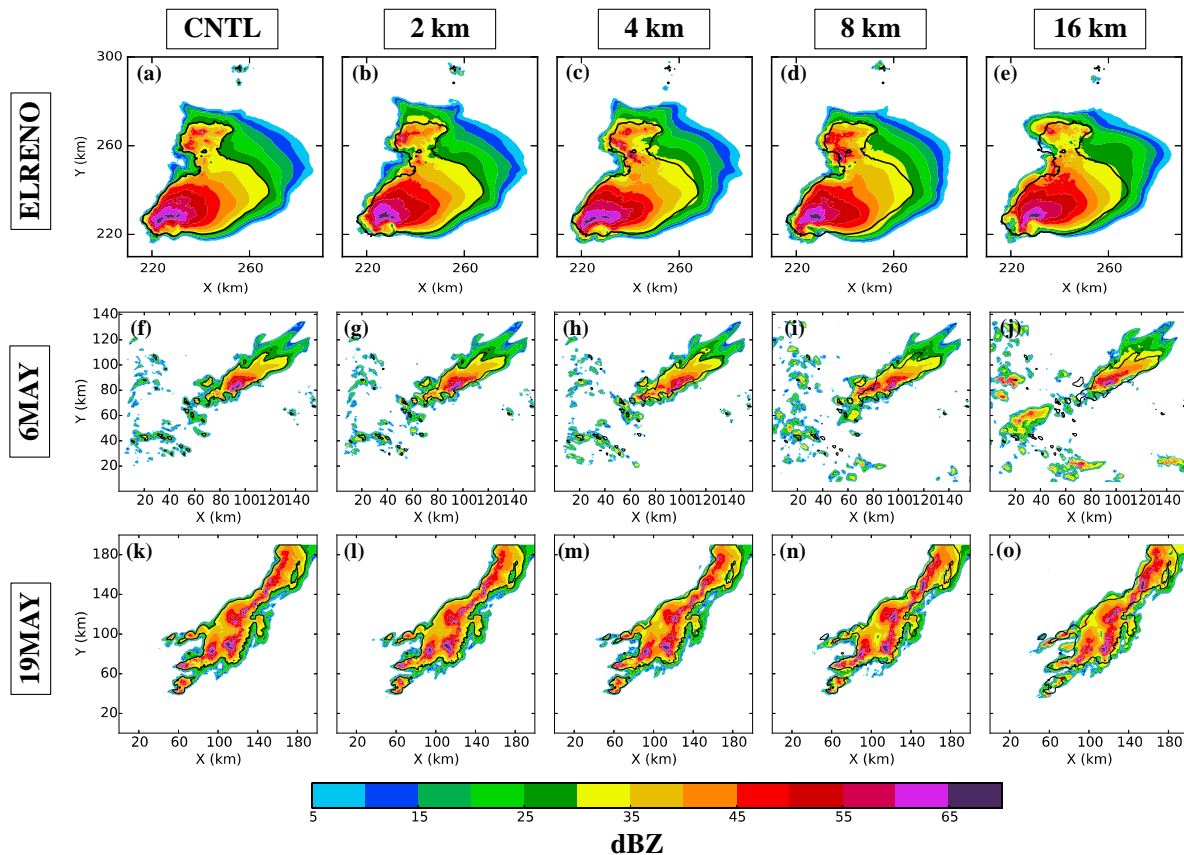
Accomplishments

1. Establishing Model Resolution Requirements for Warn-on-Forecast

Corey Potvin and Dustan Wheatley (CIMMS at NSSL), and Elisa Murillo and Montgomery Flora (NSF Research Experience for Undergraduates)

Current computational limitations prevent real-time ensemble forecasting systems from being run on convection-resolving grids. Understanding of forecast errors arising from finite model and initial condition resolution is required to optimize ensemble system design tradeoffs, guide interpretation and calibration of ensemble output, and establish model resolution requirements for Warn-on-Forecast.

In new work, idealized and full-physics simulations initialized with different degrees of filtering applied to the initial condition (IC) are compared to explore the sensitivity of supercell forecasts to initial condition resolution. In all experiments, scales removed from the IC (wavelengths < 2, 4, 8, or 16 km) regenerate within 10-20 min of model integration. While the forecast errors arising from the initial absence of these scales become quantitatively large in many instances, the qualitative storm evolution is relatively insensitive to the IC resolution. It therefore appears that adopting much finer forecast (e.g., 250-m) than analysis (e.g., 3-km) grids for data assimilation and prediction would improve supercell forecasts given limited computational resources. This motivates continued development of mixed-resolution systems. The relative insensitivity to IC resolution further suggests that convective forecasting can be more readily advanced by improving model physics and numerics and expanding extra-storm observational coverage than by increasing intra-storm observational density.



Reflectivity (dBZ; shading) ~2 km AGL at $t = 60$ min in an idealized simulation (top row) and two real-analysis-initialized simulations (middle, bottom rows). Columns from left to right: unfiltered initial conditions, and wavelengths < 2 km, 4 km, 8 km, and 16 km removed. The CNTL 30 dBZ contour is overlaid in each panel to facilitate comparison.

2. Investigating Supercell Sensitivity to Initial Conditions

Corey Potvin (CIMMS at NSSL), Montgomery Flora (OU School of Meteorology), Louis Wicker, Ted Mansell, and Rodger Brown (NSSL), Amy McGovern (OU Department of Computer Science), and Brittany Dahl (NOAA HRD)

The predictability of supercells and other deep convection is not yet thoroughly understood. Advances in understanding of intrinsic and practical predictability limits will be important for guiding the design of real-time ensemble forecasting (WoF) systems.

Work continues on assessing the sensitivity of low-level mesocyclones and tornadoes to environmental errors in 100-m idealized supercell simulations. This work has also been extended to a more realistic framework using analyses from the NSSL Experimental Warn-on-Forecast System for ensembles (NEWS-e). New ensemble analyses are generated that have reduced ensemble perturbations for one or more model state

variables (relative to the original NEWS-e analyses) and then used to initialize ensemble forecasts. These forecasts and the forecast generated from the initial NEWS-e analysis are compared to each other to assess how forecast uncertainty varies with initial condition uncertainty. Both studies are intended to advance understanding of supercell predictability, and to clarify what a WoF system can reasonably be expected to achieve in the presence of current and future environmental analysis errors.

3. Identifying and Correcting Reporting Biases in SPC Tornado Database

Corey Potvin and Patrick Skinner (CIMMS at NSSL), Chris Broyles (SPC), and Harold Brooks (NSSL)

The SPC tornado database is an indispensable resource for assessing tornado risk in the United States, and may ultimately prove critical for identifying changes in tornado characteristics due to climate change. Maximizing the value of the database, however, requires accounting for under-reporting in regions where tornadoes are more likely to escape notice. Previous studies examining reporting effects on documented tornado frequency have modeled the impact of only a single variable (e.g., population density) or of a combination of variables that are implicitly assumed to have mutually independent effects on reporting frequency. The present study, on the other hand, uses multivariable polynomial regression to make provision for inter-variable effects on tornado reporting bias. This allows us to account for such effects as the expected decrease of the influence of local population density very near NWS WFOs.

In preliminary work, we have modeled tornado reporting bias as a function of various combinations of the following variables: 1) distance from nearest 100K city (population > 100K), 2) distance from nearest 30K city, 3) distance from nearest WFO, 4) distance from nearest interstate, and 5) local population density. Of the five variables, population density is found to have the least impact on reporting bias. As expected, the reporting biases are found to be most pronounced for weaker/briefer tornadoes. Our results suggest at least a third of such tornadoes are unobserved even today. This work is ultimately intended to inform the methodology of future tornado climatology studies, and to increase the spatial resolution of tornado hazard models used by forecasters, planners, and insurance/reinsurance companies.

4. Visualization of High-Resolution Supercell Simulations

Greg Foss (TACC), Corey Potvin (CIMMS at NSSL), and Amy McGovern (OU Department of Computer Science)

Foss is developing sophisticated animations of 100-m supercell simulations generated by McGovern. Potvin is providing his scientific expertise to the generation of the simulations and the design & interpretation of the animations. The animations will support McGovern's and Potvin's efforts to use advanced spatiotemporal data mining to identify precursors of tornadoes in supercell thunderstorm simulations. Specifically, the

animations will help guide the definitions of storm objects to be extracted for data mining.

5. *Dual-Doppler Wind Retrieval*

Corey Potvin (CIMMS at NSSL), Daniel Betten, Gordon Carrie, and Elizabeth DiGangi (OU School of Meteorology), Conrad Ziegler (NSSL), Michael French (SUNY Stonybrook), Nathan Dahl (University of Miami), and Timothy Lang (NASA)

Variational dual-Doppler wind retrieval has been shown to be superior to traditional dual-Doppler retrieval techniques. It is necessary to use the most sophisticated analysis techniques available to fully exploit high-quality dual-Doppler datasets such as those collected during the VORTEX-2 experiment. Potvin's and Shapiro's variational dual-Doppler retrieval code is currently being implemented into the community Py-ART software in order to make it readily available to the entire research community. The original code is being used in four different projects led by Betten, French, DiGangi, and Dahl.

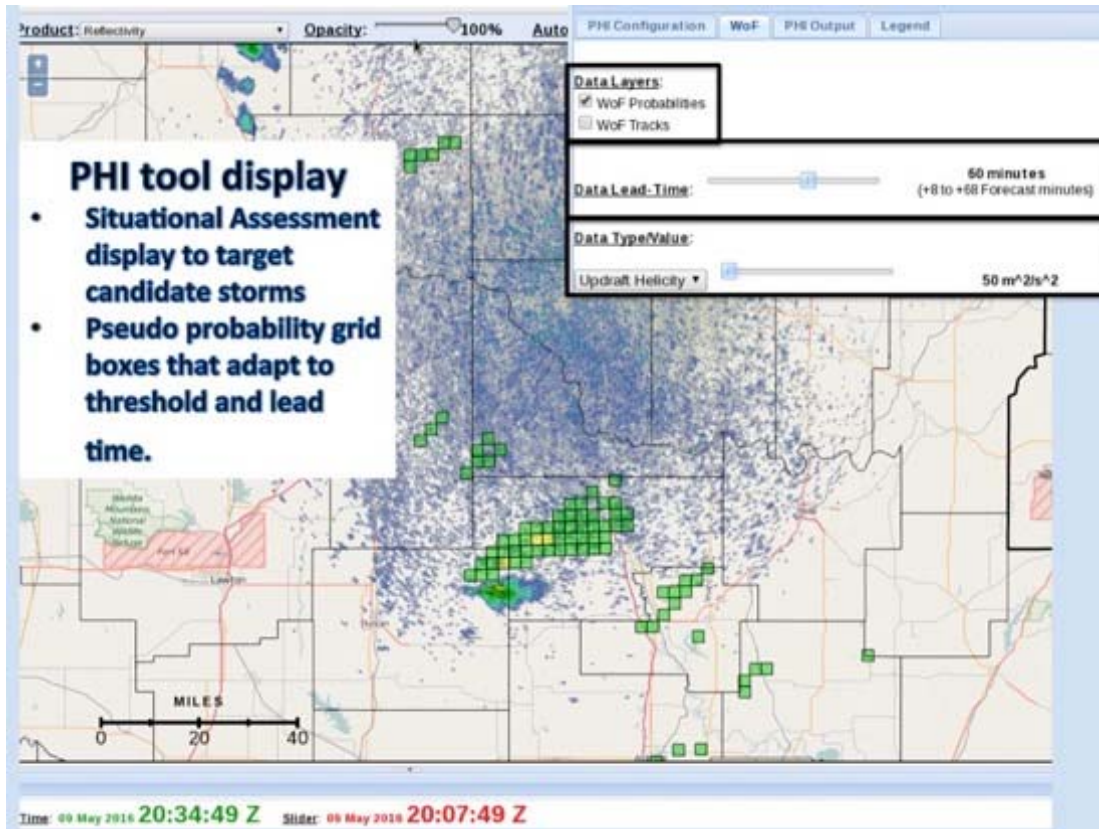
6. *Tests and Evaluation of Rapid Post-Processing and Information Extraction from Large Convection-Allowing Ensembles Applied to 0-3hr Tornado Outlooks*

James Correia Jr. (CIMMS at SPC)

The purpose of this project is to design, implement, and evaluate a new post-processing paradigm, designed for any convection-allowing modeling and ensemble system. This new paradigm will allow information extraction for severe weather forecasting, specifically tornado forecasts. This new post-processing paradigm has the benefit of being adaptable, scalable, and fast. To achieve these benefits, we propose using an object-based approach to refine gridded datasets into features of interest, a result of the data mining and information extraction, in order to achieve reduced dataset size for transmission, allow the viewing of all ensemble members, create an ability for forecasters to adapt to the problem of the day and maximize effective use of numerical guidance.

We utilized the NSSL Experimental Warn on forecast System for ensembles (NEWS-e) within the Hazardous Weather Testbed to generate tracks of rotating updrafts and low-level rotation for use during the Experimental Warning Program Probabilistic Hazard Information (PHI) experiment. In May – June 2016, nine forecasters were exposed to this information in an adaptable display designed to address the problem of the day, and allowed them to query the ensemble information contained within the tracks dataset to issue tornado PHI. The additional situational awareness provided what the forecasters called “hot spots” that they then could focus back on radar data to issue their warnings. Overall, the data and display were well received. The dataset itself was small, agile, and rapidly available.

This project is a necessary first step in achieving full use of rapidly updating, large convection-allowing ensemble systems and making them useful and usable to forecasters while producing consistent and reliable risk analyses in between the warning and watch time scales. This in turn, enables forecasters to provide effective decision support to help partners effectively mitigate the impacts of severe weather.



PHI tool display showing pseudo-probability grid (green & yellow squares) along with inset controls for querying the dataset. Queries were constrained to two variables (updraft helicity for deep rotating updrafts and low-level vorticity for mesocyclones) and multiple magnitudes. Time was also an attribute that could be set for how far out in the forecast forecasters could see the 90-minute data. Using the queries, pseudo-probabilities would be updated on the fly to see where storm features were moving, their intensity, and future location.

7. Daily NSSL WRF and NMMB Forecasts

Scott Dembek (CIMMS at NSSL), Adam Clark and Jack Kain (NSSL), and Israel Jirak (SPC)

The National Severe Storms Laboratory (NSSL) continues to use a modified version of the Weather Research and Forecasting (WRF) model for daily forecasts over the Continental United States (CONUS). These forecasts represent a valuable tool for forecasters at the Storm Prediction Center (SPC), as well as a key element in the

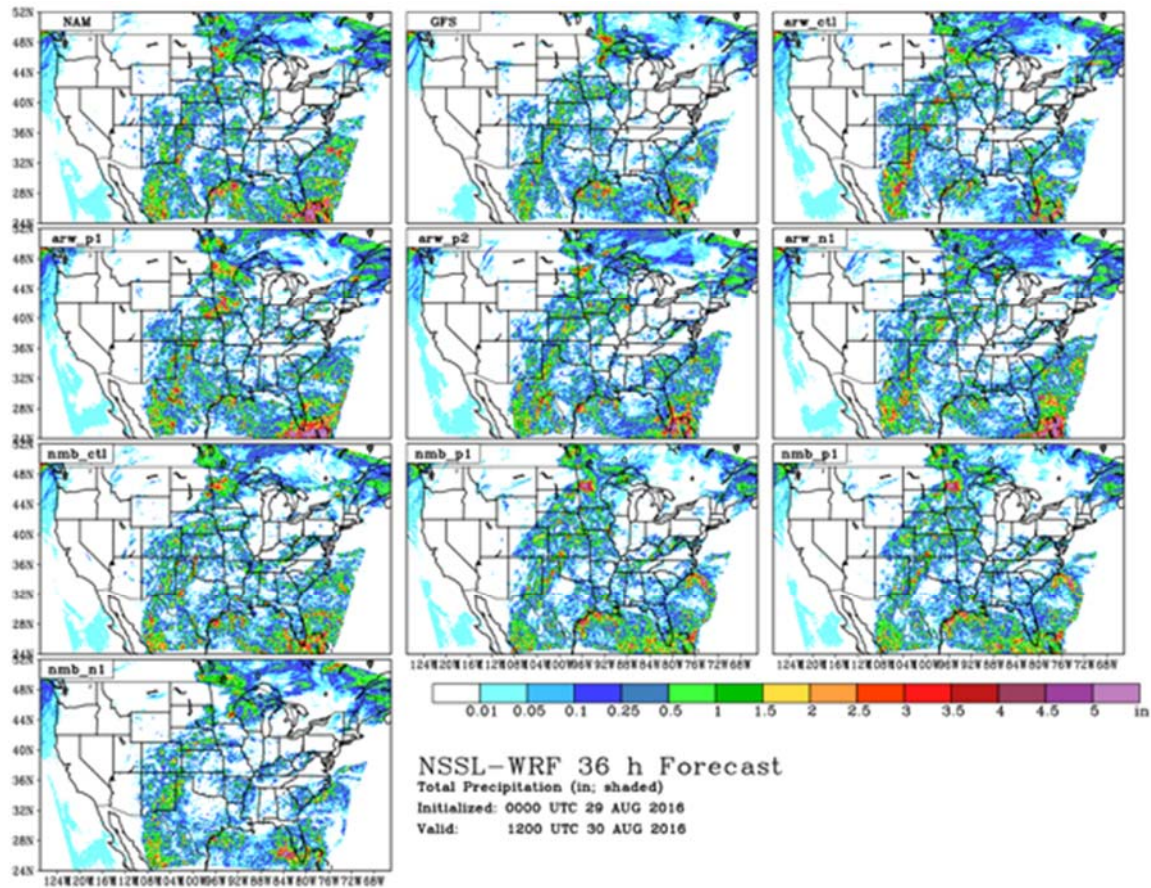
annual NOAA/Hazardous Weather Testbed Spring Forecasting Experiment. The model is run in real time twice daily at 0000 UTC and 1200 UTC, utilizing 4-km grid spacing and convection-allowing dynamics in an effort to provide unique forecast guidance for the SPC. The model is run on the Jet system at the NOAA Research and Development High Performance Computing System (RDHPCS) in Boulder, CO. The boundary conditions for the forecast are provided by the 40 km NAM model fields, and an additional NSSL WRF forecast initialized from the GFS fields is run at 0000 UTC daily for comparison purposes.

Included in the NSSL WRF forecast output is a set of unique storm-scale diagnostic fields to help SPC forecasters identify convective-scale elements like supercells and bow echoes, providing guidance related to convective initiation, mode, intensity, coverage, and evolution.

In addition to the NSSL WRF, another real-time NWP model running daily at NSSL is the NOAA Environmental Modeling System (NEMS) Nonhydrostatic Multi-scale Model on the B-grid (NMMB). The NSSL NMMB runs at 0000 UTC (following the NSSL WRF) on the Jet RDHPCS, and also covers the CONUS on a latitude-longitude grid approximating the Lambert Conformal grid used by the NSSL WRF.

Storm-scale diagnostics similar to those used in the NSSL WRF have been incorporated into the NMMB to the extent possible, allowing SPC forecasters to make direct comparisons between the resulting forecasts. Testing of the NMMB model at NSSL has helped researchers at the Environmental Modeling Center (EMC) identify a problem with low precipitation bias that was ultimately identified and eliminated for future NMMB users.

Finally, an experimental eight-member convection-allowing ensemble is being run daily at 0000 UTC on the Jet RDHPCS. This ensemble utilizes the NSSL WRF code (unvaried physics), but is initialized from a variety of NCEP's Short-Range Ensemble Forecasting (SREF) members. The SREF members used for ensemble initialization include four WRF-ARW members, and four NMMB members.



Accumulated 36-hour precipitation (inches; shaded) forecast initialized 0000 UTC 29 Aug 2016, valid 1200 UTC 30 Aug 2016, for all daily NSSL ensemble members, including the NAM-initialized WRF, the GFS-initialized WRF, and eight SREF-initialized WRF members (four WRF-ARW and four NMMB).

8. Support for the 2016 NOAA/HWT Spring Forecasting Experiment

Scott Dembek and Gerry Creager (CIMMS at NSSL), Adam Clark, Jack Kain, and Louis Wicker (NSSL), and Israel Jirak and Steve Weiss (SPC)

The 2016 NOAA/HWT Spring Forecasting Experiment (SFE) utilized a Community Leveraged Unified Ensemble (CLUE). The CLUE concept was made up of ensemble members from a variety of sources (NSSL, CAPS, NCAR, GSD, UND) with a fixed set of model specifications (e.g., grid size and spacing, and vertical levels), but with varying initial and boundary conditions, and model physics. This method of collaboration was able to bring together 65 individual ensemble members into a mega-ensemble that would be extremely challenging for any one of the SFE contributors to generate alone.

A total of 15 ensemble members were generated at NSSL, including ten using the latest version of the WRF-ARW modified to include the daily NSSL WRF diagnostic code, and five members using the NSSL-modified version of the NMMB. All codes were ported to

the Texas Advanced Computing Center (TACC) Lonestar 5 system, and run in real-time at 0000 UTC for the duration of the SFE. Significant hurdles were encountered while installing the model codes along with the latest version of the Unified Post Processor software (UPP 3.0) on the Lonestar 5 system, but collaboration with experts at TACC, the Developmental Testbed Center, CAPS, and EMC led to successful forecast production during the SFE.

9. Development and Evaluation of a Variational Technique to Assimilate Total Lightning Data

Summarized the key results in a manuscript (*Monthly Weather Review*) and collaborated with NCEP partners (Geoff DiMego, Shun Liu and Jacob Carley) to implement and test this new lightning data assimilation (LDA) technique within the GSI framework.

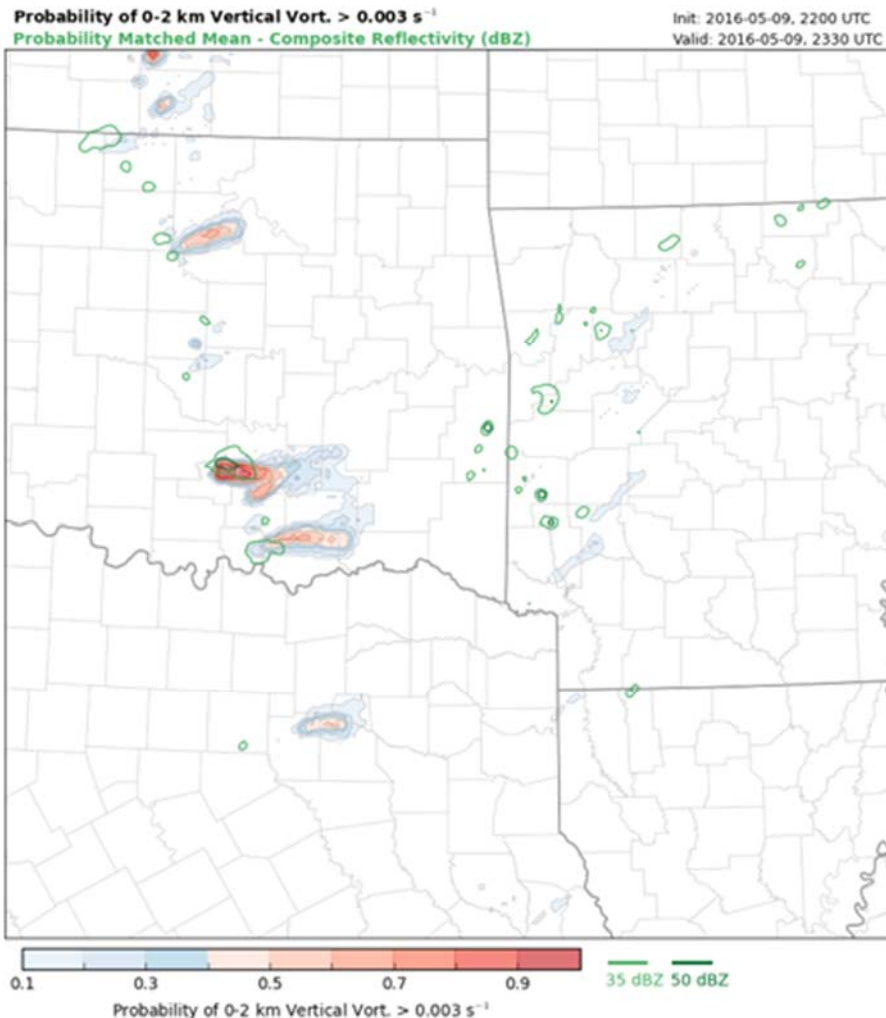
10. Development of an Automated Post Processing, Visualization, and Verification System for Warn-on-Forecast

Patrick Skinner, Dustan Wheatley, and Kent Knopfmeier (CIMMS at NSSL), and Ryan Sobash (NCAR)

The NSSL Experimental Warn-on-Forecast System for ensembles (NEWS-e) has been run in real time in order to provide probabilistic guidance of thunderstorm hazards during the springs of 2015 and 2016. The NEWS-e can produce up to a terabyte of forecast data per day and efficient post processing, visualization, and verification techniques are required to manage and interrogate the forecast data.

For the spring of 2016, a new Python-based post processing and visualization system has been developed that allows users to view NEWS-e output in real time through a web interface (see Figure). This ability to view forecast output in real time has been beneficial in identifying strengths and weaknesses of NEWS-e forecasts as well as isolating errors in the system configuration.

Additionally, an object-based verification system based on techniques published in Skinner et al. (2016) is being developed for NEWS-e forecasts of low-level rotation. Storm tracks with strong low-level rotation in NEWS-e forecasts are compared with corresponding tracks of azimuthal wind shear in Multi-Radar Multi-Sensor (MRMS) data in order to provide both summary measures of forecast skill and diagnostic information on object characteristics in forecasts and observations.



Accumulated ensemble probability of NEWS-e 0-2 km mean vertical vorticity exceeding 0.003 s^{-1} for a 90-minute forecast issued at 2200 UTC on 9 May 2016. NEWS-e Radar reflectivity at 2200 UTC is contoured in green.

11. The Impact of Observation Density on Ensemble Analyses and Forecasts of the 31 May 2013 El Reno, Oklahoma Supercell

Patrick Skinner and Corey Potvin (CIMMS), and Louis Wicker (NSSL)

Operational Warn-on-Forecast products are anticipated to be available with horizontal grid spacing on the order of 1 km; additionally they will take advantage of next-generation remote sensing observations such as those collected by phased array radars (PAR). In order to identify best practices for initializing a high-resolution ensemble forecast by assimilating dense radar observations, a series of experiments have been conducted assimilating PAR observations of the 31 May 2013 El Reno, Oklahoma, tornadic supercell.

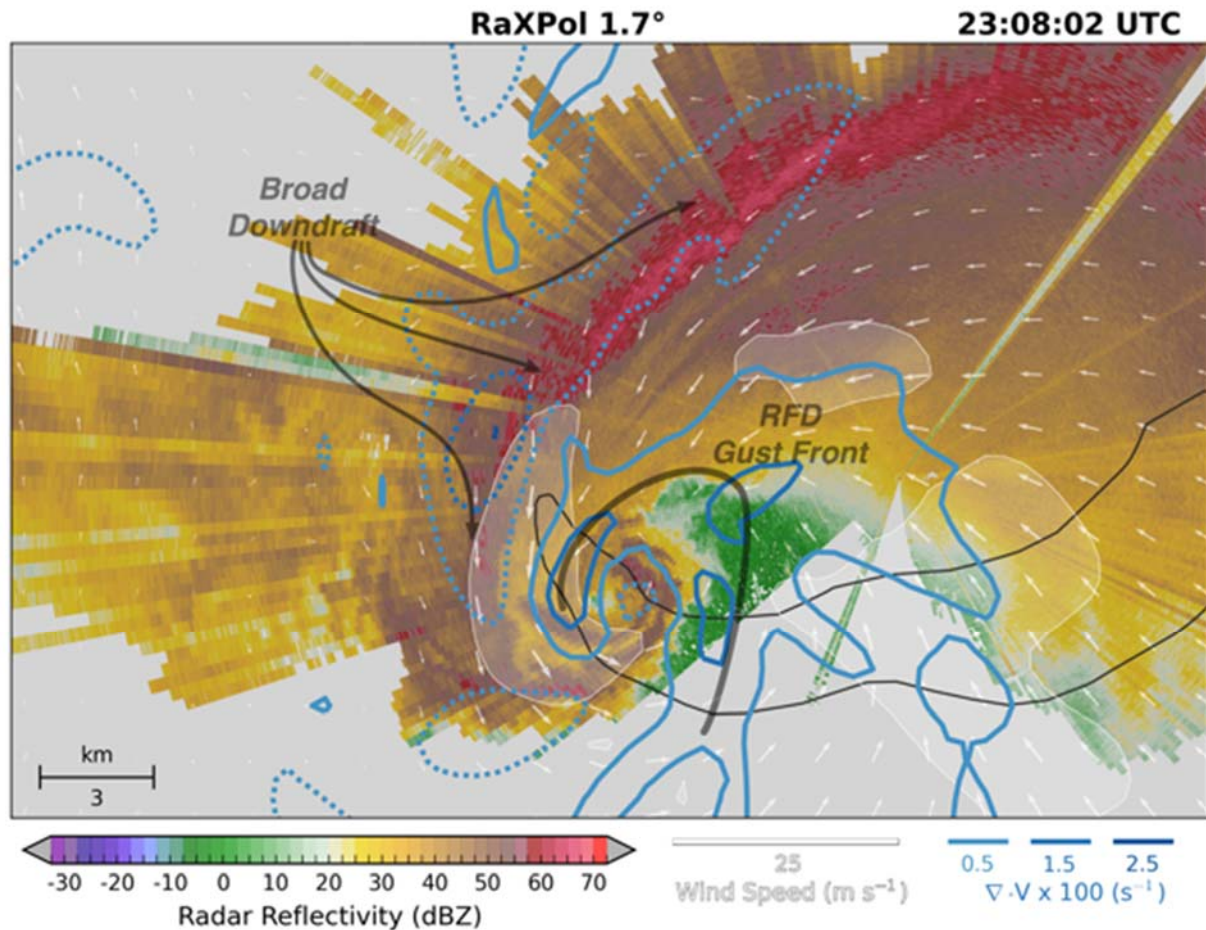
Experiments with varying observation density have identified a trade-off between reducing the amount of assimilation cycles needed to produce an accurate analysis of the El Reno supercell and interaction with model biases that can degrade forecast skill. For example, assimilation of high-density radar reflectivity observations results in a more rapid initialization of the El Reno supercell within the model; however, biases in the microphysical parameterization result in an erroneously strong cold pool that adversely affects subsequent storm-scale forecasts.

12. Ensemble Kalman Filter and Polarimetric Analysis of the 31 May 2013 El Reno, Oklahoma Supercell During Tornadogenesis

Patrick Skinner and Jeffrey Snyder (CIMMS at NSSL), Louis Wicker (NSSL), and Howard Bluestein and Kyle Thiem (OU School of Meteorology)

Polarimetric Doppler radar data with very high temporal and spatial resolution were collected by the RaXPol mobile radar preceding, during, and immediately following tornado genesis of the 31 May 2013 El Reno, Oklahoma tornado. These data have been assimilated into an ensemble of numerical models with 500 m horizontal grid spacing to retrieve the four-dimensional kinematic and thermodynamic state of the El Reno supercell during tornado genesis.

Ensemble mean analyses of the wind field have been compared with RaXPol observations to diagnose the physical processes controlling evolution of fine scale polarimetric signatures. Examples include radar signatures of an internal rear-flank downdraft momentum surge preceding tornado genesis and development of an elongated downdraft through the forward flank of the storm (see figure below) following tornado development.



RaXPol 1.7 degree radar reflectivity (dBZ) at 2308 UTC with corresponding EnKF analysis ensemble mean convergence (s^{-1}) overlain in blue contours, dashed contours represent negative values. Ensemble mean wind vectors are plotted in white with regions where wind speed is greater than 25 m s^{-1} shaded white. The rear-flank downdraft (RFD) gust front and broad downdraft extending through the forward flank are annotated.

13. Forcing Mechanisms for an Internal Rear-Flank Downdraft Momentum Surge in the 18 May 2010 Dumas, Texas, Supercell

Patrick Skinner and Corey Potvin (CIMMS at NSSL), Christopher Weiss (Texas Tech University), Louis Wicker (NSSL), and David Dowell (ESRL)

Mobile radar data collected during the second Verification of the Origin of Rotation in Tornadoes Experiment (VORTEX2) were assimilated into an ensemble of numerical models in order to diagnose the forcing mechanisms of an internal rear-flank downdraft (RFD) momentum surge. Retrieval and decomposition of the perturbation pressure field from the ensemble mean analyses revealed that the RFD surge primarily resulted from nonlinear dynamic forcing. Trajectory analyses revealed near-surface parcels within the RFD surge originated less than 1 km aloft and accelerated by means of a favorable

horizontal pressure gradient force into a localized trough within the broad-scale RFD. After crossing the trough axis, parcels encountered an adverse pressure gradient force and rapidly decelerated, resulting in the development of a convergence line along the trough axis.

14. Coherent Airstream Analysis of a Supercell Rear-Flank Downdraft in an Idealized Numerical Simulation

Ryan Hastings (NRC), Patrick Skinner (CIMMS at NSSL), and Michael Coniglio (NSSL)

An agglomerative cluster analysis is performed for parcel trajectories within the rear-flank downdraft of a simulated supercell in order to objectively identify coherent airstreams. Terms of the momentum equations are integrated along representative trajectories of each airstream in order to identify the origins and forcing mechanisms for parcels entering the low-level mesocyclone and instigating an internal rear-flank downdraft momentum surge.

15. Documenting a Rare Tornado Merger Observed in the 24 May 2011 El Reno-Piedmont, Oklahoma, Supercell

Michael French (Stony Brook), Patrick Skinner (CIMMS at NSSL), Louis Wicker (NSSL), and Howard Bluestein (OU School of Meteorology)

Observations from four Doppler radars, including high temporal resolution, volumetric data from the Mobile Weather Radar, 2005 X-Band, Phased Array (MWR-05XP) are examined to document the merger of two intense tornadoes occurring 24 May 2011. It was found that a second tornado developed in a region of strong convergence along the rear-flank gust front north of an existing tornado. The second tornado rapidly intensified and the two tornadoes were observed to make nearly a complete revolution around each other as the merger occurred. A rapid broadening and intensification of the resulting tornado vortex signature was observed immediately following the merger.

16. A Comparison of Near-Surface Buoyancy and Baroclinicity Across Three VORTEX2 Supercell Intercepts

Christopher Weiss and John Schroeder (Texas Tech University), David Dowell (ESRL), Patrick Skinner and Anthony Reinhart (CIMMS at NSSL), and Paul Markowski and Yvette Richardson (Penn State University)

Observations from a rapidly-deployable fleet of StickNet surface observing stations were examined for three deployments representing strongly tornadic, weakly tornadic, and nontornadic supercells. Buoyancy deficits throughout the entire supercell were found to be weakest in the strongly tornadic case and strongest for the nontornadic case. Additionally, narrow zones of intense baroclinic vorticity generation were documented to the north of the mesocyclone in the weakly and nontornadic cases,

which is a similar position to downdraft locations in several recent high-resolution simulations.

17. A Real-time Weather-Adaptive 3DVAR Analysis and WRF Model Forecast System with Automatic Storm Positioning and On-demand Capability

Yunheng Wang, Thomas Jones, and Gerry Creager (CIMMS at NSSL), and Jidong Gao, Louis Wicker, Jack Kain (NSSL)

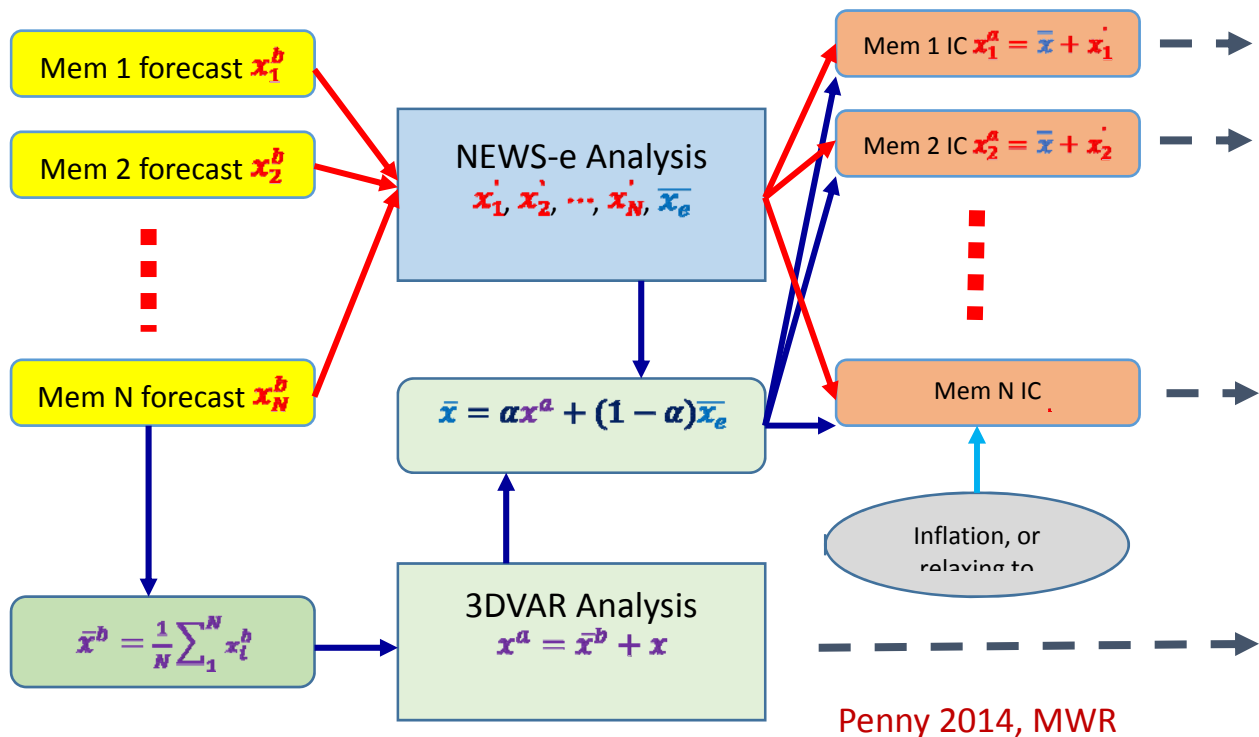
The concept for a real-time weather-adaptive 3DVAR analysis system for severe weathers detections and warnings has been well tested in the past several years (Gao et al. 2013, Smith et al. 2014). This year, we developed an interface to link the 3DVAR analysis system with the WRF model. So the analysis can be used for initializing WRF model forecasts. We also developed a real-time control system for the NOAA supported Warn-on-Forecast project (WoF). The goal for this work is to provide physically-consistent gridded analysis and forecast products to forecasters to help them make warning decisions in a timely manner. First, a storm positioning program is implemented based on NSSL WDSS-II two-dimensional composite reflectivity product. So it has the ability to automatically detect severe local hazardous weather events. Furthermore, the analysis and forecast can also be performed with on-demand capability in which end-users (e.g., forecasters or scientists) can set up the location of the analysis and forecast domain in real time based on the current weather situation. Second, the 3DVAR system incorporates available mesoscale forecasts, radar, satellite retrieved cloud water path, and traditional observations to perform a rapid analysis. This enhanced system has been tested during the 2016 Hazardous Weather Testbed (HWT) Spring Experiment period. Two types of products are generated. The first one, an analysis every 5 minutes has been produced with a floated weather-adaptive domain covered 640 km by 640 km. Then, a forecast has been launched every half hour for a 3-h WRF forecast.

18. A Hybrid Gain Ensemble Data Assimilation System for Warn-on-Forecast with the NEWS-e Ensemble Analysis and the 3DVAR Analysis System Using the WRF Forecasting Model

Jidong Gao (NSSL), Yunheng Wang, Dustan Wheatley, Kent Knopfmeier, Gerry Creager, and Patrick Skinner (CIMMS at NSSL), and Louis Wicker and Jack Kain (NSSL)

In an effort to unify the works within the Warn-on-Forecast (WoF) group, we developed a hybrid gain ensemble data assimilation system based on the NSSL Experimental WoF System for ensembles (NEWS-e) and the WRF-model based 3DVAR analysis system. With this scheme, the ensemble mean from forecast priors is used as background for the 3DVAR analysis and the analysis fields from the NEWS-e and 3DVAR are then linearly combined to produce a hybrid gain analysis around which the NEWS-e analysis ensemble is re-centered. The 3DVAR method has an advantage of incorporating weak constraints, such as mass continuity equation to help balance of different analysis variables. The 3DVAR analysis introduces climatological information on the background

error covariances for the EnKF analysis, which helps to reduce the effect of sampling noise for the ensemble analysis. The hybrid gain system is just implemented and will be tested with more cases for improvement.



Flowchart of the hybrid gain method with the NEWS-e analysis and the 3DVAR analysis.

19. Storm-Scale Data Assimilation and Ensemble Forecasting for Warn-on-Forecast

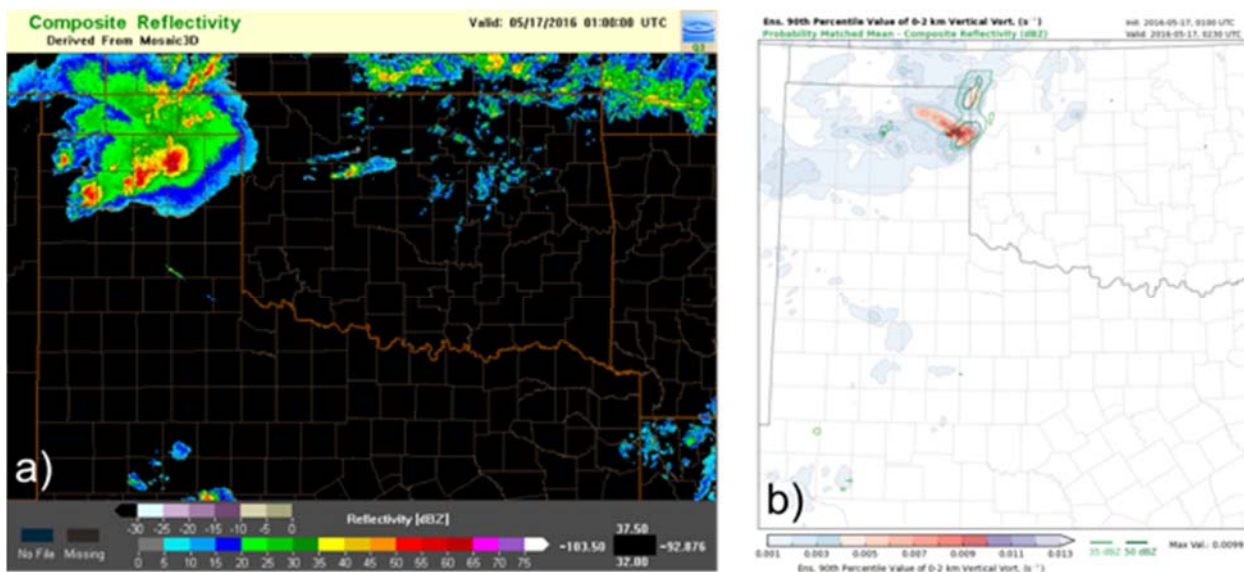
Dustan Wheatley, Kent Knopfmeier, Thomas Jones, Patrick Skinner, and Gerry Creager (CIMMS at NSSL)

The NOAA Warn-on-Forecast (WoF) research project is tasked with developing a regional 1-km storm-scale prediction system for the United States that assimilates radar, satellite, and conventional (e.g., surface) data. The proposed WoF system, to become operational sometime in the next decade, will generate new 0-3 h probabilistic forecasts 3-4 times an hour, for the purpose of predicting hazardous weather phenomena, such as thunderstorm rotation, hail, high winds, and flash flooding. A prototype system, known as the NSSL Experimental Warn-on-Forecast System for ensembles (NEWS-e), is based on the Weather Research and Forecasting (WRF) model with 3-km horizontal grid spacing for real-time experiments, and was tested during springs 2015-6 with promising results.

For spring 2016, the NEWS-e was run in real-time each day from 2 May – 3 June, which coincided with the NOAA Hazardous Weather Testbed 2016 Spring Forecast

Experiment. The starting point for each day's experiment was a 3-km, hourly cycled HRRRE under development at GSD. The 1500 UTC forecast cycle from the GSD ensemble provided initial and boundary conditions for the NEWS-e, a 36-member ensemble covering a 1000-km wide region with very frequent (sub-hourly) updates. The daily NEWS-e domain location targeted the primary region where severe weather was anticipated. Radar reflectivity and radial velocity, satellite (cloud water path retrievals), and surface data were assimilated every 15 min using the ensemble Kalman filter (EnKF) approach encoded in the Data Assimilation Research Testbed (DART).

This study is primarily focused on the short-term (i.e., 90-min) ensemble forecasts initialized from the resultant storm-scale analyses every 30 minutes during each hour of the real-time experiment. Preliminary work has evaluated the ability of model-derived measures of low-level (e.g., vorticity) and mid-level (e.g., updraft helicity) storm rotation to anticipate tornadic supercell thunderstorms and mesoscale convective systems. These results will be further compared to similar measures derived from the HRRRE, as well as the HRRR model (which is commonly used for operational storm-scale weather prediction).



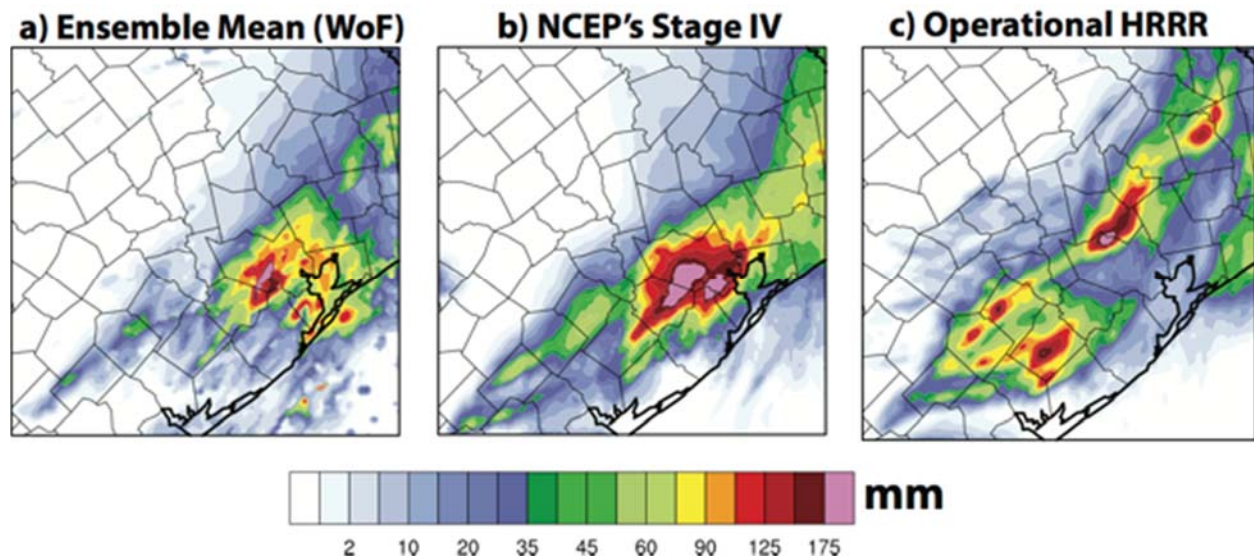
(a) Observed reflectivity and (b) ensemble 90th percentile value of 0-2 km vertical vorticity (s^{-1}) at 0100 UTC 17 May 2016. In panel (b), red triangles indicate tornado reports.

20. Short-Term (0-6 h) Flash Flood Producing Extreme Rainfall Events Using a Prototype Warn-on-Forecast System

Nusrat Yussouf, Kent Knopfmeier, and Wang (CIMMS at NSSL), and Jack Kain and Jian Zhang (NSSL)

While the main focus of WoF is tornadic events, Warn-on-Forecast type systems can be utilized for short-term probabilistic forecasts of other hazardous convective weather like

heavy rainfall and flash floods. To improve forecasts of flash floods and nowcasting convective precipitation, accurate (i.e. amount, location, and timing) quantitative precipitation forecasts (QPF) from NWP models is crucial. Therefore, to evaluate the capability of a prototype Warn-on-Forecast system in forecasting heavy rainfall, retrospective short-term (0-6 h) probabilistic ensemble forecasts of the 25th May 2015 Houston record-breaking heavy rainfall events are generated. The initial and boundary conditions for the 36-member storm-scale ensemble is obtained from the Global Ensemble Forecast System and routinely available observations from METAR, marine, mesonet, ACARS, radiosonde, satellite and WDR-88D radars will be assimilated every 15 minutes. The QPF generated from the continuous rapid update cycle ensemble are compared to observations and to rainfall estimates using extrapolation methods and the HRRR model. Results indicate that the 0-6 h rainfall forecasts from the WoF compares better with the observed rainfall in terms of location and amount. The operational HRRR is displaced and has a tendency to produce too much rainfall.



0-6 hr accumulated rainfall valid 0800 UTC 26 May 2016 from a) Probability matched mean WoF forecasts, b) NCEP's Stage IV analyses and c) operational HRRR forecasts.

21. Impact of Assimilating Department of Energy's Atmospheric Emitted Radiance Interferometer (AERI) Retrieved Temperature and Moisture Observations into a Prototype WoF Type Data Assimilation and Forecast System

Nusrat Yussouf (CIMMS at NSSL) and David Turner (NSSL)

Conducted two sets of data assimilation experiments for a 22-day period (from 25 May - 15 June 2002, IHOP field experiment) using a 36-member ensemble at 15 km grid spacing over the CONUS and 3 km grid spacing over Oklahoma and surrounding states. The Control experiment assimilates routinely available observations from METAR, radiosonde, ACARS, and marine platforms every hour and the AERI experiment assimilates AERI observations (from six sensors located in north-central Oklahoma and south Kansas) in addition to the routinely available observations (that

are assimilated in the Control experiment). Ensemble forecasts are launched from the 3-km storm-scale ensemble for convectively active days. Observations from Oklahoma mesonet, Stage IV precipitation, MRMS reflectivity and the ARM supplemental soundings are used for verification. Results do not indicate any clear improvements of the AERI experiment compared to the Control experiment. The next step is to assimilate observations every 10-min into both the experiments to see if there are any improvements in the forecasts from assimilating high temporal resolution AERI observations.

22. Computational Infrastructure Support Activities

Gerry Creager (CIMMS)

Increased storage capabilities for Warn on Forecast personnel on the Cray environment by expanding primary storage and incorporating second-tier (near-line storage) in support of research and real-time activities. Oversaw acquisition of an increment in high performance storage capacity for the Cray research computing environment, effectively doubling existing high performance storage. Worked with NSSL IT contractors to achieve a temporary second-tier (non-high performance) capacity for the Spring Forecasting Experiment and subsequent research efforts, while undertaking to specify and oversee acquisition of hardware to provide a dedicated second-tier storage facility for the Cray environment.

Acquired additional computational resources in concert with the University of Texas and the Texas Advanced Computing Center, allowing large-scale execution of the Community Leveraged Unified Ensemble experiment. Worked with TACC leadership and NSSL WRF personnel to identify requirements to support the CLUE experiment, obtain the necessary computational and storage resources, and port software to the new computing environment. NSSL was one of the first large-scale users of the TACC Cray XC40 supercomputer. CLUE is being completed with final gap-filling processing to complete the dataset at this time.

Close cooperation with NSSL IT contract personnel to support power and cooling requirements and issues in the main computing facility at the National Weather Center, resulting in better overall cooling distribution and balanced electrical loads. Supported IT in issues associated with cooling failures, poor overall cooling distribution and airflow management. Provided input and worked with OU engineering personnel to resolved these problems. Supported IT personnel in efforts to upgrade power distribution within the computing facility, as well as redistribution of loads when panel overloads were identified.

Supported acquisition, installation and configuration of post-processing systems to allow off-line analysis and post-processing of research and real time data. Identified hardware, supported purchasing process paperwork and assisted with installation of needed software, and network-attached storage configurations, for the post-processing systems.

Publications

- Fierro, A. O., A. J. Clark, E. R. Mansell, D. R. MacGorman, S. Dembek and C. Ziegler, 2015: Impact of storm-scale lightning data assimilation on WRF-ARW precipitation forecasts during the 2013 warm season over the contiguous United States. *Monthly Weather Review*, **143**, 757-777.
- Fierro, A. O., E. R. Mansell, D. R. MacGorman, and C. Ziegler, 2015: Explicitly simulated electrification and lightning within a tropical cyclone based on the environment of Hurricane Isaac (2012). *Journal of the Atmospheric Sciences*, **72**, 4167–4193.
- Fierro A. O., 2016: “Present State of Knowledge of Electrification and Lightning within Tropical Cyclones and Their Relationships to Microphysics and Storm Intensity.” Chapter 7 in *Advanced Numerical Modeling and Data Assimilation Techniques for Tropical Cyclone Predictions*, U. C. Mohanty and S. Gopalakrishnan, eds.. Co-published by Springer International Publishing, Cham, Switzerland, with Capital Publishing Company, New Delhi, India, pp. 197-220.
- Fierro, A. O., J. Gao, C. Ziegler, K. Calhoun, E.R. Mansell and D. R. MacGorman, 2016: Assimilation of flash extent data in the variational framework at convection-allowing scales: Proof-of-concept and evaluation for the short term forecast of the 24 May 2011 tornado outbreak. *Monthly Weather Review*, In Press.
- French, M. M., P. S. Skinner, L. J. Wicker, and H. B. Bluestein, 2015: Documenting a rare tornado merger observed in the 24 May 2011 El Reno-Piedmont, Oklahoma supercell. *Monthly Weather Review*, **143**, 3025–3043.
- Gallo, B. T., A. J. Clark, and S. R. Dembek, 2016: Forecasting tornadoes using convection-permitting ensembles. *Weather and Forecasting* **31**, 273–295.
- Gallo, B. T., A. J. Clark, and S. R. Dembek, 2016: CORRIGENDUM. *Weather and Forecasting*, **31**, 1407-1408.
- Jones, T. A., K. H. Knopfmeier, D. M. Wheatley, and G. J. Creager, 2016: Storm-scale data assimilation and ensemble forecasting with the NSSL Experimental Warn-on-Forecast System. Part II: Combined radar and satellite experiments. *Weather and Forecasting*, **30**, 297-327.
- McGovern, A., C. K. Potvin, and R. A. Brown, 2016: Using large-scale machine learning to improve our understanding of the formation of tornadoes. CRC Press, *In Press*.
- Potvin, C. K., and M. L. Flora, 2015: Sensitivity of idealized supercell simulations to horizontal grid spacing: Implications for Warn-On-Forecast. *Monthly Weather Review* **143**, 2998-3024.
- Shapiro, A., S. Rahimi, C. K. Potvin, and L. Orf, 2016: On the use of advection correction in trajectory analysis. *Journal of Atmospheric Science*, **72**, 4261-4280.
- Skinner, P. S., C. C. Weiss, L. J. Wicker, C. K. Potvin, and D. C. Dowell, 2015: Forcing mechanisms for an internal rear-flank downdraft momentum surge in the 18 May 2010 Dumas, Texas, supercell. *Monthly Weather Review*, **143**, 4305–4330.
- Skinner, P. S., L. J. Wicker, D. M. Wheatley, and K. H. Knopfmeier, 2016: Application of two spatial verification methods to ensemble forecasts of low-level rotation. *Weather and Forecasting*, **31**, 713-735.
- Thompson, T. E., L. J. Wicker, X. Wang, and C. K. Potvin, 2015: A comparison between the local ensemble transform Kalman filter and the ensemble square root filter for the assimilation of radar data in convective-scale models. *Quarterly Journal of the Royal Meteorological Society*, **141**, 1163-1176.
- Weiss, C. C., D. C. Dowell, J. L. Schroeder, P. S. Skinner, A. E. Reinhart, P. M. Markowski, and Y. P. Richardson, 2015: A comparison of near-surface buoyancy and baroclinity across three VORTEX2 supercell intercepts. *Monthly Weather Review*, **143**, 2736-2753.
- Wheatley, D. M., K. H. Knopfmeier, T. A. Jones, and G. J. Creager, 2015: Storm-scale data assimilation and ensemble forecasting with the NSSL Experimental Warn-on-Forecast System. Part I: Radar data experiments. *Weather and Forecasting*, **30**, 1795-1817.
- Yussouf, N., D. C. Dowell, L. J. Wicker, K. H. Knopfmeier, and D. M. Wheatley, 2015: Storm-scale data assimilation and ensemble forecasts for the 27 April 2011 severe weather outbreak in Alabama. *Monthly Weather Review*, **143**, 3044–3066.
- Yussouf, N., J. S. Kain, and A. J. Clark, 2016: Short-term probabilistic forecasts of the 31 May 2013 Oklahoma tornado and flash flood event using a continuous-update-cycle storm-scale ensemble system. *Weather and Forecasting*, **31**, 957-983.
- Zhuang Z., N. Yussouf and J. Gao, 2016: The Analyses and Forecasts of a Tornadic Supercell Outbreak using a 3DVAR System Ensemble. *Advances in Atmospheric Science*, **33**, 544-558.

NSSL Project 4 – Hydrologic Modeling Research

NOAA Technical Lead: Jonathan Gourley (NSSL)

NOAA Strategic Goal 2 – Weather-Ready Nation – Society is Prepared for and Responds to Weather-Related Events

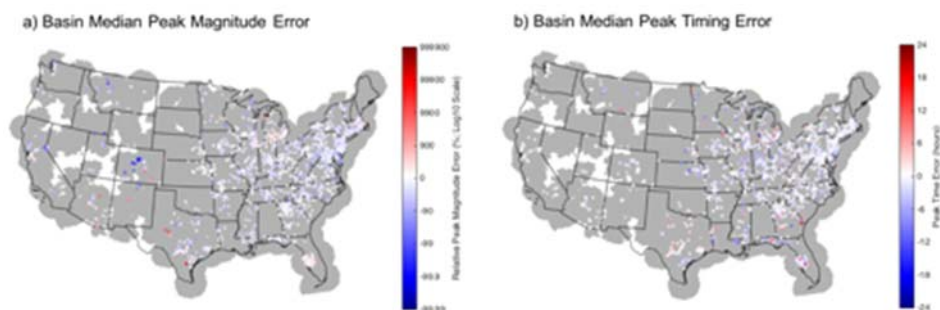
Funding Type: CIMMS Task II

Accomplishments

1. Demonstrate Real-Time Flash Flood Predictions Across the Conterminous U.S.

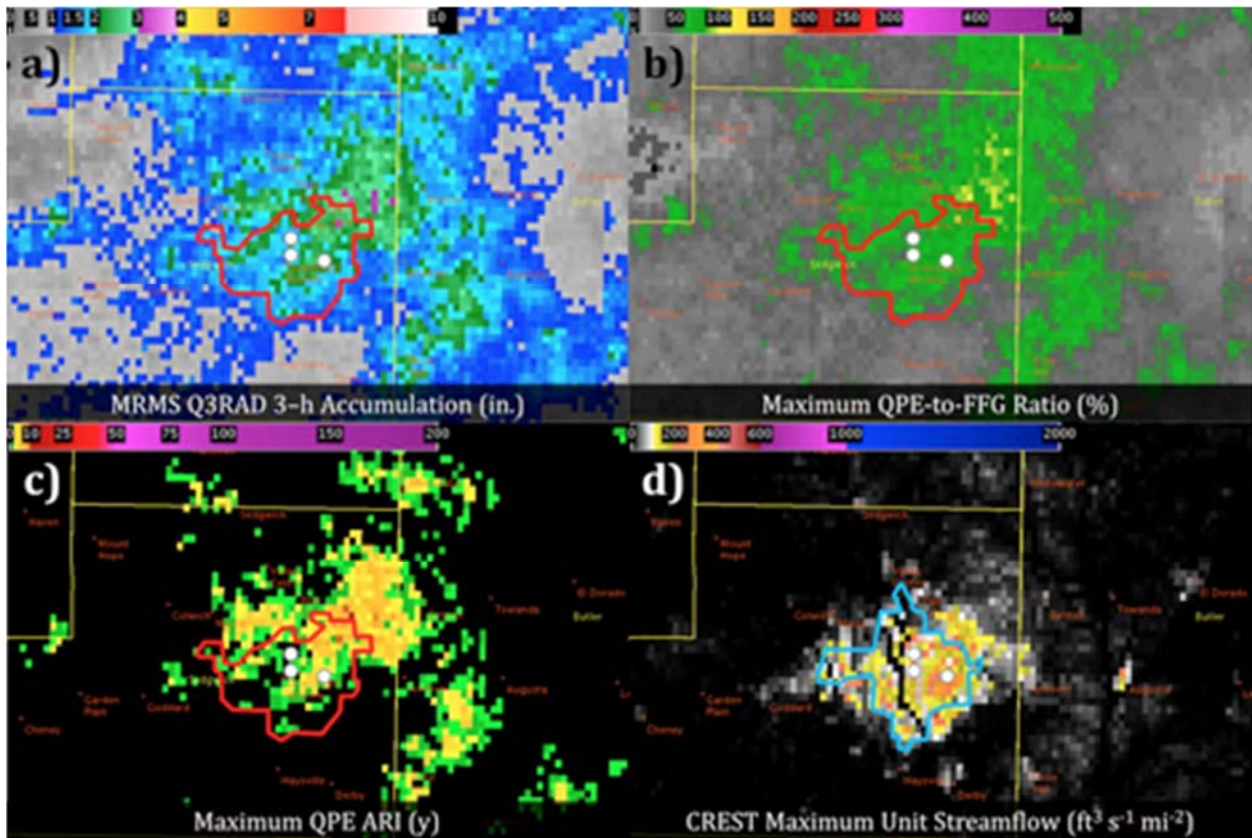
Jonathan Gourley (NSSL), and Humberto Vergara-Arrieta and Zachary Flamig (CIMMS at NSSL)

A formal evaluation of the products in the Flooded Locations and Simulated Hydrographs (FLASH) system was completed and successfully submitted for publication in the Bulletin of the American Meteorological Society (BAMS). The evaluation was based on a previous exercise performed for a period of 10 years and over 2,000 basins across the Conterminous United States (CONUS). Quality control datasets were employed to ensure a more accurate assessment of FLASH. Snow dominated basins and areas significantly affected by poor radar coverage were set aside for the evaluation. The figure below (from Gourley et al. 2016) shows a summary of peak flow simulation skill over CONUS using the Coupled Routing and Excess Storage (CREST) physics and the Kinematic Wave model in FLASH. It can be seen that, on average, FLASH underestimates the magnitude of peak flow in Colorado and the Intermountain West. No regional biases in the eastern two-thirds of the CONUS are observed. The peak flow timing shows no regional dependencies and is simulated with errors less than two hours for the majority of basins. This high skill in peak flow timing is largely attributed to the parameter estimates of the Kinematic Wave model developed by FLASH researchers (see Vergara et al. 2016).



(a) Spatial depiction of the peak magnitude error (in %) for the USGS gauged basins used in the study; (b) spatial depiction of the peak timing error (in hours). The gray-shaded regions correspond to areas that have radar coverage by the NEXRAD network within 2 km of the ground.

FLASH products were featured and tested in the HMT Multi-Radar Multi-Sensor Hydro Experiment during July – August of 2015. The figure below (from Martinaitis et al. 2016) shows a demonstration of MRMS-FLASH products at the testbed during a flash flood event on July 6 over Wichita, Kansas. CREST-based products proved their potential in highlighting flash flood threat over urbanized areas. For this particular event, the other products suggested low flash flood potential. The highlighted region of the CREST-based product displayed a good agreement with reports of extensive street flooding and water rescues of stranded motorists. One of the general conclusions by participating forecasters was the benefit of the CREST maximum unit streamflow product over urbanized regions.

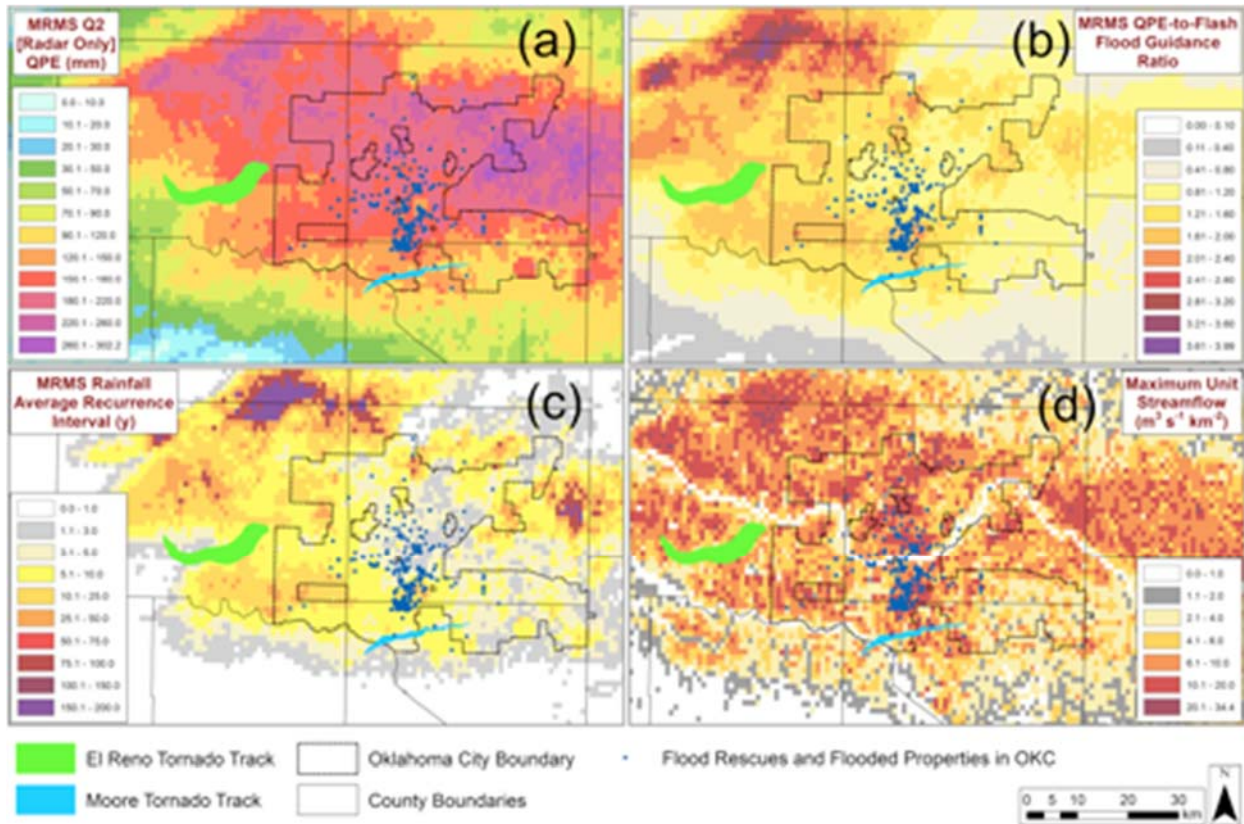


Four-panel image of (a) MRMS Q3RAD 3–h accumulation (in.), (b) maximum QPE-to-FFG ratio (%), (c) maximum QPE ARI (y), and (d) CREST maximum unit streamflow (shown in $\text{ft}^3 \text{s}^{-1} \text{mi}^{-2}$) as displayed in AWIPS-II at 2345 UTC 6 July 2015 during a flash flood event in Wichita, Kansas. The red contour in (a)–(c) represents the approximate area of CREST maximum unit streamflow values $\geq 1 \text{ m}^3 \text{ s}^{-1} \text{ km}^{-2}$ ($100 \text{ ft}^3 \text{ s}^{-1} \text{ mi}^{-2}$). The light blue contour in (d) represents the AWIPS-defined urban boundary of Wichita, Kansas. The white dots represent the real-time NWS LSRs of flash flooding.

2. Compare Skill of FLASH Model Outputs to Operational Flash Flood Guidance System

Jonathan Gourley (NSSL), and Humberto Vergara-Arrieta and Zachary Flamig (CIMMS at NSSL)

To further establish the skill of FLASH for flash flood forecasting in the United States, a quantitative comparison against the legacy operational Flash Flood Guidance (FFG) system was performed. This comparison was also presented in the Gourley et al. (2016) BAMS publication. Clark et al. (2014) had established the skill of FFG through the Critical Success Index (CSI). The maximum CSI with FFG in all River Forecast Centers was 0.20. FLASH outputs based on CREST water balance module had the best overall skill in detecting flood with a CSI of 0.38. Figure 3 (from Gourley et al. 2016) demonstrates the improvement in flash flood forecasting offered by FLASH over FFG with a case study. The flash-flooding event utilized in the study was the one associated to the May 31st 2013 tornado in Oklahoma City metropolitan area, the deadliest in the city's history and the second deadliest in the State of Oklahoma. The MRMS-to-FFG ratio product revealed estimates exceeding critical rainfall thresholds that were collocated with the highest Annual Recurrence Intervals (ARI) values. These FFG values were closer to the tornado but displaced to the North West from where most of the flash flood impacts occurred (see blue-filled circles in Fig. 3). The same MRMS quantitative precipitation estimates were used in FLASH's hydrologic model to derive the unit streamflow product shown in Fig. 3d. Unit peak discharges highlighted the OKC area with the highest concentration of impacts, demonstrating the improvements FLASH offers over FFG and the other rainfall-based products because of its capabilities in the flow routing and infiltration modules.



(a) Accumulated 24-hour rainfall estimates from the Multi Radar Multi Sensor system ending at 12 UTC 01 June 2013; (b) maximum 3-hour rainfall-to-flash flood guidance ratio from 22 UTC 31 May 2013 to 12 UTC 01 June 2013; (c) maximum 3-hour average recurrence interval of rainfall for the same times as (b); (d) maximum unit discharge forecasts from the distributed hydrologic model for the same times as in (b) and (c). The blue dots correspond to known flooding reports collected from the City of Oklahoma City, media, and social media. The reports include rescues, water in homes, street closures, and 13 fatalities. Recent tornado tracks are shown in colors as indicated in the legend.

Publications

- Argyle, E. M., J. J. Gourley, Z. L. Flamig, T. Hansen, and K. Manross, 2016: Towards a user-centered design of a weather forecasting decision support tool. *Bulletin of the American Meteorological Society*, In Press.
- Gourley, J. J., Z. Flamig, H. Vergara, P. E. Kirstetter, R. Clark III, E. Argyle, A. Arthur, S. Martinaitis, G. Terti, J. Erlingis, Y. Hong, and K. Howard, 2016: The Flooded Locations And Simulated Hydrographs (FLASH) project: Improving the tools for flash flood monitoring and prediction across the United States. *Bulletin of the American Meteorological Society*, In Press.
- Hardy, J., J.J. Gourley, P.E. Kirstetter, Y. Hong, F. Kong, and Z. Flamig, 2016: A method for probabilistic flash flood forecasting. *Journal of Hydrology*, In Press.
- Martinaitis, S. M., J. J. Gourley, Z. L. Flamig, E. M. Argyle, R. A. Clark III, A. Arthur, B. R. Smith, J. M. Erlingis, S. Perfater, and B. Albright, 2016: The HMT Multi-Radar Multi-Sensor Hydro Experiment. *Bulletin of the American Meteorological Society*, In Press.

- Vergara, H., P. E. Kirstetter, J. J. Gourley, Z. Flamig, Y. Hong, A. Arthur, and R. Kolar, 2016: Estimating a-priori kinematic wave model parameters based on regionalization for flash flood forecasting in the conterminous United States. *Journal of Hydrology*, In Press.
- Saharia, M., P. E. Kirstetter, H. Vergara, J. J. Gourley, and Y. Hong, 2016: Mapping flash flood severity in the United States. *Journal of Hydrometeorology*, Accepted.
- Saharia, M., P. E. Kirstetter, H. Vergara, J. J. Gourley, and Y. Hong, 2016: Characterization of floods in the United States. *Journal of Hydrology*, Accepted.
- Sheng, C., J. J. Gourley, Y. Hong, Q. Cao, N. Carr, P.-E. Kirstetter, J. Zhang, and Z. Flamig, 2016: Using citizen science reports to evaluate estimates of surface precipitation type. *Bulletin of the American Meteorological Society*, **97**, 187-193.
- Terti, G., I. Ruin, S. Anquetin, and J. J. Gourley, 2015: Dynamic vulnerability factors for impact-based flash flood prediction. *Natural Hazards*, **79**, 1481-1497.

NSSL Project 7 – Synoptic, Mesoscale and Stormscale Processes Associated with Hazardous Weather

NOAA Technical Leads: Lans Rothfus, Don MacGorman, Ted Mansell, Conrad Ziegler, and Jack Kain (NSSL), and Steven Weiss (SPC)

NOAA Strategic Goal 2 – Weather-Ready Nation – Society is Prepared for and Responds to Weather-Related Events

Funding Type: CIMMS Task II

Accomplishments

1. VORTEX-SE Planning and Spring 2016 Campaign

Erik Rasmussen (CIMMS at NSSL)

The VORTEX-SE activities include coordination with an inter-agency project executive committee, coordination and facilitation of field observing campaigns, and coordination of the project Scientific Steering Committee. The first VORTEX-SE science plan was developed during this reporting period. A workshop was organized and held in Huntsville, AL in November 2015, to gather input from 120 attendees regarding VORTEX-SE science objectives and priorities. Input was further refined through an online "virtual workshop". This led to the drafting of the first VORTEX-SE science plan in late winter 2016, providing input for the OAR grant competition in spring 2016.

During the winter of 2015, the first VORTEX-SE Field Campaign was designed and planned. This was a collaborative effort of over a dozen investigators who received grant support through NOAA/OAR. The field observations were collected in four intensive observing periods in March and April, 2016. This was a very quiet year for tornadoes in the southeast, and only one tornado occurred in the observing domain of northern Alabama. However, the scientifically useful observations were obtained in several scenarios of near-zero to low CAPE, but strong and evolving low-level shear. In one of the observing periods, significant CAPE developed. Storms with a variety of morphologies were observed, including short lines and supercells.

The field observing campaign highlighted a number of scientific problems associated with Southeast U.S. tornadoes, in both the physical and social/behavioral sciences. These experiences should allow the VORTEX-SE scientific community to refine and improve the project science plan in 2016/17.



VORTEX-SE investigators planning the daily operations during one of the 2016 Field Campaign Intensive Observing Periods.

2. Evaluation of Near Real-Time Preliminary Tornado Damage Paths

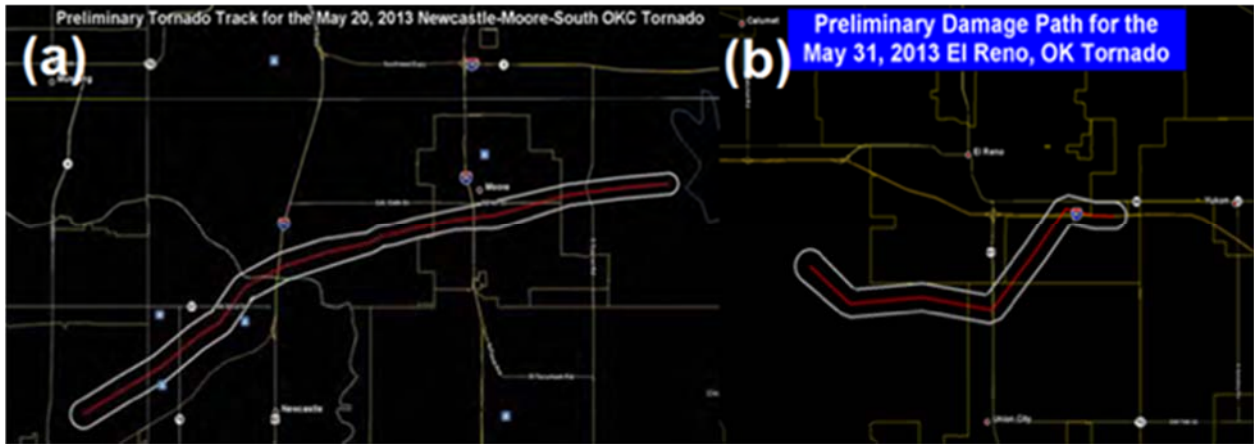
Chris Karstens (CIMMS at NSSL)

The ability to preliminarily diagnose areas damaged by a tornado was examined using both a manual and an automated approach. The manual method consists of using WSR-88D base data to track radar-indicated centroids of low-level rotation over the entirety of a tornado event. This method was developed at the National Weather Service (NWS) Weather Forecast Office (WFO) Norman, Oklahoma. According to the May 2013 Oklahoma Tornadoes and Flash Flooding Service Assessment, these preliminary damage paths were found to be beneficial to local first responders in the

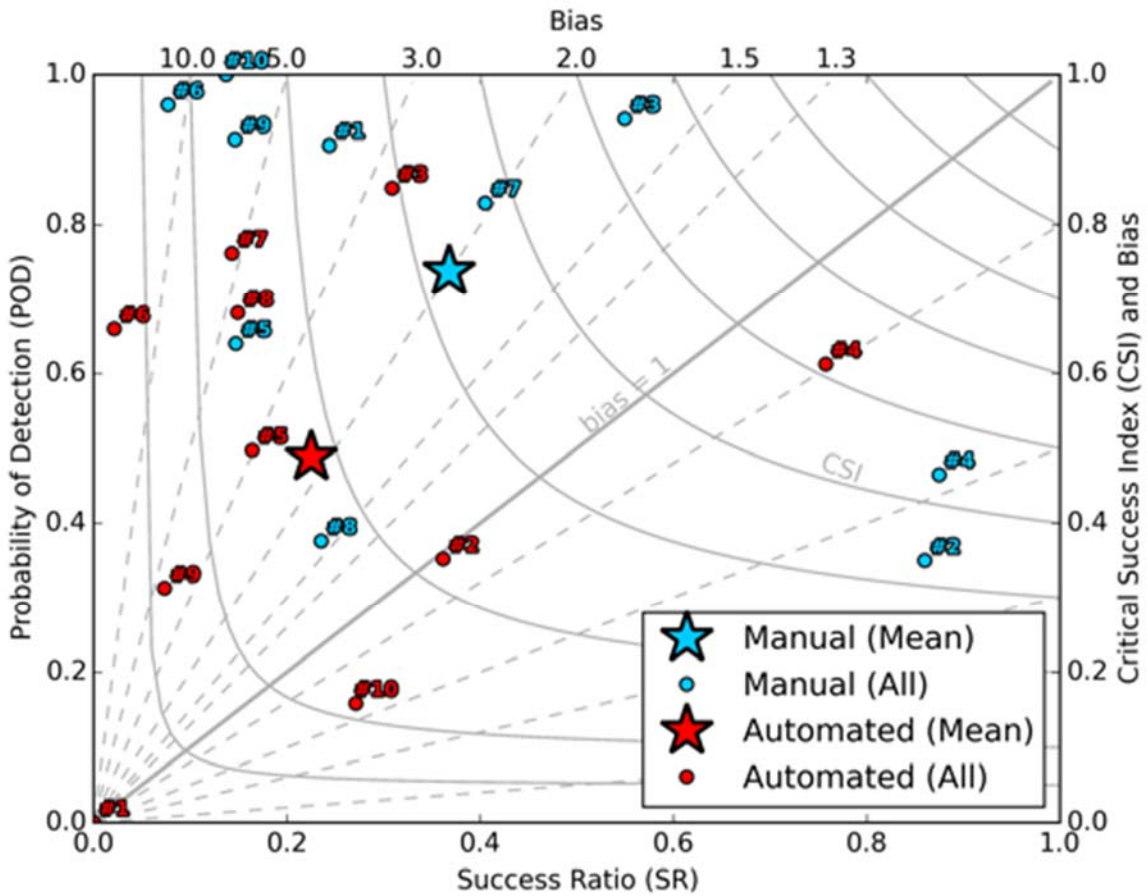
affected areas, to FEMA, and eventually to the public in graphical form via social media (first figure below). The purpose of this study was to analyze the performance of manually-derived preliminary tornado damage paths for an expanded, though limited, set of tornado events, and to compare the quality of these paths to those using an automated method using a geospatial verification technique. The automated method utilizes 0–2 km and 3–6 km AGL azimuthal shear from the Multi-Radar Multi-Sensor (MRMS) system to link together a series of strong azimuthal shear clusters and create a proposed damage path polygon.

The verification results indicate, in general, that the damage paths of the manual method do a better job of detecting areas with tornado damage, along with indicating marginally less false area, compared to the damage paths of the automated methods (second and third figures below). All methods have a high bias, indicating that the preliminary damage paths denote an area much larger than the observed damage path. The high biases are attributable to uncertainty of the exact areas with tornado damage, as the methods utilize remotely sensed data to derive a preliminary damage path. Because the exact tornado damage path cannot be known with a higher level of certainty until a damage survey is conducted, denoting large areas in the vicinity of the observed damage path seems reasonable until refinements can be made. This tradeoff is relevant when comparing the performance of the manual (available within approximately one hour after the event) and automated methods (available within a few minutes after the event). With these results it is important to be mindful of the small sample of events used in this study.

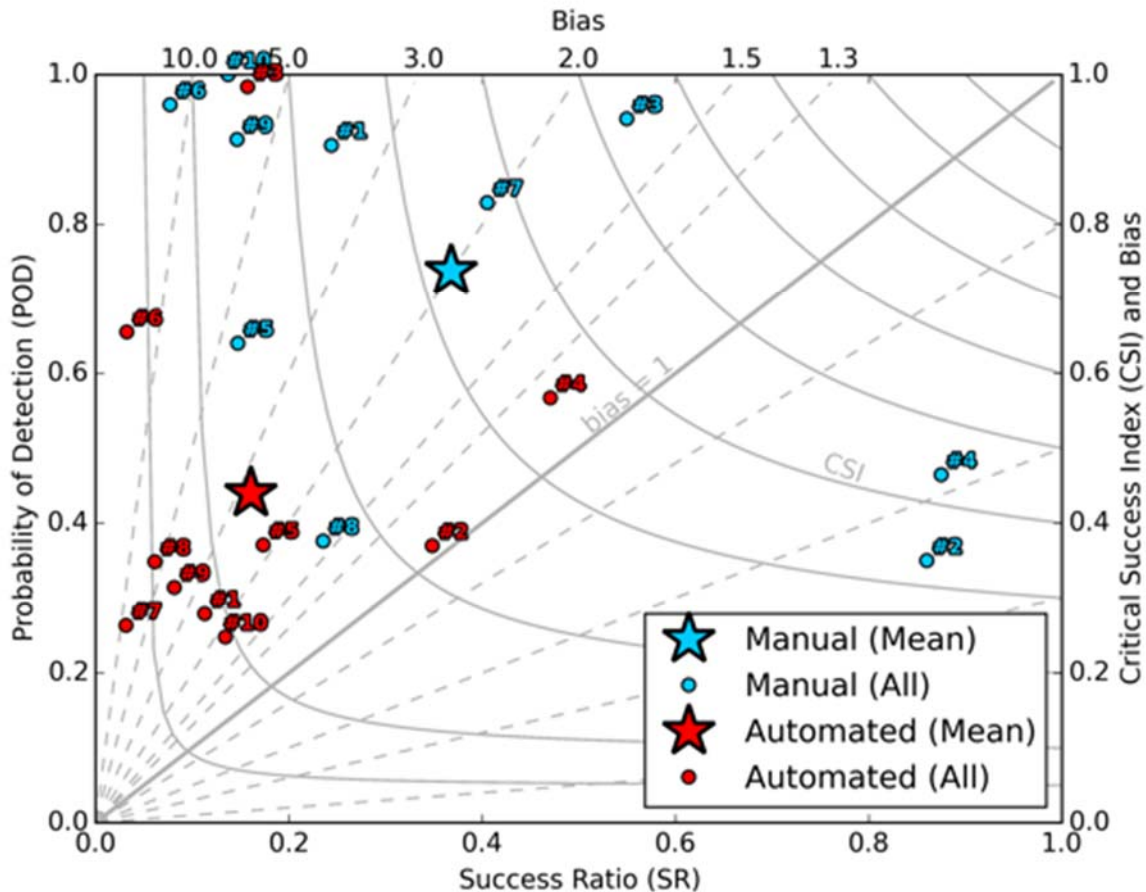
When evaluating the performance for the preliminary damage paths individually, the damage paths of the manual method had the best overall performance, followed by the automated methods using 0–2 km and 3–6 km azimuthal shear, respectively. Additionally, the metrics from damage paths using the manual method show greater variability compared to the automated method using 3–6 km AGL azimuthal shear, but similar to those using azimuthal shear from the 0–2 km layer. The larger variance of the manually-derived damage paths is likely attributable to the narrowness of these paths, given that this method is intended to denote uncertainty about the central axis of the tornado track (line) as opposed to a damage path (area). Many of the automated damage paths using the 0–2 km azimuthal shear appear to align well with the axis of observed damage paths, but the object identification appears out of sync with the observed damage path length. The degraded performance of the 3–6 km automatically-derived damage paths appears to be, in some cases, attributable to an offset in the axis of the damage path polygon, as compared to the observed damage path. This spatial offset is likely attributable to using mid-level rotation for identifying surface damage, as the two are not always correlated, especially during the later stages of a tornado.



Preliminary tornado damage paths from 20 (left) and 31 (right) May 2013 produced by WFO Norman in a GIS-compatible format.



Performance diagram for evaluating the quality of the preliminary damage paths from the manual and automated (using 0–2 km AGL azimuthal shear) methods.



As above, except using 3–6 km AGL azimuthal shear with the automated method.

Publications

Karstens, C. D., K. Shourd, D. Speheger, A. Anderson, R. Smith, D. Andra, T. M. Smith, and V. Lakshmanan, 2016: Evaluation of near real-time preliminary tornado damage paths, *Journal of Operational Meteorology*, **4**, 132-141.

3. Numerical Simulations of Electrification Processes in Tropical Cyclones and Storms

Alexander Fierro (CIMMS at NSSL) and Ted Mansell (NSSL)

The objective of this project is to conduct and, subsequently, use the output from very high-resolution real or idealized numerical simulations (350 m - 2 km) of the small-scale electrification processes within tropical cyclones (TCs) to augment our understanding on these processes and, potentially, to derive functional relationships between various lightning metrics and the microphysics/kinematics of TCs. Total lightning is emphasized because it is much better correlated to convective strength than cloud-to-ground lightning is. Lightning information is particularly critical in regions where radar data are scarce, such as over oceans where all TCs develop and eventually intensify. We implemented new physics into the NSSL COMMAS model to simulated idealized

hurricanes including rime splintering parameterizations, base state substitution code and vortex initialization. With this new code, we conducted cloud scale simulations of idealized electrified TC wherein shear or sea surface temperature were varied and compared results against a control simulation. In depth analysis of results from these simulations were also completed and submitted to an AMS journal (JAS, available upon request).

Publications

- Fierro, A. O., E. R. Mansell, D. R. MacGorman, and C. Ziegler, 2015: Explicitly simulated electrification and lightning within a tropical cyclone based on the environment of Hurricane Isaac (2012). *Journal of the Atmospheric Sciences*, **72**, 4167-4193.
- Fierro A. O., 2016: "Present State of Knowledge of Electrification and Lightning within Tropical Cyclones and Their Relationships to Microphysics and Storm Intensity." Chapter 7 in *Advanced Numerical Modeling and Data Assimilation Techniques for Tropical Cyclone Predictions*, U. C. Mohanty and S. Gopalakrishnan, eds. Co-published by Springer International Publishing, Cham, Switzerland, with Capital Publishing Company, New Delhi, India, pp. 197-220.
- Fierro, A. O., J. Gao, C. Ziegler, K. Calhoun, E. R. Mansell and D. R. MacGorman, 2016: Assimilation of flash extent data in the variational framework at convection-allowing scales: Proof-of-concept and evaluation for the short term forecast of the 24 May 2011 tornado outbreak. *Monthly Weather Review*, Accepted.

4. The Effect of Urban Environments on Storm Evolution Through a Radar-Based Climatology of the Central United States

Darrel Kingfield and Kristin Calhoun (CIMMS at NSSL)

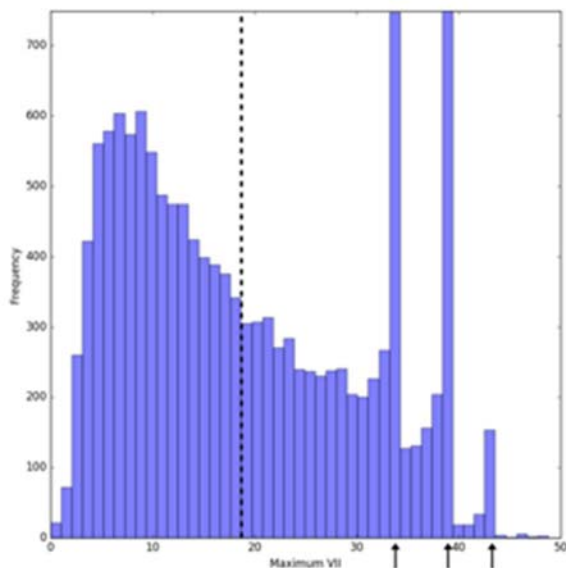
The influences urban environments have on storm development and patterns have been understudied to date, particularly for small to mid-sized cities. This study examines the role of the urban environment on the spatiotemporal characteristics of storms through a multi-year, multi-radar climatology of Weather Service Radar – 1988 Doppler (WSR-88D) radar reflectivity and algorithmic variables from 2009 to 2013 for four cities in the United States Central Plains: Minneapolis, MN, Omaha, NE, Oklahoma City, OK, and Dallas-Fort Worth, TX.

This storm-based approach allows us to better understand overall storm characteristics through larger sample statistics compared with previous studies of storm interaction with cities that typically focused on case studies or included fewer than 100 isolated storms interacting with a single city. This sample size will also allow us to better address the project questions of how city size address storm initiation, demise, track and intensity. With the expanded data set we can also address how time of year, time of day, and synoptic environment impact the effect of a city on storms.

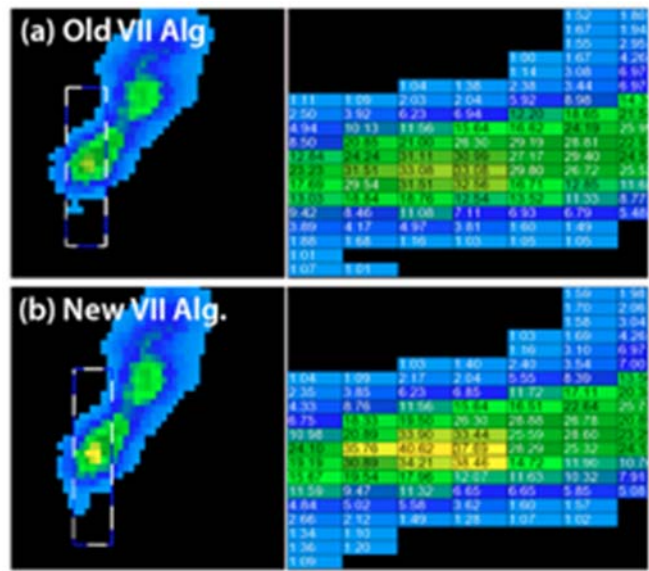
For this study, we use NSSL's Multi-Radar/Multi-Sensor (MR/MS) system to perform all data ingest and product derivations. In September 2014, the MR/MS system was deployed nationally for operational use by National Weather Service (NWS) forecast offices to enhance situational awareness during hazardous weather events. Through the application of the MR/MS framework over such a large climatology comprised of many different convective modes, this study revealed certain algorithmic performance inconsistencies that had not been measured on a smaller scale. This included updates

to the vertically integrated ice (VII) algorithm: after tracking thousands of thunderstorm objects and calculating spatial distributions of VII, we noticed two artificial peaks in this dataset (first figure below). Digging into the underlying code, we found that VII was being underestimated in thunderstorms with very strong updrafts. We re-derived the VII equation and tested it on several storms in our dataset (second figure below). As shown in the figure, this artificial limit of VII disappears with the updated algorithm and provides a more accurate estimate of frozen water in a vertical column of the atmosphere. This update was checked into the MR/MS operational baseline and will be available to NWS forecasters by September 2016.

The initial exploration of this study focused on a five-year multi-radar/multi-sensor attribute tracking analysis of 7,174 supercell storms in and around four urban domains in the Central Plains. When evaluating all of these data together, mean supercell lifetimes were longer for storms interacting with the urban domain compared supercells that missed this domain. Tracking radar-derived supercell attributes through their lifetime, a general decaying trend is observed in these variables during and after interaction with the urban domain for most combinations of variables and domains (third figure below). When compared to non-urban supercells, distributions of MESH, composite reflectivity, and other radar variables show a large amount of overlap in the ranges of values observed. The positions of radar and lightning-derived peaks on count maps exceeding certain thresholds also showed no preferred bullseye over the city with similar counts observed both upstream and downstream of the urban domain. Expansion of the dataset to include multiple storm types, additional years, convective initiation points, and additional permutations of variables and lifetime ranges are planned.



Histogram of all storm objects across the storms-cities domain that had more than 80% negative cloud-to-ground flashes (total of 13,538 storm objects). Artificial binning of the data was seen at specific values (noted by the black arrows along the x-axis) due to an error in the original VII algorithm.



Example of VII values associated with the (a) original MR/MS VII algorithm and the (b) updated VII algorithm to correct for artificial binning seen in Fig. 2 with the original algorithm. Left panels are 2D grids of the same storm object, right panels are specific grid values within the blue/white box in left panels.



MESH values extracted every 10 min. for supercells before, during, and after interaction with the urban domain as well as supercells with no interaction with the urban domain.

CIMMS Task III Project – Operation of VHF Lightning Mapping Systems to Provide Data for GOES-R GLM Verification and Algorithm Development and Testing

Don MacGorman (NSSL), Stephanie Weiss (CIMMS at NSSL), Ben Trabing, Crystal Nassir, and Dustin Jarreau (OU School of Meteorology), with collaborators Douglas Kennedy (NSSL) and Alexandre Fierro (CIMMS at NSSL)

NOAA Technical Lead: Steve Goodman (NOAA NESDIS)

NOAA Strategic Goal 2 – *Weather Ready Nation: Society is Prepared for and Responds to Weather-Related Events*

Funding Type: CIMMS Task III

Objectives

This grant was to cover part of the operating expenses of Lightning Mapping Arrays in Oklahoma (the OK-LMA) and in a region surrounding Houston, Texas (the HT-LMA). The National Severe Storms Laboratory (NSSL) and the University of Oklahoma jointly operate the Oklahoma Lightning Mapping Array (OK-LMA). Texas A&M and the University of Houston jointly operate the Houston Lightning Mapping Array (H-LMA). OK-LMA provides coverage of a region that produces supercell storms, as well as mesoscale convective complexes. The HT-LMA adds coverage of a region polluted by heavy automobile traffic and oil refineries and adds the possibility of acquiring total lightning data on hurricanes making landfall on the Gulf coast. Both systems for mapping total lightning activity will provide proxy data sets used by CIMMS scientists and GLM algorithm developers and used in various pre-launch operational tests of GLM data and algorithms. Once GOES-R GLM has undergone its initial testing and calibration and its data released for early evaluation by NOAA and NASA, the two LMAs also will be sources of ground truth data for the GLM. A second task under this grant was to finish evaluating the operational characteristics of the OK-LMA using techniques they have developed from previous grants and to prepare a manuscript describing this work for submission to a journal. These data also were to be used to begin producing a range-corrected climatology of lightning within OK-LMA's region of coverage.

Accomplishments

CIMMS, in collaboration with NSSL, continued operating the OK-LMA during the period of this grant. Furthermore, a subcontract to Texas A&M contributed toward operating expenses for the HT -LMA, which covers a coastal region and a highly polluted region. The reduced data stream produced by the networks in real time will be provided to the Hazardous Weather Testbed and the GOES-R Proving Ground for evaluating operational applications. These data, as well as archived data of the complete LMA data sets, have been and will be made available for GLM research projects and for GLM application developers.

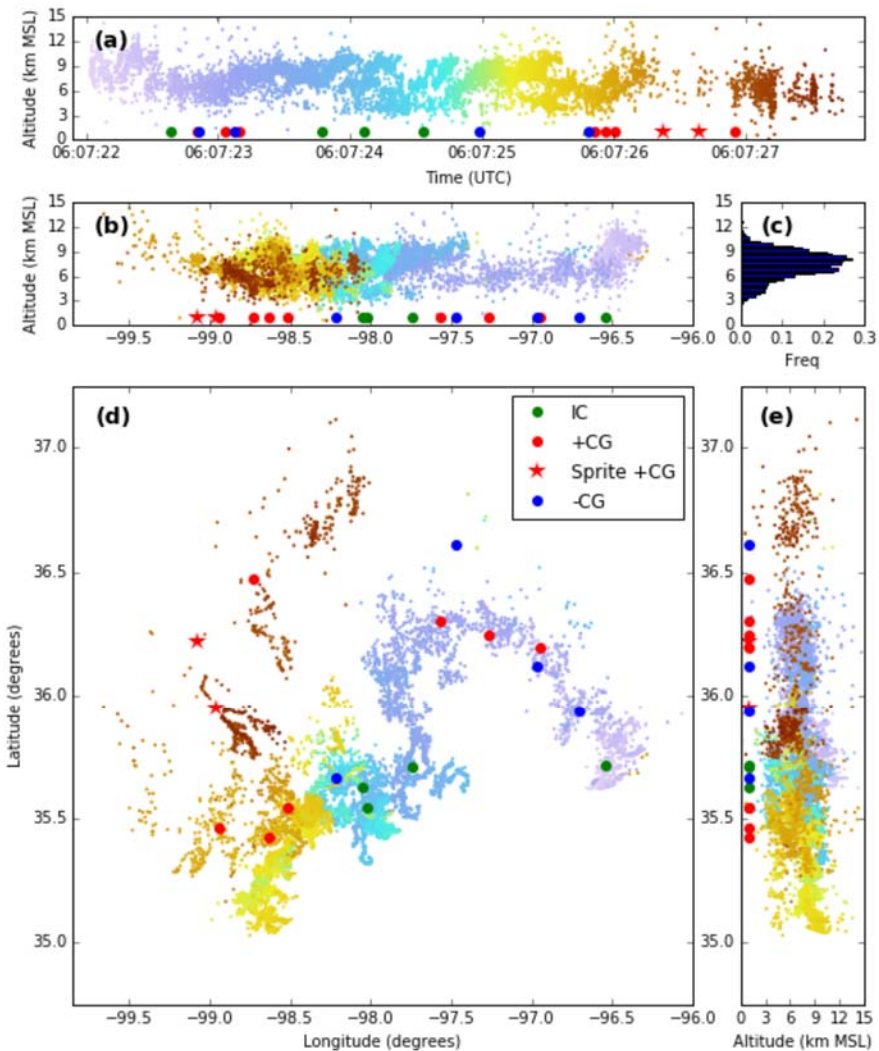
In 2016, a problem with the OKLMA in central Oklahoma prevented lightning from being mapped for part of the spring, and the problem was not discovered until later because

the technician who has been maintaining the network was required full time on another project. Steps are being taken to prevent a reoccurrence, and in fact, to improve timeliness of real-time data and overall station reliability over what has been possible previously.

Those steps include the following: (1) A solar-powered station has been purchased to replace a station we were required by the landowner to remove in 2015. The new station, which we plan to receive and install this fall or winter, is much easier to site and install and will bring the central cluster back to its full complement. (2) We have ordered replacements for the aging lightning mapping array board in the oldest stations, which have operated continuously since 2004, and plan to install them this winter. The previous board used socketed components which have become difficult to keep working properly. The new board has directly soldered components, and so should eliminate the problems caused by sockets. (3) We have purchased cell modems and will install them at all stations for next spring, so that real-time monitoring and data transmission will not be limited by the timing and occasional loss of parts of the point-to-point daisy-chain now used to transmit the station data to our central processor.

Work has been completed to develop a technique for normalizing archived lightning for range effects, and data from 2004 to the middle of 2012 have been processed to produce a lightning climatology for central Oklahoma. We plan to complete a 10-year climatology this year and to begin analyzing geographic, seasonal, and interannual variations, which we plan to publish.

Data from the OKLMA was provided to a WMO committee evaluating extreme lightning flashes. Experience from LMA's was important in developing criteria for establishing records for extreme lightning flashes, and a flash from the OKLMA was identified as having the largest spatial extent (as noted under awards) on record.



WMO record lightning flash that occurred in Oklahoma at 06:07:22 UTC on 20 June 2007. The maximum horizontal extent of the flash was 321 km (199.5 km). It began near Tulsa and traveled into far western Oklahoma. Color indicates progression in time of sources of VHF radiation for all panels. (a) Time-height plot. (b) Vertical projection in the east-west direction. (c) Altitude distribution. (d) Plan projection. (e) Vertical projection in the north-south direction. Large dots indicate points located by the National Lightning Detection Network (red, ground strikes lowering positive charge; blue, ground strikes lowering negative charge; green, in-cloud channels). The stars indicate the locations of sprites produced by the flash. (From Lang et al. 2016)

Publications

- DiGangi, E. A., D. R. MacGorman, C. L. Ziegler, D. Betten, M. Biggerstaff, M. Bowlan, C. Potvin, 2017: An overview of the 29 May 2012 Kingfisher supercell during DC3. *Journal of Geophysical Research*, Submitted.
- Lang, T. J., S. Pédeboy, W. Rison, R. S. Cervený, J. Montanyà, S. Chauzy, D. R. MacGorman, R. L. Holle, E. E. Ávila, Y. Zhang, G. Carbin, E. R. Mansell, Y. Kuleshov, T. C. Peterson, M. Brunet, F. Driouech, and D. Krahen, 2016: WMO World Record Lightning Extremes: Longest detected flash

distance and longest detected flash duration. *Bulletin of the American Meteorological Society*, In Press.

MacGorman, D. R., M. I. Biggerstaff, S. Waugh, J. T. Pilkey, M. A. Uman, D. M. Jordan, T. Ngin, W. R. Gamerota, G. Carrie, and P. Hyland, 2015: Coordinated lightning, balloon-borne electric field, and radar observations of a triggered lightning flash in North Florida. *Geophysical Research Letters*, **42**, 5635–5643.

MacGorman, D. R., M. S. Elliott, and E. A. DiGangi, 2016: Electrical discharges in the overshooting tops of thunderstorms. *Journal of Geophysical Research*, Submitted.

Waugh, S., C. L. Ziegler, D. R. MacGorman, S. E. Fredrickson, D. W. Kennedy, and W. D. Rust, 2015: A balloon-borne particle size, imaging and velocity probe for in situ microphysical measurements. *Journal of Atmospheric and Oceanic Technology*, **32**, 1562-1580.

CIMMS Task III Project – Using Total Lightning Data from BLM/GOES-R to Improve Real-Time Tropical Cyclone Genesis and Intensity Forecasts

Alexandre Fierro (CIMMS at NSSL), Ted Mansell, Conrad Ziegler, and Don MacGorman (NSSL), and Andrea Schumacher and Renate Brummer (CIRA-Colorado State University)

NOAA Technical Lead: Mark DeMaria (NOAA NCEP NHC)

NOAA Strategic Goal 2 – *Weather Ready Nation: Society is Prepared for and Responds to Weather-Related Events*

Funding Type: CIMMS Task III

Objectives

Conduct and subsequently use the output from very high-resolution numerical simulations (< 500 m) of the small-scale electrification processes within tropical cyclones (TCs) to derive functional relationships between various lightning metrics and the microphysics/kinematics of TCs. Whenever possible, these relationships will be verified against observations to ultimately develop total lightning predictors that could be used to assimilate total lightning observations directly into NHC's statistical prediction model (SHIPS). Total lightning is emphasized because it is much better correlated to convective strength than cloud-to-ground lightning is. Lightning information is particularly critical in regions where radar data are scarce, such as over oceans where all TCs develop and eventually intensify.

Accomplishments

The PI's visits to collaborators at CIRA and NHC during the first half of FY16 and subsequent meeting of the PIs during the AMS Tropical/Hurricane meeting in April 2016 resulted in the elaboration of a work plan for the remainder of the funding period. Namely, the results obtained in the high-resolution numerical simulations (< 500 m) during Year 1 (published in JAS and presented at the AMS Tropical/Hurricane meeting by the PI) needed be complemented with a new TC lightning study in the idealized framework. In this work, the PI was proposed to develop and incorporate an idealized hurricane initialization/model into the NSSL fractal-like, stochastic 3D cloud electrification model (COMMAS), which is able to explicitly resolve flash types and

polarity. Once incorporated, test how environmental parameters [e.g., shear, SST, RH etc.] influence the TC intensity and lightning activity/morphology [at the cloud scale: 500-2 km] to potentially generalize/improve the functional relationship derived in the study published in JAS during Year1. With the help of the main developer of COMMAS (Dr. Mansell), this idealized hurricane initialization/model was successfully incorporated into COMMAS during the second part of the 1st half of FY15 [i.e., November-December 2015 time frame]. During the Spring of 2016, many sensitivity simulations (on JET HPC resources) were conducted with the 3D lightning physics activated. The results motivated the inclusion of new physics into COMMAS (rime splintering parameterization) along with a improved vortex initialization procedure inspired by the Emanuel and Rotunno code available in WRF-ARW. Wind shear, relative humidity and sea surface temperature were varied using a base state substitution technique (BSS), which also was included into COMMAS (Dr. Mansell). With these model improvements, realistic lightning behaviours (evolution and patterns) were obtained. The PI recently completed a manuscript draft to be submitted to JAS summarizing the results of three main simulations: Control (wherein the TC intensifies to a steady state major TC), a shear run (deep layer shear is increased by ~ 15 m/s) and an SST cooling run.

Publications

- Fierro, A. O., E. R. Mansell, D. R. MacGorman, and C. Ziegler, 2015: Explicitly simulated electrification and lightning within a tropical cyclone based on the environment of Hurricane Isaac (2012). *Journal of the Atmospheric Sciences*, **72**, 4167-4193.
- Fierro, A. O., A. J. Clark, E. R. Mansell, D. R. MacGorman, S. Dembek, and C. Ziegler, 2015: Impact of storm-scale lightning data assimilation on WRF-ARW precipitation forecasts during the 2013 warm season over the contiguous United States. *Monthly Weather Review*, **143**, 757-777.
- Fierro A. O., 2016: "Present State of Knowledge of Electrification and Lightning within Tropical Cyclones and Their Relationships to Microphysics and Storm Intensity." Chapter 7 in *Advanced Numerical Modeling and Data Assimilation Techniques for Tropical Cyclone Predictions*, U. C. Mohanty and S. Gopalakrishnan, eds. Co-published by Springer International Publishing, Cham, Switzerland, with Capital Publishing Company, New Delhi, India, pp. 197-220.
- Fierro, A. O., J. Gao, C. Ziegler, K. Calhoun, E.R. Mansell, and D. R. MacGorman, 2016: Assimilation of flash extent data in the variational framework at convection-allowing scales: Proof-of-concept and evaluation for the short term forecast of the 24 May 2011 tornado outbreak. *Monthly Weather Review*, Accepted.

CIMMS Task III Project – Assimilating Satellite Data into NWP Models to Improve Forecasting of High Impact Weather Events

NOAA Technical Lead: Steve Goodman (NOAA/NESDIS)

NOAA Strategic Goal 2 – Weather Ready Nation: Society is Prepared for and Responds to Weather-Related Events

Funding Type: CIMMS Task III

Objectives

The multi-year goal of this research is to pave the way towards integration of the high-resolution satellite data that will be available from the GOES-R satellite in the best and

most efficient manner necessary to produce storm-scale forecasts. Emphasis is placed on assimilating cloudy satellite observations in concert with radar data observations.

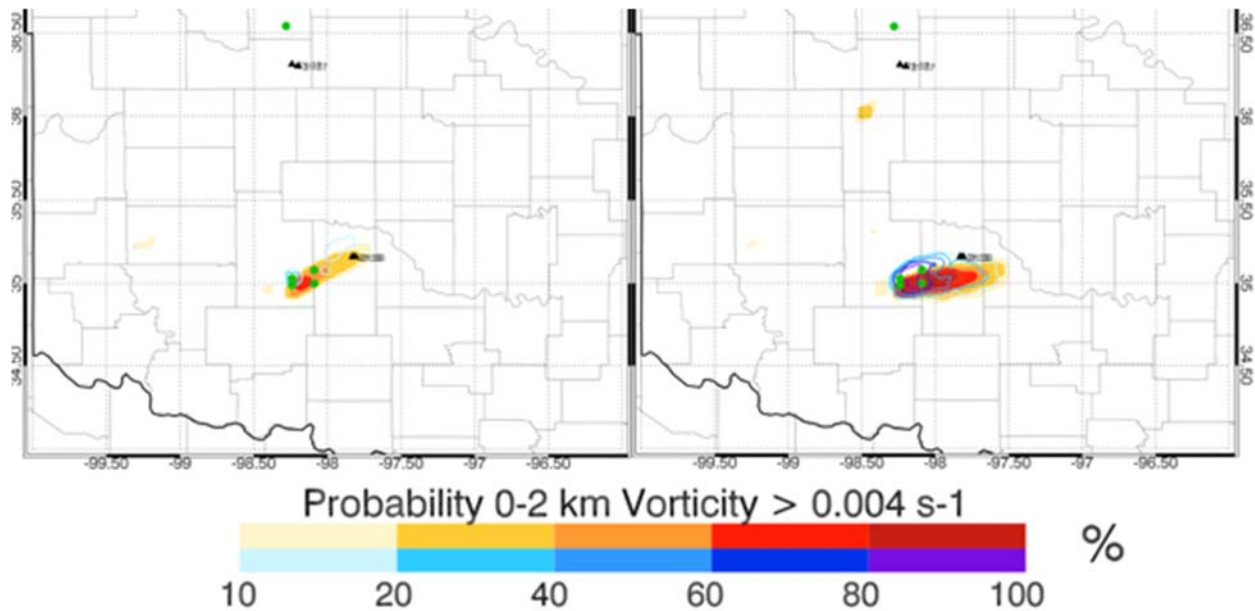
Accomplishments

1. Storm-Scale Cloud Water Path Assimilation

Thomas Jones (CIMMS at NSSL) and Patrick Minnis (NASA Langley Research Center)

Research is ongoing towards assessing the impacts of assimilating GOES cloud water path (CWP) retrievals into convection permitting models. CWP was assimilated into the NSSL experimental WoF System for ensembles (NEWS-e) during real-time testing for the 2016 HWT experiment. Assimilating these observations generally resulted in improved thermodynamic conditions over the storm-scale domain through better analysis of cloud coverage compared to radar-only experiments. These improvements often corresponded to an improved analysis of supercell storms leading to better forecasts of low-level vorticity. This positive impact was most evident for events where convection was not ongoing at the beginning of the radar and satellite data assimilation period.

Additional research has focused on determining the best methods to simultaneously assimilate both CWP and radar observations. Several instances of destructive interference were observed when assimilating both in the same location. In particular, assimilating CWP observations could weaken analyzed storm-cores in the model compared to radar-only experiments. To address this and other potential problems, a data thinning strategy was developed to remove conflicting and duplicate observations. First, clear-air reflectivity observations are removed in cloud free regions where $CWP=0 \text{ kg m}^{-2}$, since clear-air reflectivity does not necessarily correspond to cloud free conditions. Second, positive CWP retrievals where reflectivity $> 25 \text{ dBZ}$ within a column are removed since satellite observations in heavy precipitation have much higher uncertainties and do not sample the 3-D structure of precipitation features. In cases where clear air reflectivity observations exist and clouds are detected, clear-air reflectivity observations are removed within the cloud layer, but retained either above or below it. The figure below compares the probability of vorticity $> 0.004 \text{ s}^{-1}$ for a 90-minute forecast beginning at 2000 UTC 6 May 2015 using the original and thinned data sets. Using the thinned data set generates significantly higher vorticity probabilities for the central Oklahoma storm compared to the original, non-thinned, experiment.



Probability of 0-2 km AGL vertical vorticity $> 0.004 \text{ s}^{-1}$ for the 2 hour forecast period initiated at 1930 UTC for NOTHIN (left) and THIN (right).

2. GOES-R ABI Radiance Assimilation Using a Quick OSSE

Thomas Jones (CIMMS at NSSL), and Jason Otkin and Rebecca Cintineo (CIMSS-University of Wisconsin)

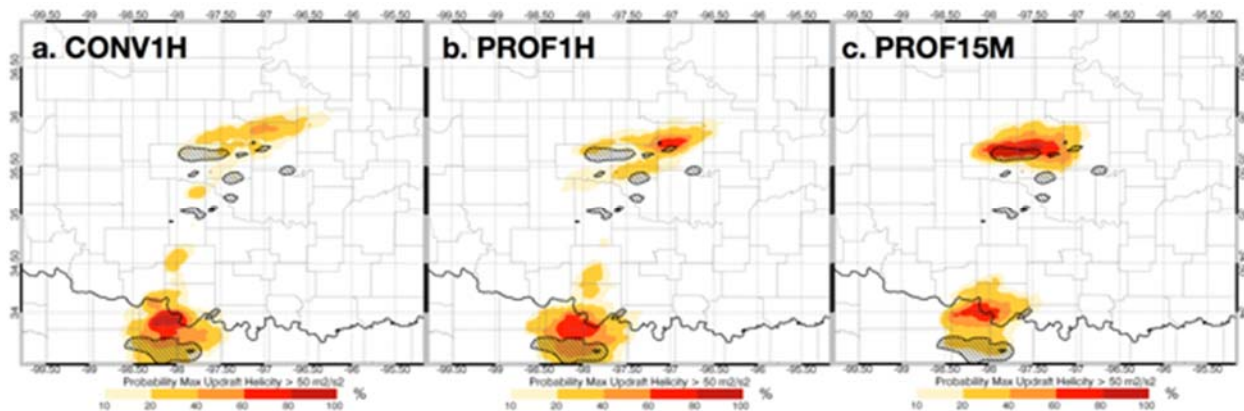
This project leads the NSSL contribution to the larger Observing System Simulation Experiment Testbed led by Robert Atlas. For our portion, assimilation tests employing different combinations of satellite, radar, and other observations are performed for a severe weather event occurring in the southern and central U.S. in June 2005. Simulated GOES-R ABI radiances and WSR-88D reflectivity and radial velocity observations were generated from a high resolution nature run. These observations were then assimilated back into an ensemble data assimilation system to determine their combined effectiveness at improvement the storm-scale analysis. The best forecasts were generated with both radar and satellite observations were assimilated into the model.

3. Hyperspectral Temperature and Humidity Profile Assimilation Using a Quick OSSE

Thomas Jones (CIMMS at NSSL), Steven Koch (NSSL), and Zhenglong Li (CIMSS-University of Wisconsin)

The research uses an Observation System Simulation Experiment (OSSE) approach to generate synthetic temperature and humidity profiles from a hypothetical geostationary-based sounder from a nature run of a high impact weather event on 20 May 2013. The

synthetic observations are then assimilated using an ensemble adjustment Kalman filter approach using hourly and 15-minute cycling to determine their effectiveness at improving the near storm environment. Results indicate that assimilating both temperature and humidity profiles reduced mid-tropospheric bias and error compared to assimilating conventional observations alone. While hourly cycling was generally effective, 15 minute cycling generally produced the lowest errors while also generating the best 2-4 hour updraft helicity forecasts of ongoing convection (figure below). The results of this study indicate the potential for significant improvement in short-term forecasting of severe storms from assimilation of hyperspectral geostationary satellite data, but more studies of this kind for different weather scenarios are needed to determine the generality of these findings.

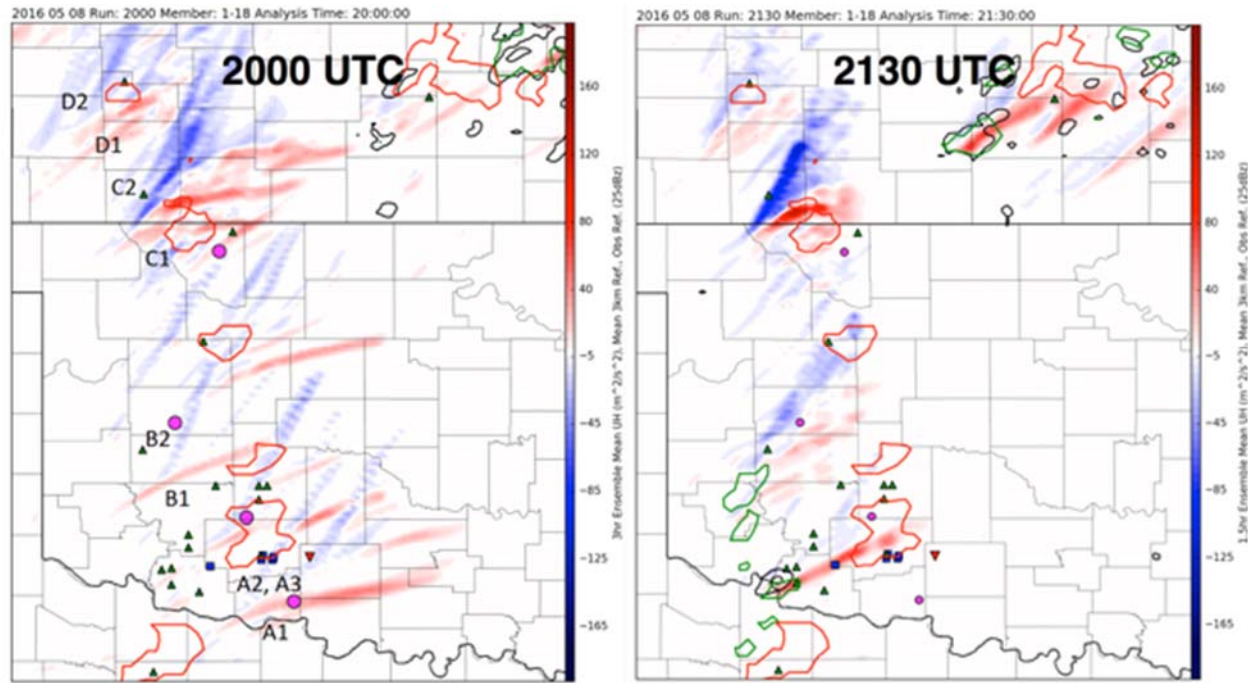


Probability of 2-5 km updraft helicity greater than 50 m² s⁻² for 4 hour forecasts initiated 2100 UTC 20 May. Hatched areas indicate location of nature run helicity greater than 50 m² s⁻² for the same time period.

4. Hollings Scholar Mentorship

Thomas Jones (CIMMS at NSSL) and Cameron Nixon (Hollings Scholar)

The Hollings Scholar Cameron Nixon analyzed the ability of the NEWS-e system to forecast left-split supercells in a mesoscale environment where both left and right splits were favorable. This environment was present over the Southern Plains during 8 May 2016 during which both left and right split supercells occurred. Both storm types produced numerous severe weather reports. Using “negative” updraft helicity, Cameron showed that the NEWS-e system can indeed forecast storm splitting and the persistence of left moving supercells in favorable environments. The figure below shows an example 3 hour forecast from 2000 UTC and 1.5 hour forecasts from 2130 UTC. Both positive (red) and negative (blue) ensemble mean updraft helicity forecasts are plotted and it is clearly evident that both left and right supercell tracks are forecast. This is an especially promising result since storm initiation had yet to occur in much of the model domain at 2000 UTC.



Mean updraft helicity for 0-3 hour forecasts beginning at 2000 UTC (left) and 1.5 hour forecasts beginning at 2130 UTC (right). Positive values (red) indicate cyclonic rotation while negative values (blue) indicate anti-cyclonic rotation. Red contours indicate location of observed reflectivity at 2300 UTC.

Publications

- Cintineo, R., J. Otkin, T. A. Jones, S. Koch, and D. Stensrud, 2016: Assimilation of synthetic GOES-R ABI infrared brightness temperatures and WSR-88D radar observations in a high-resolution OSSE. *Monthly Weather Review*, In Press.
- Jones, T. A., D. Stensrud, L. Wicker, P. Minnis, and R. Palikonda, 2015: Simultaneous radar and satellite data storm-scale assimilation using an ensemble Kalman filter approach for 24 May 2011. *Monthly Weather Review*, **143**, 165-194.
- Jones, T. A., and D. J. Stensrud, 2015: Assimilating cloud water path as a function of model cloud microphysics in an idealized simulation. *Monthly Weather Review*, **143**, 2052-2081.
- Jones, T. A., K. Knopfmeier, D. Wheatley, G. Creager, P. Minnis, and R. Palikonda, 2016: Storm-scale data assimilation and ensemble forecasting with the NSSL experimental Warn-on-Forecast system. Part II: Combined radar and satellite experiments. *Weather and Forecasting*, **30**, 297-327.
- Jones, T. A., S. Koch, and Z. Li, 2016: Assimilating synthetic hyperspectral sounder temperature and humidity retrievals to improve severe weather forecasts. *Atmospheric Research*, Accepted.

CIMMS Task III Project – Hybrid Data Assimilation for Convective-Scale “Warn-on-Forecast”

Xuguang Wang (OU School of Meteorology)

NOAA Technical Lead: Louis Wicker (NSSL)

NOAA Strategic Goal 2 – *Weather Ready Nation: Society is Prepared for and*

Responds to Weather-Related Events

Funding Type: CIMMS Task III

Objectives

A GSI-based dual resolution (DR) EnVar system is proposed and implemented for direct assimilation of radar observations. Within this system, the analysis at a sub-kilometer resolution is produced by combining the lower-resolution ensemble and the sub-kilometer first guess. This system is examined on the 8 May 2003, Oklahoma City tornadic supercell case. The DR EnVar system alleviates the southeastward bias in the tornado track forecast in the single-low-resolution (SR) EnVar system, in which both the ensemble and control are at a 2-km resolution. Detailed diagnostics suggest that the alleviated southeastward bias is due to the greater downward moving hydrometeor mixing ratios in the rear flank (RF) produced by the DR EnVar than by SR EnVar. Therefore, the tornado-like-vortices can move northeastward with the stronger outflow from the RF cold pool in the DR EnVar.

Accomplishments

1. Introduction

Relative to the number of studies on convective-scale storms, there are only a few studies which have predicted the real tornadoes or tornado-like-vortices (TLVs). Mashiko et al. (2009) simulated several convective storms in the outermost rain band mini supercell of a typhoon with quadruple nested simulations and the innermost horizontal grid spacing of 50 m. One of the simulated storms spawns a tornado, which, however, was not compared with the actual tornadoes in their study. Schenkman et al. (2012) employed three-dimensional variational data assimilation (3DVAR) cycles to initialize a mesoscale convective system (MCS) by assimilating radar and conventional observations on a 400-m grid and further launched a forecast on a nested 100-m grid. A detailed process of the tornadogenesis was provided on the 100-m simulation. Xue et al. (2014) predicted tornadoes on both 100-m grid and 50-m grid but with a northern displacement. Schenkman et al. (2014) documented the processes responsible for the tornadogenesis through the simulated tornadoes on the 50-m grid. The sensitivity of the TLVs to the microphysics schemes are also investigated by Dawson et al. (2015) utilizing a 250-m grid spacing. However, none of these studies have attempted to resolve the sub-kilometer scales within the data assimilation, and most of them used a nested high resolution grid initialized from a lower-resolution forecast/analysis, which may lose the characteristics of the fine resolution during the data assimilation.

Significant progress has been made in understanding of the convective-scale data assimilation through various data assimilation frameworks, especially for the assimilation of radial velocity and reflectivity. The cloud analysis method (Albers et al. 1996; Brewster 1996; Zhang et al. 1998; Zhang 1999; Souto et al. 2003; Xue et al. 2003; Hu et al. 2006) and digit filter (Weygandt et al. 2008) are employed to adjust the first-guess variables based on the radar reflectivity. However, too many uncertain

parameters within the cloud analysis limit its effects. Recently, ensemble Kalman filter (EnKF) is commonly used in the convective scale studies (e.g., Dowell et al. 2004; Tong and Xue 2005; Jung et al. 2008; Lei et al. 2009; Dowell et al. 2011; Yussouf et al. 2013; Johnson et al. 2015) and encouraging results have been demonstrated through direct radar data assimilation in these studies. For the variational data assimilation framework, due to the tangent linear and adjoint of the nonlinear reflectivity operators, difficulties remain in the direct assimilation of reflectivity observations. The large gradient of the cost function with respect to the small rainwater mixing ratio can prevent efficient convergence in the four dimensional variational data assimilation (4DVar) system by Sun and Crook (1997). Wang et al. (2013a, b) found in their 3DVar and 4DVar systems the underestimated hydrometeor increments are produced due to the overestimated reflectivity perturbations by its tangent linear approximation. Using the logarithm of the mixing ratio can reduce this error but can in the meantime underestimate the reflectivity perturbations (Carley 2012). To overcome these issues with the tangent linear and the adjoint of the nonlinear reflectivity operator (TLA), a new method without TLA is proposed and examined on the 8 May 2003 Oklahoma City tornadic supercell case by Wang and Wang (2016). Compared with the method with the mixing ratios as the state variables and the method with the logarithmic mixing ratios as the state variables, the newly proposed method using the reflectivity as the state variable predicts the supercell the best with a grid spacing of 2-km. These results were submitted in a peer-reviewed paper which is now in revision.

Several literatures (e.g., Gao and Xue 2008; Buehner et al. 2010; Hamill et al. 2011; Clayton et al. 2012; Kuhl et al. 2013; Schwartz et al. 2015) have documented the dual resolution (DR) hybrid or EnKF data assimilation system with a relatively cheaper computational cost than the single-high-resolution (SR) system, where the background and the ensemble have the same, high resolution. For example, Gao and Xue (2008) employed a DR EnKF system within an idealized framework. In their study, the analyses at 1-km horizontal resolution produced by SR and DR EnKF are comparable and the 4-km-resolution ensemble in DR EnKF does not significantly degrade the quality of analysis. However, perhaps due to the expense of the high resolution ensembles, very few studies have attempted to assimilate radar observations for the sub-kilometer scales with the ensemble-based data assimilation system. In the current study, a new DR EnVar system is implemented to produce the analysis at a sub-kilometer grid that combines a high resolution (HR) background (e.g., sub-kilometer) with a low resolution (LR) ensemble to produce a HR analysis, avoiding the need for a costly HR ensemble. The new method is developed with the reflectivity as the state variable based on the direct radar data assimilation method proposed by Wang and Wang (2016). The new DR EnVar system is applied on the analysis and prediction of the 8 May 2003, Oklahoma City, tornadic supercell storm.

2. Experiment Design

In this section, both GSI-based SR and DR EnVar systems are applied for the analysis and prediction of the 8 May 2003 Oklahoma City supercell case. The impacts of the two methods are studied by comparing the analyses and their subsequent tornado track

forecasts. The experiment design is described in this section followed by the results in section 3.

In this study, the SR experiment employs the same configuration with Wang and Wang (2016). A two-way coupled GSI-based SR EnVar data assimilation method with both ensemble and control at 2-km resolution is applied with a single domain (Fig. 1 outer domain). For DR experiment, the same configuration with SR experiment is also adopted except that a two-way coupled GSI-based DR EnVar data assimilation method, which runs a 500-m resolution control ingesting a 2-km ensemble, is employed on the inner domain of Fig. 1. This inner domain adopts a grid spacing of 500 m and 361×281 horizontal grid points and 50 vertical levels. The procedure of radar data assimilation and subsequent forecast for SR and DR experiments are shown in Fig. 2. Starting at 2100 UTC 8 May 2003, the radar data are assimilated every 5 minutes for a 1-h period out to 2200 UTC. One-hour forecasts are then launched from each of the 45-member analyses and the control analysis initialized at 2200 UTC. In order to reveal the impacts of introducing the sub-kilometer control analysis, the analysis at 2200 UTC in the SR experiment is downscaled to 500-m resolution first and then advanced for the 1-hour lead time.

The control forecast is updated using the EnVar where ensemble perturbations are applied to estimate the background error covariance through the use of the extended control variable method. The ensemble perturbations are updated by the ensemble smoother version of the square root filter algorithm (EnSRF; Whitaker and Hamill 2002). The analysis ensemble is further recentered around the control analysis to obtain the final ensemble analysis. As the control and ensemble are at different resolution grids in the DR experiments, the two-way nested domains are used with the feedback on in the WRF model configuration for the control forecast. The outer and inner domains of the control forecast respectively adopt the grid spacing of 2-km and 500-m. To account for the system errors, the localization and inflation are used. Cutoff radii of 12 km in the horizontal and 1.1 scale height in the vertical are used for the localization function in the EnVar and EnSRF. The posterior ensemble spread in the EnSRF is inflated to 90% of the prior ensemble spread using the Relaxation to Prior Spread (RTPS; Whitaker and Hamill 2012) inflation method. To further account for the deficiency of the spread of the first-guess ensemble in the EnSRF, both the constant inflation and additive noise (Whitaker et al. 2008; Dowell and Wicker 2009; Dowell et al. 2011; Dawson et al. 2012; Jung et al. 2012; Wang et al. 2013; Yussouf et al. 2013) are applied wherever the observed radar reflectivity exceeds 25 dBZ. The constant inflation is applied with a coefficient of 1.04 to each ensemble perturbation in every assimilation cycle. The additive noise is applied to the horizontal winds, temperature and dewpoint analyses at the first 6 cycles, and their standard deviations are 0.5 m s⁻¹, 0.5 K and 0.5 K, respectively. The horizontal and vertical length scales of 3 km are used for the perturbation smoothing function. These parameters are chosen based on our sensitivity tests. The additive perturbations are added to the analyses in order to establish the flow-dependent structure for these perturbations through the 5-minute model integration (Wang et al. 2013).

The designed experiments are listed in Table 1. SR_{thom} is a SR1 EnVar experiment applied the Thompson scheme with both ensemble and control using a 2-km grid. Experiment DR_{thom} differs from SR_{thom} in that a DR EnVar experiment is used with the high resolution control at a 500-m resolution. SR_{wsm6} is similar with SR_{thom}, except replacing the WSM6 scheme with the Thompson scheme; while DR_{wsm6} is the experiment in which the Thompson scheme used by the DR-thom is replaced by the WSM6 scheme. The comparison between SR_{xx} and DR_{xx} is used to investigate the impacts of using the SR and DR EnVar method, where xx represents the WSM6 or Thompson scheme. yy_{wsm6} and yy_{thom}, using the WSM6 and Thompson schemes, respectively, are performed to understand the sensitivity of the microphysics schemes to the reflectivity forecasts and tornado track forecasts, where yy represents the SR or DR.

3. Results

a. Impacts of the Resolution of the Ensemble and Background

To understand EnVar analysis sensitivity to the resolution of the ensemble, two experiments are performed where a single observation is assimilated. The observation is placed at -97.7W, 35.33N with 3-km AGL and the reflectivity observation is set to be 35 dBZ and have a background error standard deviation of 5 dBZ. For the two experiments, SR and DR EnVar are performed that differs by the resolution of the ensemble perturbations. The experiment SR-H is conducted using the 500-m ensemble and control whereas the experiment DR-H runs a 500-m control ingesting a 2-km ensemble. To ensure that analysis differences are solely attributed to the different ensembles, the control first guess for the single observation experiments is advanced for 5-minute from the same analysis valid at 2155 UTC.

The rainwater mixing ratio increments at 3-km AGL for SR-H and DR-H are compared in Fig. 3. The distributions of the rainwater mixing ratios are similar in the two experiments, except that the magnitude of the increments in the SR-H is greater than in the DR-H. Such similar distributions indicate the 2-km ensemble is comparable with 0.5-km ensemble to provide the ensemble covariance.

To reveal the impacts of the resolution of the control, another set of experiments are conducted. Within this set, SR and DR EnVar are performed that differs by the resolution of the control first guess. Experiment SR_{1cycle} is conducted using both ensemble and control at 2-km resolution whereas the DR_{1cycle} combines the 500-m control with 2-km ensemble. As the benefits of the higher resolution are hardly revealed through the single observation experiments, this set of experiments assimilate the KTLX radial velocity and reflectivity valid at 2155 UTC. The same 2-km ensemble first guess valid at 2155 UTC are used in both experiments. The control first guess in SR_{1cycle} at 2155 UTC is initialized from the analysis at 2150 UTC, which is also downscaled to a 500-m grid and then advanced for 5-minute to obtain the first guess used in DR_{1cycle}. The rainwater mixing ratio and downdraft analysis from SR_{1cycle} and DR_{1cycle} are shown in Fig. 4. The stronger downdraft and greater rainwater analysis are produced in

DR_1cycle analysis. Further diagnostics reveals both increment and background for downdraft and rainwater mixing ratios in the rear flank is stronger and extensive in DR_1cycle than in SR_1cycle (Fig. 5), suggesting the benefits of the higher resolution from the control.

b. Tornado Track Forecast

To evaluate the impact of using DR and SR EnVar systems on the forecasts, we verify the forecast against the observed tornado track. The simulated tornado path is represented by taking the maximum surface vorticity from all output times (Fig. 6). The tornado tracks from SR_thom (Fig. 6a) have southeastward displacement after 30-minute forecast lead time. When the DR EnVar system is applied in DR_thom (Fig. 6b), the southeast bias is significantly alleviated. For the experiments with the WSM6 scheme, DR_wsm6, in which the simulated tornado track closest to the observed track in all experiments, also alleviate the southeast bias in the SR_wsm6.

Compared with the Thompson scheme, the WSM6 scheme better forecasts the tornado track, not only in the SR EnVar framework (Fig. 6c), but also in the DR EnVar framework (Fig. 6d). SR_thom and DR_thom have more southeastward bias than SR_wsm6 and DR_wsm6, respectively. The distinct southeastward bias in the Thompson scheme is also documented by Wang and Wang (2016).

For both microphysics schemes, the DR EnVar alleviates the southeastward bias of the simulated surface tornado circulation in the SR EnVar. But the only difference between the SR_xx and DR_xx lies on the analysis field during the forecast period. The downdraft at 1 km AGL and the column-integrated rainwater mixing ratios² from all model levels in the analysis from the experiments SR_thom and DR_thom are shown in Fig. 7. Compared with SR_thom (Fig. 7a), the DR_thom (Fig. 7b) analysis produces larger amount of the rainwater mixing ratios and stronger downdraft in RF and near RF regions. The net effects are that the downward moving rainwater mixing ratios are greater in the DR_thom than in the SR_thom in the RF and near RF regions (Fig. 8), which is consistent with Fig. 5.

The different downward moving rainwater mixing ratios between the two experiments lead to the differences on their subsequent forecasts, the surface cold pool and surface tornado-like-vortices (TLVs) are shown in Fig. 9. At the 10-minute forecast lead time, relative to the SR_thom (Fig. 9a), the stronger cold pool is produced in the DR_thom (Fig. 9b), not only in the forward flank (FF), but also in the RF. After 25 minutes, the FF cold pool is becoming stronger in the SR_thom (Fig. 9c). The RF cold pool, however, is still much weaker than the DR_thom (Fig. 9d). Therefore, the outflow associated with the RF cold pool in the SR_thom is also weaker than in the DR_thom. The evolution of the RF and FF cold pool indicates the stronger outflow associated with the RF cold pool favors the northeastward motion of the TLVs; while the dominant southeastward outflow from the FF and too weak RF outflow lead to the southeastward motion of the TLVs in the SR_thom.

The surface cold pool and TLVs at 10-minute and 35-minute forecast lead time from the SR_wsm6 and DR_wsm6 are also plotted in Fig. 10. The significant RF outflow in the DR_wsm6 (Fig. 10b, d) also suggests the alleviated tornado track bias is attributed to the stronger cold pool than SR_wsm6 (Fig. 10a, c) in the RF and near RF. The better track forecast in WSM6 (Fig. 3c, d) than Thompson can also be explained by the stronger outflow in RF. Compared to Fig. 10d, the outflow in the DR_thom (Fig. 9d) is much weaker and therefore has more southeastward bias.

4. Conclusion

A series of studies have predicted the tornadoes or tornado-like-vortices (TLVs) with the sub-kilometer resolution. However, none of these studies attempted to resolve the sub-kilometer scales during the data assimilation. The ensemble based data assimilation method has been demonstrated to be useful for the convective scales by directly assimilation of the radar data. But the expense of the data assimilation using the sub-kilometer resolution can be pretty expensive. Therefore a GSI based dual resolution EnVar system is proposed by combining the lower resolution ensemble with the sub-kilometer control to produce the sub-kilometer analysis, obviating the need of the costly high resolution ensemble.

The single observation experiments for single high resolution and dual resolution EnVar reveal the 2-km ensemble is comparable to the 500-m ensemble. That is because the cross-covariance among different variables can be resolved at the lower resolution. The 1-cycle observation experiments for single low resolution and dual resolution EnVar suggest the dual resolution EnVar can benefit from the high resolution control relative to the single low resolution EnVar. The single low resolution (SR) and dual resolution (DR) EnVar are further examined on the 8 May 2008 OKC supercell storm. For both WSM6 and Thompson schemes, the DR corrects the southeastward displacement of the tornado track in SR. Detailed diagnostics suggest that stronger downdraft and greater hydrometeor mixing ratios are produced in the rear flank and near rear flank in the DR analysis than in the SR analysis; thus the cold pool and the associated outflow in the rear flank is stronger in the DR, which favors the northeastward motion of the tornado-like-vortices.

TABLE 1. List of all experiments and assimilation configuration, data resolution. See text for more details of the purpose of these experiments.

Experiment	Description
SR_thom	Single low resolution experiment using the Thompson scheme with both ensemble and control at 2-km resolution
DR_thom	Dual resolution experiment using the Thompson scheme combining the 2-km ensemble with a 500-m control
SR_wsm6	As SR_thom, but using the WSM6 scheme
DR_wsm6	As DR_thom, but using the WSM6 scheme

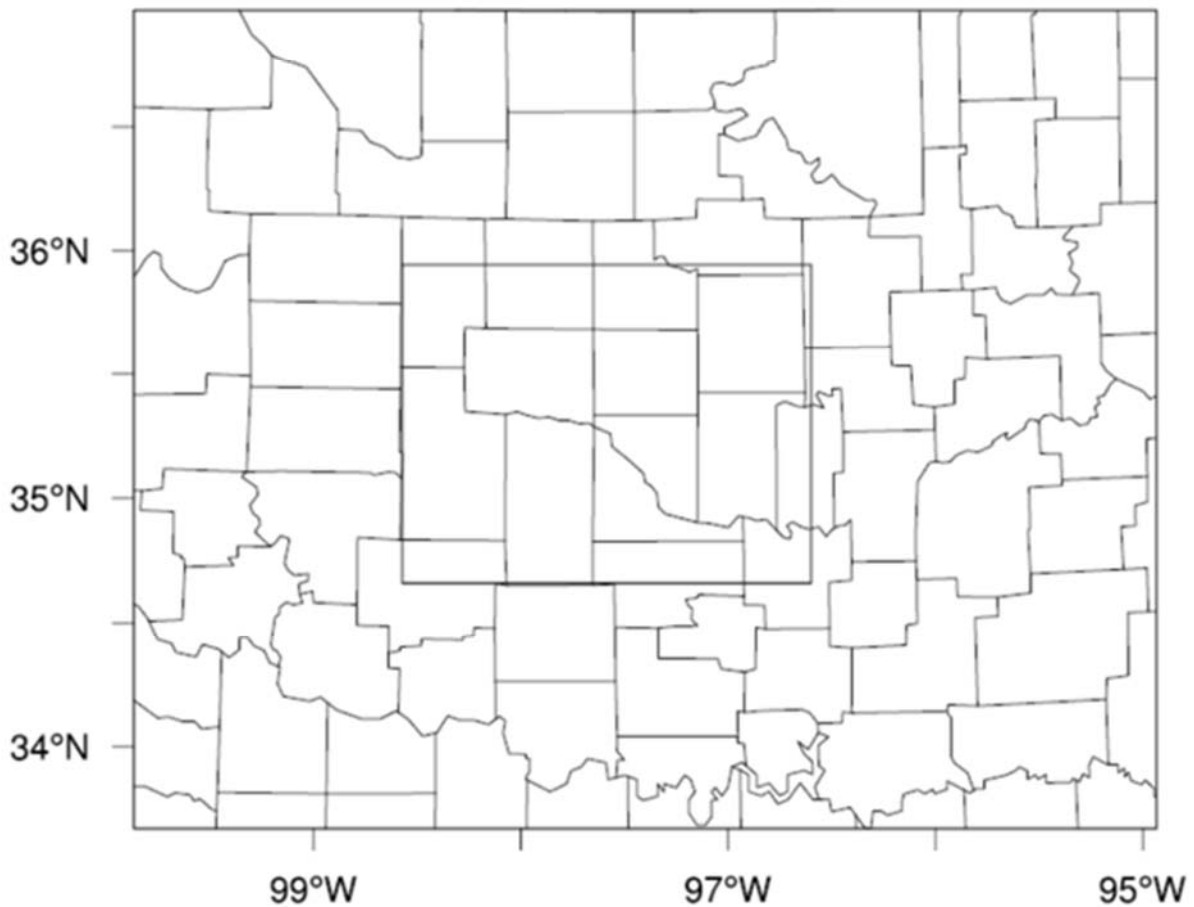


FIG.1. The outer domain with a 2-km grid for the ensemble and the control in the single-low-resolution EnVar and the inner domain with a 500-m resolution for the control in the dual resolution EnVar.

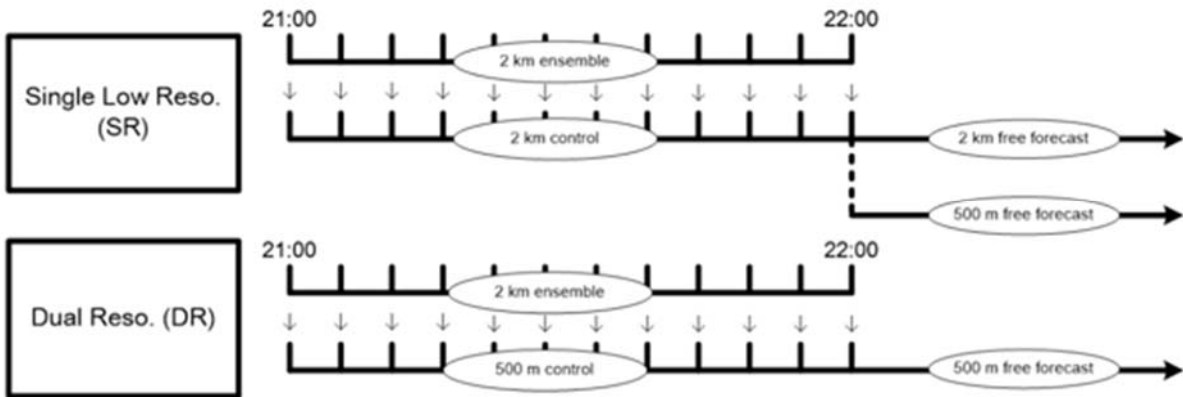


FIG. 2. Schematics of data assimilation experiment configuration. The radar data assimilation adopts the 5-minute cycling and the flow-dependent error covariance is provided by the 2-km resolution ensemble forecasts in both SR and DR EnVar. All 1-hour forecast at 500-m resolution is then initialized by the analysis at 2200 UTC after 1-hour assimilation.

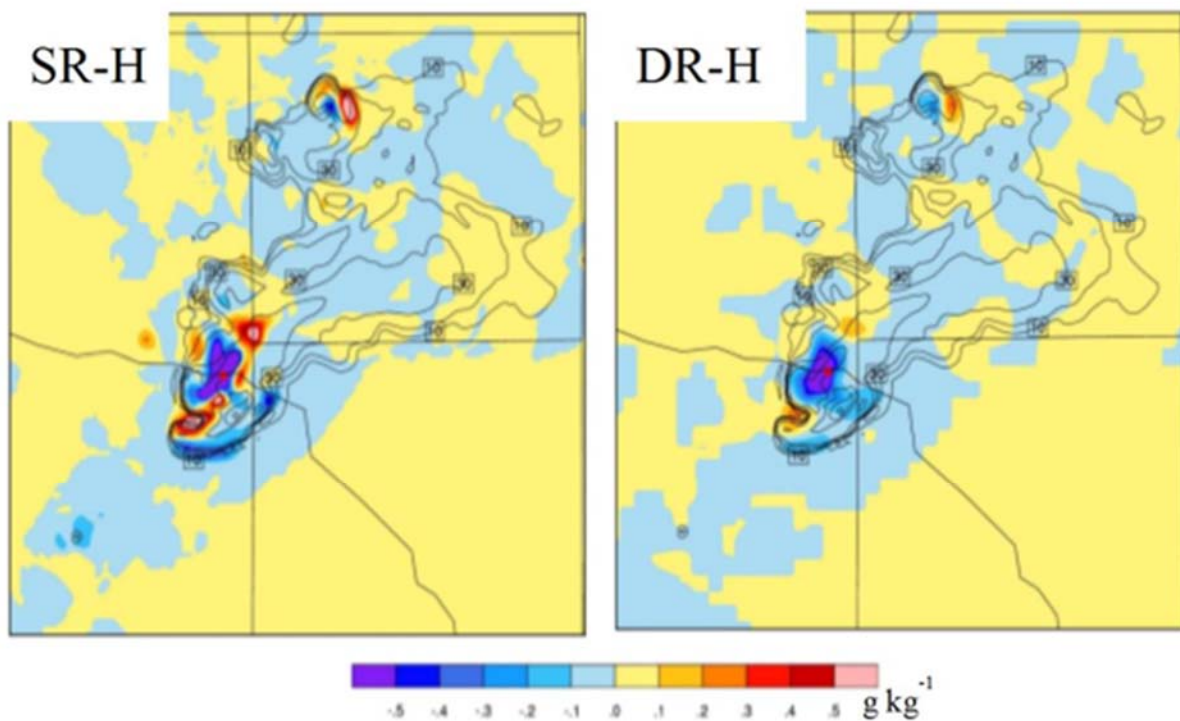


FIG.3. The increment of rainwater mixing ratios (shading; g kg^{-1}) and the reflectivity first guess (black contours from 10 dBZ to 60 dBZ at 10 dBZ interval; dBZ) at 3-km AGL for experiments SR-H and DR-H.

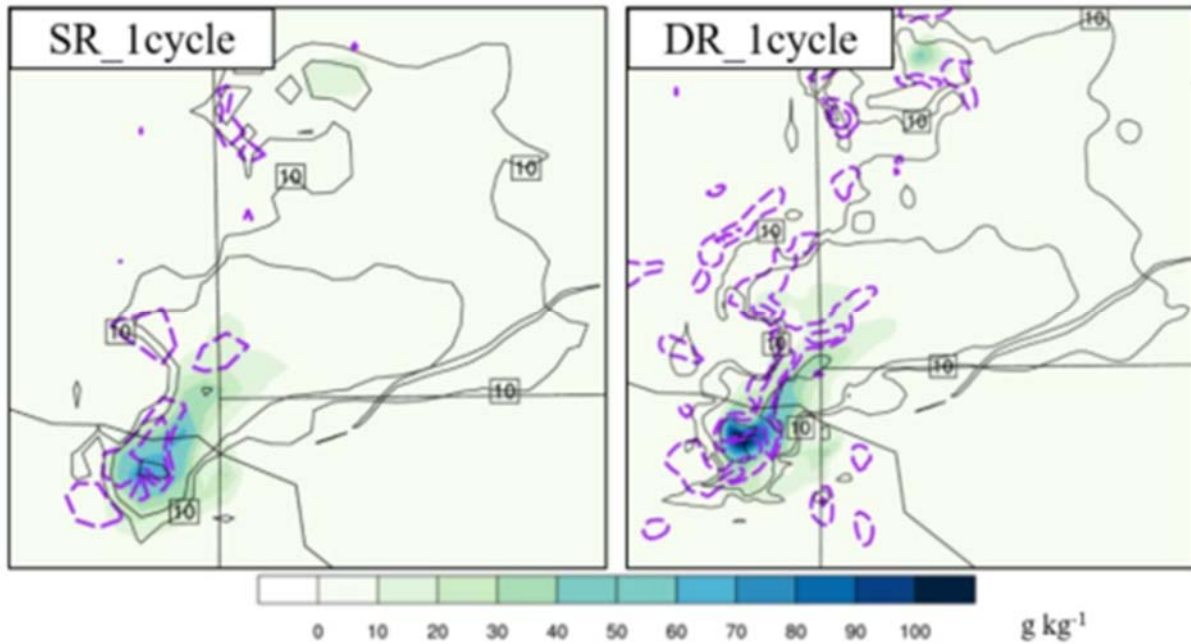


FIG. 4. The rainwater mixing ratios analysis (shading; g kg^{-1}), the downdraft analysis (purple dash contours; m s^{-1}), and the reflectivity analysis (black contours from 10 dBZ to 60 dBZ at 20 dBZ; dBZ) for the experiments SR_1cycle and DR_1cycle. The center of the tornado circulation is represented by the maximum surface vorticity (purple contours).

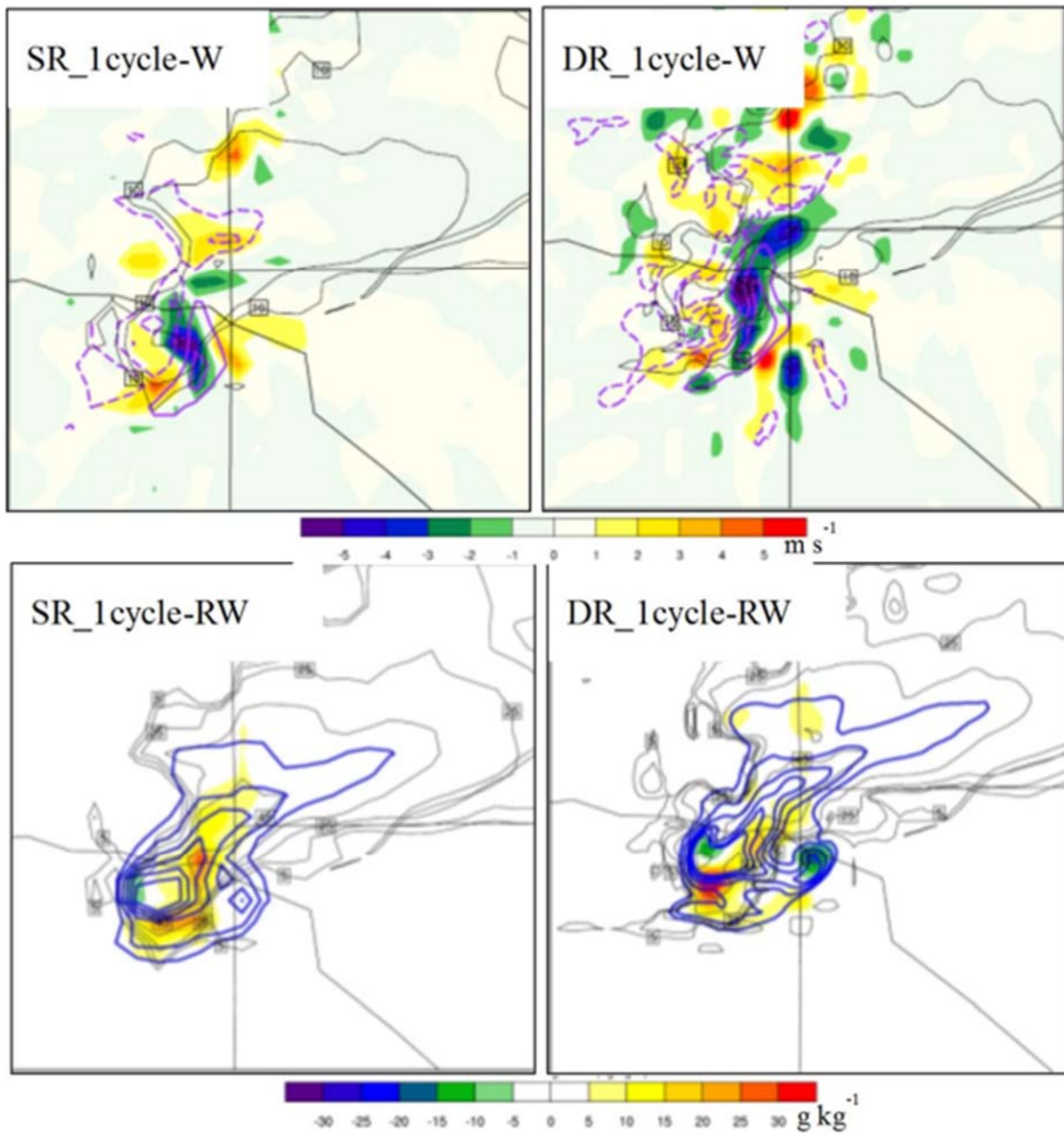


FIG. 5. The first guess downdraft (purple dash contours; m s^{-1}) for vertical velocity (W) in the upper figures and rainwater mixing ratios (blue contours; g kg^{-1}) for rainwater mixing ratios (RW) in the lower figures. The increments (shading) for the experiments SR_1cycle and DR_1cycle. The black contours are the first guess reflectivity (dBZ).

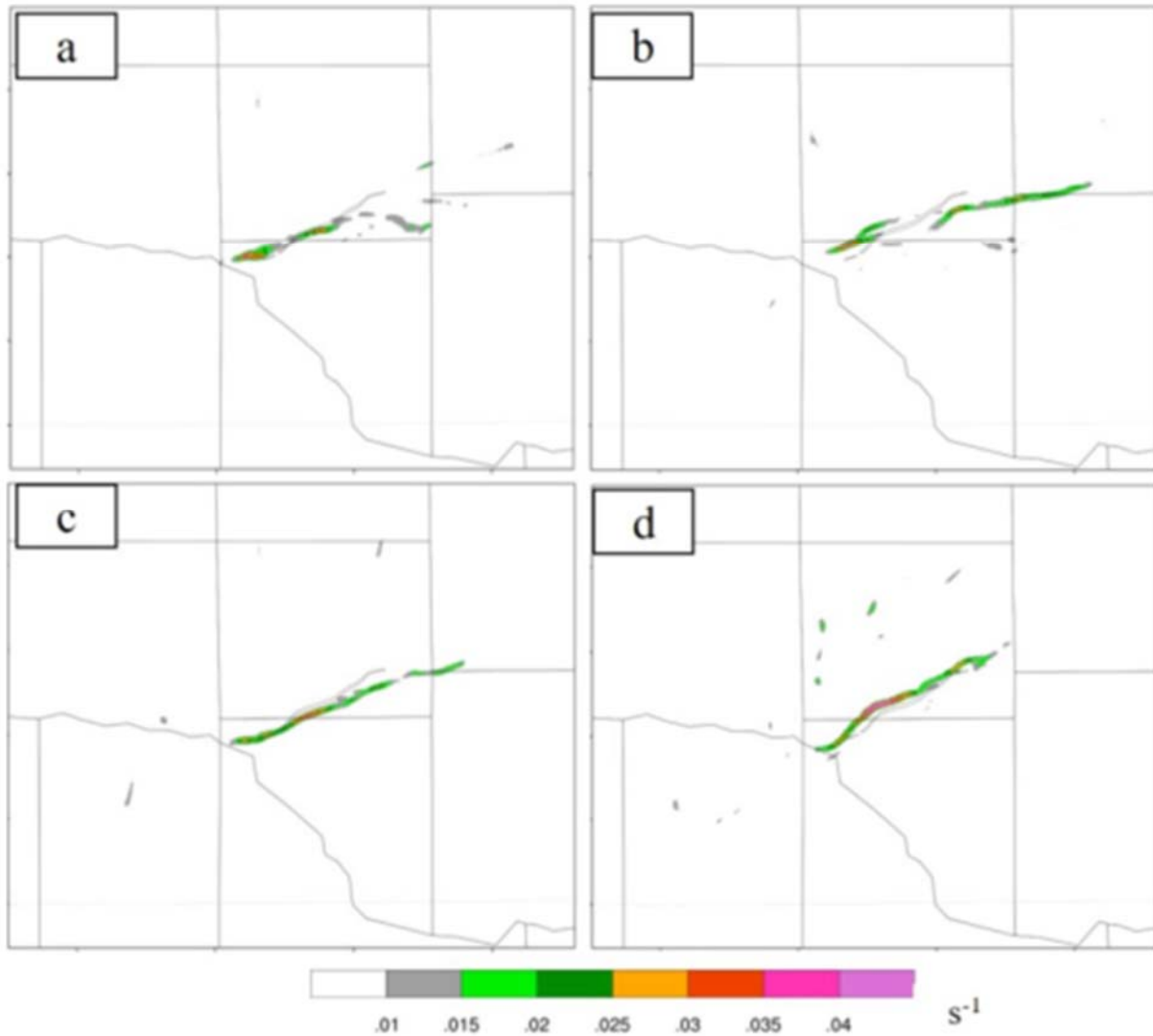


FIG. 6. Composite maximum surface vorticity (constructed by taking the maximum of the filed from all output times; s^{-1}) swaths, in shaded contours, for the period 2200-2300 UTC (3600-s model time, 60-s interval) for (a) SR_thom, (b) DR_thom, (c) SR_wsm6, and (d) DR_wsm6. The overlaid lines in each panel is the observed tornado track for reference.

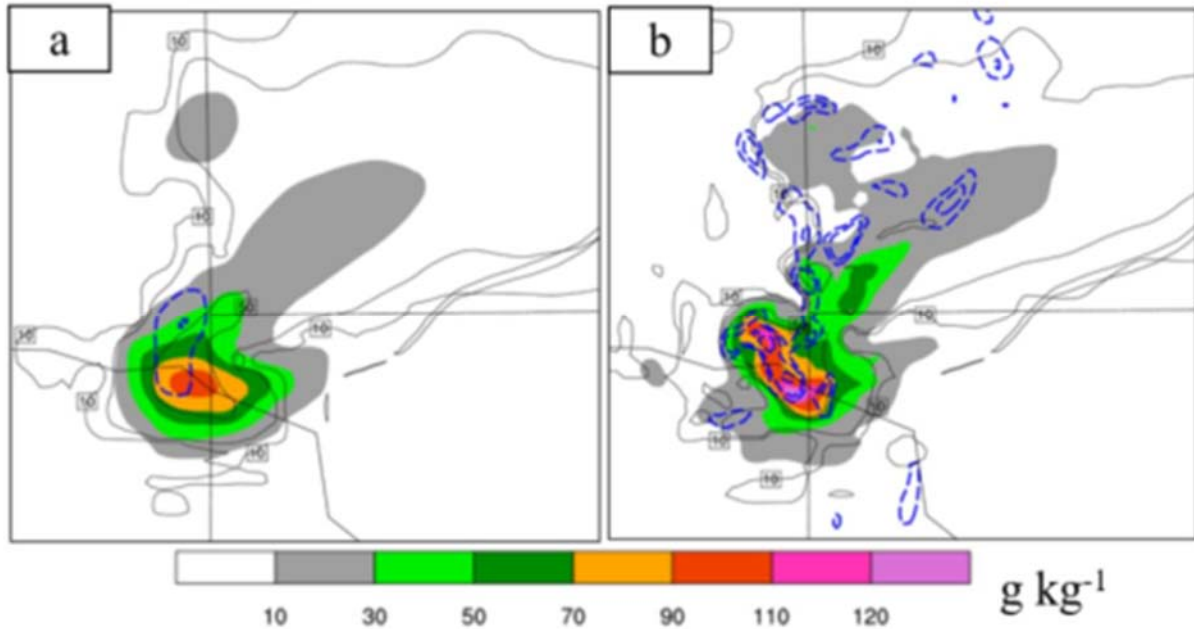


FIG. 7. Downdraft analysis (blue dash contours; $m s^{-1}$), column-integrated rainwater mixing ratios (shading; $g kg^{-1}$) and the reflectivity first guess (black contours from 10 dBZ to 60 dBZ at 20 dBZ interval; dBZ) for SR_thom (a) and DR_thom (b).

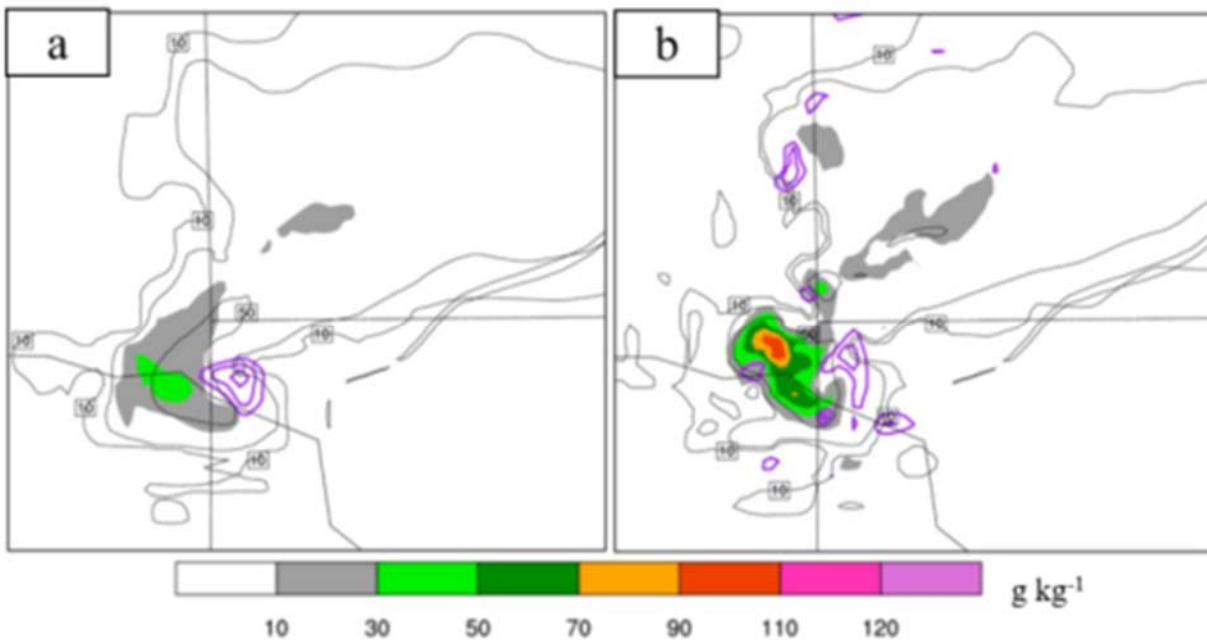


FIG. 8. Downward moving rainwater analysis (shading; $g kg^{-1}$) and the reflectivity analysis (black contours from 10 dBZ to 60 dBZ at 20 dBZ interval; dBZ) for SR_thom (a) and DR_thom (b). The center of tornado circulation is shown by the maximum vorticity in purple contours.

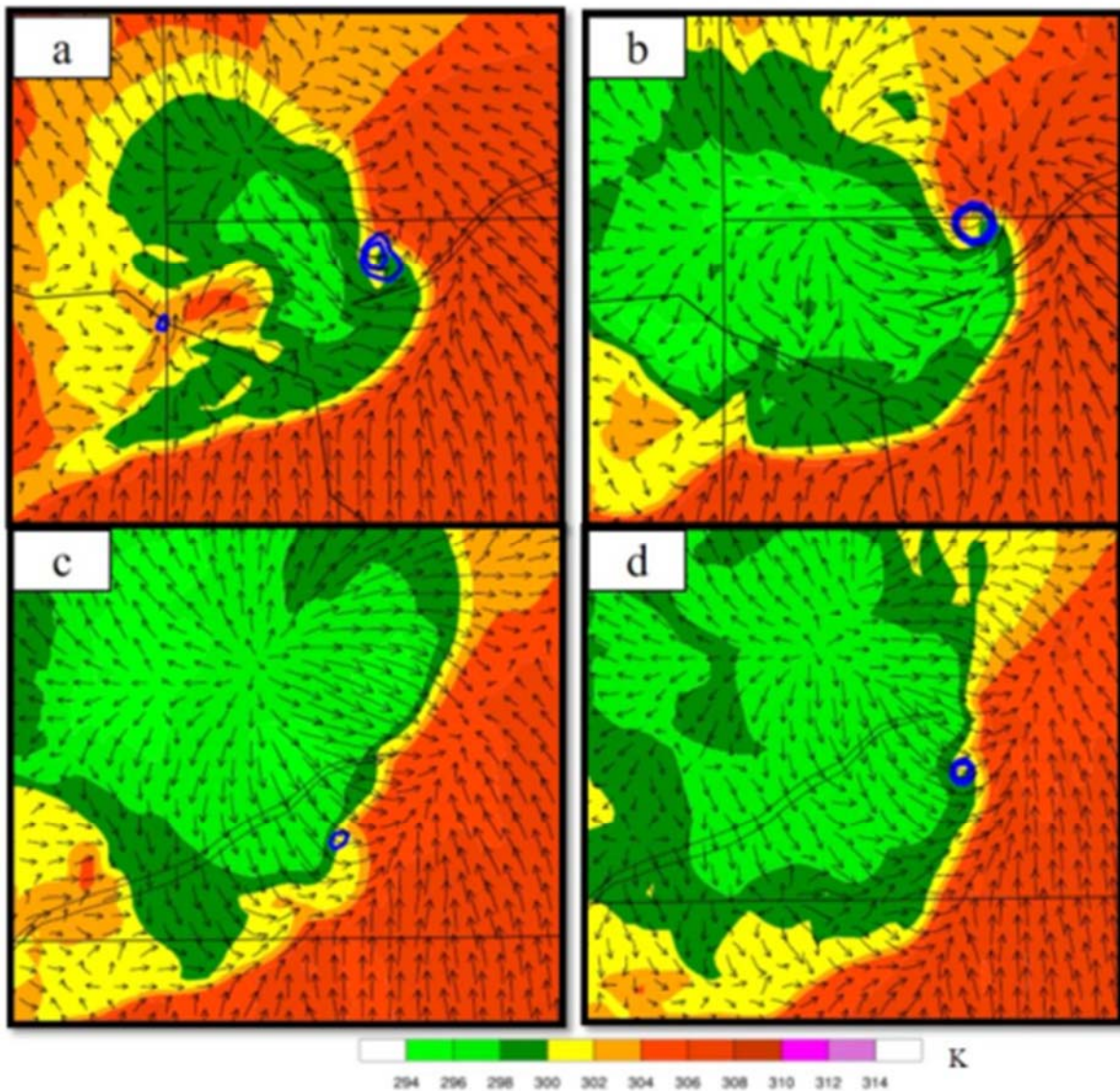


FIG. 9. Surface temperature (shading; K), wind (vector) and vorticity (blue contours; 0.05 s⁻¹ increments, starting at 0.05 s⁻¹) for SR_thom (a, c) and DR_thom (b, d) at 10-minute (a, b) and 35-minute (c, d) forecasts. The overlaid line in each panel is the observed track during 2210 UTC - 2238 UTC.

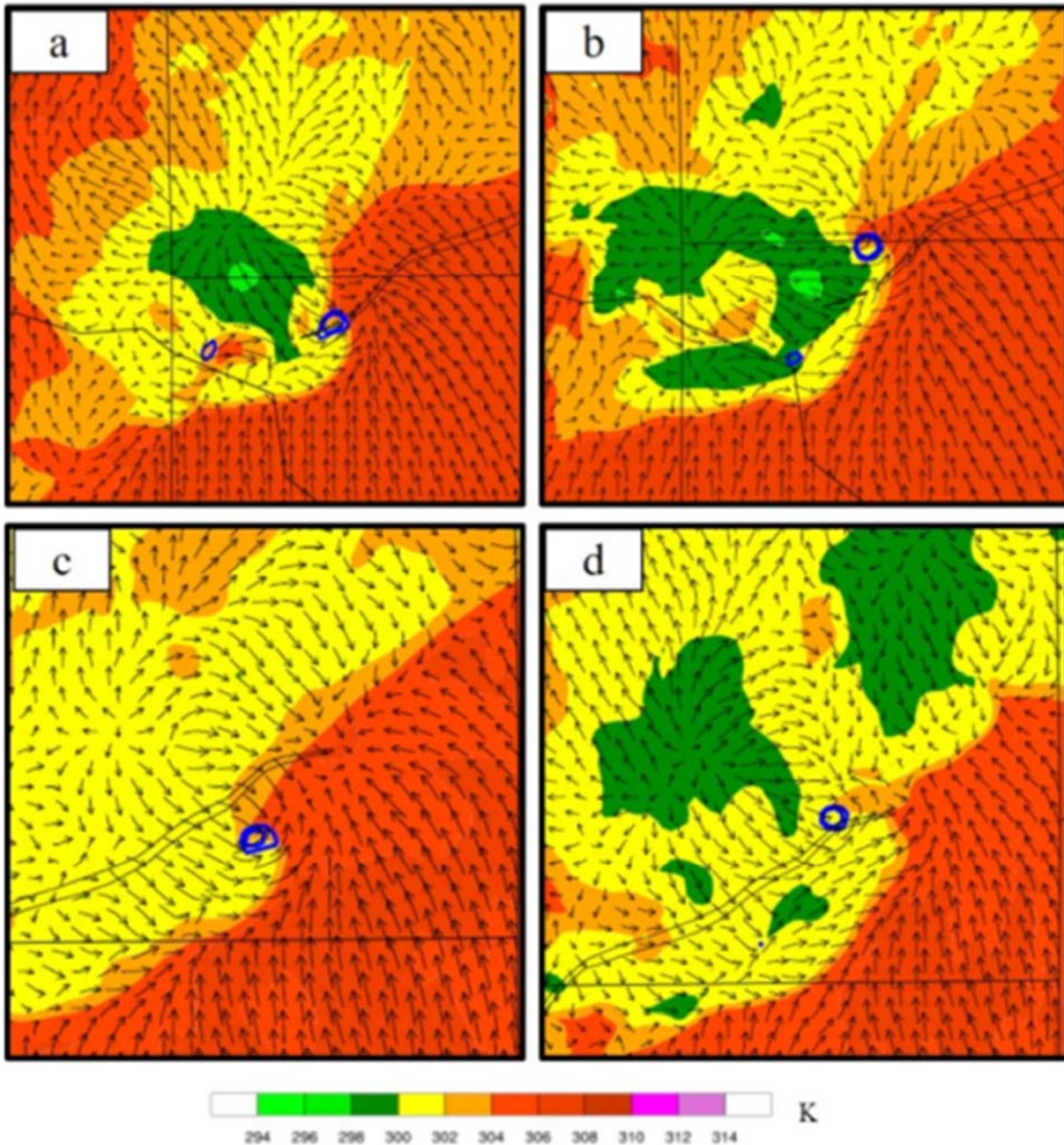


FIG. 10. Surface temperature (shading; K), wind (vector) and vorticity (blue contours; 0.05 s⁻¹ increments, starting at 0.05 s⁻¹) for SR_wsm6 (a, c) and DR_wsm6 (b, d) at 10-minute (a, b) and 35-minute (c, d) forecasts. The overlaid line in each panel is the observed track during 2210 UTC - 2238 UTC.

Publications

- Johnson, A., X. Wang, J. R. Carley, L. J. Wicker, and C. Karstens, 2015: A comparison of multiscale GSI-based EnKF and 3DVar data assimilation using radar and conventional observations for midlatitude convective-scale precipitation forecasts. *Monthly Weather Review*, **143**, 3087-3108.
- Thompson, T. E., L. J. Wicker, X. Wang, and C. Potvin, 2015: A comparison between the Local Ensemble

Transform Kalman Filter and the Ensemble Square Root Filter for the assimilation of radar data in convective-scale models. *Quarterly Journal of the Royal Meteorological Society*, **141**, 1163-1176.
Wang, Y., and X. Wang, 2016: Direct assimilation of radar reflectivity without tangent linear and adjoint of the nonlinear observation operator in GSI-based EnVar system: Methodology and experiment with the May 8th 2003 Oklahoma City tornadic supercell. *Monthly Weather Review*, In Revision.

CIMMS Task III Project – Objective Probabilistic Guidance for Severe Weather Outbreaks

Michael Richman and Lance Leslie (OU School of Meteorology)

NOAA Technical Lead: John Cortinas (NOAA OWAQ)

NOAA Strategic Goal 2 – *Weather Ready Nation: Society is Prepared for and Responds to Weather-Related Events*

Funding Type: CIMMS Task III

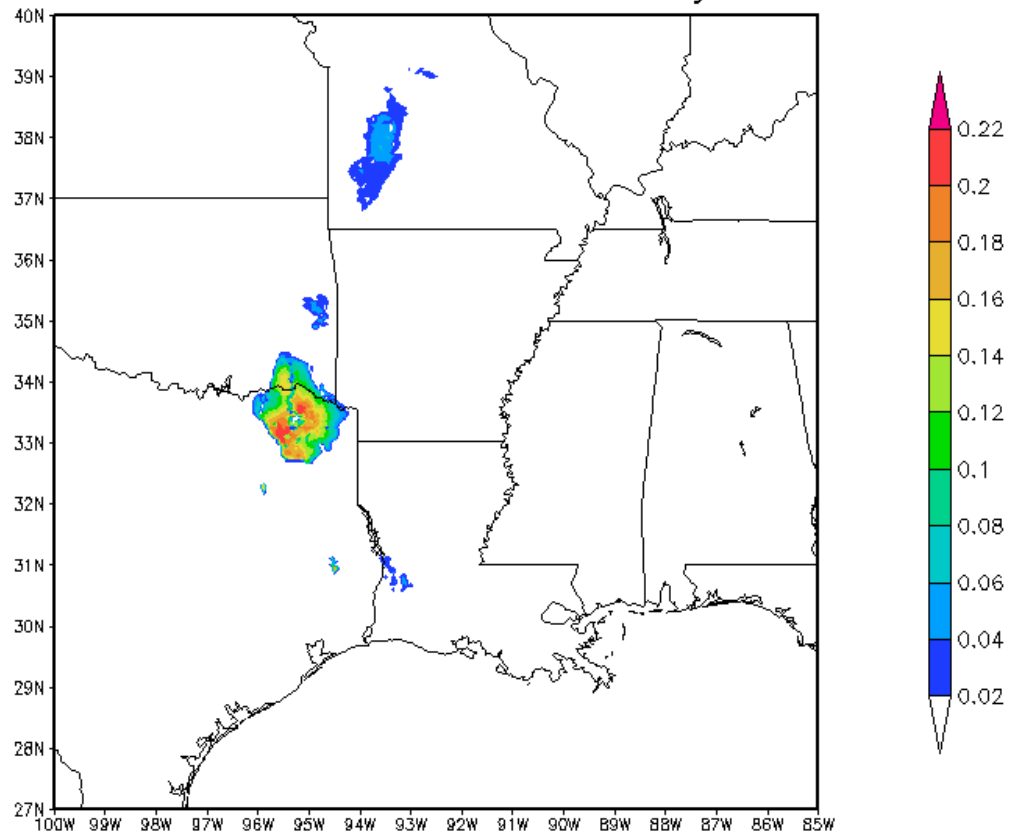
Objectives

Determine synoptic scale environments in WRF/NSSL WRF associated with outbreaks of tornadoes, hail and wind at lead times up to several days.

Accomplishments

Over the last year, efforts have been undertaken to increase the training sample size used in the objective outbreak guidance product. In particular, WRF simulations configured with the NSSL-WRF model physics and domain were run to encompass all outbreaks that extend from the initial time of the NARR database (1 January 1979 – e.g. Fig. 1) to 2009. This effectively increased the sample size from 2080 to 4852 outbreaks. From this training database effort, new training datasets derived from areal coverages of severe weather diagnostic variables on the 4852 events are formulated for use in the objective probabilistic guidance. The final steps of the work will be the completion of this training set and the objective guidance algorithm, and operational implementation by integrating current NSSL-WRF forecast fields into the guidance for identifying regions of concern and probabilistic rank forecasts.

Significant Tornado Parameter for 23 February 1979 0600 UTC



GrADS: COLA/IGES

2016-09-07-11:15

Significant tornado parameter from the first outbreak in the full 4852 outbreak training set.

Theme 3 – Forecast and Warning Improvements Research and Development

NSSL Project 5 – Hazardous Weather Testbed

NOAA Technical Leads: Alan Gerard and Jack Kain (NSSL), David Andra (OUN), and Israel Jirak (SPC)

NOAA Strategic Goal 2 – Weather-Ready Nation – Society is Prepared for and Responds to Weather-Related Events

Funding Type: CIMMS Task II

Objectives

Experimental Forecast Program (EFP) objectives include:

- Evaluate the utility of high-resolution ensemble forecast systems for severe storm guidance at both 24 and 3 hourly time scales;
- Continue improving information extraction from the ensembles and verify high-resolution forecasts.

Experimental Warning Program (EWP) objectives include:

- Evaluate the accuracy and the operational utility of new science, technology, and products in a testbed setting to gain feedback for improvements prior to their potential transition into NWS severe convective weather warning operations;
- Foster collaboration between NSSL and GOES-R scientists and operational meteorologists.

Accomplishments

The Experimental Warning Program conducted four projects during the fiscal year intended to improve severe weather warnings. Over 50 forecasters and visitors participated, spanning 12 weeks during the summer of 2015 and the spring of 2016. The Experimental Forecast Program was held over a 6-week period in spring 2016 with a similar number of participants. HWT activities are reported in other projects here, as noted below.

1. Experimental Forecast Program

James Correia Jr. (CIMMS at SPC)

This work is reported on under [SPC Project 11](#).

2. Experimental Warning Program

a. Probabilistic Hazard Information (PHI) Experiment

Chris Karstens, Darrel Kingfield, Tiffany Meyer, Gabriel Garfield, and Travis Smith (CIMMS at NSSL), and James Correia Jr. (CIMMS at SPC)

This work is reported under [NSSL Project 8](#).

b. Probabilistic Hazard Information (PHI) Hazard Services Experiment

Greg Stumpf (CIMMS at NWS/OST/MDL/DAB), and Tiffany Meyer and Darrel Kingfield (CIMMS at NSSL)

This work is reported under [OST Project 13](#).

c. GOES-R/JPSS Experiment

Bill Line (CIMMS at SPC), and Kristin Calhoun, Tiffany Meyer, and Darrel Kingfield (CIMMS at NSSL)

This work is reported under [SPC Project 11](#).

d. HMT Multi-Radar Multi-Sensor Hydro Experiment

Jonathan Gourley (NSSL), and Humberto Vergara-Arrieta, Zachary Flamig, and Tiffany Meyer (CIMMS at NSSL)

This work is reported under [NSSL Project 4](#).

e. Phased Array Radar Innovative Sensing Experiment (PARISE)

Katie Wilson, Charles Kuster, Darrel Kingfield, and Tiffany Meyer (CIMMS at NSSL), and Ziho Kang (OU School of Industrial and Systems Engineering)

This work is reported under [NSSL Project 9](#).

Publications

Karstens, C. D., G. Stumpf, C. Ling, L. Hua, D. Kingfield, T. M. Smith, J. Correia, Jr., K. M. Calhoun, K. L. Ortega, C. J. Melick, and L. P. Rothfus, 2015: Evaluation of a probabilistic forecasting methodology for severe convective weather in the 2014 Hazardous Weather Testbed. *Weather and Forecasting*, **30**, 1551-1570.

[NSSL Project 6 – Development of Technologies and Techniques in Support of Warnings](#)

NOAA Technical Lead: Alan Gerard (NSSL)

NOAA Strategic Goal 2 – *Weather-Ready Nation – Society is Prepared for and Responds to Weather-Related Events*

Funding Type: CIMMS Task II

Objectives

The primary objects for this reporting period include: (1) develop the capability to re-process and analyze 15 years' worth of WSR-88D data for use in severe local storms, hydrological, and climatological research; (2) conduct radar data quality control and develop probabilistic data displays for the Warn-on-Forecast project; (3) develop enhanced severe weather guidance for the WSR-88D radar network; and (4) enhance lightning prediction capabilities, and (5) develop warning guidance for winter weather events.

Accomplishments

1. Multi-Year Reanalysis of Remotely Sensed Storms (MYRORSS)

Kiel Ortega, Travis Smith, Holly Obermeier, Anthony Reinhart, and Chris Karstens (CIMMS at NSSL)

Data processing and quality control continued on the MYRORSS data set, with the years 2000-2011 at 90% completion.

A machine learning method was developed by Dr. Amy McGovern that predicts the duration of severe convective storms identified as objects from the MRMS composite reflectivity. A real-time and displaced real-time feed of these objects were tested and evaluated with forecasters in the Spring 2016 Probabilistic Hazard Information (PHI) experiment at the NOAA Hazardous Weather Testbed (HWT). It was found the forecasters accepted and used these predictions in approximately 75% of the forecasts produced during the experiment. This result implies that forecasters trust these predictions, or feel that the predictions are sufficient. However, evidence from prior experiments shows that forecasters rely heavily on default duration settings. Thus, some forecasters may not be giving much attention to these predictions. Further testing and evaluation, in addition to algorithm refinements, are needed to further understand the utility of these machine learning-based duration predictions. Additional work is underway to improve the automated object identification and tracking of storm clusters, which is believed to result in improvements to the duration prediction method.

2. Warn-on-Forecast

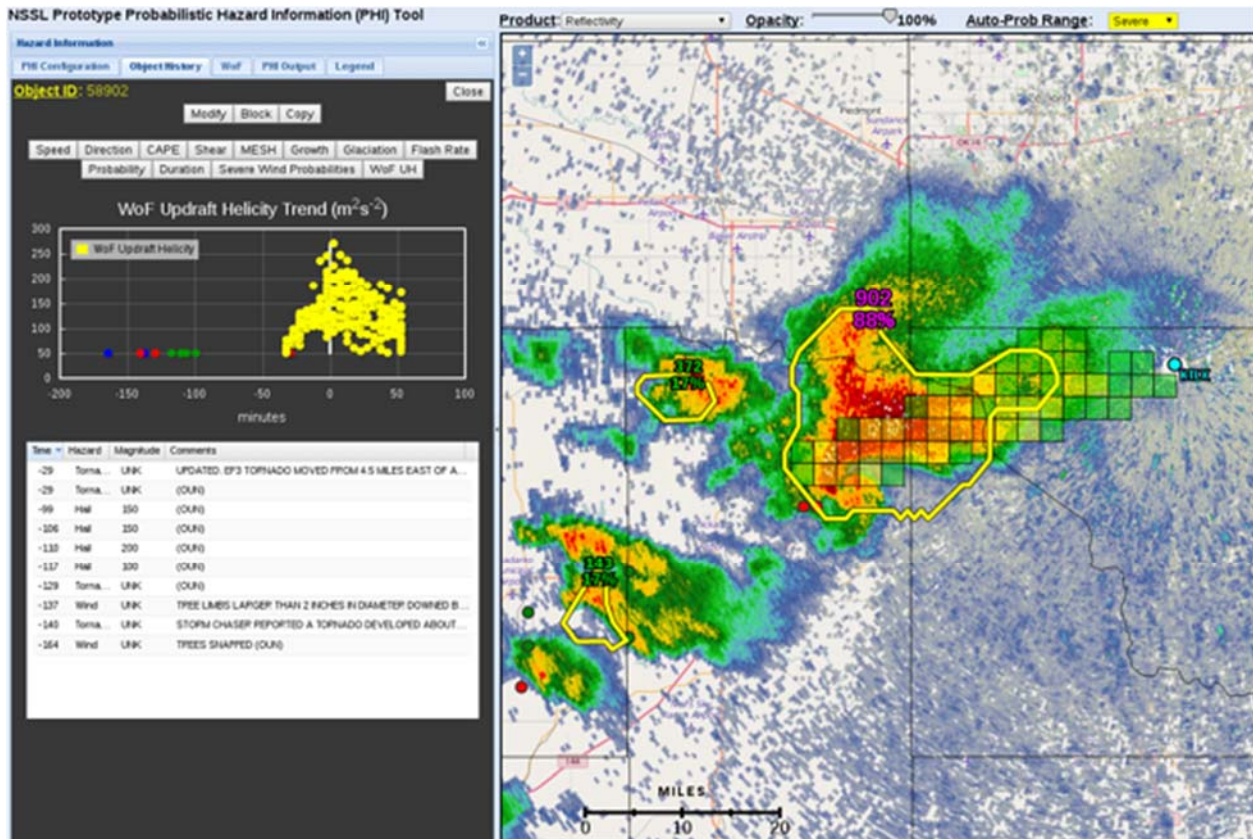
Chris Karstens (CIMMS at NSSL)

During the evaluation period, requests for automated quality-controlled radar datasets were facilitated. The source radars were primarily comprised of National Weather Service (NWS) WSR-88D radars, but also included terminal weather radars (e.g., TOKC) and research radars such as the Multiphase Phased Array Radar (MPAR) and experimental dual polarization radar (KOUN). These quality-controlled datasets were

assimilated into analyses used to drive an ensemble of Numerical Weather Prediction (NWP) models within the Warn-on-Forecast project.

Additionally, development, testing, and evaluation of probabilistic guidance from the NSSL experimental Warn-on-Forecast ensemble system (NEWS-e; Fig 1) was conducted during the Spring 2016 Probabilistic Hazard Information (PHI) experiment at the NOAA Hazardous Weather Testbed (HWT). This experiment utilizes a prototype web tool allowing forecasters to issue probabilistic forecasts for severe convective weather events (tornado, wind, hail, and lightning). The tool presented guidance derived from object-based tracking of updraft helicity and vertical vorticity. These spaghetti tracks were overlaid on the spatial display, and could be aggregated into grid point probabilities based on ensemble member agreement and filtered based on adjustable lead-time and exceedance of an adjustable variable threshold. Forecasters used this information to guide the generation of probabilistic tornado forecasts for real-time and displaced real-time weather events.

Although this guidance is still in its preliminary stages of development, it was able to give forecasters more confidence while generating forecasts. In general, forecasters lack a source of guidance that provides explicit future prediction of severe convective weather events. Thus, the NEWS-e guidance was able to fill an information void for forecasters. This was evident when the guidance showed agreement on the prediction of updraft helicity or vertical vorticity tracks, indicating a potential for tornadoes, and also when the guidance showed a lack of forecast tracks for a given storm at various forecast lead-times, indicating tornado demise or lack of sufficient rotation for the occurrence of tornadoes. Finally, the ability to adjust lead-times and variable thresholds on demand lead to improved understanding and trust of the guidance, and efforts are underway to expand these concepts to other aspects of the web tool to yield similar improvements to other sources of forecast guidance.



The Probabilistic Hazard Information tool shows a reflectivity field (right) with storm object contours and probability of severe weather within the object. Forecast trends of Updraft Helicity (upper left) and historical storm reports (lower left) for the storm cell are only a few of the analysis fields available in the tool.

3. Enhancements to WSR-88D Radar Algorithms

Kiel Ortega, Holly Obermeier, Brandon Smith, Matt Mahalik, Darrel Kingfield, Kim Elmore, and Travis Smith (CIMMS at NSSL)

a. Azimuthal Shear Products

The azimuthal shear product was re-examined for potential areas of improvements to increase product accuracy.. Three areas of improvement were identified: 1) Adjustments to governing equation from the linear least-squares derivative (LLSD) technique used to derive azimuthal shear, 2) Development of a new range-based correction technique to offset degrading accuracy of azimuthal shear with range from the radar, and 3) Restructuring of the internal code workflow and removal of obsolete code to improve efficiency.

The original LLSD equations were re-derived, retaining several terms previously neglected due to simplifications based on the geometry of the radar beam and radial grid on which azimuthal shear is calculated. In addition, the underlying pre-computation

code used to construct the LLSD kernels was re-worked to maximize efficiency, remove code redundancy, and eliminate potential errors. The updated equations produce shear values much closer to theoretical values at short range, removing artificial spikes near the radar that were caused by mathematical artifacts. One important application of azimuthal shear is rotation tracks, which uses layer-maximum azimuthal shear accumulated over time. By improving azimuthal shear calculations near the radar, rotation tracks in this region are improved significantly.

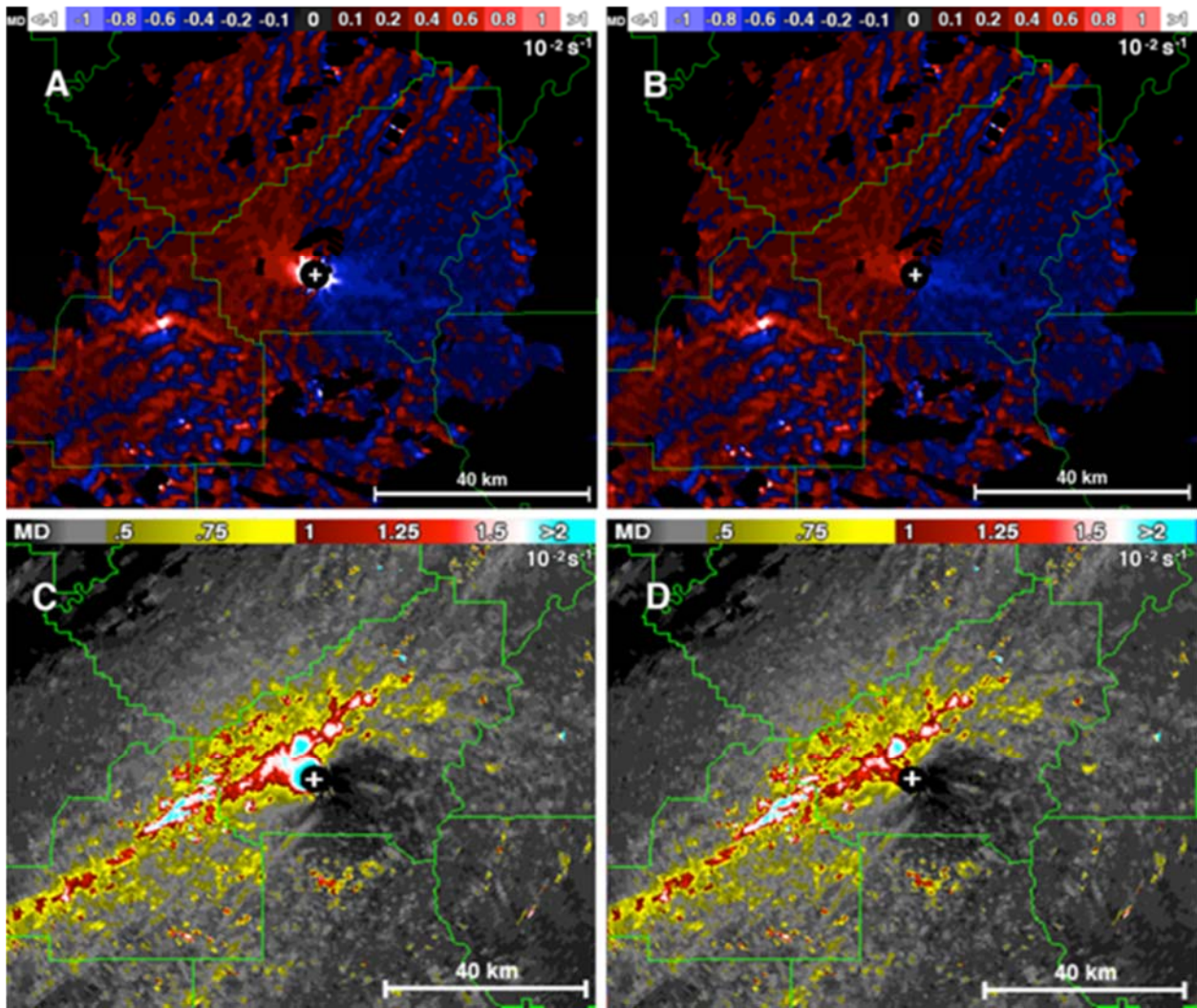
A new method of correcting azimuthal shear as a function of range was developed, replacing a previous correction method. The half-velocity, diameter, and range from radar are found for individual areas of circulation where azimuthal shear exceeds 0.008 s⁻¹. These intermediate values may be output as usable fields from the updated algorithm. These three quantities are used to identify a corresponding shear correction value derived from velocity model output, allowing for a case-by-case correction method custom-tailored to each gate that is present in the circulation itself. Implementation of a nearest-neighbor continuity check prevents erroneous azimuthal shear corrections from occurring in regions of noisy velocity data. This new shear correction helps to provide a more accurate value of azimuthal shear for areas of circulation.

The internal handling of how vertical maximum shear is calculated over a layer was improved, improving accuracy and performance. Code was cleaned and optimized for performance and consistency. Documentation of the internal workings of the algorithm was also produced.

The improved LLSD equations, updated internal handling of vertical maximum of azimuthal shear, and general cleaning/code maintenance are all part of MRMS v11 (2016). The improved azimuthal shear algorithm, as well as the new intermediate delta-velocity and diameter fields, are prepared for use in the currently under-development new mesocyclone detection algorithm (NMDA) and the new tornado detection algorithm (NTDA).

b. Hail Products

A hybrid single- and dual-polarization hail detection and sizing algorithm is being developed. The first step of the project was to adapt the enhanced Hail Detection Algorithm (HDA; Witt et al. 1998) to run in pixel-by-pixel framework on single radar data, instead of the storm-based framework it currently employs. This pixel-by-pixel algorithm produces a Maximum Expected Size of Hail (MESH) value for each pixel in the radar domain. In order to develop and evaluate the new algorithm, 268 cases in which the Severe Hazards Analysis and Verification Experiment (SHAVE) collected data were collected. The Level-II radar data was processed through the operational dual-pol preprocessing algorithm and then the new MESH algorithm was run and also the new Hail Size Discrimination Algorithm (HSDA; Ortega et al. 2016). Currently values from the HSDA and MESH are being qualitatively compared to SHAVE hail reports. Preliminary qualitative evaluations are also underway.



Comparison of instantaneous, single-scan azimuthal shear (A and B) and accumulated 60-minute rotation tracks (C and D) calculated using the legacy LLSD algorithm (A and C) and the updated LLSD algorithm (B and D) from a tornado event on 27 April 2011. Artificially high azimuthal shear associated with the legacy LLSD algorithm are mitigated using the new version.

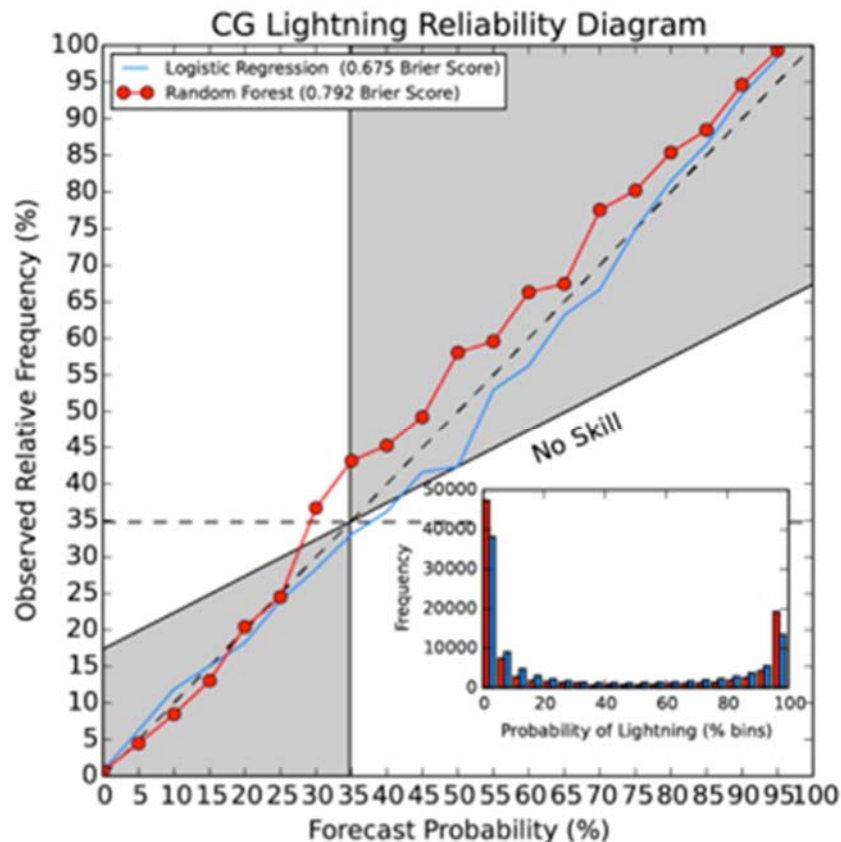
4. Development of Cloud-to-ground Lightning Probabilities

Kristin Calhoun, Tiffany Meyer, and Darrel Kingfield (CIMMS at NSSL)

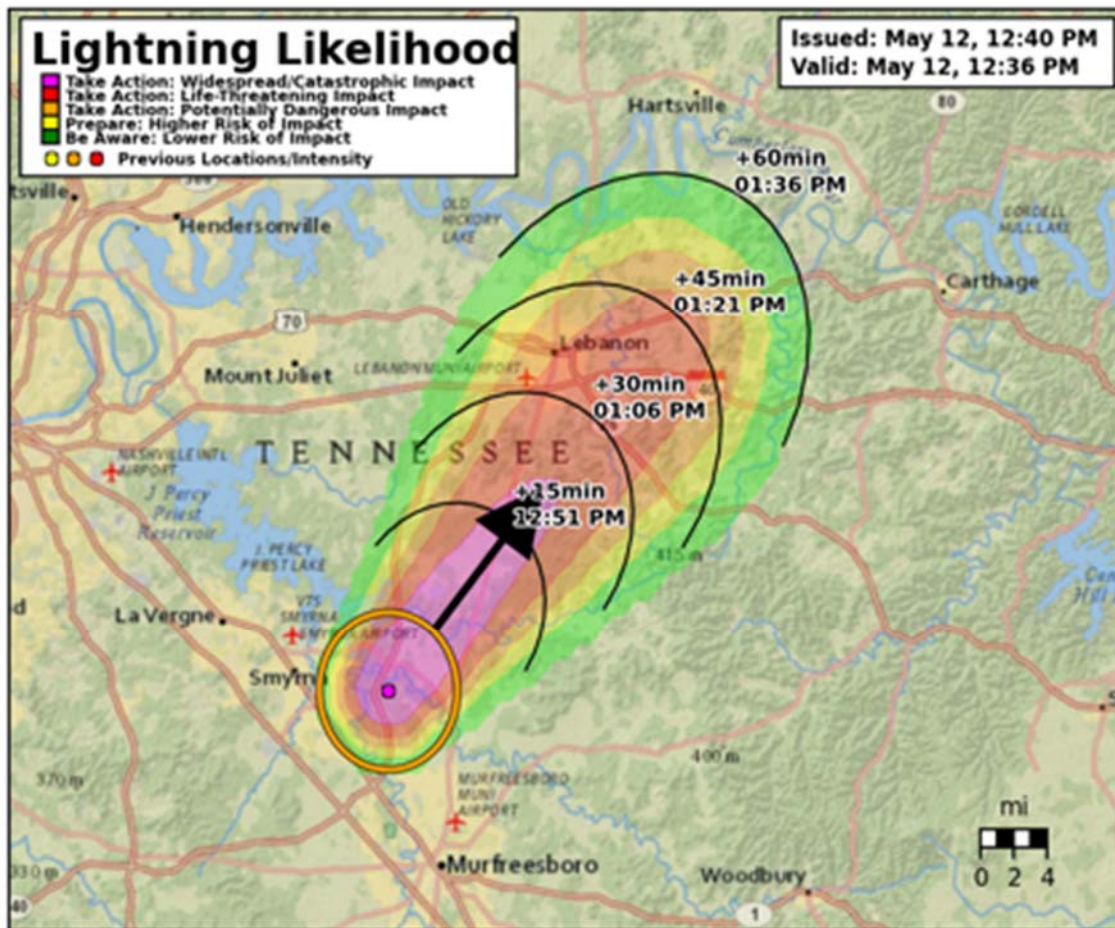
With roughly 20-25 million cloud-to-ground (CG) lightning flashes occurring across the US annually, CG lightning continues to be a significant hazard to lives and property. To date, lightning data provided to the NWS is strictly observational and provides zero lead time on future lightning occurrence. This project aims to develop multiple layers of probabilistic CG lightning guidance and sets the framework for the NWS to nowcast and communicate lightning hazard potential to the public.

During 2015, a random forest algorithm was trained using over 91,000 convective cells across 36 different days from 2014 to produce storm-based probabilities of CG lightning over a variety of forecast time intervals within the 0-1 hour period. This algorithm incorporates near storm environment information, multiple MRMS products, and lightning data from NLDN and ENTLN to generate these probabilistic CG lightning forecasts. For the 0-30 min period, these new CG probability forecasts have shown skill (Brier Skill Score of .792) and slightly underforecast (by less than 5% at probabilities greater than 25%; Fig. 1).

In addition to the 30-min storm-based probabilities noted above for future Multi-Radar/Multi-Sensor (MRMS) operational implementation, we are also developing probabilities for integration into the Probabilistic Hazard Information (PHI) tool for use by NWS forecasters in creating lightning hazard grids. These gridded CG lightning forecasts not only provide probability but also time-of-arrival and departure information (Fig. 2). Initial work with forecasters and emergency managers in the Hazardous Weather Testbed depicted great interest in these CG lightning forecasts and information.



Reliability diagram of the 0-30 min storm-based forecast of cloud-to-ground (CG) lightning versus the Observed relative frequency from the same storms using both random forest and logistic regression methodology. Frequency histogram embedded in lower right corner. Due to higher skill scores the random forest methodology was chosen for operational evaluation and implementation.



Simplified graphic of CG lightning forecast from 2016 PHI experiment using automated CG probabilistic guidance, intended for distribution through Emergency Managers and social media.

5. Winter Precipitation Observation

Heather Reeves, Alexander Ryzhkov, and John Krause (CIMMS at NSSL)

This work is a continuation effort to produce a new surface hydrometeor classification algorithm that improves upon existing strategies. We call the new algorithm the Spectral Bin Classifier (SBC). It explicitly computes the liquid-water fraction (LWF) of falling hydrometeors for a spectrum of drop sizes and uses the resulting LWF at the surface to assign the precipitation type.

Efforts this year focused on making the algorithm more computationally efficient so that it is feasible for a real-time system. We have partnered the SBC with a simple three-dimensional classifier that pre-classifies obvious cases of rain, snow, and freezing rain. This eliminates the need for the SBC to be run across the entire CONUS. Because

there appears to be a ceiling on how well the SBC performs, effort was also devoted to understanding this ceiling, why it exists and whether there are mitigation steps that can be taken to side-step it. Last, efforts were started to apply the SBC to complex terrain to improve hydrologic forecasts of run-off.

Two peer-reviewed papers have been submitted (one in press, one is conditionally accepted). Three conference presentations have also been made.

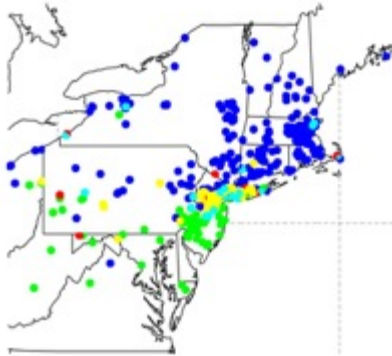
6. Discrimination Between Winter Precipitation Types Based on Spectral-Bin Microphysical Modeling

Heather Reeves, Alexander Ryzhkov, and John Krause (CIMMS at NSSL)

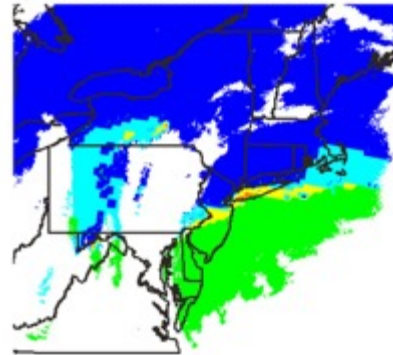
In the first, a new approach for distinguishing precipitation types at the surface, the Spectral Bin Classifier (SBC), is presented. This algorithm diagnoses six categories of precipitation: rain (RA), snow (SN), a rain/snow mix (RASN), freezing rain (FZRA), ice pellets (PL), and a freezing rain/ice pellet mix (FZRAPL). It works by calculating the liquid-water fraction (f_w) for a spectrum of falling hydrometeors given a prescribed temperature (T) and relative humidity profile.

The second paper is on the validation of forecast precipitation type. The forms of uncertainty considered are instrument/observer bias and horizontal/temporal representivity of the observations. Instrument/observer biases are assessed by comparing observations from the Automated Surface Observing Station (ASOS) and meteorological Phenomena Identification Near the Ground (mPING) networks. Relative to the augmented ASOS, mPING observations are biased toward ice pellets (PL) and away from rain (RA). Consequently, when mPING is used to validate precipitation-type forecasts, the Probabilities of Detection (PODs) for RA (PL) are decreased (increased) relative to those obtained when using augmented ASOS.

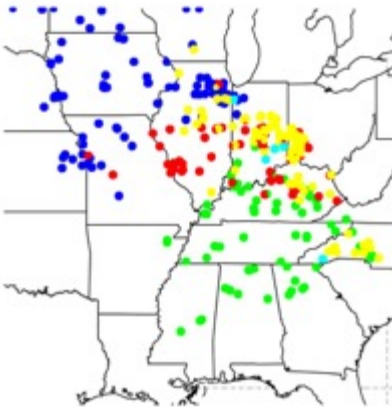
a) mPING: 1800 UTC 8 Feb 2013



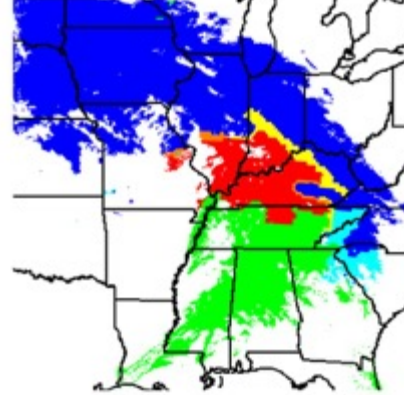
b) SBC: 1800 UTC 8 Feb 2013



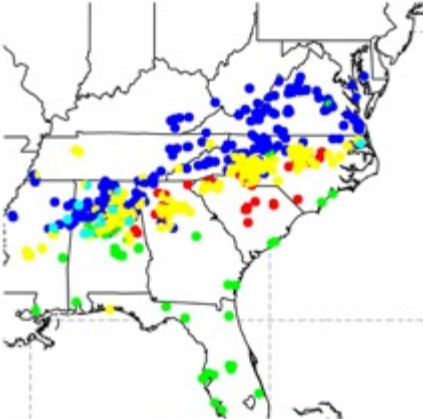
c) mPING: 0200 UTC 22 Feb 2013



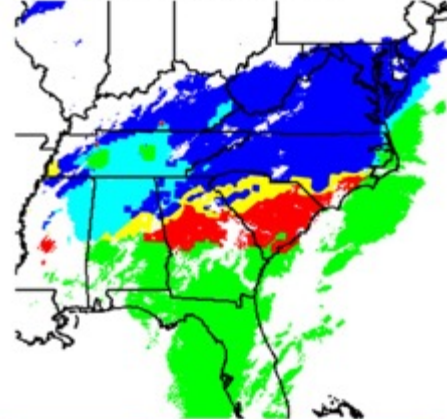
d) SBC: 0200 UTC 22 Feb 2013



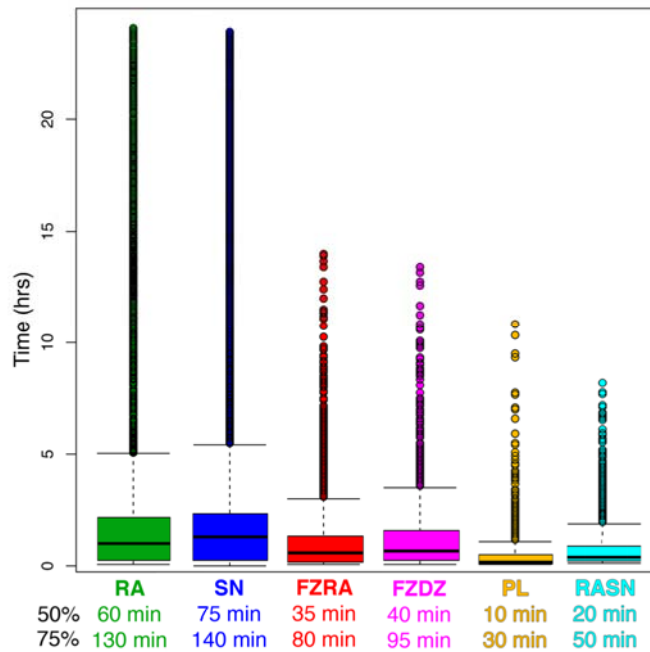
e) mPING: 2200 UTC 12 Feb 2014



f) SBC: 2200 UTC 12 Feb 2014



The (a,c,e) mPING distributions of observed precipitation type for the 2-h period surrounding the time indicated at the top of each panel and (b,d,f) the corresponding SBC analyses. In (b,d,f) only the areas with observed composite reflectivity greater than 0 dBZ are shaded.



Box-and-whisker plots showing the length of all episodes of RA, SN, FZRA, FZDZ, PL and RASN, where an episode is defined as two or more consecutive reports for the same kind of precipitation. The 50th and 75th percentiles are provided beneath the graph.

7. Facilitation of the Probabilistic Hazards Information (PHI) Prototype Experiment and the Phased Array Radar Innovative Sensing Experiment (PARISE)

Gabe Garfield (CIMMS at OUN)

Pre-experiment, a narrated weather briefing was created for PHI for each displaced real-time case (4 cases in total). Similarly for PARISE, a narrated weather briefing for each displaced real-time case (11 cases in total) was created. In each case, forecasters used these briefings to acquaint themselves with each case before beginning. Experimental procedures were tested for PARISE feedback was provided to the principal investigators, which was used to improve the project design.

Publications

- Johnson, A., X. Wang, J. Carley, L. Wicker, and C. D. Karstens, 2015: A comparison of multi-scale GSI-based EnKF and 3DVar data assimilation using radar and conventional observations for mid-latitude convective-scale precipitation forecasts. *Monthly Weather Review*, **143**, 3087-3108.
- Lakshmanan, V., C. D. Karstens, K. Elmore, S. Berkseth, and J. Krause, 2015: Which polarimetric variables are important for weather/no-weather discrimination? *Journal of Atmospheric and Oceanic Technology*, **32**, 1209-1223.
- Reeves, H. D., A. V. Ryzhkov, and J. Krause, 2016: Discrimination between winter precipitation types based on spectral-bin microphysical modeling. *Journal of Applied Meteorology and Climatology*, **55**, 1747-1761.

ROC Project 10 – Analysis of Dual Polarized Weather Radar Observations of Severe Convective Storms to Understand Severe Storm Processes and Improve Warning Decision Support

NOAA Technical Lead: Maj. David McDonald (ROC)

NOAA Strategic Goal 2 – Weather-Ready Nation – Society is Prepared for and Responds to Weather-Related Events

Funding Type: CIMMS Task II

1. Dual-Polarization Precipitation Identification

Stephen Castleberry (CIMMS at ROC), Daniel Berkowitz and Richard Murnan (ROC), and John Krause (CIMMS at NSSL)

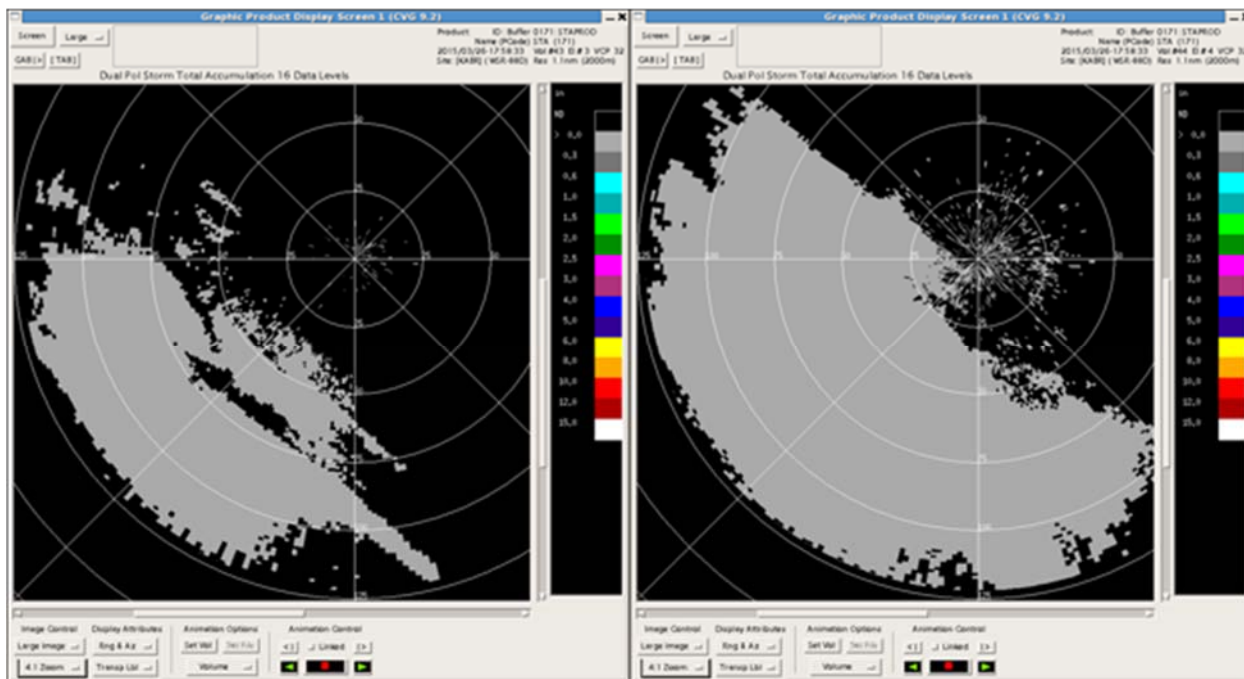
Objectives

Test, document, and optimize the Met Signal algorithm: software that was originally engineered for the ROC by NSSL scientists that identifies and filters non-meteorological targets from precipitation estimation radar products. Continue testing the software that was integrated into the Radar Product Generator (RPG) architecture during the last FY to evaluate its performance and ensure its adaptable parameters (APs) correctly perform to their anticipated sensitivities; document the results of this sensitivity testing. Develop research methods to make the software easier for end-users (such as NWS forecasters) to use, and ways to optimize the code to enhance computing efficiency and software maintainability.

Accomplishments

As noted in the FY15 report, a significant problem exists in processing and analyzing radar data to study precipitation and convective weather systems in that non-meteorological targets (wind turbines, birds, insects, vehicle traffic, etc.) can contaminate the data and cause incorrect values to be reported in various radar products, especially those related to precipitation estimation and derived dual-pol products. The Met Signal algorithm developed by NSSL scientists for the ROC is designed to identify and filter this contamination, thus improving the quality of derived dual-pol products and precipitation estimation products. After the code was fully integrated into the ROC's RPG software and deemed operational, extensive sensitivity testing was then completed to evaluate the performance of the algorithm and to ensure that varying its APs results in the desired effects (Figure 1). These tests have yielded promising results, and all aspects of the algorithm have been shown to function correctly. The results of the implementation and validation testing were then documented, summarized in a PowerPoint presentation, and then presented to the Data Quality Evaluation group at one of their weekly meetings (attended by various ROC, NSSL, and WDTD staff to name a few groups). The presentation was well received by the attendees. Currently, work is underway to optimize and increase maintainability and computing efficiency of the software, as well as to make it easier for end-users to

operate. As of now, a major logical overhaul of a key component of the software was completed to speed up its processing, and research has started on an experimental technique to automate an element of the AP selections



Comparison between Storm Total Accumulation (STA) precipitation products in units of inches using the Met Signal processing with the default adaptable parameter selection (left), and with the adaptable parameters adjusted to the lower threshold (right). The radar data used were from KABR (Aberdeen, SD) on 3/26/2015 at around 1758 UTC. This comparison illustrates that, in cases of winter weather precipitation (weaker echoes) such as this one, it is recommended that the operator reduce the Met Signal filtering threshold to the lower value to avoid “over-filtering” and removing actual precipitation targets from the data.

2. Quantitative Precipitation Estimation Analyses Tool Development

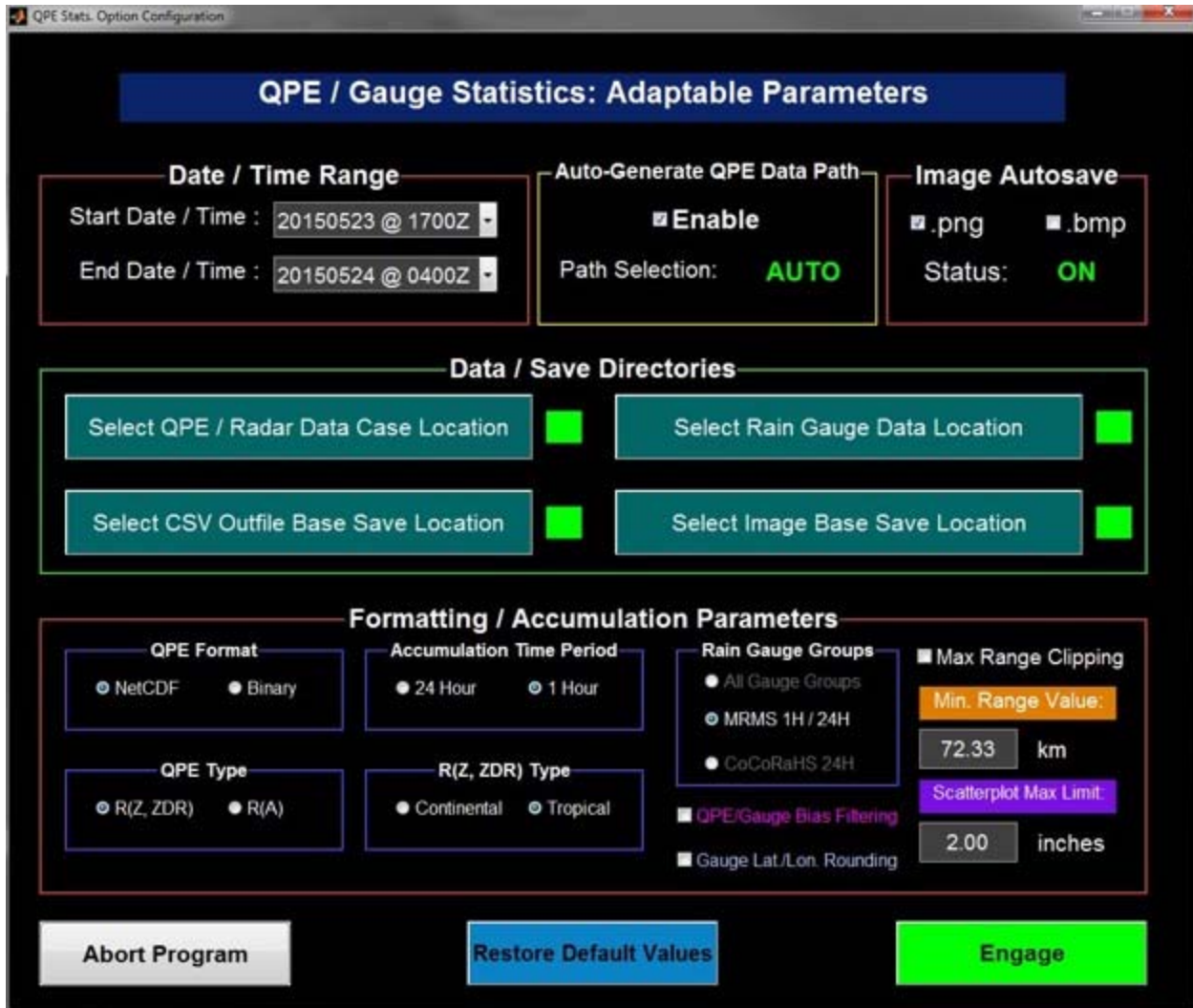
Stephen Castleberry (CIMMS at ROC), Heather Grams (CIMMS at NSSL), and Daniel Berkowitz (ROC)

Objectives

Refine software used to compare radar-derived precipitation accumulation estimates, a component of quantitative precipitation estimation (QPE), with corresponding rain gauge data (assumed to be the “ground truth”) to evaluate the sensitivity of the QPE to different $R(Z, Z_{DR})$ schemes and to various changes in the Radar Product Generator (RPG) software. To aid in evaluating these software changes and in comparing the various QPE results with rain gauge data, develop tools to enhance usability of the comparison software.

Accomplishments

As new research is performed, changes and improvements are made to the way in which dual-pol radar data are used to estimate precipitation rates and accumulations. Accordingly, as different QPE analysis techniques are developed, extensive case study testing must be performed in order to make better recommendations for which QPE adaptable parameters (APs) should be used under different meteorological conditions. For example, in the RPG software, a method in which the rainfall rate is calculated over a given time interval is given by $R \equiv R(Z, Z_{DR}) = A * (Z)^B * (Z_{DR})^C$ with units of mm hr^{-1} . Where Z is reflectivity in linear units and Z_{DR} is differential reflectivity in linear units. The coefficient A , and the exponents B and C are APs selected based on which precipitation type is to be used for the given time interval. Accordingly, the selection of these parameters can have significant impacts on the final estimated rainfall accumulation amounts over a period of time. A calculated rainfall rate that is too low would yield lower than actual accumulations, while one that is too high would overestimate the accumulations. Therefore, it is critical to test the effects of different R schemes versus the corresponding rain gauge data to evaluate the effectiveness of each under a variety of different meteorological conditions. Furthermore, changes in the RPG software dealing with QPE must also be tested to verify they produce desired results when compared to rain gauges. In order to more easily and efficiently perform the comparisons between the QPE calculations and the rain gauge data, a graphical user interface (GUI) software package was developed in Matlab (Figure 2). This package enables scientists and researchers at the ROC and NSSL to do these analyses and evaluations more quickly.



Sample Matlab GUI window that controls the input / adaptable parameter ingestion into the QPE-rain gauge statistical comparison scripts. This control panel allows the user to select the QPE data, rain gauge data, save directory locations, data type and format, $R(Z, Z_{DR})$ configuration, accumulation time interval, filtering parameters, formatting parameters, and the date-time range for the QPE-gauge comparison analysis they wish to perform. Before this software package was developed, the user had to manually type these many inputs into the command line to run the comparison scripts and ensure they were correct; this software has made the programs much easier to operate in that it automates the process of passing the inputs to the analysis scripts and performs real-time error checking to ensure the user is selecting the correct input values for the various fields.

3. 3D Modeling of Clouds to Aid in Development of a Cloud Detection Algorithm

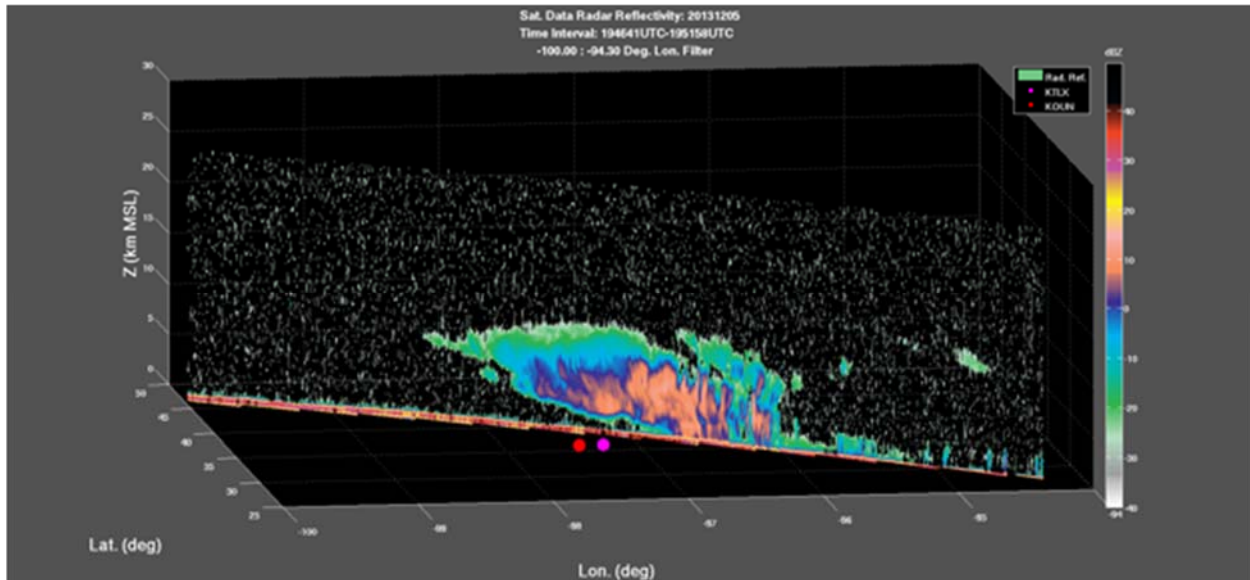
Stephen Castleberry (CIMMS at ROC), Valery Melnikov (CIMMS at NSSL), and David McDonald and Richard Murnan (ROC)

Objectives

Develop techniques to visualize and analyze cloud structures in 3D using radar data. Using the 3D visualizations of the cloud structures, assist with the development of a cloud detection algorithm (CDA) to detect these (usually low reflectivity) structures in real-time to assist forecasting, research, and aviation. Additionally, assist in the process of writing, reviewing, and commenting on a report documenting this research and explaining how the CDA was developed, how it functions, and the role the 3D representations of the cloud structures played in its creation. Further, experiment with using radar observations taken from satellites to supplement the ways in which the cloud structures are visualized in 3D.

Accomplishments

As mentioned in the FY15 report, until recently, radar data has been analyzed and visualized primarily using 2D methods such as plan position indicator (PPI) plots and range-height indicator (RHI) plots, and used primarily to study precipitation and convective weather systems. The aim here is to expand on these methods to investigate techniques to analyze and visualize radar data in 3D to foster a better understanding of the atmosphere visible to the radar, and to utilize this information to study cloud layers (non-precipitating) and other structures within the clouds, such as cloud bases and tops, cloud droplet / particle sizes and shapes, and flow patterns that could indicate turbulence. To aid in the 3D visualization aspect of this project, radar data taken from a polar orbiting satellite was also analyzed (Figure 3), along with data from the WSR-88Ds using software such as Matlab and Gibson Ridge GR2 Analyst. To summarize and apply the information obtained from these 3D visualizations and analyses, NSSL and ROC staff coordinated on writing a report describing how the resultant CDA functions and summarizing the research that led to its creation. Both parties collaborated on the writing, review / comment, and revision process of the report.



Semi-3D plot of radar reflectivity data taken from a radar antenna mounted on a polar orbiting satellite (known as CloudSat). The reflectivity data (dBZ) is plotted as a function of latitude (degrees), longitude (degrees), height (km above mean sea level - MSL), and time (UTC). The approximate domain used in this plot is approximately 25.0 to 50.0 degrees latitude, -100.0 to -94.3 degrees longitude, 0.0 to 25.0 km MSL, and across a time swath from 1946 – 1951 UTC on 12/5/2013. The reflectivity scale is from -40 to +40 dBZ since the aim is to study cloud structures which typically exhibit relatively low reflectivity values, and anything above 40 dBZ is very likely precipitation. In the feature presented in this figure, the cloud base and top boundaries are evident by the green-gray coloring pertaining to around -25 to -20 dBZ at around 4 km MSL and 8 km MSL. More dense areas of the cloud feature are evident by the ~ 10 dBZ contours reaching very low altitudes, possibly indicating the presence of fog at the surface. Furthermore, since these data were used as comparisons to those taken from weather radars, the approximate locations of the KTLX and KOUN radar sites are shown by the magenta and red dots, respectively.

4. 2-D Velocity Dealiasing Algorithm (2DVDA) Testing and Documentation

Zachary Biggs (CIMMS at ROC), Autumn Losey (Centuria Corporation), and Walter Zittel (ROC)

Objectives

Assist in documentation and maintenance of the new 2-D velocity dealiasing algorithm (2DVDA) for the National Weather Service (NWS) Radar Product Generator (RPG).

Accomplishments

During his initial phase as a CIMMS employee, Mr. Biggs worked closely with Walter Zittel and Autumn Losey on documenting and testing the new 2DVDA algorithm used in the Radar Product Generator (RPG).

2DVDA is the first velocity dealiasing program in the RPG that does not dealias radial by radial. Instead, 2DVDA accumulates an entire elevation scan before starting its work. Once an entire elevation scan has passed to 2DVDA, the program performs a “background” dealiasing on the overall velocity field using information about the vertical wind profile obtained from model data and the previous volume scan. The program then breaks down the elevation scan into regions with each region being dealiased separately. The result is a more accurately dealiased velocity field.

Because the code was given to the Radar Operations Center straight from research it had operated much as a black box. Much care has been taken by the Radar Operations Center to investigate every aspect of the 2DVDA program through its source code and to document it. My focus on this project has been the portion of the 2DVDA program that performs the dealiasing of the individual regions. By going through code carefully and developing an understanding of how it works, we have been able to create important documentation that will be useful for those needing to perform maintenance on the program.

We also tested recent changes put into the program that will aid it at times when model data is not available. One of the changes will allow 2DVDA to generate something called a “Free Atmospheric Wind” (a very rough estimate of the general flow in the atmosphere) that would aid it in dealiasing. Another change was to ensure that model data could be used more frequently (as long as it is available). This was to help during times when there were returns very far from the radar and few close. Such times proved very difficult for 2DVDA to develop any kind of estimate of the general atmospheric flow. By allowing the program to use model output more frequently there are less velocity dealiasing errors during times of convection and showers far from the radar.

5. Z-ZDR Histogram Plot investigation

Zachary Biggs (CIMMS at ROC) and Richard Murnan (ROC)

Objectives

Develop tools to visualize and analyze Z-ZDR slopes and patterns using histograms.

Accomplishments

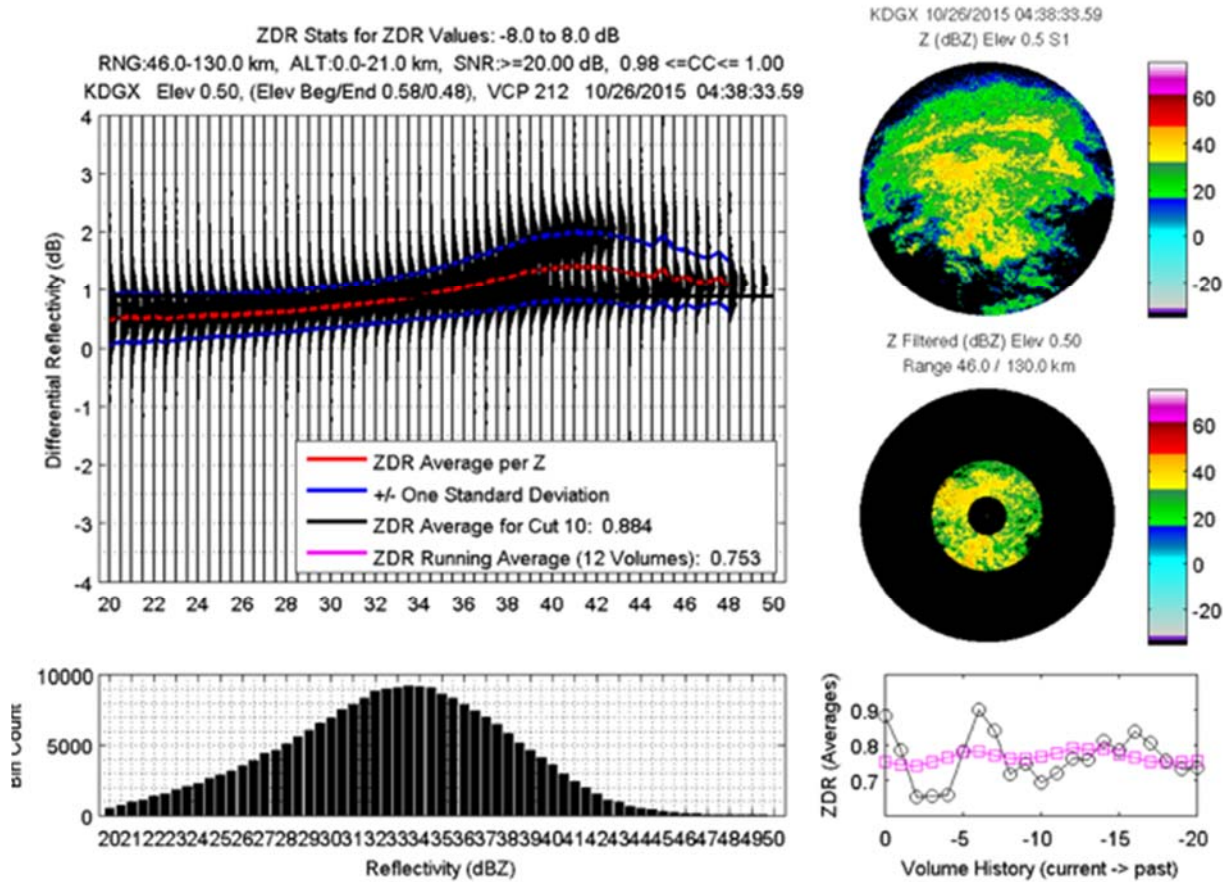
An existing program was used to make reflectivity (Z) and differential reflectivity (ZDR) slope plots using histograms and improved their performance and expanded upon their capabilities.

The Z-ZDR histogram plotter is one of the prized creations inside the Radar Operations Center Applications Branch. The program has a robust set of filters that a user can set and control via a graphical user interface (GUI) program. The GUI makes it easy to determine what portion of an elevation angle scan a user wants to examine and allows the user to filter the region using Z, ZDR, Correlation Coefficient (CC), and Signal to Noise Ratio (SNR). In this way, very specific precipitation regions can be examined. Created in Matlab the program was originally designed to monitor ZDR calibration

performance. However, because it uses histograms instead of a more typical Z-ZDR scatter plot, it became clear to me that the program could also be used to see shapes and patterns associated with various precipitation regimes.

Using tools such as Multi-Sensor-Mult-Radar (MRMS) Probability of Warm Rain (POWeR) and mPING, I selected a wide range of precipitation cases to examine using the Z-ZDR histogram plotter. From the selected cases it became clear to those of us in the ROC Applications Branch that a fixed Z-R relationship inside the WSR-88D RPG would not be appropriate for estimating rainfall during very dynamic precipitation events. In fact, a significant number of the cases examined showed quite a wide range of changes both in the histogram patterns and Z-ZDR slope for just liquid precipitation alone. One particular case from KDGX on 10/26/15 around 04:00 UTC showed a bimodal distribution for pure liquid rain in the Z values ranging from 40 to 50 dBZ as a transition zone in rainfall regimes was passing through the region (see figure below).

Based off of the KDGX 10/26/15 data case, I presented my findings to Alexander Ryzhkov, Yadong Wang, Stephen Cocks, Terry Schuur, and Pengfei Zhang, and then later at the ROC Data Quality Meeting to try to get further insight into why such dramatic differences in pure rainfall regimes were observed. I also wanted to make sure that members of the ROC and NSSL were aware of the complexities found in pure liquid precipitation. No clear answers were obtained after much discussion, but it did become apparent that the Z-R relationship needed to be more dynamic in order to keep up with rapid changes in precipitation regimes. Thus began the search for some kind of trigger mechanism that would switch the RPG Z-R relationship equation from tropical or continental based off of Z-ZDR slope and distributions.



Z-ZDR Histogram chart showing bi-modal distributions in ZDR from 38 to 45 dBZ

6. Z-ZDR Slope History Examination

Zachary Biggs (CIMMS at ROC) and Richard Murnan (ROC)

Objectives

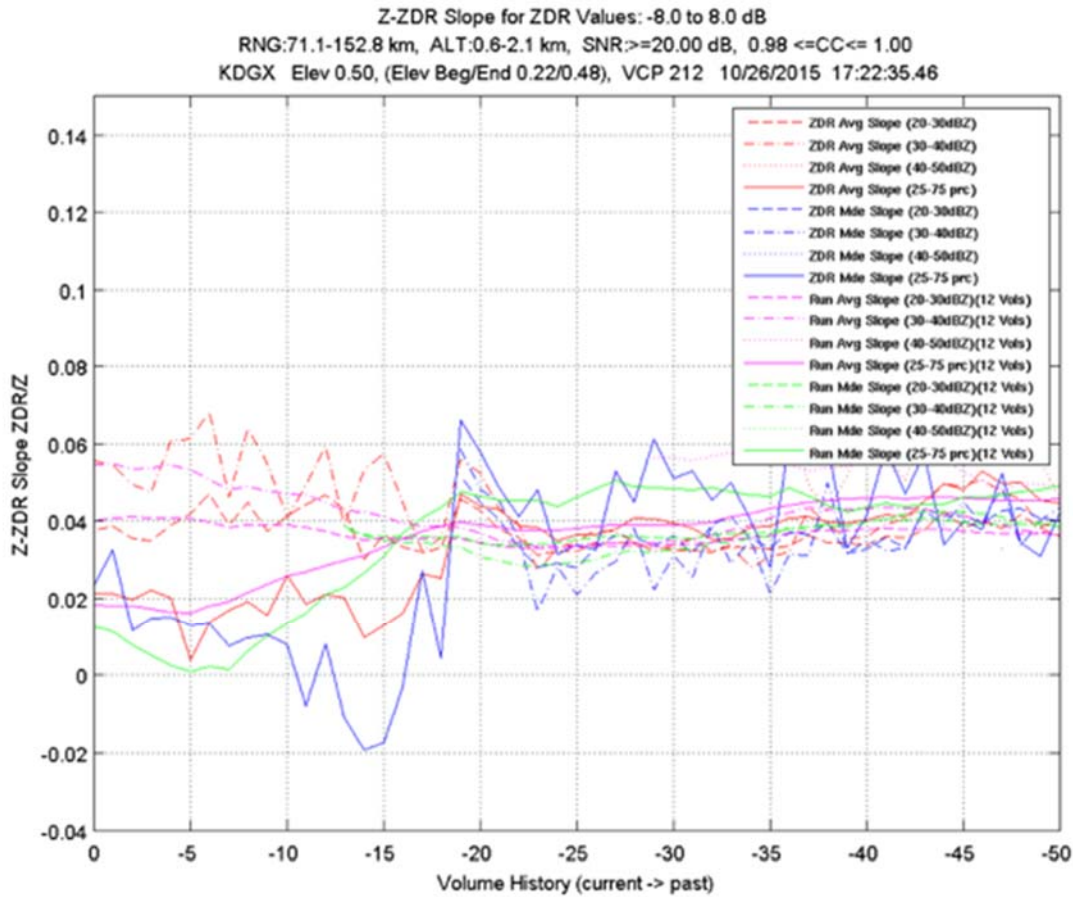
Examine Z-ZDR slope event history to see if Z-R relation can be automated.

Accomplishments

Born out of the Z-ZDR histogram plotter, a tool was created (see figure below) that plots the radar volume history of Z-ZDR slope values for the mean and mode of the Z-ZDR distributions for a number of different Z ranges. With this tool one can see transition periods where Z-ZDR slope values undergo a rapid change before settling into specific ranges of values.

To capture as much Z-ZDR slope information as possible the tool plots Z-ZDR slopes for the mean and mode ZDR per Z value for Z ranges of 20 – 30 dBZ, 30 – 40 dBZ, 40 – 50 dBZ, and the 25th – 75th Z percentile ranges. In addition, running-average values of these slopes are plotted to give additional information about the longer term trends.

The hope is that with further testing and case evaluation a method for determining when the RPG should change Z-R relationships will be determined. This would allow forecasters to focus on the meteorology and not have to worry about manually changing the Z-R relations on the fly during precipitation events.



Z-ZDR Slope Volume History Chart showing significant change in Z-ZDR slopes approximately 20 volumes before 17:22 UTC.

7. Implemented Specific Attenuation $R(A)$ Instantaneous Rainfall Rate into RPG

Zachary Biggs (CIMMS at ROC), Daniel Berkowitz and Richard Murnan (ROC), and Yadong Wang, Pengfei Zhang, and Stephen Cocks (CIMMS at NSSL)

Objectives

Create software to incorporate a new rainfall algorithm into the RPG that uses specific attenuation to calculate the rainfall rate.

Accomplishments

During the latter part of the period work was done to implement a new method of measuring the instantaneous rainfall rate (R) that depends on the specific attenuation (A) of reflectivity (Z). To see the specifics of how the method works and why it is needed see the paper “*Potential Utilization of Specific Attenuation for Rainfall Estimation, Mitigation of Partial Beam Blockage, and Radar Networking*” by Ryzhkov et al 2014. Essentially by using A instead of Z a reasonable R can be calculated in those areas where partial beam blockage is occurring.

Because of how the WSR-88D RPG is designed each radial is examined separately when calculating A for each bin (r). The first legitimate liquid precipitation bin is considered to be the starting range (r_1) of R(A) while the last legitimate liquid precipitation bin before the bottom edge of the melting layer is considered to be the ending range (r_2) of R(A). As of now I have chosen to stay out of the melting layer altogether based off of recommendations from Yadong Wang and Stephen Cocks. Once r_1 and r_2 have been identified $\Delta\Phi_{DP}$ is calculated by taking the difference in Φ_{DP} and removing any additions to $\Delta\Phi_{DP}$ from non-liquid precipitation bins between r_1 and r_2 . Equation 1 can then be used to calculate the Path Integrated Attenuation (PIA).

$$PIA = \alpha \Delta\Phi_{DP} \quad \text{Equation (1)}$$

The parameter α is calculated from the Z-ZDR slope of all liquid precipitation bins. As of now I am only using a hard coded value of 0.015 for α . In a future RPG build we hope to have α vary with time as it relates to Z-ZDR slope of the previous volume scan. When PIA has been calculated, a constant can be calculated via Equation 2. $C(\beta, PIA)$ will then be applied to all bins within that radial via Equation 5.

$$C(\beta, PIA) = e^{0.23\beta PIA} - 1 \quad \text{Equation (2)}$$

The next step is to estimate, with a finite sum, the integral $I(r_1, r_2)$ of all liquid precipitation bins between r_1 and r_2 (Equation 3) using the raw smoothed reflectivity Z_R which is pulled into the QPE algorithm from the elevation scan building program in the RPG.

$$I(r_1, r_2) = \frac{0.46\beta}{4} \sum_{i=r_1}^{r_2} Z_R(i)^\beta \quad \text{Equation (3)}$$

Because R(A) relies upon attenuation, it is imperative that the reflectivity be raw and not have any attenuation correction factor applied to it. Much work was needed to bring raw reflectivity into QPE because previous programmers did not anticipate it would be needed in the QPE program and beyond. Once the raw reflectivity was pulled into QPE a 5 gate smoothing factor was applied to it to give us Z_R .

With the above values calculated for the radial as a whole the QPE algorithm will step through each of the bins within the radial and calculate the instantaneous rainfall rate. To do this another summation must be performed via Equation 4 to retrieve the estimate of the integral $I(r, r_2)$.

$$I(r, r_2) = \frac{0.46\beta}{4} \sum_{i=r}^{r_2} Z_R(i)^\beta \quad \text{Equation (4)}$$

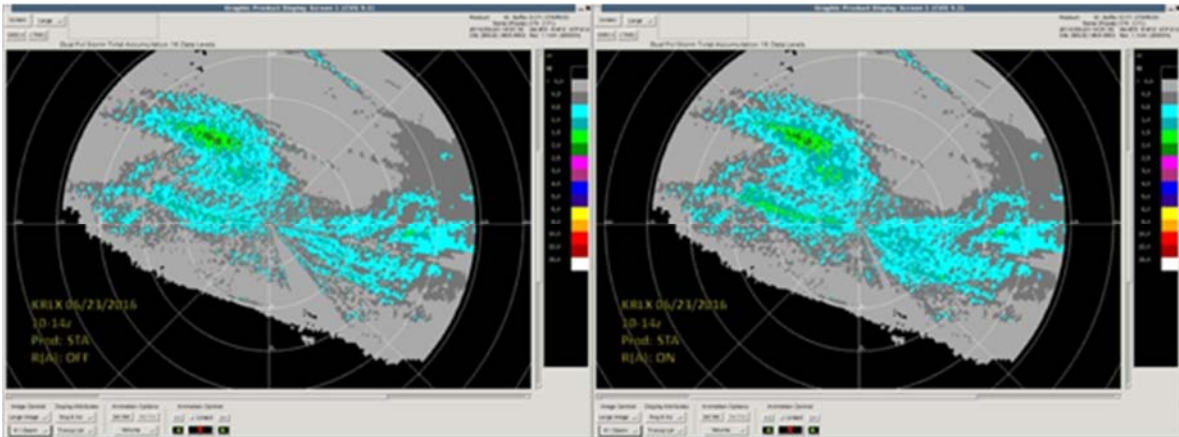
The specific attenuation value for each particular bin r is then calculated via Equation 5 and the result plugged into Equation 6 to get the instantaneous rainfall rate $R(A)$.

$$A(r) = \frac{[Z_R(r)]^\beta C(\beta, PIA)}{I(r_1, r_2) + C(\beta, PIA)I(r, r_2)} \quad \text{Equation (5)}$$

$$R(A) = \gamma A(r)^\lambda \quad \text{Equation (6)}$$

Constants β , γ , and λ were given to be 0.6, 4120, and 1.03 respectively by Ryzhkov.

So far, $R(A)$ has been tested on KRLX for the time period 6/23/16 10:00z to 14:00z. As seen in the figure below, much improvement has taken place in the heavily blocked regions to the southeast of the radar. Several more data cases need to be tested to ensure that at worst $R(A)$ does no harm to the QPE output. Once this has been established plans will be made to implement $R(A)$ into the most current RPG build cycle. Further work needs to be performed to move away from a fixed α value of 0.015 and towards an estimated α that is more representative of the rainfall regime occurring with any particular event.

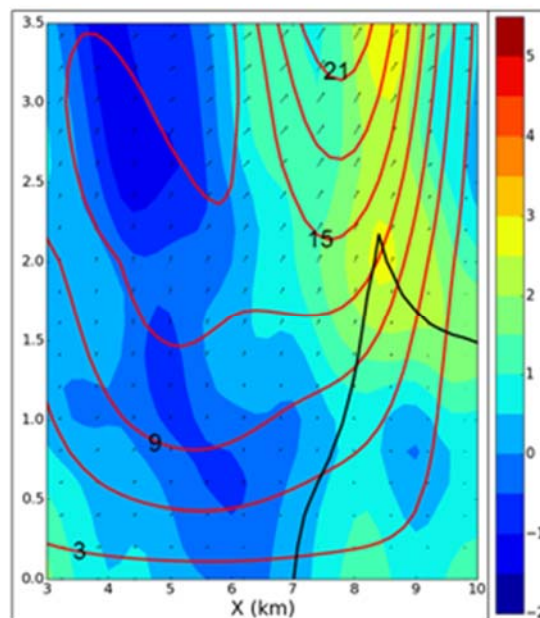


Dual-Pol Storm Total Accumulation for KRLX 6/23/16 10:00 – 14:00 UTC with $R(A)$ active on the right and inactive on the left.

8. Study of the 19 May 2013 Norman-Shawnee Tornadic Supercell

Mike French (Stony Brook University), and Don Burgess and Corey Potvin (CIMMS at NSSL)

The Norman-Shawnee Supercell produced an EF4 tornado that formed in east Norman and dissipated in extreme northwest Shawnee. Along the 40 km track there were 2 fatalities and 10 injuries. A unique aspect of the tornado is that it formed within close range (<20 km) from 6 weather radars: five fixed-site radars (KTLX, MPAR, KOUN, KCRI (S-Band), and TOKC (C-Band)), and one mobile radar (NOXP (X-Band)). Mesocyclone/updraft-scale analysis of the case has begun with Dual-Doppler from KTLX and MPAR. Zdr columns are found to compare favorably with calculated vertical velocity (see figure below). Dual-Pol Tornado Debris Signatures (TDSs) are found to compare favorably to mesocyclone vertical vorticity (not shown). The project is continuing. Tornado-scale Dual-Doppler analysis is in progress and will allow comparison of radar-derived tornado properties and Dual-Pol signatures. A separate project is looking at the kinematics of tornadogenesis. Both projects are in anticipation of a third project that will compare the analyses in the current projects to results from high-resolution Warn-on-Forecast numerical model forecasts.



Updraft overlaid on Zdr column. Color fill is Zdr magnitude (dB, scale at right), red contours are vertical velocity (m/s), and black contour is 30 dBZ reflectivity. Zdr column above 1.5 km height (at x=8-10 km) overlays the eastern portion of the supercell updraft. Below 1.5 km height, low Zdr values in the developing Tornado Debris Signature (TDS) impede the comparison of Zdr column and updraft.

SPC Project 11 – Advancing Science to Improve Knowledge of Mesoscale Hazardous Weather

NOAA Technical Leads: Russell Schneider and Steven Weiss (SPC)

NOAA Strategic Goal 2 – *Weather-Ready Nation – Society is Prepared for and Responds to Weather-Related Events*

Funding Type: CIMMS Task II

Overall Objectives

Conduct activities to maximize the diagnostic and forecast value of geostationary satellite data and products, within the SPC, HWT, and the GOES-R Proving Ground. A key component is to test and validate new satellite products associated with GOES-R, and to interact with NWS operational forecasters to prepare them for new satellite products. Emphasis will be on assessing the value of advanced satellite products for detection and short-term prediction of convective storms and associated hazards.

Support the HWT Experimental Forecast Program (EFP) and collaboration and sharing of information with the Experimental Warning Program (EWP). This involves performing research into application of new tools and applying verification techniques to convection allowing models/ensembles and experimental forecasts in near real-time within the HWT; and transferring of those activities found to be promising and of value from the HWT into daily operations at SPC. In addition, basic research is conducted to improve understanding of severe, fire, and winter weather topics that are of interest to SPC but are not related to any formal activities within the HWT. Finally, SPC partners are engaged to improve communication with the public to better mitigate the impacts of severe weather.

Develop probabilistic calibrated forecasts of cloud-to-ground (CG) lightning density through Day 8 based on input from operational numerical weather prediction models including convective allowing and ensemble models. Collaborating with NWS partners and the wildfire community is imperative to develop a broader unified probabilistic guidance suite that includes lightning occurrence and dry lightning. The probabilistic CG lightning density guidance will be distributed to NWS offices and external customers in a gridded format. The guidance will enhance the ability of fire agencies to prepare for lightning ignited wildfires by prepositioning and allocating appropriate wildfire suppression resources.

Accomplishments

1. Hazardous Weather Testbed

Chris Melick and James Correia, Jr. (CIMMS at SPC)

The 2016 Spring Forecasting Experiment was conducted 2 May-3 June with participation from more than 80 forecasters, researchers, and model developers from around the world. Building upon prior successful experiments, a main emphasis of 2016 SFE continued to be the generation of probabilistic forecasts of severe weather valid over shorter time periods than current SPC operational products. As in previous years, a suite of new and improved experimental convection allowing model (CAM) guidance contributed by our large group of collaborators was central to the generation of these forecasts. However, this year a major effort was made to coordinate CAM-based ensemble configurations much more closely instead of each group providing a separate, independently designed system. Specifically, all groups have agreed on a set of model specifications (e.g., grid-spacing, vertical levels, domain size, physics) so that the simulations contributed by each group can be used in carefully controlled experiments. Thus, the most substantial change was facilitating the conversion and post-processing of specialized CAM parameter fields (neighborhood maximum and multi-hourly maximum storm attributes) internally at SPC in order to standardize ensemble type forecast plots (e.g., probabilities, maximum value, spaghetti-“paint ball”) within the HWT. The large number of CAM members (65) at 3-km grid spacing assembled for the 2016 SFE was termed the Community Leveraged Unified Ensemble (CLUE) and provided an adaptable framework in identifying optimal configuration strategies for CAM-based ensembles (Clark et al. 2016). Ultimately, the results from a set of eight separate CLUE experiments will help provide evidence-based driven decisions in the design of the first operational CAM-based ensemble for the United States, which is planned for implementation by NOAA’s NCEP/Environmental Modeling Center (EMC).

Objective verification was performed in near real-time for the fifth consecutive year during the 2016 experiment. Forecast verification metrics were once again investigated by the participants during the five-week period of the SFE to document their usefulness in the daily evaluations of convection allowing model performance. Following the initial findings from the 2012 experiment, computations of Fractions Skill Score (FSS) for neighborhood probabilistic guidance of simulated reflectivity continued to be a valuable measure of skill from convection allowing ensembles but had now transitioned to a focus on evaluating sub-ensemble groupings within the new CLUE framework. In addition, experimental probabilistic forecasts of tornado, wind, and hail were evaluated similarly as in the 2014 and 2015 experiment by using local storm reports (LSRs) as the verification. For this purpose, CSI was calculated at two fixed probability thresholds (5% and 15%) used in SPC operational outlooks, and FSS was determined by directly comparing the probabilistic areas in the forecast to the observations.

A separate set of skill scores was generated using remotely-sensed supplemental observations of hail. Specifically, a multi-hourly, radar-derived field of maximum expected size of hail (MESH) from the MRMS system was developed to run in parallel to gauge the feasibility of alternative sources for verification. A quality control measure was applied to the hourly MESH grids using CG lightning flashes. Further, only spatially filtered grids were considered to ensure the presence of contiguous swaths in the high resolution MESH tracks. Similar to LSRs, “Practically Perfect” hindcasts were created

from the MESH to provide valuable baselines to measure the skill of the probabilistic severe hail forecasts during the 2016 experiment.

Support for various activities within the experiment included:

- Generating forecast soundings for UKMET (including SPC operations) and MPAS modeling systems,
- Ensemble forecasts of severe weather using updraft helicity objects for 3 systems (NCAR, SSEO, NSSL),
- Exploratory visualization of CAPE-shear phase space for rotating storms using the NSSL ensemble,
- Planning and support of the EWP-Probabilistic Hazard Information (PHI), and PHI-Emergency Manager projects to explore the use of PHI and its communication with emergency managers. Tailored briefings were provided for real-time cases while some graphics were provided for case study briefings.
- Grant project (***Test and Evaluation of Rapid Post-processing and Information Extraction from large Convection-Allowing Ensembles applied to 0-3hr Tornado Outlooks.***) implementation of object based, rapid post-processing techniques in warning operations for probabilistic hazard information.
- Assisted Harold Brooks (NSSL) and Kenzie Krocak (CIMMS at NSSL) on developing techniques for the extraction of time based severe weather probabilities. Concepts from these discussions resulted in the production of timing graphics of severe weather for the NCAR ensemble, using object-based techniques.

2. GOES-R and JPSS Proving Ground Activities

William Line (CIMMS at SPC)

The Storm Prediction Center (SPC) and Hazardous Weather Testbed (HWT) provide the GOES-R and JPSS Proving Ground with an opportunity to conduct pre-launch demonstrations of Baseline, Future Capabilities and experimental products associated with the next generation GOES-R geostationary and JPSS polar satellite systems. Many of these products have the potential to improve hazardous weather nowcasting and short-range forecasting. Feedback from forecasters in the SPC and HWT has led to the continued modification and development of GOES-R and JPSS algorithms.

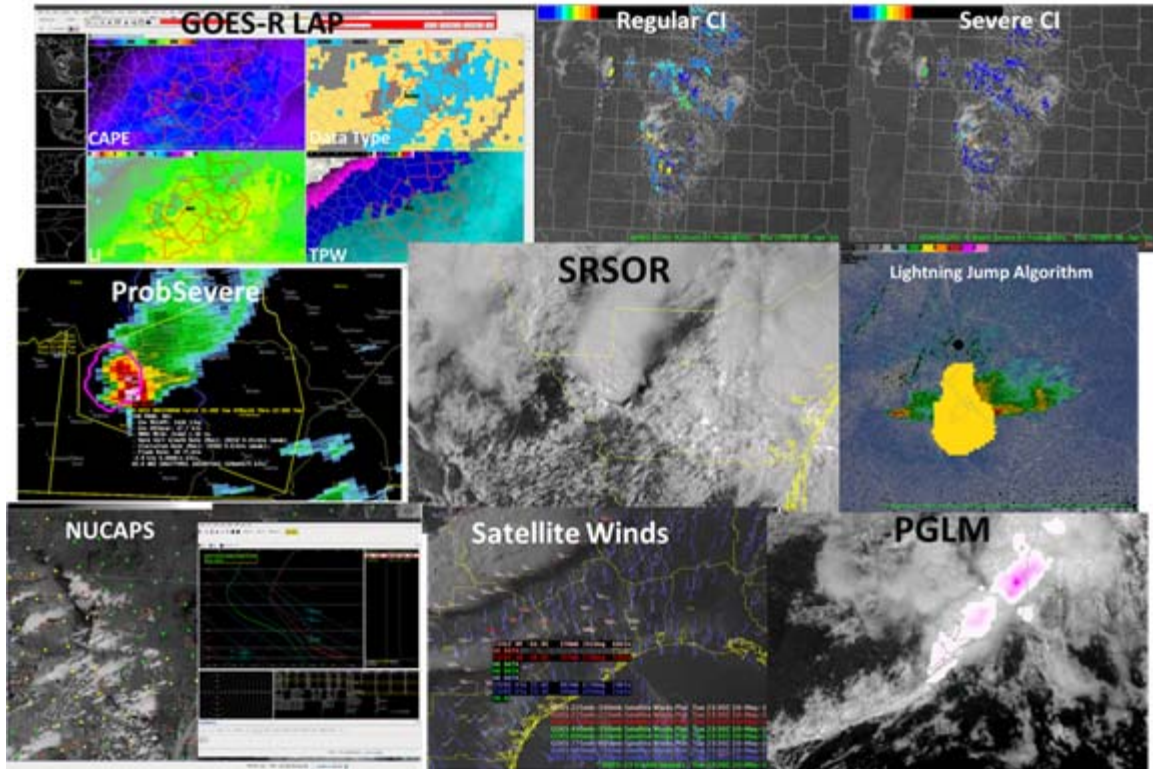
During the HWT 2016 GOES-R/JPSS Spring Experiment, GOES-R and JPSS products were demonstrated within the real-time, simulated warning operations environment of the Experimental Warning Program (EWP) using AWIPS-II (see figure below). This experiment was conducted Monday-Friday during the weeks of April 18, April 25, May 2, and May 9, and participants included a new group of three visiting NWS forecasters and one broadcast meteorologist each week. Product developers from various collaborating institutions were also in attendance to observe the activities and interact with the forecasters. Monday-Thursday included eight hour forecast/warning shifts, while Friday was a half-day dedicated to final feedback collection. During the simulated forecast shifts, the four forecasters utilized the experimental satellite products, in conjunction with operationally available meteorological data, to issue non-operational short-term

mesoscale forecast updates and severe thunderstorm and tornado warnings. Forecaster feedback was collected through the completion of daily and weekly surveys, daily and weekly debriefs, and blog posts.

GOES-R algorithms demonstrated during the HWT 2016 GOES-R/JPSS Spring Experiment included: GOES-Sounder derived all-sky Total Precipitable Water (PW), Layer PW, and Derived Atmospheric Stability Indices using the GOES-R Legacy Atmospheric Profile (LAP) algorithm from UW/CIMSS, UAH GOES-R Convective Initiation algorithm, UW/CIMSS ProbSevere Model, Pseudo-Geostationary Lightning Mapper Total Lightning products from NASA/SPoRT and the Lightning Jump algorithm from NASA/SPoRT and CIMMS/NSSL. GOES-14 1-min Super Rapid Scan Operations for GOES-R (SRSOR) imagery was available in the HWT for the full duration of the experiment, illustrating the very high frequency scanning capability of GOES-R. Parallax-corrected 1-min imagery and 10-min-updating atmospheric motion vectors were derived from the SRSOR data and also made available for forecasters to use in AWIPS-II. From the JPSS program, the NOAA Unique Combined Atmospheric Processing System (NUCAPS) temperature and moisture profiles were demonstrated in the AWIPS-II NSHARP sounding analysis program.

GOES-14 1-min SRSOR imagery was also available in SPC during three periods, including 10-21 August 2015, 1-24 February 2016, and 18 April – 14 May 2016. The SRSOR imagery was used extensively by SPC forecasters in operations when available over convectively active regions. Additional GOES-R Proving Ground products continued to be available in real-time to SPC forecasters, including the Overshooting Top Detection algorithm, Cloud Top Cooling algorithm, and NearCast Model.

The SPC has been involved in additional activities in order to prepare for the receipt and use of GOES-R data. Three GOES-R antennas were installed outside of the building in the NOAA satellite farm, and several SPC staff were trained on their use. SPC staff also tested and provided feedback on the Product Distribution and Access (PDA) interface. SPC coordinated with the TOWR-S project and participated in a GOES-R Readiness Exercise (GRE), which tested the flow of simulated GOES-R data over the SBN into AWIPS-II D2D. SPC prepared for future GOES-R readiness exercises, including the DOE-4 which would take place in July/August 2016. Results from GOES-R and JPSS product demonstrations in the SPC and HWT were documented by the satellite liaison in final reports and presented at various science meetings. Finally, the satellite liaison contributed to the development of the NWS GOES-R training plan.

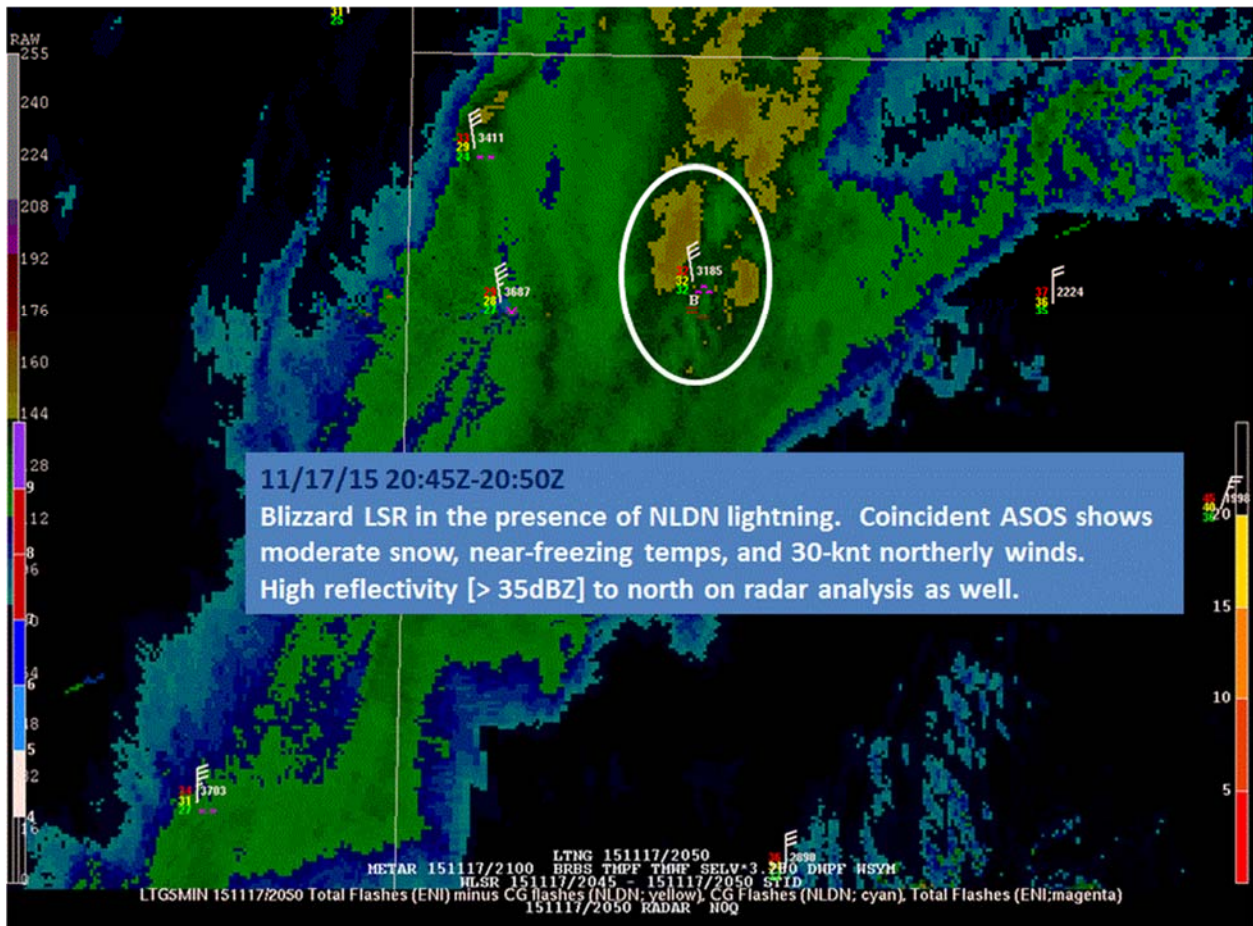


GOES-R and JPSS products and capabilities demonstrated during the HWT 2016 Spring Experiment.

3. Winter-Weather Local Storm Reports at SPC

Chris Melick (CIMMS at SPC)

Winter-Weather Local Storm Reports (LSRs) were made an available data type for viewing in the N-AWIPS N-MAP graphical user interface in SPC operations in December 2015. In order to accommodate, surface GEneral Meteorological PAckage (GEMPAK) files are created on a routine and frequent basis for recently decoded winter type LSRs. This near real-time processing is made possible via changes to the LSR Decoder to allow for event types other than those associated with Severe Thunderstorm events, including Snow, Heavy Snow, Blizzard, Sleet, Freezing Rain, and Ice Storm. One of the major advantages was providing the SPC forecasters the ability to plot and overlay the reports in near real-time with other types of observations (radar, satellite, standard surface stations, lightning detection networks) to help identify trends in precipitation type and intensity, and to assess whether convection is occurring in proximity to freezing rain, snow, or sleet (see figure below). Another benefit is the added capability to use the time-binning button/feature in N-MAP which can show accumulations and a history of the observations over a convective day (or even shorter time intervals). The development work aimed at providing forecasters a useful tool relevant to the issuance of winter weather mesoscale discussion products.



Spatial plot from N-MAP showing application of combining winter-weather LSRs with other observational datasets during a heavy snowfall event with convection. The figure has been annotated to emphasize the presence of a Blizzard LSR on November 17, 2015 coincident with other validating features in the radar analysis, lightning detection networks, and standard surface stations.

4. Cloud Flash Lightning Characteristics for Tornadoes without Cloud-to-Ground Lightning

Chris Melick (CIMMS at SPC)

Deep, robust convective updrafts are necessary for lightning production and are nearly always associated with severe thunderstorms capable of producing tornadoes. While cloud-to-ground (CG) lightning flashes are typically observed with tornadic storms, tornado events occasionally reveal a lack of CG activity, as observed by the Vaisala National Lightning Detection Network (NLDN). For instance, Guyer and Dean (2015) presented a case of an EF2 tornado that struck parts of Valdosta, Georgia, on 29 December 2014 that was not associated with any CG lightning in the vicinity leading up to, during, or immediately after the event. However, important aspects on total lighting activity, through the inclusion of cloud flashes (CF), were not presented in that study.

Current research (Melick et al. 2016) builds upon the prior work at SPC by examining United States tornado events that were not associated with CG lightning for a subset of their time period for which CF lightning data was available from Earth Networks (2013-2015). Characteristics of CF data are examined to provide a more comprehensive viewpoint of total lightning activity for these unique situations. In addition, the environmental conditions during these tornadoes are explored regarding the relationship to CF activity.

5. Lightning Density Prediction

Nicholas Nauslar (CIMMS at SPC), and Steven Weiss, Israel Jirak, and Patrick Marsh (SPC)

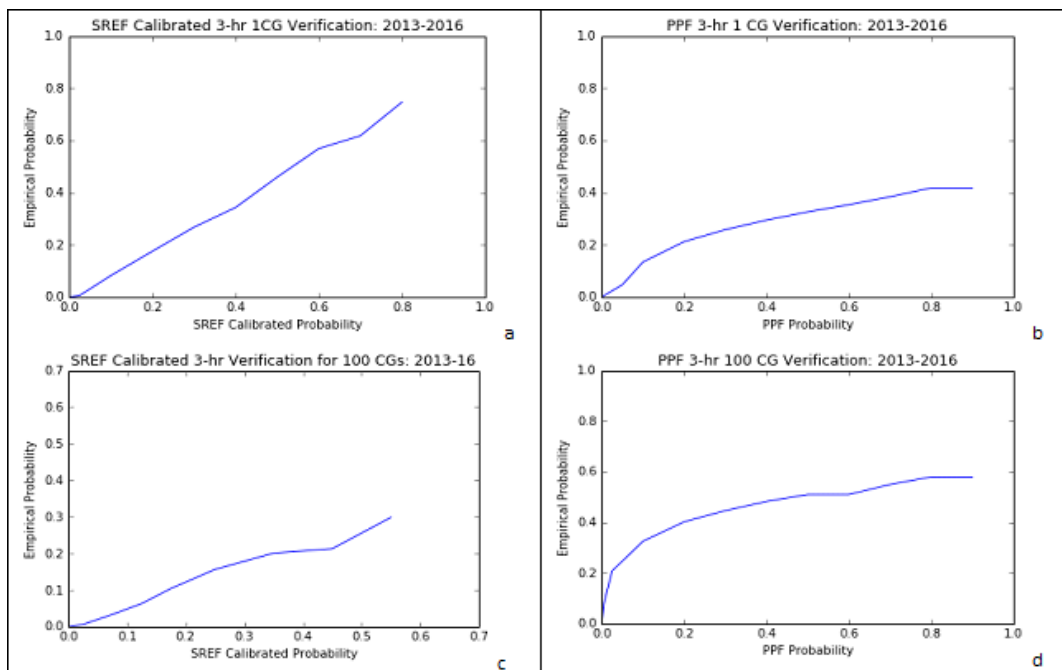
Thunderstorm and lightning guidance are imperative to fire weather forecasts, which are used by wildland fire managers when making decisions about resource allocation and suppression tactics. The Storm Prediction Center (SPC) Short Range Ensemble Forecast (SREF) calibrated thunder forecast guidance currently provides probabilistic forecasts on different temporal scales detailing the probability of one or more and 100 or more CG lightning flashes in a 40-km grid box. The SREF calibrated thunder forecast utilizes the probability of the cloud physics thunder parameter (CPTP) exceeding one and the probability of precipitation equaling or exceeding 0.01" (Pr01). Then archived CG lightning flashes are used to create calibrated probabilities based on the probability pair of CPTP greater than one and Pr01.

Verification on a 40-km grid of the SPC SREF-based calibrated probabilistic thunder guidance over parts of a three-year period for one or more CG lightning flashes demonstrates reliable and accurate forecasts and it verifies better overall than forecasts for 100 or more CG lightning flashes. A Perfect Prog technique producing thunderstorm forecasts of one or more and 100 or more CG lightning flashes, also in a 40-km grid box, using the Global Forecast System (GFS) predictors was also examined. The comparative verification results indicate the SREF calibrated thunder forecasts of one or more and 100 or more CG lightning flashes were more reliable and accurate than the Perfect Prog forecasts (see figure and table below).

The SPC SREF calibrated thunder approach was refined to improve lightning density guidance, including examination of other variables to enhance predictive skill. CPTP, most unstable and surface based convective available potential energy, lifted index, equivalent potential temperature, layered potential instability, and precipitable water were examined as potential predictors, as candidates to either replace or supplement the existing CPTP and Pr01 predictors. When examining 3-hour CG lightning totals, an inflection point emerged between 20 and 30 CG lightning flashes, and more than 80% of all 3-hour CG lightning flash totals occur below these values. The calibration method utilized for the current SREF calibrated thunder forecasts was updated and implemented on different CG lightning density thresholds ranging from 20 to 30 CG lightning flashes during 3-hour periods (out to an 87-hour forecast). Verification results

demonstrated reliable and accurate forecasts including an improvement over previous CG lightning density forecasts. However, testing of the new predictors into the forecast method did not show any measureable improvement. The new lightning density forecasts are being finalized and are projected to be available on an experimental basis in the near future.

Additionally, a forecaster survey was created to better understand operational forecasting needs and challenges pertaining to thunderstorm prediction and was distributed to NWS forecasters and USFS Predictive Services meteorologists across the US. More than 90 forecasters completed surveys, and the results are being utilized to help guide the research project and to help guide development of new lightning guidance that will better meet the needs of the user community. Consistent engagement with fire community stakeholders is ongoing.



a) *SREF Calibrated 3-hour 1 CG reliability diagram from 2013-2016; b) Perfect Prog 3-hour 1 CG reliability diagram from 2013-2016; c) SREF Calibrated 3-hour 100 CG reliability diagram from 2013-2016; d) Perfect Prog 3-hour 100 CG reliability diagram from 2013-2016.*

	SREF 1 CG	PPF 1 CG	SREF 100 CG	PPF 100 CG
Area Under the Curve (AUC)	0.908	0.849	0.901	0.646
Probability of Detection at 10%	0.684	0.401	0.165	0.036
Brier Score	0.030	0.034	0.0004	0.0003
Modified Brier Score (when a CG occurs)	0.695	0.780	0.888	0.946
Average Probability with a CG	17.911	14.211	5.854	3.261
Average Probability without a CG	2.917	1.837	1.247	0.225

Summary statistics for SREF Calibrated and Perfect Prog thunderstorm forecasts for 1 and 100 CG lightning flashes.

6. Social Science Collaboration

James Correia Jr. (CIMMS at SPC)

a. Collaboration on Applying Social Science within SPC

Organized and ran teleconferences with social scientists (Susan Jasko – California University of Pennsylvania, Kim Klockow – NOAA OWAQ, and Laura Myers – University of Alabama), SPC staff, and FEMA liaison Somer Erickson, to discuss issues of communicating to the various publics and partners, near real-time challenges of highlighting important events, and the creation, development, and use of new graphical content.

b. Continuing Work on May Tornadoes of 2013 and 2015

Our collaborative research, with units throughout OU (CASR, CAPS) and NWS (SPC and the Norman Forecast Office) continues to analyze sheltering behavior following our understanding of the response to the May 2013 tornadoes in central OK. We presented some of this work both internally and externally at the 2016 National Tornado Summit.

7. Mentoring

James Correia Jr. (CIMMS at SPC)

Hollings Scholar Jessica McDonald performed a research project on tornado forecasting using the NSSL Experimental Warn on forecast System for ensembles (NEWS-e). Jessie diagnosed local maxima in vertical vorticity and statistically explored how these profiles and the location of the vorticity maxima related to preliminary tornado reports from HWT 2016 real time experiments to help guide some of my grant work and future work geared towards helping forecasters distinguish from tornadic and non-tornadic supercells.

8. Other Activities

James Correia Jr. (CIMMS at SPC)

Developed and implemented visualizations of uncertainty for precipitation and snowfall for the Short Range Ensemble Forecast system, prototyped on the SPC website. Also, developed and applied visualizations of SPC report-based verification graphics for the SPC website for Day 1, and privately for Day 2-8. Additionally, used SPC outlook graphics to display the progression of outlooks and their verification to facilitate internal and community discussion of forecast value.

Publications

Gravelle, C. M., J. R. Mecikalski, W. E. Line, K. M. Bedka, R. A. Petersen, J. M. Sieglaff, G. T. Stano, and S. J. Goodman, 2016: Demonstration of a GOES-R satellite convective toolkit to “bridge the gap” between severe weather watches and warnings: An example from the 20 May 2013 Moore, Oklahoma, tornado outbreak. *Bulletin of the American Meteorological Society*, **97**, 69-84

Line, W. E., T. J. Schmit, D. T. Lindsey, and S. J. Goodman, 2016: Use of geostationary super rapid scan satellite imagery by the Storm Prediction Center. *Weather and Forecasting*, **31**, 483–494.

WDTD Project 12 – Warning Decision-Making Research and Training

NOAA Technical Leads: Ed Mahoney, Jami Boettcher, Brad Grant, James LaDue, Michael Magsig, and Robert Prentice, Greg Schoor, and Justin Gibbs (WDTD)

NOAA Strategic Goal 2 – Weather-Ready Nation – Society is Prepared for and Responds to Weather-Related Events

Funding Type: CIMMS Task II

Objectives

Increase expertise among NOAA/NWS personnel and their core partners on the integrated elements of the warning process. CIMMS scientists conduct applied research, develop and deliver training, and build applications to support the mission of meeting this goal. In doing so, we help NOAA/NWS warning forecasters and their core partners better serve the general public during warning operations and other hazardous weather events that require weather decision support services.

Accomplishments

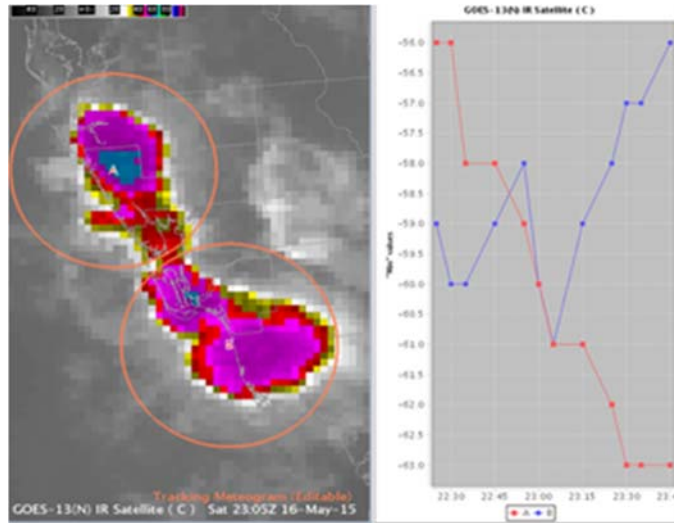
1. Advanced Weather Interactive Processing System - II (AWIPS-2) Training

Jill Hardy, Eric Jacobsen, Dale Morris, Stanislav Speransky, and Alex Zwink (CIMMS at WDTD)

By Summer 2015, National Weather Service (NWS) Weather Forecast Offices (WFOs) throughout the United States had been equipped with the AWIPS-2. This milestone led to CIMMS staff at WDTD shifting focus from AWIPS-2 transitional training to developing and updating training on feature enhancements to the system that were made during the last year. CIMMS staff at WDTD worked with NWS WDTD instructors to provide training in support of the AWIPS build update release schedule. Training released during this period covered new features, such as the Tracking Meteogram Tool, and updates to previously issued training, including the AWIPS-2 Fundamentals Course for newly hired NWS Meteorologist Interns. This latter training provides new NWS employees with a baseline understanding of the AWIPS-2 system that can be built upon when taking subsequent AWIPS training. The course uses a series of training videos, exercises, and job aids that incorporate the Weather Event Simulator - II (WES-2) Bridge to meet these training goals. Additionally, training was developed on soon to be released functionality with AWIPS Build 16.2.1 (and later builds). These lessons cover features such as the Damage Path Toolkit, Annual Recurrence Interval (ARI) displays, and Microburst Detection Algorithm and will be released in late Summer or Fall 2016.

CIMMS staff at WDTD continue to build on their high-level AWIPS-2 expertise in order to serve as focal points supporting the technical needs of the training mission of the WDTD. This expertise building includes routine baseline efforts to maintain WDTD's real-time AWIPS and development of comprehensive datasets to be used in case analysis and simulations for all WDTD training projects. CIMMS staff also operate in-house testbeds in which new software and products are tested against legacy tools. This year's internal product testing included new Multi-Radar/Multi-Sensor (MRMS) hydrology and severe weather applications, simulation capability development for the Warning Operations Course, and winter weather and river flood test cases within the WES-2 Bridge. Our AWIPS-2 testing and subsequent training development relies on close collaboration between the Radar Operations Center (ROC), National Severe Storms Laboratory (NSSL), the Hazardous Weather Testbed (HWT), the Global Systems Division (GSD), other NOAA partners, and the AWIPS contractor Raytheon.

This work is ongoing as there continues to be frequent updates to AWIPS-II. CIMMS will continue providing a vital contribution to the testing, familiarization, and training delivery of AWIPS-II features to both the NWS Office of the Chief Learning Officer (NWS/OCLO) and the entire NWS organization.



An image from the online training for AWIPS-2's Tracking Meteogram tool, published to forecasters by CIMMS staff at WDTD during FY16.

2. Geostationary Operational Environmental Satellites – R (GOES-R) Infusion into WDTD Training

Michael Bowlan, Dale Morris, and Alex Zwink (CIMMS at WDTD)

With the launch of the GOES-R rapidly approaching, NWS forecasters require training on all of the new data that they will see and can use soon in WFO operations. The Hazardous Weather Testbed (HWT) has been testing many GOES-R convective products and applications for the last few years. CIMMS staff have been preparing for the next step: Training all NWS forecasters on the GOES-R so they can incorporate those applications into their local forecasting and warning operations. A major component of this process will be the Satellite Foundational Course for GOES-R. This course will feature a series of online modules developed through a partnership of instructors from several agencies. These agencies include the Cooperative Institute for Meteorological Satellite Studies (CIMSS), the COMET Program, the Cooperative Institute for Research in the Atmosphere (CIRA), and the Short-term Prediction Research and Transition Center (SPoRT). CIMMS staff at WDTD have assisted with the planning and review of these online courses in the last year. They have also led the development of a Weather Event Simulator – II (WES-2) Bridge simulation that will support those lessons. This simulation will allow forecasters to apply lessons learned from the online courses in an Advanced Weather Interactive Processing System (AWIPS) – II environment when it is delivered in the next year.

The infusion of GOES-R products and data into WDTD courses will be another crucial component in the research to operations transfer process once the satellite is launched and becomes operational. As part of this training update initiative, CIMMS staff updated existing satellite training in the Warning Operations Course (WOC) Severe to be compatible with GOES-R at its launch. Although actual GOES-R imagery isn't available

yet, the WOC Severe lessons were updated with images from comparable satellites (and simulated GOES-R imagery from legacy satellites). These alternative images reflect some of the new science and research that has been developed with GOES-R in the last few years.

This work is ongoing. As the GOES-R becomes operational, training on these new datasets will need to be integrated across all warning-related hazard training at WDTD. CIMMS staff at WDTD will be at the forefront of this initiative.



This image shows a screen capture from one of the updated WOC Severe modules depicting estimating updraft intensity using cloud top cooling rates from satellite.

3. Experimental Warning Program & Hazardous Weather Testbed (HWT) Support

Alyssa Bates, Michael Bowlan (CIMMS at WDTD), Steve Martinaitis (CIMMS at NSSL), and Bill Line (CIMMS at SPC)

The 2016 Spring Experimental Warning Program (EWP2016) occurred from 18 April 2016 to 13 May 2016. This project tests and evaluates new applications, techniques, and products to support Weather Forecast Office (WFO) severe convective weather warning operations. Three primary projects were geared toward WFO applications in the Spring of 2016. These projects evaluated:

1. Multiple Geostationary Operational Environmental Satellites – R (GOES-R) convective products (including GOES-14 Super-Rapid Scan Test, or SRSOR, 1-minute imagery and pseudo-geostationary lightning mapper products),
2. The Joint Polar Satellite System (JPSS) NOAA-Unique CrIS/ATMS Processing System (NUCAPS) Soundings, and
3. Various Earth Networks lightning products.

Three NWS Forecasters and a broadcast meteorologist participated in the experiment one week at a time over the four week period. At the end of each week they delivered a webinar, entitled “Tales from the Testbed,” to NWS organizations and research institutions detailing their experiences. These webinars were facilitated by CIMMS staff at WDTD. CIMMS staff assisted the participants in developing and presenting a short and focused PowerPoint discussing what they learned throughout the week. Besides facilitating the webinar, CIMMS staff attended the daily weather briefings and stayed until the end of each day’s shift to help the participants with screen captures and write-ups for the webinar presentation.

In addition to facilitating these webinars for the Spring Experiment, CIMMS staff participated in two other experiments hosted at the Hazardous Weather Testbed during the past year. The first was the Hydrometeorological Testbed, which had their own experiment for three weeks in July 2015. Six different forecasters (all from WFOs and RFCs) participated each week on this experiment geared toward testing and evaluating numerous Multi-Radar/Multi-Sensor (MRMS) and Flooded Locations And Simulated Hydrographs Project (FLASH) products to support NWS WFO flash flood operations. CIMMS staff facilitated weekly webinars delivered by these forecasters and attended weather briefings throughout the experiment. The second experiment was the 2016 Hazard Services – Probabilistic Hazard Information (PHI) experiment. This experiment brought seven NWS forecasters to the HWT to test how PHI might integrate with the Hazard Services application currently under development for NWS warning operations.

CIMMS staff will continue to participate in experiments at the HWT as a facilitation expert in order to build expertise on these “research to operations” activities and identify future warning decision-making training needs for the NWS forecasters.

WDTD eLearning

Tales From the Testbed May 6, 2016 (17:29 / 22:36) Exit

JJ Wood
WFO Milwaukee/Sullivan, WI

Menu Notes

- 02 May 22:32 UTC
- 15. Parallax Correction Obscures Updraft 03 May 22:36 UTC
- 16. 1-minute Imagery & ProbSevere
- 17. ProbSevere 02 May
- 18. ProbSevere with Warning 02 May
- 19. Sparse Radar Coverage
- 20. 1-minute Vis Benefits 05 May
- 21. Legacy Atmospheric Profile (LAP) & NUCAPS
- 22. LAP Products 05 May 21 UTC
- 23. NUCAPS Profile 05 May 21 UTC
- 24. LAP Products 05 May 17 UTC
- 25. Modified Boise Sounding 05 May 12 UTC
- 26. Takeaways
- 27. Takeaways
- 28. Looking For More

Search...

LAP Products
05 May 17 UTC

PREV NEXT

This image shows a screen capture from one of the “Tales from the Testbed” webinars facilitated by CIMMS staff during the 2016 Spring Experiment (EWP 2016). The graphic in this image shows the GOES-R Legacy Atmospheric Profile products. These products show values of Convective Available Potential Energy (CAPE), Lifted Index (LI), and Precipitable Water derived from a blend of satellite and model data.

4. Multi-Radar/Multi-Sensor (MRMS) Training

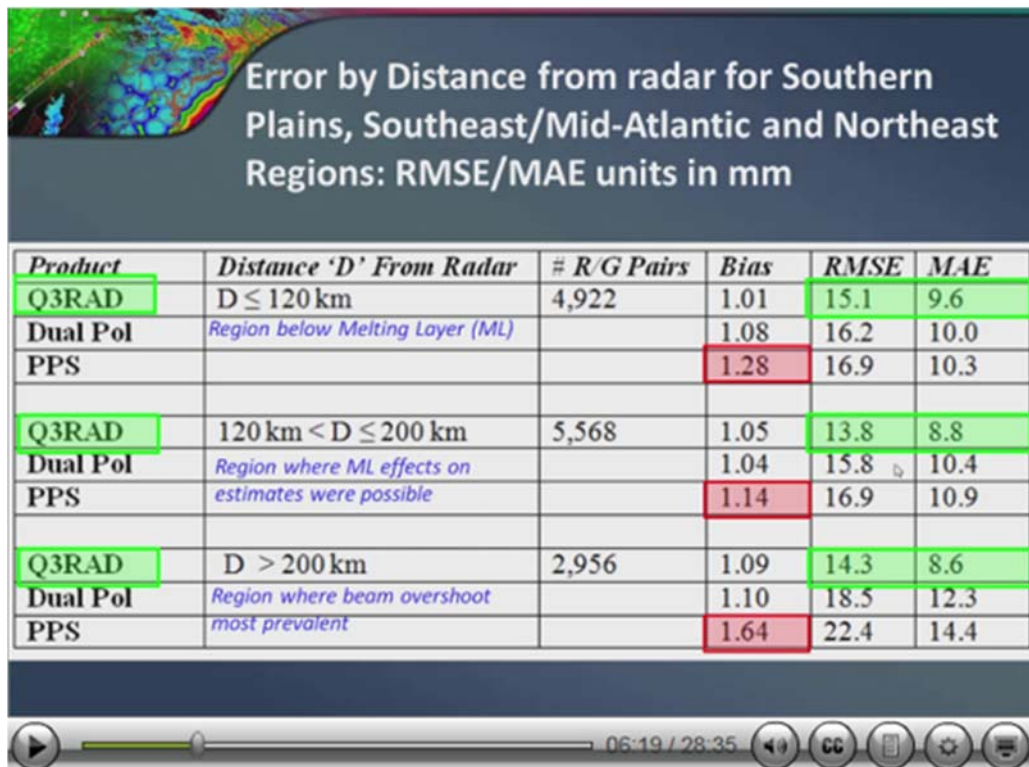
Alyssa Bates, Jill Hardy, Eric Jacobsen, Clark Payne, Chris Spannagle, Stanislav Speransky, Matt Taraldsen (CIMMS at WDTD), and Steve Martinaitis (CIMMS at NSSL)

The National Severe Storms Laboratory (NSSL) has been developing Multi-Radar/Multi-Sensor (MRMS) products over the past decade to overcome limitations inherent in single-sensor data products. Some MRMS products have been available to NWS forecasters in real-time on the Advanced Weather Interactive Processing System (AWIPS) since September 2015. CIMMS scientists have been heavily involved in testing these products in AWIPS and training for this operational deployment of the MRMS data on AWIPS across the National Weather Service (NWS).

CIMMS scientists and WDTD instructors developed the initial MRMS Products Course that was delivered in October 2014 after the web-based product deployment. Updates were made to that course for the beginning of the operational data delivery in AWIPS. In addition to the updated products course, a suite of applications-based lessons was

released to help NWS forecasters apply these products more fully into various warning operations using AWIPS. These applications lessons covered topics on the hydrology and severe weather MRMS products. Another round of new and updated products and applications lessons have been developed and are scheduled for release in late Summer 2016 as the MRMS product suite is updated.

CIMMS scientists have made significant contributions to MRMS training in other areas, as well. An in-depth reference guide provides detailed MRMS product descriptions in NWS Virtual Laboratory (VLab). This document is maintained and updated by CIMMS scientists at WDTD. Also, semi-monthly “MRMS Application of the Month” webinars are produced by WDTD with major contributions by CIMMS scientists. These half-hour webinars feature a NWS warning forecaster or NSSL research scientist showcasing a recent severe weather or hydrologic event. The presenter discusses how the various MRMS products were, or might have been, useful during the decision-making process of NWS warning operations. This work is ongoing as the MRMS product suite continues to be updated.



Slide shown is from one of the MRMS Application of the Month webinars. These webinars are hosted live, recorded and post-processed, and then made available on the WDTD web site for those who missed the live session. These sessions are just one of several ways that CIMMS scientists work collaboratively with WDTD instructors and other subject matter experts to train NWS forecasters on the MRMS products and their capabilities.

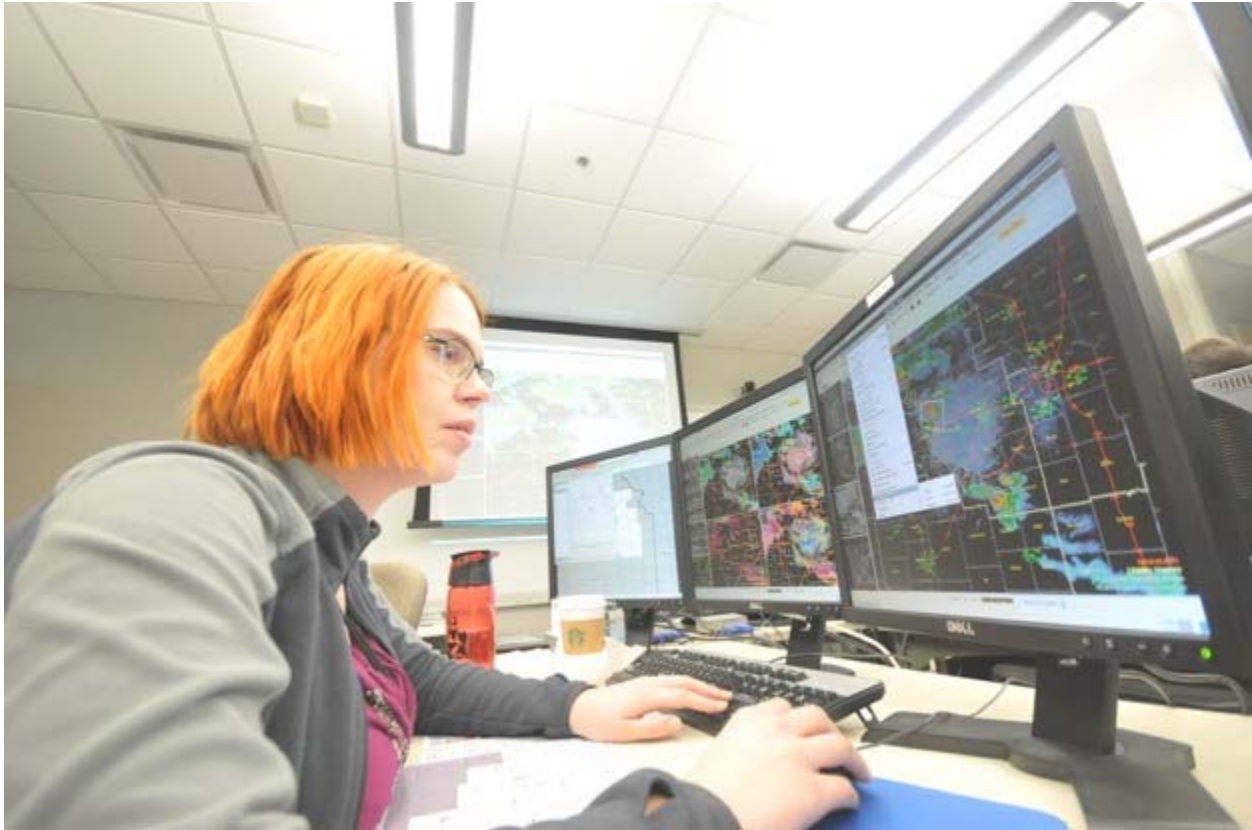
5. Radar & Applications Course (RAC)

Alyssa Bates, Michael Bowlan, Jill Hardy, Eric Jacobsen, Dale Morris, Esther Mullens, Clark Payne, Chris Spannagle, Stanislav Speransky, Matt Taraldsen, Philip Ware, Brett Williams, Andy Wood, and Alex Zwink (all CIMMS at WDTB)

The Radar & Applications Course (RAC) continues to be an area of active collaboration between CIMMS and the NWS Warning Decision Training Division. RAC teaches new NWS meteorologists a variety of topics regarding the WSR-88D and severe weather, including: radar theory, radar principles, radar data interpretation, storm interrogation techniques, and severe storm threat assessment and forecasting. The RAC is a critical piece in the development of new NWS forecasters for warning operations. The NWS requires all forecasters who may be responsible for issuing warnings in the future to complete the course. This course is taught via a combination of teletraining, web-based instruction, on-station training, and in-residence training.

CIMMS staff members are closely involved with the development of RAC. The collaborative work includes applied research on recent radar-related improvements such as MRMS and current WSR-88D capabilities to assess severe weather and flash flooding threats. As part of this training, CIMMS personnel work closely with radar engineers and software developers to determine how recent updates to different components of the WSR-88D and AWIPS impact the system as a whole. Because of the large size of this course (over 100 individual learning objects that take over 75 hours to complete), this partnership allows CIMMS staff and their WDTD collaborators to develop and update significant portions of RAC each year. The collaborative work with WDTD during these classes includes developing lecture materials, exercises, and simulations; delivering presentations, and providing expertise on warning-decision making issues to the class participants.

Another area where CIMMS staff members play a critical role with RAC is during the in-residence component of the course. During the past year, CIMMS staff upgraded WDTD's lab to Advanced Weather Interactive Processing System – II (AWIPS-2) displays using the Weather Event Simulator – II (WES-2) Bridge to play back previous weather events. This unique laboratory environment incorporates the WES-2 Bridge functions on a centralized server that controls up to 25 distributed users on a single event. The lab also features flexible configurability from single-user simulations to multi-user, collaborative simulations where groups of trainee forecasters act as a single WFO and share warning responsibilities. As part of this effort, CIMMS staff worked with WDTD instructors to develop to five full simulations, ten mini-scenarios, and two case exercises for use during the workshop portion of the RAC. Through use of this lab, RAC instructors incorporated many training environments, including workflows comparable to NWS operations, that allow them to meet the varied training needs of NWS employees in this course.



National Weather Service interns participate in one of multiple severe weather warning simulations during the Radar & Operations Course workshop held in Norman, OK.

6. Science and Operations Officers - Development and Operations Hydrologists (SOO-DOH) Facilitation Workshop/SOO Development Course

Michael Bowlan, Jill Hardy, Eric Jacobson, Dale Morris, Clark Payne, Thao Pham, Chris Spannagle, Stannislav Speransky, Philip Ware, Andy Wood, and Alex Zwink (CIMMS at WDTD)

National Weather Service (NWS) SOOs and DOHs serve an important role for WDTD distance learning. These individuals facilitate professional development for the staff in each NWS Warning Forecast Office (WFO) and River Forecast Center (RFC), throughout the U.S. Since 2011, the WDTD has provided facilitation training to the newly hired training officers in order to help them be more effective in that role. This training occurred as a three-and-a-half day “train the trainer” workshop, which is available to both new hires and, when spots are available, veteran facilitators who need refresher training. Starting in Summer 2016, this facilitation training will be combined with other SOO training, previously known as the COMET Mesoscale Analysis and Prediction course (COMAP), to be delivered at the National Weather Center. CIMMS scientists participated in the development and implementation of the final SOO-DOH Facilitation workshop as well as in the development of the inaugural SOO Development Course.

The training provided during these workshops supports the NWS training officers by improving their proficiency at coordinating, implementing, and managing local training programs and preparing them for new and upcoming science and operational technology. Participants should be able to facilitate learner-centered, performance-based training activities to help transform forecasters in their office in a way that improves performance and provided services. Topics taught during the SOO-DOH Facilitation Workshop focused on these topics, including how adults learn, using various forms of media in learning, and using the Commerce Learning Center and the Weather Event Simulator – II (WES-2) Bridge in their local training programs. The new SOO Development Course is three weeks long and covers both the previous facilitation topics as well as several scientific, technical, and human factors topics related to NWS operations. Some of these expanded topics include: infusing numerical weather prediction and remote sensing improvements into operations, transition to impact-based concept of operations, research to operations, leadership and management. CIMMS scientists serve as presenters in multiple sessions during these workshops (including sessions on gamification and root cause analysis), as well as technical advisors on WES-2 Bridge and other simulations and exercises.

This work is ongoing as the NWS continues to hire new SOOs to meet their local office training and research needs.



CIMMS staff and WDTD instructors work with SOO-DOH Facilitation Workshop participants on using the Weather Event Simulator – II (WES-2) Bridge software to conduct simulation training in their local offices.

7. Warning Operations Course (WOC) – Flash Flood, Core, and Severe Tracks

Alyssa Bates, Jill Hardy, Eric Jacobsen, Dale Morris, Esther Mullens, Thao Pham, Chris Spannagle, Matt Taraldsen, Philip Ware, Brett Williams, Andy Wood, and Alex Zwink, (CIMMS at WDTD)

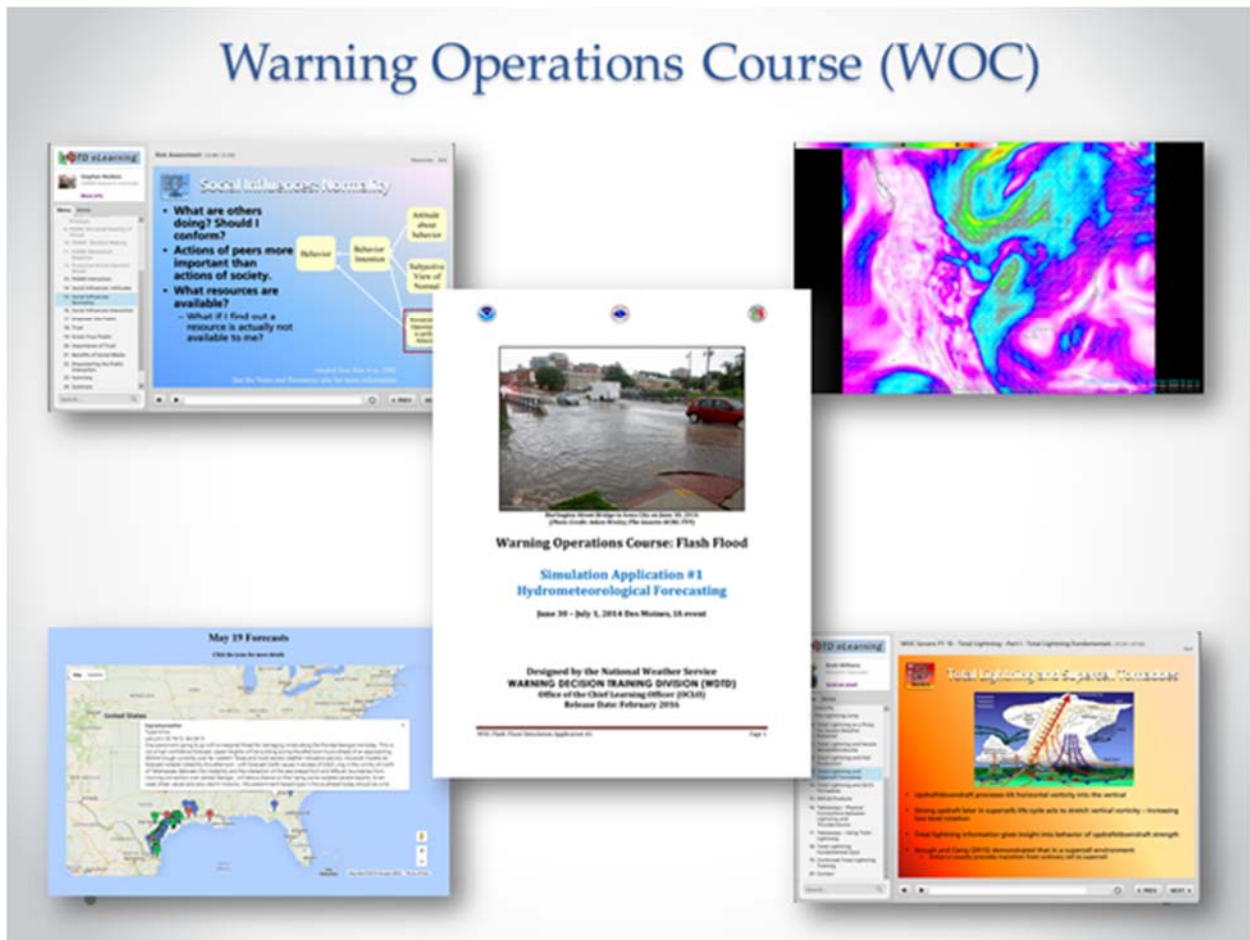
The Warning Operations Course (WOC) is a blended learning course designed to provide training on advanced warning decision-making techniques to every NWS forecaster with warning responsibility (Meteorologists and Hydrologists). CIMMS scientists have been heavily integrated into the development, delivery, and support of WDTD's WOC throughout the years. This year, WDTD offered three WOC tracks for forecasters to complete: Flash Flood, Core, and Severe.

In collaboration with WDTD instructors, CIMMS scientists made numerous changes to all three WOC tracks. These course changes include the following items:

1. WOC Flash Flood: CIMMS staff managed the delivery of the FY16 Flash Flood track. Updates for this year's course included two new lessons on the decision-making process and warning fundamentals related to Flash Flood Warnings, as well as creating two new WES-2 Bridge simulation applications and accompanying documentation. Additionally, CIMMS staff coordinated informational webinars with the Weather Prediction Center (WPC) by: reviewing webinar material, scheduling sessions, delivering announcements, hosting the webinars, and post-processing the recordings for release online. Lastly, CIMMS staff collaborated with WDTD instructors to provide NWS management with monthly reports on forecaster progress through training required of all NWS forecasters related to hydrology operations in NWS WFOs.
2. WOC Core: CIMMS personnel worked with WDTD instructors on the final delivery of the FY15 and the development and initial delivery of the FY16 course. Four of the lessons in this track were authored (and are maintained) by CIMMS personnel.
3. WOC Severe: CIMMS staff developed new lessons on total lightning, as well as managed new instructor-led training webinars, and developed a WES-2 Bridge simulation to apply what was learned in the course. Additionally, CIMMS staff created scripts, updated webpages, and managed the Severe Forecast Challenge, an applied learning exercise where forecasters apply concepts learned from the WOC Severe track in a forecasting environment. This past year, the forecast challenge included 175 NWS forecasters who issued over 4900 individual forecasts.

CIMMS scientists also contribute logistical support for all three WOC courses and their management. This support includes responding to questions from NWS forecasters, assisting local facilitators, providing certificates of completions to students, and producing statistical progress reports of students and forecast offices using the Commerce Learning Center. Lastly, CIMMS staff are actively involved in the delivery of WDTD's Storm of the Month webinars which chronicle weather event stories from the

Field. CIMMS scientists provide feedback to presenters prior to the webinars, record and run phone lines during the webinars, and then post-process and publish the webinars online. This work is ongoing.



Example visuals from each WOC track: (upper left) WOC Core lesson discusses how to handle risk assessment in operations, (lower left) WOC Severe Forecast Challenge webpage with submitted forecasts, (lower right) WOC Severe lesson discusses using total lightning data to diagnose updraft strength in supercells, (upper right) Screen capture of AWIPS data used in the WOC Flash Flood WES-2 Bridge simulation, and (middle) WOC Flash Flood WES-2 Bridge simulation application guide.

8. Weather Event Simulator (WES) - I

Alex Zwink (CIMMS at WDTD)

Although it's been fifteen years since its initial release, the CIMMS-developed Weather Event Simulator remains an important tool used in NWS forecast offices to apply training knowledge. Almost every NWS forecast office has transitioned to Advanced Weather Interactive Processing System – II (AWIPS-2). Due to this transition and the initial implementation Weather Event Simulator - 2 Bridge (WES-2 Bridge) deployment,

new WES-1 development has ceased. However, the WES-1 software (and associated hardware) needs to be maintained so offices can review archived AWIPS-1 case data. WES-1 workstation parts fail occasionally due to hardware age, too. To meet the needs of NWS forecasters, CIMMS staff provided extensive support for installation and troubleshooting of WES-1 software, hardware replacement, and case data in this transition period to the WES-2 Bridge.

This work is ongoing as NWS Weather Forecast Offices continue to rely on their WES-1 systems to review these older cases. CIMMS staff are working on a tool to convert these old cases from the WES-1 to the WES-2 Bridge format. Once that tool has been developed, then support for the WES-1 systems will cease.

9. Weather Event Simulator – II (WES-2) Bridge

Dale Morris, Alex Zwink, Thao Pham, Ali Virani, Philip Ware, Jill Hardy, Eric Jacobsen, and Chris Spannagle (CIMMS at WDTD)

CIMMS staff at WDTD have developed a training simulator compatible with the Advanced Weather Interactive Processing System – II (AWIPS-2) called the WES-2 Bridge. This simulator preserves the existing simulation functionality from the WES-1 (for use with AWIPS-1) and to support the NWS Directive 20-101 requirement for every forecaster to complete two simulations prior to each significant weather season. The WES-2 Bridge fills multiple objectives besides just being a training simulator. The WES system is the primary method staff at a local Weather Forecast Office (WFO) use to view and analyze any archived weather data from AWIPS, including supporting local research projects. The simulator software also features a streamlined method of presenting non-AWIPS information (spotter reports, video, briefings, web-based presentations, etc.) during a simulation (formerly called WESSL – the WES Scripting Language). Exploiting messaging and geospatial capabilities of the AWIPS-2 infrastructure, the updated WESSL scripting capability provides a method to engage forecasters with feedback as they complete simulations. Because of these capabilities, WES-2 Bridge is tightly integrated with many WDTD deliverables, including the Radar and Applications Course (RAC) and the Warning Operations Course (Severe and Flash Flood Tracks).

Besides developing similar capabilities as were found in WES-1, CIMMS staff developed new simulation capabilities in WES-2 Bridge that were unavailable previously. For example, simulations can now perform simulations with the AWIPS Hydrological Applications and its WFO Hydrologic Forecast System (WHFS) database (also known as the Integrated Hydrologic Forecast System, or IHFS). Also, forecasters can now use a skip feature, allowing for interval-based simulations that move sequentially through a long-duration (multi-day) event. The combination of these new features permits forecasters to train on hydrologic duties by interrogating and analyzing stream gauge observations and forecasts in a single simulation. This capability was developed in direct response to several NWS Service Assessments that mentioned that forecasters needed better tools to prepare them to use these hydrological tools for river

flooding events. In addition, several CIMMS staff collaborated with Federal WDTD instructors to develop and deliver a formal simulation to all forecast offices that demonstrated this new hydrologic simulation capability. This simulation, as well as a separate winter weather exercise, served as a test case for this new capability and provided guidance on how local offices could develop similar simulations of their own.

The “Bridge” terminology is another new component of the WES. This new system serves as a bridge (or prototype) to incorporate training functionality into the “baseline” AWIPS-2 system in the future. To support this initiative and ensure compatibility between AWIPS-2 and WES-2 Bridge, CIMMS personnel at WDTD serve as subject matter experts for the NWS AWIPS Program and for the AWIPS contractor Raytheon. The WES-2 Bridge technology represents significant engineering development because WES-2 Bridge has many requirements above and beyond the AWIPS-2 system that it operates alongside. These requirements include simultaneous availability of multiple archived data cases from multiple locations. WES-2 Bridge incorporates both DRT simulations (time-sequenced revelation of data) and case-reviews (data is displayed based on time set by the user) based on data that is locally archived at a WFO. It also supports data reprocessing to ensure compatibility with future AWIPS versions.

The WES-2 Bridge System Beta Test of the WES-2 Bridge system (hardware and software) occurred at NWS regional headquarters and four Weather Forecast Offices (WFOs) in the Summer and Fall of 2015, followed by a full-scale deployment across NWS field offices. CIMMS staff supported forecasters in the installation and initial use of the system through prepared installation instructions, training resources, reference guides, and other on-line resources. Additionally, CIMMS staff briefed the development and installation progress to NWS regional and national headquarters management throughout the process, as well as providing support during numerous help requests from local offices. This work is ongoing as CIMMS staff continue developing the simulator for more AWIPS-2 upgrades become available and to support the functionality of new and emerging datasets.

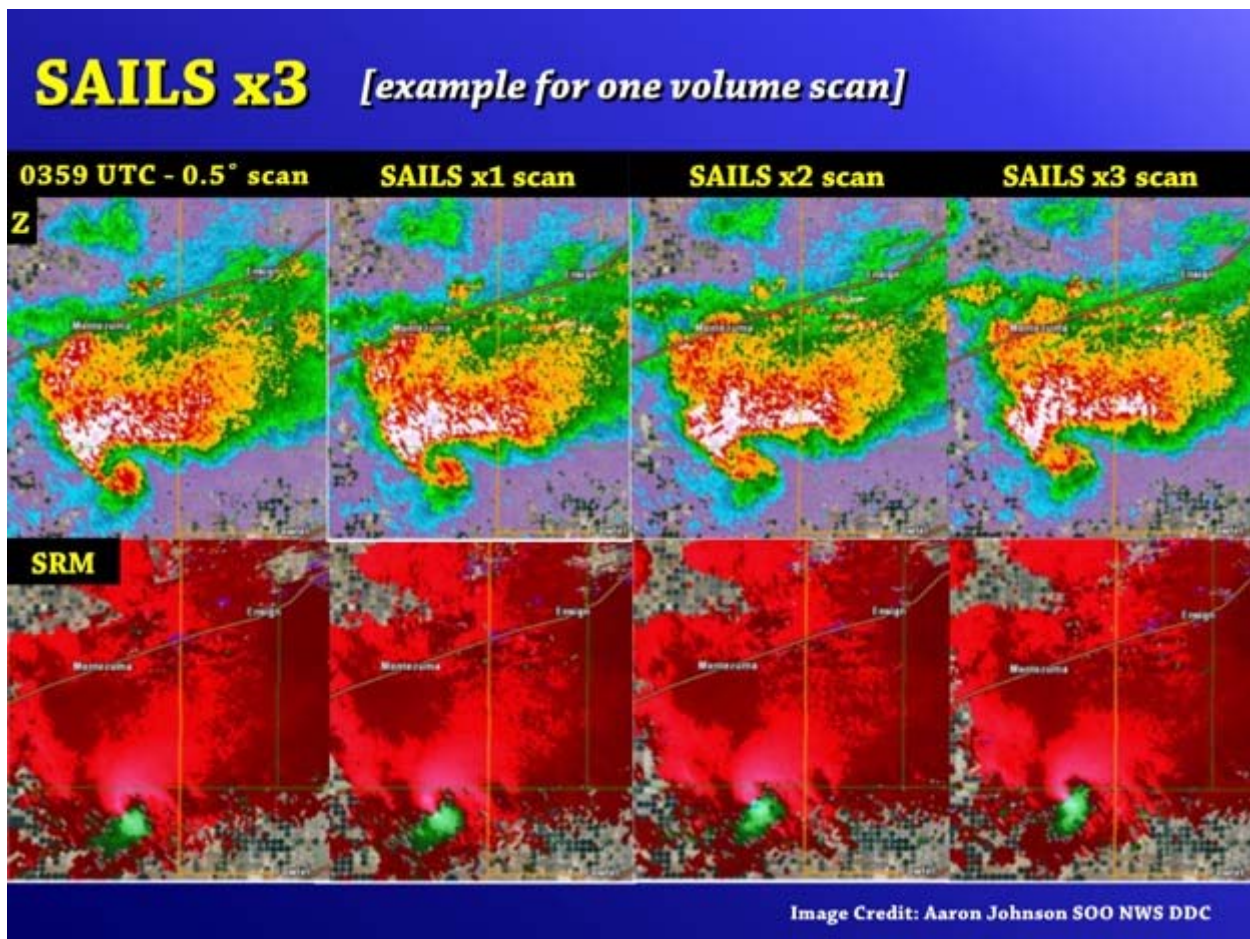


Photo shows NWS forecasters using the WES-2 Bridge for a displaced real-time simulation during a recent Radar & Applications Course (RAC) workshop. Prior to coming to this workshop, the participants used the WES-2 Bridge in their local office to learn basic functionality of the system, best practices for various tools related to warning operations, and applications of severe weather science using AWIPS-2.

10. WSR-88D Build Improvement Training

Matt Taraldsen and Andy Wood (CIMMS at WDTD)

During the past year, there was one upgrade made to the WSR-88D Radar Data Acquisition Unit (RDA) and Radar Product Generator (RPG) software. This software upgrade (Build 16.1) contained two significant updates: generation of the Raw Correlation Coefficient product and the Multiple Elevation Scan Option (MESO) Supplemental Adaptive Intra-Volume Low-Level Scan (SAILS). A second software upgrade (Build 17.0) was in Beta Test at the writing of this report. CIMMS personnel have worked closely with WDTD instructors and partners at the Radar Operations Center (ROC) during training development for NWS staff (which is also available for NWS partners). This work included supporting the software upgrade training, assisting NWS partners with training on dual-polarization radar, and collaborating with experts on guidance for optimizing Routine Product Set lists at NWS weather forecast offices (WFOs). This work is ongoing as the WSR-88D continues to receive periodic software and hardware upgrades.



This example shows a slide from the on-line training developed by WDTD for WSR-88D Build 16.1. This slide shows an example of how MESO-SAILS increases the number of low-level tilts available to forecasters when run in “SAILS x3” mode.

Publications

- Hardy, J., J.J. Gourley, P.E. Kirstetter, Y. Hong, F. Kong, and Z.L. Flamig, 2016: A method for probabilistic flash flood forecasting. *Journal of Hydrology*, In Press.
- Schroeder, A. J., J. J. Gourley, J. Hardy, J. J. Henderson, P. Parhi, V. Rahmani, K. A. Reed, R. S. Schumacher, B. K. Smith, and M. J. Taraldsen, 2016: The development of a flash flood severity index. *Journal of Hydrology*, In Press.
- National Severe Storms Laboratory, 2016: Flooded Locations and Simulated Hydrographs Project (FLASH). Available at: <http://blog.nssl.noaa.gov/flash/hwt-hydro/>
- National Severe Storms Laboratory, 2016: NOAA Hazardous Weather Testbed Spring Experiment – 2016 Tales from the Testbed. Available at: <http://hwt.nssl.noaa.gov/ewp/>
- Warning Decision Training Division, 2016: Radar & Applications Course (RAC). Available at: <http://www.wdtd.noaa.gov/courses/rac/>
- Warning Decision Training Division, 2016: Multi-Radar/Multi-Sensor (MRMS) Training. Available at: <http://www.wdtd.noaa.gov/courses/MRMS/>
- Warning Decision Training Division, 2016: Warning Operations Course (WOC). Available at: <http://www.wdtd.noaa.gov/courses/woc/>
- Warning Decision Training Division, 2016: Weather Event Simulator (WES). Available at: <http://www.wdtd.noaa.gov/tools/wes/>

Warning Decision Training Division, 2016: Weather Event Simulator II (WES-II) Bridge. Available at: <http://www.wdtd.noaa.gov/tools/wes2/>

Warning Decision Training Division, 2016: WSR-88D Build Training. Available at: <http://www.wdtd.noaa.gov/buildTraining/RPG-RDA.php>

U. S. Department of Commerce, 2016: Commerce Learning Center (CLC). Available at: <http://doc.csod.com/>

OST Project 13 – Research on Integration and Use of Multi-Sensor Information for Severe Weather Warning Operations

NOAA Technical Lead: Stephan Smith (NWS OST MDL DAB)

NOAA Strategic Goal 2 – *Weather-Ready Nation – Society is Prepared for and Responds to Weather-Related Events*

Funding Type: CIMMS Task II

Objectives

Develop multiple-radar/multiple-sensor (MRMS) severe weather warning applications and advanced display systems and transferring that technology to NWS operational systems; collaborate with the NOAA Hazardous Weather Testbed Experimental Warning Program (EWP) at the National Weather Center in Norman.

Accomplishments

1. General Overview

Greg Stumpf (CIMMS at NWS/OST/MDL/DAB)

The 12th full year of the CIMMS/NWS-Meteorological Development Laboratory (MDL) scientist position was completed during this review period. During this year, the scientist was a co-principal investigator on an independent experiment for the Experimental Warning Program's (EWP) spring experiments in the NOAA Hazardous Weather Testbed (HWT) (described in Accomplishment #2). The EWP is a proving ground for evaluating new applications, technology, and services designed to improve NWS short-fused (0-2 hour) hazardous convective weather warning decisions. The CIMMS/MDL scientist remained the liaison between the HWT and NWS-MDL. He continues to collaborate with National Severe Storms Laboratory (NSSL) scientists who are involved in the EWP, including attending scientific and technical meetings and retreats, and is the coordinator of a weekly brown-bag lunch devoted toward EWP-related topics. At these brown bag lunches, there are local and remote guest speakers, software demonstrations, and general discussions on recent severe weather episodes.

The CIMMS/MDL scientist continues to be involved with the severe weather warning R&D activities at CIMMS and NSSL and served as a co-principal investigator and subject matter expert for the multiple-radar / multiple-sensor (MRMS) severe weather warning products. The process to transfer MRMS technology to operations at the

National Center for Environmental Prediction was completed in FY15, and the CIMMS/MDL scientist has been involved in the following activities related to the MRMS tech transfer, 1) development manager for creating the capability to display operational MRMS products in the National Weather Service AWIPS2 system, and, 2) supporting the collaborative MRMS “community” on the NOAA Virtual Laboratory (VLab).

2. Probabilistic Hazard Information (PHI)

Greg Stumpf (CIMMS at NWS/OST/MDL/DAB), and Chris Karstens and Brandon Smith (CIMMS at NSSL)

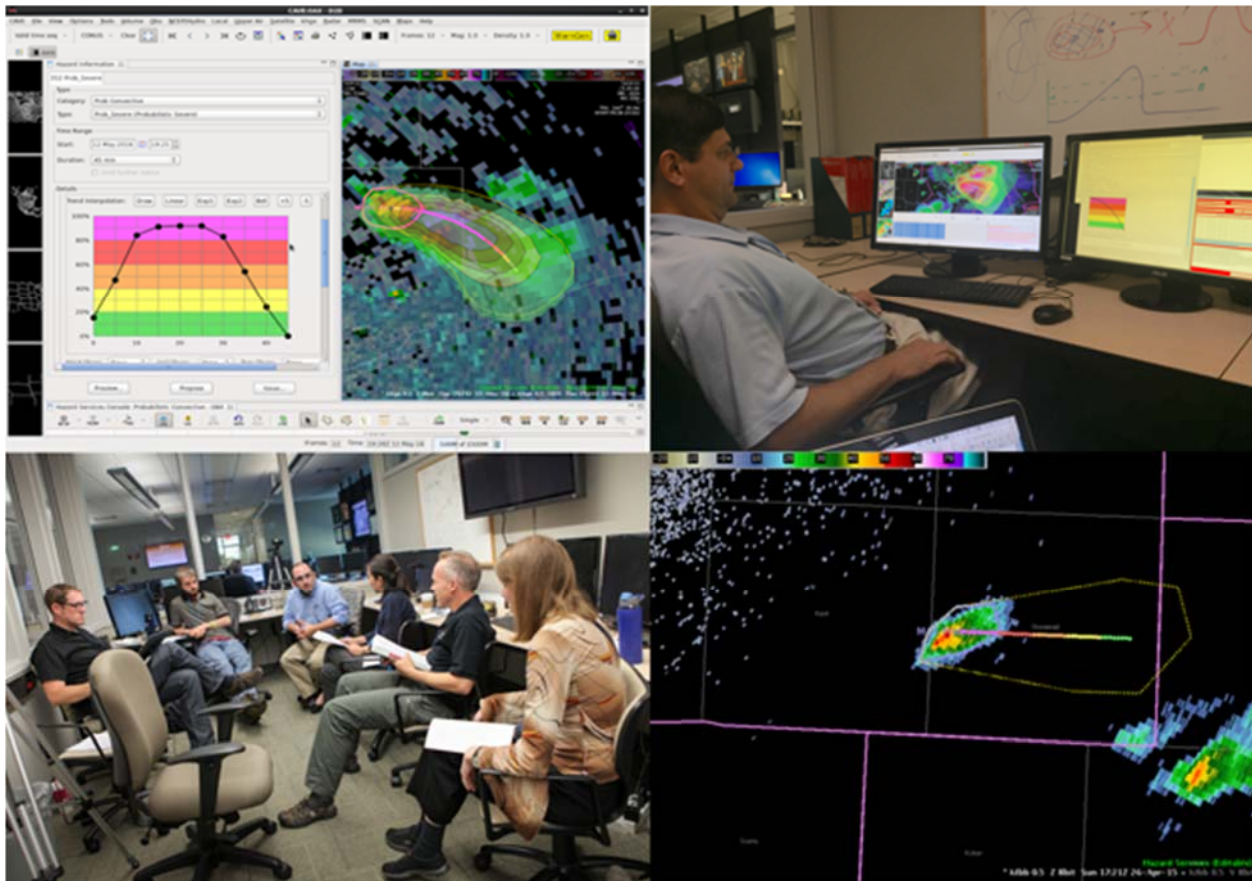
The activities reported in this section are related to a USWRP R2O grant that was awarded to several agencies to fund initial research and development activities for the Forecasting A Continuum of Environmental Threats (FACETs) initiative to change the severe weather forecast and warning paradigm for the NWS. The CIMMS/MDL scientist is involved in two of the subprojects on this grant.

The CIMMS/MDL scientist is co-team leader, along with a NOAA/ESRL/Global Systems Division (GSD) software engineer, to transfer the technology of the NSSL-developed Probabilistic Hazard Information (PHI) Prototype tool. The PHI-Prototype has been under development since 2013 and has been tested in the NOAA HWT during the springs of 2014, 2015, and 2016. Feedback on the software design, operational use, and human factors workload, was used to improve the prototype each year. MRMS products were available within the PHI tool to aid in the forecaster decision making process. Beginning after the 2015 experiment, GSD software developers and meteorologists began implementing the PHI Tool concepts into AWIPS2 Hazard Services, a new application platform from which all NWS watches, warnings, and advisories will be issued in the new future. The CIMMS/MDL scientist led a 3-week NOAA HWT experiment conducted in the spring of 2016 with visiting NWS forecasters to test this new Hazard Services – PHI (HS-PHI) application. This included helping guide the GSD software development, selection of archive case scenarios designed to train forecasters on the HS-PHI software and PHI concepts, and test various operational decision making situations including inter-office collaboration. Warning Decision Training Division scientists also collaborated on the experiment, in order to start the process of developing best operational practices. The first figure below shows a screen capture of the HS-PHI application, as well as forecasters and researchers working together in the experiment.

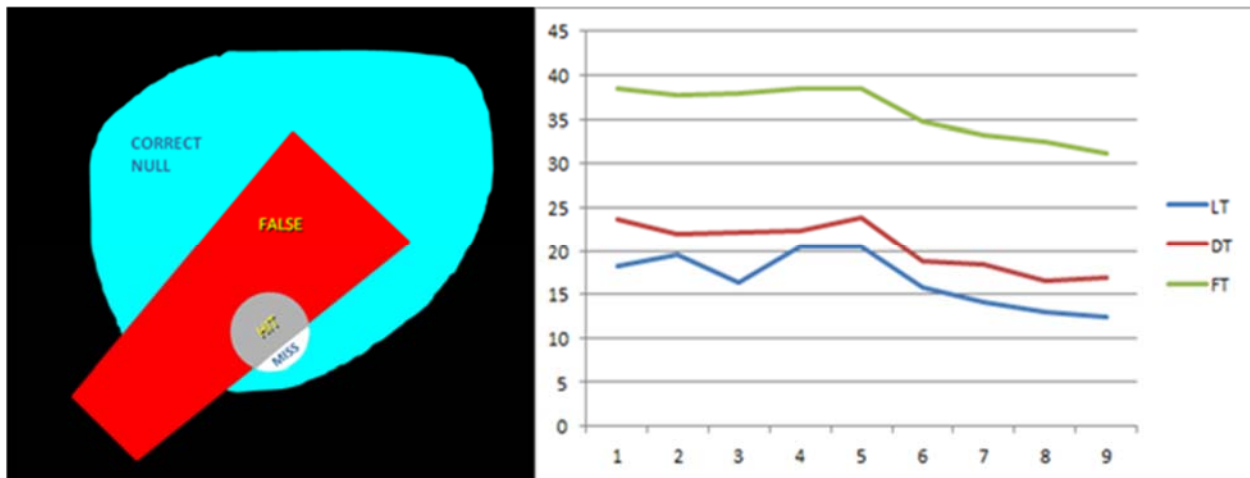
The CIMMS/MDL scientist is co-investigator, along with scientists at NOAA/ESRL/GSD, to develop a real-time verification system for the PHI Tool, which will use 1) a new way to blend, in real-time, remotely-sensed data from the MRMS system with live storm reports, and 2) innovative warning verification techniques that have been under development for several years, which include new measures such as False Alarm Area and False Alarm Time in verified warnings as well as location-specific lead- and departure-time. A gridded verification system for tornado warnings was completed. The system scores tornado warnings against ground observations of tornadoes on a 1

km² x 1 min grid (left panel of second figure below), and calculates grid-based Probability of Detection, False Alarm Ratio, Lead Time, and new metrics False Alarm Area, False Alarm Time, and Departure Time. The system has been run on the entire storm-based Tornado Warning and Local Storm Report database from October 2007 – December 2015. Statistics broken down by year, month, and hour of the day have been computed. Initial results show that Lead Time, Departure Time, and False Alarm Time have been steadily decreasing over this period (right panel of second figure below).

The CIMMS/MDL scientist serves as the lead reporter on the various aspects of the PHI project at MDL quarterly status briefings.



Images from the Hazard Services – Probabilistic Hazard Information (HS-PHI) 2016 spring experiment in the NOAA Hazardous Weather Testbed. Clockwise from top-left: a) screen capture of the HS-PHI application, showing a probabilistic severe weather “plume”, the forecasted probability trend, and other software controls, b) visiting NWS forecaster issuing PHI using the software, c) one of many group discussions between forecasters, developers, human factors experts, and trainers, and d) image of a downstream plume on an incipient severe thunderstorm.



Left: Schematic showing how the gridded verification scheme divides warning areas, storm observation areas (tornado, wind, or hail), storm areas (reflectivity), overlap areas, and areas outside of all. Misses (white) are where there are observation grid points and no warning grid points. False Alarms (red) are where there are warning grid points but no observation grid points. Hits (grey) are where there is a union of observation and warning grid points. Correct Nulls (cyan) are where there are no observation and no grid points, but there is storm reflectivity. All other points (black) are not scored. Right: Trend of Lead Time (LT), Departure Time (DT), and False Alarm Time (FT) over the 9 years of the study (1=2007, ..., 9=2015).

3. MRMS Product Display for AWIPS2

Greg Stumpf (CIMMS at NWS/OST/MDL/DAB) and Darrel Kingfield (CIMMS at NSSL)

The operational MRMS system at NCEP went online and began disseminating data to the weather enterprise, including the National Weather Service, on 1 October 2014. The CIMMS/MDL scientist is the development manager overseeing an NSSL employee doing the software coding. One new version of source code was delivered to AWIPS2 during FY16, which included display of new products provided by MRMS version 11. This was delivered for AWIPS2 Build 16.2.2 (deployed to the field by September 2016). In the role of the MRMS display development manager for AWIPS2, the CIMMS/MDL scientist continues to work with with NCEP implementation teams to monitor MRMS data transmission latency.

4. MRMS in the NOAA Virtual Laboratory (VLab)

Greg Stumpf (CIMMS at NWS/OST/MDL/DAB)

The CIMMS/MDL scientist is the site owner of the MRMS community in the NOAA Virtual Laboratory (VLab). He developed the design and layout of the collaboration community and manages the development community. The scientist coordinated the development of an MRMS product Wiki in the VLab, designed as a basis for official NWS/WDTB training documentation. In addition, the CIMMS/MDL scientist serves on

the VLab Support Team, to help design, develop, and implement the NWS VLab as a whole. The CIMMS/MDL scientist leads the bi-monthly NOAA VLab Community and Project Owners' Meetings.

Publications

- Jiang, H., S. Albers, I. Jankov, D. Birkenheuer, Z. Toth, Y. Xie, G. Stumpf, D. Kingfield, B. Motta, M. Scotten, and J. Picca, 2015: Real-time applications of the variational version of the Local Analysis and Predication System (vLAPS). *Bulletin of the American Meteorological Society*, **96**, 2045-2057.
- Karstens, C. D., G. Stumpf, C. Ling, L. Hua, D. Kingfield, T. M. Smith, J. Correia, Jr., K. Calhoun, K. Ortega, C. Melick, and L. P. Rothfusz, 2015: Evaluation of a probabilistic forecasting methodology for severe convective weather in the 2014 Hazardous Weather Testbed. *Weather and Forecasting*, **30**, 1551-1570.

NWSTC Project 14 – Forecast Systems Optimization and Decision Support Services Research Simulation and Training

NOAA Technical Leads: Jeff Zeltwanger (OCLO) and Kim Runk (NWS Operations Proving Ground - OPG)

NOAA Strategic Goal 2 – Weather-Ready Nation – Society is Prepared for and Responds to Weather-Related Events

Funding Type: CIMMS Task II

Objectives

1. Forecast Systems Optimization

Sub-Objective 1: Provide end-user training for meteorologists and hydrologists using Advanced Weather Interactive Processing System (AWIPS) in the NWS. This includes updating previously created training to more useful and functional products.

Sub-Objective 2: Support and maintain end-user training for meteorologists and hydrologists using the Community Hydrologic Prediction System (CHPS) in the NWS. This includes updating previously created training to more useful and functional products.

Sub-Objective 3: Create and deliver training for Broadcast Message Handler (BMH) for both the Operational Testing and Evaluation (OT&E) period, and for deployment. This sub-objective is a result of the Hurricane Sandy Assessment objective, "Improve availability and accessibility of NWS data and information for NOAA Weather Radio."

Sub-Objective 4: Create and deliver a course to aid those NWS employees that report data errors using the National Centers for Environmental Information (NCEI) Datzilla ticketing system.

Sub-Objective 5: Support Hazard Services instructors and technical leads as they strive to reduce AWIPS II warning tools, by creating a tool that provides all warning services. Supporting this effort includes staying up-to-date on progress and providing ideas for future training.

2. NWS Proving Ground Operational Service Delivery Simulations

Sub-Objective 1: Evaluate AWIPS performance and gather NWS forecaster feedback from using multiple spectral bands and derived combination imagery, or “Red-Green-Blue” (RGB) imagery, available on the Japanese Meteorological Agency’s Himawari-8 satellite as a proxy for the Geostationary Operational Environmental Satellite R-Series (GOES-R). Fifteen of the 16 spectral bands on Himawari-8 are identical to the spectral bands GOES-R will have.

Sub-Objective 2: Collaborate with the Aviation Weather Testbed (AWT) on a project to assess Digital Aviation Services, specifically to evaluate whether there is an optimal methodology for generating gridded forecast elements using AWIPS’s Graphical Forecast Editor (GFE) that can serve as a foundation for the creation of WFO products for aviation partners. This was stage one of a two stage evaluation.

3. Impact Based Decision Support Services Research and Development

Sub-Objective 1: Prepare all operational NWS employees for providing decision support services from their offices. To accomplish this goal, operational employees need online training. This is the main goal behind the Impact-Based Decision Support Services Professional Development Series.

Sub-Objective 2: Prepare NWS employees for deployment in the field, and train them to communicate weather information to the public and partners effectively. Accomplishing this is the main goal of the Impact-Based Decision Support (IDSS) Deployment Boot Camp residence course.

Sub-Objective 3: Transform the IDSS residence course into a traveling version, and teach concepts to any national center or regional office that requests it.

Sub-Objective 4: Conduct or assist with training sessions outside of IDSS Deployment Boot Camp that continues learning in communication best practices. This may include guest speaking in other residence courses in Kansas City, or consulting with offices or individuals as requested.

Sub-Objective 5: To support Weather-Ready Nation goals, conduct training on impact-based decision support services as applicable specifically to hurricane messaging. This is the primary function of the Effective Hurricane Messaging Course hosted in Miami, Florida.

4. Advanced Training Development

Sub-Objective 1: Develop expertise in useful technology, best practices, and methodologies in effort to produce better training and share information. This might include attending professional development training and conferences, and pushing the boundaries of instructional design, training, and technology.

Sub-Objective 2: Help OCLO and OPG employees grow and learn new tools for training and collaboration.

Sub-Objective 3: Reach out to others in the agency through various methods, and spread information about available training, professional development, and the roles NWS “staff play” in a Weather Ready Nation.

Sub-Objective 4: Use expertise to join and help OCLO and OPG focal point teams.

Sub-Objective 5: Help develop and maintain an OCLO Intern Program to aid in training development while providing outreach services to the community.

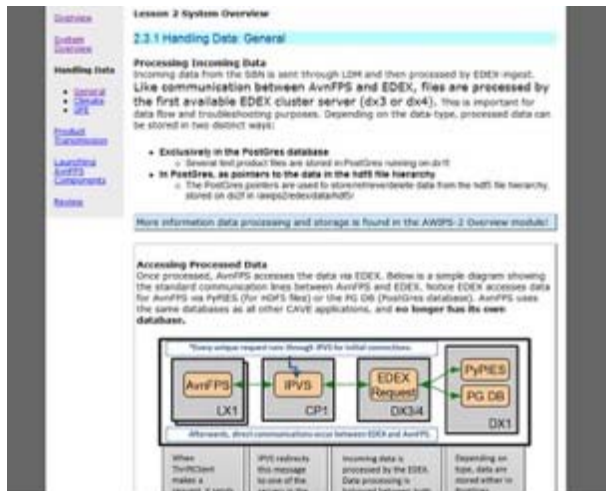
Accomplishments

1. Forecast Systems Optimization

a. Sub-Project 1: Advanced Weather Interactive Processing System (AWIPS II) and Graphical Forecast Editor (GFE) Distance Learning

Sarah Grana (CIMMS at NWSTC), Jeffrey Zeltwanger and Hattie Wiley (OCLO), and Bill Gery (NWS Central Region HQ)

Distance learning modules for AWIPS II applications and GFE have aged. Over the past year, Sarah Grana updated the GFE Focal Point courses (four total), Collaboration Tool Training, and Data Delivery Training. This included updating the HTML contents to HTML5 format, removing and replacing Adobe Flash-based interactions, converting Adobe Captivate presentation to Articulate Engage interactions, updating quizzes, reworking Camtasia video productions, and collaborating with subject-matter experts on updating content.



Before



After

A sample AWIPS course (left) in the old format and the AvnFPS AWIPS course (right) in the new format.

b. Sub-Project 2: Community Hydrologic Prediction System (CHPS) Distance Learning

Sarah Grana (CIMMS at NWSTC), Doug Streu and Hattie Wiley (OCLO), and Teresa Murphy (NWS HQ)

A carry-over from last reporting period, Sarah Grana continued updating CHPS distance learning modules. This included updating five additional courses. Course changes included updating the HTML contents to HTML5 format, removing and replacing Adobe Flash-based interactions, converting Adobe Captivate presentation to Articulate Engage interactions, updating quizzes, and reworking Camtasia video productions.

c. Sub-Project 3: Broadcast Message Handler (BMH) Training

Sarah Grana, Megan Taylor, and Denise Balukas (CIMMS at NWSTC), Teresa Murphy (NWS HQ), and Doug Streu, Jeffrey Zeltwanger, Jim Poole, Hattie Wiley, and Jerry Griffin (OCLO), Greg Noonan (NWS Central Region HQ), and Teresa Murphy, Steve Schotz, Joel Nathan, Jim Buchman, Joe Fiore, Bert Viloria, and Sanford Garrard (NWS HQ)

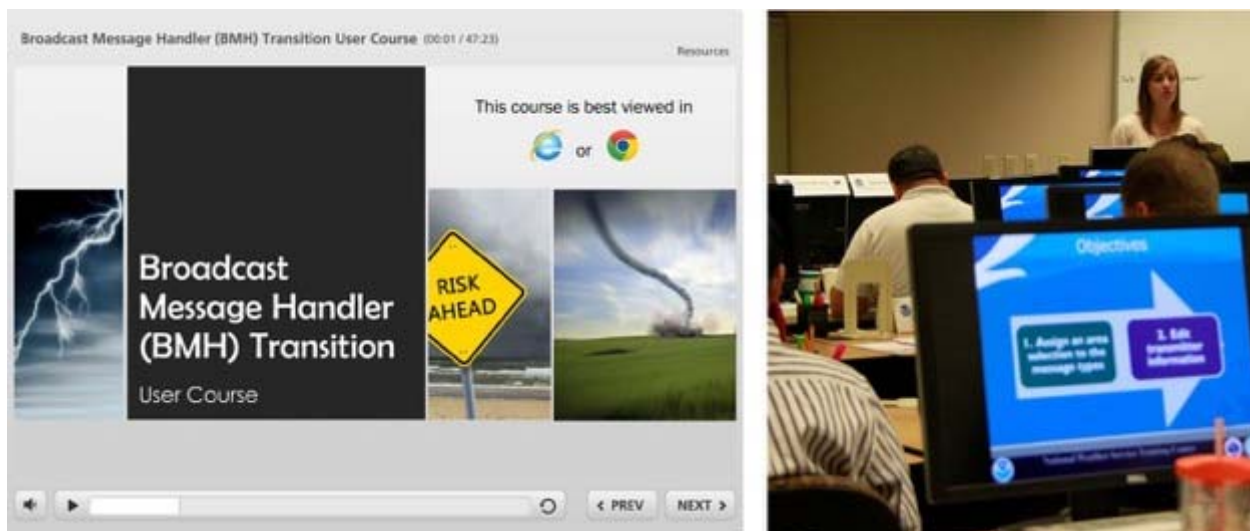
Perhaps one of the largest projects in this reporting period, Broadcast Message Handler (BMH) is a software and hardware update that replaces the Console Replacement System for NOAA Weather Radio. Training on this new system is a continuation of the project that began last reporting period. CIMMS Sarah Grana, Megan Taylor, and Denise Balukas helped develop two types of training:

Operational Testing & Evaluation (OT&E) Training: Sarah Grana wrote most of the lesson plans, gathered images, wrote exercises, wrote job sheets, put binders together,

and taught a large portion of the OT&E Focal Point residence course. Additionally, she helped write, review, gather images, and create quizzes and final exams for the online OT&E User Training. Megan Taylor assisted in this stage by consulting during the writing phases, and building the online training course with provided materials. The OT&E phase ended on January 28, 2016. And:

Deployment Training: The second type of training developed was for general deployment training. Sarah Grana wrote the content, gathered images, built the training, recorded audio, created videos, created job sheets, and created quizzes/exams for both the Deployment Focal Point and Deployment User Training courses. Megan Taylor and Denise Balukas assisted in this process by conducting thorough reviews of the content. Both courses were available online by February 24, 2016.

Training development was the primary mission during this reporting period for this project. However, Sarah Grana was also charged with general BMH-related tasks such as setting up software, reviewing modification notes and manuals, troubleshooting the system, writing reports, assisting other BMH subject-matter experts, instructing demos in related OCLO courses, attending conference calls, and testing.



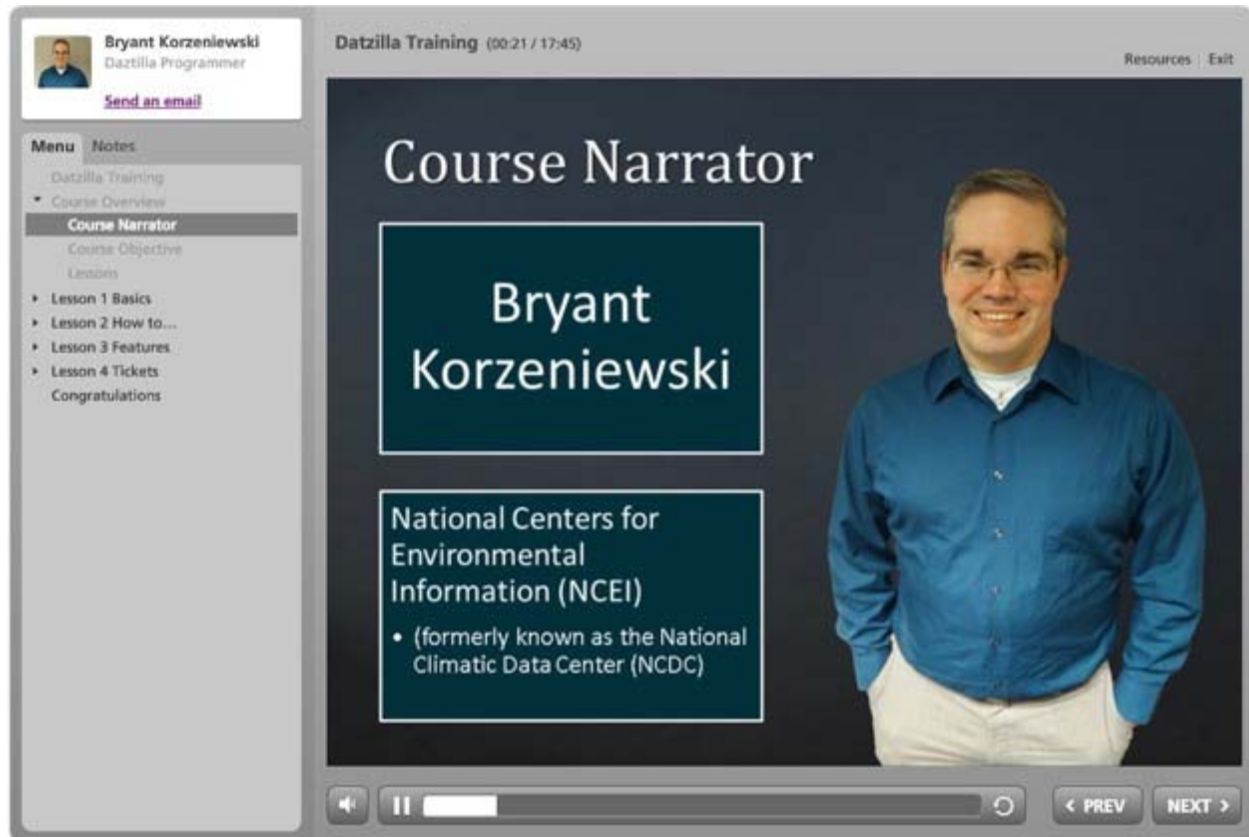
Screenshot of the Broadcast Message Handler (BMH) online user training (Left). Sarah Grana teaching in OT&E focal point course (Right).

d. Sub-Project 4: Datzilla User Training Course

Megan Taylor (CIMMS at NWSTC), Hattie Wiley (OCLO), Bryant Korzieneiwski (NWS NCEI), and Jim Zdrojewski (NWS HQ)

A continuation from the previous reporting period, the OCLO created a user course for the Datzilla data error ticketing system. Megan Taylor kicked off this project with analysis and information gathering with Bryant Korzieneiwski and Jim Zdrojewski. Then, the project went to the NWSTC Instructional Designer, Hattie Wiley, for content, design,

and development. The course went live in Fall 2015. Updates to the course are anticipated within the next year.



Screenshot of the Datzilla Training course.

e. Sub-Project 5: Hazard Services Training

Sarah Grana (CIMMS at NWSTC), Dave Cokely (OCLO), and Tom Piper and Bob Rood (NWS HQ)

Hazard Services is a team of technical leads (and instructors) striving to reduce AWIPS warning tools, and integrate them into one program. This project remained in the planning phase through the duration of the previous and current reporting period. Sarah Grana audited calls and helped instructor Dave Cokely assess future training needs.

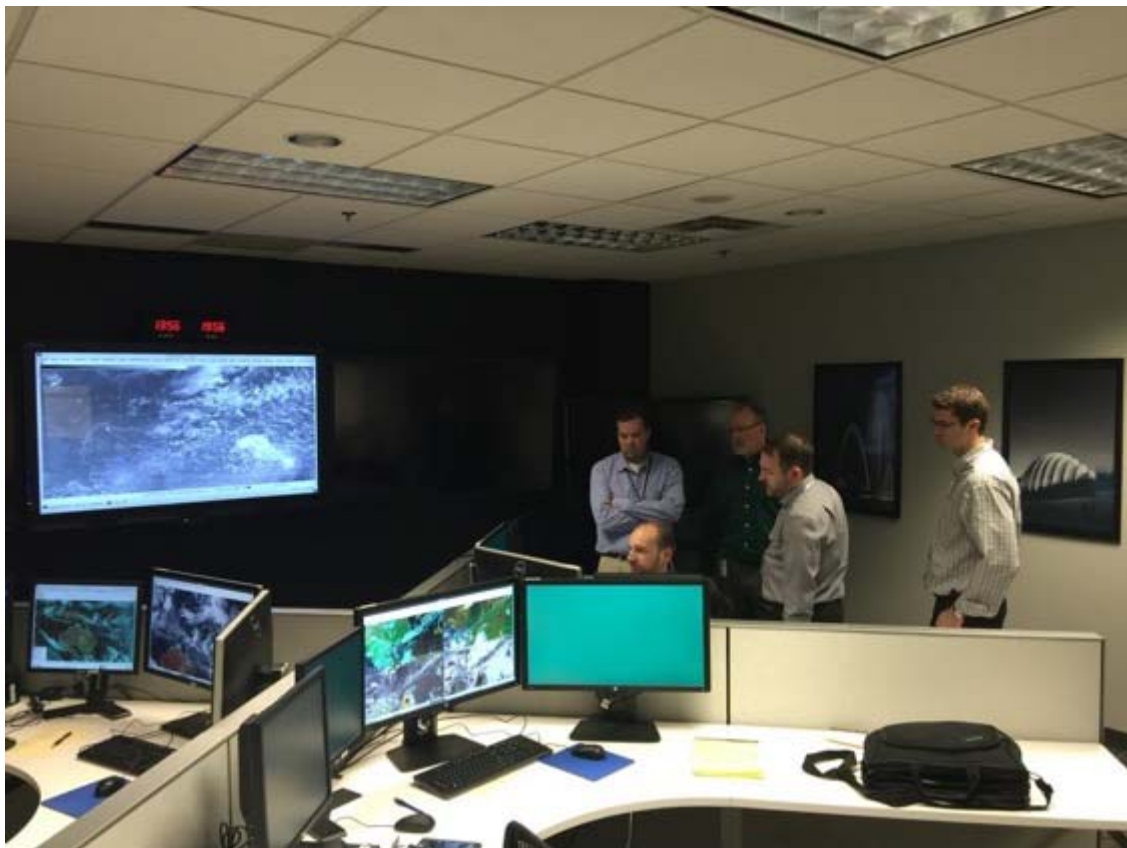
2. NWS Proving Ground Operational Service Delivery Simulations

a. Sub-Project 1: Himawari-8 RGB Products and Multiple Spectral Band Imagery Evaluation

Katie Crandall and Derrick Snyder (CIMMS at NWSTC), Chad Gravelle (CIMSS-University of Wisconsin), Kim Runk (OPG), and Jack Richardson (OCLO and OPG Contractor), Matthew Foster (NWS Central Region HQ), and NASA SPoRT staff

As part of the preparation for the 2016 launch of the GOES-R satellite, OPG conducted an evaluation of RGB products available on the Himawari-8 satellite, which has similar capabilities to what GOES-R will have. Sixteen spectral channels from Himawari-8, as well as several RGB products created by NASA SPoRT, are now flowing to the OPG's AWIPS-II workstation. NWS forecasters provided feedback on using multiple spectral bands and RGB imagery in the forecast process. For this evaluation, RGB imagery was generated "on the fly" using the EPDT RGB Plugin. The evaluation used imagery from the Himawari-8 Advanced Imager (AHI) which is a proxy for the GOES-R Advanced Baseline Imager (ABI).

Along with planning and executing the evaluation Katie Crandall and Derrick Snyder performed specific job tasks: Crandall – (1) developed surveys to collect feedback from forecasters; (2) recorded and transcribed audio recording of group discussions; (3) analyzed evaluation data and made that data accessible to other OPG members; and (4) helped with creating evaluation reports and findings for NWS management. Snyder – (1) collected and prepared satellite data sets for use in AWIPS-II; (2) configured AWIPS-II to optimize performance for NWS forecasters; and (3) led training exercises with NWS forecasters to analyze satellite data.



OPG staff and NWS forecasters discussing Himawari-8 imagery during the first week of a three week RGB and multiple spectral band imagery evaluation.



OPG staff and NWS forecasters discussing Himawari-8 imagery during the second week of a three week RGB and multiple spectral band imagery evaluation.



OPG staff and NWS forecasters discussing Himawari-8 imagery during the third week of a three week RGB and multiple spectral band imagery evaluation.

Sub-Project 2: Collaborate with the Aviation Weather Testbed (AWT) on Digital Aviation Services Evaluation (Part 1)

Katie Crandall and Derrick Snyder (CIMMS at NWSTC), Chad Gravelle (CIMSS-University of Wisconsin), Kim Runk (OPG), Jack Richardson (OCLO and OPG Contractor), Matthew Foster (NWS Central Region HQ), Steve Lack, Austin Cross, and Joshua Scheck (AWC), Benjamin Schwedler (CIRA-Colorado State University), Cammye Sims (NWS ASB), Aviation Weather Testbed, and ESRL Global Systems Division

The OPG collaborated with the Aviation Weather Testbed (AWT) using Digital Aviation Services to assess whether there is an optimal methodology for generating grids that can serve as a foundation for the creation of WFO products for aviation partners. Multiple methodologies are used today and anecdotal evidence suggests a broad range of opinions about the workload required to achieve the quality needed for terminal aerodrome forecast (TAF) production. The first set of evaluations focused on comparing and contrasting the existing methodologies for both meteorological quality and forecaster workload impact, across a variety of weather hazards and geographical locations. Some cases were archived simulations from a two-week period that coincided with the AWT Winter Experiment in February 2016. This allowed OPG to compare two different starting points for the scenarios: CONSShort and a national CIG/VIS grid generated by AWC. Live data was also used during the evaluation.

Along with planning and executing the evaluation Katie Crandall and Derrick Snyder performed specific job tasks: Crandall – (1) developed surveys to collect feedback from forecasters; (2) created detailed maps with aviation TAF locations and airport information; (3) recorded and transcribed audio recordings of group discussions; (4) analyzed evaluation data and made that data accessible to other OPG members; and (5) helped create evaluation reports and findings to NWS management. Snyder – (1) assisted in configuring AWIPS-II to test various methods of TAF production, using archived “displaced real-time” cases and using live data; (2) obtained GFE and AvnFPS configuration files from Weather Forecast Offices to allow for TAF production; and (3) obtained archived meteorological data sets (radar, model, surface observations, etc.) to run archived simulations using AWIPS-II.



OPG staff and NWS forecasters discussing methodology during the first week of a two week Digital Aviation Services evaluation.



OPG staff, AWC staff, and NWS forecasters collaborating during the second week of a two week Digital Aviation Services evaluation.

3. Impact-Based Decision Support Services Research and Development

As part of the Weather-Ready Nation initiative, the NWS is undergoing a change in culture. Part of this change includes providing more impact-based decision support services to NWS core partners and improving communication to partners and the public. During this reporting period, numerous training initiatives occurred in effort to support this need. These include:

a. Sub-Project 1: Impact-Based Decision Support Services (IDSS) Professional Development Series

Megan Taylor and Denise Balukas (CIMMS at NWSTC), Jeffrey Zeltwanger, Marco Bohorquez, Doug Streu, Jerry Griffin, Hattie Wiley, and Cathy Burgdorf (OCLO), Kim Runk (OPG), Derek Deroche (NWS Central Region HQ), and Numerous NWS HQ and Region PDS Team Members

While the previous reporting period was focused on planning for the IDSS PDS, this reporting period signifies the beginning of training development. This is one of the largest training initiatives in some time and it is highly visible across the agency. The overall plan for the curriculum is:

- Professional Competency Unit 1 - Intro to IDSS Basics and Incident Command Structure (FEMA)
- Professional Competency Unit 2 - Customer-Focused Support
- Professional Competency Unit 3 - Effective Communication
- Professional Competency Unit 4 - Operating within ICS & NIMS
- Professional Competency Unit 5 - Partnership Building
- Professional Competency Unit 6 - Threat Assessment & Risk Communication
- Professional Competency Unit 7 - Deployment-Ready Task Book
- Professional Competency Unit 8 - Advanced ERS for Complex Incidents
- Professional Competency Unit 9 - ERS Endorsements

PCUs 1-3 are required for all operational NWS employees regardless of location or office type. PCUs 4-7 are for those operational employees wishing to be “deployment-ready.” PCUs 8-9 involve advanced studies into specific types of incidents.

Planning for courses within the first three PCUs began in late August 2015. During the fall, Megan Taylor, with assistance from Jeff Zeltwanger and Hattie Wiley, researched and performed analysis regarding existing NWS courses related to IDSS concepts, analyzed audience type, need, gaps, etc. for the new training series. During that time, Megan took numerous courses to evaluate for potential use. During the winter of 2015-2016, Megan Taylor and Denise Balukas, continued to refine the course list, goals, and objectives. At the end of this period, a proposal was sent to the PDS Team and NWS Mission Delivery Council for approval. Course development began in Spring 2016, with Denise Balukas focused on “Effective Presentations,” and Megan Taylor focused on “Fundamentals of Communication: Body Language.” Megan Taylor also began project

management at this point, helping Doug Streu with his course on “Phases of Emergency Management” and Hattie Wiley with a course on “Designing Weather Visuals.” Both Megan Taylor and Denise Balukas provided thorough reviews at various stages of course development. OU CIMMS Katie Crandall, Derrick Snyder, and Sarah Grana also helped by acting in training videos for the Body Language course, and reviewing any developed training components.

As of the end of this reporting period, the Body Language course has received final comments and is near completion. A plan and outline is finished for the Phases of Emergency Management course. After some brainstorming and re-organizing, both the Effective Presentations and Designing Weather Visuals course will be broken up, with various pieces in draft form. During all phases of development, Megan Taylor and Denise Balukas will be heavily involved in researching, writing content, designing training, collaborating with the IDSS PDS Team and subject-matter experts, reviewing modules designed by other instructors, and managing the project as a whole while various others provide pieces of training.



Screenshot of the Body Language Course (Top-Left) and screenshot of the Effective Presentation Course (Bottom-Left) for the IDSS PDS.

b. Sub-Project 2: Conduct IDSS Deployment Boot Camp

Megan Taylor, Denise Balukas, Sarah Grana, Katie Crandall, and Derrick Snyder (CIMMS at NWSTC), Jeff Zeltwanger, Marco Bohorquez, and Doug Streu (OCLO), Kim Runk (OPG), and Derek Deroche and Chris Foltz (NWS Central Region HQ)

The popular Impact-Based Decision Support Services Deployment Boot Camp was held three times during the reporting period. The goal behind these courses is to prepare NWS employees for deployment in the field and train them to communicate weather information to partners and the public. Beginning the next reporting period, this course will be built into the IDSS Professional Development Series (Sub-Project 1).

Megan Taylor has been involved in the training since 2012, and continues to help plan and organize the course. Megan created a new booklet, and redesigned many of the course presentations. Additionally, she taught Plain Language (Sept. only), Media Training (all offerings), Communications (March only), and Partner and Public Briefings (March only). She also continues to act as a reporter during the full-day simulation. During this reporting period, Denise Balukas observed the first course in November, and provided feedback. Thereafter, she also became heavily involved in planning and organizing the course. She took over the maintenance of the new course booklet. Denise also took over the Plain Language topic and taught the session in March. Additionally, she helped with the simulation both by acting as a unit advisor in all offerings, and by helping the simulation lead (Doug Streu) create and refine documentation for the event.

Sarah Grana, Katie Crandall, and Derrick Snyder played newspaper reporters in the full-day simulation and participate in the mock-press conference.



Katie Crandall (Top-Left) and Sarah Grana (Top-Right) give feedback about the media component of the simulation. Denise Balukas (Bottom-Left) listens as instructions for the simulation are given. Megan Taylor (Bottom-Right) polls the participants with a paper clicker tool.

c. Sub-Project 3: Conduct Custom Traveling Versions of the IDSS Deployment Boot Camp

Megan Taylor, Denise Balukas, and Sara Grana (CIMMS at NWSTC), Jeff Zeltwanger, Marco Bohorquez, and Doug Streu (OCLO), Kim Runk (OPG), Charlie Woodrum (NWS HQ), Dave Snider (NOAA Alaska TV), and Aimee Fish and Jeff Oslensky (NWS Alaska Region HQ)

Given the continued success of the IDSS Deployment Boot Camp, the OCLO had another request for a customized, traveling version of the course. Megan Taylor, Denise Balukas, Sarah Grana, Marco Bohorquez, and Kim Runk traveled to Anchorage, Alaska in April 2016, and hosted the course. Megan Taylor was part of the initial planning team. She helped edit, design, or assist in the development of many course presentations, handouts, and additional documents. She also helped manage the overall project using Trello, a project management software. She taught Media Training, Graphics for Public Presentations, and acted as Handler in the full-day simulation. Megan was also heavily involved in the writing, editing, and executing of the simulation. Denise Balukas helped manage, edit, and prepare course documents. She also taught the Plain Language session, reviewed course documents prepared by others, participated in team calls, and acted as Unit Advisor during the full-day simulation. Sarah Grana helped review course documents, taught Fundamentals of Human Communication, and acted as Unit Advisor in the full-day simulation.



Denise Balukas (Top-Left) provides assistance during an activity. Megan Taylor (Top-Right) conducts an interview practice session. Sarah Grana (Bottom) teaches communication to the class.

d. Sub-Project 4: Conduct Additional IDSS-Related Training Sessions

Because IDSS training is needed in many avenues of operational life in the NWS, additional training opportunities were pursued and continued during this reporting period. These additional sessions included:

i. IDSS Virtual Conference Webinars

Megan Taylor and Denise Balukas (CIMMS at NWSTC), Jeff Zeltwanger and Marco Bohorquez (OCLO), Charlie Woodrum (NWS Pacific Region HQ), and Numerous Guest Speakers

NWS Headquarters and OCLO hosted numerous IDSS Virtual Conference webinars over the reporting period. These webinars focused on a different topic each time, and gave numerous guest speakers a chance to share some IDSS best practices with the agency. Denise Balukas attended all offerings. Megan Taylor attended most offerings, and processed all resulting videos for publishing on YouTube.

ii. Warning Coordination Meteorologist (WCM) Development Course

Megan Taylor (CIMMS at NWSTC), Doug Streu, Dave Cokely, Jerry Griffin, and Jeff Zeltwanger (OCLO), and Numerous Guest Speakers

IDSS concepts such as communication and customer service are essential to the role of Warning Coordination Meteorologist (WCM). During the reporting period, one WCM Development Course was held in Fall 2015, and preparations began for another. Megan Taylor consulted during the planning phase of the 2015 course. She taught Body Language and Effective Presentations during the 2015 course, as well as acted as a reporter during the full-day simulation. For the 2016 course, Megan has participated in some planning discussions and will teach 2-3 subjects in December.

iii. NWS Public Speaking Video Series and Coaching

Megan Taylor (CIMMS at NWSTC), Cathy Burgdorf and Jeff Zeltwanger (OCLO), Brooke Bingaman (NWSFO Sacramento), Renee Wise (NWSFO Aberdeen), and Dave Snider (NOAA Alaska TV)

The OCLO was approached with a project in late summer 2015. Three WFO public speaking SMEs (Brooke Bingaman, Renee Wise, and Dave Snider) wanted to create a set of public speaking “how-to” videos in conjunction with a new coaching program. The OCLO decided to move forward. Megan Taylor and Cathy Burgdorf filmed the proposed videos in January 2016. To do so, they also had to install a new cove green screen for maximum filming area. Megan directed the video shoot, and conducted discussions on planning the new coaching program. She began building the coaching website and reviewed videos as they were edited by Cathy Burgdorf. The project will likely be completed in late 2016 or early 2017.

iv. WFO Media Training/Personal Consultation

Megan Taylor (CIMMS at NWSTC), Albert Pietrycha (NWSFO Pleasant Hill), Audra Hennecke (NWSFO Topeka), John Koch (NWS Eastern Region Headquarters), Jeff Zeltwanger (OCLO), and Additional Field Office Employees

Several forecast offices requested Megan Taylor's media training services in this reporting period. During the WFO media training sessions, Megan Taylor teaches media training concepts (as well as some basic communication). She then interviews each employee either in person or via Skype. She provides the employees with verbal (and written if requested) feedback to help improve his/her interviewing skills. Megan conducted these sessions for WFO Pleasant Hill (Oct. 2015), WFO Topeka (Dec. 2015) and WFO Philadelphia (June 2016), the later of which was in preparation for supporting the Democratic National Convention. Megan also coaches individuals in media training and public speaking concepts. Due to the private nature of these sessions, names are not available.

v. Office of Marine and Aviation Operations Midgrade

Megan Taylor (CIMMS at NWSTC), Scott Tessmer and David Hall (NWS OMAO), Jenna Dalton (CIRA-OMAO), and Keli Pirtle (NOAA Norman Partners)

To maintain consistency in training, Scott Tessmer (Chief Learning Officer, OMAO) requested Megan Taylor assist with media training for the OMAO Midgrade Course. Megan worked with David Hall and Keli Pirtle in establishing common goals for this training. Megan also conducted in-class interview practice and individualized feedback.

vi. Graphics Consultation

Megan Taylor and Katie Crandall (CIMMS at NWSTC) and Derek Deroche and Brian Walawender (NWS Central Region Headquarters)

Keeping IDSS principles and basic graphic design concepts in mind, Megan Taylor and Katie Crandall have consulted in various instances on Central Region Headquarters social media and website projects. One example of such is the Impacts Warnings automatically disseminated on Twitter.

vii. Cooperative Network Operations Course

Megan Taylor (CIMMS at NWSTC) and Marco Bohorquez (OCLO)

Because IDSS concepts such as communication are vital to the success of the Cooperative Observer Program, Megan Taylor continues to prepare materials and teach communications in the Cooperative Network Operations residence course. Megan taught in the March 2016 offering and will teach another session in the fall.



At the top, a screenshot (Top-Left) from WFO communications presentation and a screenshot (Top-Right) of the new Twitter impacts warnings. On the bottom, a still image of Brooke Bingaman (Bottom-Left) preparing to film a segment on body language and a still of Megan Taylor (Bottom-Right) teaching in WCM Class.

e. Sub-Project 5: Conduct Effective Hurricane Messaging Course

Denise Balukas (CIMMS at NWSTC), Marco Bohorquez and Shannon White (OCLO), Dan Brown (National Hurricane Center), Jen McNatt (NWS Southern Region Headquarters), Matt Moreland and Andy Devanas (NWSFO Key West), John Koch (NWS Eastern Region Headquarters), David Sharp (NWSFO Melbourne), and Lance Wood (NWSFO Houston)

The EHM course supports the goal of Weather Ready Nation. Like the Deployment Boot Camp, one of the primary objectives of the EHM is that students gain the ability to effectively communicate weather and water threats, impacts, forecasts, and other technical information to both the public (primarily through media interviews and social media) and to core NWS partners such as emergency management and Coast Guard (through various means including remote and on-site briefings). Another primary goal of both Boot Camp and EHM is to instill the importance of developing the trust of core

partners and of fostering deep and lasting relationships with these partners. Because of the unique nature of the hurricane threat, the EHM has hazard-specific components related to the appropriate use and messaging of the National Hurricane Center's tropical cyclone products which are addressed during the course.

Denise Balukas observed the course in April 2016 at the National Hurricane Center in Miami, Florida. From that point forward, Denise has been involved with the planning and development of future EHM course offerings as the OCLO takes over the course. She meets with facilitators and assists with developing objectives, facilitating discussion between experts, facilitators, and instructors, and aides in refining the feedback strategy for the course. Denise will be developing a course booklet (similar to the deployment boot camp booklet) for upcoming EHM courses.



The yearly storm track board at the National Hurricane Center for the 2015 hurricane season.

4. Advanced Training Development

The OU CIMMS stationed in the OCLO and OPG building must maintain a level of expertise in many areas in order to fully support the local NWS staff. This may mean

developing new or more advanced skills, training others in the office, participating in outreach, or joining one of the building teams. The activities relevant to this objective is as follows:

a. Sub-Project 1: Develop Expertise in Technology, Best Practices, and Methodologies to Better Fulfill Roles and Help Others.

i. Conferences

- Summer Institute on Distance Learning & Instructional Technology (SIDLIT) - Megan Taylor, Sarah Grana
- National Weather Association Annual Meeting (Oklahoma City) - Megan Taylor, Sarah Grana, Katie Crandall - Poster Presentation, Derrick Snyder - Poster Presentation.
- American Meteorological Society Annual Meeting (New Orleans) - Sarah Grana, Derrick Snyder - Oral Presentation, Katie Crandall - Oral Presentation
- American Meteorological Society Bi-Annual Tropical Meteorology Conference (Puerto Rico) - Denise Balukas - Oral Presentation (Presented for Denise Balukas by Dr. Elizabeth Ritchie)
- International Associate for Public Participation (IAP2) in Portland, OR - Sarah Grana
- Skillpath Conference for Women (Kansas City) - Megan Taylor, Sarah Grana, Katie Crandall, Denise Balukas
- NWS IDSS Virtual Conference (Online) - Megan Taylor, Sarah Grana, Denise Balukas
- Missouri Academy of Science Annual Meeting (Jefferson City) - Katie Crandall - Oral Presentation
- NWS Pleasant Hill, MO Integrated Warning Team Workshop - Megan Taylor, Katie Crandall, Derrick Snyder
- NWS Pleasant Hill, MO Winter Weather Workshop - Katie Crandall - Oral Presentation, Megan Taylor - Attended, Derrick Snyder

ii. Office Visits

- Portland, OR WFO - Sarah Grana
- Pleasant Hill, MO WFO - Megan Taylor, Sarah Grana, Derrick Snyder, Katie Crandall
- Topeka, KS WFO - Megan Taylor
- Anchorage, AK WFO - Megan Taylor, Sarah Grana, Denise Balukas
- Alaska River Forecast Center (RFC) - Megan Taylor, Sarah Grana, Denise Balukas
- Alaska Aviation Weather Unit (AAWU) - Megan Taylor, Sarah Grana, Denise Balukas
- National Hurricane Center, FL - Denise Balukas

iii. NWS/NOAA Training

- Radar and Applications Course (Norman) - Sarah Grana, Derrick Snyder, Katie Crandall
- Warning Operations Course – Core and Severe (Online) - Sarah Grana, Derrick Snyder, Megan Taylor (core only), Denise Balukas (partial core)
- Media Training - Denise Balukas, Derrick Snyder
- Introduction to Tropical Cyclone Storm Surge (Online) - Denise Balukas
- Storm Surge and Datums (Online) - Denise Balukas
- Use of Probabilistic Surge Guidance in Local Storm Surge Forecasting (Online) - Denise Balukas
- Forecasting Tropical Cyclone Storm Surge (Online) - Denise Balukas
- Determining Onset and Risk of Tropical Cyclone Winds (Online) - Denise Balukas
- Tropical Cyclone Forecast Uncertainty (Online) - Denise Balukas
- Use of Probabilistic Guidance in Local Tropical Cyclone Wind Forecasting (Online) - Denise Balukas
- NOAA Communicating Risks in High-Impact Events - Denise Balukas

iv. Online Training

- FEMA online training (100, 200, 700, & 800) - Sarah Grana, Denise Balukas, Megan Taylor (100 only)
- FEMA Communications Training - Denise Balukas
- Instructional System Design: The ADDIE Model Online tutorial - Denise Balukas
- Skillsoft Active Listening - Denise Balukas, Megan Taylor
- Skillsoft Online Advanced PowerPoint Technical Tutorials - Denise Balukas, Megan Taylor
- Skillsoft Plain Writing Act - Denise Balukas
- CDC Crisis and Emergency Risk Communication - Denise Balukas, Megan Taylor
- Skillsoft Creating Presentations in PowerPoint 2013 - Megan Taylor
- Skillsoft Business Grammar: Common Usage Errors - Megan Taylor
- Skillsoft Team and Customer Relationships - Megan Taylor
- Skillsoft Written Communication - Megan Taylor
- Skillsoft Developing Strong Customer Relationships - Megan Taylor
- Skillsoft Customer-focused Interaction- Megan Taylor
- Skillsoft Customer Service Fundamentals: Building Rapport in Customer Relationships - Megan Taylor
- Skillsoft Communication Skills - Megan Taylor
- Skillsoft Building Peer Relationships - Megan Taylor
- Coursera Survey Data Collection and Analytics - Katie Crandall

v. Internal Training

- Instructional Design Training (by Hattie Wiley) - Sarah Grana, Denise Balukas, Megan Taylor
- Writing Basics (bi-weekly)
- Designing visuals (monthly)
- Annual Instructional Design Refresher - Sarah Grana, Denise Balukas, Megan Taylor
- Articulate Training - Denise Balukas
- Rapid Protocol Design Training - Sarah Grana, Denise Balukas, Megan Taylor
- DOC Active Shooter Training - Sarah Grana, Denise Balukas, Megan Taylor

vi. Additional Training

- Community Emergency Response Team training (CERT) (Kansas City) - Denise Balukas



Photos taken from various conferences throughout the reporting period.

b. Sub-Project 2: Help NWSTC Employees Learn New Tools and Methodologies for Training and Collaboration

The following is a list of internal training conducted, job sheets created, or reviews completed by the OU CIMMS stationed in Kansas City in effort to train or assist OCLO/OPG employees.

i. Internal Training

- On-Boarding Denise Balukas - Sarah Grana, Megan Taylor
- Articulate Quizmaker for NWS Training Center Employees - Sarah Grana
- Changing Passwords & FTP Help - Sarah Grana
- Designing Visuals (1 session) - Megan Taylor
- Apple TV & iPad Integration and Training - Megan Taylor
- GoTo Meeting Quick Help Sheets - Megan Taylor
- Google Apps Training (in person, online, one-on-one) - Megan Taylor
- New Instructor Training: Body Language - Megan Taylor
- Trello for Project Management - Megan Taylor
- Plickers - Paper Cards for Classroom Polling - Megan Taylor
- Survey Design Training - Katie Crandall

ii. Course Reviews/Assistance

- Governance for NWS Employees (Review) - Megan Taylor, Sarah Grana,
- Appropriations for NWS Employees (Review) - Megan Taylor, Sarah Grana, Denise Balukas
- Handling Space Weather Inquiries (Review) - Megan Taylor, Sarah Grana, Denise Balukas
- NWS 101: New Hire Orientation (Materials Creation) - Megan Taylor, Denise Balukas
- Leadership Academy (Materials Update for 3 classes) - Megan Taylor
- Leadership Academy (Taught Body Language) - Megan Taylor
- Server Transition (Planning Sessions) - Megan Taylor
- Photography (Fill-In As Needed) - Megan Taylor
- YouTube Videos (Uploaded for Several Instructors) - Megan Taylor

c. Sub-Project 3: Reach Out to the Agency to Spread Information about Training

Megan Taylor (CIMMS at NWSTC), and John Ogren and Jeff Zeltwanger (OCLO)

The only sub-project regarding outreach during this reporting period is the New OCLO video and brochure. During the previous reporting period, Megan Taylor worked on a video to announce the change from the NWS Training Division to the NWS Office of the Chief Learning Officer. During this reporting period, Megan Taylor finished and published the final video. She also created QR code cards linking to the video to pass out at conferences, and an OCLO brochure explaining the office, divisions within, and functions. To watch the video, visit: <https://youtube/dQaMdSwIEj4>.

d. Sub-Objective 4: Use Expertise to Join and Help OCLO and OPG Focal Point Teams

Recycling Focal Point - Sarah Grana was in charge of recycling toner, contacting recycling company, and ensuring the building has opportunities to recycle various items. Denise Balukas is taking over the duties for the next reporting period.

Social Media Team - Megan Taylor (team lead) posts all social media activity via Facebook and YouTube. She is also working on expanding platforms and combining efforts with other OCLO divisions. Katie Crandall (team member) assists with reviewing posts and submitting ideas.

Intranet Team - Megan Taylor (team lead) created the NWSTC intranet and continues to maintain it. She also leads several others as they maintain pages on the site.

Apple Device Team - Megan Taylor (team lead) introduced two iPads and two Apple TVs during the reporting period. She leads a team of two others, who monitor, administer, and check out the devices. This team also helps teach others how to use them.

Virtual Lab Focal Point - Katie Crandall updated the Virtual Lab site and spent time training on Virtual Lab for the OPG

Google Applications Trainer/Troubleshooter - Megan Taylor (team lead), Sarah Grana (team member), and Jeff Zeltwanger ensure staff can use Google Applications (Gmail, Calendar, Drive, etc.), and understand any updates. They also help troubleshoot and answer questions when needed.

Internet/Training Portal - Megan Taylor assists Hattie Wiley in maintaining and updating the NWSTC webpage and the OCLO training portal.



Logos from a few of the internal teams in which Katie Crandall, Sarah Grana, Derrick Snyder, Denise Balukas, and Megan Taylor participate.

Sub-Objective 5: Help Develop and Maintain an OCLO Intern Program to Aid in Training Development While Providing Outreach Services to the Community

Megan Taylor and Denise Balukas (CIMMS at NWSTC) and Hattie Wiley (OCLO)

For the first time, the OCLO is welcoming student interns to help with projects while gaining valuable real-world experience. Hattie Wiley led the project during this reporting period. Denise Balukas helped create a contact list to connect the OCLO with local universities and educational establishments. Megan Taylor created several position openings, organize documentation, and a webpage. She also attended Park University's career fair in effort to recruit interns. You can see more information at the NWSTC website here: <http://www.nwstc.noaa.gov/homepage/news.html>

Publications

- Crandall, K. L., P. S. Market, A. R. Lupo, L. P. McCoy, R.J. Tillott, and J. J. Abraham, 2016: The application of diabatic heating in Q-vectors for the study of a North American cyclone event. *Advances in Meteorology*, Article ID 2908423, 11 pages.
- Gravelle, C. M., K. J. Runk, K. L. Crandall, and D. W. Snyder, 2016: Forecaster evaluations of high temporal satellite imagery for the GOES-R era at the NWS Operations Proving Ground. *Weather and Forecasting*, **31**, 1157-1177.

CIMMS Task III Project – The GOES-R GLM Lightning Jump Algorithm: A National Field Test for Operational Readiness

Kristin Calhoun and Darrel Kingfield (CIMMS at NSSL)

NOAA Technical Lead(s): Dan Lindsay and Andy Heidinger (NOAA NESDIS)

NOAA Strategic Goal 2 – *Weather Ready Nation: Society is Prepared for and Responds to Weather-Related Events*

Funding Type: CIMMS Task III

Objectives

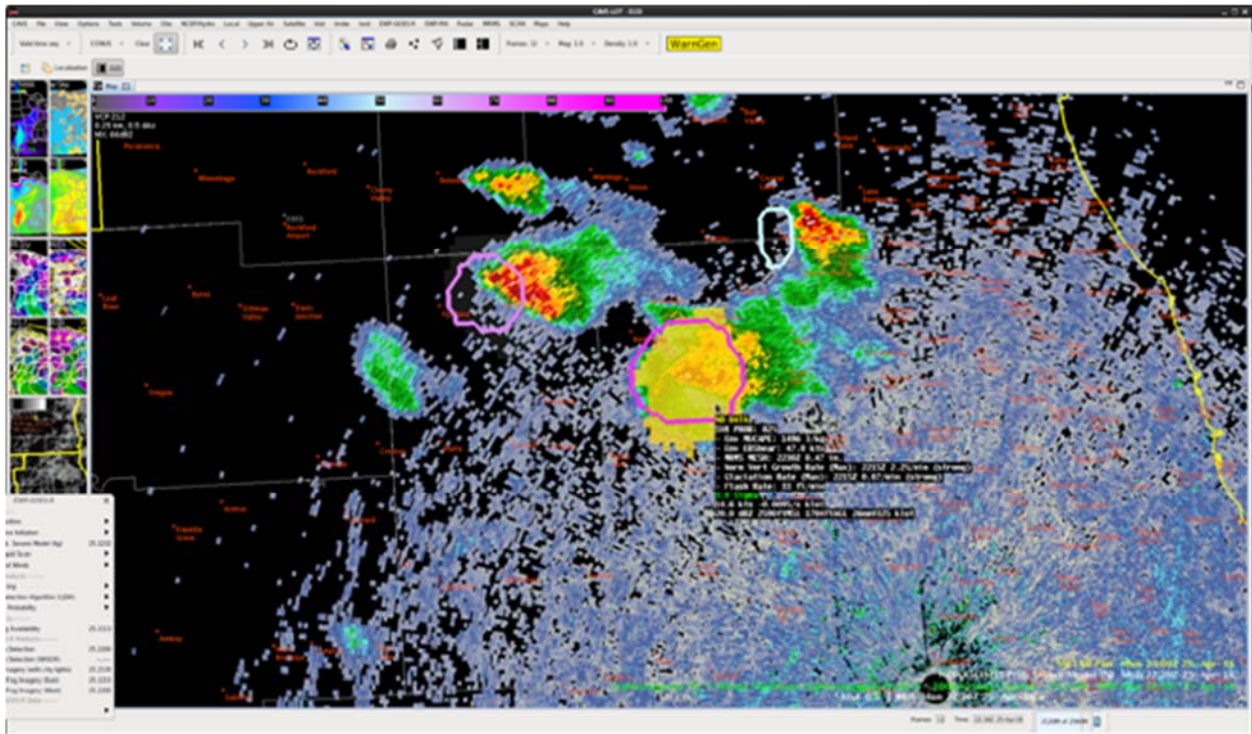
A fully automated, real-time Lightning Jump Algorithm (LJA) is being developed and tested for National Weather Service implementation in collaboration with the University of Alabama-Huntsville. The LJA is designed to highlight rapid intensification in thunderstorms preceding severe weather such as tornadoes, hail and straight-line winds at the surface by tens of minutes. While the GOES-R Geostationary Lightning Mapper (GLM) provides a general path to operations for the use of continuous total lightning observations and the lightning jump concept over a hemispheric domain, the operational implementation for the Hazardous Weather Testbed (HWT) of the LJA pre-GLM is being produced using data from the Earth Networks Total Lightning Network (ENTLN) and Lightning Mapping Array data on localized domains.

Accomplishments

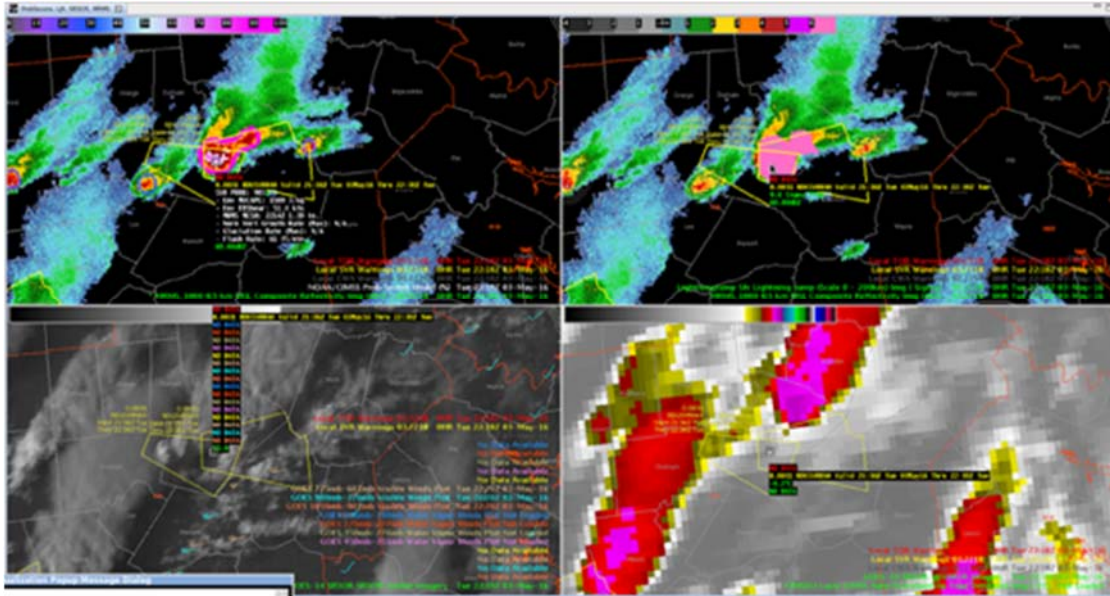
A final evaluation of the algorithm was completed in the HWT during Spring of 2016 as part of the GOES-R Proving Ground. Forecasters continued to find it useful in severe and hazardous weather monitoring, particularly when used in tandem with the “ProbSevere” product (two

figures below). Both a 1-min update and a 5-min max product (new in 2016 and created based on previous feedback) were evaluated by forecasters; one was not greatly preferred to the others as individual forecasters generally gravitated to one or the other depending on the operational focus of the day. Feedback showed desire that both products move forward into NWS operations.

An initial test of transition to NCEP for operations implementation was made as part of the Multi-Sensor/Multi-radar (MRMS) platform. This initial testing showed difficulty in regard to the amount of memory available to keep up with the storm-tracking and data ingest in a real-time manner as was provided in the HWT. Based on this initial testing, the storm-tracking algorithm is being revised to reduce the amount of memory needed at the operational center. The algorithm is expected to be part of the 2017 MRMS operational system.



Forecaster screenshot from AWIPSII during HWT evaluation on 25 Apr 2016. Forecaster chose to issue warning on this storm at 2230 due to increase of ProbSevere (pink outline) to 82% and corresponding lightning jump of 3-sigma (yellow region) at the same time, shortly after warning issued 1" hail was reported west of the Chicago metro region with this storm.



4-panel configuration of forecaster display from AWIPSII during HWT evaluation on 3 May 2016 in Wake County, NC. Forecaster had high confidence in extending the warning due 9 sigma lightning jump (pink region, top right) and 98% value from ProbSevere (top left).

Publications

Chronis, T., L. D. Carey, C. J. Schultz, E. V. Schultz, K. M. Calhoun, and S. J. Goodman, 2015: Exploring Lightning Jump Characteristics. *Weather and Forecasting*, **30**, 23-37.

CIMMS Task III Project – Development of Short-Range Real-Time Analysis and Forecasting System Based on the ARPS for Taiwan Region

Ming Xue, Fanyou Kong, Keith Brewster, and Chong-Chi Tong (CAPS at OU)

NOAA Technical Lead: Fanthune Moeng (NOAA GSD)

NOAA Strategic Goal 2 – Weather Ready Nation: Society is Prepared for and Responds to Weather-Related Events

Funding Type: CIMMS Task III

Objectives

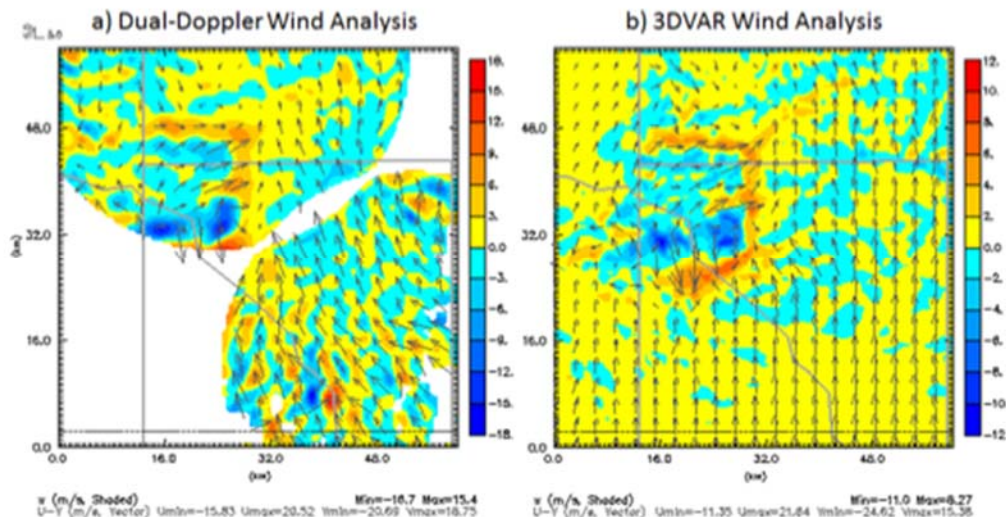
Investigate the impact of radar data assimilation on the analysis and simulation of a continental downburst case using the ARPS 3DVAR and cloud analysis system, and study different microphysics schemes and their impact on the prediction of the downburst-associated storm features.

Accomplishments

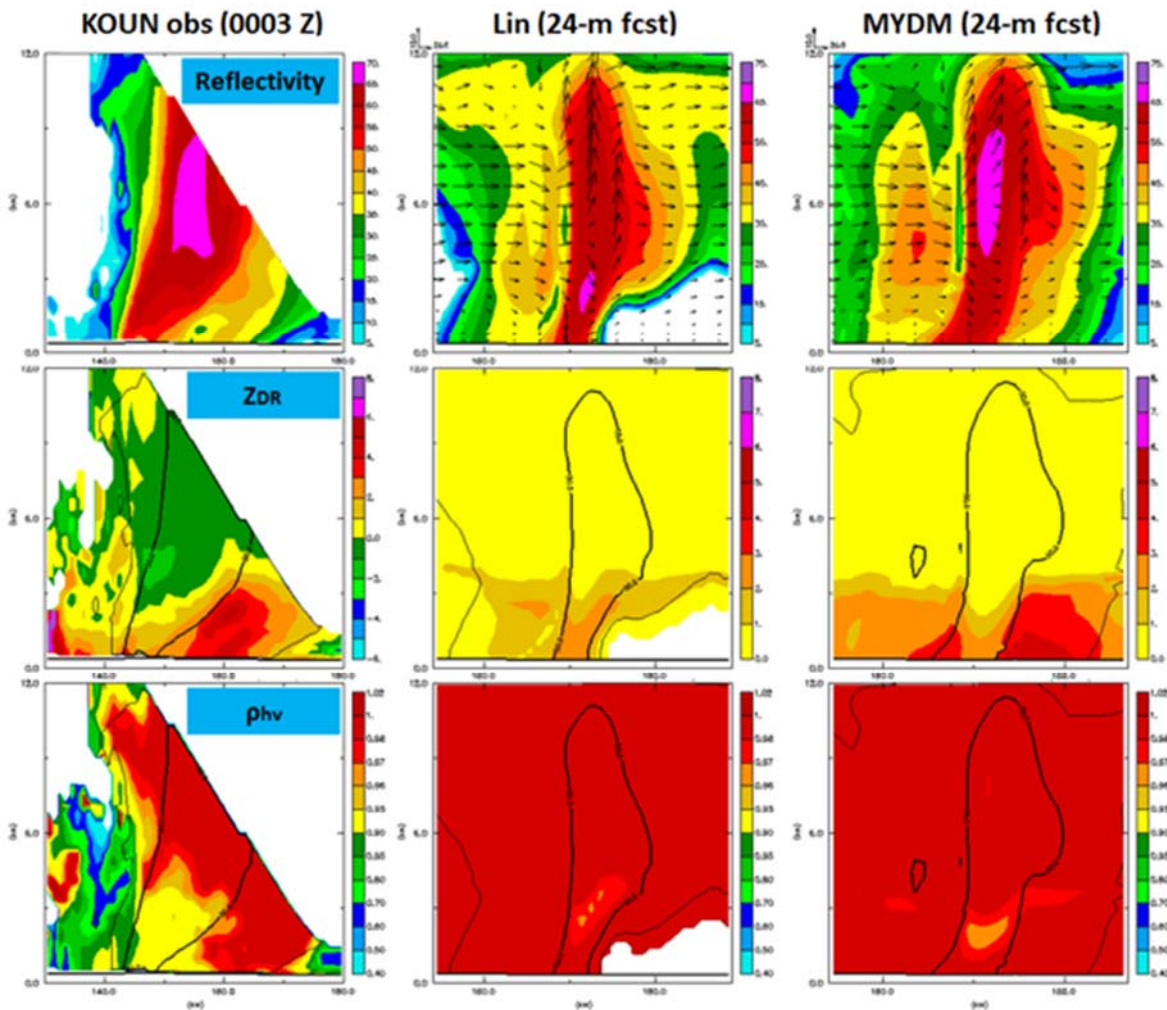
The project is in a no-cost extension period (FY16). The effectiveness of the ARPS three dimensional variational (3DVAR) data assimilation (DA) scheme in analyzing

radar radial velocity data for the 15 June 2011 Oklahoma downburst case was investigated. Our result shows great consistency between the 3DVAR analysis (realized at 500 m grid spacing) and dual-Doppler wind analysis wind fields around the downburst location (Fig. 1). However, it is found that the extreme values of vertical velocity (w) from the 3DVAR analysis is smaller than the counterparts from the dual-Doppler analysis, primarily due to the mass continuity constraint that is included in the 3DVAR analysis process.

The same downburst case was further studied using the ARPS 3DVAR and cloud analysis system. Radar radial velocity and reflectivity, Oklahoma Mesonet observation, and the radiosonde data at Norman, OK are assimilated. Two different microphysics parameterization schemes, the Lin single-moment scheme (Lin et al. 1983) and the Milbrandt and Yau double-moment scheme (referred to as MYDM hereafter; Milbrandt and Yau 2005), are applied and their impacts on the downburst simulation are preliminarily examined. Result shows the MYDM scheme is capable of providing better storm structure in terms of more realistic polarimetric signatures (PSs). Fig. 2 provides both the simulation and observation of various radar variables in the cross section over the main storm. On the Z_{DR} simulation, the MYDM is found to well capture the vertically extended Z_{DR} columns as well as the midlevel Z_{DR} ring surrounding the intense convective core, which are known as the results of size sorting mechanism. On the contrary, most high Z_{DR} values monotonically coincide with the high Z values in the Lin simulation, owing to the lack of independence between mixing ratio and N_0 in the single-moment scheme. Further, the MYDM outperforms the Lin in terms of a more pronounced midlevel ρ_{hv} ring which better resembles its counterpart in real observation. As this feature mainly characterizes the melting process of ice-phase particles, its importance is thus expected for more accurate prediction of the downburst, in which the loading effect of the heavy raindrops and hails is prominent according to the observation.



Horizontal winds (vectors) and vertical velocity (shaded) at 1 km AGL from (a) dual-Doppler analysis and (b) 3DVAR analysis at 0025 UTC 15 June 2011 (occurrence of the downburst at Norman, Oklahoma).



Radar variables Z (upper row), Z_{DR} (middle row), and ρ_{hv} (lower row) of cross sections over the downburst-associated storm by KOUN observation (left panel) simulation experiments Lin (middle panel) and MYDM (right panel). Forecast winds of both experiments are overlaid on Z plots in vectors, while the Z of 20 dBZ (thin contours) and 50 dBZ (thick contours) are overlaid on both Z_{DR} and ρ_{hv} plots.

CIMMS Task III Project – Contribution to Model Development and Enhancement Research Team by the Center for Analysis and Prediction of Storms

Ming Xue, Gang Zhao, and Chengsi Liu (CAPS at OU)

NOAA Technical Lead: Stan Benjamin (NOAA ESRL GSD)

NOAA Strategic Goal 2 – Weather-Ready Nation: Society is Prepared for and Responds to Weather-Related Events

Funding Type: CIMMS Task III

Objectives

Develop and test an ensemble Kalman filter (EnKF) and GSI-based EnKF/3DVAR hybrid data assimilation system suitable for operational implementation for the Rapid Refresh (RAP) forecasting system; establish radar data assimilation capabilities in the EnKF and hybrid systems and eventually apply the systems to the High Resolution Rapid Refresh (HRRR) system.

Accomplishments

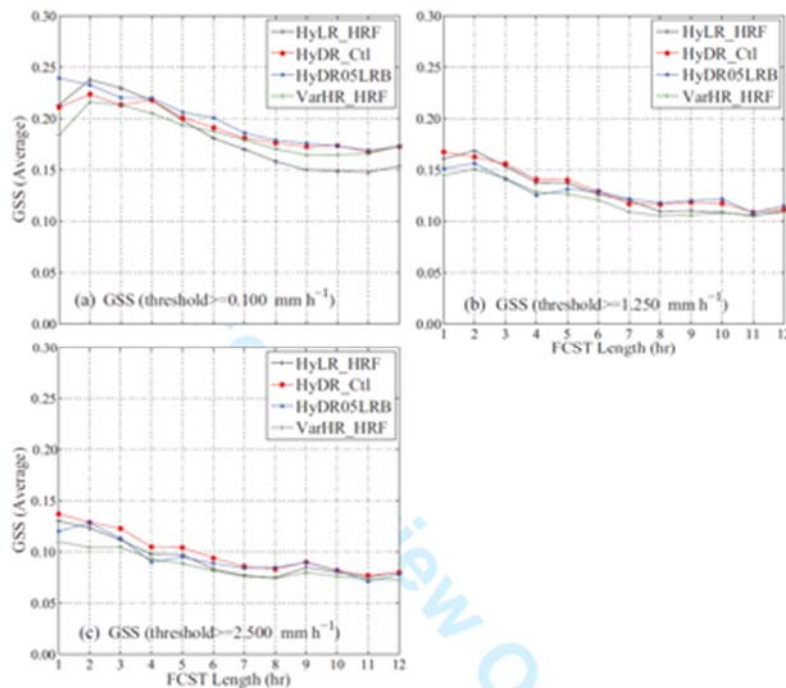
Pan et al. (2016) established a regional dual-resolution (DR) (40/13km) ensemble square-root filter (EnSRF) – 3D ensemble variational (3DEnVar) coupled hybrid data assimilation (DA) system. The DR hybrid system utilizes lower-resolution (LR) ensemble perturbations from the EnKF system, which is documented in Zhu et al. (MWR 2013) and Pan et al. (2014 MWR), to get the flow-dependent background error covariance, and within each DA cycle performs a higher-resolution (HR) 3DEnVar hybrid analysis then a HR deterministic forecast for use as the background at the next analysis time. The DR DA system is tested with 3-hour cycles over the same 9-day testing period used in Zhu et al. (MWR 2013) and Pan et al. (MWR 2014). The HR forecast of DR hybrid is compared with those using the operational GSI 3DVar run at 13 km grid spacing, and those launched from interpolated 40-km LR hybrid (HyLR-HRF) and EnSRF analyses (EnLR_HRF). The optimized DR hybrid system significantly outperforms the 13-km GSI-3DVar. Its forecasts are also better than those from interpolated LR hybrid analyses for the humidity and wind but not for temperature. For precipitation forecasts, the DR hybrid always outperforms GSI-3DVar, and outperforms the LR hybrid except for the initial period and for low thresholds (see first figure below). The humidity fields are improved most.

Zhu et al (2016) investigate the impacts of assimilating satellite radiance data by using the regional GSI-based EnKF DA system, which is established and tested with operational RAP configuration but without satellite radiance assimilated in Zhu et al (2013 MWR). The satellite radiance data include those of the Advanced Microwave Sounding Unit (AMSU), the Atmospheric Infrared Sounder Radiance (AIRS), the Microwave Humidity Sounder (MHS) and the High-resolution Infrared Radiation Sounder (HIRS) data. As in Zhu et al. (2013 MWR), the EnKF system is run at a horizontal grid spacing of ~40 km and impacts on forecasts up to 18 hours are examined. Positive impacts of radiance data are obtained after tuning the radiance bias correction with appropriate data thinning. Among the radiance datasets, AMSU-A and AIRS data show the greatest positive impacts. AMSU-A data improves the forecasts of all verified variables especially for wind while AIRS data greatly improve the forecasts of humidity. When all radiance data are assimilated, the forecasts are improved even more. Parallel experiments are also performed with GSI 3DVar, and positive impacts are also obtained but forecasts from the EnKF analyses are consistently better than those from the 3DVar analyses. Precipitation forecast skills on the downscaled 13 km grid are also improved with radiance assimilation.

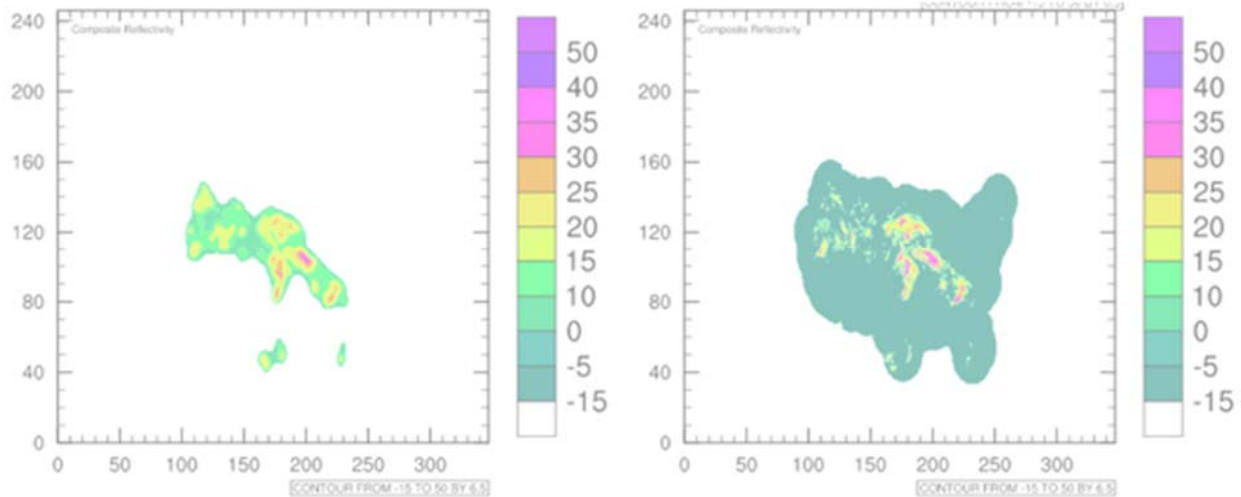
Another important piece of work is the development of capabilities to directly assimilate radar reflectivity data within the GSI 3DVar and GSI En3DVar systems,

based on reflectivity observation operators that involve ice hydrometeors. The reflectivity observation operator used in CAPS ensemble variational data assimilation system was adopted into GSI 3DVAR system. The use of log of hydrometeor mixing ratios was found to lead to more accurate analyses. The tiled NSSL radar reflectivity mosaic observation data was combined and can be analyzed directly into GSI 3DVAR. The preliminary analysis results with direct assimilation of radar reflectivity mosaic observation are reasonable (see second figure below). Now CAPS is working on adding the capability of assimilating reflectivity into GSI-based EnKF system, which is also needed to establish hybrid reflectivity assimilation capabilities based on GSI.

CAPS also coupled the GSI-based EnKF system with the ARPS EnKF system and WRF-ARW model to perform CONUS 3-km grid EnKF DA experiments in real-time for 2016 Hazard Weather Testbed (HWT) Spring Experiment. The GSI-based EnKF was used to assimilate conventional observations used in operational RAP in hourly cycles from 1800 to 0000 UTC while the ARPS EnKF was used from 2300 to 0000 UTC at 15 minute intervals assimilating all WSR-88D radar data. The final EnKF analyses were used to initialize 36-hour deterministic and ensemble forecasts. Preliminary verifications suggest that the forecasts launched from the EnKF analyses are more skillful than the forecasts launched a one-time analysis using the ARPS 3DVAR/cloud analysis system at 0000 UTC, at least for short range precipitation forecasts.



Average precipitation GSSs of 13-km forecasts as a function of forecast length for thresholds (a) 0.1 mm h⁻¹, (b) 1.25 mm h⁻¹, and (c) 2.5 mm h⁻¹ for HyDR_Ctl, HyDR05LRB and VarHR_HRF.



The right panel shows the radar observations, which is the radar composite reflectivity mosaic on 2010051023, the left panel shows the composite reflectivity of GSI-3DVar analysis with zero hydrometer in background.

Publications

- Pan, Y., M. Xue, K. Zhu, and M. Wang, 2016: A GSI-based dual-resolution coupled EnSRF-3DVar hybrid data assimilation system for the operational Rapid Refresh Model. *Advances in Atmospheric Sciences*, Conditionally Accepted.
- Zhu, K., M. Xue, Y. Pan, M. Hu, S. G. Benjamin, S. S. Weygandt, and H. Liu, 2016: The impact of assimilating polar-orbiting satellite radiance data using GSI-based ensemble Kalman filter and GSI 3DVar for a rapid refresh configuration. *Journal of Advances in Modeling Earth Systems*, Submitted.

CIMMS Task III Project – Advanced Data Assimilation and Prediction Research for Convective-Scale “Warn-on-Forecast”

Ming Xue, Youngsun Jung, Tim Supinie, Chengshi Liu, Nathan Snook, and Rong Kong (CAPS at OU)

NOAA Technical Lead: Louis Wicker (NSSL)

NOAA Strategic Goal 2 – Weather-Ready Nation: Society is Prepared for and Responds to Weather-Related Events

Funding Type: CIMMS Task III

Objectives

As a partner of the WoF project, CAPS focuses most of its efforts on developing, refining and applying ensemble-based data assimilation systems to storm-scale deterministic and probabilistic predictions. Efforts will also be made to develop a hybrid ensemble-variational data assimilation system that seeks to combine the strengths of both variational and ensemble methods. Specific objectives for CAPS over the past year include: (1) the development and applications of convective-scale ensemble data

assimilation methods and systems; and (2) participation in inter-comparisons of DA methods on selected cases.

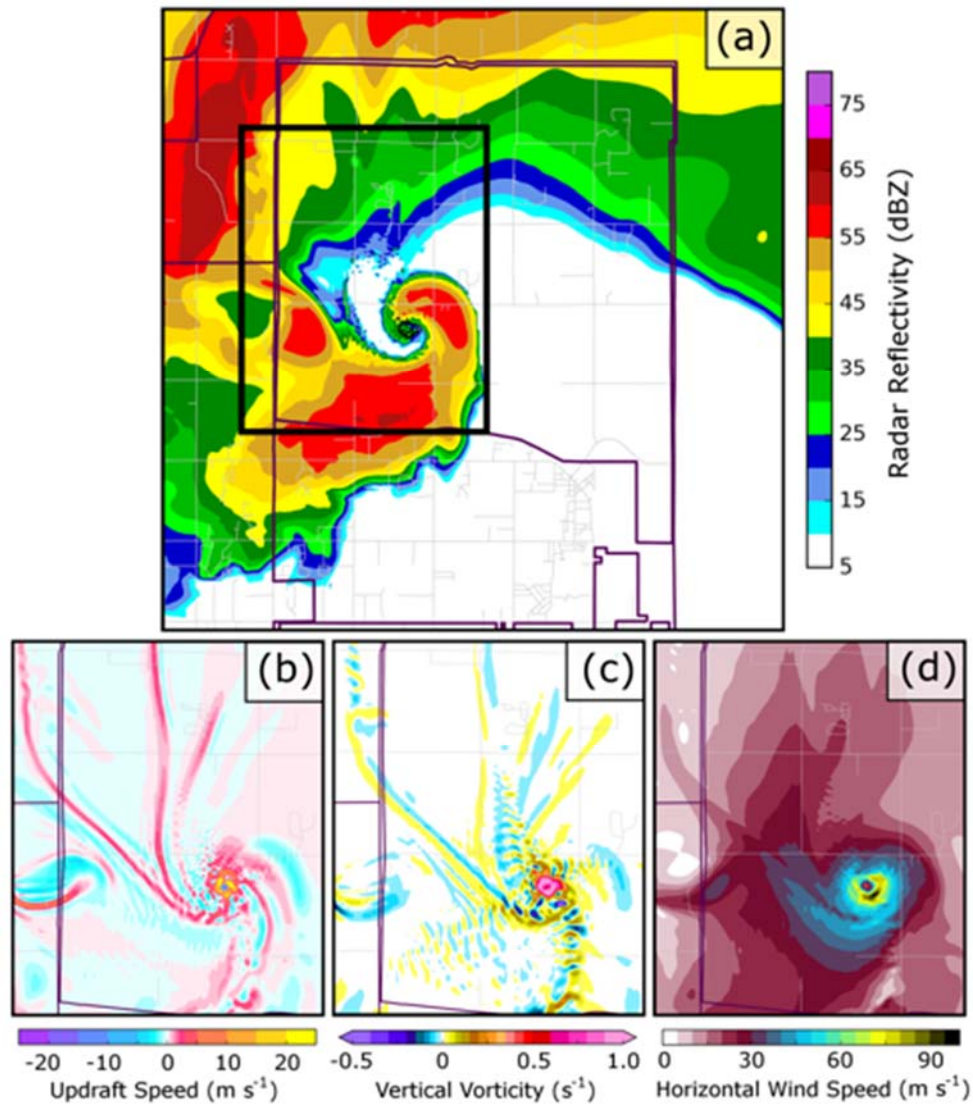
Accomplishments

The invariant background error profile for microphysical variables in ARPS-3DVar/EnVar was replaced with the temperature-dependent background error profile. The OSSE results indicate that reflectivity assimilation produces more reasonable analyses of both liquid and ice hydrometeors when the temperature-dependent background error profile is used. To allow different background error decorrelation lengths for clear and precipitation reflectivity, a double-pass procedure that assimilates clear and precipitation reflectivity in successive steps was developed in the ARPS-3DVar/EnVar framework. This double-pass procedure was found to be more effective in suppressing spurious echoes. Those results were reported in Liu et al (2016) and Rong et al (2016). The ARPS-EnVar has recently been parallelized, and a real-case study using this parallel version is underway. In addition, four ensemble four-dimensional variational algorithms were compared, and their relations within a unified framework were described and published in Liu and Xue (2016). Also, the 4DEnVAR that does not require an adjoint model was implemented within the ARPS variational DA framework during the reporting period.

During the 2016 Hazardous Weather Testbed Spring Experiment organized by NSSL and SPC, CAPS successfully carried out cycled GSI-EnKF DA combined with CAPS's EnKF DA over the CONUS domain with 3-km grid spacing, assimilating conventional and WSR-88D radar data in real time. Ensemble forecasts of surface precipitation from 12 selected days for the non-cycled 3DVAR-based ensemble and the cycled GSI+EnKF-based ensemble were verified against MRMS hourly precipitation. The preliminary results suggest that the EnKF-based ensemble produced forecasts as skillful as the 3DVAR-based ensemble for short-term forecasts (≤ 12 hours).

An ensemble forecast was performed and evaluated for the 20 May 2013 Newcastle-Moore EF5 tornado and its parent storm, consisting of six members with 50-m horizontal grid spacing. In addition to examining predicted tornadic vortices in individual members (see figure below), probabilistic forecast products were produced, predicting the probability of a tornado passing within 1 km of a point using surface wind and/or vorticity criteria. A manuscript reporting initial results is currently in internal review and will be submitted for publication soon (Snook et al. 2016a). The tornado forecast ensemble described above was nested within a 40 member forecast ensemble using 500 m resolution. The results of the 500 m ensemble forecast have been used to facilitate and develop methods for producing and verifying 0-2 hour forecasts of hail, including use of dual-polarimetric radar observations as a supplemental source of verification information in addition to surface hail reports. The 500 m ensemble, when assimilating radar and surface observations using a suitable EnKF configuration, was found to produce skillful 0-90 minute hail forecasts using a variety of metrics (Snook et al. 2016b).

A study comparing the results of assimilating MPAR data versus assimilating WSR-88D data for a supercell case from Oklahoma on 22 May 2011 has been completed using the CAPS's 4DEnSRF DA system. Compared to assimilating 88D data, assimilating MPAR data was found to produce better analyses and forecasts over shorter assimilation periods, while results for the experiments were similar for longer assimilation periods. A paper reporting these results has been submitted for publication (Supinie et al. 2016).



Plots of (a) radar reflectivity, (b) vertical wind speed, (c) vertical vorticity, and (d) horizontal wind speed at 10 m above the surface in the region of the tornadic circulation in an individual ensemble member at 2040 UTC. The thick black box shown in panel (a) indicates the region shown in panels (b), (c), and (d). City borders are indicated in dark purple, and roads are shown in light gray.

Publications

- Liu, C. and M. Xue, 2016: Relationships among four-dimensional hybrid ensemble-variational assimilation algorithms with full and approximate ensemble covariance localization. *Monthly Weather Review*, **144**, 591-606.
- Snook, N., Y. Jung, J. Brotzge, B. Putnam, and M. Xue, 2016: Prediction and ensemble forecast verification of hail in the supercell storms of 20 May 2013. *Weather and Forecasting*, **31**, 811-825.
- Supinie, T., N. Yussouf, Y. Jung, M. Xue, J. Cheng, and S. Wang, 2016: Comparison of the analysis and forecasts of a tornadic supercell storm from assimilating phased array radar and WSR-88D observations, *Weather and Forecasting*, Submitted.
- Yussouf, N., J. Cheng, Y. Jung, M. Xue, and S. Wang, 2016: Comparison of the analyses and forecasts of a tornadic supercell storm from assimilating phased array radar and WSR-88D observations. *Monthly Weather Review*, Submitted.

CIMMS Task III Project – National Sea Grant Weather & Climate Extension Specialist Activities

Kodi Monroe (CIMMS at NSSL), Lans Rothfusz and Alan Gerard (NSSL), and Sam Bush (OU Department of Civil Engineering and Environmental Science)

NOAA Technical Lead: Jonathan Pennock (NOAA Sea Grant)

NOAA Strategic Goal 2 – *Weather-Ready Nation – Society is Prepared for and Responds to Weather-Related Events; and*

NOAA Strategic Goal 1 – *Climate Adaptation and Mitigation: An Informed Society Anticipating and Responding to Climate and its Impacts, and Weather-Ready Nation – Society is Prepared for and Responds to Weather-Related Events*

Funding Type: CIMMS Task III

Objectives

Connect NSSL research with the Sea Grant Extension Network; lead the Coastal and Inland Flooding Observation and Warning (CI-FLOW) project to predict total water level for coastal watersheds; develop a capacity to forecast high-impact threats for coastal communities using the FACETs framework and methodologies.

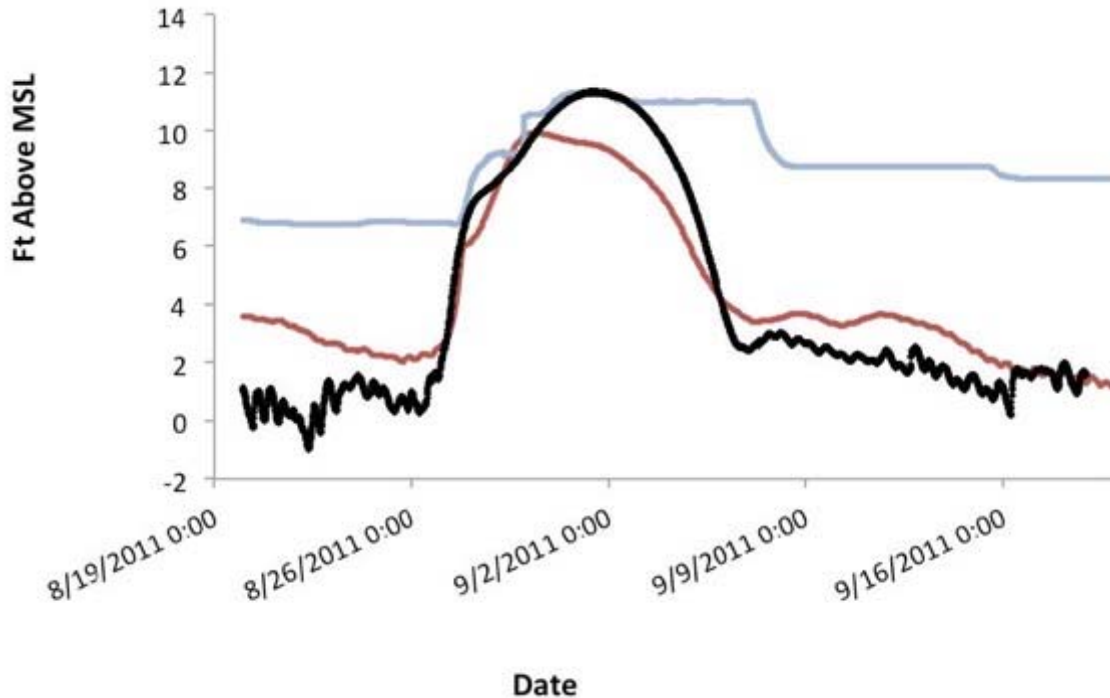
Accomplishments

The Sea Grant Weather & Climate Extension Specialist at CIMMS/NSSL leads NOAA's CI-FLOW project and actively participates in NSSL's hydrometeorological research activities. During the 2015 and 2016 Atlantic hurricane seasons, the CI-FLOW collaborators maintained the real-time coupled modeling system. Quantitative precipitation estimates produced by the NSSL MRMS system provided input data to the 128-member ensemble of the National Weather Service (NWS) Hydrologic Lab-Research Distributed Hydrologic Model (HL-RDHM). Discharge information from HL-RDHM served as upstream boundary conditions for the ADvanced CIRCulation (ADCIRC) hydrodynamic model to incorporate freshwater contributions into coastal water level simulations. Real-time simulations of coastal water levels are available every

six hours on the Coastal Emergency Risks Assessment (<http://nc-cera.renci.org/>) web site.

The Sea Grant Weather & Climate Extension Specialist collaborated with colleagues at OU and NOAA's Coast Survey Development Laboratory to continue a research project on the use of one- and two-dimensional hydraulic models within the CI-FLOW system. This research helps quantify the benefits of a coupled model system that can be more broadly implemented into NWS operations for the Gulf and Atlantic coasts. OU researchers set up a model of the Tar River basin and collected and generated hindcast model forcing data for three test cases - Hurricane Isabel, Hurricane Irene, and Hurricane Floyd. Comparative hindcasts were performed on proposed coupling methods. Results from Hurricane Irene indicate that the one-dimensional hydraulic model predicts low-flow conditions more accurately than the two-dimensional hydraulic model; however, the two-dimensional model predicts the peak water heights and flows more accurately than the one-dimensional model. Current work includes looking at other cases to determine if these trends hold, addressing how and where the hydraulic model might best be incorporated in CI-FLOW, and determining the benefits this coupling can provide in terms of time and accuracy. Initial tests of the time requirements of the different models indicates that the runtime can be reduced by at least half when the one-dimensional hydraulic model is used as middleware in place of an extended two-dimensional model.

The Sea Grant Weather & Climate Extension Specialist is actively participating in NOAA's Storm Surge Roadmap Team, the Great Lakes Coastal Storms Program, and the committee for Living With Extreme Weather: A Workshop to Integrate Understanding and Improve Societal Response. The Extension Specialist also served on a joint technical review panel for Illinois-Indiana and Wisconsin Sea Grant Programs' call for proposals to address knowledge and data gaps related to coastal community resiliency in response to severe weather events. During the 2016 Hazardous Weather Testbed (HWT) Probabilistic Hazard Information (PHI) experiment, the Extension Specialist served as the technical lead and weather producer for the broadcaster room. In collaboration with the South Central Climate Science Center, the Extension Specialist served as a subject matter expert on the impacts of climate change on the water cycle for the massive open online course called "Managing for a Changing Climate".



Water surface elevation predicted by the ADCIRC model (blue) and HEC-RAS (red) model, and observed at the USGS gauge 02084000, Greenville, NC (black) during Hurricane Irene.

CIMMS Task III Project – Prototyping and Evaluating Key Network-of-Networks Technologies

Fred Carr, Nicholas Gasperoni, and Andrew Osborne (OU School of Meteorology), and Keith Brewster (OU CAPS)

NOAA Technical Lead: Curtis Marshall (NWS Office of Observations)

NOAA Strategic Goal 2 – Weather Ready Nation: Society is Prepared for and Responds to Weather-Related Events

Funding Type: CIMMS Task III

Objectives

Conduct Observation System Experiments (OSEs) using data denial and other methods to assess the relative utility of conventional and new observation sources for mesoscale and storm-scale weather forecasting. The Dallas-Fort Worth Urban Testbed, which is home to several novel data sources, is used for this testing.

Accomplishments

In this project we have identified five high impact weather events for study and are using three different data assimilation and forecast tools. Significant progress was made in

producing quality analyses and forecasts for the events and in utilizing some of the newest observation datasets into the analyses systems. New data ingest and pre-processing systems were created to handle data from the GST Mobile Platform Environmental data (MoPED) and Understory Weather automated surface observations.

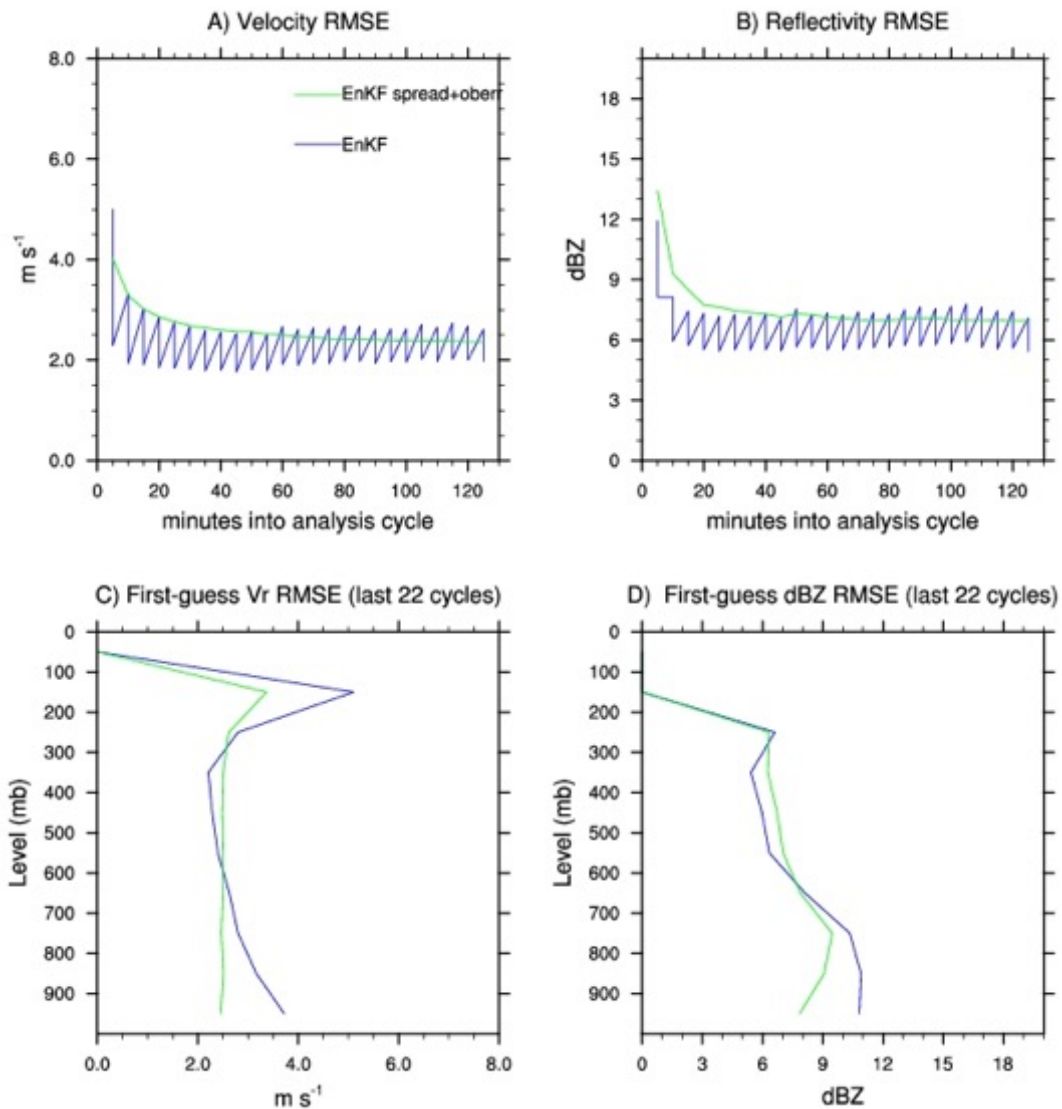
Case 1: May 15, 2013 Cleburne, Texas Tornado: Previous work on this case using the CAPS Advanced Regional Prediction System (ARPS) 3DVAR and ARPS forecast model had produced an excellent forecast with 1-km and 400-m resolution grids. Work was done to apply the CAPS 3DVAR and Weather Research and Forecasting Model (WRF-ARW) model to this case, and after some tuning of the WRF-ARW configuration, similar results were obtained using all data. Data denial experiments showed a positive impact from non-conventional observation types, resulting in better RMS errors in several analyzed variables and better quality of storm structure when those data are included.

Case 2: 26 December 2015 Rowlett, Texas Tornado: An excellent result at 1-km had been obtained in the CAPS DFW Testbed real-time 1-km forecast for this case. Applying the ARPS-3DVAR and WRF-ARW in place of ARPS required some tuning of forecasts, but similar results now have been replicated. Data denial experiments are being set-up for this case.

Case 3: 11 April 2016 Hailstorm: This storm produced hail up to 10 cm (4 in) in diameter in the northern part of the Dallas/Ft Worth Testbed. Analyses using 3DVAR and ARPS are being tuned to produce the best forecast using all data.

Case 4: 3 April 2014 Hail and Tornadoes in North Texas. For this case the GSI-EnKF system is being applied. Experiments were reconfigured to a two-way nested domain at 12-km and 2.4-km resolution for outer and inner grids, respectively, to avoid downscaling issues previously encountered when interpolating from the coarse SREF and GEFS initial conditions. Conventional observations are assimilated every 3 hours for 4 cycles total on the outer grid to obtain a quality larger scale depiction of the event. Software was written to convert all the non-conventional data to the PREPBUFR format that is used in this system. A number of modifications were made to the analysis and forecast configuration, particularly the EnKF settings, to produce a clean analysis and forecast with proper error and ensemble spread during the 5-minute cycling assimilation window on the inner grid. These include modifications to assimilate both clear-air and precipitation observations from radar simultaneously with other testbed data to effectively suppress spurious storm development during the cycling window while correctly representing pre-existing convection within the domain. Other modifications include varying localization width based on observation types and extending the cycling window another hour to produce a final analysis with proper convection initiation (CI) timing. The final analysis shows areas of strong moisture convergence and low CIN near the locations where CI occurs in reality. Next will proceed with data denial experiments. Analysis will include evaluating ensemble forecasts for members with and without CI and comparing the differences that led to CI.

Case 5: 23 March 2016 Squall Line: This case was selected for testing the possible benefit of the high resolution assimilation for CI and storm propagation. Testing and analysis is planned for the next FY.



Root-mean-square differences (RMSE) from observations (blue) and ensemble spread (green) during the GSI EnKF assimilation on the inner (2.4 km) grid for the 3 April 2014 case. A) Velocity, B) Reflectivity. First-guess RMSE vertical profile in the last 22 cycles C) Velocity, D) Reflectivity.

Publications

- Carlaw, L. B., J. A. Brotzge, and F. H. Carr, 2015: Investigating the impacts of assimilating surface observations on high-resolution forecasts of the 15 May 2013 tornado event. *Electronic Journal of Severe Storms Meteorology*, **10**, 1-34.
- Gasperoni, N. A., and X. Wang, 2015: Adaptive localization for the ensemble-based observation impact estimate using regression confidence factors. *Monthly Weather Review*, **143**, 1981-2000.

Theme 4 – Impacts of Climate Change Related to Extreme Weather Events

CIMMS Task III Project – The Assimilation, Analysis, and Dissemination of Pacific Rain Gauge Data (PACRAIN)

Mark Morrissey and Susan Postawko (OU School of Meteorology), and J. Scott Greene (OU Department of Geography and Environmental Sustainability)

NOAA Technical Leads: David Legler (NOAA Climate Program Office) and Howard Diamond (NOAA National Center for Environmental Information)

NOAA Strategic Goal 1 – *Climate Adaptation and Mitigation: An Informed Society Anticipating and Responding to Climate and its Impacts*

Funding Type: CIMMS Task III

Objectives

Tropical rainfall data taken over both land and ocean are particularly important to the understanding of the climate system. Not only is it a tracer of latent heat, it is vital to the understanding of ocean properties as well, including latent and sensible heat flux, salinity changes and concomitant local ocean circulation changes. In addition, rain gauge observations from low-lying atolls are required to conduct verification exercises of the TAO/TRITON buoy-mounted rain gauges, which are funded by NOAA's Ocean Climate Observing Program (OCO). Tropical island rainfall is also required for verification work by satellite rainfall algorithm programs funded by NASA, NOAA and various international programs.

This project supports the NOAA effort to “build and sustain the global climate observing system that is needed to satisfy the long-term observational requirements of the operational forecast centers, international research programs, and major scientific assessments”. Our current and future efforts include expanding our mission to collect, analyze, verify and disseminate global rainfall data sets and products deemed useful for Operational Forecast Centers, International Research Programs and individual researchers in their scientific endeavors. Housed in the National Weather Center at OU, the Comprehensive Pacific rainfall Database and the Schools of the Pacific Rainfall Climate Experiment (SPaRCE) have built upon work from past NOAA-supported projects to become a unique location for scientists to obtain scarce rain gauge data and to conduct research into verification activities. These data are continually analyzed to produce error-assessed rainfall products and are easily assessable via our web page (<http://pacrain.evac.ou.edu/>). We remain actively involved in research of the tropical rainfall process using data obtained from this project.

Accomplishments

1. Development of a New Gridded Surface Tropical Pacific Rainfall Product

A set of 0.25-degree monthly rainfall grids, derived wholly from surface observations contained in the PACRAIN database has been produced. This product will be the subject of a forthcoming journal article, as well as an AMS presentation at the January, 2017 AMS annual meeting. The abstract for the poster presentation should appear under the 21st Conference on Integrated Observing and Assimilation Systems for the Atmosphere, Oceans, and Land Surface, once abstracts are viewable. These grids are important in the sense that they are ‘uncontaminated’ by remotely sensed rainfall estimates which are ‘calibrated’ via surface observations. The relatively fine resolution of the PACRAIN grids allows for aggregation and valid comparison to model output and to remotely sensed estimates, both of which are inherently areal-averaged in terms of their statistical properties. These gridded rainfall estimates were generated using statistical and spatial analysis using Kriging, and employ only rainfall observations taken at locations where orographic effects can safely be taken as non-existent (e.g., atoll stations.) The PACRAIN grids have not been released yet, as the method used to produce them is currently being subject to cross validation and other statistical analysis, but the initial Version 1 product will be vetted and released within the next few months.

2. Tipping Bucket Rain Gauge Project

Rain rate measurements over open ocean regions are very important in the assessment of satellite rain algorithms and climate change and modeling of physical processes. Until recently, no Pacific island rainfall measurements have been available at resolutions less than one hour. In another example of our ability to leverage additional resources from the University of Oklahoma toward this project, we have collected a series of MetONE rain gauges tipping bucket gauges that equipped with data loggers. These were sent to various PIMS for setup and testing. We have received rainfall tip data back from many PIMS and these data are inserted into the PACRAIN database. These data are particularly important in the understanding of basic physics underlying tropical rain systems and consequently, play an important part in enhancing the accuracy of global climate models. These data too are all included in the PACRAIN database. Although we have had problems with collecting and analyzing as much of this data as we would have liked, we are still confident that we will be able to have enough information and analysis to produce a refereed journal paper on our research efforts with these data.

3. Investigation into Differences Observed Between the PACRAIN Data and the Global Historical Climate Network

The primary purpose is to include PACRAIN into the GHCH and use the PACRAIN project to build and search for new and existing Pacific island rain gauge data that are not found easily (i.e. such as on the GTS).

The GHCN dataset is maintained by the National Climatic Data Center as a compilation of climate data from around the world. However, several unforeseen difficulties have resulted in some significant differences in the data records between corresponding sites in the GHCN and the PACRAIN data set. The efforts are ongoing and a technical paper outlining the differences is under preparation.

4. Database Status

During the last year over 74,000 daily and monthly rainfall records from 971 sites have been added to the PACRAIN database.

- The database contains over 3 million daily and monthly observations (see figure below). Data begin in January 1874.
- All data are available at <http://pacrain.evac.ou.edu>. The database was last updated in September 2016. Data availability varies by site.
- Data are not available in real time and thus are not distributed via GTS. Data are collected for climate research and frequently arrive from very remote locales after several months.
- Data access is verified at least monthly with each regular update. Users are encouraged to report access problems so that they can be corrected as soon as possible. Database availability for the past year has been over 99.99%.

5. Outreach and Education

For the past 25 years the Schools of the Pacific Rainfall Climate Experiment (SPaRCE) project at the University of Oklahoma has been working directly with elementary and high school teachers, as well as other organizations (such as the Secretariat of the Pacific Regional Environment Programme) around the Pacific. During this time, we have also worked informally with the Pacific island meteorological services to aid them with their own local educational outreach projects. The SPaRCE program is uniquely situated to be able to both continue collaborating directly with schools, and to aid the meteorological personnel in the islands to develop easily understood educational materials that can be used in a variety of circumstances. Over the past year we have worked on updating many of the SPaRCE materials to include more recent/relevant information on topics such as ENSO, global climate change, cyclones, cyclone preparation brochure, etc.

Continued funding for the SPaRCE program will be used to provide Pacific island meteorological services with low-cost rain gauges for their cooperative observer networks, and to support our undergraduate student to work with meteorological service personnel to develop and deliver educational materials aimed at both potential cooperative observers as well as the general public.

2015-16 progress related to the SPARCE Program:

- Met previous year's objectives. Presently 25 schools actively participating. SPaRCE data are available via a dedicated online interface at <http://sparce.evac.ou.edu/>.
- We continue to receive new interest from schools and have, for example, received new data from schools in the Marshall Islands.
- A quarterly SPaRCE newsletter is published and distributed to participants and other interested parties.
- We have sent out additional recruitment packets to over 100 Pacific Island schools and organizations.
- We continue to work with Pacific meteorological services to enroll more schools

We continue with our updating of the SPaRCE Workbooks. This is nearly complete with up to date scientific information and new color photos and visuals.

Theme 5 – Societal and Socioeconomic Impacts of High Impact Weather Systems

NSSL Project 8 – Warning Process Evolution and Effective Communication to the Public

Chris Karstens (CIMMS at NSSL), James Correia, Jr. (CIMMS at SPC), and Gabe Garfield (CIMMS at OUN)

NOAA Technical Lead: Lans Rothfusz (NSSL)

NOAA Strategic Goal 2 – *Weather-Ready Nation: Society is Prepared for and Responds to Weather-Related Events*

Funding Type: CIMMS Task II

Overall Objectives

Improve various aspects of weather warnings (guidance, decision-making) both in the short, medium, and long terms.

Accomplishments

The 2016 HWT Probabilistic Hazard Information (PHI) Experiment was conducted during the weeks of May 9-13, May 23-27, and June 6-10. During this experiment, participants worked in an integrated warning team: forecasters were tasked with issuing experimental probabilistic forecasts for real-time and displaced real-time severe convective events, and Emergency Managers (EMs) and broadcasters used this experimental information to make simulated decisions. After each event, researchers brought the three groups together for discussions focused on particular elements of the forecast information (e.g., tools, probabilities, visualization, communication) and how each element could be improved.

In 2014, when NWS forecasters were the only participants, it was learned that manual generation and maintenance of object-based probabilistic forecasts becomes problematic when there are 4-5 or more hazard areas to manage simultaneously, presenting a potential limitation to the amount of information that can be updated and passed along to users. In an ideal framework, information would be passed along to users without obstructive workload constraints. In 2015, automated, object-based guidance was introduced to combat this workload issue for the forecasters while striving to understand and optimize elements of forecast information for the EMs. Initially, the goals were to identify various levels of forecaster-automation and to sense whether or not an optimal human-machine mix exists. Additionally, EMs were added in 2015 to explore key decision-maker needs through the usage of PHI, and to begin a co-creation process among researchers, developers, forecasters, and users.

In 2015 it was learned that the optimal human-machine mix is one in which the automated system maintains and updates geographic hazard areas (i.e., objects) while

forecasters override various attributes (e.g., storm motion, forecast duration, probabilities, communication) of the forecast. This strategy gives forecasters more time to analyze radar and other observations while communicating more quality forecast information. In addition, no warning decisions were made by forecasters; they only provided probabilistic information regarding the tornado and wind/hail hazards to the EMs. The presence of EMs provided forecasters an audience for their communication, as well as feedback as to what kinds of information about storms were helpful for decision-making. Through testing and evaluation, a few critical limitations were identified with this work strategy for forecasters. In particular, automated object identification and tracking is not a steady process. Hazard areas are not always immediately identified and maintained, and thus, the tracking is sometimes unjustifiably (and sometimes justifiably) discontinuous. When presented with these situational impasses, forecasters preferentially assumed control of the object as a way to eliminate the error, but the reversion to manual usage resurfaces the aforementioned workload issues, thus limiting information flow. The challenge for 2016 was to develop and test tools that get forecasters through these impasses to maintain operating in the optimal human-machine mix mode. Additionally, EMs and forecasters independently realized the potential of a short forecast discussion to provide critical information needed by the EMs for sense-making, and thus, decision-making. The meaning the forecasters could add by typing a short discussion was critical. Identification of this critical communication element led to an expansion of efforts focusing on the communication (e.g., formatting, colors, wording) of hazardous weather information to key decision-makers in 2016.

For 2016, three types of automated guidance were available to forecasters. These included the NOAA/CIMSS ProbSevere model for the occurrence of any severe (tornadoes, wind, and hail), the NSSL Experimental Warn-on-Forecast System for ensembles (NEWS-e) for tornadoes, and early algorithm development occurring at CIMMS/NSSL for lightning. In addition to having EM participants, Broadcast Meteorologists participated by using PHI to decide whether and when to do simulated cut-ins to programming on an internal TV broadcast. Week one of the experiment began with forecaster tools identical to those from 2015 to re-identify challenges associated with automated object identification and tracking, particularly when the tracking breaks. This breakage occurs when the original object cannot be identified on the successive data layer, and will manifest as one of three potential situations: (1) the original object disappears; (2) the original object is replaced with a new object or set of objects; and (3) the original object is merged with another previously identified object or set of objects.

To address these three tracking issues, a tactic was developed to reintroduce any forecaster-modified object that undergoes a tracking failure back into the spatial display while automatically masking any overlapping object not being maintained by the forecaster. At this juncture, the forecaster is presented with the power to decide how to proceed, depending on which of the three tracking situations have been incurred. In situation #1, the forecaster can take no action or expire the object. In situations #2 and #3, the forecaster can repair the broken object tracking by transferring attributes from one object (original) to another (new object(s) that automatically replaced the original).

Usage with this new tactic quickly revealed new results and additional challenges. In convective events, particularly those with minimal spatial coverage, where tracking issues happen intermittently, the tactic appears to work well. Forecasters are able to overcome the three situational impasses quickly and decisively without interrupting the flow of information to users. However, some convective events appear to trigger these tracking situations frequently and randomly, leading to additional workload to maintain a coherent geospatial representation of the hazard areas. It is hypothesized that adjustments to the object identification and tracking algorithm may alleviate a significant portion of these issues. Preparations are underway to investigate how, if at all, such changes can improve upon the robustness of the current object identification and tracking configuration. However, it is clear that tracking discontinuities are an innate predicament of tracking convective hazard areas. It is also apparent that the previously identified optimal human-machine mix mode is likely optimal for most convective modes and evolutions, but clearly not for all. Thus, forecasters need tools that effectively allow them to transfer between various modes of usage with automated object-based guidance. This conditional usage concept is a topic that will be investigated further in the next experiment.

In addition to working through the object identification and tracking challenges, forecasters were presented with first guess probabilistic trends within the automated object-based guidance. These trends were created from probabilistic predictions from machine learning algorithms, extending through an assumed or predicted duration of predictability. It was hypothesized that these automated predictions would help forecasters in making their probabilistic trend predictions. Usage with this information revealed that forecasters find the automated predictions to be helpful in prioritizing which hazards to engage for generating forecasts for users, with the highest priority given to hazard areas associated the highest predicted probabilistic values. Such hazard areas were typically assigned a warning, whereas hazard areas with lower probabilistic predictions were typically assigned a significant weather advisory. EMs and broadcast meteorology participants used both severe and sub-severe information in their decision making. EMs carefully watched the trends in probabilities, and depending upon circumstance, they made decisions based first on time, second on severity. For example, if a dorm at a university requires 18 minutes to get students to safe areas on the lowest floors, that EM might make a decision ahead of a warning because more time is required than a typical warning lead time. Broadcasters could better prepare for cut-in decisions, and while a sub-severe storm generally did not merit a cut-in to programming, the broadcast meteorologists found the information useful to confirm their own assessments of the storms.

Additionally, forecasters were given the ability to adjust the first guess probabilistic predictions. It was found that adjustments were made frequently (greater than 90% of the time) and the probabilistic trends were typically adjusted to higher values that extended through the assigned duration. However, verification efforts performed from the 2014 experiment indicate that such adjustments result in detrimental reliability, drifting into over-forecasting with little or no skill. These adjustments appear motivated

by the precautionary principle, and were used as a means to reinforce the communication of a warning and drive desired action. Although these actions appear well intentioned with perhaps some communicative merit (discussed later), the intentional distortion of probabilities implies some level of unjustified mistrust of the guidance, and inevitably leads to misunderstanding and misuse of the probabilistic information. Efforts are underway to improve forecasters understanding of the automated guidance by assessing its seasonal skill and envisioning new capabilities for visualizing its underlying reasoning and training information. Additionally, the definition of the probabilistic trend will be simplified to reflect forecast confidence in an effort to address the reliability of the combined forecaster-automated probabilistic forecast system.

Forecaster creation and adjustment toward precautionary probabilistic trends was also partially motivated by interaction with users through the integrated warning team. When the traditional notion of warnings was removed in 2015, users (only EMs that year) struggled with the understanding and intention of probabilities for severe convective events. In pre-week surveys they clearly expressed an understanding that warnings have a range of likelihood of verifying. They've not had to operationalize and use that understanding, however, and were initially unsure they knew how to apply these likelihoods and how to do it well. As they gained some comfort in thinking about how probability might link to action, they pointed out that they might act on a much lower probability when high-end severe weather was expected than on a marginal day, when it was unclear whether storms would reach severe criteria. Ultimately, they strongly expressed the need for the meteorologists to make the meteorological assessment regarding whether a storm merited a warning. EMs need warnings: their standard operating plans have elements (e.g., sounding outdoor warning sirens) based upon those warnings from the NWS. Reinserting traditional warning information into the PHI system in 2016 helped forecasters and users re-establish necessary and (apparently) effective elements of the current warning system (i.e., do no harm). Broadcasters, who first participated in 2016, conveyed that warnings are a lowest-common denominator type of information for the public. In recognition of these needs, the system design will be re-strategized such that generation and consumption of warnings and significant weather advisories are initially prioritized, with probabilistic information initially treated as supplemental information.

The reinsertion of traditional warning information in 2016 was supplemented with a test of prototypes from the Hazard Simplification Project. The tested prototypes changed the overall format to a simple, essentially bulleted form. They included specification of forecaster confidence and severity level in addition to standard information on what, where, and when to expect severe weather. One prototype also changed wording from the current "Advisory" and "Warning" to "Be aware" and "Take action." TV broadcasters found the wording initially difficult to adapt to on air; shifting language to action words and phrases was possible but restricted many of the ways broadcasters currently speak. EMs also found the wording difficult because they talk to their city/county personnel, as well as neighboring EMs (for mutual aid purposes), about warnings. Prototypes also included a color to specify warning level, and all prototypes attempted

to use color in some way. Green was universally dismissed as a first hazard level; green should mean "okay."

Finally, the reinsertion of traditional warning information allowed forecasters and users to focus on new forecast elements associated with the PHI system. Savvy users not only have well-developed plans of action, but, as mentioned earlier, have estimated the amount of time it takes to execute these plans. Thus, time of arrival information, in addition to traditional warning and probabilistic information, meets important needs of this subset of users. However, providing accurate and reliable timing information *requires* a dedication on the part of the forecaster to provide frequent updates to the hazard location, movement, and its various attributes (e.g., severity, intensity, history of reports, forecast information), as well as an increased attention to the geospatial specification of the hazard areas. This critical process of providing frequent updates is a concept we've termed "continuous flow of information," and it is sought out or calculated (if necessary) by our EMs and broadcasters. Because the PHI system completes some tasks for the forecasters, they are able to use their time to focus on meteorological assessment and communication. In other words, frequent updates are possible. Observations of forecasters working high-impact tornado events show evidence that forecasters can naturally identify and utilize the capability of providing continuous flow of information while using geospatially precise objects within the PHI system. Additionally, the optimal human-machine mix mode directly supports these concepts, but as previously noted, more work is needed to better situate the forecaster with the guidance. EMs found the increased precision of PHI objects over traditional warning polygons extremely helpful, and stated they would have tolerance for unexpected changes in the information. The next iteration of this joint experiment will likely give emphasis to the "continuous flow of information" concept, in addition to continuing to challenge forecasters and users to consider the more insightful elements of the PHI system.

Publications

Karstens, C. D., G. Stumpf, C. Ling, L. Hua, D. Kingfield, T. M. Smith, J. Correia, Jr., K. M. Calhoun, K. L. Ortega, C. J. Melick, and L. P. Rothfus, 2015: Evaluation of a probabilistic forecasting methodology for severe convective weather in the 2014 Hazardous Weather Testbed. *Weather and Forecasting*, **30**, 1551-1570.

NSSL Project 9 – Evaluating the Impact of New Technologies, Data, and Information in the Operational Forecasting Environment

NOAA Technical Lead: Pamela Heinselman (NSSL)

NOAA Strategic Goal 2 – Weather-Ready Nation – Society is Prepared for and Responds to Weather-Related Events

Funding Type: CIMMS Task III

Objectives

Design, prepare for, and execute the 2015 Phased Array Radar Innovative Sensing Experiment (PARISE).

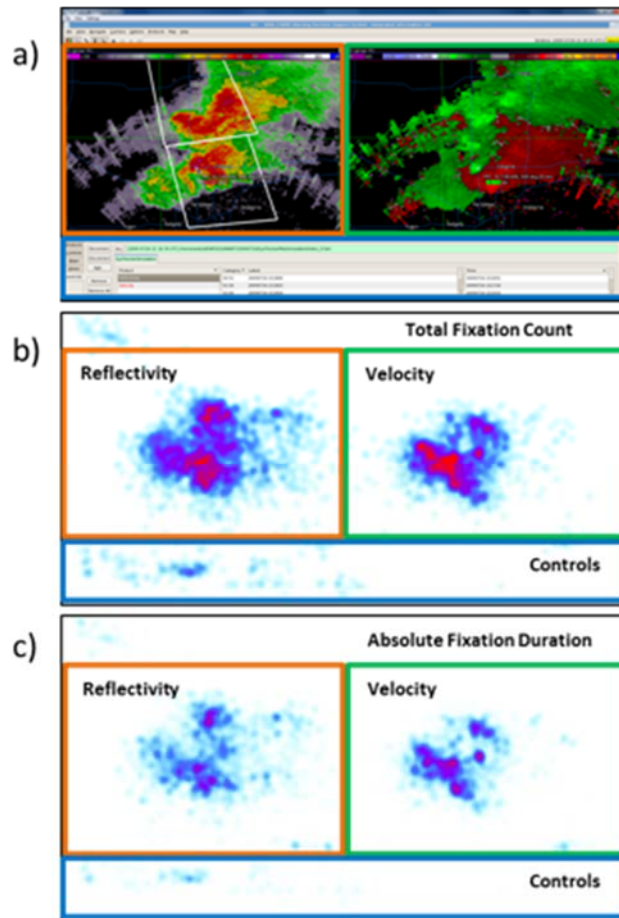
Accomplishments

1. Eye-Tracking Pilot Study

Katie Wilson (CIMMS at NSSL and OU School of Meteorology), Pam Heinselman (NSSL), and Zihong Kang (OU School of Industrial and Systems Engineering)

A pilot study was designed to collect and examine a NWS forecaster's eye gaze data for the first time. Eye gaze data was collected using a Tobii TX300 eye-tracking system. The forecaster worked one weather event, after which he also provided retrospective recall data about his warning decision process. Together, the eye gaze data and retrospective recall data were analyzed. This analysis showed that a signal associated with a changing cognitive process (as observed in the retrospective recall) was evident in the eye fixation measure trends. Being able to track trends in eye fixation measures as the case evolved also provided interesting insight into the forecasters' cognitive processes as the weather event evolved (figure below). This pilot study will appear as an Inbox Article in the *Bulletin of the AMS* November 2016 issue, and provided motivation for the use of eye-tracking methods in the 2015 Phased Array Radar Innovative Sensing Experiment (PARISE).

This work was presented on at the National Weather Association 2015 Annual Meeting and the 2016 Student Research and Creativity Day, with both presentations winning oral awards.



The Warning Decision Support System-Integrated Information (WDSSII) display divided into three areas of interest: reflectivity (left panel, orange box), velocity (right panel, green box), and controls (bottom panel, blue box). Heat maps were created for the (b) total fixation count and (c) absolute fixation duration for the entire case. Within the heat maps, red values indicate a higher fixation count and absolute fixation duration, and blue colors indicate a lower fixation count and shorter absolute fixation duration.

2. The 2015 Phased Array Radar Innovative Sensing Experiment (PARISE)

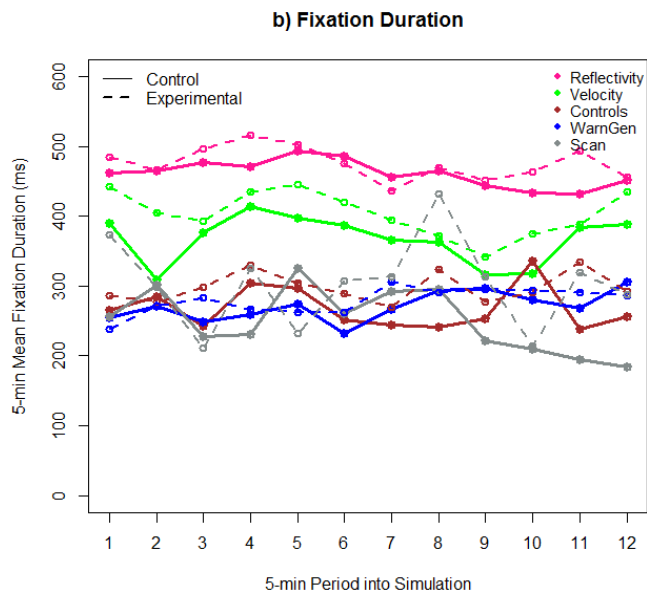
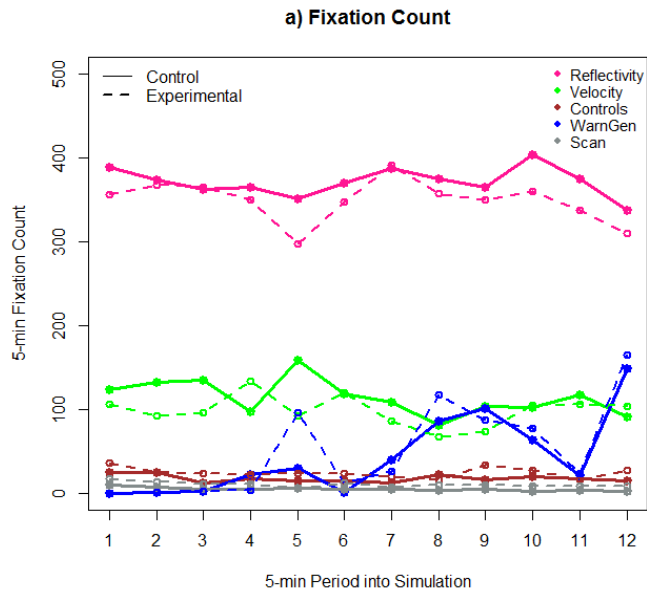
Katie Wilson (CIMMS at NSSL and OU School of Meteorology), Pam Heinselman (NSSL), Ziho Kang (OU School of Industrial and Systems Engineering), and Charles Kuster, Darrel Kingfield, and Tiffany Meyer (CIMMS at NSSL)

The 2015 PARISE was comprised of three experimental components: the traditional experiment, the eye-tracking experiment, and focus groups. The traditional experiment expanded on previous PARISE work by increasing the sample size in number of participants and number of cases worked. In total, 30 NWS forecasters participate in this experiment (representing 25 WFOs), and all forecasters worked nine cases. These cases were split into three types: null, severe hail and/or wind, and tornado. Based on random group assignment, forecasters worked each of the three case types independently using 1-min, 2-min, and 5-min PAR updates in simulated real time.

Following the cases, forecasters provided retrospective recalls of their warning decision processes, and provided cognitive workload ratings for each 5-min period using the instantaneous self-assessment tool. Performance, warning characteristics, and workload rating analysis has been completed for this portion of the 2015 PARISE. The performance results have been presented on at the 2016 AMS and NWA annual meetings by Pam Heinselman. We recently submitted a paper to Weather and Forecasting that discusses the experimental design and results of the traditional experiment.

Forecasters also participated in the eye-tracking experiment using either 1-min or 5-min PAR updates during a one-hour long severe hail and wind event. The experimental design and early results regarding average group differences in forecasters' fixation measures (separated by update speed) were presented on at the 2016 AMS and NWA annual meetings by Katie Wilson (first figure below). The former presentation won an oral award, and this work has also been recognized by the NWA through Wilson's award of the Dr. Roderick A. Scofield scholarship in the summer of 2016. Analysis of this data is currently underway, and Wilson plans to investigate similarity and differences in forecasters' interrogation of radar data based on update speed through scanpath analysis methods.

The third and final portion of the 2015 PARISE was the focus groups (second figure below). In total, six focus groups were carried out, with five forecasters participating in each. The focus groups were held once all other elements of the experiment were completed. Forecasters were invited to share their thoughts, opinions, and feedback on use of 1-min, 2-min, and 5-min phased array radar updates. Pre-identified questions drove the majority of the discussion, but forecasters also raised interesting topics regarding use of dual-polarization radar data with faster updates, and what potential adaptations would have to take place for a WFO to use rapid-update radar data in real-life warning operations. Analysis of this focus group data will take place in spring 2017.



Group median 5-min fixation counts and mean fixating durations for each 5-min period of the one-hour long case for experimental (dashed) and control (solid) participants for the five defined areas of interest.



Focus group discussions with NWS forecasters after they had completed the 2015 PARISE experiments.

Publications

Bowden, K. A., P. L. Heinselman, D. M. Kingfield, and R. P. Thomas, 2015: Impacts of phased-array radar data on forecaster performance during severe hail and wind events. *Weather and Forecasting*, **30**, 389-404.

Heinselman, P., D. LaDue, D. M. Kingfield, and R. Hoffman, 2015: Tornado warning decisions using phased array radar data. *Weather and Forecasting*, **30**, 57-78.

Wilson, K. A., P. L. Heinselman, and Z. Kang, 2016: Exploring applications of eye tracking in operational meteorology research. *Bulletin of the American Meteorological Society*, In Press.

CIMMS Task III Project – Collaborative Research: Understanding the Current Flow of Weather Information and Associated Uncertainty, and Their Effect on Emergency Managers and the General Public

Daphne LaDue (OU CAPS) and Jack Friedman (OU CASR)

NOAA Technical Lead: Steve Koch and Erik Rasmussen (NSSL)

NOAA Strategic Goal 2 – *Weather Ready Nation: Society is Prepared for and Responds to Weather-Related Events*

Funding Type: CIMMS Task III

Objectives

This project is designed to complement physical science research and development efforts from the 2016 VORTEX SE field project: without a baseline of how three types of users of meteorological data* currently behave, the introduction of new technologies may result in unanticipated challenges. Further, this research can help NOAA prioritize when to introduce new technologies into NWS operations. This report addresses two of the three components in this collaborative research project: NWS forecasters and Emergency Managers. Our collaborator at the University of Alabama is addressing the third component: publics.

Accomplishments

1. Forecaster-Oriented Research

Qualitative, ethnographic research was conducted with forecasters from the NWS Huntsville Weather Forecasting Office during the 2015-2016 VORTEX-SE experiment. The lead ethnographic researcher (Friedman) conducted interviews with forecasters, observed forecaster interaction, behavior, and decision-making before, during, and after severe weather events in order to consider how “local forecaster knowledge” influences and shapes the ways in which operational forecasters in the southeast might be able to predict, interpret, and communicate tornado risks in the highly unstable and complex atmospheric conditions that shape southeastern tornado systems. Friedman, an anthropologist who has conducted research on various aspects of severe weather since 2011, approached this research by layering four overlapping research methods and analytics within his research design. First, he conducted *forecaster background interviews* with a majority of the forecasters at the WFO in order to gather general information about their views of risk and reliability and confidence related to different aspects of the work of modern meteorology (numerical model guidance, radar, social media, etc.). Second, pre- and post-event specific interviews were conducted with forecasters regarding severe weather events that were targeted for study during the Spring 2016 VORTEX Intensive Observation Periods (IOPs). Third, in situ observations were conducted in the WFO before, during, and after severe weather events that were the target of VORTEX IOPs. These in situ observations were recorded in written field notes and included both intra-office communication, planning, and activities as well as communication that occurred between the WFO and its partners (emergency managers, other decision makers, and the media) and the publics (via traditional media (NWS watches, warnings, and written products) as well as social media). Finally, fourth, the study included active “digital ethnography,” involving Dr. Friedman’s graduate research assistant (Melissa Wagner) recording and communicating (often in real-time) relevant online communication and data regarding the severe weather, including NWS products, NWS chat, social media, radar images, traditional media, etc. All of these data were recorded using Storify to automate some of the capture of social media.

97 recorded interviews were conducted between February 2, 2016 and May 1, 2016 with forecasters at the Huntsville NWS WFO. 14 background interviews were conducted with individual forecasters at the WFO (average ~75 minutes each). These background

interviews gathered forecasters' personal and professional backgrounds as well as forecasters' perceptions of uncertainties in and beliefs about 1) numerical model guidance, 2) sensing technologies, 3) region-specific challenges for forecasting severe weather in the southeast, 4) how publics understand weather science, and 5) social media. In addition to the person-centered, background interviews, 83 event-specific interviews (pre-/post-observed event interviews, average ~18 minutes each) were conducted with WFO forecasters during 8 observed events (1 pre-VORTEX event; 7 VORTEX events). 64 out of 83 (>77%) event-specific interviews involved both pre- and post-interviews with the same interviewee (the remaining 17 (<21%) involved either a pre- or post-interview, usually due to a research subject being scheduled to be off of work either on the day before or after an event that they worked; there were also 2 "ad hoc" interviews with subjects regarding tangential, but related, topics).

Interviews were transcribed and coded, drawing on inductive methods (similar to grounded theory) to identify recurrent and connected themes that emerged in the interviewees' talk. In the background interviews, 6 broad thematic "master themes" were identified, with a total of 34 specific sub-themes coded using TAMS Analytic, a free, open-access qualitative-coding program. The event-specific, pre- and post-interviews were manually coded and recorded in Excel spreadsheets focused on four key themes: 1) what was/would be most difficult to predict about an event, 2) what the interviewee was most confident about regarding an event, 3) how the interviewee judged model guidance for an event pre- and post-event, and 4) the interviewee's overall impressions, descriptions, and predictions related to an event. The use of Excel spreadsheets was possible because these event-specific interviews tended to be much shorter than the background interviews (~18 minutes vs. ~75 minutes) and were significantly more structured interviews. The spreadsheet approach also allowed easier visual and analytical comparisons of pre- and post-event discourse across individual research subjects.

2. Emergency Manager-Oriented Research

This portion of the work builds upon prior work by LaDue on how emergency managers are currently receiving, understanding, and using information about severe weather in their preparation and response activities. The previous work included geographically distributed participants from many states east of the Rocky Mountains and was a basis for understanding emergency manager decision making in NOAA's Hazardous Weather Testbed under experimental warning-type information during the 2015 and 2016 Prototype Probabilistic Hazard Information projects. This new work focuses on the VORTEX SE study domain in northern Alabama. This portion of the study began with background interviews that included a critical incident technique element, pre-post interviews around VORTEX SE intensive operations periods (IOP), and, when possible, observations of EM operations during VORTEX SE IOPs.

A pre-VORTEX SE trip was taken in order to meet and establish relationships with emergency managers across the VORTEX SE study domain. Most of the resulting 14 background interviews were conducted during that trip. Each lasted between 1–2 hours,

and were conducted with emergency management directors, deputy directors, and officers. A few additional interviews were added during VORTEX SE travel. These interviews were designed to learn about emergency managers' standard operating procedures, typical practices, and experiences with weather events in their areas. These were conducted with a mix of general social science and critical incident interview techniques. Pre-post interviews were attempted around each VORTEX SE IOP, but these proved more difficult than for Friedman, where the NWS office is a 24/7 operation (by Alabama statute, the only weather conditions under which emergency operations centers (EOC) are *required* to open outside of normal hours is when the county is under a tornado watch). Emergency management offices are a weekday, daytime operation outside of active response periods, and emergency managers are frequently out of the office with meetings, training workshops, and other mitigation and recovery activities (two aspects of emergency management not explicitly included in this work). In the end, 20 pre-post interviews were achieved for five of the IOPs, with six as matching pairs (meaning the same person was reached both pre- and post-event). The final, and key activity, was observing EM operations. This was possible during any event for which a tornado watch was issued (one event), or when a VORTEX SE IOP occurred during weekday hours (two events). For the remaining IOPs LaDue stayed within 10 minutes of the county EOC within the focus of that IOP, ready to engage in observations if weather conditions worsened and the EOC opened. For the final two IOPs, which occurred on a weekend, LaDue was able to observe operations in the incident command center of an outdoor arts and music festival. In addition to the planned activities, a number of informants from schools, law enforcement, and fire departments were engaged in informal discussions in preparation for 2017 VORTEX SE, which will extend this work beyond the EM to his/her constituencies.

Background and pre-post interviews were partially transcribed and notes were taken. The subsequent data-driven thematic analysis has thus far yielded four major themes. Pre-post interviews showed a variety of anticipation levels, with the highest anticipation being for an event that remained sub-severe in northern Alabama.

CIMMS Task III Project – Implementation of a Drought App for Mobile Devices

Mark Shafer (OCS at OU) and Mike Wolfinbarger (Weather Decision Technologies, Inc.)

NOAA Technical Lead: Claudia Nierenberg (NOAA Climate Program Office)

NOAA Strategic Goal 1 – *Climate Adaptation and Mitigation: An Informed Society Anticipating and Responding to Climate and its Impacts*

Funding Type: CIMMS Task III

Objectives

A mobile drought app is being developed by Weather Decision Technologies, a private firm located in Norman, Oklahoma, under funding previously provided on a project, *Drought Risk Management for the United States* (described next). This project is to

complete development of the app, including iPhone and Android platforms, and make it freely available for download.

Accomplishments

The iPhone prototype app is still under development on the previous grant. This must be completed before funds from this grant can be used to complete the app development and port it to the Android platform. The prototype app should be available for beta testing in Fall 2016 with an expected operational app for both iPhone and Android platforms by Spring 2017.

CIMMS Task III Project – Drought Risk Management for the United States

Mark Shafer (OCS at OU), and Michael Hayes, Mark Svoboda, Cody Knutson, Tsegaye Tadesse, Deborah Bathke, and Brian Fuchs (National Drought Mitigation Center)

NOAA Technical Lead: Chad McNutt (NOAA NIDIS Program Office)

NOAA Strategic Goal 1 – *Climate Adaptation and Mitigation: An Informed Society Anticipating and Responding to Climate and its Impacts*

Funding Type: CIMMS Task III

Objectives

The overall goal of the project is to improve drought risk management across the United States. To accomplish this goal, the project builds upon partnerships between the Southern Climate Impacts Planning Program (SCIPP), National Drought Mitigation Center (NDMC), and National Integrated Drought Information System (NIDIS). The project will develop new tools and procedures and test them in the Southern Plains Drought Early Warning System being developed by NIDIS. Specific objectives of the project include: (1) Improving and expanding drought monitoring activities; (2) Engaging the NIDIS Preparedness Community Technical Working Group activities; (3) Examining drought planning assistance; (4) Continued development of Regional Drought Early Warning System assistance; (5) Conducting a regional drought event assessment; and (6) Communication and dissemination activities.

Accomplishments

Improving and Expanding Drought Monitoring Activities. NDMC is now ingesting additional data feeds (SNOTEL, SCAN), including soil moisture and satellite-based tools, into products used for the U.S. Drought monitor. NDMC has conducted several case studies to validate the new data sources. NDMC is collaborating with Canadian scientists to expand the scope of VegDRI (Vegetation Drought Response Index).

Engaging the NIDIS Preparedness Community Technical Working Group. A meeting for the NIDIS Early Preparedness Communities (EPC) was held in Lincoln, NE April 28-29, 2016, the first such meeting since 2011. The meeting assessed the status of Early Warning Systems as input into the revision of NIDIS' Implementation Plan. Participation in planning and conduct of several other meetings has occurred under this objective:

Wildfire Management Workshop (October 21-22, 2015 in Boise, ID); Rural Futures Conference (October 2015); Multi-Hazard Drought/Flood Tournament (September 17, 2015, Floresville, TX, with the U.S. Army Corps of Engineers and San Antonio River Authority).

Drought Planning Strategies. “Managing Drought Risk on the Ranch” workshops and webinars have continued engagement with livestock producers and extension personnel and investigated expansion to crop producers. One of the workshops was hosted by the Chickasaw Nation in Sulphur, OK and involved 80 individuals from 12 tribes. SCIPP and NDMC collaborated with the Arkansas Natural Resources Commission to begin a state drought planning effort in Arkansas. The planning process included co-hosting a workshop on June 8, 2016 in Little Rock, AR.

Regional Drought Early Warning Systems. NDMC participated in developing the Missouri River Basin Regional Drought Early Warning System (RDEWS), participated in the Midwest RDEWS, and collaborated with the Carolinas Integrated Regional Sciences and Assessments team on developing an enhanced system for collecting volunteer drought observations in the Coastal Carolina RDEWS. NDMC and SCIPP continued collaboration on the Southern Plains RDEWS, which included conducting a workshop on the rapid shift from extreme drought to record floods in 2015 (October 2015, Fort Worth, TX).

Drought Event Assessments. NDMC is leading development of an assessment of the 2010-2015 Southern Plains drought, in collaboration with SCIPP, NOAA Regional Climate Services, and USDA Climate Hub.

Communication and Dissemination Activities. SCIPP and Weather Decisions Technologies are collaborating on developing a mobile drought app for the iPhone. The app is currently in prototype stage and should go to a limited group for beta testing in Fall 2017. A companion app for Android and Google platforms is being developed under a separate project. Other communication activities included publishing a quarterly DroughtScape publication, monthly drought and impacts summaries, participation in the Drought Portal redesign, and cross-agency expansion of NIDIS and NDMC tools into EDEN and USDA Extension systems.



Trevor Timberlake, Engineer Supervisor for the Arkansas Natural Resources Commission, leads a group discussion on how drought impacts Arkansas.

CIMMS Task III Project – Baseline of Public Responsiveness to Uncertainty in Forecasts

Carol Silva (OU CRCM), Hank Jenkins-Smith (OU National Institute for Risk and Resilience – NIRR – and Department of Political Science), Joseph Ripberger (OU CRCM, NIRR, and Department of Political Science)

NOAA Technical Lead: John Cortinas (NOAA OWAQ)

NOAA Strategic Goal 2 – *Weather Ready Nation: Society is Prepared for and Responds to Weather-Related Events*

Funding Type: CIMMS Task III

Objectives

Over the three year course of this project, CRCM will develop a conceptual design for independently evaluating the extent to which NWS initiatives/products change the way end users interact with, interpret, and respond to new types of information about extreme weather. To enable this evaluation, the proposed project will: (1) establish a scientifically defensible baseline measure of public responsiveness to NWS warnings, watches, and advisories under the current WWA paradigm; and (2) develop a protocol for repeatedly measuring (monitoring) public responsiveness to NWS warnings, watches, and advisories as FACETs initiatives/products come to fruition. The data necessary for establishing the baseline measure and evaluation protocol will come from an independent and ongoing weather survey program that is managed, paid for, and owned by the CRCM. The empirical foundation of this program is a national survey of the U.S. public that is statistically weighted against the U.S. Census to ensure that all segments of the population are accounted for in the analysis.

Accomplishments

During the first year of the project, social scientists at CRCM drew upon previous research, theories, and techniques in the social and behavioral sciences to design a survey instrument that systematically measures the extent to which members of the U.S. public receive, comprehend, and respond to NWS warnings, watches, and advisories under the current WWA paradigm. They also statistically analyzed the reliability and validity of the instrument using data from an independent and ongoing survey, called the Meso-Scale Integrated Socio-geographic Net (M-SISNet), which is implemented and managed by researchers at CRCM and funded by National Science Foundation. Based on this analysis, the scientists have begun to design the pilot survey instrument that will be used to establish baseline measures of reception, comprehension, and response under the current WWA paradigm. This survey will be implemented during the second year of the project as part of an independent and ongoing weather survey program that is managed, paid for, and owned by the CRCM.

Public Affairs and Outreach

NOAA Partners Communications, Public Affairs, and Outreach

NOAA Technical Leads: Lans Rothfusz (NSSL) and Keli Pirtle (NOAA Public Affairs)

NOAA Engagement Enterprise – *An Engaged and Educated Public with an Improved Capacity to Make Scientifically Informed Environmental Decisions*

Funding Type: CIMMS Task II

Objectives

Communicate CIMMS and NSSL research to OU, OAR, NOAA, Department of Commerce leadership, U.S. Congress, decision makers, partners, collaborators, and the public.

Accomplishments

1. NOAA and OAR Data Calls – Tanya Schoor (CIMMS)

- Report significant papers– Alert NOAA leadership to published papers determined to be significant by NSSL leadership.
 - Work with authors to write a summary of each significant paper.
 - NSSL reported **16** significant papers in FY2016.
- Fact check total publication numbers against NOAA HQ's for accuracy.
- Report numbers for Quarterly Education performance taskers.

2. Legislative Affairs – Tanya Schoor (CIMMS)

- Work with NSSL and CIMMS management to revise fact sheets used to brief members of the U.S. Congress and their staffers during NOAA Day on The Hill and the CI Directors' Legislative Affairs Day.
- NOAA in Your State – Legislative Affairs maintains a spreadsheet of NOAA Activities in each state to use when briefing the U.S. Congress. This list is updated each year.
- Work with Legislative Affairs to develop an annual Congressional Plan for NSSL.

3. NOAA and OAR Communications – Tanya Schoor (CIMMS)

- **OAR Hot Items** Describe new NSSL research and activities. Hot items are posted on the OAR Hub, where the OAR Communications team reviews and chooses significant topics to be included in the Department of Commerce Secretary's Weekly Report. **14** Hot Items were submitted on behalf of NSSL in FY2016.
- **Department of Commerce Secretary's Weekly Report** – Significant OAR Hot Items are condensed into a few sentences to be included into the Department of

Commerce Secretary's Weekly Report. Work with HQ to ensure the accuracy of these items. In FY2016, 2 NSSL OAR Hot Items were included in the Weekly Report.

- **OAR Editorial Board** – Serve on the OAR Editorial Board that meets each Monday to review the accuracy and clarity of items to be sent to the Executive Management Team and the Secretary of Commerce. Discuss potential social media items.

4. NSSL Project Fact Sheets – Tanya Schoor (CIMMS)

- Fact Sheets are 1-2 page handouts on NSSL projects used to give visitors and guests a “take-away” message. 6 NSSL Fact Sheets were designed, written, edited, or updated in FY2016.

5. NSSL Research and Projects on Social Media – Tanya Schoor (CIMMS)

- NSSL's Facebook and Twitter accounts are very popular. New content is published daily based on monthly themes and partner posts are shared as appropriate. NSSL also has Flickr and Instagram accounts.

6. NSSL Outreach Emails – Tanya Schoor (CIMMS)

- The public submits questions to NSSL via the NSSL Outreach email account. In FY2016, 159 emails and 12 written letters were received and answered.

7. NSSL Website – Vicki Farmer (ACE) and Tanya Schoor (CIMMS)

- Review and update NSSL website content as needed.
- Track and post awards.

8. Back-up NOAA Weather Partners Public Affairs – Keli Pirtle (NOAA) and Tanya Schoor (CIMMS)

- Field media calls and questions while the NOAA Public Affairs Officer is on AL or out of the office.

9. Education and Outreach – Patrick Hyland (OU)

- Lead public and school tours of NOAA offices in the National Weather Center.
- Plan and organize National Weather Festival activities.
- Facilitate educational outreach opportunities

CIMMS at WDTD Outreach

Alyssa Bates, Michael Bowlan, Jill Hardy, Eric Jacobsen, Chris Spannagle, Philip Ware, Andy Wood, and Alex Zwink (CIMMS at WDTD)

CIMMS staff at WDTD regularly engaged in various outreach activities during the past year. Some of the activities involved partnerships with other organizations in the National Weather Center. Some of these outreach activities include:

- Working support “shifts” at the NWS Norman Weather Forecast Office (WFO) during severe weather events;
- Participating in the planning and presentation of the National Weather Festival;
- Volunteering with other National Weather Center organizations during the Norman United Way Day of Caring; and
- Giving a mini-workshop to School of Meteorology students on warning fundamentals.

Other outreach activities involving CIMMS staff at WDTB included:

- Developing grade-level appropriate meteorology lessons and presenting them to elementary school students;
- Discussing NWS warning issuance with a civic group;
- Giving presentations to undergraduate student groups on dual-polarization radar; and
- Visiting elementary and middle school career days to discuss common activities of meteorologists.



Skype session led by CIMMS instructor (lower right-hand corner of photo) for civic group in Marysville, KS (in main part of image).

Appendix A

AWARDS AND HONORS

The following awards or other notable achievements occurred in the past fiscal year:

Date	Awardee	Award	Reason/Topic
7/30/15	Megan Taylor	Innovation in Teaching Award	Nominated for this award at the Summer Institute for Distance Learning and Instructional Technology (SIDLIT)
9/24/15	Andy Wood	2015 Dean's Award for Outstanding Service	Recognized for his exceptional support of severe weather education and outreach to the National Weather Service (NWS), NOAA, and key partners of the Weather-Ready Nation initiative
10/21/15	HWT Team at NWC, including CIMMS	Larry R. Johnson Special Award, NWA Annual Meeting	Awarded to an individual or group that has made significant contributions to the field of operational meteorology
10/21/15	Race Clark and Galatea Terti	1st and 2nd place, respectively, in the graduate student poster contest at the NWA Annual Meeting	Race's poster was titled "Towards Hazard Services Recommenders for Flash Flood Forecasting," while Galatea presented "Target the warnings: Probabilistic flash flood casualties prediction."
10/21/15	Katie (Bowden) Wilson	Best Graduate Student Oral Presentation	"Eye-tracking during the Forecaster Warning Decision Process: A Pilot Experiment." Co-authors were Pam Heinselman and Ziho Kang.
11/1/15	Jill Hardy	Selected to the "30 Under 30" panel at Eliot Maisie's Learning 2015 Conference	The 30 Under 30 Program aims to support young talent, who will become the next generation of learning leaders, and offers a platform to share ideas and network with peers.
2/2/16	Katie (Bowden) Wilson	1st Place Winner, Oral Presentation Category in the 32 nd EIPT Conference Student Competition at the AMS Annual Meeting	"Eye-Tracking Applications to Assess Impacts of Phased Array Radar Data on Forecasters' Cognitive Processes"
2/6/16	Tomer Burg (REU Student)	3rd place in the 32 nd EIPT Conference Student Competition - AMS Annual Meeting	"Assessing the Skill of Updated Precipitation Type Diagnostics for Rapid Refresh with mPING"
2/9/16	Greg Blumberg	Second place in the oral presentation category at the 32 nd EIPT Conference Student Competition	"Monitoring the Evolution of Deep Convection Through the Use of Ground-Based Spectral Infrared Thermodynamic Sounders" w/ Univ. of Wisconsin/CIMMS' Timothy Wagner and NSSL's Dave Turner
2/9/16	David Harrison and Christopher Karstens	Honorable Mention in the 11 th Symposium on Societal Applications: Policy, Research and Practice (11SOCIETY) Student Competition	"A Statistical Overview of Operational Storm-Based Warnings"

2/9/16	Mallory Paige Row, and S. M. Cavallo and D.D. Turner	2nd place winner in the 28 th Conference on Climate Variability and Change	"Synoptic and Local Influences on a Summertime, Long-Lived, Mixed-Phase Cloud Event Over Summit, Greenland: A Modeling Perspective"
2/9/16	Ryan A. Lagerquist, and A. McGovern, V. Lakshmanan, and Travis Smith	3rd place winner in the 14 th Conference on Artificial and Computational Intelligence and its Applications to the Environmental Sciences Student Competition	"Real-time Prediction of Damaging Straight-line Winds Produced by Thunderstorms"
3/4/16	Katie (Bowden) Wilson	1st Place Winner, OU Student Research and Creativity Day	
3/4/16	Race Clark	McNair's Choice in Science Award at OU Student Research and Creativity Day	
4/11/16	Christopher Karstens	Best Paper award for 7 th Annual TBPG workshop	For his presentation on "Forecaster Decision-Making with Automated Probabilistic Guidance in the 2015 Hazardous Weather Testbed Probabilistic Hazard Information experiment"
4/11/16	Katie (Bowden) Wilson	2016 Yoshi Sasaki Award	For Best M.S. Publication: Bowden, K., P. Heinselman, D. M. Kingfield, and R. Thomas, 2015: Impacts of phased array radar data on forecaster performance during severe hail and wind events. <i>Wea. Forecasting</i> ,30, 389–404.
5-6/16	Megan Taylor	"Emerging Training Leader to Watch" by Training Magazine	Award is given to those who "inspired and engaged their organizations with stellar leadership skills, business acumen, and innovation." Full article at: https://pubs.royle.com/publication/?i=300711 , p. 33.
7/1/16	Heather Reeves	AMS Service Award	In recognition of her creativity in developing and administering the "Mountain Meteorology Webinar" at the AMS Conference on Mountain Meteorology (27 June – 1 July 2016)

9/14/16	Katie (Bowden) Wilson	Dr. Roderick A. Scofield Scholarship in Meteorology, National Weather Association Annual Meeting	
9/14/16	MRMS Team at CIMMS	Larry R. Johnson Special Award, NWA Annual Meeting	Awarded to an individual or group that has made significant contributions to the field of operational meteorology

Appendix B

PUBLICATION SUMMARY*

	CIMMS Lead Author				NOAA Lead Author				Other Lead Author			
	2008-09	2009-10	2010-11	2011-12	2008-09	2009-10	2010-11	2011-12	2008-09	2009-10	2010-11	2011-12
Peer Reviewed	52	32	28	31	13	28	32	13	45	40	44	35

	CIMMS Lead Author				NOAA Lead Author				Other Lead Author			
	2012-13	2013-14	2014-15	2015-16	2012-13	2013-14	2014-15	2015-16	2012-13	2013-14	2014-15	2015-16
Peer Reviewed	32	57	60	62	8	9	7	5	45	44	40	52

**Publication numbers are approximate.*

Appendix C

PERSONNEL SUMMARY – NOAA FUNDED RESEARCH ONLY

Category	Number	B.S.	M.S.	Ph.D.
Research Scientist	80	4	41	35
Visiting Scientist	2		2	
Postdoctoral Fellow	10			10
Research Support Staff	17	7	10	
Administrative	2	1	1	
Total (>50% support)	111	12	54	45
Undergraduate Students	23			
Graduate Students (current degree)	46	23	23	
Employees that receive <50% NOAA Funding (not including students)	56	8	9	39
Located at Lab	NSSL-83, WDTD-16, ROC-9, SPC-7, NWSTC-5, OUN-1			
Obtained NOAA employment within the last year	2			

Appendix D

COMPILATION OF CIMMS-RELATED PUBLICATION 2015-16

Publications compiled here were reported for projects funded under Cooperative Agreement NA11OAR4320072.

Peer-Reviewed Journal Articles, Books, and Book Chapters *Published, In Press, or Accepted*

- Argyle, E. M., J. J. Gourley, Z. L. Flamig, T. Hansen, and K. Manross, 2016: Towards a user-centered design of a weather forecasting decision support tool. *Bulletin of the American Meteorological Society*, In Press.
- Bluestein, H., and J. Snyder, 2015: An observational study of the effects of dry air produced in dissipating convective storms on the predictability of severe weather. *Weather and Forecasting*, **30**, 79-114.
- Bluestein, H. B., J. C. Snyder, and J. B. Houser, 2015: A multi-scale overview of the El Reno, Oklahoma, tornadic supercell of 31 May 2013. *Weather and Forecasting*, **30**, 525-552.
- Bluestein, H., M. French, J. Snyder, and J. Houser, 2016: Doppler-radar observations of anticyclonic tornadoes in cyclonically rotating, right-moving supercells. *Monthly Weather Review*, **144**, 1591-1616.
- Boodoo, S., D. Hudak, A. Ryzhkov, P. Zhang, N. Donaldson, D. Sills, and J. Reid, 2015: Quantitative precipitation estimation from a C-Band dual-polarized radar for the July 08 2013 flood in Toronto, Canada. *Journal of Hydrometeorology*, **16**, 2027-2044.
- Borowska, L., G. Zhang, and D. S. Zrnica, 2015: Considerations for oversampling in azimuth on the phased array weather radar. *Journal of Atmospheric and Oceanic Technology*, **32**, 1614-1629.
- Borowska, L., G. Zhang, and D. S. Zrnica, 2016: Spectral processing for step scanning phased array radars, *IEEE Trans. On Geoscience and Remote Sensing*, **54**, 4534-4543.
- Bowden, K. A., P. L. Heinselman, D. M. Kingfield, and R. P. Thomas, 2015: Impacts of phased-array radar data on forecaster performance during severe hail and wind events. *Weather and Forecasting*, **30**, 389-404.
- Cao, Q., M. Knight, A. Ryzhkov, P. Zhang, and N. Lawrence, 2016: Differential phase calibration of linearly polarized weather radar for accurate measurements of circular depolarization ratio. *IEEE Transactions on Geosciences Remote Sensing*, Accepted.
- Carlaw, L. B., J. A. Brotzge, and F. H. Carr, 2015: Investigating the impacts of assimilating surface observations on high-resolution forecasts of the 15 May 2013 tornado event. *Electronic Journal of Severe Storms Meteorology*, **10**, 1-34.
- Carlin, J., 2015: Weather radar polarimetry. *Physics Today*. Available at <http://scitation.aip.org/content/aip/magazine/physicstoday/news/10.1063/PT.5.4011.jsessionid=4pginrtbms1m9.x-aip-live-02>.

- Carlin, J., A. Ryzhkov, J. Snyder, and A. Khain, 2016: Hydrometeor mixing ratio retrievals for storm-scale radar data assimilation: Utility of current equations and potential benefits of polarimetry. *Monthly Weather Review*, **144**, 2981-3001.
- Chronis, T., L. D. Carey, C. J. Schultz, E. V. Schultz, K. M. Calhoun, and S. J. Goodman, 2015: Exploring Lightning Jump Characteristics. *Weather and Forecasting*, **30**, 23-37.
- Cintineo, R., J. Otkin, T. A. Jones, S. Koch, and D. Stensrud, 2016: Assimilation of synthetic GOES-R ABI infrared brightness temperatures and WSR-88D radar observations in a high-resolution OSSE. *Monthly Weather Review*, In Press.
- Cocks, S. B., S. M. Martinaitis, B. Kaney, J. Zhang, and K. Howard, 2016: MRMS QPE performance during the 2013/14 cool season. *Journal of Hydrometeorology*, **17**, 791-810.
- Crandall, K. L., P. S. Market, A. R. Lupo, L. P. McCoy, R. J. Tillott, and J. J. Abraham, 2015: The application of diabatic heating in Q-vectors for the study of a North American cyclone event. *Advances in Meteorology*, Article ID 2908423, 11 pages.
- Curtis, C., M. Yeary, and J. Lake, 2016: Adaptive beamforming to mitigate ground clutter on the National Weather Radar Testbed phased array radar. Accepted by *IEEE Transactions on Geoscience and Remote Sensing*, **54**, 1282-1291.
- Diederich, M., S. Troemel, A. Ryzhkov, P. Zhang, and C. Simmer, 2015: Use of specific attenuation for rainfall measurements at X-band radar wavelengths. Part I: Radar calibration and partial beam blockage estimation. *Journal of Hydrometeorology*, **16**, 487-502.
- Diederich, M., S. Troemel, A. Ryzhkov, P. Zhang, and C. Simmer, 2015: Use of specific attenuation for rainfall measurements at X-band radar wavelengths. Part II: Rainfall estimates and comparison with rain gauges. *Journal of Hydrometeorology*, **16**, 503-516.
- Elmore, K. L., H. M. Grams, D. Apps, and H. D. Reeves, 2015: Verifying forecast precipitation type with mPING. *Weather and Forecasting*, **30**, 656-667.
- Fierro A. O., 2016: "Present State of Knowledge of Electrification and Lightning within Tropical Cyclones and Their Relationships to Microphysics and Storm Intensity." Chapter 7 in *Advanced Numerical Modeling and Data Assimilation Techniques for Tropical Cyclone Predictions*, U. C. Mohanty and S. Gopalakrishnan, eds. Co-published by Springer International Publishing, Cham, Switzerland, with Capital Publishing Company, New Delhi, India, pp. 197-220.
- Fierro, A. O., A. J. Clark, E. R. Mansell, D. R. MacGorman, S. Dembek and C. Ziegler, 2015: Impact of storm-scale lightning data assimilation on WRF-ARW precipitation forecasts during the 2013 warm season over the contiguous United States. *Monthly Weather Review*, **143**, 757-777.
- Fierro, A. O., E. R. Mansell, D. R. MacGorman, and C. Ziegler, 2015: Explicitly simulated electrification and lightning within a tropical cyclone based on the environment of Hurricane Isaac (2012). *Journal of the Atmospheric Sciences*, **72**, 4167-4193.
- Fierro, A. O., J. Gao, C. Ziegler, K. Calhoun, E. R. Mansell and D. R. MacGorman, 2016: Assimilation of flash extent data in the variational framework at convection-allowing scales: Proof-of-concept and evaluation for the short term forecast of the 24 May 2011 tornado outbreak. *Monthly Weather Review*, Accepted.
- French, M. M., P. S. Skinner, L. J. Wicker, and H. B. Bluestein, 2015: Documenting a rare tornado merger observed in the 24 May 2011 El Reno-Piedmont, Oklahoma supercell. *Monthly Weather Review*, **143**, 3025-3043.

- Fulton, C., and A. Mirkamali, 2015: A computer-aided technique for the analysis of embedded element patterns of cylindrical arrays [EM Programmer's Notebook]. *IEEE Antennas and Propagation Magazine*, **57**, 132-138.
- Fulton, C., M. Yeary, D. Thompson, J. Lake, and A. Mitchell, 2016: Digital phased arrays: Challenges and opportunities. *Proceedings IEEE, Special Issue on Phased Arrays*, **104**, 487-503.
- Gallo, B. T., A. J. Clark, and S. R. Dembek, 2016: Forecasting tornadoes using convection-permitting ensembles. *Weather and Forecasting* **31**, 273–295.
- Gallo, B. T., A. J. Clark, and S. R. Dembek, 2016: CORRIGENDUM. *Weather and Forecasting*, **31**, 1407-1408.
- Gasperoni, N. A., and X. Wang, 2015: Adaptive localization for the ensemble-based observation impact estimate using regression confidence factors. *Monthly Weather Review*, **143**, 1981-2000.
- Giangrande, S., T. Toto, A. Bansemer, M. Kumjian, S. Mishra, and A. Ryzhkov, 2016: Insights into riming and aggregation processes as revealed by aircraft, radar, and disdrometer observations for a 27 April 2011 widespread precipitation event. *Journal of Geophysical Research*, **121**, 5846-5863.
- Gourley, J. J., Z. Flamig, H. Vergara, P. E. Kirstetter, R. Clark III, E. Argyle, A. Arthur, S. Martinaitis, G. Terti, J. Erlingis, Y. Hong, and K. Howard, 2016: The Flooded Locations And Simulated Hydrographs (FLASH) project: Improving the tools for flash flood monitoring and prediction across the United States. *Bulletin of the American Meteorological Society*, In Press.
- Grams, H. M., P.-E. Kirstetter, and J. J. Gourley, 2016: Naive Bayesian precipitation type retrieval from satellite using a cloud top and ground radar matched climatology. *Journal of Hydrometeorology*, Accepted.
- Gravelle, C. M., J. R. Mecikalski, W. E. Line, K. M. Bedka, R. A. Petersen, J. M. Sieglaff, G. T. Stano, and S. J. Goodman, 2016: Demonstration of a GOES-R satellite convective toolkit to “bridge the gap” between severe weather watches and warnings: an example from the 20 May 2013 Moore, OK tornado outbreak. *Bulletin of the American Meteorological Society*, **97**, 69-84.
- Gravelle, C. M., K. J. Runk, K. L. Crandall, and D. W. Snyder, 2016: Forecaster evaluations of high temporal satellite imagery for the GOES-R era at the NWS Operations Proving Ground. *Weather and Forecasting*, **31**, 1157-1177.
- Hardy, J., J.J. Gourley, P.E. Kirstetter, Y. Hong, F. Kong, and Z. Flamig, 2016: A method for probabilistic flash flood forecasting. *Journal of Hydrology*, In Press.
- Heinselman, P., D. LaDue, D. M. Kingfield, and R. Hoffman, 2015: Tornado warning decisions using phased array radar data. *Weather and Forecasting*, **30**, 57-78.
- Houser, J., H. B. Bluestein, and J. C. Snyder, 2015: Rapid-scan, polarimetric, Doppler radar observations of tornadogenesis and tornado dissipation in a tornadic supercell: the “El Reno, Oklahoma” storm of 24 May 2011. *Monthly Weather Review*, **143**, 2685-2710.
- Houser, J., H. Bluestein, and J. Snyder, 2016: A fine-scale radar examination of the tornadic debris signatures and weak reflectivity band associated with a large, violent tornado. *Monthly Weather Review*, In Press.
- Ilotoviz, E., N. Benmoshe, A. Khain, V. Phillips, and A. Ryzhkov, 2016: Effect of aerosols on freezing drops, hail, and precipitation in a mid-latitude storm. *Journal of Atmospheric Science.*, **73**, 109-144.

- Issa Lélé M., L. M. Leslie, and P. J. Lamb, 2015: Analysis of low-level atmospheric moisture transport associated with the West African monsoon. *Journal of Climate*, **28**, 4414-4430.
- Ivić, I. R., 2016: A technique to improve copolar correlation coefficient estimation. *IEEE Transactions on Geoscience and Remote Sensing*, **54**, 5776–5800.
- Ivić, I., and R. Doviak, 2016: Evaluation of phase coding to mitigate differential reflectivity bias in polarimetric PAR, *IEEE Transactions on Geoscience and Remote Sensing*, **54**, 431-451.
- Jiang, H., S. Albers, I. Jankov, D. Birkenheuer, Z. Toth, Y. Xie, G. Stumpf, D. Kingfield, B. Motta, M. Scotten, and J. Picca, 2015: Real-time applications of the variational version of the Local Analysis and Prediction System (vLAPS). *Bulletin of the American Meteorological Society*, **96**, 2045-2057.
- Johnson, A., X. Wang, J. R. Carley, L. J. Wicker, and C. Karstens, 2015: A comparison of multiscale GSI-based EnKF and 3DVar data assimilation using radar and conventional observations for midlatitude convective-scale precipitation forecasts. *Monthly Weather Review*, **143**, 3087-3108.
- Jones, T. A., D. Stensrud, L. Wicker, P. Minnis, and R. Palikonda, 2015: Simultaneous radar and satellite data storm-scale assimilation using an ensemble Kalman filter approach for 24 May 2011. *Monthly Weather Review*, **143**, 165-194.
- Jones, T. A., and D. J. Stensrud, 2015: Assimilating cloud water path as a function of model cloud microphysics in an idealized simulation. *Monthly Weather Review*, **143**, 2052-2081.
- Jones, T. A., K. Knopfmeier, D. Wheatley, G. Creager, P. Minnis, and R. Palikonda, 2016: Storm-scale data assimilation and ensemble forecasting with the NSSL experimental Warn-on-Forecast system. Part II: Combined radar and satellite experiments. *Weather and Forecasting*, **30**, 297-327.
- Jones, T. A., S. Koch, and Z. Li, 2016: Assimilating synthetic hyperspectral sounder temperature and humidity retrievals to improve severe weather forecasts. *Atmospheric Research*, Accepted.
- Kaltenboeck, R., and A. Ryzhkov, 2016: A freezing rain storm explored with a C-band polarimetric weather radar using the QVP methodology. *Meteorologische Zeitschrift*, Accepted.
- Karimkashi, S., and G. Zhang, 2015: Optimizing radiation patterns of a cylindrical polarimetric phased-array radar for multimissions. *IEEE Transactions On Geoscience and Remote Sensing*, **53**, 2810-2818.
- Karstens, C. D., G. Stumpf, C. Ling, L. Hua, D. Kingfield, T. M. Smith, J. Correia, Jr., K. M. Calhoun, K. L. Ortega, C. J. Melick, and L. P. Rothfus, 2015: Evaluation of a probabilistic forecasting methodology for severe convective weather in the 2014 Hazardous Weather Testbed. *Weather and Forecasting*, **30**, 1551-1570.
- Karstens, C. D., K. Shourd, D. Speheger, A. Anderson, R. Smith, D. Andra, T. M. Smith, and V. Lakshmanan, 2016: Evaluation of near real-time preliminary tornado damage paths, *Journal of Operational Meteorology*, **4**, 132-141.
- Krause, J., 2016: A simple algorithm to discriminate between meteorological and non-meteorological radar echoes. *Journal of Atmospheric and Oceanic Technology*, **33**, 1875-1885.
- Kumjian, M., S. Mishra, S. Giangrande, T. Toto, A. Ryzhkov, and A. Bansemmer, 2016: Polarimetric radar and aircraft observations of saggy bright band during MC3E. *Journal of Geophysical Research, Atmospheres*, **121**, 3584-3607.

- Kurdzo, J. M., D. J. Bodine, B. L. Cheong, and R. D. Palmer, 2015: High-temporal resolution polarimetric X-band Doppler radar observations of the 20 May 2013 Moore, Oklahoma tornado. *Monthly Weather Review*, **143**, 2711-2735.
- Kuster, C. M., P. L. Heinselman, and M. Austin, 2015: 31 May 2013 El Reno tornadoes: Advantages of rapid-scan phased-array radar data from a warning forecaster's perspective. *Weather and Forecasting*, **30**, 933-956.
- Kuster, C. M., P. L. Heinselman, and T. J. Schuur, 2016: Rapid-update radar observations of downbursts occurring within an intense multicell thunderstorm of 14 June 2011. *Weather and Forecasting*, **31**, 827-851.
- Lakshmanan, V., C. D. Karstens, K. Elmore, S. Berkseth, and J. Krause, 2015: Which polarimetric variables are important for weather/no-weather discrimination? *Journal of Atmospheric and Oceanic Technology*, **32**, 1209-1223.
- Lang, T. J., S. Pédeboy, W. Rison, R. S. Cervený, J. Montanyà, S. Chauzy, D. R. MacGorman, R. L. Holle, E. E. Ávila, Y. Zhang, G. Carbin, E. R. Mansell, Y. Kuleshov, T. C. Peterson, M. Brunet, F. Driouech, and D. Krahen, 2016: WMO World Record Lightning Extremes: Longest detected flash distance and longest detected flash duration. *Bulletin of the American Meteorological Society*, In Press.
- Lei, L., G. Zhang, R. Doviak, and S. Karimkashi, 2015: Comparison of theoretical biases in estimating polarimetric properties of precipitation with weather radar using parabolic reflector, or planar and cylindrical arrays, *IEEE Transactions On Geoscience and Remote Sensing*, **53**, 4313-4327.
- Line, W. E., T. J. Schmit, D. T. Lindsey, and S. J. Goodman, 2016: Use of geostationary super rapid scan satellite imagery by the Storm Prediction Center. *Weather and Forecasting*, **31**, 483-494.
- Liu, C. and M. Xue, 2016: Relationships among four-dimensional hybrid ensemble-variational assimilation algorithms with full and approximate ensemble covariance localization. *Monthly Weather Review*, **144**, 591-606.
- MacGorman, D. R., M. I. Biggerstaff, S. Waugh, J. T. Pilkey, M. A. Uman, D. M. Jordan, T. Ngin, W. R. Gamerota, G. Carrie, and P. Hyland, 2015: Coordinated lightning, balloon-borne electric field, and radar observations of a triggered lightning flash in North Florida. *Geophysical Research Letters*, **42**, 5635-5643.
- Martinaitis, S. M., S. B. Cocks, Y. Qi, B. T. Kaney, J. Zhang, and K. Howard, 2015: Understanding winter precipitation impacts on automated gauge observations within a real-time system. *Journal of Hydrometeorology*, **16**, 2345-2363.
- Martinaitis, S. M., J. J. Gourley, Z. L. Flamig, E. M. Argyle, R. A. Clark III, A. Arthur, B. R. Smith, J. M. Erlingis, S. Perfater, and B. Albright, 2016: The HMT Multi-Radar Multi-Sensor Hydro Experiment. *Bulletin of the American Meteorological Society*, In Press.
- McGovern, A., C. K. Potvin, and R. A. Brown, 2016: *Using Large-Scale Machine Learning to Improve Our Understanding of the Formation of Tornadoes*. CRC Press, In Press.
- Melnikov, V., and D. S. Zrnić, 2015: On the alternate transmission mode for polarimetric phased array weather radar. *Journal of Atmospheric and Oceanic Technology*, **32**, 220-233.
- Melnikov, V., R. Doviak, and D. Zrnic, 2015: A method to increase the scanning rate of phased-array weather radar. *IEEE Transactions in Geosciences Remote Sensing*, **53**, 5634-5643.

- Melnikov, V., D. Zrnić, D. Burgess, and E. Mansell, 2015: Vertical extent of thunderstorm inflows revealed by polarimetric radar. *Journal of Atmospheric and Oceanic Technology*, **32**, 1860-1865.
- Melnikov, V., M. Istok, and J. Westbrook, 2015: Asymmetric radar echo patterns from insects. *Journal of Atmospheric and Oceanic Technology*, **32**, 659-674.
- Nai, F., S. M. Torres, and R. D. Palmer, 2016: Adaptive beamspace processing for phased-array weather radars. *IEEE Transactions on Geoscience and Remote Sensing*, **54**, 5688-5698.
- Ortega, K., J. Krause, and A. Ryzhkov, 2016: Polarimetric radar characteristics of melting hail. Part III: Validation of the algorithm for hail size discrimination. *Journal of Applied Meteorology and Climatology*, **55**, 829-848.
- Otkin, J. A., M. Shafer, M. Svoboda, B. Wardlow, M. C. Anderson, C. Hain, and J. Basara, 2015: Facilitating the use of drought early warning information through interactions with agricultural stakeholders. *Bulletin of the American Meteorological Society*, **96**, 1073-1078.
- Oue, M., M. Galletti, J. Verlinde, A. Ryzhkov, Y. Lu, and N. Bharadwaj, 2016: Use of X-band differential reflectivity measurements to study shallow Arctic mixed-phase clouds. *Journal of Applied Meteorology and Climatology*, **55**, 403-424.
- Peppler, R. A., 2016: "They could tell what the weather was to be in advance." Native Oklahoma weather and climate insights from the archive. *Chronicles of Oklahoma*, Accepted.
- Peppler, R. A., K. E., Kehoe, J. W. Monroe, A. K. Theisen, and S. T. Moore, 2016: "The ARM Data Quality Program." Chapter 12 in *The Atmospheric Radiation Measurement (ARM) Program. Meteorological Monographs*, American Meteorological Society, 12.1-12.14.
- Peppler, R. A., K. E. Klockow, and R. D. Smith, 2016: "Hazardscapes: Perceptions of tornado risk and the role of place in central Oklahoma." In *PLACE Attachment: A Geographic Perspective*, J. S. Smith, ed., Accepted.
- Phillips, V., A. Khain, N. Benmoshe, E. Ilotoviz, and A. Ryzhkov, 2015: Theory of time-dependent freezing. Part II. Scheme for freezing raindrops and simulations by a cloud model with spectral bin microphysics. *Journal of the Atmospheric Sciences*, **72**, 262-286.
- Potvin, C. K., and M. L. Flora, 2015: Sensitivity of idealized supercell simulations to horizontal grid spacing: Implications for Warn-On-Forecast. *Monthly Weather Review*, **143**, 2998-3024.
- Qi, Y., S. Martinaitis, J. Zhang, and S. Cocks, 2016: A real-time automated quality control of hourly rain gauge data based on multiple sensors in MRMS system. *Journal of Hydrometeorology*, **17**, 1675-1691.
- Reeves, H., A. Ryzhkov, and J. Krause, 2016: Discrimination between winter precipitation types based on spectral-bin microphysical modeling. *Journal of Applied Meteorology and Climatology*, **55**, 1747-1761.
- Ripberger, J. T., C. L. Silva, H. C. Jenkins-Smith, D. E. Carlson, M. James, and K. G. Herron, 2015: False alarms and missed events: The impact and origins of perceived inaccuracy in tornado warning systems. *Risk Analysis*, **35**, 44-56.
- Ripberger, J. T., C. L. Silva, H. C. Jenkins-Smith, and M. James, 2015: The influence of consequence-based messages on public responses to tornado warnings. *Bulletin of the American Meteorological Society*, **96**, 577-590.

- Ryzhkov, A., P. Zhang, H. Reeves, M. Kumjian, T. Tschallener, C. Simmer, and S. Troemel, 2016: Quasi-vertical profiles – a new way to look at polarimetric radar data. *Journal of Atmospheric and Oceanic Technology*, **33**, 551-562.
- Saharia, M., P. E. Kirstetter, H. Vergara, J. J. Gourley, and Y. Hong, 2016: Mapping flash flood severity in the United States. *Journal of Hydrometeorology*, Accepted.
- Saharia, M., P. E. Kirstetter, H. Vergara, J. J. Gourley, and Y. Hong, 2016: Characterization of floods in the United States. *Journal of Hydrology*, Accepted.
- Schroeder, A. J., J. J. Gourley, J. Hardy, J. J. Henderson, P. Parhi, V. Rahmani, K. A. Reed, R. S. Schumacher, B. K. Smith, and M. J. Taraldsen, 2016: The development of a flash flood severity index. *Journal of Hydrology*, In Press.
- Shapiro, A., S. Rahimi, C. K. Potvin, and L. Orf, 2016: On the use of advection correction in trajectory analysis. *Journal of the Atmospheric Sciences*, **72**, 4261-4280.
- Sheng, C., J. J. Gourley, Y. Hong, Q. Cao, N. Carr, P.-E. Kirstetter, J. Zhang, and Z. Flamig, 2016: Using citizen science reports to evaluate estimates of surface precipitation type. *Bulletin of the American Meteorological Society*, **97**, 187-193.
- Sisterson, D. L., R. A. Peppler, T. S. Cress, P. J. Lamb, and D. D. Turner, 2016: "The ARM Southern Great Plains (SGP) Site." Chapter 6 in, *The Atmospheric Radiation Measurement (ARM) Program. Meteorological Monographs*, American Meteorological Society, 6.1-6.14.
- Skinner, P. S., L. J. Wicker, D. M. Wheatley, and K. H. Knopfmeier, 2016: Application of two spatial verification methods to ensemble forecasts of low-level rotation. *Weather and Forecasting*, **31**, 713-735.
- Skinner, P. S., C. C. Weiss, L. J. Wicker, C. K. Potvin, and D. C. Dowell, 2015: Forcing mechanisms for an internal rear-flank downdraft momentum surge in the 18 May 2010 Dumas, Texas, supercell. *Monthly Weather Review*, **143**, 4305-4330.
- Smith, T. M., V. Lakshmanan, G. J. Stumpf, K. L. Ortega, K. Hondl, K. Cooper, K. M. Calhoun, D. M. Kingfield, K. L. Manross, R. Toomey, and J. Brogden, 2016: Multi-Radar Multi-Sensor (MRMS) severe weather and aviation products: Initial operating capabilities. *Bulletin of the American Meteorological Society*, Early Online Release.
- Snook, N., Y. Jung, J. Brotzge, B. Putnam, and M. Xue, 2016: Prediction and ensemble forecast verification of hail in the supercell storms of 20 May 2013. *Weather and Forecasting*, **31**, 811-825.
- Snyder, J., A. Ryzhkov, M. Kumjian, J. Picca, and A. Khain, 2015: Developing a Z_{DR} column detection algorithm to examine convective storm updrafts. *Weather and Forecasting*, **30**, 1819-1844.
- Snyder, J., and A. Ryzhkov, 2015: Automated detection of polarimetric tornado debris signatures. *Journal of Applied Meteorology and Climatology*, **54**, 1861-1870.
- Tanamachi, R. L., P. L. Heinselman, and L. J. Wicker, 2015: Impacts of a storm merger on the 24 May 2011 El Reno, Oklahoma tornadic supercell. *Weather and Forecasting*, **30**, 501-524.
- Terti, G., I. Ruin, S. Anquetin, and J. J. Gourley, 2015: Dynamic vulnerability factors for impact-based flash flood prediction. *Natural Hazards*, **79**, 1481-1497.

- Thompson, T. E., L. J. Wicker, X. Wang, and C. K. Potvin, 2015: A comparison between the local ensemble transform Kalman filter and the ensemble square root filter for the assimilation of radar data in convective-scale models. *Quarterly Journal of the Royal Meteorological Society*, **141**, 1163-1176.
- Torres, S. M. and C. D. Curtis, 2015: The impact of range oversampling processing on tornado velocity signatures obtained from WSR-88D super-resolution data. *Journal of Atmospheric and Oceanic Technology*, **32**, 1581-1592.
- Torres, S., R. Adams, C. Curtis, E. Forren, D. Forsyth, I. Ivić, D. Priegnitz, J. Thompson, and D. Warde, 2016: Adaptive-weather-surveillance and multifunction capabilities of the National Weather Radar Testbed Phased-Array Radar. *IEEE Proceedings*, **104**, 660-672.
- Troemel, S., A. Ryzhkov, M. Diederich, K. Muhlbauer, C. Simmer, S. Kneifel, and J. Snyder, 2016: Multi-sensor characterization of mammatus clouds. *Monthly Weather Review*, Accepted.
- Vergara, H., P. E. Kirstetter, J. J. Gourley, Z. Flamig, Y. Hong, A. Arthur, and R. Kolar, 2016: Estimating a-priori kinematic wave model parameters based on regionalization for flash flood forecasting in the conterminous United States. *Journal of Hydrology*, In Press.
- Wakimoto, R. M., N. T. Atkins, K. M. Butler, H. B. Bluestein, K. Thiem, J. C. Snyder, and J. B. Houser, 2015: Photogrammetric analysis of the 2013 El Reno tornado combined with mobile X-band polarimetric radar data. *Monthly Weather Review*, **143**, 2657-2683.
- Wakimoto, R., N. Atkins, K. Butler, H. Bluestein, K. Theim, J. Snyder, J. Houser, and J. Wurman, 2016: Aerial damage survey of the 2013 El Reno tornado combined with mobile radar data. *Monthly Weather Review*, **144**, 1749-1776.
- Wang, Y., J. Zhang, P.-L. Chang, and Q. Cao, 2015: Radar vertical profile of reflectivity correction with TRMM observations using a neural network approach. *Journal of Hydrometeorology*, **16**, 2230-2247.
- Wang, Y., J. Zhang, P. Chang, C. Langston, B. Kaney, L. Tang, 2016: Operational C-Band Dual-Polarization radar QPE for the subtropical complex terrain of Taiwan. *Advances in Meteorology*, 1-15.
- Waugh, S., C. L. Ziegler, D. R. MacGorman, S. E. Fredrickson, D. W. Kennedy, and W. D. Rust, 2015: A balloon-borne particle size, imaging and velocity probe for in situ microphysical measurements. *Journal of Atmospheric and Oceanic Technology*, **32**, 1562-1580.
- Weiss, C. C., D. C. Dowell, J. L. Schroeder, P. S. Skinner, A. E. Reinhart, P. M. Markowski, and Y. P. Richardson, 2015: A comparison of near-surface buoyancy and baroclinity across three VORTEX2 supercell intercepts. *Monthly Weather Review*, **143**, 2736-2753.
- Wheatley, D. M., K. H. Knopfmeier, T. A. Jones, and G. J. Creager, 2015: Storm-scale data assimilation and ensemble forecasting with the NSSL experimental Warn-on-Forecast system. Part I: Radar data experiments. *Weather and Forecasting*, **30**, 1795-1817.
- Wilson, K. A., P. L. Heinselman, and Z. Kang, 2016: Exploring applications of eye tracking in operational meteorology research. *Bulletin of the American Meteorological Society*, In Press.
- Xie, X., R. Evaristo, S. Troemel, P. Saavedra, C. Simmer, and A. Ryzhkov, 2016: Radar observation of evaporation and implications for quantitative precipitation and cooling rate estimation. *Journal of Atmospheric and Oceanic Technology*, **33**, 1779-1792.

- Yu, X., Y. Zhang, A. Patel, A. Zahrai, and M. Weber, 2016: An implementation of real-time phased array radar fundamental functions on DSP-focused, high-performance embedded computing platform. *Aerospace: Special Issue – Radar and Aerospace*, Accepted.
- Yussouf, N., D. C. Dowell, L. J. Wicker, K. H. Knopfmeier, and D. M. Wheatley, 2015: Storm-scale data assimilation and ensemble forecasts for the 27 April 2011 severe weather outbreak in Alabama. *Monthly Weather Review*, **143**, 3044–3066.
- Yussouf, N., J. S. Kain, and A. J. Clark, 2016: Short-term probabilistic forecasts of the 31 May 2013 Oklahoma tornado and flash flood event using a continuous-update-cycle storm-scale ensemble system. *Weather and Forecasting*, **31**, 957-983.
- Zhang, G. 2016: *Weather Radar Polarimetry*. CRC Press.
- Zhang, J., K. Howard, C. Langston, B. Kaney, Y. Qi, L. Tang, H. Grams, Y. Wang, S. Cocks, S. Martinaitis, A. Arthur, K. Cooper, J. Brogden, and D. Kitzmiller, 2016: Multi-Radar Multi-Sensor (MRMS) quantitative precipitation estimation: Initial operating capabilities. *Bulletin of the American Meteorological Society*, **97**, 621-637.
- Zhuang Z., N. Yussouf and J. Gao, 2016: The Analyses and Forecasts of a Tornadic Supercell Outbreak using a 3DVAR System Ensemble. *Advances in Atmospheric Science*, **33**, 544-558.
- Zrnica, D., V. Melnikov, R. Doviak, and R. Palmer, 2015: Scanning strategy for the Multifunction Phased-Array Radar to satisfy aviation and meteorological needs. *Geosciences Remote Sensing Letters, IEEE*, **12**, 204-208.

Appendix E

NOAA COMPETITIVE AWARD RECIPIENT REPORTS

and

NOAA HURRICANE SANDY COMPETITIVE AWARD RECIPIENT REPORTS

*These reports are presented in the format provided by the respective PIs directly to their NOAA Program Managers. **They appear in a separate file to this document.***